frontiers | Research Topics

Root development: Towards understanding regulatory networks and complex interactions between cell populations

Edited by
Svetlana Shishkova, Ling Huang, Ramiro Esteban Rodriguez, Daniela Ristova and Raffaele Dello Ioio

Published in
Frontiers in Plant Science

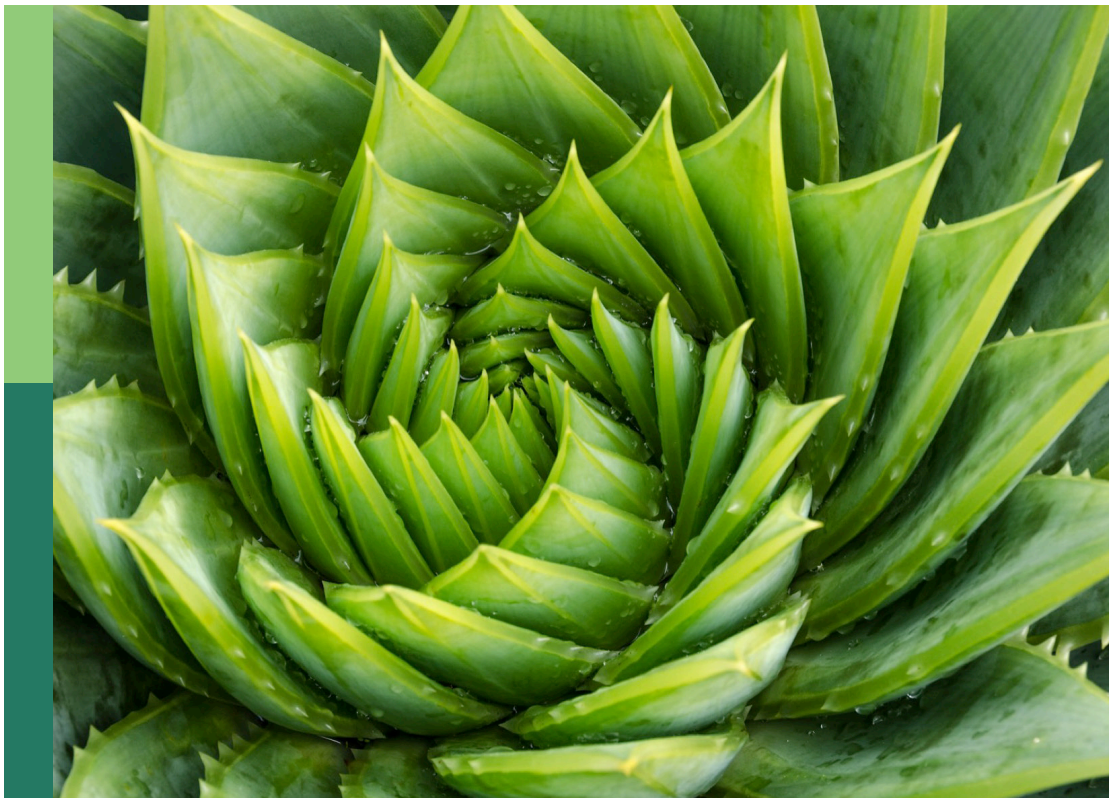

ISSN 1664-8714
ISBN 978-2-83251-390-3
DOI 10.3389/978-2-83251-390-3

About Frontiers

Frontiers is more than just an open access publisher of scholarly articles: it is a pioneering approach to the world of academia, radically improving the way scholarly research is managed. The grand vision of Frontiers is a world where all people have an equal opportunity to seek, share and generate knowledge. Frontiers provides immediate and permanent online open access to all its publications, but this alone is not enough to realize our grand goals.

Frontiers journal series

The Frontiers journal series is a multi-tier and interdisciplinary set of open-access, online journals, promising a paradigm shift from the current review, selection and dissemination processes in academic publishing. All Frontiers journals are driven by researchers for researchers; therefore, they constitute a service to the scholarly community. At the same time, the *Frontiers journal series* operates on a revolutionary invention, the tiered publishing system, initially addressing specific communities of scholars, and gradually climbing up to broader public understanding, thus serving the interests of the lay society, too.

Dedication to quality

Each Frontiers article is a landmark of the highest quality, thanks to genuinely collaborative interactions between authors and review editors, who include some of the world's best academicians. Research must be certified by peers before entering a stream of knowledge that may eventually reach the public - and shape society; therefore, Frontiers only applies the most rigorous and unbiased reviews. Frontiers revolutionizes research publishing by freely delivering the most outstanding research, evaluated with no bias from both the academic and social point of view. By applying the most advanced information technologies, Frontiers is catapulting scholarly publishing into a new generation.

What are Frontiers Research Topics?

Frontiers Research Topics are very popular trademarks of the *Frontiers journals series*: they are collections of at least ten articles, all centered on a particular subject. With their unique mix of varied contributions from Original Research to Review Articles, Frontiers Research Topics unify the most influential researchers, the latest key findings and historical advances in a hot research area.

Find out more on how to host your own Frontiers Research Topic or contribute to one as an author by contacting the Frontiers editorial office: frontiersin.org/about/contact

Root development: Towards understanding regulatory networks and complex interactions between cell populations

Topic editors

Svetlana Shishkova — National Autonomous University of Mexico, Mexico
Ling Huang — Salk Institute for Biological Studies, United States
Ramiro Esteban Rodriguez — CONICET Instituto de Biología Molecular y Celular de Rosario (IBR), Argentina
Daniela Ristova — University of Cologne, Germany
Raffaele Dello Ioio — Sapienza University of Rome, Italy

Citation

Shishkova, S., Huang, L., Rodriguez, R. E., Ristova, D., Ioio, R. D., eds. (2023). *Root development: Towards understanding regulatory networks and complex interactions between cell populations*. Lausanne: Frontiers Media SA. doi: 10.3389/978-2-83251-390-3

Table of contents

frontiers | Frontiers in Plant Science

TYPE Editorial
PUBLISHED 06 January 2023
DOI 10.3389/fpls.2022.1108367

OPEN ACCESS

EDITED AND REVIEWED BY
Hironaka Tsukagoshi,
Meijo University, Japan

*CORRESPONDENCE
Svetlana Shishkova
svetlana.shishkova@ibt.unam.mx

†PRESENT ADDRESS
Ling Huang,
Neomorph, Inc., San Diego, CA,
United States

SPECIALTY SECTION
This article was submitted to Plant Development and EvoDevo, a section of the journal Frontiers in Plant Science

RECEIVED 26 November 2022
ACCEPTED 23 December 2022
PUBLISHED 06 January 2023

CITATION
Shishkova S, Huang L, Rodríguez RE, Ristova D and Dello Ioio R (2023) Editorial: Root development: Towards understanding regulatory networks and complex interactions between cell populations.
Front. Plant Sci. 13:1108367.
doi: 10.3389/fpls.2022.1108367

Editorial: Root development: Towards understanding regulatory networks and complex interactions between cell populations

Svetlana Shishkova[1]*, Ling Huang[2†], Ramiro Esteban Rodríguez[3], Daniela Ristova[4] and Raffaele Dello Ioio[5]

[1]Departamento de Biologa Molecular de Plantas, Instituto de Biotecnología, Universidad Nacional Autónoma de México, Cuernavaca, Mexico, [2]Integrative Genomics and Bioinformatics Core, Salk Institute for Biological Studies, La Jolla, CA, United States, [3]Instituto de Biología Molecular y Celular de Rosario (IBR) - National Scientific and Technical Research Council and Universidad Nacional de Rosario, Rosario, Argentina, [4]Institute for Plant Sciences, Cologne Biocenter, University of Cologne, Cologne, Germany, [5]Dipartimento di Biologia e Biotecnologie, Sapienza Università di Roma, Rome, Italy

KEYWORDS

root growth, cell proliferation and differentiation, root plasticity, root system architecture, gene regulatory networks

Editorial on the Research Topic
Root development: Towards understanding regulatory networks and complex interactions between cell populations

The root system architecture is pivotal for soil exploration and plant adaptation and survival. For this reason, the genetic control of root development (reviewed, e.g., in Bennett and Scheres, 2010; Slovak et al., 2016) is under enormous selection pressure at various scales, from tissue patterning to branching of the below-ground root system, which can be even more extensive than the above-ground shoot system.

Various aspects of root development are discussed in this collection, including the role of hormonal cross-talk in root development in general, as well as auxin, peptide hormones, ROS homeostasis and cell-wall proteins, in particular. Also, traits of the root system architecture and differences in ground tissue patterning between species are discussed, among other subjects.

Plant hormones are main protagonists in the control of root development. In this special issue Zluhan-Martínez et al. and García-Gómez et al. underpin their role in root patterning and growth, shedding light on the cross-talk among several hormones and cell proliferation and patterning. While García-Gómez et al. highlight how hormones interact with master regulators of stem cell activity to maintain stem cell identity, Zluhan-Martínez et al. report the most recent findings on cell proliferation and differentiation.

The phytohormone auxin influences root development in multiple ways and at many levels, being a signal that induces drastic changes in gene expression. The AUXIN RESPONSE FACTOR (ARF) family proteins are the transcription factors at the end of the auxin signaling cascade. Kirolinko et al. report on the participation of the ARF2, ARF3 and ARF4 from *Medicago truncatula* in lateral root and nitrogen-fixing nodule development, thus expanding our knowledge of the participation of the miR390-tasiARF-ARF regulatory node to this model legume species.

Plant peptide hormones participate in signaling cascades by binding to specific membrane receptor kinases. Like traditional plant hormones, later-described peptide hormones also have diverse regulatory roles in plant development and physiology. Hussain et al. identify that a peptide hormone family member *PAMP-INDUCED PEPTIDE 2* (*PIP2*) in *Arabidopsis thaliana* regulates both root and hypocotyl elongation. As *PIP2* is an auxin responsive gene, it provides another remarkable example on how cross-talk between traditional plant hormones and plant peptide hormones collectively regulates plant growth and development.

Besides traditional plant hormones and peptide hormones, other compounds act as internal and external cues to regulate plant root development and mediate its response to environmental changes.

Reactive Oxygen Species (ROS) were initially conceived as dangerous by-products of oxygen metabolism in aerobic organisms, while by now their role in development and signaling pathways is clearly established. In this Research Topic, Mase and Tsukagoshi review the role of ROS homeostasis in root development and integrate their signaling role with plant hormones and transcription factors. The authors provide an extensive description of the multiple aspects of root development modulated by ROS, among them the promotion of the polar tip growth of the root hairs. In line with this, Kim et al. identify and characterize in rice a regulatory module composed of a Rho-type GTPase of Plants (ROP/Rac) that interacts with a particular ROP-guanine nucleotide exchange factor and a respiratory burst oxidase to promote root growth in rice.

Transcription factors from plant-specific AP2/ERF superfamily play essential roles in many aspects of plant development and stress response. Wang et al. demonstrate that the overexpression of *PagERF16* in *Populus alba* × *P. glandulosa* hybrids results in an increase in root diameter and volume. On the other hand, *PagERF16* overexpression lines were sensitive to salt stress, showing a decrease in the total root length in comparison with WT hybrid lines.

Although representing a minor proportion of the plant cell wall constituents, structural proteins are essential components. These include proline rich proteins, glycine-rich proteins, extensins and arabinogalactan proteins (AGP), the latter being glycoproteins with galactose and arabinose as the most abundant sugar moieties. Hromadová et al. review in this Research Topic the multiple roles of cell-wall localized AGPs in root development, stress response and in mediating the interaction with other organisms.

Plants show a large interspecific diversity in root radial patterning (Di Ruocco et al., 2018). *Arabidopsis thaliana* ground tissue patterning has been widely used to understand the molecular basis of radial patterning in roots. In their review Hernandez-Coronado and Ortiz-Ramirez first describe the molecular mechanisms governing radial patterning of the ground tissue in the *A. thaliana* root meristem. Subsequently, they highlight how these findings allowed the comprehension of the molecular basis of root radial patterning diversity among different plant species.

The root system has crucial importance for plant development and fitness, yet the root traits were rarely part of plant breeding strategies. Deja-Muylle et al. report a comprehensive study of 17 root system architecture (RSA) traits in 241 *Arabidopsis thaliana* accessions grown in large plates, as well as in rhizotrons. They identified an overall correlation of *in vitro* RSA traits and RSA traits of plants grown in soil, but not for all accessions, suggesting that later stages of root development can be shaped uniquely by the environment. Additionally, the authors report many known and newly identified genome-wide associations for 14 root traits.

Root system architecture is also a focus of González-Sánchez et al. study. They recorded the dynamics of RSA of closely related and more divergent species from a large genus *Mammillaria* belonging to the Cactaceae family. Determinate growth of cacti primary and lateral roots (Shishkova et al., 2013) allowed to follow root growth in 12 cm square petri plates during more than five months after seed germination. The authors conclude that the phenotypic outcome of microevolution of *Mammillaria* RSA partially recapitulates the patterns generated at the macroevolutionary level in this genus.

Development of fully functional root system has evolutionary significance that enabled plants to colonize lands. Fang et al. in their review, focus on the importance of the evolution of lycophyte roots (*Selaginella*) with an emphasis on root apical meristem (RAM) organization, root branching, and auxin control of root development. Moreover, exploiting genomics and transcriptomics knowledge the authors stress the importance of auxin homeostasis in *Selaginella* root development, and pin-point developmental genes and protein families that play crucial role in lycophytes evolution.

Single-cell RNA-sequencing (scRNA-seq) has been shown to be a powerful tool to profile transcriptional signatures at unprecedented resolution to unravel cell identity and reconstruct gene regulatory networks (GRN) (Minne et al., 2022). Serrano-Ron et al. summarize different strategies used for scRNA-seq and demonstrates how it can be useful to understand the molecular mechanism of lateral root formation, a field that remains largely unexplored by the current knowledge.

In conclusion, the thirteen articles in this collection highlight multiple features of root development from the molecular and cellular level to the whole root-system level in model and non-model plant species.

Author contributions

All authors of the Editorial wrote and approved it for publication and contributed to the Research Topic.

Funding

SS acknowledges support from the DGAPA-PAPIIT-UNAM (IN210221) and CONACyT (CF2019-304301).

Acknowledgments

We thank all the authors and reviewers that have participated in this topic.

Conflict of interest

The authors declare that this work was conducted in the absence of any commercial or financial relationships that could be construed as a potential conflict of interest.

Publisher's note

All claims expressed in this article are solely those of the authors and do not necessarily represent those of their affiliated organizations, or those of the publisher, the editors and the reviewers. Any product that may be evaluated in this article, or claim that may be made by its manufacturer, is not guaranteed or endorsed by the publisher.

References

Bennett, T., and Scheres, B. (2010). Root development-two meristems for the price of one? *Curr. Top. Dev. Biol.* 91, 67–102. doi: 10.1016/S0070-2153(10)91003-X

Di Ruocco, G., Di Mambro, R., and Dello Ioio, R. (2018). Building the differences: a case for the ground tissue patterning in plants. *Proc. R. Soc. B.* 285, 20181746. doi: 10.1098/rspb.2018.1746

Minne, M., Ke, Y., Saura-Sanchez, M., and De Rybel, B. (2022). Advancing root developmental research through single-cell technologies. *Curr. Opin. Plant Biol.* 65, 102113. doi: 10.1016/j.pbi.2021.102113

Shishkova, S., Las Peñas, M. L., Napsucialy-Mendivil, S., Matvienko, M., Kozik, A., Montiel, J., et al. (2013). Determinate primary root growth as an adaptation to aridity in cactaceae: towards evolution and genetic control of the trait. *Ann. Bot.* 112, 239–252. doi: 10.1093/aob/mct100

Slovak, R., Ogura, T., Satbhai, S. B., Ristova, D., and Busch, W. (2016). Genetic control of root growth: From genes to networks. *Ann. Bot.* 117, 9–24. doi: 10.1093/aob/mcv160

frontiers in Plant Science

REVIEW
published: 03 March 2021
doi: 10.3389/fpls.2021.628491

Hormonal Regulation of Stem Cell Proliferation at the *Arabidopsis thaliana* Root Stem Cell Niche

*Mónica L. García-Gómez[1,2], Adriana Garay-Arroyo[1,2], Berenice García-Ponce[1], María de la Paz Sánchez[1] and Elena R. Álvarez-Buylla[1,2]**

[1] Laboratorio de Genética Molecular, Desarrollo y Evolución de Plantas, Departamento de Ecología Funcional, Instituto de Ecología, Universidad Nacional Autónoma de México, Ciudad de México, Mexico, [2] Centro de Ciencias de la Complejidad, Universidad Nacional Autónoma de México, Ciudad de México, Mexico

The root stem cell niche (SCN) of *Arabidopsis thaliana* consists of the quiescent center (QC) cells and the surrounding initial stem cells that produce progeny to replenish all the tissues of the root. The QC cells divide rather slowly relative to the initials, yet most root tissues can be formed from these cells, depending on the requirements of the plant. Hormones are fundamental cues that link such needs with the cell proliferation and differentiation dynamics at the root SCN. Nonetheless, the crosstalk between hormone signaling and the mechanisms that regulate developmental adjustments is still not fully understood. Developmental transcriptional regulatory networks modulate hormone biosynthesis, metabolism, and signaling, and conversely, hormonal responses can affect the expression of transcription factors involved in the spatiotemporal patterning at the root SCN. Hence, a complex genetic–hormonal regulatory network underlies root patterning, growth, and plasticity in response to changing environmental conditions. In this review, we summarize the scientific literature regarding the role of hormones in the regulation of QC cell proliferation and discuss how hormonal signaling pathways may be integrated with the gene regulatory network that underlies cell fate in the root SCN. The conceptual framework we present aims to contribute to the understanding of the mechanisms by which hormonal pathways act as integrators of environmental cues to impact on SCN activity.

Keywords: root stem cell niche, quiescent center, stem cell regulation, gene regulatory networks, plant development, hormonal regulation

OPEN ACCESS

Edited by:
Raffaele Dello Ioio, Sapienza University of Rome, Italy

Reviewed by:
Renze Heidstra, Wageningen University and Research, Netherlands
Yanhai Yin, Iowa State University, United States

***Correspondence:**
Elena R. Álvarez-Buylla
elenabuylla@protonmail.com

Specialty section:
This article was submitted to Plant Development and EvoDevo, a section of the journal Frontiers in Plant Science

Received: *12 November 2020*
Accepted: *12 January 2021*
Published: *03 March 2021*

Citation:
García-Gómez ML, Garay-Arroyo A, García-Ponce B, Sánchez MP and Álvarez-Buylla ER (2021) Hormonal Regulation of Stem Cell Proliferation at the Arabidopsis thaliana Root Stem Cell Niche. Front. Plant Sci. 12:628491. doi: 10.3389/fpls.2021.628491

INTRODUCTION

Stem cells (SCs) are undifferentiated cells that can self-renew and produce progeny that replenishes and regenerates the tissues of multicellular organisms (Alvarado and Yamanaka, 2014). The root stem cell niche (SCN) of *Arabidopsis thaliana* (*Arabidopsis* hereafter) has a relatively simple structure, a stereotypical number of SCs, and a highly regular pattern of cell divisions (Dolan et al., 1993) (**Figure 1A**), making it a unique model to characterize the dynamics of SC activity in living organs. The SCN is located at the root apex and consists of the quiescent center (QC) and the stem or initial cells (ICs) (Barlow, 1978; Dolan et al., 1993; Barlow, 1997; Heidstra and Sabatini, 2014). Depending on their position relative to the QC, ICs produce cells that will become part of

the different tissues of the root (Dolan et al., 1993) (**Figure 1A**). The cortex/endodermis initials, the provascular initials, and the epidermis and lateral root cap initials produce cells that will populate the meristem, whereas the distal ICs produce cells of the columella (Dolan et al., 1993). The QC cells divide at a much lower rate than the ICs, although the frequency of division increases with the age of the plant (Timilsina et al., 2019). Clonal and time-lapse analyses have shown that QC divisions are asymmetric and replace different sets of ICs at different frequencies (Kidner et al., 2000; Wachsman et al., 2011; Cruz-Ramírez et al., 2013; Rahni and Birnbaum, 2019). Most QC cell divisions are periclinal (**Figure 1B**), producing two daughter cells that are positioned at different distances from the provascular cells of the root apical meristem (Cruz-Ramírez et al., 2013). The two daughter cells retain the activity of a QC marker for several days, until eventually one cell differentiates into a columella initial (Cruz-Ramírez et al., 2013). This indicates that QC cell divisions are symmetrical and produce identical cells, and that a cell fate asymmetry takes place after the division event. In this scenario, signals from the niche microenvironment might be instructive for this cell fate decision making. For instance, the production of columella initials is an emergent outcome of a system-level mechanism that considers the feedback regulation between the gene regulatory network in each cell and constraints in the expression pattern and intercellular mobility of the transcription factor SHORT ROOT (SHR) (**Box 1**; García-Gómez et al., 2020). The QC cells can also produce other types of ICs (Kidner et al., 2000; Rahni and Birnbaum, 2019); for instance, anticlinal QC divisions produce cortex/endodermis initials (**Figure 1B**; Rahni and Birnbaum, 2019). The QC cells are considered a reserve of multipotent SCs that can actively divide and replace lost or damaged initials and meristematic cells (Heyman et al., 2014). Interestingly, the root SCN organization in two SC populations with differing proliferative activities and generative potential is common to SCN of plants and animals (Barlow, 1978; Barlow, 1997; Jiang and Feldman, 2005; Li and Clevers, 2010), suggesting that this could be a generic feature of SCN organization.

The frequency of QC cell divisions changes with the developmental age of the seedlings in *Arabidopsis* and other plant species (Baum et al., 2002; Jiang and Feldman, 2005; Chen et al., 2011; Timilsina et al., 2019) and also shows variation in different *Arabidopsis* accessions (Aceves-García et al., 2016). Additionally, QC divisions can be stimulated in response to the availability of nutrients (Sánchez-Calderón et al., 2005), upon root meristematic damage and by genotoxic treatments (Cruz-Ramírez et al., 2013; Heyman et al., 2013). Plant hormones can be regulated by developmental and environmental cues at different levels, including metabolism, signaling, crosstalk, and transport, offering potential mechanisms to integrate external information into the regulation of SCN activity. The role of hormones as mediators between these cues and the regulation of SC activity in the root SCN is likely to be linked to the gene regulatory network that underlies QC identity and activity. In this case, plant hormonal responses could be channeled toward a common regulatory module to regulate the division at the QC according to the requirements of the plant.

In this review, we summarize current evidence regarding the regulation of QC cell division in the root SCN of *Arabidopsis*, focusing on how hormones interact with transcriptional regulatory networks implied in QC activity. We recapitulate on the transcription factors that have been identified as important regulators of QC specification; we summarize the information about the mitotic activity of the QC cells under optimal growth conditions, the role of reactive oxygen species (ROS), and several cell cycle components in the quiescence of the QC cells. We then discuss the effects of auxin, cytokinin (CK), brassinosteroids (BRs), and abscisic acid (ABA) on the division of the QC cells and on the expression of cell identity regulators. The existence of recurrent regulatory targets led us to discuss how hormonal responses may be channeled toward the genetic–hormonal regulatory network that underlies the acquisition of the cell identity and proliferative profiles in the root SCN, and how it can possibly constitute a developmental module to regulate SC activity in response to changing environmental conditions.

GENETIC REGULATORS OF QC CELL IDENTITY IN THE ROOT SCN

Several transcription factors have been identified as important regulators of QC cell identity; these also play important roles in the establishment of the radial pattern of the root and in the maintenance of the RAM. One of these regulators is the GRAS transcription factor *SHR* that is expressed in the provascular tissues at the RAM (**Figure 2A**; Benfey et al., 1993; Scheres et al., 1995; Helariutta et al., 2000). SHR moves to the endodermis, the cortex/endodermis ICs, and the QC (Nakajima et al., 2001), where it induces *SCARECROW* (*SCR*) expression (Cui et al., 2007). SCR and SHR form a heterodimer that localizes in the cell

BOX 1 | A system-level mechanism regulating the asymmetric division of QC cells.

The QC cells are considered a reserve of multipotent SCs that can produce all cell types in the root (Heyman et al., 2014), yet most QC cell divisions produce columella initials (Cruz-Ramírez et al., 2013). In a recent study, a mathematical model of genetic regulation in the root SCN was used to understand the mechanism behind this biased production of columella (García-Gómez et al., 2020). A perturbation analysis of a genetic regulatory model was used to identify the regulators that can cause cell state transitions *in silico* (García-Gómez et al., 2020); this represents the transition from one cell type to another. SHR was identified as a regulator that causes the transition from the QC to the columella initials state and thus as a candidate regulator that could be behind the asymmetric division of the QC cell. The constraints in SHR expression pattern, intercellular mobility, and nuclear retention in the cells of the RAM were studied in a multilevel model that recovered the dynamics reported upon QC cell divisions (Cruz-Ramírez et al., 2013), namely, that a periclinal QC cell division produces two QC cells, which over time develop differences in their intracellular levels of SHR due to their different proximity to the source of SHR. The intracellular SHR levels in each daughter cell are then interpreted by their regulatory networks, and for one daughter cell, this results in a transition to the columella initials state, resulting in asymmetry in cell fate (García-Gómez et al., 2020). The model also predicted that an increase in the availability of SHR causes a shift from asymmetric to symmetric QC cell divisions, increasing the pool of undifferentiated QC cells in the root SCN (García-Gómez et al., 2020).

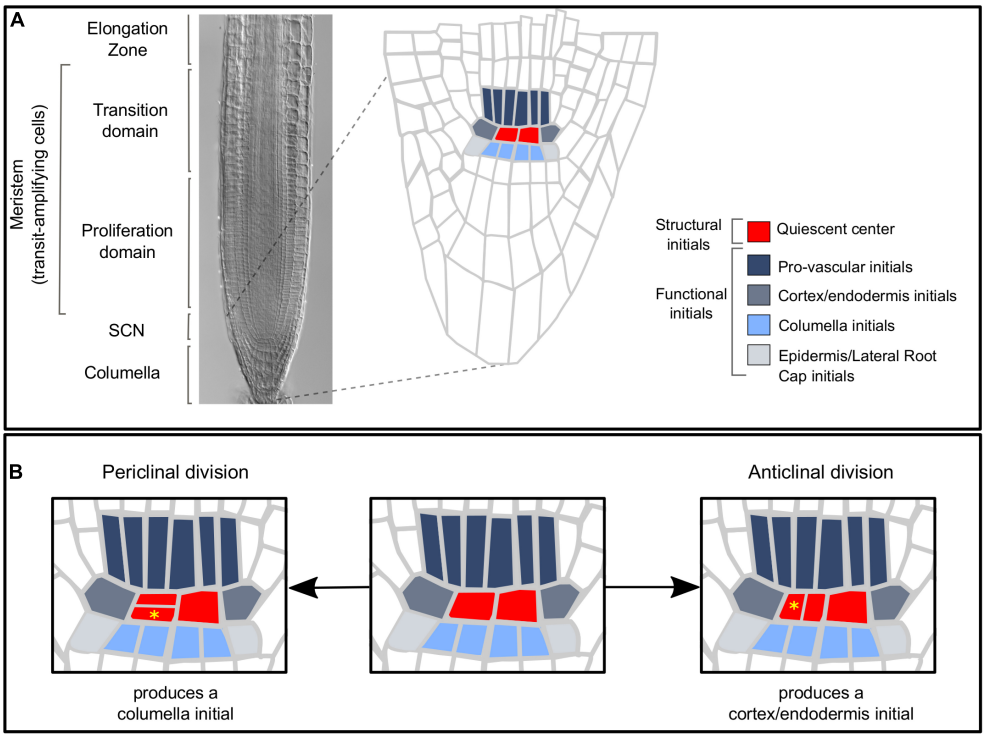

FIGURE 1 | (A) The root apical meristem is composed of the SCN, the proliferation domain, and the transition domain (Ivanov and Dubrovsky, 2013). The SCN houses the QC cells and the ICs [structural and funcional initials, respectively (Barlow, 1997)] which divide asymmetrically and produce cells of different root tissues. The QC cells produce most root tissues and are considered a reserve of multipotent stem cells. **(B)** QC divisions can be periclinal or anticlinal and produce columella initials or cortex/endodermis initials, respectively. Yellow asterisks mark the daughter cells that replace an initial cell in each case.

nucleus and restricts SHR's intercellular movement (Cui et al., 2007). The SCR/SHR protein complex regulates the expression of genes necessary for the specification of the endodermis, the cortex/endodermis ICs, and the QC cells (Sabatini et al., 2003; Sarkar et al., 2007; Welch et al., 2007; Moreno-Risueno et al., 2015). Additionally, SHR forms heterodimers with JACKDAW (JKD), MAGPIE (MGP), and BLUEJAY (BLJ) transcription factors, forming different protein complexes that localize in the cell nucleus (Long et al., 2015; Long et al., 2017). It has been shown that the endodermis, cortex/endodermis initials, and the QC cells are enriched in different protein complexes containing SHR, SCR, and JKD (Long et al., 2017; Clark et al., 2020), which could be providing specificity in the genes that are regulated by SHR in the different cells of the adjacent layer to the provasculature (Long et al., 2015, 2017; Moreno-Risueno et al., 2015). Loss-of-function mutants in *scr* and *shr* have defects in the asymmetric division of the cortex/endodermis ICs, and the roots display a single layer of ground tissue (Di Laurenzio et al., 1996). Moreover, these mutants have defects in the specification of the QC and the ICs differentiate, leading to premature consumption of the meristem (Benfey et al., 1993; Sabatini et al., 2003; Sarkar et al., 2007).

The AP2-type PLETHORA transcription factors (PLT1, PLT2, PLT3, and PLT4/BABY BOOM [BBM]) are important regulators for root meristem maintenance (Aida et al., 2004; Galinha et al., 2007; Mähönen et al., 2014). The *PLT* transcription factors are highly expressed in the cells of the root SCN, including the QC (**Figure 2B**), and their expression is positively regulated by the high auxin levels in these cells (Aida et al., 2004; Galinha et al., 2007). A protein gradient of PLTs is created along the RAM because of cell growth and proliferation occurring in the meristem, as well as their intercellular movement (Mähönen et al., 2014). In this way, high PLT levels maintain the root SCN, intermediate levels maintain cell proliferation in the meristem, and low levels correlate with the beginning of cell differentiation (Mähönen et al., 2014). In the double-mutant *plt1 plt2*, the QC cells show defects in the expression of specific QC makers and display QC division events, indicating a loss of QC cell identity and its characteristic quiescent state (Aida et al., 2004).

Another important regulator of the root SCN is *WUSCHEL-related homeobox 5* (*WOX5*), a homeodomain transcription factor that is specifically expressed in the QC cells (**Figure 2A**; Sarkar et al., 2007). Mutant plants with non-functional WOX5 lack the expression of several QC-specific markers and display differentiation of the distal ICs (Sarkar et al., 2007; Ding and Friml, 2010). The expression of *WOX5* depends on the activity of the radial regulators SCR and SHR and the longitudinal PLT regulators mentioned in the previous paragraphs. The *scr* and *shr* mutants lack *WOX5* expression and display severe root growth defects (Sarkar et al., 2007), whereas in the case of *plt*, a multiple mutant has an expanded expression of *WOX5* compared to WT plants (Sarkar et al., 2007; Zhai et al., 2020). Recently, it was

shown that PLT and SCR form a protein complex with teosinte-branched cycloidea PCNA (TCP) transcription factor to directly regulate *WOX5* expression and the identity of the QC cells (Shimotohno et al., 2018), thus showing a mechanism for the convergence of these regulatory pathways (**Figure 2C**). Moreover, SCR forms a transcriptional complex with SEUSS (SEU) at the promoter of *WOX5* (**Figure 2C**), in which SEU acts as a scaffold protein that recruits SET DOMAIN GROUP 4 (SDG4), a SET domain methyltransferase (Zhai et al., 2020). The transcriptional complex SCR-SEU-SDG4 is implicated in the deposition of the H3K4me3 epigenetic mark in the promoter of *WOX5*, critical for its expression and for QC specification (Zhai et al., 2020). *SCR* expression itself seems to be reduced in *seu* mutants, suggesting the existence of a positive feedback loop in the regulation of *WOX5* in the QC (Zhai et al., 2020).

Auxin is an important regulator of *WOX5*, and alterations in its distribution, for example, by altering its polar transport, result in the expression of *WOX5* in the endodermal cells of the meristem (Sabatini et al., 1999; Mähönen et al., 2014). Auxin signaling regulates *WOX5* positively and negatively through different auxin response factors (ARFs): MP (ARF5) is necessary for its expression, whereas ARF10/16 represses it (Sarkar et al., 2007; Ding and Friml, 2010). Interestingly, *MP* and *ARF10* are not expressed homogenously in the RAM (Rademacher et al., 2011), suggesting that the cellular context could be important to define the effect of auxin over *WOX5* (García-Gómez et al., 2017). Particularly, *MP* is expressed in the QC cells but not *ARF10* (Rademacher et al., 2011; Truskina et al., 2020), which raises the hypothesis that particular ARF profiles could be important for the auxin regulation of *WOX5* expression in these cells. Hence, it is of interest to uncover the mechanisms behind the expression patterns of these ARFs in the RAM in order to understand the specificity of auxin responses in the root meristem; however, there is still no evidence about it. Regulatory links between RAM patterning mechanisms and the auxin signaling components were postulated and put to the test through a mathematical model (García-Gómez et al., 2017). The hypothetical interactions analyzed with the model imply that the heterodimers formed between SHR and its interaction partners JKD and MGP might be involved in the regulation of *MP* and *ARF10*, namely, that the SHR-JKD heterodimer represses the expression of *ARF10*, whereas the SHR-MGP heterodimer represses the expression of *MP* (García-Gómez et al., 2017). These hypotheses are based on the bioinformatics prediction that SHR represses *ARF10* and *MP* expression (Levesque et al., 2006), on the binding of JKD to the promoter of *ARF10* (Moreno-Risueno et al., 2015), and the fact that *ARF10* and *JKD* are expressed on non-overlapping domains in the RAM, and the same for *MP* and *MGP* (Welch et al., 2007; Rademacher et al., 2011). The study of these hypothetical interactions in the context of a mathematical regulatory network model of the RAM showed that they are necessary to recover attractors (steady states) with the expression patterns of *MP* and *ARF10*, as observed in the cells of the root meristem, including the QC cells (García-Gómez et al., 2017). In the model, the recovered activity configurations allow the expression of *WOX5* in the QC cells, but not in the other RAM cells. The results from the model strongly suggest that the expression patterns of the ARF transcription factors define the effect of auxin over *WOX5*: cells of the RAM with different ARF10 and MP expression profiles will exhibit different auxin responses; some may activate *WOX5*, whereas other will repress it. The proposed links between patterning mechanisms and hormonal signaling pathways may be critical for understanding how cells will respond to auxin and may constitute a generic mechanism for the spatial specificity of hormonal responses in plant development. Interestingly, it has been shown that the chromatin of several ARFs is constitutively open for transcription, and a series of transcriptional repressors affect their expression (Truskina et al., 2020). Under such a scenario, SHR-JKD and SHR-MGP could act as the repressors that are behind the expression patterns of *ARF10* and *MP*, respectively, and that underlie the spatial specificity of their activity in the RAM.

Another important regulator of *WOX5* is REPRESSOR OF WUSCHEL1 (ROW1), a PHD domain-containing protein that has been shown to restrict *WOX5* expression to its characteristic position at the center of the root SCN (Zhang et al., 2015). WOX5 activity in the QC cells is important for the maintenance of the ICs (van den Berg et al., 1997; Ding and Friml, 2010), and in the case of the distal ICs, this is achieved, in part, via the non-cellular autonomous activity of WOX5 (Pi et al., 2015). WOX5 moves from the QC cells to the distal ICs where it recruits corepressors and a histone deacetylase to repress the expression of *CYCLING DOF FACTOR 4* (*CDF4*), which promotes the terminal differentiation of the columella cells (Pi et al., 2015). WOX5 also moves toward the provascular initials, where it has been proposed to negatively regulate the expression of *SHR* (Clark et al., 2020).

CELL CYCLE REGULATION OF THE QC CELLS

The QC cells divide in optimal growth conditions (Timilsina et al., 2019), albeit at a lower frequency compared to the surrounding ICs and meristematic cells (Wachsman et al., 2011; Cruz-Ramírez et al., 2013). In a pioneering article by Clowes (1956), it was estimated that the QC cells in maize roots display a quarter of DNA synthesis compared to meristematic cells (Clowes, 1956), which is in remarkable accordance to what has been reported for *Arabidopsis* (Cruz-Ramírez et al., 2013). This similarity in the division frequencies suggests the existence of generic patterns of cell cycle regulation in the root meristem of different plant species.

In *Arabidopsis*, root growth is not compromised by genetic perturbations that result in alterations in the division patterns of the QC cells, suggesting that low division rate of the QC cells is not strictly necessary for the function and the organization of the root meristem under optimal growth conditions (Vanstraelen et al., 2009; González-García et al., 2011; Cruz-Ramírez et al., 2013; Savina et al., 2020; Wang et al., 2020). The division of the QC cells has been shown to increase in frequency in older *Arabidopsis* seedlings (Timilsina et al., 2019), and it can also be actively modulated to cope with the current needs of the root. For instance, as a response to changes in hormonal activity,

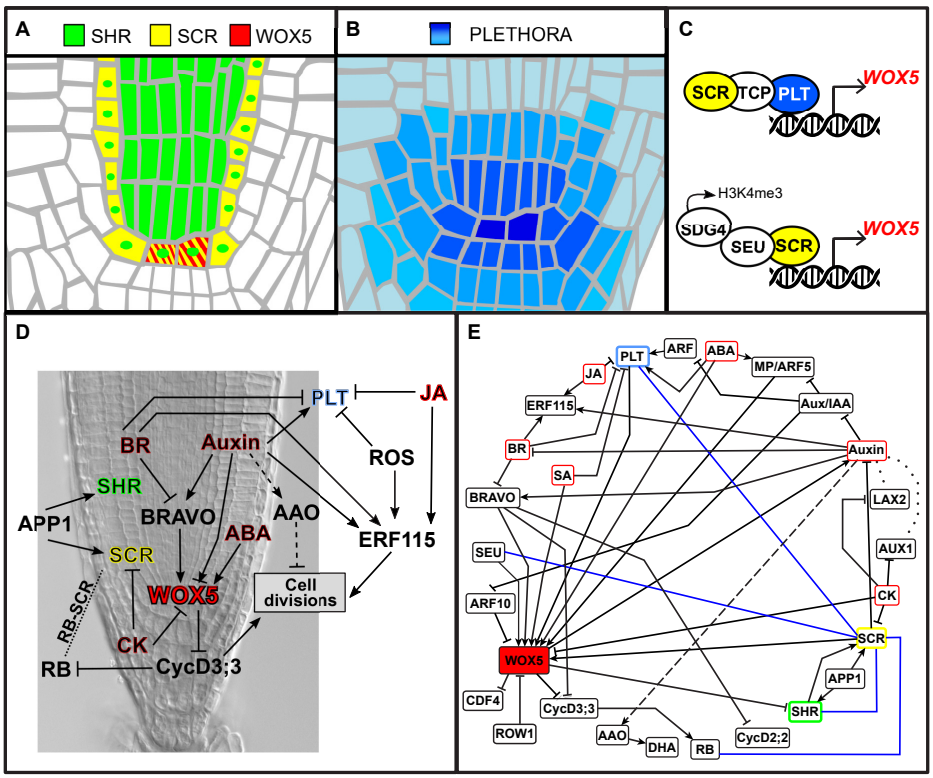

FIGURE 2 | Expression and activity domains of the main genetic regulators of the QC cells fate. In **(A)**, SHR, SCR, and WOX5, and in **(B)**, the PLT family of transcription factors. **(C)** Protein complexes that bind to the regulatory regions of *WOX5* promoter. **(D)** Schematic representation of some of the regulatory interactions underlying the division of the QC cells. **(E)** Network depicting the regulatory interactions underlying QC divisions discussed throughout this review. The blue lines indicate protein–protein interactions; dotted lines indicate the role of auxin influx transporters, and the dashed line between auxin and AAO indicates that this particular regulation was observed in maize roots.

limiting phosphate conditions (Sánchez-Calderón et al., 2005), genotoxic treatments that cause cell death of the proliferating cells of the meristem (Cruz-Ramírez et al., 2013; Heyman et al., 2013; Vilarrasa-Blasi et al., 2014), or after the excision of the root cap (Ponce et al., 2005). In the case of QC cell divisions that occur as a response to meristematic damage, it is unknown what non–cell-autonomously mechanism is involved in the modulation of QC cell divisions. A potential mechanism to achieve this could be the directional signaling from mature cells of the meristem to the SCs to maintain cell fate (van den Berg et al., 1995), although this possibility requires further investigation.

The regulation of QC cell divisions, as a response to endogenous or environmental signals, must ultimately impact on the activity of the regulators that underlie the progression of the different phases of the cell cycle (Polyn et al., 2015; Ortiz-Gutiérrez et al., 2015). Interestingly, the transcription factor WOX5 directly inhibits the expression of *CYD3;3* (Forzani et al., 2014), implying a direct regulatory link between a QC cell fate transcription factor and a regulator of the progression of the cell cycle. D-type cyclins (CYCD) form a complex with A-type cyclin-dependent kinases to regulate the commitment point at G1/S transition through the phosphorylation and inactivation of retinoblastoma-related (RBR) protein, to release E2F transcriptional factor (Polyn et al., 2015); these are necessary steps for the transition to the S phase of the cell cycle. Otherwise, RBR activity maintains a quiescent state of the QC cells (Wildwater et al., 2005; Cruz-Ramírez et al., 2013). RBR in the QC maintains its low proliferative state, and consequently seedlings with no RBR activity in the QC display cell divisions (Cruz-Ramírez et al., 2013). This regulation of QC cell proliferation is mediated by the interaction of RBR and SCR (Cruz-Ramírez et al., 2013). Disruption of this interaction yields QC divisions (Cruz-Ramírez et al., 2013), thus establishing a regulatory circuit of cell cycle and cell fate regulators that modulate QC cell divisions. The repression of *CYCD3;3* by WOX5 explains the extended G1 phase and low mitotic rate of the QC cells. Interestingly, local expression of *CYCD1;1* and of *CYCD3;3* in the QC using the *WOX5* promoter showed that only CYCD3;3 is able to significantly induce cell division in the embryonic QC (Forzani et al., 2014). Additionally, *CYCD6;1*, which is part of a regulatory circuit that regulates the asymmetric cell division of the cortex/endodermis IC, is not expressed in the QC cells (Sozzani et al., 2010; Cruz-Ramírez et al., 2013). Hence, CYCD proteins might be part of cell type–specific programs of cell cycle regulation, which could underlie the varying proliferation rates in different tissues (de Almeida Engler et al., 2009).

BOX 2 | Hormone signal transduction basics.

- Auxin

Auxin regulates a high variety of plant developmental processes, including cell proliferation in the root meristem and the maintenance of the root SCN (Sabatini et al., 1999; Ishida et al., 2010). The auxin signaling pathway is composed of the family of ARF and Aux/IAA transcription factors that regulate the expression of auxin-responsive genes (Ulmasov et al., 1999; Okushima et al., 2005; Guilfoyle and Hagen, 2007). The auxin signaling pathway is elicited when the hormone binds to its coreceptors, the transport inhibitor response1/auxin signaling F-box protein1-5 (TIR1/AFB) and its substrates, the Aux/IAA proteins (Dharmasiri et al., 2005; Calderon Villalobos et al., 2012). TIR1/AFB are components of the SKP1/Cullin/F-box protein ($SCF^{TIR1/AFB}$) ubiquitin ligase complex, and auxin produces a conformational change that favors its interaction with the Aux/IAA proteins, promoting their ubiquitination and eventual degradation (Xu et al., 2007). In this way, auxin frees the ARF transcription factors from the repressive action of Aux/IAA, so that they can regulate the expression of auxin-responsive genes.

Auxin displays a concentration gradient along the longitudinal axis of the root with a maximum at the QC cells (Sabatini et al., 1999; Sarkar et al., 2007; Petersson et al., 2009; Brunoud et al., 2012). This gradient correlates with the cellular activities of the cells along the RAM: the highest auxin concentration is found in the SCN, where cells have low division rates; the proliferation domain has high auxin concentration, and cells divide actively, and then in the transition domain, where auxin levels decrease, and cells stop dividing (Blilou et al., 2005; Mähönen et al., 2014). Auxin distribution in the root is the result of the regulation of auxin metabolism, conjugation, and transport, the latter mediated by efflux and influx proteins that actively move auxin between cells (Petersson et al., 2009; Vanneste and Friml, 2009; Liu et al., 2017). Auxin can enter cells passively and also through the activity of the auxin influx proteins AUX1, LAX1, LAX2, and LAX3, which are expressed in different tissues of the root (Swarup et al., 2005; Péret et al., 2012). The family of PIN-FORMED (PIN) proteins are auxin efflux transporters that play a major role in the generation of auxin distribution patterns throughout development (Blilou et al., 2005). In the root, the PIN efflux transporters are polarly localized in the cell membranes, forming a rootward auxin flux through the vascular tissues. At the columella, PINs redistribute auxin laterally, connecting it with a shootward flux through the outside root tissues (Blilou et al., 2005). This PIN distribution forms a transport network that underlies the distribution of auxin in a gradient with a maximum in the position of the QC cells (Blilou et al., 2005; Grieneisen et al., 2007). The distribution of auxin in the root meristem is tightly regulated and can be modulated by complex mechanisms that regulate *PIN* expression and PIN localization and the regulation of auxin metabolism that fine-tunes the patterns of auxin accumulation in the cells (Gonzali et al., 2005; Liu et al., 2017).

- Cytokinin

Plant cells sense CK via a two-component signaling pathway similar to the phosphorelay system found in bacteria (Santner et al., 2009). The CK receptors, *Arabidopsis* His kinase 2 (AHK2), AHK3 and cytokinin response 1 (CRE1)/AHK4, are transmembrane proteins that autophosphorylate upon CK binding and transfer the phosphoryl group to *Arabidopsis* His-phosphotransfer proteins (AHP). Eventually, AHP proteins translocate to the nucleus and the signal is transferred to the Arabidopsis response regulators (ARRs) transcription factors. There are four types of ARR proteins based on their protein similarity (To et al., 2007). Type B ARRs positively regulate the expression of CK responsive genes, including the type A ARRs that repress CK signaling. Additionally, the type B ARRs promote the expression of the cytokinin response factor (CRF) family of transcription factors (Rashotte et al., 2006). The CRF proteins accumulate in the nucleus depending on the activity of AHP proteins to regulate the expression of CK-responsive genes (Rashotte et al., 2006). The type C ARRs have phosphatase activity and are thought to regulate CK signaling negatively by removing the phosphoryl group from type B and type A ARRs (Kiba et al., 2004). The fourth group corresponds to the *Arabidopsis* pseudoresponse regulators that has been shown to participate in the regulation of the circadian rhythm (To et al., 2007).

(Continued)

BOX 2 | Continued

- Brassinosteroids

The steroid hormones BRs are perceived in the plasma membrane by a group of leucine-rich repeat receptor-like kinase (LRR-RKL) receptors (brassinosteroid insensitive 1, BRI, and brassinosteroid receptor-like 1 BRL1 and BRL3 in *Arabidopsis*) that, upon BR binding, elicit a signal transduction cascade that inhibits BR-insensitive 2 (BIN2) (Zhu et al., 2013). In the absence of BR, BIN2 phosphorylates the transcription factors EMS suppressor 1 (BES1) and brassinazole-resistant 1 (BZR1), blocking their ability to bind their DNA targets (Belkhadir et al., 2014). Upon BR binding by the receptors, a signaling cascade is induced that ultimately results in dephosphorylation and increased nuclear localization of BES1/BZR1, which can in turn regulate the expression of BR-responsive genes (Belkhadir et al., 2014).

- Abscisic Acid

The ABA signaling pathway is elicited when the hormone binds to the PYR/PYL/RCAR receptor proteins that release SnRK2s kinases from PP2Cs inhibition, thereby activating the ABF/AREB transcription factors to regulate the expression of ABA-responsive genes (Santner et al., 2009).

Protein degradation processes regulate the progression of the cell cycle (Gutierrez, 2009), and they have been found important for the control of QC cell divisions (Ueda et al., 2004; Vanstraelen et al., 2009). For example, *HALTED ROOT* (*HLR*) encodes a subunit of the ubiquitin 26S proteasome, and the *hlr* mutant displays dividing QC cells and a loss of the expression of characteristic markers of these cells (Ueda et al., 2004). It has been shown that the *hlr* mutant is defective in auxin signaling, as the degradation of IAA17 is compromised (Ueda et al., 2004). IAA17 is a member of the family of AUX/IAA repressors (**Box 2**), which interact with the ARF transcription factors and impede them to regulate the expression of auxin-responsive genes (Ulmasov et al., 1997, 1999; Okushima et al., 2005; Guilfoyle and Hagen, 2007). Notably, IAA17 and WOX5 act in the same regulatory pathway in the QC cells (Ding and Friml, 2010; Tian et al., 2014). An IAA17 gain-of-function mutant has altered auxin levels in the QC cells, multiple layers of the distal ICs, and an expanded *WOX5* expression domain (Ding and Friml, 2010; Tian et al., 2014). This phenotype clearly shows that if the degradation of IAA17 is compromised, as observed in the *hlr* mutant, there will be defects in the organization of the QC cells and the SCN (Ueda et al., 2004). The defects of the IAA17 gain-of-function mutant concerning the restriction in the expression of *WOX5* could be related to the regulation of MP and ARF10, as both interact with this particular AUX/IAA repressor (Vernoux et al., 2011; Piya et al., 2014) and both regulate *WOX5*, as it was mentioned in the previous section.

The CELL CYCLE SWITCH 52 A1 (CCS52A1) and CCS52A2 protein isoforms are components of the ANAPHASE-PROMOTING COMPLEX/CYCLOSOME (APC/C) that targets several cell cycle proteins for degradation, important for cell cycle progression and mitosis (Vanstraelen et al., 2009). Interestingly, APC regulates mitotic arrest in the QC and also the onset of endocycle in the transition domain of the root meristem (Vanstraelen et al., 2009; Heyman et al., 2013; Takahashi and Umeda, 2014). In the *ccs52a2* loss-of-function mutant, the QC cells divide more frequently than in wild-type plants,

and the meristem is eventually exhausted (Vanstraelen et al., 2009; Heyman et al., 2013). One of the regulatory targets of CCS52A2 is ETHYLENE RESPONSE FACTOR 115 (ERF115), whose expression is observed prior to the division of QC cells (Heyman et al., 2013). ERF115 activates the expression of *phytosulfokine5* (*PSK5*), a peptide hormone that induces QC cell divisions (Heyman et al., 2013). Overexpression of *ERF115* results in a marked increase in the frequency of QC cell divisions in the root SCN, indicating that it is a positive regulator of QC mitotic activity. Although *ERF115* has been annotated as an ethylene response factor, its expression is actually not regulated by ethylene. Instead it is induced by ROS signaling (Kong et al., 2018) and brassinolide (BL) treatment (Heyman et al., 2013). Notably, QC cell divisions still take place in *erf115* mutants treated with BL (Heyman et al., 2013), indicating that BR also promotes cell divisions independently of ERF115 (Vilarrasa-Blasi et al., 2014).

Recently, it was found that ULTRAPETALA1 (ULT1), described as a trithorax (TrxG) component, is also required for QC cell divisions, evidencing the participation of the epigenetic factors in this process (Ornelas-Ayala et al., 2020).

REDOX REGULATION OF QC CELL DIVISION

Redox regulation plays a critical role in the organization of the RAM in *Arabidopsis* (Tsukagoshi et al., 2010), but its role in the QC is not so clear. In this section, we include research studies from maize regarding the function of redox regulation in the QC cells, in order to provide insights of its role in *Arabidopsis*.

In maize roots, the boundary between the QC and the proliferating cells of the meristem is marked by a drastic change in the redox cellular state (Kerk and Feldman, 1995; Jiang et al., 2003). The position of the QC in the root apex is characterized by an oxidizing environment with high levels of dehydroascorbic acid (DHA) and glutathione disulfide, whereas a reduced state is detected in the neighboring cells in the RAM with high levels of ascorbic acid (AA) and glutathione (GSH) (Kerk and Feldman, 1995; Jiang et al., 2003). The redox profiles of the quiescent SCs and the proliferative meristematic cells could be important in the definition of these zones of contrasting mitotic activity. This notion is supported by experiments in which the QC cells start dividing in maize roots treated with AA, whereas cells become arrested in the G1 phase of the cell cycle when roots are treated with an inhibitor of AA biosynthesis (Kerk and Feldman, 1995, and references therein), indicating the importance of the redox status in the regulation of QC cell divisions.

Reduced compounds such as AA and GSH, which are enriched in meristematic cells of maize, are necessary for the progression of many generic cellular processes including the transition from G1 to S phase of the cell cycle, metabolic reactions, and protein synthesis (Kerk and Feldman, 1995; Vernoux et al., 2000; Jiang and Feldman, 2005; De Tullio et al., 2010). The molecular mechanism behind these effects may involve these molecular species acting as second messengers in signaling pathways (Apel and Heribert, 2004) and in the regulation of protein activity and conformation. In *Arabidopsis*, this could be mediated through the oxidation/reduction of cysteine residues in enzymes and transcription factors (De Tullio et al., 2010), which potentially could modulate the information processing capabilities of the cells. AA has been suggested to affect ethylene biosynthesis (Arrigoni and Tullio, 2000). As ethylene induces QC cell division (Ortega-Martínez et al., 2007), this potentially represents another mechanism by which the redox status of the cell regulates QC cell division.

In *Arabidopsis*, several reports indicate the importance of the redox status of the QC cells in the maintenance of their low mitotic rate. For instance, the *app1* mutant, a mutant in a mitochondrial ATPase, has altered levels of reactive oxygen species (ROS) in the cells of the RAM and displays an increase in QC cell division (Yu et al., 2016; Kong et al., 2018). Interestingly, this phenotype is accompanied by a reduction in the expression of the transcription factors *SCR* and *SHR* (Yu et al., 2016). Salicylic acid (SA) is a hormone that plays an important role in plant defense, and it induces QC cell divisions in a dose-dependent manner (Wang et al., 2020). The SA-induced cell divisions are mediated by an increase in ROS levels the RAM and a downregulation of *PLT1*, *PLT2*, and *WOX5* in the QC cells (Wang et al., 2020). It was also previously shown that increased ROS levels cause a downregulation of *PLT* genes, a higher expression of *ERF115*, among other factors (Kong et al., 2018). Altogether, these studies in *Arabidopsis* indicate a key role of redox regulation in QC cell divisions and show the existence of interesting links between QC cell identity and its proliferative state.

It is remarkable that in neural SCs, ROS production in mitochondria has also been shown to regulate SC fate by regulating the expression of key developmental genes (Khacho et al., 2016), suggesting that this could be a generic mechanism for the control SC activity as a response of the internal redox state of the cells.

HORMONAL REGULATION OF QC MITOTIC ACTIVITY

Auxin and CK, as well as BR and ABA, have antagonistic roles in different developmental contexts, including the division of the QC cells in the root SCN. In this section, we review the regulatory crosstalk between these two pairs of antagonistic hormones. All interactions were included in a network that illustrates the complexity underlying QC cell division (**Figure 2E**). Other plant hormones such as gibberellins are not included in this review because it has been demonstrated to regulate root growth independently of the activity of the SCN (Achard et al., 2009; Ubeda-Tomás et al., 2009; González-García et al., 2011).

Auxin and CK Antagonism in the Regulation of the QC Cell Divisions

In the root SCN, WOX5 promotes auxin accumulation in the QC by inducing the expression of the auxin biosynthetic enzymes *YUCCA1* (Tian et al., 2014), *tryptophan aminotransferase of arabidopsis1* (TAA1; Savina et al., 2020), and by repressing the expression of auxin conjugation genes (Gonzali et al.,

2005). As *WOX5* expression is induced by auxin in the QC (Sarkar et al., 2007), this establishes an auxin—WOX5-positive feedback loop in these cells. Moreover, SCR controls auxin levels in the QC cells by indirectly repressing the expression of *ASB1* (*ANTHRANILATE SYNTHASE BETA SUBUNIT 1*), an enzyme involved in auxin biosynthesis (Moubayidin et al., 2013). Consequently, in the *scr-1* mutant, the auxin content is dramatically increased, and the SCN is disorganized (Moubayidin et al., 2013). This suggests that auxin levels have to be actively modulated in the QC cells, to maintain appropriate levels for the long-term organization of the root SCN.

In the QC cells, auxin indirectly promotes low division rates through the positive regulation of *WOX5*, maintaining low levels of *CYCD3;3* in these cells (**Figure 2D**). A study from maize suggests another mechanism by which auxin may impact on QC cell divisions. In maize roots, auxin promotes the expression and the activity of the enzyme ascorbate oxidase (*AAO*), which oxidizes AA to DHA (Kerk and Feldman, 1995). *AAO* expression is high in the QC, moderate in the meristem, and absent in the mature root (Kerk and Feldman, 1995), correlating with the auxin concentration gradient along the RAM. As mentioned in the previous section, in maize, the QC cells have a redox status different to that of the meristem cells. The spatial distribution of auxin and *AAO* along the RAM suggests that the redox status of the cells may be established, at least in part, by auxin. In support of this idea, maize roots treated with 1-*N*-naphtylphthalamic acid (NPA), an inhibitor of auxin efflux transport, display changes in auxin distribution, and the QC becomes less oxidized (Jiang et al., 2003). This change in the redox state of the QC preceded the incorporation of the nucleotide analog, BrdU, strongly suggesting that this change in the redox status of the QC cells underlies the increase in their proliferation rate (Jiang et al., 2003). Based on these results, it was proposed that high levels of auxin in the QC cells regulate the redox status of the cells and maintain low proliferation rates of the QC cells (Jiang et al., 2003). It remains to be determined if this redox regulation also occurs in *Arabidopsis*. Experiments in *Arabidopsis* indicate that SA-induced QC cell divisions are accompanied by an increase in ROS levels and a decrease in auxin signaling in the QC cells (Wang et al., 2020), thus suggesting the existence of a mechanism similar to the one described in maize roots.

Cytokinins have an antagonistic function to auxin in different developmental processes. For instance, the crosstalk between these hormones regulates the balance between proliferation and differentiation in the RAM (Moubayidin et al., 2009; Su et al., 2011; Aichinger et al., 2012; Rodriguez-Villalon and Hardtke, 2014). In the QC, these hormones also have antagonistic role as CK induces cell division. Plants with increased CK signaling display ectopic division of the QC cells (Zhang et al., 2011, 2013). For example, the *arr3,4,5,6,7,8,9,15* loss-of-function multiple mutant in numerous type A ARRs results in CK hypersensitivity and a higher rate of cell division in the QC compared with wild-type plants (Zhang et al., 2011). This phenotype is accompanied by the differentiation of the distal ICs and mild alterations in the auxin response of the QC, indicating that type A ARRs are necessary for maintaining appropriate activity of the QC (Zhang et al., 2011).

Wild-type roots treated with exogenous CK and CK oxidase mutants (*ckx3* and *ckx5*) with elevated endogenous levels of CK also show an increase in QC cell division (Zhang et al., 2013). Expression analyses showed that *WOX5* and *SCR*, as well as the auxin influx transporters *AUX1* and *LAX2*, are down-regulated in the QC of these mutants (Zhang et al., 2013). Interestingly, ARR1 (type B ARR) directly binds to the promoter of *LAX2,* which is expressed in the provascular tissues and the QC cells (Péret et al., 2012), and the QC cells divide in the *lax2* mutant (Zhang et al., 2013). Furthermore, in roots treated with exogenous CK, *LAX2* expression is repressed, resulting in dampening auxin accumulation in the QC cells. Hence, the induction of QC cell division by CK could be an indirect result of lowering auxin levels in the QC. This evidence agrees with a notion where high auxin concentration in the QC promotes a state of no cell divisions. It is interesting that CK levels in the QC cells are rather low, whereas these increase in the neighboring cells (Zhang et al., 2013; Zürcher et al., 2013; Antoniadi et al., 2015), suggesting that a tight spatial regulation of CK metabolism and signaling is important to maintain the QC cells.

Effects of BRs and ABA in the Regulation of QC Cell Divisions

Treating wild-type seedlings with exogenous L-brassinolide (BL) induces the division of the QC cells and the differentiation of distal ICs in a dose-dependent manner (González-García et al., 2011; Fàbregas et al., 2013). Accordingly, the gain-of-function *bzr1-1d* has actively dividing QC cells even if BR biosynthesis is blocked (Chaiwanon and Wang, 2015). Two of the three known BR receptors, namely, BRL1 and BRL3, are detected mainly in the root SCN (Fàbregas et al., 2013), and the*ir* loss-of-function mutants show a reduction in the division rate of the QC cells in comparison with wild-type seedlings (Fàbregas et al., 2013). The protein of the third BR receptor, BRI1, is detected in the root meristem but not in the QC (van Esse et al., 2011; Fàbregas et al., 2013). Interestingly, despite this apparent absence of BRI1 in the QC cells, it is necessary for BR-induced QC cell divisions, as in the *bri1-116* mutant the divisions were completely abolished in roots treated with BL (Vilarrasa-Blasi et al., 2014).

The nuclear accumulation of BES1 and BZR1 can be used as a marker of the activity of the BR signaling. In the SCN, these proteins accumulate mostly in the cytoplasm indicating that the BR signaling pathway is not active in these cells (Chaiwanon and Wang, 2015). As the QC cells of young *Arabidopsis* roots are mitotically quiescent, endogenous mechanisms to maintain BR signaling low in these cells may exist. Based on current evidence, this might be mediated by a low accumulation of BRI1 protein in the QC cells (van Esse et al., 2011; Fàbregas et al., 2013) and by the auxin-dependent increased local BR catabolism in the root SCN area (Chaiwanon and Wang, 2015).

Brassinosteroids signaling negatively affects the expression of a significant number of QC-enriched genes, suggesting that loss of QC identity is linked to an increase in its proliferation (Chaiwanon and Wang, 2015). The MYB transcription factor BRASSINOSTEROIDS AT VASCULAR AND ORGANIZING

CENTER (BRAVO) was identified as the only BR-regulated gene that is a direct target of BES1 and BZR1 in the proximal ICs and the QC cells (Vilarrasa-Blasi et al., 2014). *BRAVO* expression is reduced upon BL treatment in a time- and dose-dependent manner, and this reduction occurs before the BL-induced QC cell divisions (Vilarrasa-Blasi et al., 2014). The *bravo* loss-of-function mutant has increased mitotic activity of the QC cells and a dramatic reduction in the expression of *WOX5* and other QC markers (Vilarrasa-Blasi et al., 2014). In the roots of ectopic expression inducible lines of *BRAVO*, several cell cycle genes are downregulated including *CYCD2;2* and *CYCD3;3*, providing clues of the mechanism by which BRAVO may impact on the cell cycle progression to repress QC divisions. Intriguingly, loss-of-function *wox5-1* mutants show resistance to BR with respect to QC cell proliferation (González-García et al., 2011), indicating that WOX5 is a crucial regulator for the BR-induced QC divisions. This evidence supports a conceptual model where QC cell identity is intimately linked with cell division. In the case of BR, the activation of QC cell divisions may be mediated, in part, by relieving the WOX5-dependent inhibition of *CYCD3;3* (**Figure 2D**). As both BRAVO and WOX5 regulate negatively the expression of *CYCD3;3* (Forzani et al., 2014; Vilarrasa-Blasi et al., 2014), it is tempting to speculate that BRAVO acts through WOX5 in the regulation of QC mitotic activity. Additionally, as BRAVO affects the expression of other cell cycle regulators, it is likely that it also regulates QC cellular quiescence through a parallel pathway (Vilarrasa-Blasi et al., 2014).

On the other hand, ABA has been reported to maintain the quiescent state of the QC cells. Indeed, the low division rate of the QC cells is compromised in ABA-deficient and ABA-insensitive mutants, and in wild-type plants treated with fluridone, an inhibitor of ABA biosynthesis (Zhang et al., 2010). Roots of these plants display increased differentiation of distal ICs, and in some cases, the QC cells had starch granules (Zhang et al., 2010), suggesting that the function and identity of the QC are severely compromised. On the contrary, exogenous ABA treatment induced the quiescence of the QC cells, reduced distal IC differentiation, and increased the expression of root SCN regulators, as *PLT2*, *MP,* and *WOX5* (Zhang et al., 2010). WOX5 mediates the effect of ABA in preventing distal IC differentiation, as treatment of *wox5-1* mutants with either ABA or fluridone no longer altered the differentiation pattern of distal IC (Zhang et al., 2010). Moreover, it has been reported that overexpression of *WOX5* (*35S:WOX5*) potentiates ABA effects related to the additional distal ICs files (Sarkar et al., 2007; Zhang et al., 2010). Surprisingly, distal ICs became differentiated when *35S:WOX5* plants were treated with fluridone, strongly suggesting that the effect of WOX5 over distal ICs depends on ABA availability (Zhang et al., 2010). Altogether, the mentioned evidence indicates that ABA promotes the quiescence of the QC cells, in part by promoting the expression of *WOX5* among other transcription factors, and there might exist a mutual interdependency between ABA and WOX5 to regulate the differentiation of distal ICs.

In summary, the antagonistic effects of BR and ABA on QC cell division are mediated in part by the regulation of QC cell factors, including WOX5. Interestingly, ABA treatment causes a slight increase of *BRAVO* expression (Vilarrasa-Blasi et al., 2014), suggesting that it could be a mediator of BR and ABA responses in the QC cells, although it remains to be determined if this is indeed the case.

AN INTEGRATIVE REGULATORY MODULE FOR QC CELL IDENTITY AND CELL DIVISIONS

The regulatory interactions related to the division of the QC cells described in the previous sections were integrated in a regulatory network that might constitute a developmental module of SC regulation (**Figure 2E**). Through this conceptual framework, it is possible to get insight into how each hormone is affecting the activity of the other elements of the network, and then understand how the system overall is responding to hormonal alterations. For instance, it can be noticed that WOX5 is a recurrent target in the hormonal regulation of QC cell division, making it a central component of the proposed regulatory module (**Figure 2E**). This convergent regulation of a QC-specific transcription factor suggests that the regulation of QC cell division by hormonal signaling pathways is intimately linked with QC cell identity (**Figure 2**). In this regard, it is remarkable that WOX5 directly represses *CYCD3;3* (Forzani et al., 2014) because this establishes a direct link between cell fate regulation in the QC and mitotic quiescence. However, the low proliferation state of the QC cells might be maintained by other means, for example, by the activity of the proteasome (Ueda et al., 2004; Vanstraelen et al., 2009), through the direct regulation of various cell cycle components (Vilarrasa-Blasi et al., 2014), or, as suggested by studies from maize, by the regulation of the redox status of the cells (Kerk and Feldman, 1995; Jiang et al., 2003).

The notion that hormones are channeled toward a common regulatory module to adjust QC cell divisions is supported by reported antagonistic effects on the regulation of QC genes and of QC cell division. For example, auxin and BR have antagonistic effects in the regulation of QC quiescence, and most of the genes that are repressed by BR in the QC are induced by auxin (Chaiwanon and Wang, 2015). *BRAVO* and all *PLTs* are part of the genes regulated differentially by both auxin and BR (Chaiwanon and Wang, 2015), thus establishing a mechanism by which both hormones impact on the cell fate of the QC cells (**Figures 2D,E**). Auxin also promotes the expression of BR catabolic enzymes in order to maintain BR low levels in the root meristem cells and establishing auxin and BR domains with no overlapping responses (Chaiwanon and Wang, 2015). Thus, there are many ways in which this hormonal crosstalk takes place, and its study can be aided through a network approach.

In the case of auxin and CK, this pair of hormones has antagonistic roles in the regulation of cell division in both the RAM and in the QC cells. Intriguingly, auxin promotes cell proliferation in the meristem and mitotic quiescence in the QC (Kerk and Feldman, 1995; Ishida et al., 2010; Chaiwanon and Wang, 2015), whereas CK promotes the opposite (Dello ioio et al., 2008; Zhang et al., 2013). This indicates that there is a general antagonism between auxin and CK that is independent of the tissue context (**Table 1**). The regulatory crosstalk between auxin

and CK is not necessarily conserved in the root meristem and the QC (reviewed in Garay-Arroyo et al., 2012; **Table 1**). For example, CK induces the expression of the Aux/IAA repressor *SHY2* to regulate meristem size, and this is a key point in the regulatory crosstalk between auxin and CK (Dello ioio et al., 2008), but SHY2 is not involved in the regulation of CK-induced QC cell division (Zhang et al., 2013). Therefore, how the hormonal regulatory modules act in the meristematic cells and in the QC, and how they are coupled remain to be uncovered. The opposite effects of these hormones in the meristem and the QC could be due to quantitative variations in its levels and the specific gene activity profile in each context (Fridman et al., 2014; Vragović et al., 2015). Thus, considering the gene regulatory network that underlies the acquisition of different fates in the RAM could be very instrumental to understand the opposite effects of these hormones in the different zones of the root apex (García-Gómez et al., 2017).

It is interesting that there are mutants with RAM defects, which display QC cell divisions despite maintaining *WOX5* expression, indicating that, although it is a central component in the hormonal regulation of QC cell division, it is not enough to maintain a quiescence cell state. Examples of this are the *ccs52a2* loss-of-function mutant (Vanstraelen et al., 2009), BR gain-of-function signaling mutants (González-García et al., 2011), a mutant with SA overaccumulation (Wang et al., 2020), a down-regulation of *rbr* in the QC cells (Cruz-Ramírez et al., 2013), and mutants affecting folate metabolism (Reyes-Hernández et al., 2014) and threonine synthesis (Reyes-Hernández et al., 2019). As reviewed here, other important regulators of QC divisions include the redox status of the cells (Kerk and Feldman, 1995; Jiang et al., 2003) and BRAVO, which controls the expression of several cell cycle genes (Vilarrasa-Blasi et al., 2014). This could constitute parallel ways in which the division of the QC cells can be modulated independently of WOX5. As we learn more about the effects of hormones on the activity of the cell fate regulators of the root SCN, these could be integrated into the network to assess their effect on the other key elements of QC cell regulation (**Figure 2E**).

Regarding jasmonic acid (JA), a report showed that it induces QC cell proliferation, and it has been suggested to be through the control of the transition from the G2 to M phase of the cell cycle (Chen et al., 2011). Additionally, JA signaling inhibits the expression of the auxin-responsive genes *PLT1* and *PLT2* (Chen et al., 2011), and recent reports show that it promotes QC cell division through the RBR-SCR regulatory circuit and ERF115 (Zhou et al., 2019), thus connecting JA signaling with the regulatory module controlling cell fate and division in the QC. Moreover, auxin induces the expression of *ERF115* during regeneration as QC cell divisions take place (Zhou et al., 2019), indicating a multistability of auxin signaling in the regulation of QC cell divisions. Ethylene also promotes the proliferation of the QC cells, but the molecular mechanism is currently unknown (Ortega-Martínez et al., 2007). It has been reported that this ethylene effect on QC cell division is achieved independently of auxin, BR, CK, and JA (Chen et al., 2011; Heyman et al., 2013; Zhang et al., 2013). Curiously, in maize roots, NPA-induced QC cell divisions are reverted by cotreatment with an ethylene precursor ACC, indicating a regulatory interaction between these hormones in the regulation of the QC (Ponce et al., 2005). In this study, it is suggested that this might be a non–cell-autonomous effect mediated by a deregulation of auxin transport (Ponce et al., 2005).

Finally, the hormonal regulatory interactions that underlie QC cellular quiescence are non-linear and occur in a multicellular context, so an integrative approach of regulatory networks could aid in understanding these interactions (Azpeitia and Alvarez-Buylla, 2012; García-Gómez et al., 2020).

TABLE 1 | Hormonal regulatory effects in the QC and root meristem cells.

Hormone	Link to primary metabolism	Effect in the QC	Effect in the meristem	Regulation of SCN transcription factors	Other regulated genes at the root tip	References
Brassinosteroids	—	Proliferation	Proliferation and differentiation	WOX5, PLT1, PLT2, BBM, and AGL42.	BRAVO and KRP2	González-García et al., 2011; Vilarrasa-Blasi et al., 2014; Vragović et al., 2015; Chaiwanon and Wang, 2015
Abscisic acid	—	Quiescence	Proliferation and differentiation	WOX5, MP, and PLT2		Zhang et al., 2010
Auxin	Tryptophane	Quiescence	Proliferation	WOX5, PLT1, PLT2, BBM, and BRAVO	AAO (in maize roots) and BR catabolic enzymes	Kerk and Feldman, 1995; Aida et al., 2004; Galinha et al., 2007; Sarkar et al., 2007; Chaiwanon and Wang, 2015
Cytokinin	Adenine	Proliferation	Differentiation	WOX5 and SCR	LAX2, SHY2 and CCS52A1	Dello ioio et al., 2008; Takahashi and Umeda, 2014; Zhang et al., 2013
Jasmonic acid	Isoleucine	Proliferation	Differentiation	PLT1 and PLT2		Chen et al., 2011
Ethylene	Methionine	Proliferation	—	—	TAA1	Stepanova et al., 2008

PERSPECTIVES

The interconnection of hormonal signaling pathways, regulators of cell division, and the cell identity of the QC cells is an exciting matter of research that could reveal systemic mechanisms by which SC activity in plants is dynamically modulated to adapt to changing environmental and physiological conditions. Although this is of interest to the field of plant development, recent reports in animal SCNs are finding features that are also present in plant SCNs (Li and Clevers, 2010), and thus, what we learn about the QC regulation could potentially uncover generic regulatory mechanisms of SCs. Some of the most remarkable similarities between plant and animal SCNs are the coexistence of two adjoining populations of SCs with different proliferation rates (Barlow, 1978, 1997; Jiang and Feldman, 2005; Li and Clevers, 2010) and also the dual role of SCs that can act as organizers and also maintain their progeny undifferentiated (van den Berg et al., 1997; Pardo-Saganta et al., 2015). The functional meaning of SCs acting both as the organizer of the SCN and as SCs, as is the case for the QC in the root SCN, is possibly related to the self-organizing properties of the SCNs and the dynamic regulation of its size at the organ level. Furthermore, the existence of a population of SCs with different division rates results in the preservation of this population of cells for longer times, protecting them against deleterious mutations that otherwise might spread to the whole tissue (Clowes, 1956; Scadden, 2006). The root SCN is a well-described niche at the anatomical level, and we have a good understanding of the regulatory networks that underlie the acquisition of cell identity and hormonal profiles. Thus, the root SCN is a model system to describe the constraints of hormonal regulation of SCs activity that will then be instrumental to understand how the same may be occurring in other systems. The conceptual framework we presented in this review constitutes an important step toward this goal.

AUTHOR CONTRIBUTIONS

All authors listed have made a substantial, direct and intellectual contribution to the work, and approved it for publication.

FUNDING

This study was financed with the following grants: Programa de Apoyo a Proyectos de Investigación e Innovación Tecnológica Universidad Nacional Autónoma de México (UNAM-DGAPA-PAPIIT http://dgapa.unam.mx/index.php/impulso-a-la-investigacion/papiit): IN200920, IN203220, IN206220, IN211721, and Consejo Nacional de Ciencia y Tecnología (CONACyT): 102959 and 102987. The funders had no role in study design, data collection and analysis, decision to publish, or preparation of the manuscript.

ACKNOWLEDGMENTS

We acknowledge the help from Diana Belén Sánchez-Rodríguez with various logistical tasks.

REFERENCES

Aceves-García, P., Álvarez-Buylla, E. R., Garay-Arroyo, A., García-Ponce, B., Muñoz, R., and de la Paz Sánchez, M. (2016). Root architecture diversity and meristem dynamics in different populations of *Arabidopsis thaliana*. *Front. Plant Sci.* 7:858. doi: 10.3389/fpls.2016.00858

Achard, P., Gusti, A., Cheminant, S., Alioua, M., Dhondt, S., Coppens, F., et al. (2009). Gibberellin signaling controls cell proliferation rate in *Arabidopsis*. *Curr. Biol.* 19, 1188–1193. doi: 10.1016/j.cub.2009.05.059

Aichinger, E., Kornet, N., Friedrich, T., and Laux, T. (2012). Plant stem cell niches. *Annu. Rev. Plant Biol.* 63, 615–636. doi: 10.1146/annurev-arplant-042811-105555

Aida, M., Beis, D., Heidstra, R., Willemsen, V., Blilou, I., Galinha, C., et al. (2004). The PLETHORA genes mediate patterning of the *Arabidopsis* root stem cell niche. *Cell* 119, 109–120. doi: 10.1016/j.cell.2004.09.018

Alvarado, A. S., and Yamanaka, S. (2014). Rethinking differentiation: stem cells, regeneration, and plasticity. *Cell* 157, 110–119. doi: 10.1016/j.cell.2014.02.041

Antoniadi, I., Plačková, L., Simonovik, B., Doležal, K., Turnbull, C., Ljung, K., et al. (2015). Cell-type-specific cytokinin distribution within the *Arabidopsis* primary root apex. *Plant Cell* 27, 1955–1967. doi: 10.1105/tpc.15.00176

Apel, K., and Heribert, H. (2004). Reactive oxygen species: metabolism, oxidative stress, and signal transduction. *Annu. Rev. Plant Biol.* 55, 373–399. doi: 10.1146/annurev.arplant.55.031903.141701

Arrigoni, O., and De Tullio, M. C. (2000). The role of ascorbic acid in cell metabolism: between gene-directed functions and unpredictable chemical reactions. *J. Plant Physiol.* 157, 481–488. doi: 10.1016/S0176-1617(00)80102-9

Azpeitia, E., and Alvarez-Buylla, E. R. (2012). A complex systems approach to *Arabidopsis* root stem-cell niche developmental mechanisms: from molecules, to networks, to morphogenesis. *Plant Mol. Biol.* 80, 351–363. doi: 10.1007/s11103-012-9954-6

Barlow, P. W. (1978). "The concept of the stem cell in the context of plant growth and development," in *Stem Cells and Tissue Homeostasis*, (Cambridge: Cambridge University. Press), 87–113.

Barlow, P. W. (1997). "Stem cells and founder zones in plants, particularly their roots," in *Stem Cells*, ed C. S. Poten (London: Academic), 29–57. doi: 10.1016/B978-012563455-7/50003-9

Baum, S. F., Dubrovsky, J. G., and Rost, T. L. (2002). Apical organization and maturation of the cortex and vascular cylinder in*Arabidopsis thaliana* (*Brassicaceae*) roots. *Am. J. Bot.* 89, 908–920. doi: 10.3732/ajb.89.6.908

Belkhadir, Y., Yang, L., Hetzel, J., Dangl, J. L., and Chory, J. (2014). The growth–defense pivot: crisis management in plants mediated by LRR-RK surface receptors. *Trends Biochem. Sci.* 39, 447–456. doi: 10.1016/j.tibs.2014.06.006

Benfey, P. N., Linstead, P. J., Roberts, K., Schiefelbein, J. W., Hauser, M. T., and Aeschbacher, R. A. (1993). Root development in *Arabidopsis*: four mutants with dramatically altered root morphogenesis. *Development* 119, 57–70.

Blilou, I., Xu, J., Wildwater, M., Willemsen, V., Paponov, I., Friml, J., et al. (2005). The PIN auxin efflux facilitator network controls growth and patterning in *Arabidopsis* roots. *Nature* 433, 39–44. doi: 10.1038/nature03184

Brunoud, G., Wells, D. M., Oliva, M., Larrieu, A., Mirabet, V., Burrow, A. H., et al. (2012). A novel sensor to map auxin response and distribution at high spatio-temporal resolution. *Nature* 482, 103–106. doi: 10.1038/nature10791

Calderón Villalobos, L. I. A. C., Lee, S., De Oliveira, C., Ivetac, A., Brandt, W., Armitage, L., et al. (2012). A combinatorial TIR1/AFB–Aux/IAA co-receptor system for differential sensing of auxin. *Nat. Chem. Biol.* 8, 477–485. doi: 10.1038/nchembio.926

Chaiwanon, J., and Wang, Z. Y. (2015). Spatiotemporal brassinosteroid signaling and antagonism with auxin pattern stem cell dynamics in *Arabidopsis* roots. *Curr. Biol.* 25, 1031–1042. doi: 10.1016/j.cub.2015.02.046

Chen, Q., Sun, J., Zhai, Q., Zhou, W., Qi, L., Xu, L., et al. (2011). The basic helix-loop-helix transcription factor MYC2 directly represses PLETHORA

expression during jasmonate-mediated modulation of the root stem cell niche in *Arabidopsis*. *Plant Cell Online* 23, 3335–3352. doi: 10.1105/tpc.111.089870

Clark, N. M., Fisher, A. P., Berckmans, B., Van den Broeck, L., Nelson, E. C., Nguyen, T. T., et al. (2020). Protein complex stoichiometry and expression dynamics of transcription factors modulate stem cell division. *Proc. Natl. Acad. Sci. U.S.A.* 117, 15332–15342. doi: 10.1073/pnas.2002166117

Clowes, F. A. L. (1956). Localization of nucleic acid synthesis in root meristems. *J. Exp. Bot.* 7, 307–312. doi: 10.1093/jxb/7.3.307

Cruz-Ramírez, A., Díaz-Triviño, S., Wachsman, G., Du, Y., Arteága-Vázquez, M., Zhang, H., et al. (2013). A SCARECROW-RETINOBLASTOMA protein network controls protective quiescence in the *Arabidopsis* root stem cell organizer. *PLoS Biol.* 11:e1001724. doi: 10.1371/journal.pbio.1001724

Cui, H., Levesque, M. P., Vernoux, T., Jung, J. W., Paquette, A. J., Gallagher, K. L., et al. (2007). An evolutionarily conserved mechanism delimiting SHR movement defines a single layer of endodermis in plants. *Science* 316, 421–425. doi: 10.1126/science.1139531

de Almeida Engler, J., De Veylder, L., De Groodt, R., Rombauts, S., Boudolf, V., De Meyer, B., et al. (2009). Systematic analysis of cell-cycle gene expression during *Arabidopsis* development. *Plant J.* 59, 645–660. doi: 10.1111/j.1365-313X.2009.03893.x

De Tullio, M. C., Jiang, K., and Feldman, L. J. (2010). Redox regulation of root apical meristem organization: connecting root development to its environment. *Plant Physiol. Biochem.* 48, 328–336. doi: 10.1016/j.plaphy.2009.11.005

Dello ioio, R., Nakamura, K., Moubayidin, L., Perilli, S., Taniguchi, M., Morita, M. T., et al. (2008). A genetic framework for the control of cell division and differentiation in the root meristem. *Science* 322, 1380–1384. doi: 10.1126/science.1164147

Dharmasiri, N., Dharmasiri, S., and Estelle, M. (2005). The F-box protein TIR1 is an auxin receptor. *Nature* 435, 441–445. doi: 10.1038/nature03543

Di Laurenzio, L., Wysocka-Diller, J., Malamy, J. E., Pysh, L., Helariutta, Y., Freshour, G., et al. (1996). The SCARECROW gene regulates an asymmetric cell division that is essential for generating the radial organization of the *Arabidopsis* root. *Cell* 86, 423–433. doi: 10.1016/S0092-8674(00)80115-4

Ding, Z., and Friml, J. (2010). Auxin regulates distal stem cell differentiation in *Arabidopsis* roots. *Proc. Natl. Acad. Sci. U.S.A.* 107, 12046–12051. doi: 10.1073/pnas.1000672107

Dolan, L., Janmaat, K., Willemsen, V., Linstead, P., Poethig, S., Roberts, K., et al. (1993). Cellular organisation of the *Arabidopsis thaliana* root. *Development* 119, 71–84.

Fàbregas, N., Li, N., Boeren, S., Nash, T. E., Goshe, M. B., Clouse, S. D., et al. (2013). The BRASSINOSTEROID INSENSITIVE1–LIKE3 signalosome complex regulates *Arabidopsis* root development. *Plant Cell* 25, 3377–3388. doi: 10.1105/tpc.113.114462

Forzani, C., Aichinger, E., Sornay, E., Willemsen, V., Laux, T., Dewitte, W., et al. (2014). WOX5 suppresses CYCLIN D activity to establish quiescence at the center of the root stem cell niche. *Curr. Biol.* 24, 1939–1944. doi: 10.1016/j.cub.2014.07.019

Fridman, Y., Elkouby, L., Holland, N., Vragović, K., Elbaum, R., and Savaldi-Goldstein, S. (2014). Root growth is modulated by differential hormonal sensitivity in neighboring cells. *Genes Dev.* 28, 912–920. doi: 10.1101/gad.239335.114

Galinha, C., Hofhuis, H., Luijten, M., Willemsen, V., Blilou, I., Heidstra, R., et al. (2007). PLETHORA proteins as dose-dependent master regulators of *Arabidopsis* root development. *Nature* 449, 1053–1057. doi: 10.1038/nature06206

Garay-Arroyo, A., De La Paz Sánchez, M., García-Ponce, B., Azpeitia, E., and Álvarez-Buylla, E. R. (2012). Hormone symphony during root growth and development. *Dev. Dyn.* 241, 1867–1885. doi: 10.1002/dvdy.23878

García-Gómez, M. L., Azpeitia, E., and Álvarez-Buylla, E. R. (2017). A dynamic genetic-hormonal regulatory network model explains multiple cellular behaviors of the root apical meristem of *Arabidopsis thaliana*. *PLoS Comput. Biol.* 13:e1005488. doi: 10.1371/journal.pcbi.1005488

García-Gómez, M. L., Ornelas-Ayala, D., Garay-Arroyo, A., García-Ponce, B., de la Paz Sánchez, M., and Álvarez-Buylla, E. R. (2020). A system-level mechanistic explanation for asymmetric stem cell fates: *Arabidopsis thaliana* root niche as a study system. *Sci. Rep.* 10, 1–16.

González-García, M. P., Vilarrasa-Blasi, J., Zhiponova, M., Divol, F., Mora-García, S., Russinova, E., et al. (2011). Brassinosteroids control meristem size by promoting cell cycle progression in *Arabidopsis* roots. *Development* 138, 849–859. doi: 10.1242/dev.057331

Gonzali, S., Novi, G., Loreti, E., Paolicchi, F., Poggi, A., Alpi, A., et al. (2005). A turanose-insensitive mutant suggests a role for WOX5 in auxin homeostasis in *Arabidopsis thaliana*. *Plant J.* 44, 633–645. doi: 10.1111/j.1365-313X.2005.02555.x

Grieneisen, V. A., Xu, J., Marée, A. F., Hogeweg, P., and Scheres, B. (2007). Auxin transport is sufficient to generate a maximum and gradient guiding root growth. *Nature* 449, 1008–1013. doi: 10.1038/nature06215

Guilfoyle, T. J., and Hagen, G. (2007). Auxin response factors. *Curr. Opin. Plant Biol.* 10, 453–460. doi: 10.1016/j.pbi.2007.08.014

Gutierrez, C. (2009). The *Arabidopsis* cell division cycle. *Arabidopsis Book* 7:e0120. doi: 10.1199/tab.0120

Heidstra, R., and Sabatini, S. (2014). Plant and animal stem cells: similar yet different. *Nat. Rev. Mol. Cell Biol.* 15, 301–312. doi: 10.1038/nrm3790

Helariutta, Y., Fukaki, H., Wysocka-Diller, J., Nakajima, K., Jung, J., Sena, G., et al. (2000). The SHORT-ROOT gene controls radial patterning of the *Arabidopsis* root through radial signaling. *Cell* 101, 555–567. doi: 10.1016/S0092-8674(00)80865-X

Heyman, J., Cools, T., Vandenbussche, F., Heyndrickx, K. S., Van Leene, J., Vercauteren, I., et al. (2013). ERF115 controls root quiescent center cell division and stem cell replenishment. *Science* 342, 860–863. doi: 10.1126/science.1240667

Heyman, J., Kumpf, R. P., and De Veylder, L. (2014). A quiescent path to plant longevity. *Trends Cell Biol.* 24, 443–448. doi: 10.1016/j.tcb.2014.03.004

Ishida, T., Adachi, S., Yoshimura, M., Shimizu, K., Umeda, M., and Sugimoto, K. (2010). Auxin modulates the transition from the mitotic cycle to the endocycle in *Arabidopsis*. *Development* 137, 63–71. doi: 10.1242/dev.035840

Ivanov, V. B., and Dubrovsky, J. G. (2013). Longitudinal zonation pattern in plant roots: conflicts and solutions. *Trends Plant Sci.* 18, 237–243. doi: 10.1016/j.tplants.2012.10.002

Jiang, K., and Feldman, L. J. (2005). Regulation of root apical meristem development. *Annu. Rev. Cell Dev. Biol.* 21, 485–509. doi: 10.1146/annurev.cellbio.21.122303.114753

Jiang, K., Meng, Y. L., and Feldman, L. J. (2003). Quiescent center formation in maize roots is associated with an auxin-regulated oxidizing environment. *Development* 130, 1429–1438. doi: 10.1242/dev.00359

Kerk, N. M., and Feldman, N. J. (1995). A biochemical model for the initiation and maintenance of the quiescent center: implications for organization of root meristems. *Development* 121, 2825–2833.

Khacho, M., Clark, A., Svoboda, D. S., Azzi, J., MacLaurin, J. G., Meghaizel, C., et al. (2016). Mitochondrial dynamics impacts stem cell identity and fate decisions by regulating a nuclear transcriptional program. *Cell Stem Cell* 19, 232–247. doi: 10.1016/j.stem.2016.04.015

Kiba, T., Aoki, K., Sakakibara, H., and Mizuno, T. (2004). *Arabidopsis* response regulator, ARR22, ectopic expression of which results in phenotypes similar to the wol cytokinin-receptor mutant. *Plant Cell Physiol.* 45, 1063–1077. doi: 10.1093/pcp/pch128

Kidner, C., Sundaresan, V., Roberts, K., and Dolan, L. (2000). Clonal analysis of the *Arabidopsis* root confirms that position, not lineage, determines cell fate. *Planta* 211, 191–199. doi: 10.1007/s004250000284

Kong, X., Tian, H., Yu, Q., Zhang, F., Wang, R., Gao, S., et al. (2018). PHB3 maintains root stem cell niche identity through ROS-responsive AP2/ERF transcription factors in *Arabidopsis*. *Cell Rep.* 22, 1350–1363. doi: 10.1016/j.celrep.2017.12.105

Levesque, M. P., Vernoux, T., Busch, W., Cui, H., Wang, J. Y., Blilou, I., et al. (2006). Whole-genome analysis of the SHORT-ROOT developmental pathway in *Arabidopsis*. *PLoS Biol.* 4:e143. doi: 10.1371/journal.pbio.0040143

Li, L., and Clevers, H. (2010). Coexistence of quiescent and active adult stem cells in mammals. *Science* 327, 542–545. doi: 10.1126/science.1180794

Liu, Y., Xu, M., Liang, N., Zheng, Y., Yu, Q., and Wu, S. (2017). Symplastic communication spatially directs local auxin biosynthesis to maintain root stem cell niche in *Arabidopsis*. *Proc. Natl. Acad. Sci. U.S.A.* 114, 4005–4010. doi: 10.1073/pnas.1616387114

Long, Y., Smet, W., Cruz-Ramírez, A., Castelijns, B., de Jonge, W., Mähönen, A. P., et al. (2015). *Arabidopsis* BIRD zinc finger proteins jointly stabilize tissue boundaries by confining the cell fate regulator SHORT-ROOT and contributing to fate specification. *Plant Cell* 27, 1185–1199. doi: 10.1105/tpc.114.132407

Long, Y., Stahl, Y., Weidtkamp-Peters, S., Postma, M., Zhou, W., Goedhart, J., et al. (2017). In vivo FRET–FLIM reveals cell-type-specific protein interactions in *Arabidopsis* roots. *Nature* 548, 97–102. doi: 10.1038/nature23317

Mähönen, A. P., Ten Tusscher, K., Siligato, R., Smetana, O., Díaz-Triviño, S., Salojärvi, J., et al. (2014). PLETHORA gradient formation mechanism separates auxin responses. *Nature* 515, 125–129. doi: 10.1038/nature13663

Moreno-Risueno, M. A., Sozzani, R., Yardımcı, G. G., Petricka, J. J., Vernoux, T., Blilou, I., et al. (2015). Transcriptional control of tissue formation throughout root development. *Science* 350, 426–430. doi: 10.1126/science.aad1171

Moubayidin, L., Di Mambro, R., and Sabatini, S. (2009). Cytokinin–auxin crosstalk. *Trends Plant Sci.* 14, 557–562. doi: 10.1016/j.tplants.2009.06.010

Moubayidin, L., Di Mambro, R., Sozzani, R., Pacifici, E., Salvi, E., Terpstra, I., et al. (2013). Spatial coordination between stem cell activity and cell differentiation in the root meristem. *Dev. Cell* 26, 405–415. doi: 10.1016/j.devcel.2013.06.025

Nakajima, K., Sena, G., Nawy, T., and Benfey, P. N. (2001). Intercellular movement of the putative transcription factor SHR in root patterning. *Nature* 413, 307–311. doi: 10.1038/35095061

Okushima, Y., Mitina, I., Quach, H. L., and Theologis, A. (2005). AUXIN RESPONSE FACTOR 2 (ARF2): a pleiotropic developmental regulator. *Plant J.* 43, 29–46. doi: 10.1111/j.1365-313X.2005.02426.x

Ornelas-Ayala, D., Vega-León, R., Petrone-Mendoza, E., Garay-Arroyo, A., García-Ponce, B., and Álvarez-Buylla, E. R. (2020). ULTRAPETALA1 maintains *Arabidopsis* root stem cell niche independently of *ARABIDOPSIS TRITHORAX1*. *New Phytol.* 225, 1261–1272. doi: 10.1111/nph.16213

Ortega-Martínez, O., Pernas, M., Carol, R. J., and Dolan, L. (2007). Ethylene modulates stem cell division in the *Arabidopsis thaliana* root. *Science* 317, 507–510. doi: 10.1126/science.1143409

Ortiz-Gutiérrez, E., García-Cruz, K., Azpeitia, E., Castillo, A., de la Paz Sanchez, M., and Álvarez-Buylla, E. R. (2015). A dynamic gene regulatory network model that recovers the cyclic behavior of *Arabidopsis thaliana* cell cycle. *PLoS Comput. Biol.* 11:e1004486. doi: 10.1371/journal.pcbi.1004486

Pardo-Saganta, A., Tata, P. R., Law, B. M., Saez, B., Chow, R. D. W., Prabhu, M., et al. (2015). Parent stem cells can serve as niches for their own daughter cells. *Nature* 523, 597–601. doi: 10.1038/nature14553

Péret, B., Swarup, K., Ferguson, A., Seth, M., Yang, Y., Dhondt, S., et al. (2012). AUX/LAX genes encode a family of auxin influx transporters that perform distinct functions during *Arabidopsis* development. *Plant Cell* 24, 2874–2885. doi: 10.1105/tpc.112.097766

Petersson, S. V., Johansson, A. I., Kowalczyk, M., Makoveychuk, A., Wang, J. Y., Moritz, T., et al. (2009). An auxin gradient and maximum in the *Arabidopsis* root apex shown by high-resolution cell-specific analysis of IAA distribution and synthesis. *Plant Cell* 21, 1659–1668. doi: 10.1105/tpc.109.066480

Pi, L., Aichinger, E., van der Graaff, E., Llavata-Peris, C. I., Weijers, D., Hennig, L., et al. (2015). Organizer-derived WOX5 signal maintains root columella stem cells through chromatin-mediated repression of CDF4 expression. *Dev. Cell* 33, 576–588. doi: 10.1016/j.devcel.2015.04.024

Piya, S., Shrestha, S. K., Binder, B., Stewart, C. N. Jr., and Hewezi, T. (2014). Protein-protein interaction and gene co-expression maps of ARFs and Aux/IAAs in *Arabidopsis*. *Front. Plant Sci.* 5:744. doi: 10.3389/fpls.2014.00744

Polyn, S., Willems, A., and De Veylder, L. (2015). Cell cycle entry, maintenance, and exit during plant development. *Curr. Opin. Plant Biol.* 23, 1–7. doi: 10.1016/j.pbi.2014.09.012

Ponce, G., Barlow, P. W., Feldman, L. J., and Cassab, G. I. (2005). Auxin and ethylene interactions control mitotic activity of the quiescent centre, root cap size, and pattern of cap cell differentiation in maize. *Plant Cell Environ.* 28, 719–732. doi: 10.1111/j.1365-3040.2005.01318.x

Rademacher, E. H., Möller, B., Lokerse, A. S., Llavata-Peris, C. I., van den Berg, W., and Weijers, D. (2011). A cellular expression map of the *Arabidopsis* AUXIN RESPONSE FACTOR gene family. *Plant J.* 68, 597–606. doi: 10.1111/j.1365-313X.2011.04710.x

Rahni, R., and Birnbaum, K. D. (2019). Week-long imaging of cell divisions in the *Arabidopsis* root meristem. *Plant Methods* 15:30.

Rashotte, A. M., Mason, M. G., Hutchison, C. E., Ferreira, F. J., Schaller, G. E., and Kieber, J. J. (2006). A subset of *Arabidopsis* AP2 transcription factors mediates cytokinin responses in concert with a two-component pathway. *Proc. Natl. Acad. Sci. U.S.A.* 103, 11081–11085. doi: 10.1073/pnas.0602038103

Reyes-Hernández, B. J., Shishkova, S., Amir, R., Quintana-Armas, A. X., Napsucialy-Mendivil, S., Cervantes-Gamez, R. G., et al. (2019). Root stem cell niche maintenance and apical meristem activity critically depend on THREONINE SYNTHASE1. *J. Exp. Bot.* 70, 3835–3849. doi: 10.1093/jxb/erz165

Reyes-Hernández, B. J., Srivastava, A. C., Ugartechea-Chirino, Y., Shishkova, S., Ramos-Parra, P. A., Lira-Ruan, V., et al. (2014). The root indeterminacy-to-determinacy developmental switch is operated through a folate-dependent pathway in *Arabidopsis thaliana*. *New Phytol.* 202, 1223–1236. doi: 10.1111/nph.12757

Rodriguez-Villalon, A., and Hardtke, C. S. (2014). "Auxin and its henchmen: hormonal cross talk in root growth and development," in *Auxin and Its Role in Plant Development*, eds E. Zažímalová, J. Petrášek, and E. Benková (Vienna: Springer), 245–264. doi: 10.1007/978-3-7091-1526-8_12

Sabatini, S., Beis, D., Wolkenfelt, H., Murfett, J., Guilfoyle, T., Malamy, J., et al. (1999). An auxin-dependent distal organizer of pattern and polarity in the *Arabidopsis* root. *Cell* 99, 463–472. doi: 10.1016/S0092-8674(00)81535-4

Sabatini, S., Heidstra, R., Wildwater, M., and Scheres, B. (2003). SCARECROW is involved in positioning the stem cell niche in the *Arabidopsis* root meristem. *Genes Dev.* 17, 354–358. doi: 10.1101/gad.252503

Sánchez-Calderón, L., López-Bucio, J., Chacón-López, A., Cruz-Ramírez, A., Nieto-Jacobo, F., Dubrovsky, J. G., et al. (2005). Phosphate starvation induces a determinate developmental program in the roots of *Arabidopsis thaliana*. *Plant Cell Physiol.* 46, 174–184. doi: 10.1093/pcp/pci011

Santner, A., Calderon-Villalobos, L. I. A., and Estelle, M. (2009). Plant hormones are versatile chemical regulators of plant growth. *Nat. Chem. Biol.* 5, 301–307. doi: 10.1038/nchembio.165

Sarkar, A. K., Luijten, M., Miyashima, S., Lenhard, M., Hashimoto, T., Nakajima, K., et al. (2007). Conserved factors regulate signalling in *Arabidopsis thaliana* shoot and root stem cell organizers. *Nature* 446, 811–814. doi: 10.1038/nature05703

Savina, M. S., Pasternak, T., Omelyanchuk, N. A., Novikova, D. D., Palme, K., Mironova, V. V., et al. (2020). Cell dynamics in WOX5-overexpressing root tips: the impact of local auxin biosynthesis. *Front. Plant Sci.* 11:169. doi: 10.3389/fpls.2020.560169

Scadden, D. T. (2006). The stem-cell niche as an entity of action. *Nature* 441, 1075–1079. doi: 10.1038/nature04957

Scheres, B., Di Laurenzio, L., Willemsen, V., Hauser, M. T., Janmaat, K., Weisbeek, P., et al. (1995). Mutations affecting the radial organisation of the *Arabidopsis* root display specific defects throughout the embryonic axis. *Development* 121, 53–62.

Shimotohno, A., Heidstra, R., Blilou, I., and Scheres, B. (2018). Root stem cell niche organizer specification by molecular convergence of PLETHORA and SCARECROW transcription factor modules. *Genes Dev.* 32, 1085–1100. doi: 10.1101/gad.314096.118

Sozzani, R., Cui, H., Moreno-Risueno, M. A., Busch, W., Van Norman, J. M., Vernoux, T., et al. (2010). Spatiotemporal regulation of cell-cycle genes by SHORTROOT links patterning and growth. *Nature* 466, 128–132. doi: 10.1038/nature09143

Stepanova, A. N., Robertson-Hoyt, J., Yun, J., Benavente, L. M., Xie, D. Y., Doležal, K., et al. (2008). TAA1-mediated auxin biosynthesis is essential for hormone crosstalk and plant development. *Cell* 133, 177–191. doi: 10.1016/j.cell.2008.01.047

Su, Y. H., Liu, Y. B., and Zhang, X. S. (2011). Auxin–cytokinin interaction regulates meristem development. *Mol. Plant* 4, 616–625. doi: 10.1093/mp/ssr007

Swarup, R., Kramer, E. M., Perry, P., Knox, K., Leyser, H. O., Haseloff, J., et al. (2005). Root gravitropism requires lateral root cap and epidermal cells for transport and response to a mobile auxin signal. *Nat. Cell Biol.* 7, 1057–1065. doi: 10.1038/ncb1316

Takahashi, N., and Umeda, M. (2014). Cytokinins promote onset of endoreplication by controlling cell cycle machinery. *Plant Signal. Behav.* 9, 1812–1817. doi: 10.4161/psb.29396

Tian, H., Wabnik, K., Niu, T., Li, H., Yu, Q., Pollmann, S., et al. (2014). WOX5–IAA17 feedback circuit-mediated cellular auxin response is crucial for the patterning of root stem cell niches in *Arabidopsis*. *Mol. Plant* 7, 277–289. doi: 10.1093/mp/sst118

Timilsina, R., Kim, J. H., Nam, H. G., and Woo, H. R. (2019). Temporal changes in cell division rate and genotoxic stress tolerance in quiescent center cells of *Arabidopsis* primary root apical meristem. *Sci. Rep.* 9, 1–9. doi: 10.1007/978-94-010-0936-2_1

To, J. P., Deruère, J., Maxwell, B. B., Morris, V. F., Hutchison, C. E., Ferreira, F. J., et al. (2007). Cytokinin regulates type-A *Arabidopsis* response regulator activity and protein stability via two-component phosphorelay. *Plant Cell Online* 19, 3901–3914. doi: 10.1105/tpc.107.052662

Truskina, J., Han, J., Chrysanthou, E., Galvan-Ampudia, C. S., Lainé, S., Brunoud, G., et al. (2020). A network of transcriptional repressors modulates auxin responses. *Nature* 589, 116–119. doi: 10.1038/s41586-020-2940-2

Tsukagoshi, H., Busch, W., and Benfey, P. N. (2010). Transcriptional regulation of ROS controls transition from proliferation to differentiation in the root. *Cell* 143, 606–616. doi: 10.1016/j.cell.2010.10.020

Ubeda-Tomás, S., Federici, F., Casimiro, I., Beemster, G. T., Bhalerao, R., Swarup, R., et al. (2009). Gibberellin signaling in the endodermis controls *Arabidopsis* root meristem size. *Curr. Biol.* 19, 1194–1199. doi: 10.1016/j.cub.2009.06.023

Ueda, M., Matsui, K., Ishiguro, S., Sano, R., Wada, T., Paponov, I., et al. (2004). The HALTED ROOT gene encoding the 26S proteasome subunit RPT2a is essential for the maintenance of *Arabidopsis* meristems. *Development* 131, 2101–2111. doi: 10.1242/dev.01096

Ulmasov, T., Hagen, G., and Guilfoyle, T. J. (1999). Activation and repression of transcription by auxin-response factors. *Proc. Natl. Acad. Sci. U.S.A.* 96, 5844–5849. doi: 10.1073/pnas.96.10.5844

Ulmasov, T., Murfett, J., Hagen, G., and Guilfoyle, T. J. (1997). Aux/IAA proteins repress expression of reporter genes containing natural and highly active synthetic auxin response elements. *Plant Cell* 9, 1963–1971. doi: 10.1105/tpc.9.11.1963

van den Berg, C., Willemsen, V., Hage, W., Weisbeek, P., and Scheres, B. (1995). Cell fate in the *Arabidopsis* root meristem determined by directional signalling. *Nature* 378, 62–65. doi: 10.1038/378062a0

van den Berg, C., Willemsen, V., Hendriks, G., Weisbeek, P., and Scheres, B. (1997). Short-range control of cell differentiation in the *Arabidopsis* root meristem. *Nature* 390, 287–289. doi: 10.1038/36856

van Esse, G. W., Westphal, A. H., Surendran, R. P., Albrecht, C., van Veen, B., Borst, J. W., et al. (2011). Quantification of the brassinosteroid insensitive1 receptor in planta. *Plant Physiol.* 156, 1691–1700. doi: 10.1104/pp.111.179309

Vanneste, S., and Friml, J. (2009). Auxin: a trigger for change in plant development. *Cell* 136, 1005–1016. doi: 10.1016/j.cell.2009.03.001

Vanstraelen, M., Baloban, M., Da Ines, O., Cultrone, A., Lammens, T., Boudolf, V., et al. (2009). APC/CCCS52A complexes control meristem maintenance in the *Arabidopsis* root. *Proc. Natl. Acad. Sci. U.S.A.* 106, 11806–11811. doi: 10.1073/pnas.0901193106

Vernoux, T., Brunoud, G., Farcot, E., Morin, V., Van den Daele, H., Legrand, J., et al. (2011). The auxin signalling network translates dynamic input into robust patterning at the shoot apex. *Mol. Syst. Biol.* 7:508. doi: 10.1038/msb.2011.39

Vernoux, T., Wilson, R. C., Seeley, K. A., Reichheld, J. P., Muroy, S., Brown, S., et al. (2000). The ROOT MERISTEMLESS1/CADMIUM SENSITIVE2 gene defines a glutathione-dependent pathway involved in initiation and maintenance of cell division during postembryonic root development. *Plant Cell* 12, 97–109. doi: 10.1105/tpc.12.1.97

Vilarrasa-Blasi, J., González-García, M. P., Frigola, D., Fàbregas, N., Alexiou, K. G., López-Bigas, N., et al. (2014). Regulation of plant stem cell quiescence by a brassinosteroid signaling module. *Dev. Cell* 30, 36–47. doi: 10.1016/j.devcel.2014.05.020

Vragović, K., Sela, A., Friedlander-Shani, L., Fridman, Y., Hacham, Y., Holland, N., et al. (2015). Translatome analyses capture of opposing tissue-specific brassinosteroid signals orchestrating root meristem differentiation. *Proc. Natl. Acad. Sci. U.S.A.* 112, 923–928. doi: 10.1073/pnas.1417947112

Wachsman, G., Heidstra, R., and Scheres, B. (2011). Distinct cell-autonomous functions of RETINOBLASTOMA-RELATED in *Arabidopsis* stem cells revealed by the brother of brainbow clonal analysis system. *Plant Cell* 23, 2581–2591. doi: 10.1105/tpc.111.086199

Wang, Z., Rong, D., Chen, D., Xiao, Y., Liu, R., Wu, S., et al. (2020). Salicylic acid promotes quiescent center cell division through ROS accumulation and down-regulation of PLT1, PLT2, and WOX5. *J. Integr. Plant Biol.* doi: 10.1111/jipb.13020. [Epub ahead of print].

Welch, D., Hassan, H., Blilou, I., Immink, R., Heidstra, R., and Scheres, B. (2007). *Arabidopsis* JACKDAW and MAGPIE zinc finger proteins delimit asymmetric cell division and stabilize tissue boundaries by restricting SHORT-ROOT action. *Genes Dev.* 21, 2196–2204. doi: 10.1101/gad.440307

Wildwater, M., Campilho, A., Perez-Perez, J. M., Heidstra, R., Blilou, I., Korthout, H., et al. (2005). The RETINOBLASTOMA-RELATED gene regulates stem cell maintenance in *Arabidopsis* roots. *Cell* 123, 1337–1349. doi: 10.1016/j.cell.2005.09.042

Xu, T., Calderon-Villalobos, L. I. A., Michal, S., Zheng, C., Robinson, C. V., Estelle, M., et al. (2007). Mechanism of auxin perception by the TIR1 ubiquitin ligase. *Nature* 446, 640–645. doi: 10.1038/nature05731

Yu, Q., Tian, H., Yue, K., Liu, J., Zhang, B., Li, X., et al. (2016). A P-loop NTPase regulates quiescent center cell division and distal stem cell identity through the regulation of ROS homeostasis in *Arabidopsis* root. *PLoS Genet.* 12:e1006175. doi: 10.1371/journal.pgen.1006175

Zhai, H., Zhang, X., You, Y., Lin, L., Zhou, W., and Li, C. (2020). SEUSS integrates transcriptional and epigenetic control of root stem cell organizer specification. *EMBO J.* 39:e105047. doi: 10.15252/embj.2020105047

Zhang, H., Han, W., De Smet, I., Talboys, P., Loya, R., Hassan, A., et al. (2010). ABA promotes quiescence of the quiescent centre and suppresses stem cell differentiation in the *Arabidopsis* primary root meristem. *Plant J.* 64, 764–774. doi: 10.1111/j.1365-313X.2010.04367.x

Zhang, W., Swarup, R., Bennett, M., Schaller, G. E., and Kieber, J. J. (2013). Cytokinin induces cell division in the quiescent center of the *Arabidopsis* root apical meristem. *Curr. Biol.* 23, 1979–1989. doi: 10.1016/j.cub.2013.08.008

Zhang, W., To, J. P., Cheng, C. Y., Eric Schaller, G., and Kieber, J. J. (2011). Type-A response regulators are required for proper root apical meristem function through post-transcriptional regulation of PIN auxin efflux carriers. *Plant J.* 68, 1–10. doi: 10.1111/j.1365-313X.2011.04668

Zhang, Y., Jiao, Y., Liu, Z., and Zhu, Y. X. (2015). ROW1 maintains quiescent centre identity by confining WOX5 expression to specific cells. *Nat. Commun.* 6:6003. doi: 10.1038/ncomms7003

Zhou, W., Lozano-Torres, J. L., Blilou, I., Zhang, X., Zhai, Q., Smant, G., et al. (2019). A jasmonate signaling network activates root stem cells and promotes regeneration. *Cell* 177, 942–956. doi: 10.1016/j.cell.2019.03.006

Zhu, J. Y., Sae-Seaw, J., and Wang, Z. Y. (2013). Brassinosteroid signalling. *Development* 140, 1615–1620. doi: 10.1242/dev.060590

Zürcher, E., Tavor-Deslex, D., Lituiev, D., Enkerli, K., Tarr, P. T., and Müller, B. (2013). A robust and sensitive synthetic sensor to monitor the transcriptional output of the cytokinin signaling network in planta. *Plant Physiol.* 161, 1066–1075. doi: 10.1104/pp.112.211763

Conflict of Interest: The authors declare that the research was conducted in the absence of any commercial or financial relationships that could be construed as a potential conflict of interest.

frontiers in Plant Science

ORIGINAL RESEARCH
published: 08 April 2021
doi: 10.3389/fpls.2021.659061

Auxin Response Factor 2 (ARF2), ARF3, and ARF4 Mediate Both Lateral Root and Nitrogen Fixing Nodule Development in *Medicago truncatula*

*Cristina Kirolinko[1], Karen Hobecker[1†], Jiangqi Wen[2], Kirankumar S. Mysore[2], Andreas Niebel[3], Flavio Antonio Blanco[1] and María Eugenia Zanetti[1]**

[1] Instituto de Biotecnología y Biología Molecular, Departamento de Ciencias Biológicas, Facultad de Ciencias Exactas, Universidad Nacional de La Plata, Centro Científico y Tecnológico-La Plata, Consejo Nacional de Investigaciones Científicas y Técnicas, La Plata, Argentina, [2] Noble Research Institute LLC, Ardmore, OK, United States, [3] Laboratoire des Interactions Plantes-Microorganismes, INRAE, CNRS, Université de Toulouse, Castanet-Tolosan, France

Auxin Response Factors (ARFs) constitute a large family of transcription factors that mediate auxin-regulated developmental programs in plants. *ARF2*, *ARF3*, and *ARF4* are post-transcriptionally regulated by the microRNA390 (miR390)/*trans*-acting small interference RNA 3 (*TAS3*) module through the action of *TAS3*-derived *trans*-acting small interfering RNAs (ta-siRNA). We have previously reported that constitutive activation of the miR390/*TAS3* pathway promotes elongation of lateral roots but impairs nodule organogenesis and infection by rhizobia during the nitrogen-fixing symbiosis established between *Medicago truncatula* and its partner *Sinorhizobium meliloti*. However, the involvement of the targets of the miR390/*TAS3* pathway, i.e., *MtARF2, MtARF3, MtARF4a*, and *MtARF4b*, in root development and establishment of the nitrogen-fixing symbiosis remained unexplored. Here, promoter:reporter fusions showed that expression of both *MtARF3* and *MtARF4a* was associated with lateral root development; however, only the *MtARF4a* promoter was active in developing nodules. In addition, up-regulation of *MtARF2*, *MtARF3*, and *MtARF4a/b* in response to rhizobia depends on Nod Factor perception. We provide evidence that simultaneous knockdown of *MtARF2, MtARF3, MtARF4a*, and *MtARF4b* or mutation in *MtARF4a* impaired nodule formation, and reduced initiation and progression of infection events. Silencing of *MtARF2, MtARF3, MtARF4a*, and *MtARF4b* altered mRNA levels of the early nodulation gene nodulation signaling pathway 2 (*MtNSP2*). In addition, roots with reduced levels of *MtARF2, MtARF3, MtARF4a*, and *MtARF4b,* as well as *arf4a* mutant plants exhibited altered root architecture, causing a reduction in primary and lateral root length, but increasing lateral root density. Taken together, our results suggest that these ARF members are common key players of the morphogenetic programs that control root development and the formation of nitrogen-fixing nodules.

Keywords: auxin response factors, legumes, Nod Factor, miR390, nodulation, root architecture, symbiosis, tasiARFs

OPEN ACCESS

Edited by:
Svetlana Shishkova, National Autonomous University of Mexico, Mexico

Reviewed by:
Henk Franssen, Wageningen University and Research, Netherlands
Anthony Bishopp, University of Nottingham, United Kingdom

****Correspondence:***
María Eugenia Zanetti
ezanetti@biol.unlp.edu.ar

†Present address:
Karen Hobecker, TUM School of Life Sciences Weihenstephan, Technical University of Munich, Munich, Germany

Specialty section:
This article was submitted to Plant Development and EvoDevo, a section of the journal Frontiers in Plant Science

Received: *26 January 2021*
Accepted: *02 March 2021*
Published: *08 April 2021*

Citation:
Kirolinko C, Hobecker K, Wen J, Mysore KS, Niebel A, Blanco FA and Zanetti ME (2021) Auxin Response Factor 2 (ARF2), ARF3, and ARF4 Mediate Both Lateral Root and Nitrogen Fixing Nodule Development in Medicago truncatula. Front. Plant Sci. 12:659061. doi: 10.3389/fpls.2021.659061

INTRODUCTION

Auxins play essential roles in diverse aspects of plant growth and development, including cell elongation, cell polarity, vascular tissue differentiation, embryo patterning, apical dominance, and leaf shape (Salehin et al., 2015). Auxins also control root system architecture by inhibiting primary root growth and promoting the emergence and growth of lateral roots (Overvoorde et al., 2010). In plants belonging to the nitrogen-fixing clade, which includes the orders Fabales, Fagales, Rosales, and Cucurbitales (Doyle, 2011), these phytohormones play major roles regulating the root nodule symbiosis (Kohlen et al., 2018). Lateral roots serve for soil anchoring as well as water and nutrient acquisition, whereas nodules are the result of a symbiotic relationship with nitrogen-fixing bacteria that allow these plants to overcome nitrogen deficiencies in the soil. It has been proposed that the program of nodule organogenesis, which is activated by bacteria-derived signals known as Nodulation (Nod) factors, has co-opted the endogenous developmental program of root and lateral root development during evolution (Bishopp and Bennett, 2019; Soyano et al., 2021). Up-regulation of meristematic markers such as *WUSCHEL-RELATED HOMEOBOX 5* and *PLETHORA* has been observed during nodule formation (Osipova et al., 2012; Franssen et al., 2015). Notably, two recent reports conducted in *Lotus japonicus* and *Medicago truncatula* provided substantial evidence that the program of lateral root formation has been recruited to contribute to nodule formation in legumes (Schiessl et al., 2019; Soyano et al., 2019). Moreover, although both organs differ in the environmental stimuli and function, their developmental programs converged in the generation and interpretation of auxin maximum (Herrbach et al., 2014; Xiao et al., 2014; Schiessl et al., 2019). In addition, it was recently shown that *Nuclear Factor YA* (*NF-YA*) genes are important regulators of auxin signaling during nodule development *via* the direct control of *SHORT INTERNODES/STYLISH* (*STY*) transcription factor genes and their downstream targets, *YUCCA1* and *YUCCA11*, involved in auxin biosynthesis (Shrestha et al., 2020). This implies that auxin biosynthesis, signaling, and responses must be integrated with the nodulation program, which is initiated by the LysM domain receptor kinases MtNFP (Nod Factor Perception, Amor et al., 2003) and MtLYK3 (Smit et al., 2007) in *M. truncatula* and followed by the activation of a number of transcription factors such as the ERF transcription factor MtERN1 (Ethylene response factor Required for Nodulation 1) (Middleton et al., 2007) and the three subunits of the NF-Y heterotrimeric complex (Combier et al., 2006; Laporte et al., 2014; Baudin et al., 2015). Auxins also interact with the ethylene signaling pathway during root nodule symbiosis, since the ethylene-insensitive *sikle* (*skl*) mutant, which forms numerous infection threads (ITs) and nodules under symbiotic conditions (Penmetsa and Cook, 1997), also exhibited altered auxin transport during nodulation (Prayitno et al., 2006).

Auxin signaling and responses are mediated by multiple members of the Auxin Response Factor (ARF) family of transcription factors and the Aux/IAA proteins. ARF proteins, which have been classified as transcriptional activators or repressors based on sequence analysis and transient expression assays, mediate transcriptional regulation by binding the Auxin response elements (AuxRE) in the promoters of auxin-responsive genes (Ulmasov et al., 1999; Tiwari et al., 2003). At low auxin concentrations, ARF activators form heterodimers with Aux/IAA proteins, which repress auxin-responsive genes by recruiting the TOPLESS repressor. At high auxin concentration, Aux/IAA proteins are ubiquitinated by the SCF E3 ubiquitin ligase complex and targeted to degradation *via* the 26S proteasome, releasing ARF repression and promoting ARF-mediated transcriptional activation of auxin-responsive genes (Guilfoyle and Hagen, 2007).

Depending on the species, plant genomes contain a variable number of ARF members, e.g., 23 ARF members in Arabidopsis, 39 members in *Populus trichocarpa,* 25 members in *Oryza sativa*, 22 members in *Zea mays* (Finet et al., 2013), 24 members in *M. truncatula*, and 51 members in *Glycine max* (Shen et al., 2015). A comprehensive phylogenetic analysis of the ARF family in all major living division of land plants—including eudicots, monocots, gymnosperms, and bryophytes—indicated that ARF genes split into three main clades during evolution: clade A, clade B, and clade C (Finet et al., 2013). In Arabidopsis, ARF activators were clustered mainly in clade A (including AtARF5, AtARF6, AtARF7, and AtARF8), whereas most ARF repressors were divided into both clades B (including AtARF1, AtARF2, AtARF3, AtARF4, and AtARF9) and C (including AtARF10, AtARF16, and AtARF17) (Finet et al., 2013). Several members of the ARF family have been implicated in distinct steps of the formation of lateral roots. In Arabidopsis, single mutants in *AtARF7* or *AtARF19* showed a mild reduction in lateral root number, whereas double *arf7/arf19* mutants exhibited a marked reduction in the development of lateral root primordia, suggesting that these two members of the ARF family might display a certain degree of redundancy in lateral root initiation (Okushima et al., 2005; Wilmoth et al., 2005). *AtARF5* was also implicated in the development of lateral roots. Loss-of-function *arf5* mutants displayed a substantial reduction in the number of emerged lateral roots but exhibited clustering of lateral root primordia, leading to the suggestion that lateral root formation is subjected to a bimodular auxin response control: a first module composed by AtARF7/AtARF19 controls lateral root initiation and a second module involving AtARF5 is required for proper organogenesis of lateral roots (De Smet et al., 2010). Genetic evidence revealed that other ARF members could function as negative regulators of lateral root development. For example, Arabidopsis *arf10/arf16* double mutants produced an increased number of lateral roots (Wang et al., 2005). Interestingly, ARF10, ARF16, and ARF17 have also been involved in the development of nitrogen-fixing nodules and the infection by rhizobia in legumes. Overexpression of the microRNA160, which targets *ARF10*, *ARF16*, and *ARF17* transcripts, leads to a reduction in the number of nodules in *G. max* and *M. truncatula* roots (Bustos-Sanmamed et al., 2013; Turner et al., 2013; Nizampatnam et al., 2015). In addition, three *M. truncatula arf16a-Tnt1* insertional mutants exhibited a reduced number of infection events upon inoculation with its symbiotic partner *Sinorhizobium meliloti* (Breakspear et al., 2014).

ARF2, *ARF3*, and *ARF4* are post-transcriptionally regulated by the action of the *trans*-acting small interference RNAs (tasiRNAs)—referred to as tasiARFs—derived from the evolutionarily conserved pathway involving the microRNA390 (miR390) and the *trans*-acting small interference RNA 3 (*TAS3*) transcript (Xia et al., 2017). These members of the ARF family were also implicated in lateral root development in mono- and dicotyledonous species. In Arabidopsis, *arf2*, *arf3*, and *arf4* single mutant plants or plants expressing an artificial microRNA that simultaneously knock down *AtARF2*, *AtARF3*, and *AtARF4* exhibited longer lateral roots and lower lateral root density (Marin et al., 2010; Yoon et al., 2010). Congruently, plants that overproduce tasiARFs—by either activation tagging or overexpression of the *TAS3* gene—also produced longer lateral roots. In *P. trichocarpa*, overexpression of a tasiARF-resistant form of *PtARF4* suppressed lateral root elongation and reduced lateral root density, whereas knockdown of *PtARF4* enhances both lateral root growth and density under normal and salt stress conditions (He et al., 2018). Conversely, Lu et al. (2018) showed that overexpression of *TAS3* in *O. sativa*, which efficiently reduced *OsARF3* mRNA levels, increased the number of lateral roots. These studies indicated that, albeit species-specific differences, the miR390/*TAS3* pathway and its targets *ARF2*, *ARF3*, and *ARF4* play essential roles in the development of lateral roots.

In a previous work, we have shown that the miR390/*TAS3* pathway also mediates the development of nitrogen-fixing nodules (Hobecker et al., 2017). Activation of this pathway by overexpression of miR390b in *M. truncatula* roots led to enhanced lateral root growth, but impaired nodule organogenesis and reduced infection by the nitrogen-fixing bacteria *S. meliloti*. Conversely, inactivation of the miR390/*TAS3* pathway by either expression of a target mimic of miR390 or mutation in the gene encoding ARGONAUTE7—the argonaute protein that binds miR390—increased the density of infection events and the number of nodules and altered their spatial distribution (Hobecker et al., 2017). Thus, the miR390/*TAS3* module functions as a positive modulator of lateral root development and a negative modulator of nodulation in *M. truncatula*. However, whether this pathway operates through their target transcripts *MtARF2, MtARF3*, *MtARF4a*, and *MtARF4b* and the implications of these transcription factors in the development of lateral root organs have not been investigated in legumes. Here, we used *M. truncatula* roots with simultaneous knockdown of *MtARF2, MtARF3*, *MtARF4a*, and *MtARF4b*, as well as an *arf4a Tnt1* insertional mutant, to show that these members of the ARF family contribute to modulation of root architecture and the development of nitrogen-fixing nodules.

MATERIALS AND METHODS

Biological Material

Wild-type (WT) *M. truncatula* Jemalong A17 seeds were obtained from INRA Montpellier, France[1]. *M. truncatula arf4a Tnt-1* insertional mutant seeds were obtained from the Noble Research Institute LLC. *nfp*, *nf-ya1*, *ern1*, and *skl* mutants were previously described (Amor et al., 2003; Middleton et al., 2007; Laporte et al., 2014; and Penmetsa and Cook, 1997, respectively). *S. meliloti* strain 1021 (Meade and Signer, 1977) or the same strain expressing RFP (Tian et al., 2012) were used for root inoculation as in Hobecker et al. (2017). *Agrobacterium rhizogenes* strain Arqua1 was used for hairy root transformations (Quandt et al., 1993).

Constructs for Plant Transformation

The *pMtARF3:GUS-GFP* construct was generated by amplifying the 1,958-bp region upstream of the translational initiation codon of *MtARF3* using the pMtARF3 F and pMtARF3 R primers listed in **Supplementary Table 1**. The resulting DNA fragment was cloned into the pENTR/D-TOPO vector (Thermo Scientific) and then recombined into the Gateway-compatible binary vector pKGWFS7,0 (Karimi et al., 2002) using LR Clonase according to the manufacturer's instructions (Thermo Scientific). The *pMtARF4:GUS-GFP* construct was previously generated by Hobecker et al. (2017). The *ARF2/3/4a/4b* RNAi construct was generated by PCR amplification of an *MtARF3* fragment that contains the binding sites for tasiARFs. PCR was conducted using cDNA from *M. truncatula* roots as template, the *MtARF2/3/4* RNAi F and *MtARF2/3/4* RNAi R primers (**Supplementary Table 1**) and *pfu* DNA polymerase (Promega). The *GUS* RNAi construct was generated by amplification of a β-*glucuronidase* (*GUS*) fragment using the pKGWFS7,0 vector (Karimi et al., 2002) as template and *GUS* RNAi F and *GUS* RNAi R primers listed in **Supplementary Table 1**. The *GUS* RNAi and *ARF2/3/4a/4b* RNAi amplified fragments were cloned into the pENTR/D-TOPO (Thermo Scientific) vector and then recombined into the destination vector pK7GWIWG2D (II) (Karimi et al., 2007) to produce *GUS* RNAi and *ARF2/3/4a/4b* RNAi constructs, respectively, following manufacturer's instructions (Thermo Fisher). The pK7GWIWG2D (II) destination vector contains the *rolD:gfp* gene for the detection and selection of transgenic hairy roots; therefore, only roots with detectable GFP fluorescence (more than 80% of the roots) were taken into account for expression and phenotypic analyses. All constructs were verified by sequencing. Binary vectors were introduced into *A. rhizogenes* Arqua1 (Quandt et al., 1993) by electroporation.

Growth of *Medicago truncatula*, Hairy Root Transformation, Inoculation With Rhizobia and NF Treatment

Seeds were surface sterilized and germinated on 10% (w/v) agar plates at 25°C in the dark for 24 h. Transgenic roots were generated by *A. rhizogenes*-mediated transformation essentially as previously described (Boisson-Dernier et al., 2001) and transferred to Petri dishes containing agar Fahraeus media (Fahraeus, 1957) supplemented with 8 mM KNO_3 and 12.5 μg/ml of kanamycin for 7 days. Seedlings were grown at 25°C in a 16/8-h day/night cycle with radiation of 200 $\mu mol\ m^{-2}\ s^{-1}$ using mixed lighting containing four OSRAM

[1]http://www.montpellier.inra.fr

cool daylight L36W/765 tubes per one OSRAM FLUORA L36W/77 tube. For root architecture analysis, composite plants, consisting of a non-transgenic shoot and transgenic hairy roots, were transferred to slanted boxes containing Fahraeus media supplemented with 8 mM KNO_3 and grown under the conditions described above for 15 days. For inoculation with rhizobia, plants that developed hairy roots were transferred to slanted boxes containing Fahraeus media free of nitrogen covered with sterile filter paper. Germinated seedlings of WT and the *arf4a* mutant were transferred to Petri dishes containing agar Fahraeus media free of nitrogen for rhizobia inoculation or to the same media supplemented with 8 mM KNO_3 and grown for 7 or 15 days for root and shoot developmental phenotypic analysis. For rhizobia inoculation, 7 days after transplantation to slanted boxes, seedlings were inoculated with 10 ml of a 1:1,000 dilution of *S. meliloti* 1021 (Meade and Signer, 1977) or the same strain expressing RFP culture grown in liquid TY media until OD_{600} reached 0.8 or with 10 ml of water as a control (mock treatment). The excess of liquid was removed 1 h after inoculation, and seedlings were incubated vertically under the growth conditions described above. For Nod Factor treatment, WT, *nfp, nf-ya1, ern1*, and *skl* mutants were grown on slanted boxes containing Fahraeus media free of nitrogen for 7 days and then treated with 10 ml of a suspension of 10^{-8} M of NFs purified from *S. meliloti* or with 10 ml of water as a mock-treatment.

Tissue Expression Analysis Using Promoter:Reporter Fusions

Composite plants transformed with the *pMtARF3:GFP-GUS* or *pMtARF4a:GFP-GUS* were transferred to square petri dishes (12 cm × 12 cm) containing slanted agar-Fahraeus medium. GFP fluorescence of roots was visualized with an inverted microscope (Olympus IX51) using UV light with appropriate filters for GFP. For detection of GFP and RFP fluorescence in *S. meliloti* inoculated roots and in nodules, confocal microscopy was performed at 5 and 9 dpi with an *S. meliloti* strain expressing RFP (Tian et al., 2012) using an inverted SP5 confocal microscope (Leica Microsystems). GFP and RFP were excited using 488- and 543-nm lasers, and emissions were collected from 498 to 552 nm and from 578 to 626 nm, respectively. Images were processed with the LAS Image Analysis software (Leica Microsystems).

Phenotypic Analyses

For analysis of root architecture, germinated WT and *arf4a* mutant seedings, as well as composite *GUS* RNAi and *ARF2/3/4a/4b* RNAi plants generated by *A. rhizogenes*-mediated transformation, were transferred to slanted boxes containing agar-Fahraeus medium supplemented with 8 mM KNO_3. The number of lateral roots per centimeter of primary root and the length of primary and lateral roots were determined at 7 and 15 days after germination (dag) for WT and *arf4a* mutant plants. The length of aerial part and the number of true leaves of WT and *arf4a* mutants were also determined at 7 and 15 dag. For *GUS* RNAi and *ARF2/3/4a/4b RNAi* composite plants, each root that emerged directly from the sectioned site of the non-transgenic root inoculated with *A. rhizogenes* was considered an independent transgenic primary root in the hairy root system. Only first-order lateral roots that emerged from each independent transgenic primary root were considered to estimate lateral root length and density. The number of lateral roots per centimeter of transgenic primary root and the length of transgenic primary and lateral roots were determined at 15 days after transplantation. For the determination of shoot dry weight, the aerial part of composite plants was dried at 80°C for 24 h and weighed using an analytical balance. Three independent biological replicates were performed. For nodulation analysis, WT, *arf4a* mutants, or composite plants transformed with the *GUS* RNAi or *ARF2/3/4a/4b* RNAi construct were transferred to slanted boxes containing nitrogen-free Fahraeus medium and inoculated with *S. meliloti* 1021 7 days after transplantation. The number of nodules was recorded at different time points after inoculation with *S. meliloti* as previously described (Hobecker et al., 2017). Nodules were classified as pink (nitrogen-fixing mature nodules) or white (immature nodules) according to Traubenik et al. (2020). Only roots containing nodules were considered for the quantification and classification of pink and white nodules. Shoot dry weight and shoot length were determined at 21 dpi with *S. meliloti*. Three independent biological replicates were performed. For analysis of infection events, *GUS* and *ARF2/3/4a/4b* RNAi plants of 14 days after transformation or WT and *arf4a* plants of 14 dag were transferred to petri dishes containing agar-Fahraeus medium free of nitrogen. Seven days after transplantation, roots were inoculated with the *S. meliloti* strain expressing RFP (Tian et al., 2012) and grown as described above. Infection events were visualized, quantified, and classified at 7 dpi in an Olympus IX51 inverted microscope. Infection events were classified as microcolonies, ITs that end in the root hair, ITs that reached the base of the epidermal root hair, or ITs that reached and ramified in the cortical cells. Three independent biological replicates were performed. In all cases, statistical significance of the differences for each parameter was determined by unpaired two-tailed Student's *t* tests for each construct or for the WT vs. the *arf4a* mutant line.

RNA Extraction, RT-PCR, and RT-qPCR

Total RNA extraction was performed with Trizol according to the manufacturer's instructions (Thermo Fisher). RNA concentration was determined by measuring OD_{260} using a Nanodrop ND-1000 (Nanodrop Technologies) and RNA integrity was evaluated by electrophoresis 1.2% (w/v) agarose gels stained with ethidium bromide. Total RNA was treated with DNase I according to the manufacturer's instructions (Promega) and subjected to first-strand cDNA synthesis using M-MLV reverse transcriptase (Promega). Expression analysis was performed by RT-qPCR using the iQ SBR Green Supermix kit (BioRad) and the CFX96 qPCR system (BioRad) as previously described (Blanco et al., 2009). For each pair of primers, the presence of a unique product of the expected size was verified on 1.2% (w/v) agarose gels stained with ethidium bromide. In all cases, negative controls without template or without RT were included. Expression values were normalized to *MtHIS3L*, which has been validated by GNORM software (Vandesompele et al., 2002), as reported previously by Ariel et al. (2010) and

Reynoso et al. (2013). Primers used for RT-qPCR are listed in **Supplementary Table 1**. For detection of *MtARF4a* mRNAs by semiquantitative RT-PCR on WT and the *arf4a* mutant roots, a pair of primers specific for *MtARF4a* (MtARF4a F and MtARF4a R) were used, which are listed in **Supplementary Table 1**.

Sequence Alignment and Phylogenetic Analysis

All members of the Arabidopsis ARF family were retrieved from the TAIR database[2]. *M. truncatula* ARF members were retrieved from the recently released version of the *M. truncatula* genome MtrunA17r5.0-ANR[3] (Pecrix et al., 2018). Amino acid and nucleotide alignments were generated with the Clustal Omega algorithm available at EMBL-EBI[4] and decorated with BOXSHADE[5]. The phylogenetic tree was generated with MEGA X (Kumar et al., 2018) using the Neighbor-Joining method (Saitou and Nei, 1987). The percentage of replicate trees in which the associated taxa clustered together in the bootstrap test (10,000 replicates) was computed as described by Felsenstein (1985). The evolutionary distances were computed using the p-distance method (Nei and Kumar, 2000).

Accession Numbers

Sequence data from this article can be found at the *M. truncatula* genome Mt4.0v1 or MtrunA17r5.0-ANR databases under the following accession numbers, respectively: *MtARF2* (Medtr8g100050 or MtrunA17_Chr8g0385791), *MtARF3* (Medtr2g014770 or MtrunA17_Chr2g0282961), *MtARF4a* (Medtr4g060460 or MtrunA17_Chr4g0029671), *MtARF4b* (Medtr2g093740 or MtrunA17_Chr2g0326281), *MtARF16a* (Medtr1g094960 or MtrunA17_Chr1g0199681), *MtARF19a* (Medtr2g018690 or MtrunA17_Chr2g0301251), *MtNSP1* (Medtr8g020840 or MtrunA17_Chr8g0344101), *MtNSP2* (Medtr3g072710 or MtrunA17_Chr3g0114841), *MtNIN* (Medtr5g099060 or MtrunA17_Chr5g0448621), *MtERN1* (Medtr7g085810 or MtrunA17_Chr7g0253424), *MtNF-YA1* (MtrunA17_Chr1g0148951), *MtENOD40* (MtrunA17_Chr8g0368441), *MtNFP* (MtrunA17_Chr5g0403371), and *MtSKL* (MtrunA17_Chr5g0427621).

RESULTS

MtARF3 and *MtARF4a* Are Expressed During Lateral Root Development, but Only *ARF4a* Is Transcribed During the Root Nodule Symbiosis

Considering that expression of the *MIR390* promoter was associated with the development of lateral roots and nodules, we aimed to characterize the spatial and temporal expression pattern of the targets of the miR390/*TAS3* pathway during the development of both types of lateral organs. Previous phylogenetic analysis of the ARF family using ESTs or the Mt3.5 version of the *M. truncatula* genome identified single genes as putative orthologs of Arabidopsis *AtARF2* and *AtARF3*, referred to as *MtARF2* and *MtARF3*, respectively, and two genes evolutionarily closer to Arabidopsis *AtARF4*, designated as *MtARF4a* and *MtARF4b* (Zhou et al., 2013; Shen et al., 2015). Proteins encoded by *MtARF4a* and *MtARF4b* exhibited 75% of identity to each other (**Supplementary Figure 1**). Here, we generated a phylogenetic tree that includes all members of the Arabidopsis ARF family, and MtARF2, MtARF3, MtARF4a, and MtARF4b. In addition, the tree includes *M. truncatula* ARF members that have been involved in root development and nodulation in this legume, i.e., MtARF10, MtARF16, and MtARF17 (Bustos-Sanmamed et al., 2013; Breakspear et al., 2014), as well as best *M. truncatula* homologs of ARF members implicated in these processes in other plant species, such as AtARF5, AtARF7, and AtARF19 in lateral root development (Okushima et al., 2005; Wilmoth et al., 2005; De Smet et al., 2010) and GmARF6 and GmARF8 in nodulation (Wang et al., 2015). The amino acid sequences of *M. truncatula* ARF members were retrieved from the recently released version of the *M. truncatula* genome MtrunA17r5.0-ANR (Pecrix et al., 2018). This phylogenetic analysis verified that MtARF2, MtARF3, MtARF4a, and MtARF4b clustered in the same clades as their Arabidopsis counterparts (**Supplementary Figure 2**). Inspection of public RNA-sequencing data reported by Schiessl et al. (2019) indicated that *MtARF4a* increased at 5 days after spot-inoculation with droplets of a *S. meliloti* suspension, whereas *MtARF4b* decreased at all time points after inoculation (**Supplementary Figure 3**). On the other hand, *MtARF3* transcript levels significantly increased in fully emerged lateral roots (72 h after induction of lateral root formation) but decreased at 7 days after spot-inoculation with rhizobia, whereas *ARF2* levels did not increase neither during lateral root development nor after spot-inoculation with rhizobia (**Supplementary Figure 3**). To better characterize the spatial expression pattern of *ARF* genes during lateral root and nodule formation promoter:*GUS-GFP* transcriptional fusions were generated for *MtARF3* and *MtARF4a* (*pMtARF3:GFP-GUS* and *pMtARF4:GFP-GUS*, respectively). Despite several attempts using different combinations of primers based on either the *M. truncatula* genome v4.0 or v5.0, we were unable to amplify a promoter region of *ARF2*. Introduction of *pMtARF3:GFP-GUS* and *pMtARF4a:GFP-GUS* constructs into *M. truncatula* hairy roots revealed that both promoters were active in the vascular tissue of the primary roots, as well as in the vasculature and the meristematic region of lateral roots. *pMtARF3* and *pMtARF4a* expression was also detected in lateral root primordia prior to emergence and in emerged lateral roots (**Figure 1**). To evaluate the expression of *pARF3* and *pARF4* during symbiosis, hairy roots harboring *pMtARF3:GFP-GUS* or *pMtARF4a:GFP-GUS* were inoculated with a *S. meliloti* strain that expresses the red fluorescent protein (RFP) (Tian et al., 2012). This strain allows visualizing the root hairs that contain an IT, i.e., the tubular structure that allows the bacteria to cross the epidermis and reach the dividing cells of the nodule primordia, as well as infected

[2]https://www.arabidopsis.org/

[3]https://medicago.toulouse.inra.fr/MtrunA17r5.0-ANR/

[4]https://www.ebi.ac.uk/Tools/msa/clustalo/

[5]http://sourceforge.net/projects/boxshade/

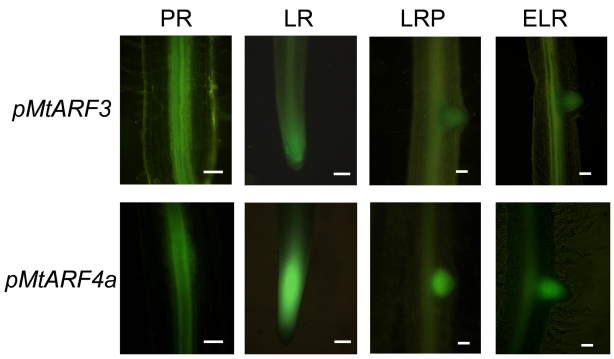

FIGURE 1 | Promoter:reporter fusion expression analysis of *MtARF3* and *MtARF4a* in primary and lateral roots. Expression of the *GFP* reporter gene in roots transformed with the *pMtARF3:GUS-GFP* (upper panels) or the p*MtARF4a:GUS-GFP* (bottom panels) construct was detected in the vasculature of the primary root (PR) and lateral root (LR), in lateral root primordia (LRP) prior to emergence and in emerged lateral roots (ELR). Bars = 50 μm.

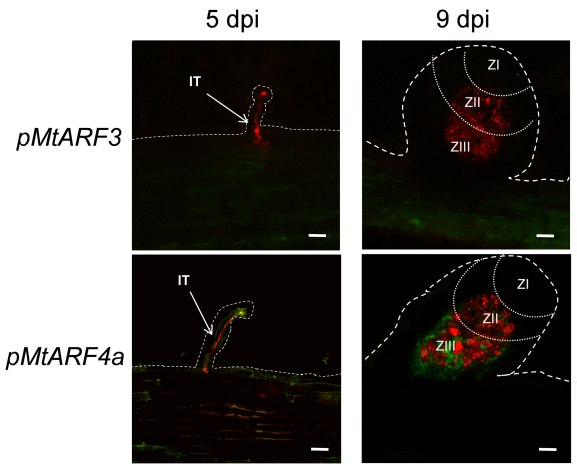

FIGURE 2 | Promoter:reporter fusion expression analysis of *MtARF3* and *MtARF4a* at different stages of the symbiotic interaction with *S. meliloti.* GFP fluorescence was analyzed in roots transformed with the *pMtARF3:GUS-GFP* (upper panels) or the *pMtARF4a:GUS-GFP* (bottom panels) construct at 5 days post-inoculation (dpi) and in developing nodules at 9 dpi with a strain of *S. meliloti* that expressed the red fluorescent protein (RFP). Dashed lines mark the epidermal cells of roots and nodules. Dotted lines separate different nodule zones. ZI, meristematic zone; ZII, infection zone; ZIII, fixation zone; IT, infection thread. Bars = 50 μm.

cells of the nodule. Upon rhizobia inoculation, GFP fluorescence was not detected in the infected root hair or in the adjacent epidermal cells at 5 dpi, or in the infected or non-infected cells of developing nodules of 9 dpi when roots were transformed with the *pMtARF3:GFP-GUS* construct (**Figure 2**). On the other hand, expression of GFP driven by *pMtARF4a* promoter was found in the root hair containing elongating ITs and in the epidermal cells surrounding the infected root hair at 5 dpi, as well as in the non-infected cells that surround infected cells of nodules of 9 dpi (**Figure 2**), in agreement with previous results (Hobecker et al., 2017). Thus, the promoter reporter analysis presented here revealed that the activity of both *pMtARF3* and *pMtARF4a* is associated with lateral root development. However, only *pMtARF4a* seems to be responsive to rhizobial infection and active in developing nodules, consistently with the mRNA expression pattern described in spot-inoculation experiments (Schiessl et al., 2019).

Up-Regulation of *MtARF2*, *MtARF3*, and *MtARF4a/b* mRNAs Depends on the Nod Factor Signaling Pathway

Previously, we have shown that mRNA levels of *MtARF2*, *MtARF4a/b*, and, to a lesser extent, *MtARF3* increased in *M. truncatula* roots upon inoculation with *S. meliloti* (Reynoso et al., 2013; Hobecker et al., 2017). Here, we investigated whether the Nod Factors (NFs) and their signaling pathway were responsible for up-regulation of this set of ARFs during symbiosis. Roots of WT plants were treated with purified NFs from *S. meliloti* for 48 h. Reverse transcription quantitative PCR (RT-qPCR) analysis revealed that these ARFs were extensively up-regulated by NFs; *MtARF2* and *MtARF4a/b* mRNA levels increased by more than 25-fold in NF-treated roots as compared to mock-inoculated WT roots, whereas the increase was 12-fold for *MtARF3* transcripts (**Figure 3**). Interestingly, mRNA levels of none of these *ARFs* were significantly up-regulated upon NF treatment in the *nfp* mutant, a loss-of-function mutant in the *MtNFP* gene involved in NF reception (Amor et al., 2003), albeit levels of *MtARF2* and *MtARF3* were slightly higher in this mutant than in WT under mock inoculation conditions. In addition, up-regulation of *MtARF2* and *MtARF3* or *MtARF4a/b* in response to NFs was partially or completely impaired, respectively, in mutants of the transcription factor *MtNF-YA1*. Up-regulation of *MtARF2* and *MtARF3* mRNA levels was not impaired in *ern-1* and *skl* mutants (**Figures 3A,B**). Moreover, *MtARF2* mRNA levels increased to a higher extent in *skl* mutants as compared to WT plants, which might be consistent with the enhanced auxin transport observed in *skl* (Prayitno et al., 2006). On the other hand, up-regulation of *MtARF4a/b* in response to NFs was partially impaired in *ern1* and unaffected in *skl* mutants (**Figure 3C**). Altogether, these results suggest that induction of these ARFs, notably of *MtARF4a/b*, depends on NF perception and requires the function of the MtNF-YA1 transcription factor.

Knockdown of *MtARF2, MtARF3, MtARF4a*, and *MtARF4b* and Mutation of *MtARF4a* Reduce Nodulation and Infection by Rhizobia

To elucidate whether these three ARF members play a role in the control of nodule formation and/or rhizobial infection in *M. truncatula*, we applied an RNA interference (RNAi) strategy to simultaneously knock down *MtARF2, MtARF3, MtARF4a,* and *MtARF4b*. The fragment used for RNAi was designed in an mRNA region highly conserved across *MtARF2, MtARF3, MtARF4a*, and *MtARF4b* that includes the tasiARFs target sites (**Supplementary Figure 4**). Introduction of the *ARF2/3/4a/4b*

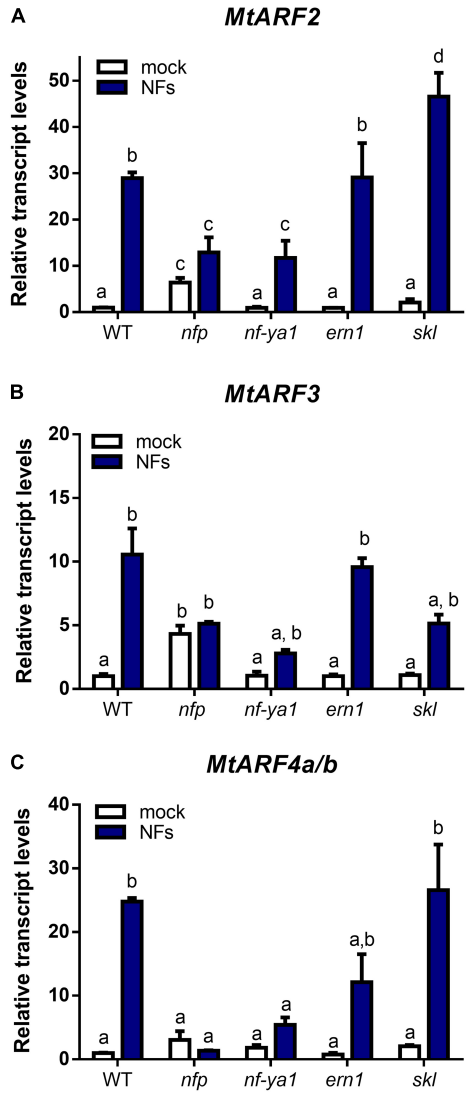

FIGURE 3 | *MtARF2*, *MtARF3*, and *MtARF4a/b* are up-regulated by Nod Factors and depends on *MtNFP* and *MtNF-YA1* genes. Transcript levels of *MtARF2* **(A)**, *MtARF3* **(B)**, and *MtARF4a/b* **(C)** were analyzed in root tissue of WT and *nfp, nf-ya1*, *ern1*, and *skl* mutant plants treated with 10^{-8} M purified Nod Factors (NFs, blue bars) or water (mock, white bars) for 48 h. Expression levels were determined by RT-qPCR and normalized to the levels of the *MtHIS3L* transcript. Values are expressed relative to the WT mock-treated sample, which was set at 1. Different letters above the bars indicate statistically significant differences between samples in an unpaired two-tailed Student's *t* test with a p value ≤ 0.05.

RNAi construct in *M. truncatula* hairy roots reduced by 80, 70, and more than 90% *MtARF2*, *MtARF3*, and *MtARF4a/b* mRNA levels, respectively, relative to the levels of *GUS* RNAi roots used as the control (**Figure 4A**). However, this RNAi construct did not decrease levels of *MtARF16a* or *MtARF19a* (**Supplementary Figure 5**), evidencing the specificity of the RNAi approach. Reductions of *MtARF2, MtARF3, MtARF4a*, and *MtARF4b* transcript levels significantly impacted nodulation, reducing the number of nodulated plants, as well as the number of nodules formed over the time in hairy roots (**Table 1** and **Figure 4B**). These differences were observed as early as 7 dpi, with a 70% reduction in the number of nodules formed in *ARF2/3/4a/4b* RNAi as compared with *GUS* RNAi plants, but continued over the time course of the experiment, with nearly a 50% reduction in the number of nodules at 21 dpi. However, the percentage of nodules that acquired the characteristic pink color caused by expression of leghemoglobin upon the onset of nitrogen fixation was not affected by knockdown of *MtARF2, MtARF3, MtARF4a*, and *MtARF4b* (**Figure 4C**). These results suggest that silencing of these *ARFs* negatively affects nodule formation, but once formed, these nodules develop the nitrogen fixation zone characteristic of indeterminate nodules. To evaluate whether infection by rhizobia was affected by knockdown of *MtARF2, MtARF3, MtARF4a*, and *MtARF4b*, the number of infection events and their progression were evaluated in hairy roots inoculated with the RFP-expressing *S. meliloti* strain. Knockdown of *MtARF2, MtARF3*, and *MtARF4a/b* caused a significant reduction in the total density of infection events, i.e., the number of infection events per centimeter of root (**Figure 4D**). A more notable effect was observed in the progression of the infection events, with 58% of the infection events remaining at the microcolony stage and only 10% of the ITs reaching the dividing cortical cells in *ARF2/3/4a/4b* RNAi roots, whereas over 50% of the infection events reached the base of the epidermal cells or reached the cortex in *GUS* RNAi roots (**Figure 4E**). Thus, these results indicate that simultaneous silencing of *MtARF2, MtARF3, MtARF4a*, and *MtARF4b* interferes not only with the initiation of infection events but also with their progression to the dividing cortical cell beneath the infection site. In addition, *ARF2/3/4a/4b* RNAi composite plants grown in the absence of nitrogen exhibited reduced shoot length and shoot dry weight as compared to *GUS* RNAi at 21 dpi with *S. meliloti* (**Figures 4F,G**, respectively), presumably because of poor nodulation and impaired infection that compromises nitrogen fixation.

Since the *MtARF4a* promoter was active during bacterial infection and nodule formation and up-regulation of *ARF4a/b* was completely impaired in *nfp* and *nf-ya1* mutants, we analyzed the symbiotic phenotype caused by a mutation in the *MtARF4a* gene. A mutant carrying the *Tnt1* insertion within the first exon of the *MtARF4a* gene (*arf4a*) was obtained by screening the collection available at Noble Research Institute LLC (Tadege et al., 2008; Cheng et al., 2014). Semiquantitative RT-PCR analysis revealed that levels of *MtARF4a* mRNAs were undetectable in *arf4a* mutants, whereas WT plants accumulated noticeable levels of *MtARF4a* transcripts (**Figure 5A**). Upon inoculation with rhizobia, the *arf4a* mutant developed a significantly lower number of nodules as compared with WT plants (**Figure 5B**). In agreement with what was observed in *ARF2/3/4a/4b* RNAi roots, roots of *arf4a* mutants exhibited a significant reduction in the density of the infection events (**Figure 5C**) as well as in their progression. In the *arf4a* mutants, 45% of the infection events remained at the microcolony stage and only 20% reached the root cortex, whereas in WT roots, nearly 55% of the infection events reached the cortical cells (**Figure 5D**). Reduced nodule formation and bacterial infection also impacted the development of the aerial part of the *arf4a* plants grown in the absence

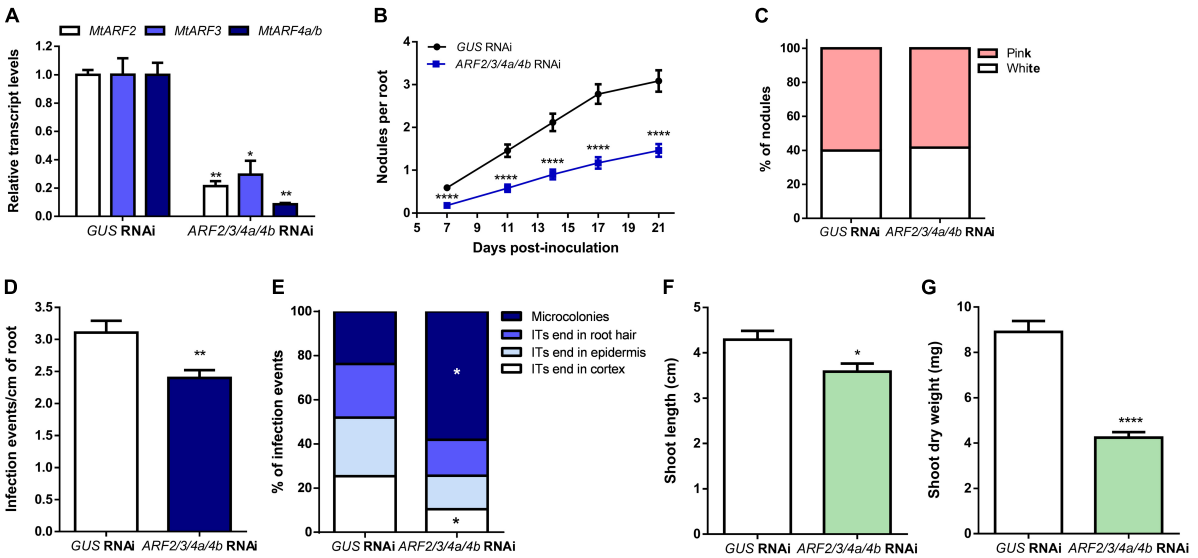

FIGURE 4 | Simultaneous knockdown of *MtARF2, MtARF3, MtARF4a*, and *MtARF4b* impaired nodule formation and infection by rhizobia. **(A)** Expression levels of *MtARF2*, *MtARF3*, and *MtARF4a/b* transcripts in *GUS* RNAi and *ARF2/3/4a/4b* RNAi roots. Expression values were determined by RT-qPCR, normalized to *MtHIS3L*, and expressed relative to the *GUS* RNAi sample, which was set at 1. Each bar represents the mean ± SE of three biological replicates (whole root tissue from at least three composite plants were collected in each biological replicate) with three technical replicates each. Asterisks indicate statistically significant differences between *GUS* and *ARF2/3/4a/4b* RNAi roots in an unpaired two-tailed Student's *t* test (*$p \leq 0.05$, **$p \leq 0.01$). **(B)** Time-course nodule formation in *GUS* and *ARF2/3/4a/4b* RNAi roots upon inoculation with *S. meliloti*. Error bars represent mean ± SE of three independent biological replicates, each with at least 50 roots. Four asterisks indicate statistically significant differences between *GUS* and *ARF2/3/4a/4b* RNAi roots in an unpaired two-tailed Student's *t* test with a *p* value ≤ 0.0001. **(C)** Percentage of pink and white nodules developed in *GUS* RNAi and *ARF2/3/4a/4b* RNAi roots at 21 dpi. Bars represent the mean ± SE of three independent biological replicates. More than 68 nodules from more than 15 independent plants per construct were quantified in each biological replicate. **(D)** Density of infection events in *GUS* and *ARF2/3/4a/4b* RNAi roots at 7dpi with a *S. meliloti* strain expressing the RFP protein. Each bar represents the mean ± SE of three biological replicates, each with more than 25 transgenic roots. The asterisks indicate statistically significant differences between *GUS* and *ARF2/3/4a/4b* RNAi roots in an unpaired two-tailed Student's *t* test with a *p* value ≤ 0.01. **(E)** Progression of infection events in *GUS* and *ARF2/3/4a/4b* RNAi roots. Infection events were classified as microcolonies, infection threads (ITs) that end in the root hair, in the epidermal cell layer, or reach the cortex at 7 dpi. Each category is presented as the percentage of total infection events. Data are representative of three independent biological replicates, each with more than 25 transgenic roots. The asterisk indicates that the percentage of microcolonies and ITs that end in cortex was significant different between *GUS* and *ARF2/3/4a/4b* RNAi roots in an unpaired two-tailed Student's *t* test with a *p* value ≤ 0.05. **(F,G)** Shoot length **(F)** and shoot dry weight **(G)** measured in *GUS* and *ARF2/3/4a/4b* RNAi composite plants grown on free-nitrogen slanted agar-Fahraeus at 21 dpi with *S. meliloti*. Error bars represent the mean ± SE of three biological replicates, each performed with more than 10 composite plants. Asterisks denote a statistically significant difference between *GUS* and *ARF2/3/4a/4b* RNAi composite plants in an unpaired two-tailed Student's *t* test (*$p \leq 0.05$, ****$p \leq 0.0001$).

of nitrogen, which exhibited reduced shoot length and dry weight as compared with WT plants under symbiotic conditions (**Figures 5E,F**).

Knockdown of *MtARF2, MtARF3, MtARF4a*, and *MtARF4b* Impairs Expression of Nodulation Signaling Pathway 2

Since silencing of *MtARF2, MtARF3, MtARF4a*, and *MtARF4b* or mutations in *MtARF4a* affected nodule formation and bacterial infection, we tested whether the expression of key genes of the nodulation signaling pathway is affected in plants with reduced levels of *MtARF2*, *MtARF3*, and *MtARF4a/b* transcripts (**Figure 6**). Transcript levels of the A and C subunits of the heterotrimeric transcription factor NF-Y accumulated to significantly higher levels in response to *S. meliloti* (>60- and >100-fold induction for *MtNF-YA1* and *MtNF-YC1*, respectively) with no significant differences between *ARF2/3/4a/4b* RNAi and *GUS* RNAi roots. A similar scenario was found for transcripts of *MtERN1*, which accumulated more than 10-fold upon inoculation with *S. meliloti* as compared to mock in both *ARF2/3/4a/4b* RNAi and *GUS* RNAi roots. However, mRNA levels of the GRAS transcription factor nodulation signaling pathway 2 (MtNSP2) accumulated to a significantly lower extent in *ARF2/3/4a/4b* RNAi roots than in *GUS* RNAi roots after inoculation with *S. meliloti*, indicating that MtARF2, MtARF3, MtARF4a, and/or MtARF4b transcription factors might be required for full activation of *MtNSP2*, in agreement with that previously reported by Hobecker et al. (2017).

Knockdown of *MtARF2, MtARF3, MtARF4a*, and *MtARF4b* and Mutations in *MtARF4a* Alter Root Architecture

Recent studies have evidenced that genes required for lateral root development were co-opted for the nodulation program in legume plants, including those involved in auxin biosynthesis, signaling, and responses (Schiessl et al., 2019; Soyano et al., 2019). Thus, we investigated whether *MtARF2*, *MtARF3*, and

TABLE 1 | Number and percentage of plants with nodules.

Days post-inoculation	*GUS* RNAi	*ARF2/3/4a/4b* RNAi
7	44/108 (40.8%)	21/134 (15.7%)
11	80/108 (74.1%)	45/134 (33.6%)
14	85/108 (78.7%)	56/134 (41.8%)
17	88/108 (81.5%)	74/134 (55.2%)
21	96/108 (88.9%)	84/134 (62.7%)

MtARF4a/b members play a role in the control of root development in *M. truncatula* by analyzing the architecture of roots with reduced levels of *MtARF2*, *MtARF3*, and *MtARF4a/b* transcripts. Root architecture of *ARF2/3/4a/4b* RNAi roots was severely affected when plants were grown for 15 days under nitrogen availability. *ARF2/3/4a/4b* RNAi caused a significant reduction in the length of primary and lateral root but enhanced by more than twofold the lateral root density—i.e., the number of lateral roots per primary root centimeter—as compared with control *GUS* RNAi roots (**Figures 7A–D**). In addition, the dry weight of the shoot was reduced in these plants, most likely because of the limited growth of primary and lateral roots (**Figure 7E**). In accordance, *arf4a* mutants also exhibited a pronounced and significant reduction in primary and lateral root length as well as a significant increase in lateral root density as compared with WT plants at 7 and 15 dag when grown in the presence of nitrogen (**Figures 8A–C** and **Supplementary Figures 6A–C**, respectively). This indicates that *MtARF4a* might act as a modulator that promotes the elongation of primary and lateral roots but limits the formation of new lateral root in *M. truncatula*. On the other hand, *arf4a* mutant plants exhibited a pleiotropic phenotype in the aerial part (**Figure 8D**), with a significant reduction in shoot length (**Figure 8E** and **Supplementary Figure 6D**) and the number of true leaves (**Figure 8F** and **Supplementary Figure 6E**). Moreover, in plants of 15 dag, the shape and organ separation of the trifoliate leaves was also affected in *arf4a* mutants, with leaflets closer to each other as compared with WT plants (**Supplementary Figure 6F**). These results indicate that mutation in *MtARF4a* not only altered the root architecture, but also the shoot development in *M. truncatula*. Altered compound leaf patterning was previously observed in *M. truncatula ago7* mutants, which exhibited reduced levels of *MtARF2, MtARF3*, and *MtARF4a/b* (Zhou et al., 2013), as well as in plants that overexpresses *MtARF3* (Peng et al., 2017). Based on the results presented here, *MtARF4a* might have a direct role in shoot development, or alternatively, the shoot developmental defects observed in *arf4a* mutant plants might be the consequence of the altered growth of primary and lateral roots.

DISCUSSION

ARF-Mediated Control of Nodule Organogenesis and Root Architecture

Auxin biosynthesis, signaling, and response are crucial for the developmental programs that control root architecture and the formation of symbiotic nodules (Overvoorde et al., 2010; Lin et al., 2020). Different lines of evidence revealed that there are extensive overlaps in the signaling components and developmental processes that lead to the formation of both types of organs, including those activated by auxin; however, there are also remarkable differences (reviewed by Kohlen et al., 2018). Different ARF members modulate root architecture in legume and non-legume species, some of which promote root development, while others exert inhibitory effects in root development. Here, we found that *M. truncatula* roots with reduced levels of *MtARF2, MtARF3, MtARF4a*, and *MtARF4b* or an *arf4a* single mutant exhibited shorter primary and lateral roots but enhanced lateral root density (**Figures 7**, **8**), suggesting that these ARFs might function in promoting primary and lateral root growth and inhibiting the inception of lateral roots. We have previously shown that reduction of *MtARF2, MtARF3, MtARF4a*, and *MtARF4b* levels produced by overexpression of miR390 promotes elongation of lateral roots without affecting primary root length or lateral root density (Hobecker et al., 2017). This suggests either that miR390 mediates lateral root growth by acting through a pathway that is independent of *MtARF2, MtARF3, MtARF4a*, and *MtARF4b* or that the drastic reduction in the three *ARF* transcript levels caused by RNAi (70–90% depending on the *ARF* mRNA) or null levels of *MtARF4a* results in a distinct and more severe root phenotype than activation of the miR390/*TAS3* pathway by overexpression of miR390, which reduced *ARF* mRNA levels by only 50–80%. The phenotype observed here in *M. truncatula* contrasts with that previously described by Marin et al. (2010) in Arabidopsis, where the authors showed that plants expressing an artificial miRNA that simultaneously knock down the three ARFs (aMIR-ARFs) exhibited longer lateral roots. In addition, individual *arf2*, *arf3*, and *arf4* Arabidopsis mutants showed a mild enhancement in primary and lateral root length as compared to WT plants, whereas *arf3* and *arf4* mutants had reduced lateral root density (Marin et al., 2010). On the other hand, expression of an RNAi that targets *PtARF4* in *P. trichocarpa* increased both lateral root length and density under normal or salt stress conditions (He et al., 2018), whereas overexpression of *OsTAS3* in *O. sativa*, which results in a reduction in ARF levels, yielded denser lateral roots (Lu et al., 2018). Thus, it seems that distinct plant species respond with different alteration of root architecture to the reduction or loss of *ARF2, ARF3*, and/or *ARF4*. These species-specific determination mechanisms have been previously observed in leaf development, where alteration in the production of tasiARFs results in highly variable phenotypic response depending on the species such as wiry leaves in tomato (Yifhar et al., 2012), cylindrical leaves in *O. sativa* (Douglas et al., 2010), reduced number of leaflets in *L. japonicus* (Yan et al., 2010), and lobed leaf margin and widely spaced lateral shoot organs in *M. truncatula* (Zhou et al., 2013). Species-specific phenotypic variation in root architecture has also been observed in response to the lack or reduction of *ARF10/16/17* levels. In Arabidopsis, an *arf10/arf16* double mutant or a miR160-overexpressing line exhibited more lateral roots and reduced primary root growth (Mallory et al., 2005; Wang et al., 2005), whereas reduction of *MtARF10/16/17* levels by

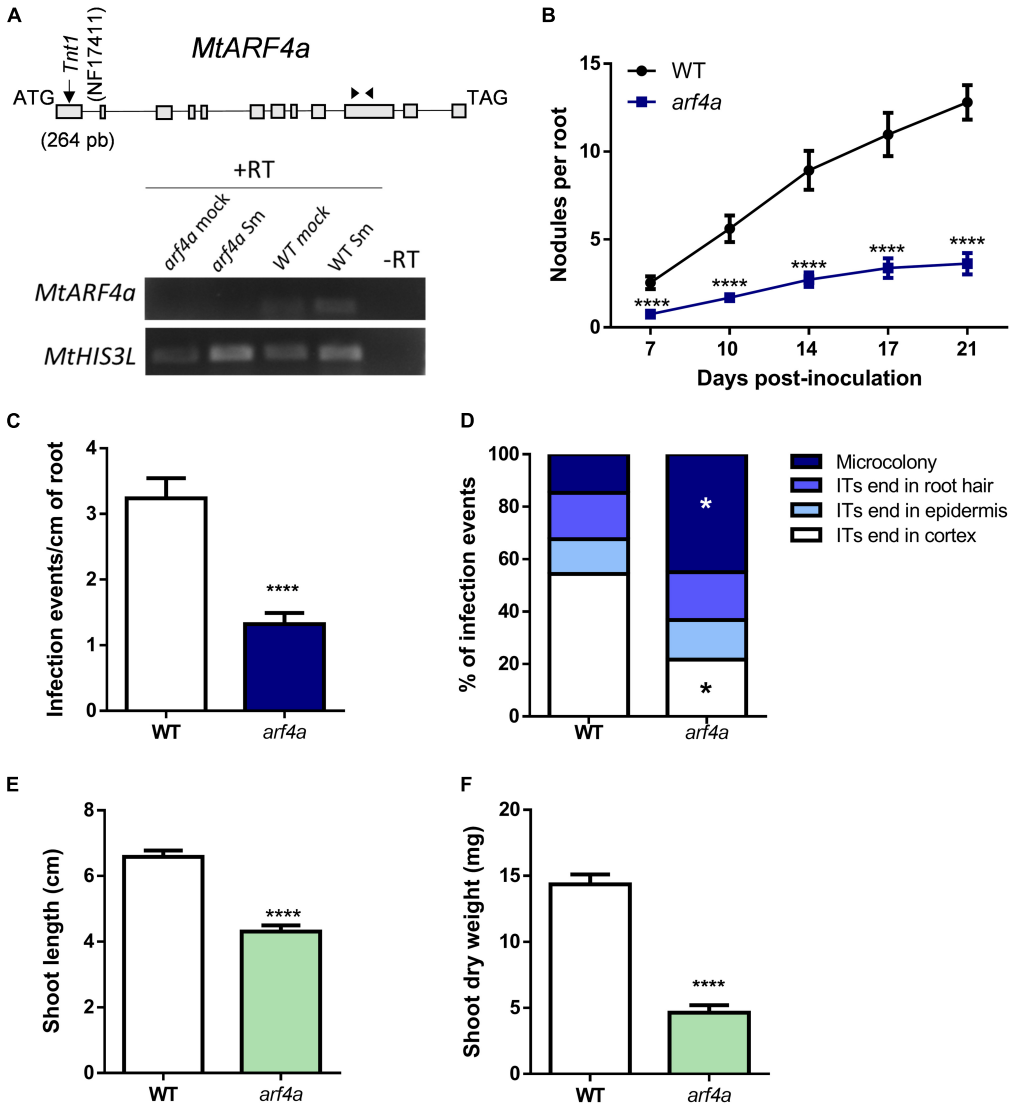

FIGURE 5 | A *Tnt1* insertional mutant in *MtARFa* gene (*arf4a*) exhibited reduced nodulation and infection by rhizobia. **(A)** Schematic representation of *MtARF4a* gene model and the insertion of the *Tnt1* transposon (upper panel). The gene model is composed of 12 exons (gray blocks) and 11 introns (lines). The position of the *Tnt1* insertion within the first exon in the NF17411 mutant line is indicated in base pairs (bp) with a black arrow. Black arrowheads indicate the position of MtARF4a F and MtARF4a R primers specific for *ARF4a* (listed in **Supplementary Table 1**) used for RT-PCR analysis. Expression levels of *MtARF4a* and *MtHIS3L* were determined by semiquantitative RT-PCR using 35 and 25 cycles, respectively, on WT and NF17411 (*arf4a*) roots at 48 hpi with *S. meliloti* (Sm) or water (mock) (lower panel). **(B)** Time-course nodule formation in roots of WT and *arf4a* plants upon inoculation with *S. meliloti*. Error bars represent the mean ± SE of three biological replicates, each performed with at least ten plants. Four asterisks indicate statistically significant differences between WT and *arf4a* mutant roots in an unpaired two-tailed Student's *t* test with a *p* value ≤ 0.0001. **(C)** Density of infection events developed at 7 dpi in WT and *arf4a* mutant roots. Error bars represent the mean ± SE of three biological replicates each performed with at least 10 plants. Four asterisks indicate statistically significant differences between WT and *arf4a* mutant roots in an unpaired two-tailed Student's *t* test with a *p* value ≤ 0.0001. **(D)** Progression of infection events in WT and *arf4a* mutant roots. Infection events were classified as microcolonies or ITs that end in the root hair, in the epidermal cell layer, or reach the cortex at 7 dpi. Each category is presented as the percentage of total infection events. Results are representative of three biological replicates, each with more than 10 plants. The asterisk indicates that the percentage of microcolonies and ITs that end in cortex was significantly different in an unpaired two-tailed Student's *t* test between WT and *arf4a* roots with $p \leq 0.05$. **(E,F)** Shoot length **(E)** and shoot dry weight **(F)** measured in WT and *arf4a* mutant plants grown on free-nitrogen slanted agar-Fahraeus at 21 dpi with *S. meliloti*. Error bars represent the mean ± SE of three biological replicates, each performed with more than 10 plants. Four asterisks denote a statistically significant difference between WT and *arf4a* plants in an unpaired two-tailed Student's *t* test with a *p* value ≤ 0.0001.

overexpression of miR160 in *M. truncatula* did not alter lateral root formation or elongation but instead affected primary root growth by altering the organization of the root apical meristem (Bustos-Sanmamed et al., 2013).

In the root nodule symbiosis, members of the ARF family exert either positive or negative roles on nodule number and rhizobial infection. *GmARF8a* and *GmARF8b* function as negative regulators of nodule formation in *G. max* (Wang

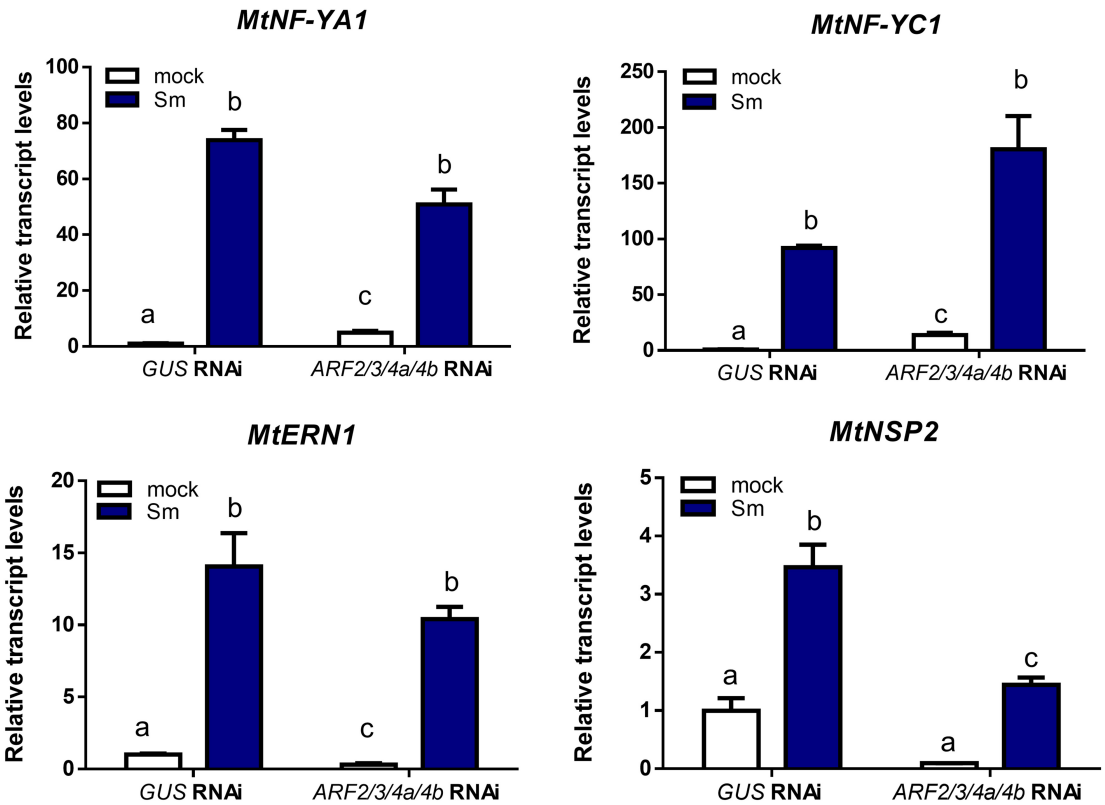

FIGURE 6 | Simultaneous knockdown of *MtARF2, MtARF3, MtARF4a*, and *MtARF4b* interfered with up-regulation of *NSP2* by rhizobia inoculation. Transcript levels of early nodulation markers *MtNF-YA1*, *MtNF-YC1*, *MtERN1*, and *MtNSP2* in *GUS* and *ARF2/3/4a/4b* RNAi roots at 48 h post-inoculation (hpi) with *S. meliloti* (Sm, blue bars) or water (mock, white bars) were determined by RT-qPCR, normalized to *MtHIS3L*, and expressed relative to the *GUS* RNAi mock sample. Different letters indicate statistically significant differences in an unpaired two-tailed Student's *t* test with a p value ≤ 0.05.

et al., 2015). On the other hand, *GmARF10*, *GmARF16*, and *GmARF17*, which are post-transcriptionally repressed by miR160, acts as positive regulators of nodule formation in both determinate and indeterminate nodule-forming species *G. max* (Turner et al., 2013; Nizampatnam et al., 2015) and *M. truncatula* (Bustos-Sanmamed et al., 2013), respectively. Here, we showed that the *MtARF2, MtARF3, MtARF4a*, and *MtARF4b* members of the B clade of the ARF family are required for proper nodule formation and development in *M. truncatula* (**Table 1** and **Figures 4B,C**). This indicates that in addition to members of the C clade, such as *MtARF10, MtARF16*, and *MtARF17*, *MtARF2, MtARF3*, and *MtARF4* can act as positive regulators of indeterminate nodule formation. These results are in agreement with those previously obtained by overexpression of miR390 in *M. truncatula* (Hobecker et al., 2017). Although our RNAi strategy effectively silenced *MtARF2, MtARF3*, and *MtARF4a/b*, expression data indicated that *MtARF4a* was the main ARF transcriptionally activated by rhizobia among these three ARF members (**Figure 2** and **Supplementary Figure 3**). Unfortunately, the high similarity of nucleotide sequences of *MtARF2*, *MtARF3, MtARF4a*, and *MtARF4b* transcripts made it unfeasible to design RNAi constructs specific for each member, preventing us to dissect the individual contribution of *MtARF2*, *MtARF3*, and *MtARF4b* to the root architecture and nodulation phenotype. However, the single *arf4a* mutant showed a very similar nodulation phenotype than that observed by simultaneous silencing of *ARF2/3/4a/4b* (**Figures 4B**, **5B**), suggesting that *MtARF4a* has a preponderant function in nodule formation. This reduction in nodule number observed in *ARF2/3/4a/4b* RNAi roots or in the *arf4a* mutant might be due to a decrease in auxin signaling and response, which is also correlated with the reactivation of cell divisions in the root cortex that promote nodule organogenesis (Kohlen et al., 2018). Intriguingly, it has been suggested that *LjARF2, LjARF3*, and *LjARF4* can potentially act as negative regulators of nodulation in *L. japonicus*, since their expression is enhanced in *reduced leaflet3/argonaute7* (*rel3/ago7*) mutants, which are impaired in nodule formation (Li et al., 2014). If this is the case, the contrasting results found in *L. japonicus* (Li et al., 2014) and *M. truncatula* (Hobecker et al., 2017 and this study) suggest that the role of these ARFs in nodulation might be also subjected to species-specific determinant mechanisms. Further analysis in other legume species will certainly help to elucidate whether the mode of action of these ARFs is different in determinate and indeterminate nodule-forming species.

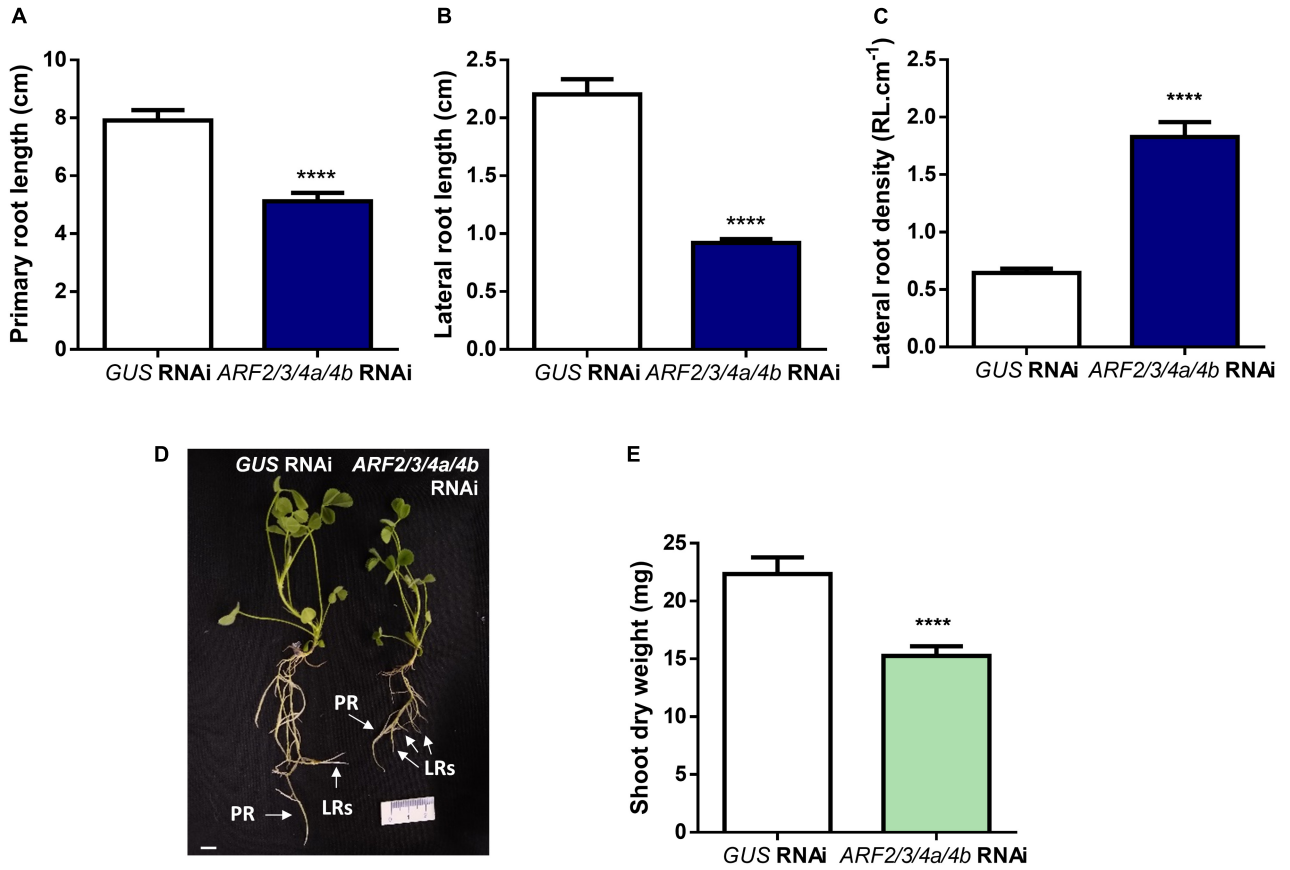

FIGURE 7 | Knockdown of *MtARF2, MtARF3, MtARF4a*, and *MtARF4b* altered root architecture. **(A–C)** Length of independent primary transgenic roots **(A)** and lateral root **(B)** and density of lateral roots **(C)** were measured in *GUS* and *ARF2/3/4a/b* RNAi roots at 15 days after transplantation to square petri dishes slanted agar-Fahraeus medium supplemented with 8 mM KNO_3. Error bars represent mean ± SE of three independent biological replicates with more than 20 roots in each experiment. Four asterisks indicate statistically significant differences between *GUS* RNAi and *ARF2/3/4a/4b* RNAi roots in an unpaired two-tailed Student's *t* test with a *p* value ≤ 0.0001. **(D)** Image of *GUS* and *ARF2/3/4a/4b* RNAi composite plants illustrating the shorter primary and lateral roots observed in *ARF2/3/4a/4b* RNAi roots. Each root that emerged directly from the sectioned site of the non-transgenic roots inoculated with *A. rhizogenes* was considered independent transgenic primary root (PR), whereas first-order roots that emerged from each independent transgenic primary root were considered lateral roots (LRs) in the hairy root system. Scale bar: 1 cm. **(E)** Shoot dry weight measured in *GUS* and *ARF2/3/4a/4b* RNAi composite plants at 15 days after transplantation to square petri dishes slanted agar-Fahraeus medium supplemented with 8 mM KNO_3. Error bars represent mean ± SE of three independent biological replicates with more than 10 composite plants in each experiment. Four asterisks indicate statistically significant differences between *GUS* and *ARF2/3/4a/4b* RNAi composite plants in an unpaired two-tailed Student's *t* test with a *p* value ≤ 0.0001.

As for other *ARF* genes involved in both lateral root architecture and nodule formation (e.g., *ARF8* and *ARF10/16/17*), the possibility that the symbiotic phenotype observed in *arf4a* mutants might be a consequence of alteration in root architecture and/or shoot development cannot be excluded. However, the nodulation phenotype of *arf4a* mutants—with over 70% reduction in nodule number as compared to WT (**Figure 5B**)—was more severe than the root architecture phenotype, where lateral root length was reduced by 20% but the number of lateral roots increased by 35% as compared to WT (**Figure 8**). Considering that nodules formed mainly in lateral roots, the total lateral root system for nodule formation is not drastically altered in *arf4a* mutants; thus, it seems unlikely that root architecture was the cause of the symbiotic phenotype. Remarkably, infection by rhizobia, which can be genetically separated from nodule organogenesis (Oldroyd et al., 2011), was also severely impaired in *arf4a* mutants (**Figures 5C,D**), supporting a role for *MtARF4a* in the root nodule symbiosis.

ARFs and Their Role in Rhizobial Infection

Infection by rhizobia can be arrested either at the initiation stage or during the progression of the infection events toward the dividing cortical cells that will form the nodule primordium. Here, we found that silencing of *MtARF2, MtARF3, MtARF4a*, and *MtARF4b* or mutation of *MtARF4a* in *M. truncatula*, resulted in a moderate reduction in the density of infection events, but a severe impairment of the progression of these events to root cortex (**Figures 4D,E**, **5C,D**). The infection phenotype observed here using an RNAi strategy or the *arf4a* mutant was more

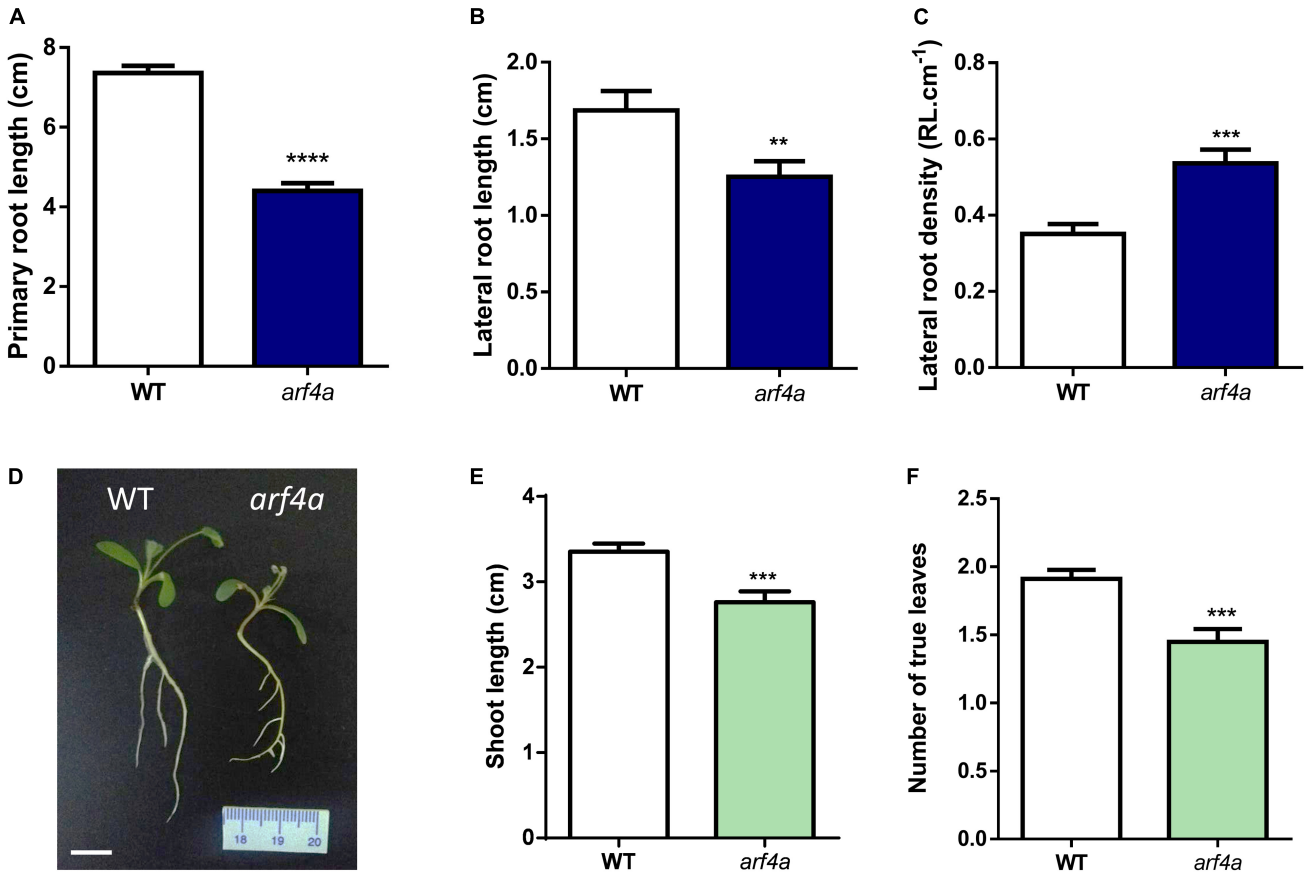

FIGURE 8 | The *arf4a* mutant exhibited altered root and shoot development. **(A–C)** Primary root length **(A)**, lateral root length **(B)**, and lateral root density **(C)** were measured in WT and *arf4a* mutant plants at 7 days after germination (dag). Plants were grown on slanted agar-Fahraeus medium supplemented with 8 mM KNO_3. Error bars represent mean ± SE of three biological replicates, each with at least 10 plants. Asterisks denote statistically significant differences between WT and *arf4a* plants in an unpaired two-tailed Student's *t* test (**$p \leq 0.01$, ***$p \leq 0.001$, and ****$p \leq 0.0001$). **(D)** Image of WT and *arf4a* mutant plants at 7 dag illustrating the shorter primary and lateral roots observed in *arf4a* mutant roots. Scale bar: 1 cm. **(E,F)** Shoot length **(E)** and number of true leaves **(F)** measured in WT and *arf4a* mutant at 7 dag. Plants were grown on slanted agar-Fahraeus medium supplemented with 8 mM KNO_3. Error bars represent mean ± SE of three biological replicates, each with at least 10 plants. Three asterisks denote a statistically significant difference between WT and *arf4a* plants in an unpaired two-tailed Student's *t* with a *p* value ≤ 0.001.

pronounced than that observed by Hobecker et al. (2017), since overexpression of miR390 reduced the density of infection events but not their progression. This might be explained considering that the RNAi is more effective in reducing *ARF* transcript levels than overexpression of miR390 (70–90 vs. 50–80% depending on the *ARF*). Previously, Breakspear et al. (2014) have shown that mutations in *MtARF16a* also affected infection by rhizobia in *M. truncatula*, mostly caused by a decrease in the formation of pockets containing microcolonies and elongating ITs. Thus, *MtARF16* seems to be required for the initiation of infection rather than for elongation and ramification of ITs. Our results indicate that *MtARF4a* participate not only in the initiation but also in the elongation and ramification of ITs, since the majority of infection events were arrested at the microcolony stage and only a minor proportion of the ITs reached the dividing cortex (**Figure 5D**). A recent study in *L. japonicus* using a *DR5:GUS* reporter or a LjDII auxin sensor—consisting of the DII domain of Arabidopsis AtIAA28 and nuclear—localized triple YFP—has demonstrated that auxins accumulate specifically in rhizobium-infected root hairs and, moreover, that this accumulation is dependent on the NF signaling (Nadzieja et al., 2018). In addition, the same study revealed that components of the auxin biosynthetic pathway are up-regulated specifically in the rhizobia infected root hairs. In *M. truncatula*, inoculation with *S. meliloti* induced *DR5:GUS* reporter in both infected and uninfected root hairs over the entire infection zone and up-regulated a number of genes involved in auxin signaling and response such as *MtGH3*, *MtSAUR1*, and *MtARF16a* (Breakspear et al., 2014). The promoter:*GFP* analysis presented here has shown that *MtARF4a*, but not *MtARF3*, is expressed in the infected root hairs and in epidermal surrounding cells (**Figure 2**), supporting the notion that auxin signaling and response have a crucial role in promoting infection events in epidermal cells. This requirement for auxin signaling might be related to changes in cell-cycle progression that increase extensibility of the cell wall during IT formation in the root hairs (Breakspear et al., 2014; Lin et al., 2020).

ARFs and the Nod Factor Signaling Pathway

We have found that the expression of *MtARF2*, *MtARF3*, and *MtARF4/b* was activated in response to NFs, and that this activation requires the Nod Factor Receptor MtNFP and the MtNF-YA1 transcription factor (**Figure 3**), suggesting that this set of ARFs might act downstream of NF-Y in the NF signaling pathway. *MtNFP* was also required for timely activation of miR160 in *M. truncatula*, which targets *MtARF10*, *MtARF16*, and *MtARF17* (Bustos-Sanmamed et al., 2013). Conversely, NF perception-dependent expression has been described for the miR167 in *G. max*, which targets *GmARF8a/b*, since accumulation of this miRNA in response to rhizobia was impaired in the non-nodulating mutant defective in the NF receptor *GmNFR1α* (Wang et al., 2015). Thus, it seems that modulation of the expression of different members of the ARFs family is dependent on NF signaling pathway in legumes. In addition, silencing of *MtARF2, MtARF3, MtARF4a*, and *MtARF4b* did not affect the up-regulation of *MtNF-YA1* and *MtNF-YC1* in response to rhizobia (**Figure 6**), supporting the notion that these ARF members act downstream of the NF-Y complex. On the other hand, we have found that *MtARF2, MtARF3, MtARF4a*, and *MtARF4b* are required for full induction of *MtNSP2* in response to *S. meliloti* (**Figure 6**), indicating that these ARFs might intercept the Nod signaling pathway acting upstream of MtNSP2. This agrees with previous results that showed that roots overexpressing miR390, which have reduced levels of *MtARF2, MtARF3, MtARF4a*, and *MtARF4b*, failed to up-regulate *MtNSP1* and *MtNSP2* in *M. truncatula* in response to rhizobia (Hobecker et al., 2017). In *G. max*, GmARF8a/b can potentially act as negative regulators of *GmNSP1* and other symbiotically related genes (Wang et al., 2015). On the other hand, *G. max* roots with reduced levels of miR160, which targets *ARF10/16/17*, exhibited greater induction of *GmNSP1* upon inoculation with its symbiotic partner *Bradyrhizobium japonicum*, indicating that *GmARF10*, *GmARF16*, and *GmARF17* can act as positive regulators of *GmNSP1* (Nizampatnam et al., 2015). These results indicate that different ARF members intercept the nodulation signaling pathway acting either as positive or negative regulators of distinct components required for nodulation, such as *NSP1* and *NSP2*. Further analysis will help to elucidate whether ARFs can act as direct activators or repressors of *NSP1* and *NSP2*. Interestingly, recent studies on the Arabidopsis AtARF5 revealed a new paradigm to explain the ARF-mediated transcriptional response to auxin. In addition to the auxin−mediated degradation of Aux/IAA proteins that releases ARF repression, ARFs can potentially act as pioneer transcription factors by recruiting chromatin remodeling proteins that promote a chromatin permissive configuration at auxin-regulated loci (e.g., *PLETHORA*), allowing proximal *cis*−AuxREs to become accessible to form higher-order transcriptional complexes, and adding a new layer of complexity to the auxin transcriptional response (Kornet and Scheres, 2009; Wu et al., 2015; Chandler, 2016). Undoubtedly, more research is needed to clarify which loci are targeted by *MtARF2, MtARF3, MtARF4a*, and *MtARF4b* and the mechanisms by which these ARFs mediate auxin response in the root nodule symbiosis. The results presented here regarding the positive role of these ARF members in nodulation and its crosstalk with the nodulation signaling pathway represent an initial step toward the elucidation of such mechanisms.

DATA AVAILABILITY STATEMENT

The raw data supporting the conclusions of this article will be made available by the authors, without undue reservation.

AUTHOR CONTRIBUTIONS

MZ and FB conceived the research, conceptualized the study, and supervised the study. CK, KH, MZ, FB, and AN designed the experiments. CK, KH, and AN performed the experiments. JW, KM, and AN contributed to the biological material. CK, KH, FB, and MZ analyzed the data. CK, MZ, and FB wrote the original draft of the article. CK, KH, AN, FB, and MZ reviewed and edited the article. AN, FB, and MZ acquired funding. All authors contributed to the article and approved the submitted version.

FUNDING

This study was financially supported by the Agencia Nacional de Promoción Científica y Tecnológica, Argentina through PICT2016-0582 and PICT2017-0581 granted to MZ and PICT2016-0333 and PICT2017-0069 granted to FB. The study was also funded by a IAL (International Associated Laboratory) NOCOSYM project funded by Centre National de la Recherche Scientifique (CNRS) granted to AN and MZ. Development of *M. truncatula Tnt1* mutant population was, in part, funded by the National Science Foundation, United States (DBI-0703285 and IOS-1127155) to KM. MZ and FB are members of Consejo Nacional de Investigaciones Científicas y Técnicas (CONICET). CK and KH were recipients of CONICET fellowships.

ACKNOWLEDGMENTS

We would like to thank Claudio Mazzo for assistance with the preparation of transgenic roots and Mauricio Reynoso for advice on growing *arf4a* mutants and critical reading of the manuscript. We would also like to thank the CNRS of France for funding visiting programs between France and Argentina.

SUPPLEMENTARY MATERIAL

The Supplementary Material for this article can be found online at: https://www.frontiersin.org/articles/10.3389/fpls.2021.659061/full#supplementary-material

REFERENCES

Amor, B. B., Shaw, S. L., Oldroyd, G. E., Maillet, F., Penmetsa, R. V., Cook, D., et al. (2003). The NFP locus of *Medicago truncatula* controls an early step of Nod factor signal transduction upstream of a rapid calcium flux and root hair deformation. *Plant J.* 34, 495–506. doi: 10.1046/j.1365-313x.2003.01743.x

Ariel, F., Diet, A., Verdenaud, M., Gruber, V., Frugier, F., Chan, R., et al. (2010). Environmental regulation of lateral root emergence in *Medicago truncatula* requires the HD-Zip I transcription factor HB1. *Plant Cell* 22, 2171–2183. doi: 10.1105/tpc.110.074823

Baudin, M., Laloum, T., Lepage, A., Ripodas, C., Ariel, F., Frances, L., et al. (2015). A phylogenetically conserved group of nuclear factor-Y transcription factors interact to control nodulation in legumes. *Plant Physiol.* 169, 2761–2773.

Bishopp, A., and Bennett, M. J. (2019). Turning lateral roots into nodules. *Science* 366, 953–954. doi: 10.1126/science.aay8620

Blanco, F. A., Meschini, E. P., Zanetti, M. E., and Aguilar, O. M. (2009). A small GTPase of the Rab family is required for root hair formation and preinfection stages of the common bean-Rhizobium symbiotic association. *Plant Cell* 21, 2797–2810. doi: 10.1105/tpc.108.063420

Boisson-Dernier, A., Chabaud, M., Garcia, F., Becard, G., Rosenberg, C., and Barker, D. G. (2001). Agrobacterium rhizogenes-transformed roots of *Medicago truncatula* for the study of nitrogen-fixing and endomycorrhizal symbiotic associations. *Mol. Plant Microbe Interact.* 14, 695–700. doi: 10.1094/mpmi.2001.14.6.695

Breakspear, A., Liu, C., Roy, S., Stacey, N., Rogers, C., Trick, M., et al. (2014). The root hair "infectome" of *Medicago truncatula* uncovers changes in cell cycle genes and reveals a requirement for Auxin signaling in rhizobial infection. *Plant Cell* 26, 4680–4701. doi: 10.1105/tpc.114.133496

Bustos-Sanmamed, P., Mao, G., Deng, Y., Elouet, M., Khan, G. A., Bazin, J., et al. (2013). Overexpression of miR160 affects root growth and nitrogen-fixing nodule number in *Medicago truncatula*. *Funct. Plant Biol.* 40, 1208–1220. doi: 10.1071/fp13123

Chandler, J. W. (2016). Auxin response factors. *Plant Cell Environ.* 39, 1014–1028. doi: 10.1111/pce.12662

Cheng, X., Wang, M., Lee, H. K., Tadege, M., Ratet, P., Udvardi, M., et al. (2014). An efficient reverse genetics platform in the model legume *Medicago truncatula*. *New Phytol.* 201, 1065–1076.

Combier, J. P., Frugier, F., De Billy, F., Boualem, A., El-Yahyaoui, F., Moreau, S., et al. (2006). MtHAP2-1 is a key transcriptional regulator of symbiotic nodule development regulated by microRNA169 in *Medicago truncatula*. *Genes Dev.* 20, 3084–3088. doi: 10.1101/gad.402806

De Smet, I., Lau, S., Voss, U., Vanneste, S., Benjamins, R., Rademacher, E. H., et al. (2010). Bimodular auxin response controls organogenesis in *Arabidopsis*. *Proc. Natl. Acad. Sci. U.S.A.* 107, 2705–2710. doi: 10.1073/pnas.0915001107

Douglas, R. N., Wiley, D., Sarkar, A., Springer, N., Timmermans, M. C. P., and Scanlon, M. J. (2010). *Ragged seedling2* encodes an ARGONAUTE7-like protein required for mediolateral expansion, but not dorsiventrality, of maize leaves. *Plant Cell* 22, 1441–1451. doi: 10.1105/tpc.109.071613

Doyle, J. J. (2011). Phylogenetic perspectives on the origins of nodulation. *Mol. Plant Microbe Interact.* 24, 1289–1295. doi: 10.1094/mpmi-05-11-0114

Fahraeus, G. (1957). The infection of clover root hairs by nodule bacteria studied by a simple glass slide technique. *J. Gen. Microbiol.* 16, 374–381. doi: 10.1099/00221287-16-2-374

Felsenstein, J. (1985). Confidence limits on phylogenies: an approach using the bootstrap. *Evolution* 39, 783–791. doi: 10.2307/2408678

Finet, C., Berne-Dedieu, A., Scutt, C. P., and Marlétaz, F. (2013). Evolution of the ARF gene family in land plants: old domains, new tricks. *Mol. Biol. Evol.* 30, 45–56. doi: 10.1093/molbev/mss220

Franssen, H. J., Xiao, T. T., Kulikova, O., Wan, X., Bisseling, T., Scheres, B., et al. (2015). Root developmental programs shape the *Medicago truncatula* nodule meristem. *Development* 142, 2941–2950. doi: 10.1242/dev.120774

Guilfoyle, T. J., and Hagen, G. (2007). Auxin response factors. *Curr. Opin. Plant Biol.* 10, 453–460.

He, F., Xu, C., Fu, X., Shen, Y., Guo, L., Leng, M., et al. (2018). The MicroRNA390/TRANS-acting short interfering RNA3 module mediates lateral root growth under salt stress via the auxin pathway. *Plant Physiol.* 177, 775–791. doi: 10.1104/pp.17.01559

Herrbach, V., Rembliere, C., Gough, C., and Bensmihen, S. (2014). Lateral root formation and patterning in *Medicago truncatula*. *J. Plant Physiol.* 171, 301–310. doi: 10.1016/j.jplph.2013.09.006

Hobecker, K. V., Reynoso, M. A., Bustos-Sanmamed, P., Wen, J., Mysore, K. S., Crespi, M., et al. (2017). The MicroRNA390/TAS3 pathway mediates symbiotic nodulation and lateral root growth. *Plant Physiol.* 174, 2469–2486. doi: 10.1104/pp.17.00464

Karimi, M., Depicker, A., and Hilson, P. (2007). Recombinational cloning with plant gateway vectors. *Plant Physiol.* 145, 1144–1154. doi: 10.1104/pp.107.106989

Karimi, M., Inze, D., and Depicker, A. (2002). GATEWAY vectors for *Agrobacterium*-mediated plant transformation. *Trends Plant Sci.* 7, 193–195. doi: 10.1016/s1360-1385(02)02251-3

Kohlen, W., Ng, J. L. P., Deinum, E. E., and Mathesius, U. (2018). Auxin transport, metabolism, and signaling during nodule initiation: indeterminate and determinate nodules. *J. Exp. Bot.* 69, 229–244. doi: 10.1093/jxb/erx308

Kornet, N., and Scheres, B. (2009). Members of the GCN5 histone acetyltransferase complex regulate PLETHORA-mediated root stem cell niche maintenance and transit amplifying cell proliferation in *Arabidopsis*. *Plant Cell* 21, 1070–1079. doi: 10.1105/tpc.108.065300

Kumar, S., Stecher, G., Li, M., Knyaz, C., and Tamura, K. (2018). MEGA X: molecular evolutionary genetics analysis across computing platforms. *Mol. Biol. Evol.* 35, 1547–1549. doi: 10.1093/molbev/msy096

Laporte, P., Lepage, A., Fournier, J., Catrice, O., Moreau, S., Jardinaud, M. F., et al. (2014). The CCAAT box-binding transcription factor NF-YA1 controls rhizobial infection. *J. Exp. Bot.* 65, 481–494. doi: 10.1093/jxb/ert392

Li, X., Lei, M., Yan, Z., Wang, Q., Chen, A., Sun, J., et al. (2014). The REL3-mediated TAS3 ta-siRNA pathway integrates auxin and ethylene signaling to regulate nodulation in *Lotus japonicus*. *New Phytol.* 201, 531–544. doi: 10.1111/nph.12550

Lin, J., Frank, M., and Reid, D. (2020). No home without hormones: how plant hormones control legume nodule organogenesis. *Plant Commun.* 1:100104. doi: 10.1016/j.xplc.2020.100104

Lu, Y., Feng, Z., Liu, X., Bian, L., Xie, H., Zhang, C., et al. (2018). MiR393 and miR390 synergistically regulate lateral root growth in rice under different conditions. *BMC Plant Biol.* 18:261. doi: 10.1186/s12870-018-1488-x

Mallory, A. C., Bartel, D. P., and Bartel, B. (2005). MicroRNA-directed regulation of *Arabidopsis* AUXIN RESPONSE FACTOR17 is essential for proper development and modulates expression of early auxin response genes. *Plant Cell* 17, 1360–1375. doi: 10.1105/tpc.105.031716

Marin, E., Jouannet, V., Herz, A., Lokerse, A. S., Weijers, D., Vaucheret, H., et al. (2010). miR390, *Arabidopsis* TAS3 tasiRNAs, and their AUXIN RESPONSE FACTOR targets define an autoregulatory network quantitatively regulating lateral root growth. *Plant Cell* 22, 1104–1117. doi: 10.1105/tpc.109.072553

Meade, H. M., and Signer, E. R. (1977). Genetic mapping of *Rhizobium meliloti*. *Proc. Natl. Acad. Sci. U.S.A.* 74, 2076–2078. doi: 10.1073/pnas.74.5.2076

Middleton, P. H., Jakab, J., Penmetsa, R. V., Starker, C. G., Doll, J., Kalo, P., et al. (2007). An ERF transcription factor in *Medicago truncatula* that is essential for Nod factor signal transduction. *Plant Cell* 19, 1221–1234. doi: 10.1105/tpc.106.048264

Nadzieja, M., Kelly, S., Stougaard, J., and Reid, D. (2018). Epidermal auxin biosynthesis facilitates rhizobial infection in *Lotus japonicus*. *Plant J.* 95, 101–111. doi: 10.1111/tpj.13934

Nei, M., and Kumar, S. (2000). *Molecular Evolution and Phylogenetics*. New York, NY: Oxford University Press.

Nizampatnam, N. R., Schreier, S. J., Damodaran, S., Adhikari, S., and Subramanian, S. (2015). microRNA160 dictates stage-specific auxin and cytokinin sensitivities and directs soybean nodule development. *Plant J.* 84, 140–153. doi: 10.1111/tpj.12965

Okushima, Y., Overvoorde, P. J., Arima, K., Alonso, J. M., Chan, A., Chang, C., et al. (2005). Functional genomic analysis of the AUXIN RESPONSE FACTOR gene family members in *Arabidopsis thaliana*: unique and overlapping functions of ARF7 and ARF19. *Plant Cell* 17, 444–463. doi: 10.1105/tpc.104.028316

Oldroyd, G. E., Murray, J. D., Poole, P. S., and Downie, J. A. (2011). The rules of engagement in the legume-rhizobial symbiosis. *Annu. Rev. Genet.* 45, 119–144. doi: 10.1146/annurev-genet-110410-132549

Osipova, M. A., Mortier, V., Demchenko, K. N., Tsyganov, V. E., Tikhonovich, I. A., Lutova, L. A., et al. (2012). Wuschel-related homeobox5 gene expression

and interaction of CLE peptides with components of the systemic control add two pieces to the puzzle of autoregulation of nodulation. *Plant Physiol.* 158, 1329–1341. doi: 10.1104/pp.111.188078

Overvoorde, P., Fukaki, H., and Beeckman, T. (2010). Auxin control of root development. *Cold Spring Harb. Perspect. Biol.* 2:a001537. doi: 10.1101/cshperspect.a001537

Pecrix, Y., Staton, S. E., Sallet, E., Lelandais-Briere, C., Moreau, S., Carrere, S., et al. (2018). Whole-genome landscape of *Medicago truncatula* symbiotic genes. *Nat. Plants* 4, 1017–1025.

Peng, J., Berbel, A., Madueño, F., and Chen, R. (2017). AUXIN response FACTOR3 regulates compound leaf patterning by directly repressing PALMATE-LIKE PENTAFOLIATA1 expression in *Medicago truncatula*. *Front. Plant Sci.* 8:1630. doi: 10.3389/fpls.2017.01630

Penmetsa, R. V., and Cook, D. R. (1997). A legume ethylene-insensitive mutant hyperinfected by its rhizobial symbiont. *Science* 275, 527–530. doi: 10.1126/science.275.5299.527

Prayitno, J., Rolfe, B. G., and Mathesius, U. (2006). The Ethylene-insensitive sickle mutant of *Medicago truncatula* shows altered auxin transport regulation during nodulation. *Plant Physiol.* 142, 168–180. doi: 10.1104/pp.106.080093

Quandt, H. J., Pühler, A., and Broer, I. (1993). Transgenic root nodules of Vicia hirsuta: a fast and efficient system for the study of gene expression in indeterminate-type nodules. *Mol. Plant Microbe Interact.* 6, 699–706. doi: 10.1094/mpmi-6-699

Reynoso, M. A., Blanco, F. A., Bailey-Serres, J., Crespi, M., and Zanetti, M. E. (2013). Selective recruitment of mRNAs and miRNAs to polyribosomes in response to rhizobia infection in *Medicago truncatula*. *Plant J.* 73, 289–301. doi: 10.1111/tpj.12033

Saitou, N., and Nei, M. (1987). The neighbor-joining method: a new method for reconstructing phylogenetic trees. *Mol. Biol. Evol.* 4, 406–425.

Salehin, M., Bagchi, R., and Estelle, M. (2015). SCFTIR1/AFB-based auxin perception: mechanism and role in plant growth and development. *Plant Cell* 27, 9–19. doi: 10.1105/tpc.114.133744

Schiessl, K., Lilley, J. L. S., Lee, T., Tamvakis, I., Kohlen, W., Bailey, P. C., et al. (2019). Nodule inception recruits the lateral root developmental program for symbiotic nodule organogenesis in *Medicago truncatula*. *Curr. Biol.* 29, 3657.e5–3668.e5.

Shen, C., Yue, R., Sun, T., Zhang, L., Xu, L., Tie, S., et al. (2015). Genome-wide identification and expression analysis of auxin response factor gene family in *Medicago truncatula*. *Front. Plant Sci.* 6:73. doi: 10.3389/fpls.2015.00073

Shrestha, A., Zhong, S., Therrien, J., Huebert, T., Sato, S., Mun, T., et al. (2020). *Lotus japonicus* nuclear factor YA1, a nodule emergence stage-specific regulator of auxin signalling. *New Phytol.* 229, 1535–1552. doi: 10.1111/nph.16950

Smit, P., Limpens, E., Geurts, R., Fedorova, E., Dolgikh, E., Gough, C., et al. (2007). Medicago LYK3, an entry receptor in rhizobial nodulation factor signaling. *Plant Physiol.* 145, 183–191. doi: 10.1104/pp.107.100495

Soyano, T., Liu, M., Kawaguchi, M., and Hayashi, M. (2021). Leguminous nodule symbiosis involves recruitment of factors contributing to lateral root development. *Curr. Opin. Plant Biol.* 59:102000. doi: 10.1016/j.pbi.2020.102000

Soyano, T., Shimoda, Y., Kawaguchi, M., and Hayashi, M. (2019). A shared gene drives lateral root development and root nodule symbiosis pathways in *Lotus*. *Science* 366, 1021–1023. doi: 10.1126/science.aax2153

Tadege, M., Wen, J., He, J., Tu, H., Kwak, Y., Eschstruth, A., et al. (2008). Large-scale insertional mutagenesis using the Tnt1 retrotransposon in the model legume *Medicago truncatula*. *Plant J.* 54, 335–347. doi: 10.1111/j.1365-313x.2008.03418.x

Tian, C. F., Garnerone, A. M., Mathieu-Demaziere, C., Masson-Boivin, C., and Batut, J. (2012). Plant-activated bacterial receptor adenylate cyclases modulate epidermal infection in the *Sinorhizobium meliloti*-Medicago symbiosis. *Proc. Natl. Acad. Sci. U.S.A.* 109, 6751–6756. doi: 10.1073/pnas.1120260109

Tiwari, S. B., Hagen, G., and Guilfoyle, T. (2003). The roles of auxin response factor domains in auxin-responsive transcription. *Plant Cell* 15, 533–543. doi: 10.1105/tpc.008417

Traubenik, S., Reynoso, M. A., Hobecker, K., Lancia, M., Hummel, M., Rosen, B., et al. (2020). Reprogramming of root cells during nitrogen-fixing symbiosis involves dynamic polysome association of coding and noncoding RNAs. *Plant Cell* 32, 352–373. doi: 10.1105/tpc.19.00647

Turner, M., Nizampatnam, N. R., Baron, M., Coppin, S., Damodaran, S., Adhikari, S., et al. (2013). Ectopic expression of miR160 results in auxin hypersensitivity, cytokinin hyposensitivity, and inhibition of symbiotic nodule development in soybean. *Plant Physiol.* 162, 2042–2055. doi: 10.1104/pp.113.220699

Ulmasov, T., Hagen, G., and Guilfoyle, T. J. (1999). Activation and repression of transcription by auxin-response factors. *Proc. Natl. Acad. Sci. U.S.A.* 96, 5844–5849. doi: 10.1073/pnas.96.10.5844

Vandesompele, J., De Preter, K., Pattyn, F., Poppe, B., Van Roy, N., De Paepe, A., et al. (2002). Accurate normalization of real-time quantitative RT-PCR data by geometric averaging of multiple internal control genes. *Genome Biol.* 3:research0034.1.

Wang, S., Tiwari, S. B., Hagen, G., and Guilfoyle, T. J. (2005). AUXIN RESPONSE FACTOR7 restores the expression of auxin-responsive genes in mutant *Arabidopsis* leaf mesophyll protoplasts. *Plant Cell* 17, 1979–1993. doi: 10.1105/tpc.105.031096

Wang, Y., Li, K., Chen, L., Zou, Y., Liu, H., Tian, Y., et al. (2015). MicroRNA167-directed regulation of the auxin response factors GmARF8a and GmARF8b is required for soybean nodulation and lateral root development. *Plant Physiol.* 168, 984–999. doi: 10.1104/pp.15.00265

Wilmoth, J. C., Wang, S., Tiwari, S. B., Joshi, A. D., Hagen, G., Guilfoyle, T. J., et al. (2005). NPH4/ARF7 and ARF19 promote leaf expansion and auxin-induced lateral root formation. *Plant J.* 43, 118–130. doi: 10.1111/j.1365-313x.2005.02432.x

Wu, M. F., Yamaguchi, N., Xiao, J., Bargmann, B., Estelle, M., Sang, Y., et al. (2015). Auxin-regulated chromatin switch directs acquisition of flower primordium founder fate. *eLife* 4:e09269.

Xia, R., Xu, J., and Meyers, B. C. (2017). The emergence, evolution, and diversification of the miR390-TAS3-ARF pathway in land plants. *Plant Cell* 29, 1232–1247. doi: 10.1105/tpc.17.00185

Xiao, T. T., Schilderink, S., Moling, S., Deinum, E. E., Kondorosi, E., Franssen, H., et al. (2014). Fate map of *Medicago truncatula* root nodules. *Development* 141, 3517–3528. doi: 10.1242/dev.110775

Yan, J., Cai, X., Luo, J., Sato, S., Jiang, Q., Yang, J., et al. (2010). The REDUCED LEAFLET genes encode key components of the trans-acting small interfering RNA pathway and regulate compound leaf and flower development in Lotus japonicus. *Plant Physiol.* 152, 797–807. doi: 10.1104/pp.109.140947

Yifhar, T., Pekker, I., Peled, D., Friedlander, G., Pistunov, A., Sabban, M., et al. (2012). Failure of the tomato trans-acting short interfering RNA program to regulate AUXIN RESPONSE FACTOR3 and ARF4 underlies the wiry leaf syndrome. *Plant Cell* 24, 3575–3589. doi: 10.1105/tpc.112.100222

Yoon, E. K., Yang, J. H., Lim, J., Kim, S. H., Kim, S. K., and Lee, W. S. (2010). Auxin regulation of the microRNA390-dependent transacting small interfering RNA pathway in *Arabidopsis* lateral root development. *Nucleic Acids Res.* 38, 1382–1391. doi: 10.1093/nar/gkp1128

Zhou, C., Han, L., Fu, C., Wen, J., Cheng, X., Nakashima, J., et al. (2013). The trans-acting short interfering RNA3 pathway and no apical meristem antagonistically regulate leaf margin development and lateral organ separation, as revealed by analysis of an argonaute7/lobed leaflet1 mutant in *Medicago truncatula*. *Plant Cell* 25, 4845–4862. doi: 10.1105/tpc.113.117788

Conflict of Interest: JW and KM were employed by the company Noble Research Institute LLC.

The remaining authors declare that the research was conducted in the absence of any commercial or financial relationships that could be construed as a potential conflict of interest.

frontiers in Plant Science

REVIEW
published: 26 April 2021
doi: 10.3389/fpls.2021.659155

Integrative Roles of Phytohormones on Cell Proliferation, Elongation and Differentiation in the *Arabidopsis thaliana* Primary Root

*Estephania Zluhan-Martínez[1†], Brenda Anabel López-Ruíz[1†], Mónica L. García-Gómez[1,2], Berenice García-Ponce[1], María de la Paz Sánchez[1], Elena R. Álvarez-Buylla[1,2] and Adriana Garay-Arroyo[1,2]**

[1] Laboratorio de Genética Molecular, Desarrollo y Evolución de Plantas, Departamento de Ecología Funcional, Instituto de Ecología, Universidad Nacional Autónoma de México, Ciudad de México, Mexico, [2] Centro de Ciencias de la Complejidad, Universidad Nacional Autónoma de México, Ciudad de México, Mexico

The growth of multicellular organisms relies on cell proliferation, elongation and differentiation that are tightly regulated throughout development by internal and external stimuli. The plasticity of a growth response largely depends on the capacity of the organism to adjust the ratio between cell proliferation and cell differentiation. The primary root of *Arabidopsis thaliana* offers many advantages toward understanding growth homeostasis as root cells are continuously produced and move from cell proliferation to elongation and differentiation that are processes spatially separated and could be studied along the longitudinal axis. Hormones fine tune plant growth responses and a huge amount of information has been recently generated on the role of these compounds in Arabidopsis primary root development. In this review, we summarized the participation of nine hormones in the regulation of the different zones and domains of the Arabidopsis primary root. In some cases, we found synergism between hormones that function either positively or negatively in proliferation, elongation or differentiation. Intriguingly, there are other cases where the interaction between hormones exhibits unexpected results. Future analysis on the molecular mechanisms underlying crosstalk hormone action in specific zones and domains will unravel their coordination over PR development.

Keywords: hormones, Arabidopsis, root apical meristem, primary root, cell proliferation, cell elongation, cell differentiation

OPEN ACCESS

Edited by:
Ramiro Esteban Rodriguez, CONICET Instituto de Biología Molecular y Celular de Rosario (IBR), Argentina

Reviewed by:
Riccardo Di Mambro, University of Pisa, Italy
Miguel Angel Moreno-Risueno, Center for Plant Biotechnology and Genomics, National Institute of Agricultural and Food Research and Technology, Spain

***Correspondence:**
Adriana Garay-Arroyo
agaray@iecologia.unam.mx

† These authors have contributed equally to this work

Specialty section:
This article was submitted to Plant Development and EvoDevo, a section of the journal Frontiers in Plant Science

Received: *27 January 2021*
Accepted: *24 March 2021*
Published: *26 April 2021*

Citation:
Zluhan-Martínez E, López-Ruíz BA, García-Gómez ML, García-Ponce B, de la Paz Sánchez M, Álvarez-Buylla ER and Garay-Arroyo A (2021) Integrative Roles of Phytohormones on Cell Proliferation, Elongation and Differentiation in the Arabidopsis thaliana Primary Root. Front. Plant Sci. 12:659155. doi: 10.3389/fpls.2021.659155

INTRODUCTION

Plant development depends on three interlinked processes: cell proliferation, elongation and differentiation, that can be studied *in vivo* in *Arabidopsis thaliana* (hereafter Arabidopsis) roots. Roots are an excellent model to study the balance between cell division, elongation and differentiation as these processes are spatially separated along the main axis (Scheres and Wolkenfelt, 1998). The organization from the tip of the root to the base of the stem consists of different tissues and zones, starting with the columella, which confers soil abrasion resistance,

followed by the MZ, the Elongation Zone (EZ) and the Differentiation Zone (DZ) (**Figure 1**; Baluška et al., 1996; Verbelen et al., 2006; Ivanov and Dubrovsky, 2013; Salvi et al., 2020). The MZ is the region within the root where cells are produced, and it consists of the Stem Cell Niche (SCN), the Proliferation Domain (PD) and the Transition Domain (TD) (Baluška et al., 1994, 2010; Verbelen et al., 2006; Ivanov and Dubrovsky, 2013; Salvi et al., 2020; **Figure 1**). The SCN has a central organizer known as the Quiescent Center (QC) surrounded by stem cells that divide to self-renew and to provide cells that will populate either the PD or the columella, in the case of the distal stem cells (Dolan et al., 1993; Van den Berg et al., 1995; Van Den Berg et al., 1997; Benfey and Scheres, 2000; **Figure 1**). In the MZ, the cells divide 4 to 6 times and then they transit to the EZ where there is a rapid longitudinal expansion, until eventually the cells reach the DZ where they acquire their final characteristics (Dolan et al., 1993; Barrada et al., 2015; **Figure 1**). In addition, the primary root (PR) of Arabidopsis has a very simple radial organization with cell types arranged around the innermost vascular tissues; the epidermis is the most external layer, followed by the cortex, the 40 endodermis, the pericycle and the vascular tissues in the center. The lateral root cap protects the 41 epidermis at the very root tip, and it is only present in the Meristematic Zone (MZ) (Dolan et al., 1993).

Roots are essential for anchorage, water and nutrients uptake, for the establishment of symbiotic associations with different organisms and for environmental sensing (Hodge, 2009). Therefore, root development is highly plastic in response to an ever-changing environment where the hormones participate in all plant developmental processes and exhibit cell types, organs and tissues-specific responses (Gray, 2004; Hodge, 2009; Sánchez-Calderón et al., 2013). Information regarding the biosynthesis, conjugation, transport, catabolism, perception and signal transduction pathways of auxin, abscisic acid (ABA), brassinosteroid (BR), strigolactone (SL), gibberellic acid (GA), cytokinin (CK), jasmonic acid (JA), salicylic acid (SA) and ethylene have been widely studied, and details were summarized in **Supplementary Figure 1** and **Supplementary Tables 1**, **2**. Moreover, the participation of them in Arabidopsis PR development has been widely studied either in mutants of loss or gain-of-function (LoF or GoF; **Supplementary Table 3** to see the root phenotype); by treatments with chemicals that change their concentration or distribution as well as by using hormonal-response gene constructs (Tanimoto, 2005; Jung and McCouch, 2013; Qin et al., 2019; Waidmann et al., 2020). Not surprisingly, the function of each hormone is spatially regulated and depends specifically on the organ and the plant developmental stage (Wang and Irving, 2011). Despite the huge amount of information generated in the last two decades on the effect of hormones in PR growth, their participation in all domains and zones have still not been fully integrated (Takatsuka and Umeda, 2014). Hormones regulate cell division and cell elongation in Arabidopsis roots and the length of either the MZ and the fully elongated cells, are two sensitive and quantitative parameters to evaluate their participation in PR growth (Rahman et al., 2000; Okamoto et al., 2008; Tapia-López et al., 2008; Garay-Arroyo et al., 2013; Chaiwanon et al., 2016; Moubayidin et al., 2016; Cajero Sánchez et al., 2018). To shed light on this matter, in this review we summarize and discuss the information regarding the effect of diverse hormones in each developmental zone that comprise the PR.

Hormone Function in the Meristematic Zone

As mentioned above, the MZ consists of two different domains: the proliferation domain (PD) and the transition domain (TD) (Verbelen et al., 2006; Ivanov and Dubrovsky, 2013; Salvi et al., 2020; **Figure 1**).

Hormone Control of Cell Division in the Proliferation Domain

As the proliferation domain (PD) is where most cells are produced (Ivanov and Dubrovsky, 2013; García-Gómez et al., 2017; **Figure 2B**) and most studies do not differentiate between the PD and the TD and treat them as the MZ, we will interpret the reported meristematic data as PD unless otherwise is indicated.

In the root auxin, GA and SL are hormones that promote cell division in the MZ. Regarding auxin, it has a maximum concentration in the QC cells where it is synthesized, high in the PD and relatively low in the EZ and the DZ (Blilou et al., 2005; Vieten et al., 2005; Petersson et al., 2009; Brunoud et al., 2012; Band et al., 2014). Application of low auxin levels (200 nM IAA) stimulate mitotic activity resulting in a larger MZ (Růzička et al., 2009; **Figure 2B**). In addition, the double LoF mutant in the auxin biosynthetic genes *WEI8*/*TAA1* and *TAR2* (*wei8 tar2*) does not have an identifiable MZ and the treatment with IAA, partially re-establish the meristem (Brumos et al., 2018). Auxin distribution in the MZ depends mainly on the action of the PIN-FORMED (PIN) proteins that are auxin efflux carriers differentially distributed in root tissues and this, in turn, regulates MZ size (Blilou et al., 2005; Vieten et al., 2005; **Figure 2A**). PIN proteins have phosphorylation-dependent polar localization in the plasma membrane and the overexpression of the protein kinase *PINOID* (*PID*) induces a basal-to-apical shift in PIN1, PIN2 and PIN4 localization in the MZ cells, altering the gradient of auxin and triggering a collapse of the MZ (Friml et al., 2004). A similar phenotype has been seen in the LoF of the protein phosphatase 2A (*PP2A*) that regulates apical-to-basal PIN cell localization (Michniewicz et al., 2007). The redundant function of the PIN proteins makes their analyses difficult and the single LoF mutants of *PIN* genes (*PIN1*, *2*, *3*, *4* and *7*) hardly affect MZ size while the double and triple mutants diminish it (Blilou et al., 2005). Contrary to the plasma membrane PIN proteins, the LoF mutants of *PIN5* and *PIN-LIKES 6* (*PILS6*), that are auxin carriers localized in the endoplasmic reticulum, have enlarged meristems; accordingly, the OE of anyone of both genes, have shorter meristems compared to WT (Mravec et al., 2009; Di Mambro et al., 2019; Feraru et al., 2019).

PLETHORA (PLT) genes are transcription factors (TF) induced and regulated downstream of the auxin signaling pathway and function in a dose-dependent manner to maintain cell proliferation in the PD (Galinha et al., 2007; Mähönen et al., 2014; Santuari et al., 2016; Scheres and Krizek, 2018; **Figure 2B**). *PLT1*, *PLT2*, *PLT3* and *PLT4* (*BABY BOOM*, *BBM*) are expressed

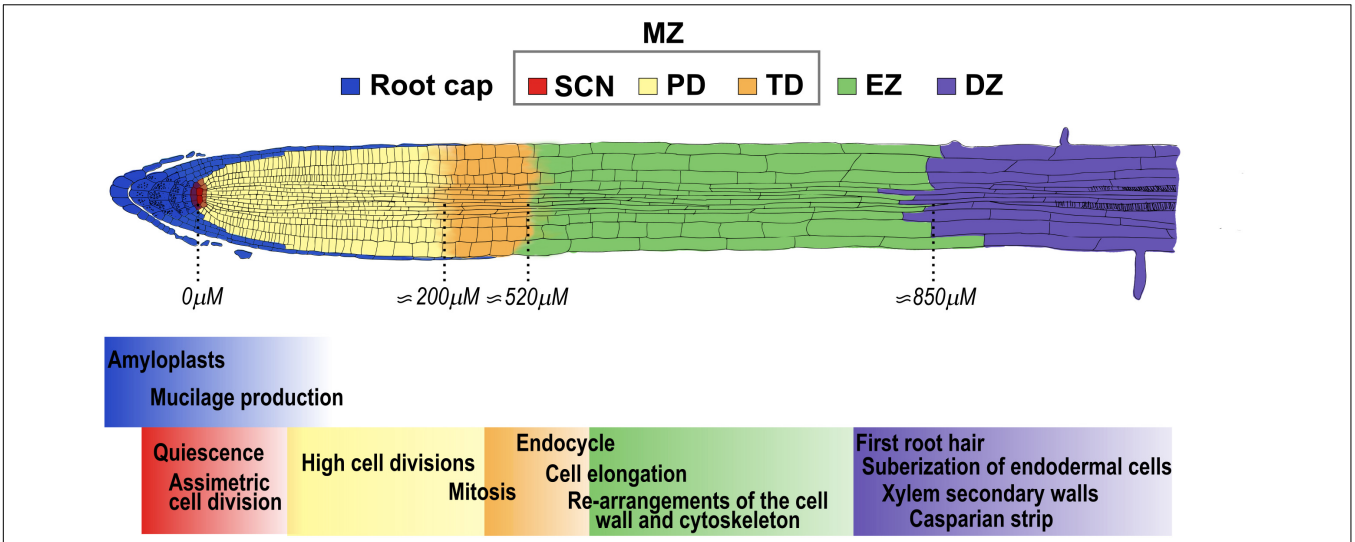

FIGURE 1 | Arabidopsis primary root developmental zones and domains. The root is composed from its tip along the longitudinal axis by the stem cell niche (SCN-red) that consists of stem cells that surround the Quiescent Center. The primary root is divided in three developmental zones: the meristematic zone (MZ), that includes the SCN, the proliferation domain (PD-yellow) and the transition domain (TD-orange); the elongation zone (EZ-green) and the differentiation zone (DZ-purple). The root cap (blue) surrounds the tip of the root until the end of the MZ. The approximate distance from the QC to the end of the PD, TD and EZ at 5 days after germination (5dag) WT seedlings is indicated below (Verbelen et al., 2006). The cellular functions that occur in each of the developmental zones and domains of the root are highlighted with the color that corresponds to each developmental stage.

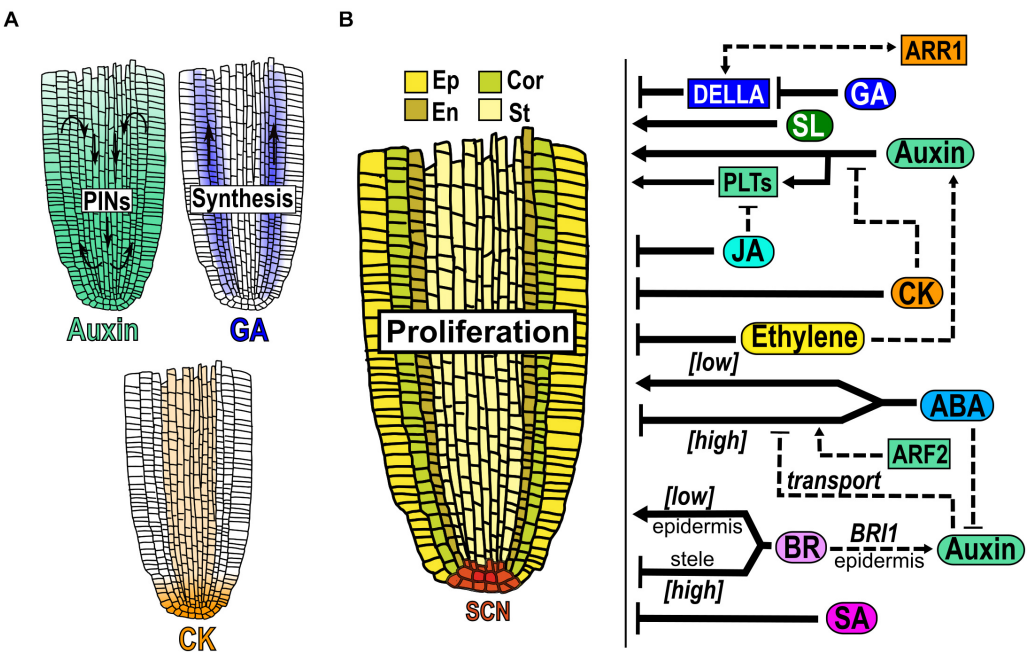

FIGURE 2 | Hormone function in the proliferation domain. **(A)** Hormones accumulation in the MZ. The auxin gradient (green) is established by the transport network formed by PIN efflux proteins and GA (blue) produced in the PD moves upwards this zone. GA is synthesized mainly in cortex and endodermis cells and CK (light orange) in vascular tissue. **(B)** Structure of the PD: the stem cell niche (SCN red) at the base produces cells that are incorporated to the PD where they proliferate at a high rate in either the epidermis (Ep), cortex (Cor), endodermis (En) and stele (St). At the right of the Figure is depicted the hormonal regulation (black arrows) and crosstalk (dotted arrows) over the MZ growth.

in the COL, SCN and PD, their proteins form gradients all over the PR and function redundantly to control meristem size (Galinha et al., 2007; Mähönen et al., 2014). Also, high levels of *PLT2* are related with slow division rates in the SCN, intermediate levels are required to maintain high cell division in the MZ, and low levels promote cell expansion and differentiation; in addition,

the OE of *PLT2* has a larger MZ (Galinha et al., 2007; Mähönen et al., 2014). The double mutant of *PLT1* and *PLT2* has a short MZ and the quadruple mutant (*PLT1*, *PLT2*, *PLT3* and *BBM*) is rootless (Aida et al., 2004; Galinha et al., 2007).

Besides, *MONOPTEROS* (*MP)/ARF5*, an auxin response factor, positively regulates the expression of miR390, which mediates the auxin responses in the MZ (Dastidar et al., 2019); its LoF mutant is rootless while the weak *mp/arf5* allele (*mpS319)* has short MZ in postembryonic development (Berleth and Jurgens, 1993; Konishi et al., 2015). Furthermore, the auxin signaling repressor *IAA3/SHORT HYPOCOTYL 2 (SHY2)* regulates the size of the MZ, since the GoF mutant of this gene (*shy2-2)* has a reduced MZ with less cells, while the LoF mutant (*shy2-31*) has a larger MZ than WT (Dello Ioio et al., 2008b; Moubayidin et al., 2010).

GA is produced in the meristem where the cortex and the endodermis are important sites of its biosynthesis (**Figure 2A**). This hormone is required for cell division and the EZ requires GA production or action from the MZ for cell elongation (Barker et al., 2020; **Figure 2B**). Besides, GA is a promoter of cell proliferation and addition of the biological active GA, increases the size of the MZ whereas the treatment with paclobutrazol (PAC), an inhibitor of GA synthesis, results in a reduced MZ (Ubeda-Tomás et al., 2009; Moubayidin et al., 2010, 2016; **Figure 2B**). GA modulates the MZ size via a DELLA dependent mechanism as the GA-deficient mutant *ga1-3* displays a reduction in MZ size which can be reverted when crossed with the quadruple LoF mutant of the negative regulators of GA signal transduction, the DELLAs *GIBBERELLIC ACID INSENSITIVE* (*GAI*), *REPRESSOR OF GA1-3* (*RGA*), *RGA-LIKE1* (*RGL1*), and *RGL2* (*gai-t6 rga-t2 rgl1-1 rgl2-1*) (**Figure 2B**). Indeed, *GAI* transcript accumulation in the endodermis of the MZ is sufficient to reduce the MZ size partially by enhancing the levels of two cell cycle inhibitors: *KIP-RELATING PROTEIN 2* (*KRP2*) and *SIAMESE* (*SIM*) (Ubeda-Tomás et al., 2008, 2009; Achard et al., 2009). The expression of the TF *SCARECROW* (*SCR*) in the endodermis of the LoF *scr-1* mutant, partially reestablishes the MZ size of the mutant (Sabatini, 2003). Interestingly, GA application increases the MZ size in WT plants but not in the *scr* mutant, showing that SCR is required to mediate this GA effect (Moubayidin et al., 2016). Additionally, epistatic genetic analysis showed that *RGA* and *SCR* participate in different signaling pathways controlling MZ size despite the fact that SCR controls the stability of this DELLA protein (Moubayidin et al., 2016).

In addition, treatment with the synthetic SL analog GR24 (2.5μM) increases PD size, compared to untreated plants (Ruyter-Spira et al., 2011; **Figure 2B**). Besides, the SL signaling mutant of *MORE AXILLARY GROWTH 2* (*max2*), the SL biosynthesis mutants *max1* and *CAROTENOID CLEAVAGE DIOXYGENASE 8* (*max4*), have shorter meristems than WT plants (Ruyter-Spira et al., 2011).

Conversely, CK, ethylene, JA and SA are hormones that inhibit cell division in the PD/MZ. CK concentration is lower in the MZ compared to the SCN (Antoniadi et al., 2015; **Figure 2A**). This hormone negatively controls the MZ size and positively the meristematic cell differentiation in a dose-dependent manner (Dello Ioio et al., 2007; Ishida et al., 2010; Takahashi et al., 2013; Street et al., 2015; **Figure 2B**). Diminishing CK levels and/or signaling results in a larger MZ and a delay in the onset of endoreplication as exemplified by the triple LoF mutant of isopentenyl transferase enzymes (IPTs) (*ipt3 ipt5 ipt7*) and in mutants affecting either the CK signal transduction pathway (*ARABIDOPSIS HISTIDINE KINASE 3/4* (*AHK3/4*) or type B *ARR1/12*) or by causing an increase in CK catabolism by the OE of *CYTOKININ OXIDASE/DEHYDROGENASE* (*CKX*) (Werner et al., 2003; Dello Ioio et al., 2007; Ishida et al., 2010; Takahashi et al., 2013; Street et al., 2016). Moreover, the double mutant (*phb phv*) of the LoF of *PHABULOSA* (*PHB*) and *PHAVOLUTA* (*PHV*), that are members of the TFs HD-ZIPII family, has a longer meristem than WT plants in control conditions and the CK treatment restores the root phenotype to WT (Dello Ioio et al., 2012).

Ethylene, as CK, negatively regulates the MZ size in a dose-dependent manner (Street et al., 2015; Zdarska et al., 2019; **Figure 2B**). Furthermore, ethylene reduces the activity of a cell cycle reporter (*CYCB1;1-GUS*) in the PD, which is reverted by the co-treatment with an ethylene inhibitor (1-methylcyclopropene, 1-MCP). Interestingly, *CYCB1;1* expression is not affected in response to ethylene, suggesting post-transcriptional regulation (Street et al., 2015). In addition, the LoF of the *CONSTITUTIVE TRIPLE RESPONSE 1* (*CTR1-2*), a negative regulator of ethylene pathway, has a shorter MZ. Consistently, the LoF mutant *etr1-1*, an ethylene insensitive mutant, has longer MZ than WT plants (Street et al., 2015; Méndez-Bravo et al., 2019; Zdarska et al., 2019).

JA treatment reduces the MZ size in a *COI1*/*MYC2* dependent manner (**Figure 2B**) by repressing the expression of cell cycle genes like *CYCB1;1*, *CYCLIN DEPENDENT KINASE A;1* (*CDKA;1)*, *KRP1* and *PROLIFERATING CELL NUCLEAR ANTIGEN* (*PCNA1)* (Chen et al., 2011). Similarly, SA treatment reduces the MZ size (**Figure 2B**) and the expression of *CYCB1;1* (Pasternak et al., 2019).

Additionally, ABA and BR can either promote or inhibit PD/MZ activity in a dose-dependent fashion. Low exogenous ABA concentrations (0.5 μM) increases the MZ size (Zhang et al., 2010), whereas high concentrations (30 μM) inhibit it compared to control conditions (Yang et al., 2014; **Figure 2B**). Interestingly, the MZ size inhibition by ABA can be partially recovered by the co-treatment with the reducing agent glutathione (GSH), suggesting that ABA controls the MZ size through reactive oxygen species (ROS) regulation (Yang et al., 2014). Curiously, it has been reported that local application of ABA to the shoot, in a concentration that when applied to the roots inhibits MZ size (2 μM), positively regulates the MZ size compared to control conditions (Xie et al., 2020). This ABA effect is mediated by the long-range transport of auxin from the shoot to the root, that promotes cell division in the MZ (Xie et al., 2020).

Plants treated with high concentrations of 0.4–4 nM of BR, have a shorter MZ than untreated plants, whilst 0.04nM of BR increase the MZ size (González-García et al., 2011; Chaiwanon and Wang, 2015; Li et al., 2020; **Figure 2B**). Accordingly, low BR concentrations (50 pM) could rescue MZ length whereas higher concentrations (1 nM and 100 nM) reduce the MZ size in the BR-deficient mutant *dwf4* (González-García et al., 2011;

Chaiwanon and Wang, 2015). Also, low endogenous BR levels or high BR response that can be obtained either with mutations in BR biosynthesis and signaling genes (*de-etiolated 2* (*det2-1*), *bri1-5, BES1-RNAi* or the GoF mutant *bin2*-1) or with the GoF of *BRI1-EMS-SUPPRESSOR 1* (*BES1; bes1-D*), with enhanced BR signaling, lead to plants with shorter MZ than WT (González-García et al., 2011; Hacham et al., 2011). Concordantly, the triple LoF mutant of the negative regulator *BRASSINOSTEROID INSENSITIVE 2* (*BIN2)* and its two homologs *BIN2-LIKE1* (*BIL1)* and *BIL2* (*bin2-3 bil1 bil2*) show a larger MZ (González-García et al., 2011; Li et al., 2020). In addition, the BR-insensitive mutant *bri1-116*, has a shorter MZ than WT, due to a decrease in the cell cycle progression that can be reverted to WT plants in the double mutant with the OE of *CYCD3;1* (*bri1-116 CYCD3;1*OE) (González-García et al., 2011; Hacham et al., 2011). Interestingly, the BR effect over the meristem cell proliferation or cell differentiation depends on the cell type where it is active: in the epidermis, BR signaling is necessary to induce the number of proliferating cells whilst in the stele it promotes cell differentiation (Hacham et al., 2011; Vragović et al., 2015). Furthermore, the MZ length of the single mutant of the receptor *BRASSINOSTEROID INSENSITIVE 1* (*BRI1; bri1*) and the triple mutant of *BRI1* with *BRI1 LIKE1* (*BRL1*) and *BRL3* (*bri1 brl1 brl3*) are bigger than WT if *BRI1* is expressed in the epidermal non-hair-cells (Hacham et al., 2011; Vragović et al., 2015; **Figure 2B**). Also, the expression of the GoF of *BRASSINAZOLE RESISTANT 1* (*BZR1; bzr1-1D*) or *BRI1* in the epidermis in the *bri1* LoF mutant background can rescue the MZ size (Chaiwanon and Wang, 2015). Contrarily, the expression in the stele of *BRI1* counteracts the proliferation induced by epidermal *BRI1* expression (Vragović et al., 2015; **Figure 2B**). All these data suggest the importance not only of BR dosage but also the cell type where it is active to control the MZ size.

The CK and auxin crosstalk is well described, and it is known to regulate the MZ size by controlling the transition from proliferation to elongation (Salvi et al., 2020). CK interferes with auxin responses and transport in the MZ as follow: *SHY2/IAA3* is positively regulated by ARR1 and is sufficient to mediate ARR1 function in the MZ size, because the OE of *ARR1* in the LoF mutant *shy2-31*, does not show a MZ reduction. In addition, the double mutants, *arr1-3 shy2-2* and *arr1-3 shy2-31* have the same MZ size than the single *arr1-3* mutant (Dello Ioio et al., 2008b). Moreover, SHY2 in turn, negatively regulates the expression of the efflux auxin transporters (PINs) (Dello Ioio et al., 2008b). Besides, the MZ size of the double and triple auxin influx transport with CK signaling mutants, *aux1 arr12* and *aux1 arr1 arr12*, is higher than *aux1* single mutant and WT plants but identical to the single *arr12* or the double *arr1 arr12* CK signaling mutants, suggesting that CK is epistatic to auxin in this phenotype (Street et al., 2016; **Figure 2B**) (more details on CK-auxin crosstalk are also described in the TD section). Additionally, the tryptophan (Trp) synthesis gene *ANTHRANILATE SYNTHASE B1 (ASB1)*, which is expressed in the MZ, is also regulated by CK via ARR1 (Moubayidin et al., 2013).

JA negatively regulates the expression of *PLT1* and *PLT2* genes through the direct repression by the TF *MYC2* (**Figure 2B**). Interestingly, the double mutant *plt1-4 plt2-2* is less inhibited by JA application than WT, but the hormone still reduces the MZ size of this mutant (Chen et al., 2011) suggesting the existence of also a PLT-dependent mechanism by which JA regulates the meristem.

CK participates in the ethylene inhibition of the MZ size as the LoF mutants of the CK TFs, *ARR1* and *ARR3*, are less responsive to ethylene inhibition of MZ size than WT plants and it has been described that CK induces ethylene biosynthesis (Chae et al., 2003; Street et al., 2015; Zdarska et al., 2019). Interestingly, the ethylene-insensitive mutants (*etr1-1* and *ein2-1*) reduce the MZ responsiveness only at low CK concentrations (0.1 and 1 μm) but not at high CK levels (10μm) (Street et al., 2015). Moreover, the co-treatment with an ethylene inhibitor (1-MCP) partially alleviates the CK inhibition of the MZ size compared to plants only treated with CK, confirming a role for ethylene in cytokinin response in the MZ size (Street et al., 2015; **Figure 2B**).

Compared to CK and JA, that negatively impact on auxin function in the MZ, ethylene enhances local IAA production (**Figure 2B**) by promoting the transcript accumulation of two genes that participate in auxin biosynthesis, *WEI8/TAA1* and *TAR2* (Stepanova et al., 2008). Moreover, ethylene application or the LoF of *CTR1,* stimulates *AUX1* and *PIN2* expression and promotes auxin movement throughout the PD, especially from the root tip to the TD and EZ. This auxin re-distribution is not observed in the auxin transport (*aux1)* and synthesis *(wei2* and *wei7)* mutants, where the co-treatment with ethylene promotes auxin accumulation strictly limited to cells of the COL and part of the PD (Stepanova et al., 2005, 2007; Rùžièka et al., 2007; Swarup et al., 2007; Méndez-Bravo et al., 2019; **Figure 2B**). In addition, the *pin2* LoF mutant has a longer MZ, but the double mutant *ctr1-1eir1-1*(*pin2*) has a total absence of the MZ (Méndez-Bravo et al., 2019).

Regarding auxin and its crosstalk with the biphasic hormones that participate in the MZ, it has been shown that the induction of cell proliferation in the MZ caused by *BRI1* expression in epidermis is achieved by increasing the auxin concentration in this zone through the upregulation of auxin transporters (Vragović et al., 2015; **Figure 2B**). Besides, mutations in the auxin biosynthesis (*taa1*) or the efflux transport (*pin2*) genes revert the enlarged MZ size observed when *BRI1* is overexpressed only in the epidermis in the triple mutant *bri1 brl1 brl3* (Vragović et al., 2015). Furthermore, the MZ size of the triple *PILS* mutant (*pils235*) is more whereas the OE of *PILS5* is less inhibited to BR treatment than WT plants (Sun et al., 2010).

ABA downregulates the levels of auxin response in the PD (He et al., 2012; **Figure 2B**). Also, *ARF2* positively regulates MZ size in response to ABA, since its length is considerably reduced in the *arf2-101* mutants treated with ABA (**Figure 2B**). Besides, *arf2-101 pin4-3* and *arf2-101 pin1-1* double mutants, have a larger MZ than the single mutant (*arf2-10*1), suggesting that *PIN1* and *PIN4* counteract the ABA effects in the MZ size of *arf2-101* (Promchuea et al., 2017; **Figure 2B**). ABA negatively regulates *PLT1* and *PLT2* expression through *ARF2*, and the OE of *PLT2* in *arf2-101* mutant enhances MZ size compared to either the single mutant or the OE line and this phenotype can be partially inhibited by ABA treatment (Promchuea et al., 2017).

During the early stages of meristem development, GA regulates the MZ size by suppressing CK signaling (Moubayidin et al., 2010). GA targets the degradation of the DELLA protein RGA that positively regulates the expression of *ARR1* and *SHY2* thus repressing CK signaling and inducing auxin responses in the MZ. Also, auxin negatively regulates the expression of *SHY2* that down regulates PINs expression and, therefore, auxin movement (Dello Ioio et al., 2008b; Moubayidin et al., 2010; **Figure 2B**). In addition, in the single *arr1-3* and in the double *arr1-3 arr12-1* CK signaling mutants, the promoter effect of GA or the inhibitor effect of PAC at 5 dag, is lost and the MZ size is as in control conditions (Moubayidin et al., 2010; **Figure 2B**). Furthermore, the induction of ARR1 protein translocation into the nucleus causes a reduction in root MZ size that can be reverted by GA treatment that depletes DELLAs from PR cells (Marín-de la Rosa et al., 2015). These data suggest that the interaction between type-B ARR, DELLA and auxin transport proteins are required to establish the MZ size.

Transition Domain Regulation by Hormones

The cell cycle of the transition domain (TD) cells is changing from cell division to endoreduplication, in which cells undergo several cycles of DNA replication with no cytokinesis (Verbelen et al., 2006; Bhosale et al., 2018; Salvi et al., 2020; **Figure 3A**). Moreover, these cells continue to grow at the same rate as in the PD but the frequency of division decreases resulting in the coexistence of cells that may still divide with others that undergo endoreduplication and are relatively larger than those in the PD (Ivanov and Dubrovsky, 2013). TD cells also have re-arrangements of the cell wall and cytoskeletal organization, high fluxes of ions, auxin and oxygen, and a high rate of vesicle recycling and vacuolization, to prepare for the fast elongation that takes place in the EZ (Verbelen et al., 2006; Baluška and Mancuso, 2013; Salvi et al., 2020). In addition, TD integrates external and internal signals, including hormonal responses, to determine cell fate and root growth (Baluška et al., 2010; Baluška and Mancuso, 2013; Kong et al., 2018). In this domain, the root cell elongation is controlled, among others, by α-expansins which are proteins that are activated by low apoplastic pH and allow the loosening of the cell wall and turgor−driven cell expansion (Cosgrove, 2005; Pacifici et al., 2018). Changes in the TD have been quantified as TD cell number, TD position regarding its distance from the QC or through the meristematic cell transition to elongation that can either reduced or increment the MZ (Dello Ioio et al., 2007, 2008b; Di Mambro et al., 2017; Pacifici et al., 2018).

It has been described that auxin, ABA and SL inhibit the transition from proliferation to elongation. An auxin minimum in the TD is necessary for the transition to elongation and perturbation of this minimum changes the TD position and the MZ size (Di Mambro et al., 2017; Kong et al., 2018; **Figure 3B**). In addition, lowering auxin levels reduces mitosis downregulating the expression of mitotic cell cycle genes and increasing the endocycle (Ishida et al., 2010; **Figure 3A**). As in the PD, PIN expression and distribution are also important in the TD to create the auxin reflux along the meristem (Blilou et al., 2005; Verbelen et al., 2006; Petrášek and Friml, 2009; Baluška et al., 2010; Salvi et al., 2020). Accordingly, different mutants defective in biosynthesis, transport or signaling of auxin, promotes the transition from mitotic to endocycle regulation and the TD appears proximally to the QC whereas increasing auxin levels, delays the onset to endocycling and elongation (Ishida et al., 2010; **Figure 3A**). Interestingly, the OE of *CYCA2;3* partially reverts the early entry into the endocycle and the short meristem induced by the auxin antagonist (2-(1H-Indol-3-yl)-4-oxo-4-phenyl-butyric acid; PEO-IAA) (Ishida et al., 2010). Also, the mutant of *GRETCHEN HAGEN 3.17* (*GH3.17; gh3.17–1*), a gene that encodes an IAA amino acid synthase conjugating auxin with amino acids to decrease the free auxin levels, shows an increment of free auxin and has a TD that appear distally with a delay in the onset to endocycling and cell differentiation (Di Mambro et al., 2017). Accordingly, the OE of *GH3.17* decreases auxin levels, and the position of the TD appears proximally with a premature transition to cell elongation compared to WT (Di Mambro et al., 2017).

ABA also suppresses the differentiation and positively regulates RAM size; application of ABA (0.5μM) increases the cell number in the TD resulting in a longer meristem. Accordingly, fluridone treatment, an inhibitor of ABA, reduces the TD cell number and the MZ size (Zhang et al., 2010; Takatsuka and Umeda, 2019; **Figure 3A**). Similarly, treatment with SL (2.5μM), increases the size of the TD and the cell number and decreases the cell length in the TD, compared to untreated plants, suggesting an effect of SL in the regulation of cell relative growth in the TD (Ruyter-Spira et al., 2011; **Figure 3A**).

CK, BR and ethylene are hormones that promote the transition from proliferation to elongation. CK synthesis and signaling genes such as *IPT7*, *ARR1* and *ARR12*, are expressed in the vascular tissue of the TD where CK regulates cell differentiation by antagonizing auxin signaling (Miyawaki et al., 2004; Dello Ioio et al., 2007; Salvi et al., 2020; **Figure 3B**). It has been described that the specific expression of *CKX1*, which catalyzes the degradation of CK, in the vascular tissue of the TD, results in an enlargement of the MZ and a delay in cell differentiation (Dello Ioio et al., 2007). Also, elevated CK levels change the position of the TD closer to the QC, leading to a shorter meristem, whilst low CK displaces the TD distally to the QC, generating a longer meristem (Dello Ioio et al., 2007). The treatment with CK reduces the number of TD cells and the CK signaling mutants *ahk3/4* and *arr2* have more TD cells than WT (Takatsuka et al., 2018; Takatsuka and Umeda, 2019; **Figure 3A**). Besides, CK stimulates the transition to endocycling through the positive and direct regulation of the anaphase promoting complex/cyclosome (APC/C) activator *CELL CYCLE SWITCH PROTEIN 52A* (*CCS52A1*) expression by ARR2 (**Figure 3A**; Takahashi et al., 2013).

Several expansins and H^+-ATPases regulate cell growth in the TD and their expression depends partially on CK signaling (Pacifici et al., 2018). Besides, CK also participates in the reorganization of actin, which is involved in cell elongation that begins in the TD (Takatsuka et al., 2018). Moreover, the GoF of *PHB* (*phb-1d*), has a short meristem and the TD is closer to the QC compared to WT plants and, interestingly, the expression of *CKX1* in the TD is sufficient to restore the MZ size in *phb-1d/* + mutant indicating that *PHB* functions on TD

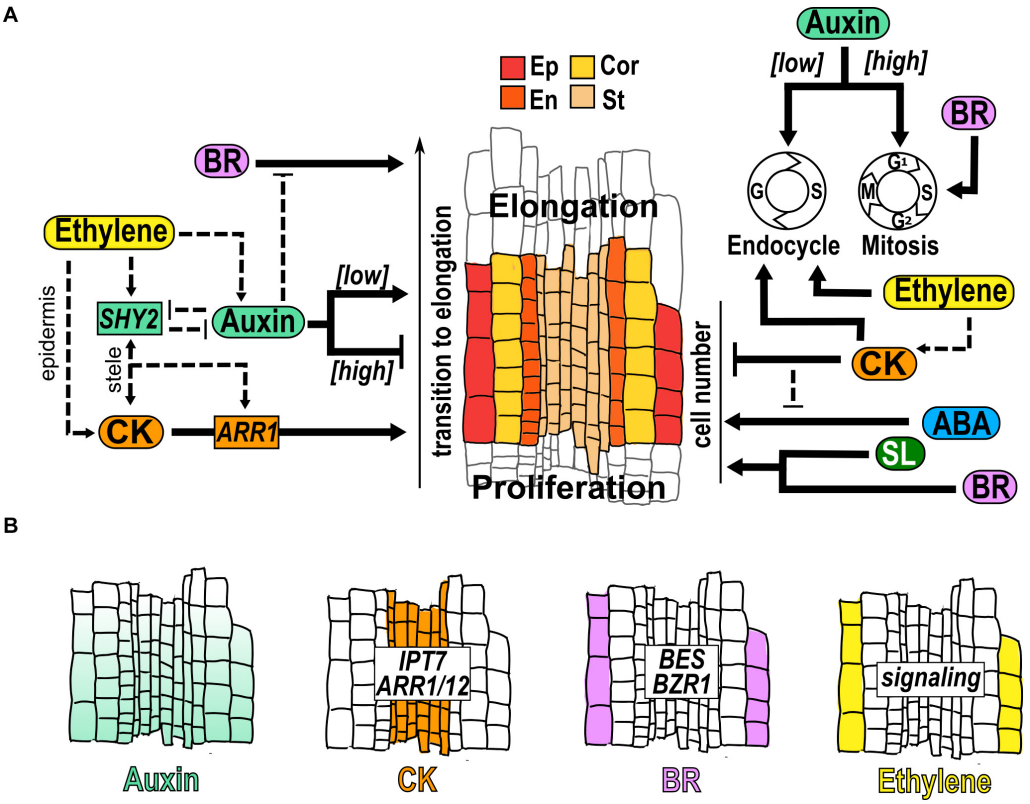

FIGURE 3 | Hormone function in the transition domain. **(A)** Structure of the TD that is a region flanked by the dividing cells of the PD and the elongating cells in the EZ. The cells of different tissues are indicated: epidermis (Ep), cortex (Cor), endodermis (En) and stele (St); and hormonal regulation (black arrows) and crosstalk (dotted arrows) over the control of the transition to elongation, the TD cell number and the control of endocycle, conformed by Gap (G) and Synthesis (S); and Mitosis (M), conformed by Gap1 (G1), S, Gap2 (G2) and M is indicated. **(B)** Hormone accumulation (different colors), expression pattern of genes and hormonal pathways that participate in the TD.

are dependent on CK (Dello Ioio et al., 2012). Furthermore, *PHB* enhances the CK biosynthesis inducing the expression of *IPT7* in the pro-vascular cells of the meristem and it has been suggested that CK moves to the TD and promotes the transition of cells from the TD to the EZ (Bishopp et al., 2011; Dello Ioio et al., 2012).

In the TD, BR functions as a promoter of the transition from proliferation to elongation (**Figure 3A**). Accordingly, *bri1* mutant has a defective cell cycle activity and cell expansion, that leads to a significantly reduced TD, with less and shorter cells compared to WT (Hacham et al., 2011). Moreover, a similar phenotype is detected in the BR biosynthesis mutant *constitutive photomorphogenesis and dwarfism* (*cpd*), with few cells in the TD (Hacham et al., 2011; **Figure 3A**). In this domain, BR signaling is high in the two outermost cell types (epidermis and lateral root cap) but BR responsive genes are only high in the epidermis (Vragović et al., 2015). The concentration of the proteins encoded by the TFs *BZR1* and *BES* is highest in the epidermal cells of the TD and a gene construction that expresses the activated *BZR1* in the TD epidermis, rescues the reduction of MZ and EZ that occurs in *bri1-116* mutant (Chaiwanon and Wang, 2015; **Figure 3B**).

Ethylene treatment induces a rapid increase in endoreduplication and nuclear area in the TD compared to control conditions (**Figure 3A**) and this increment in endoreduplication is not present in the ethylene insensitive mutants (*etr1-1* and *ein2-50*) in response to ethylene (Street et al., 2015). It would be interesting to investigate if this regulation over endoreduplication affects the length and/or the number of TD cells.

In the TD an interplay between diverse hormones occurs; two of the most characterized that participate in the establishment and maintenance of this domain, are auxins and CK that are interlinked and act antagonistically (Dello Ioio et al., 2008a; Di Mambro et al., 2017; Kong et al., 2018; Salvi et al., 2020). This crosstalk relies on several mechanisms: ARR1 and ARR12 up-regulate the transcript accumulation of the auxin signaling repressor *IAA3/SHY2*, which is expressed in the vasculature of the TD (**Figure 3A**). SHY2 down regulates the transcript accumulation of several auxin efflux transporters affecting the accumulation and distribution of auxin in the TD (Dello Ioio et al., 2008b; Moubayidin et al., 2010; Takahashi et al., 2013; **Figure 3A**). In addition, auxin mediates the degradation of SHY2 that upregulates *IPT5* and *ARR1* transcript accumulation and CK biosynthesis in the vascular

bundle of the TD (Dello Ioio et al., 2008b; Moubayidin et al., 2013) (**Figure 3A**).

Moreover, in the epidermal cells of the TD, BZR1 target genes tend to be induced by BR but repressed by auxin and the application of IAA causes a diminished nuclear accumulation of BZR1 and its subsequent localization in the cytoplasm, which is associated with low BR signaling (Chaiwanon and Wang, 2015; **Figure 3A**). Interestingly, ethylene also induces the expression of *SHY2* that is indispensable for the negative effect of ethylene on the MZ size (Street et al., 2015) (**Figure 3A**). Ethylene signaling response is detected in the epidermis of the TD (**Figure 3B**) where it regulates the pH of the apoplast via positive regulation of auxin biosynthesis and responsiveness in the root tip, showing the interdependence of ethylene and auxin to regulate root growth (Vaseva et al., 2018; **Figure 3A**). Furthermore, the CK-responsive construct (*pTCSn:GFP*) is also induced by ethylene predominately in the epidermal cells of the TD and it is abolished in the *etr1-1* mutant but not in *ein2-1* mutant, indicating that ethylene regulation of CK is via *ETR1* pathway but independently of the canonical *EIN2* pathway (Zdarska et al., 2019).

Finally, ABA treatment (0.5 and 10 μM) enhances the number of cells in the TD in WT plants but not in the *ahk3/4* and *arr2* mutants that show a similar number as in control conditions (Takatsuka and Umeda, 2019; **Figure 3A**).

Hormone Function in the Elongation Zone

The cells in the elongation zone (EZ) have a rapid anisotropic growth accompanied by cell wall loosening, endoreduplication and changes in the organization of the microtubules (Dolan and Davies, 2004). In the EZ the cells do not divide and can increase their length three times in only 3 h (Verbelen et al., 2006; Salvi et al., 2020; **Figure 1**). Recently, it was discovered that in seedlings where the shoot is removed, the EZ is displaced toward the root tip, indicating that the aerial part of the plant can send signals to maintain root growth (Baskin et al., 2020). In addition, hormones regulate the expression and function of enzymes that participate in cell wall modifications in the EZ similarly to what happened in TD cells (Wu and Cosgrove, 2000; Somssich et al., 2016; Barbez et al., 2017; Dietrich, 2018). As we will discuss below, many hormones are involved in the regulation of cell elongation.

In the EZ, GA and BR are hormones that act as positive regulators of cell elongation. GA is synthesized mainly in the endodermal cells of the MZ but the bioactive GA is accumulated in the endodermal, cortical and epidermal cells of the EZ where it contributes to the regulation of cell elongation (Ubeda-Tomás et al., 2008; Shani et al., 2013; Rizza et al., 2017; Barker et al., 2020; **Figure 4A**); but GA-responses in the endodermis are sufficient to regulate cell expansion (Ubeda-Tomás et al., 2008; Rizza et al., 2019). Also, it has been proposed that the levels of GA in the EZ have a graded distribution due to dilution given the rapid cell growth, resulting in a subsequent increase in DELLAs concentration toward the end of the EZ that could function as a mechanism to terminate the elongation (Band et al., 2012). Lowering GA levels, with PAC, an inhibitor of GA synthesis, or blocking the GA response in endodermis, using a GA-insensitive mutant form of the DELLA protein GAI, provokes a reduction in cell elongation (Ubeda-Tomás et al., 2008, 2009; Band et al., 2012; **Figure 4B**).

Application of BR (100 nM) promotes cell elongation in the EZ and the BR signaling proteins *BZR1* and *BES* concentrate at high levels in the epidermal cells of this zone (Chaiwanon and Wang, 2015; **Figure 4A**). Besides, BR acts a positive regulator of cell elongation, since the LoF mutants *bri1-116* and the triple mutant *bri1 brl1 brl3* have a significantly shorter elongated cells, while the OE of *BRI1* and *bes1-D* have larger fully elongated cells than WT plants (González-García et al., 2011; Hacham et al., 2011; Kang et al., 2017; **Figure 4B**). Moreover, in the BR-deficient mutant, *dwf4*, the treatment with either low or high BR concentrations can rescue the size of the fully elongated cells (Chaiwanon and Wang, 2015). In addition, BZR1 is maintained at high levels in the nucleus in the EZ, promoting cell elongation via upregulation of genes induced by BR as cell-wall proteins and its expression in the epidermis rescues the size of the fully elongated cells of the *bri1-116* mutant phenotype (Chaiwanon and Wang, 2015), indicating that it is its main site of action (**Figure 4A**). Interestingly, *BRI1* expression promotes cell elongation of hair (trichoblasts) cells while inhibits in non-hair (atrichoblasts) cells (Hacham et al., 2011; Fridman et al., 2014; Vragović et al., 2015).

Several hormones such as CK, Ethylene, JA, SA and auxin, act as negative regulators of cell elongation. CK application reduces cell elongation (**Figure 4B**; Beemster and Baskin, 2000) and re−organized the cortical microtubules at the EZ from a transversal to an oblique disposition, which is associated with termination of cell expansion (Montesinos et al., 2020). Furthermore, the length of the completely elongated cells is larger in *arr1 arr12* double mutants than in WT plants (Street et al., 2016; **Figure 4B**). Similarly, application of either the ethylene precursor 1-aminocyclopropane-1-carboxylic acid (ACC), SA or JA inhibits cell elongation compared to WT plants (Rùžièka et al., 2007; Chen et al., 2011; Pasternak et al., 2019; **Figure 4B**). Moreover, the single or double LoF mutants of the JA negative regulator, *NOVEL INTERACTOR OF JAZZ* (*NINJA)* and of the gene that encodes the enzyme ALLENE OXIDASE SYNTHASE (AOS), have shorter fully elongated cells than WT plants (Acosta et al., 2013).

Auxin conjugation and auxin perception/signaling are important for apoplast acidification and promotion of cell elongation; the inducible expression of *GH3.6*, the triple mutant of the auxin receptors *TRANSPORT INHIBITOR RESPONSE1* (*TIR1*)*/Auxin-Binding F box* (*AFB*s) (*tir1afb2afb3*), the GoF of *bodenlos* (*iaa12/bdl*) mutant and the double mutant *arf10 arf16*, have a higher apoplastic pH with smaller EZ epidermal cells compared to WT (Barbez et al., 2017). Interestingly, the root cell elongation is also inhibited using a high IAA concentration (250nm) or in the OE of *YUC6* compared to control conditions, probably by a transitory alkalinization of the apoplast (Barbez et al., 2017; **Figure 4B**). Moreover, cells in the EZ have transversal microtubules that are more sensitive to auxin−driven reorientation of the microtubule network to longitudinal disposition than in other PR zones leading to a reduced cellular elongation rate (Montesinos et al., 2020). Additionally, many different PIN mutants have a

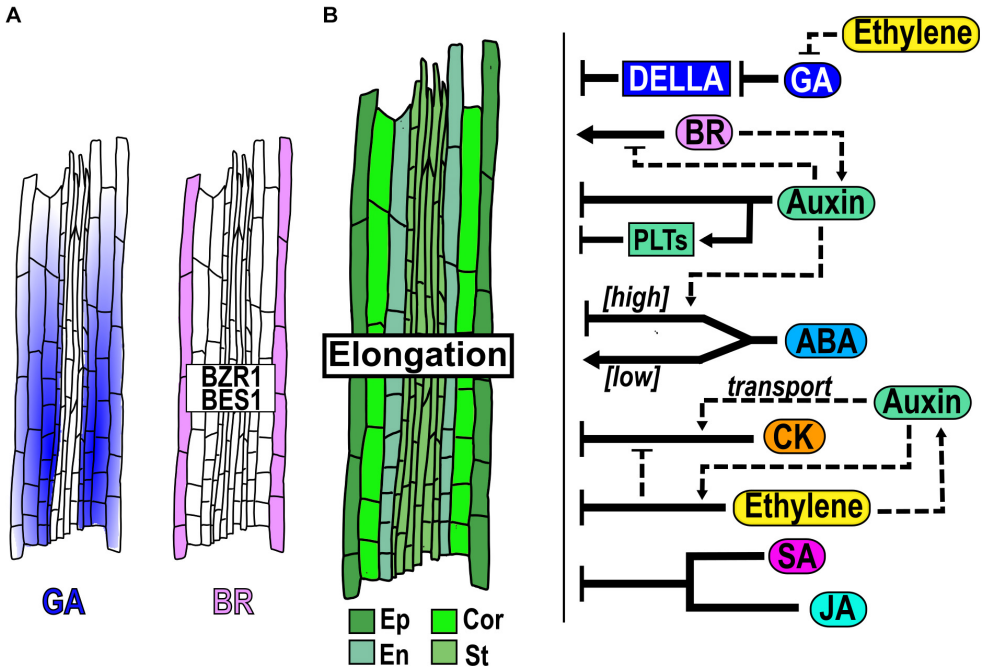

FIGURE 4 | Hormone function in the elongation zone homeostasis. **(A)** Hormone accumulation and expression pattern of genes that participate in the EZ. **(B)** Structure of the EZ, with cells from different tissues: epidermis (Ep), cortex (Cor), endodermis (En) and stele (St) and hormonal regulation (black arrows) and crosstalk (dotted arrows) function in the EZ.

reduction in the cell elongation size compared to WT and high levels of *PLT2* expression or PLT2 protein in the EZ inhibit cell elongation (Galinha et al., 2007; Mähönen et al., 2014) (Blilou et al., 2005).

In addition, the treatment with high levels of ABA (30μM) significantly reduces cell elongation, while low levels of ABA treatment (100 nM) increase it (Dietrich et al., 2017; Promchuea et al., 2017; **Figure 4B**). Furthermore, the *snrk2.2 snrk2.3* double mutant of the ABA signaling kinase is insensitive to the promotion of cell elongation at low (100 nM) ABA levels (Dietrich et al., 2017). Interestingly, the application of ABA (2μM) in the shoot promotes a significant increment in root cell elongation compared to control conditions. This might be mediated by long-distance transport of an output of the ABA signaling transduction pathway in the shoot, since this hormone does not diffuse into the roots (Xie et al., 2020).

There is an interplay between different hormones in the regulation of cell elongation. For instance, ABA treatment reduces the cell elongation of the *arf2-101* mutant, compared to WT plants, but does not alter the cell number (Promchuea et al., 2017). In the case of auxin and its interaction with ABA, the double mutants *arf2-101 pin1-1* and *arf2-101 pin4-3* have longer cells in the EZ than the *arf2-101* single mutant in response to ABA treatment (Promchuea et al., 2017; **Figure 4B**).

As described above, BR induce cell elongation, whilst auxin deficiency or high exogenous or endogenous concentrations, inhibits it (Barbez et al., 2017). Accordingly, auxin treatment induces cytoplasmic localization of BZR1 in the EZ reducing its nuclear accumulation that results in a decrease in BR signaling in this zone (Chaiwanon and Wang, 2015). While BR treatment (100 nM) promotes cell elongation, the co-treatment of BL with high auxin (5μM) enhances the inhibitory effect of auxin over cell elongation (Chaiwanon and Wang, 2015; **Figure 4B**).

Auxin interacts with CK and ethylene, which also function as negative regulators of cell elongation. The influx carrier AUX1 is required for the CK responses as the *aux1* mutant is insensible to CK inhibition of cell elongation compared to the WT (Street et al., 2016; **Figure 4B**). Additionally, the completely elongated cells of *aux1 arr12* and *aux1 arr1 arr12* mutants are also insensitive to CK inhibition compared to WT plants and control conditions, whereas the *arr12* single mutant has the same CK sensitivity as the WT, regarding the length of elongated cells (Chaiwanon and Wang, 2015). Also, high concentrations of ethylene inhibit epidermal cell elongation and this inhibition is dependent on the promotion of the basipetal auxin transport mediated by AUX1 and PIN2, as well as by the auxin biosynthesis in the EZ (Růžička et al., 2007; Swarup et al., 2007) (**Figure 4B**). Moreover, auxin function in the EZ makes cells more sensitive to ethylene; high auxin levels in the TD activate ethylene signaling in the EZ and represses cell elongation (Stepanova et al., 2007). Besides, ethylene effects on cell elongation are diminished in the *pin2/eir1-1, aux1-T* mutants and in the OE line of *PIN1,* indicating a key role of basipetal auxin transport in such responses (Růžička et al., 2007).

Interestingly, ethylene seems to act as a negative regulator of cell elongation by inhibiting GA uptake, accumulation and distribution in the endodermis of the EZ (Shani et al., 2013; **Figure 4B**). Furthermore, CK regulates the inhibition of cell

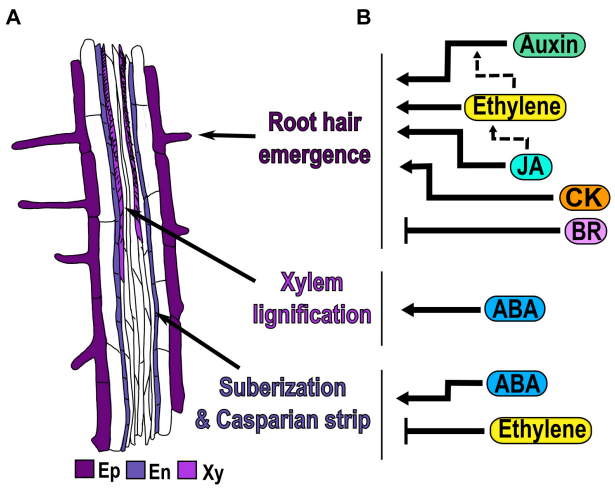

FIGURE 5 | Hormonal regulation of cell differentiation. **(A)** Morphological markers of cell differentiation are the emergence of the first epidermal (Ep) root hair, the xylem (Xy) lignification, the suberization of endodermal (En) cells and the presence of the Casparian strip. **(B)** Hormone regulation (black arrows) and crosstalk (dotted arrows) in each of the three differentiation processes.

elongation partially in an ethylene dependent pathway since the ethylene insensitive *ein2* mutant shows less reduction on cell elongation in the EZ in response to CK compared to WT (Street et al., 2016; **Figure 4B**).

Differentiation Zone Regulation by Hormones

In the differentiation zone (DZ) the cells stop elongating and acquire the final characteristics of mature cells (**Figure 1B**). One of the morphological markers of the beginning of the DZ is the appearance of the first epidermal root hair (Dolan et al., 1993; Verbelen et al., 2006; Cajero Sánchez et al., 2018; Salvi et al., 2020; **Figure 5A**). Epidermal cells differentiate into trichoblasts and atrichoblasts, depending on their contact with the underlying cortical cells: cells contacting two cortical cells develop root hairs, whereas non-hair cells overlie just in one cortical cell (Schiefelbein et al., 2009; Shibata and Sugimoto, 2019). In Arabidopsis, these cells are organized in alternated files, with the hair cells files regularly separated by two non-hair cell files (Ishida et al., 2008). Other morphological characteristics of differentiated root cells are the formation of xylem secondary walls in the pro-vasculature, and the Casparian strip and suberization of endodermal cells (Dolan et al., 1993; Somssich et al., 2016; Cajero Sánchez et al., 2018; **Figure 5A**).

In this section we focus on the function of hormones in the emergence of root hairs, the lignification of xylem cells and the suberization of endodermal cells as developmental processes that take place in the DZ (**Figure 5A**). There are other excellent reviews that have information regarding root hair elongation (Carol and Dolan, 2002; Libault et al., 2010; Salazar-Henao et al., 2016; Vissenberg et al., 2020) and vascular patterning (Kondo et al., 2014; Smet and De Rybel, 2016; Vaughan-Hirsch et al., 2018; Ramachandran et al., 2020), processes that will not be addressed here.

Auxin, ethylene, CK and JA are hormones that act as positive regulators of root hair emergence in the DZ. The Arabidopsis hairless mutant *root hair defective 6 (rhd6)* can be rescued by the treatment with auxins, CK or ethylene that cause an increase in the frequency of root hairs (Masucci and Schiefelbein, 1996; Rahman et al., 2002; Zhang et al., 2016). Moreover, auxin is required for the initiation of root hairs and consequently, the GoF mutant *iaa17/axr3-1,* defective in auxin signaling, has no root hairs (Masucci and Schiefelbein, 1996; Knox et al., 2003; Lee and Cho, 2013; Shibata and Sugimoto, 2019; **Figure 5B**). In addition, in the recessive *aux1-7* mutant of an auxin influx transporter, only 30% of the epidermal cells develop root hairs, compared to 40% in WT; accordingly, the treatment with either NAA or the chromosaponin I (CSI), a compound that improves auxin uptake, increments the percentage of root hair-bearing cells in *aux1-7* (Rahman et al., 2002). In the null allele of *AUX1*, *aux1-22,* CSI application does not improve root hair formation, showing that CSI needs AUX1 to regulate root hair density (Rahman et al., 2002).

Ethylene application induces ectopic hair formation in atrichoblast cells (Cao et al., 1999; Dolan, 2001; Le et al., 2001; Zhang et al., 2016; **Figure 5B**). Consequently, inhibitors of ethylene biosynthesis (AVG) and perception (Ag^{+}), block root hair formation in all cells (Tanimoto et al., 1995; Masucci and Schiefelbein, 1996; **Figure 5B**). Likewise, the *ethylene overproducer 3* (*eto3)* mutant, that produces elevated levels of ethylene, and the constitutively ethylene-responsive mutant *ctr1* both develop hairs in the epidermal cells in the position of atrichoblasts (Masucci and Schiefelbein, 1996; Cao et al., 1999). Furthermore, it has been described that ethylene promotes the initiation of root hairs via the interaction of ethylene signaling EIN3/EIL1, with the proteins encoded by the genes involved in root hair initiation and growth like *RHD6* and its respective paralog: *RHD6-LIKE (RSL1)* (Feng et al., 2017). In the *rhd6 rsl1* double mutant, with a hairless phenotype, the ACC treatment produces bulges that are characteristic of root hair initiation, and the quadruple mutant *ein3 eil1 rhd6 rsl1* do not produce these bulges even with ACC treatment (Feng et al., 2017). Auxin and ethylene seem to independently regulate root hair density as NAA application to *ein2-1* increases the frequency of root hairs (Rahman et al., 2002), whereas the root hairs density decreases with the auxin inhibitor 1-NOA in this mutant. Furthermore, the double mutant *aux1-7 ein2* has a frequency of root hairs emergence lower than the WT; and the single mutants with NAA treatment completely restores the root hair phenotype to WT (Rahman et al., 2002; **Figure 5B**).

The application of JA increases root hair density, while perturbation in JA perception/signaling as in the *coi1-2* mutant, causes a decrease in root hair frequency (Zhu et al., 2006, 2011; **Figure 5B**). Interestingly, the JA-induced root hair development is inhibited by the co-treatment with the ethylene inhibitors, AVG or Ag +, as well as in the *etr1-1* mutant, showing that these two hormones act in the same pathway regulating root hair density (Zhu et al., 2006, 2011; **Figure 5B**).

Conversely, BR is a hormone that acts as a negative regulator of root hair emergence, since the application of BR reduces the formation of root hair in trichoblasts, whereas the treatment with the BR inhibitor, brassinazole (Brz), leads to the formation of root hairs in atrichoblasts cells (Cheng et al., 2014; **Figure 5B**). In mutants related to BR synthesis: *det2-1*, *cpd,* a cytochrome P450 enzyme, and in the LoF of *BRI1* (*bri1-116*), the hair density is higher due to the presence of more hair files, suggesting that atrichoblast files change their fate to trichoblast. Therefore, plants with an increased BR signaling, as the OE of *BRI1* and the triple mutant of *BIN2* and their paralogs, (*bin2-3 bil1 bil2*), have fewer root hairs than WT, because many trichoblasts cells do not develop root hairs (Cheng et al., 2014).

ABA is a hormone that acts as a positive regulator of xylem differentiation and suberization of endodermal cells in the DZ. Mutants with reduced ABA levels (*aba2-1* and *aba3-1)* and plants treated with fluridone, have discontinuous or absent xylem strands compared to WT and this phenotype is reversed by ABA treatment (Ramachandran et al., 2018; **Figure 5B**). ABA is also involved in the lignification of the Casparian strip and suberization of endodermal cells, which are characteristics of differentiated endodermal cells. In response to ABA, the Casparian strip appears closer to the end of the TD compared to control conditions, showing that ABA promotes early endodermal differentiation (Bloch et al., 2019; **Figure 5B**). Moreover, suberin biosynthesis in endodermal cells is induced by ABA treatment, through the enhanced expression of the *GLYCEROL-3-PHOSPHATE ACYL-TRANSFERASE 5* (*GPAT5)*, a suberin biosynthesis enzyme (Barberon et al., 2016). Accordingly, mutants of ABA biosynthesis and response (*aba2*, *aba insensitive 3 [abi3], abi4* and *abi5*) have a delay in suberin deposition that is formed in a discontinuous pattern (Barberon et al., 2016; **Figure 5B**).

Ethylene is a hormone that acts as a negative regulator in suberization of endodermal cells in the DZ. Contrary to the effect of ethylene as a promoter of root hair emergence; the application of ACC reduces the suberin accumulation in newly differentiated endodermal cells via *GPAT5* (Barberon et al., 2016; **Figure 5B**). Interestingly, ACC also triggers the degradation of pre-existing suberin in already differentiated endodermal cells creating a patchy suberin pattern in the endodermis compared to control conditions (Barberon et al., 2016). Accordingly, mutants defective in the ethylene-signaling pathway, *ein3* and *etr1,* have enhanced suberization, while *ctr1* mutant, with constitutive ethylene response, has less suberization compared to WT (Barberon et al., 2016; **Figure 5B**).

Hormonal Regulation of Columella Development

The columella (COL) and the lateral root cap (LRC) comprise the root cap that protects the epidermis and the SCN in the MZ. The root cap acts as an integrator of environmental information that is then transmitted to other root cells and provides lubrication that facilitates root tip penetration to the soil by secreting polysaccharide-based mucilage (Wen et al., 2007; Kumpf and Nowack, 2015). COL cells are localized at the root tip below the SCN and are organized in cell files of increasing size departing from the columella stem cells (CSCs) (**Figure 6A**). Columella differentiated cells contain amyloplasts (plastids with starch) that participate in root gravitropism and are excellent markers of columella cell differentiation (Dolan et al., 1993; Kumpf and Nowack, 2015; **Figures 1**, **6A**). Moreover, COL has a controlled cell file number homeostasis with a high cell turnover that maintains a constant cell file number showing the tight coupling of cell proliferation, differentiation and detachment (Kumpf and Nowack, 2015; Kumar and Iyer-Pascuzzi, 2020). The regulation of cell proliferation and cell differentiation of the COL is maintained by a well-documented signaling gene regulatory network centered in the activity of *WUSCHEL-RELATED HOMEOBOX 5* (*WOX5*), a homeodomain TF expressed in the QC cells. WOX5 moves from the QC cells to the CSCs, where it negatively regulates *CYCLING DOF FACTOR 4* (*CDF4)* expression, that promotes CSCs differentiation (Pi et al., 2015). Thus, WOX5 constitutes a mobile signal emanating from the QC cells, to maintain the columella initials in an undifferentiated state. Besides, *CLAVATA3/EMBRYO-SURROUNDING REGION 40 (CLE40)*, that modulates CSCs differentiation, also acts as a negatively regulator of *WOX5* expression via the receptor-like kinase *ARABIDOPSIS CRINKLY 4 (ACR4*) (Stahl et al., 2009; Drisch and Stahl, 2015; Richards et al., 2015). In addition, PLTs positively regulate *WOX5* expression to maintain the CSCs fate (Shimotohno et al., 2018). Interestingly, in this regulatory network WOX5 excludes the NAC [NO APICAL MERISTEM (NAM), ATAF, and CUP SHAPED COTYLEDON (CUC)] TF SOMBRERO (SMB), from the CSCs to promote differentiation (Bennett et al., 2014.). Moreover, it has been reported that other members of the NAC family of TFs like *FEZ* inhibits differentiation while *BEARSKIN1 (BRN1)* and *BRN2*, participate in COL cell detachment (Willemsen et al., 2008; Bennett et al., 2010; Kumar and Iyer-Pascuzzi, 2020). This latter process requires cellulases (Del Campillo et al., 2004; **Figure 6A**) and when cell division is repressed by either hydroxyurea or aphidicolin treatments, the cell detachment process stops and the number of differentiated columella cell files remains constant (Dubreuil et al., 2018). Also, removing the root cap, using a root cap specific promoter that drives the expression of the diphtheria toxin that kills cells, shows abnormal root growth with short meristem, fewer files of differentiated columella cells and abnormal phenotypes in the remaining columella files, showing the importance of this tissue in overall root development (Tsugeki and Fedoroff, 1999).

The participation of auxin, CK, ABA, BR, JA and SA, have been documented in the CSCs differentiation being auxin and CK two hormones that are highly accumulated in COL (Antoniadi et al., 2015; Dubreuil et al., 2018). Auxin homeostasis in the columella is affected by both long-range auxin transport and from local root synthesis (Dombrecht et al., 2007). The polar transport of auxin in the root generates a graded auxin distribution in the MZ which creates a maximum of auxin concentration and response in the QC cells followed by the CSCs and the outermost columella layer, separated by cell files with lower auxin responses (Petersson et al., 2009; De Rybel et al., 2012; Dubreuil et al., 2018; Kumar and Iyer-Pascuzzi, 2020;

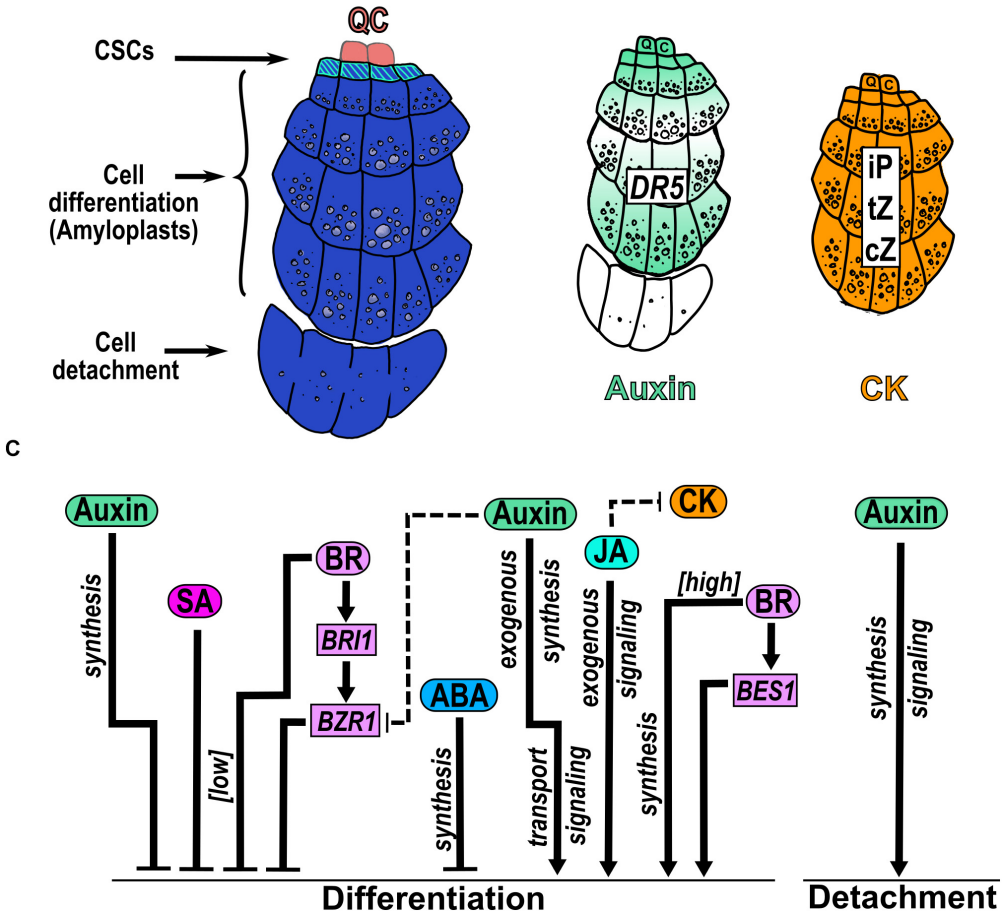

FIGURE 6 | Hormonal regulation of CSC differentiation and COL detachment. **(A)** The columella (COL) is below the QC and is arranged in cell files of increasing size. The columella stem cells (CSCs) remain undifferentiated and originate COL differentiated cells that accumulate starch granules in amyloplasts. The last COL cell file is sloughed off from the root. **(B)** Presence of hormones in COL reported by the auxin response (DR5) and measurement of different CK types. **(C)** Hormone function over CSCs differentiation and COL sloughing. The comments that are nearby arrows indicate if the hormone was applied exogenously under [high] or [low] concentrations or if the regulation depends on genes that participate in hormone synthesis, transport or signaling. Dotted arrows indicate the hormonal crosstalk.

Figure 6B). The expression of tryptophan monooxygenase (*iaaM*), an *Agrobacterium tumefaciens* auxin biosynthesis gene, in the outermost COL cell layers, shows an increased number of attached COL cells (Dubreuil et al., 2018), indicating a role of auxin in the cell-cell separation process. Regarding CK, its nucleotides; ribosides, as isopentenyladenine (iP), cis-zeatin (cZ) and trans-zeatin (tZ); and its conjugates are found at high concentrations in both the CSCs and the differentiated COL cells. Accordingly, several genes that participate in auxin and CK homeostasis are expressed in COL (De Rybel et al., 2012; Antoniadi et al., 2015; **Figure 3B**).

The application of the synthetic auxin, 1-naphthaleneacetic acid (NAA), promotes differentiation of CSCs (Ding and Friml, 2010; **Figure 6B**). Besides, auxin transport, biosynthesis and signaling are required to promote CSCs differentiation; as the quadruple *PIN* mutant (*pin1 pin3 pin4 pin7*) completely aborted columella growth (Dubreuil et al., 2018); and the single mutants of *pin4, pin3* and *pin7*, the double mutant *arf10arf16,* mutants defective in tryptophan-dependent auxin biosynthesis genes as *YUCCA* (*yuc*) and *TAA1* (*wei8*), and mutants defective in auxin signaling as *INDOLE-3-ACETIC ACID INDUCIBLE 17*/*AUXIN RESISTANT 3* (*iaa17*/*axr3*) have multiple layers of CSCs (Friml et al., 2002; Ding and Friml, 2010). Likewise, the double mutant *arf10 arf16* shows detachment defects of the outermost COL cells (Wang et al., 2005; **Figure 6B**). Intriguingly, the LoF mutants of another allele of *TAA1* ($taa1^{ckrc1-1}$) and the auxin biosynthesis anthranilate synthase double mutant (*asa1 asb1*), have a reduced COL size attributed to both less cell division and cell detachment (Dubreuil et al., 2018), contrary to what was reported by Ding and Friml (2010). As Dubreuil et al. (2018) did not analyze CSCs number and/or the presence of amyloplast in COL differentiated cells and only measure COL size, it is difficult to compare the two studies and it would be interesting to perform the same experimental procedures to analyze the auxin levels in each *TAA1* allele, to understand the auxin roles in CSCs differentiation.

Additionally, auxin participates in the regulatory network of COL promoting cell differentiation mediated by the repression of *WOX5* by ARF10 and ARF16 that restricts its expression to the QC cells (Ding and Friml, 2010). Moreover, auxin also promotes *WOX5* expression, through PLT to maintain the CSC fate (Shimotohno et al., 2018). At the same time, WOX5 regulates positively the expression of the auxin biosynthetic gene *YUC1* (Tian et al., 2014). The OE of *WOX5* increases auxin levels in PR and generates extra layers of CSCs, contrary to the phenotype of NAA application (Sarkar et al., 2007; Tian et al., 2014). Besides, in the LoF mutant of *WOX5* the CSCs are differentiated, opposite to the phenotype of auxin mutants mentioned above (Sarkar et al., 2007). Therefore, there is a multistability in the responses of WOX5 to auxin, such that the effect of auxin may depend on the cellular context in COL development (García-Gómez et al., 2017).

To our knowledge, the concentration profile of other hormones has not been quantified in COL, but their participation has been studied either by their application or by using LoF or GoF mutants.

JA promotes premature differentiation of CSCs and, consequently, an increasing number of COL cell layers with amyloplasts (**Figure 6C**). Curiously, the CSCs marker *J2341* is found in several columella cell layers under this condition indicating an increase in the cell files with CSCs identity (Chen et al., 2011). Besides, JA perception/signaling is necessary to induce CSCs differentiation as the mutants of *MYC2* and *COI1* do not differentiate under JA application. Accordingly, the RNA interference lines of a negative regulator of JA signaling (*JAZ10*) shows more CSCs differentiation compared to WT plants (Chen et al., 2011). Interestingly, exogenous application of JA reduces the signal of the CK-responsive marker *ARR5:GFP* in COL (Jang et al., 2019; Vázquez-Chimalhua et al., 2019) suggesting an antagonistic crosstalk between JA and CK (**Figure 6C**).

Otherwise, ABA and SA function as negative regulators of CSCs differentiation. Inhibition of ABA biosynthesis by fluridone, promotes CSCs differentiation and ABA induces the expression of *WOX5* and *PLT2* that are genes involved in COL development (Zhang et al., 2010; **Figure 6C**). Also, addition of low SA levels (30μM) produces an enlargement of CSCs area with two to four disorganized extra CSCs tiers whereas at higher SA levels (150 μM), COL architecture changes to bigger cells that lack starch granules (Pasternak et al., 2019; **Figure 6C**).

BR is a hormone that regulates CSCs differentiation in a dose-dependent manner; at low concentrations, BR inhibits CSCs differentiation and reduces the number of COL cells layers; in contrast, higher concentrations of BR have the opposite effects (González-García et al., 2011; Lee et al., 2015; **Figure 6C**). Also, BR signaling mediated by the positive regulators *BES1* and *BZR1*, have opposite functions on CSC differentiation i.e., the GoF mutant of *BES1* (*bes1-D*) enhances CSCs differentiation, while the GoF mutant (*bzr1-D*) enhances the number of CSCs layers with less COL differentiate cell layers (Lee et al., 2015; **Figure 6C**). Moreover, the mutant of the receptor *BRI1* (*bri1-116*) shows the same phenotype as *bes1-D* while the LoF of *de-etiolated 1* (*det1-2*), which participates in BR biosynthesis, has the same *bzr1-D* phenotype (Lee et al., 2015; **Figure 6C**). These results show that higher BR concentrations as well as the BES-mediated perception/signaling pathway stimulates CSC differentiation while lower BR concentrations and the BZR-mediated signaling pathway inhibits it (Lee et al., 2015; **Figure 6C**). Interestingly, it has been reported that BES acts as a transcriptional activator (Yin et al., 2005) whereas BZR1 as a repressor (He et al., 2005) so it would be very interesting to determine cell type specific BR target genes in different hormone concentrations and signaling and biosynthesis mutants. In addition, the lack of CSCs layers of *bri1-116* could be rescued by the OE of the D-Type Cyclin *CYCD3;1*, which promotes supernumerary layers of CSCs, in the double mutant (*bri1-116 CYCD3;1OE).* Accordingly, BR treatment in the OE of *CYCD3;1* plant, enhances the CSCs differentiation suggesting that BR regulates this phenotype through cell cycle regulation (González-García et al., 2011; Lee et al., 2015).

Besides, BR and auxin act antagonistically in columella development. The *bzr1-D* mutant phenotype, with additional layers of CSCs, is reverted into plants with more CSCs differentiation using NAA treatments (Lee et al., 2015; **Figure 6C**). Moreover, the inhibition of local auxin biosynthesis by L-kynurenine in the QC increases the nuclear accumulation and TF activity of *BZR1-YFP* in CSCs suggesting that the BZR1 pattern and nuclear accumulation is regulated by the auxin gradient (Chaiwanon and Wang, 2015). Interestingly, the nuclear accumulation of BZR1 causes extra divisions in the QC (Lee et al., 2015) that could affect the cell file number of CSCs.

The hormone participation in the regulation of the NAC TFs and their involvement in the regulatory network for COL development has not been addressed, different hormones might be regulating the expression of the NACs as their phenotypes in COL development are very similar. For instance, *fez* mutant promotes CSCs differentiation (Willemsen et al., 2008; Hong et al., 2015) and this phenotype is detected in the GoF mutant of *BES1,* in high BR, auxin or JA treatment and in auxin mutants. Contrary, the *smb-3* reduces CSCs differentiation as it is observed in the treatment with low BR and SA, as well as in BR signaling mutants and in auxin and ABA synthesis mutants (Willemsen et al., 2008; Ding and Friml, 2010; Chen et al., 2011; Lee et al., 2015). Furthermore, in the *brn1-1 brn2-1* double mutant, the COL cells fail to detach as is observed in auxin signaling mutants (Wang et al., 2005).

In brief, JA promotes COL cell differentiation while ABA and SA delay it. Interestingly, SA has a dose-dependent regulation over COL architecture that is not observed in any other zone or domain of the root. Furthermore, BR acts in a dose-dependent manner: at low concentrations repress, while at high concentration promotes, CSCs differentiation (**Figure 6C**). Besides, auxin can either promote or inhibit CSCs differentiation. Finally, auxin is the only hormone that participates in cell detachment, proliferation and differentiation (**Figure 6C**).

Lateral Root Cap Regulation by Hormones

The Lateral Root Cap (LRC) is the cell file that surrounds and protects the external part of the MZ of the root and is derived from the LRC/epidermis stem cells (**Figure 1**; Dolan et al., 1993;

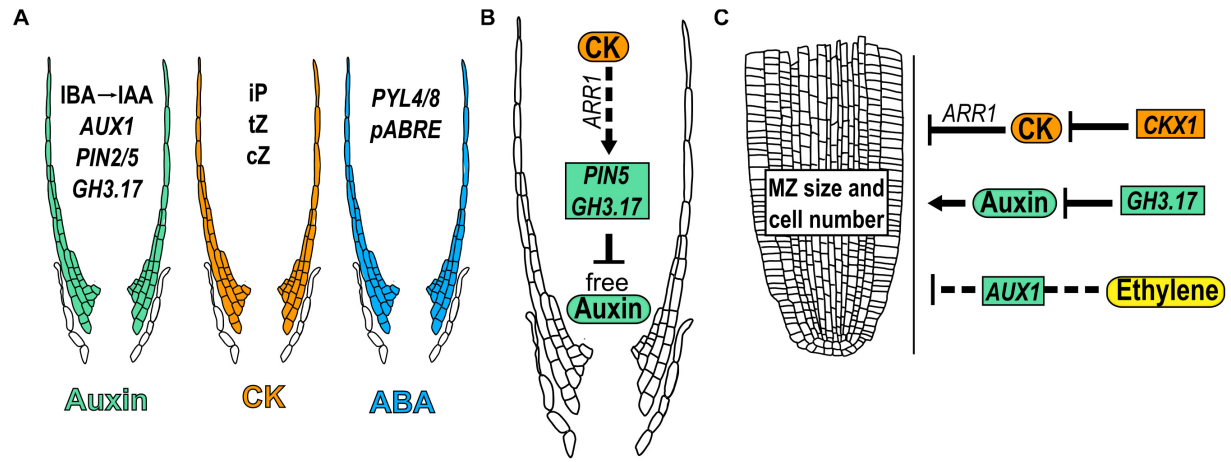

FIGURE 7 | Hormone function in meristem size through lateral root cap. **(A)** Presence of different hormone forms and expression of related genes that participate in lateral root cap growth. **(B)** Regulatory crosstalk between auxin and CK in the lateral root cap development. **(C)** Hormonal regulations in LRC that modulate meristem size. Dotted arrows indicate the hormonal crosstalk.

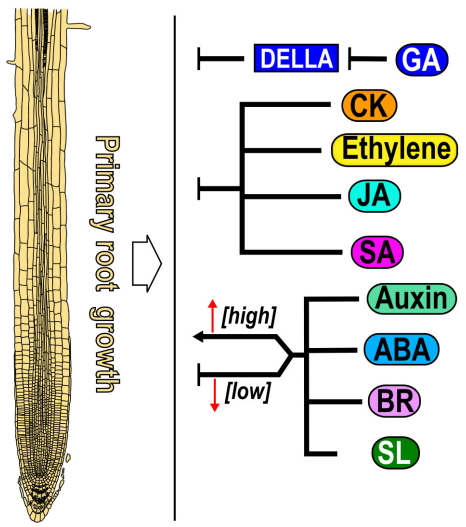

FIGURE 8 | Effect of nine hormones in primary root growth. Gibberellic acid (GA) is a positive regulator, whereas auxin, abscisic acid (ABA), brassinosteroid (BR) and strigolactone (SL) act both as promoters and repressors of primary root growth in a dose-dependent manner. Cytokinin (CK), ethylene, jasmonic acid (JA) and salicylic acid (SA) are negative regulators of PR growth (black arrows). For all Figures, directed arrows represent positive whereas blunt arrows indicate negative regulation over root growth.

Kumpf and Nowack, 2015). The cells of the LRC divide anticlinally and eventually die as part of a genetically controlled cell death program (PCD) upon reaching the EZ (Fendrych et al., 2014; Kumpf and Nowack, 2015; Huysmans et al., 2018). Hormone function over LRC development has been studied through changes in the MZ size (Xuan et al., 2016; Di Mambro et al., 2019).

CK and auxin-related proteins that participate in their transport or signaling, have been detected in the LRC cells (Antoniadi et al., 2015; Di Mambro et al., 2019). In the case of auxins, the expression in the LRC of the auxin influx transporter, *AUX1* and the efflux transporter *PIN2,* are required to mobilize the auxins from the MZ till the beginning of the EZ (Swarup et al., 2001; Feraru and Friml, 2008; **Figure 7A**). The endoplasmic reticulum auxin transporter *PIN5* is expressed in the LRC and transports auxin from the cytoplasm into the lumen of the endoplasmic reticulum; its OE results in decreased levels of free auxin in the LRC (Mravec et al., 2009; Di Mambro et al., 2019). In addition, *GH3.17* is expressed in the LRC and in EZ epidermal cells where it reduces free auxin levels (Di Mambro et al., 2019; **Figure 7A**). Additionally, outer LRC cells constitute a local source of auxin produced from indole-3-butyric acid (IBA) (Xuan et al., 2015). Regarding CK, the most active (iP, cZ, and tZ) precursors and conjugated forms, are accumulated at very high levels in LRC cells suggesting its restricted metabolism in these cells (Antoniadi et al., 2015; **Figure 7A**). Interestingly, *PIN5* and *GH3.17* are positively regulated by CK in the LRC through *ARR1* suggesting that auxins concentration and distribution in LRC cells are dynamically controlled by CK (Di Mambro et al., 2019; **Figure 7B**).

The expression of the ABA receptors *PYRABACTIN RESISTANCE–LIKE 4* (*PYL4*), *PYL8* as well as the ABA-responsive element reporter (*pABRE_A:GFP)* are expressed in the LRC in early stages of root growth (Antoni et al., 2013; Belda-Palazon et al., 2018; Wein et al., 2020; **Figure 7A**).

Furthermore, hormonal concentrations in the LRC affect the development of other parts of the root; the presence of auxin and CK in the LRC affects the MZ size. In addition, the expression of *GH3.17* using the inducible LRC specific line (J2632), reduces meristem size while the mutant *gh3.17-1* displays an enlarged meristem; interestingly, the complementation of the *gh3.17-1* mutant, with the specific expression of *GH3.17* in the LRC, rescued this phenotype (Di Mambro et al., 2019; **Figure 7C**). Contrary to auxin, reducing the CK levels in LRC by using the J2632 reporter line to drive the expression of the gene

that participates in its catabolism, *CKX1*, increases MZ size; accordingly, *ARR1* induction (with a high CK response) in the LRC (J2632 line), decreases the MZ size (Di Mambro et al., 2019; **Figure 7C**). Furthermore, CK regulates the expression of *GH3.17* in the LRC through *ARR1* (Di Mambro et al., 2019). These data suggest that auxin and CK levels in the LRC are determinant for the control of MZ size and that the effect of auxin in LRC is partially controlled by CK.

Furthermore, the PR growth regulated by ethylene depends on the transport of auxin via the LRC, as the expression of *AUX1* in LRC cells using the line *M0013 >>AUX1*, is enough to re-establish the ethylene inhibition of root growth in *aux1* mutant (Swarup et al., 2007; **Figure 7C**).

In summary, the LRC is a structure that protects but also regulates root MZ size and PR development. High levels of CK in the LRC inhibits while low levels of auxin promote the MZ size and the downregulation of auxin by CK in the LRC, partially controls its effect as a promoter of root MZ size.

CONCLUSION

The balance between cell proliferation, elongation and differentiation is crucial for root growth and is dynamically adjusted depending on external and internal factors such as phytohormones. This review describes how nine hormones alone or in crosstalk, determine the different activities found in zones and domains of the Arabidopsis PR as despite the spatio-temporal roles over PR growth of the different hormones, it is difficult to understand how their synthesis, distribution and sensing accounts for their function in cell and tissue patterning. The PR growth is regulated in a dose-dependent manner; where low concentrations promote it and high concentrations inhibit it by auxin, ABA, BR, and SL (Müssig et al., 2003; Ruyter-Spira et al., 2011; Li et al., 2017; Waidmann et al., 2020; **Figure 8**), CK, ethylene, JA and SA act as negative regulators of PR growth (Medford et al., 1989; Le et al., 2001; Pasternak et al., 2005; Rùžièka et al., 2007; Kuderová et al., 2008; Chen et al., 2011; **Figure 8**) and GA is the only hormone that functions as a positive regulator of PR growth as different GA loss-of-function mutants and plants treated with an inhibitor of GA synthesis (Paclobutrazol, PAC) have shorter roots than WT (Fu and Harberd, 2003; Griffiths et al., 2006; Ubeda-Tomás et al., 2008, 2009; **Figure 8**).

PR growth is determined by the balance between cell proliferation and elongation. Accordingly, hormones that promote (GA) or inhibit (CK, ethylene, JA and SA) these two processes produce longer or shorter PRs, respectively. It is also possible that the readout of a hormone is not so straight such that one of these two cell processes compensate for the other, or that a gradient of concentration determines the root patterning as with auxin where it is found a maximum of concentration in the SCN followed by intermediate levels in the MZ and low levels in the EZ. Moreover, low levels of BR are important for MZ maintenance while BR signaling in the epidermal cells of the TD is necessary to promote cell elongation. Interestingly, hormone function also could be determined in each domain, zone or organ by changing the threshold of concentration where cells and tissues respond. Low concentrations of auxin, ABA, SL and BR promote while high concentration inhibit PR growth and the same occurs for ABA and BR in PD activity, for auxin in the TD to induce the transition to elongation and for ABA in cell elongation. Curiously, BR dose-dependent participation in CSCs, functions in opposite ways, low concentrations and the BZR1-mediated signaling pathway inhibit, while high concentration as well as the activation of the BES1 signaling pathway promotes CSCs differentiation. In addition, the BR effect over cell proliferation depends on the particular cell type where it is active; in the epidermis of the MZ, BR signaling is necessary to induce the MZ size, whilst in the stele it promotes cell differentiation. Furthermore, the MZ length of the single mutant of *bri1* and the triple mutant of *bri1 brl1 brl3* are bigger than WT if *BRI1* is expressed in the epidermal non-hair-cells. All these data suggest the importance not only of BR dosage but also the cell type where it is active to control the MZ size.

Moreover, we would like to highlight some important hormone crosstalks that are relevant to the activity and growth of the different zones and domains. A well-known crosstalk is the one where CK interacts antagonistically with auxin in the transition from the MZ to the TD and to the EZ where higher CK levels and lower auxin levels are necessary for endoreduplication. Interestingly, auxin and CK negatively regulate cell elongation and positively regulate root hair emergence suggesting different interactions between these two hormones in zones and domains. Also, ethylene inhibits the MZ size, promotes the early transition to EZ and suppresses cell elongation by both enhancing auxin biosynthesis and transport to the EZ, and inhibiting GA accumulation in the endodermis of the EZ.

It would be interesting to analyze how roots dynamically integrate all hormonal signals between the different zones and domains to alter the molecular processes underneath the changes in the ratio between cell proliferation, elongation and differentiation, to fully understand the PR development.

AUTHOR CONTRIBUTIONS

EZ-M, BL-R, and AG-A conceived and wrote the review. BG-P, MP, MG-G, and EÁ-B helped in writing and editing the review. All authors have read and agreed to the published version of the manuscript.

FUNDING

This study was financed with the following grants: AG-A, BG-P, MP, and EÁ-B received funding from UNAM-DGAPA-PAPIIT (IN200920, IN206220, IN203220, and IN211721) and CONACyT 102959 (AG-A) and 102987 (MP). EZ-M is a Ph.D. student from: Programa de Doctorado en Ciencias Biomédicas, Universidad Nacional Autónoma de México (UNAM) and has received a

CONACyT fellowship (579738). BL-R received a postdoctoral fellowship from CONACyT (489444).

ACKNOWLEDGMENTS

We would like to thank Dr. Diana Beléìn Sáìnchez Rodrìguez for logistical and technical support, to Dr. José López-Bucio (Universidad Michoacana de San Nicolás de Hidalgo) for comments on the manuscript and to the two reviewers that helped to improve this review.

SUPPLEMENTARY MATERIAL

The Supplementary Material for this article can be found online at: https://www.frontiersin.org/articles/10.3389/fpls.2021.659155/full#supplementary-material

REFERENCES

Achard, P., Gusti, A., Cheminant, S., Alioua, M., Dhondt, S., Coppens, F., et al. (2009). Gibberellin signaling controls cell proliferation rate in *Arabidopsis*. *Curr. Biol.* 19, 1188–1193. doi: 10.1016/j.cub.2009.05.059

Acosta, I. F., Gasperini, D., Chetelat, A., Stolz, S., Santuari, L., and Farmer, E. E. (2013). Role of NINJA in root jasmonate signaling. *Proc. Natl. Acad. Sci. U.S.A.* 110, 15473–15478. doi: 10.1073/pnas.1307910110

Aida, M., Beis, D., Heidstra, R., Willemsen, V., Blilou, I., Galinha, C., et al. (2004). The PLETHORA genes mediate patterning of the *Arabidopsis* root stem cell niche. *Cell* 119, 109–120. doi: 10.1016/j.cell.2004.09.018

Antoni, R., Gonzalez-Guzman, M., Rodriguez, L., Peirats-Llobet, M., Pizzio, G. A., Fernandez, M. A., et al. (2013). Pyrabactin resistance1-LIKE8 plays an important role for the regulation of abscisic acid signaling in root. *Plant Physiol.* 161, 931–941. doi: 10.1104/pp.112.208678

Antoniadi, I., Plačková, L., Simonovik, B., Doležal, K., Turnbull, C., Ljung, K., et al. (2015). Cell-type-specific cytokinin distribution within the *arabidopsis* primary root apex. *Plant Cell* 27, 1955–1967. doi: 10.1105/tpc.15.00176

Baluška, F., Barlow, P. W., and Kubica, Š (1994). Importance of the post-mitotic isodiametric growth (PIG) region for growth and development of roots. *Plant Soil* 167, 31–41. doi: 10.1007/BF01587595

Baluška, F., and Mancuso, S. (2013). Root apex transition zone as oscillatory zone. *Front. Plant Sci.* 4:354. doi: 10.3389/fpls.2013.00354

Baluška, F., Mancuso, S., Volkmann, D., and Barlow, P. W. (2010). Root apex transition zone: a signalling-response nexus in the root. *Trends. Plant. Sci.* 15, 402–408. doi: 10.1016/j.tplants.2010.04.007

Baluška, F., Volkmann, D., and Barlow, P. W. (1996). Specialized zones of development in roots: view from the cellular level. *Plant Physiol.* 112, 3–4. doi: 10.1104/pp.112.1.3

Band, L. R., Úbeda-Tomás, S., Dyson, R. J., Middleton, A. M., Hodgman, T. C., Owen, M. R., et al. (2012). Growth-induced hormone dilution can explain the dynamics of plant root cell elongation. *Proc. Natl. Acad. Sci. U. S. A.* 109, 7577–7582. doi: 10.1073/pnas.1113632109

Band, L. R., Wells, D. M., Fozard, J. A., Ghetiu, T., French, A. P., Pound, M. P., et al. (2014). Systems analysis of auxin transport in the *Arabidopsis* root apex. *Plant Cell* 26, 862–875. doi: 10.1105/tpc.113.119495

Barberon, M., Vermeer, J. E. M., De Bellis, D., Wang, P., Naseer, S., Andersen, T. G., et al. (2016). Adaptation of root function by nutrient-induced plasticity of endodermal differentiation. *Cell* 164, 447–459. doi: 10.1016/j.cell.2015.12.021

Barbez, E., Dünser, K., Gaidora, A., Lendl, T., and Busch, W. (2017). Auxin steers root cell expansion via apoplastic pH regulation in *Arabidopsis thaliana*. *Proc. Natl. Acad. Sci. U. S. A.* 114, E4884–E4893. doi: 10.1073/pnas.1613499114

Barker, R., Fernandez Garcia, M. N., Powers, S. J., Vaughan, S., Bennett, M. J., Phillips, A. L., et al. (2020). Mapping sites of gibberellin biosynthesis in the *Arabidopsis* root tip. *New Phytol.* 229, 1521–1534. doi: 10.1111/nph.16967

Barrada, A., Montané, M. H., Robaglia, C., and Menand, B. (2015). Spatial regulation of root growth: placing the plant TOR pathway in a developmental perspective. *Int. J. Mol. Sci.* 16, 19671–19697. doi: 10.3390/ijms160819671

Baskin, T. I., Preston, S., Zelinsky, E., Yang, X., Elmali, M., Bellos, D., et al. (2020). Positioning the root elongation zone is saltatory and receivesinput from the shoot. *Science* 23:101309. doi: 10.1016/j.isci.2020.101309

Beemster, G. T. S, and Baskin, T. I, (2000). Stunted plant 1 mediates effects of cytokinin, but not of auxin, on cell division and expansion in the root of *Arabidopsis*. *Plant Physiol.* 124, 1718–1727. doi: 10.1104/pp.124.4.1718

Belda-Palazon, B., Gonzalez-Garcia, M. P., Lozano-Juste, J., Coego, A., Antoni, R., Julian, J., et al. (2018). PYL8 mediates ABA perception in the root through non-cell-autonomous and ligand-stabilization–based mechanisms. *Proc. Natl. Acad. Sci. U. S. A.* 115, E11857–E11863. doi: 10.1073/pnas.1815410115

Benfey, P. N., and Scheres, B. (2000). Root development. *Curr. Biol.* 10, R813–R815. doi: 10.1016/S0960-9822(00)00814-9

Bennett, T., van den Toorn, A., Sanchez-Perez, G. F., Campilho, A., Willemsen, V., Snel, B., et al. (2010). Sombrero, Bearskin1, and Bearskin2 regulate root cap maturation in *Arabidopsis*. *Plant Cell* 22, 640–654. doi: 10.1105/tpc.109.072272

Bennett, T., van den Toorn, A., Willemsen, V., and Scheres, B. (2014). Precise control of plant stem cell activity through parallel regulatory inputs. *Development* 141, 4055–4064. doi: 10.1242/dev.110148

Berleth, T., and Jurgens, G. (1993). The role of the monopteros gene in organising the basal body region of the *Arabidopsis* embryo. *Development* 118, 575–587.

Bhosale, R., Boudolf, V., Cuevas, F., Lu, R., Eekhout, T., Hu, Z., et al. (2018). A spatiotemporal DNA endoploidy map of the *Arabidopsis* root reveals roles for the endocycle in root development and stress adaptation. *Plant Cell* 30, 2330–2351. doi: 10.1105/tpc.17.00983

Bishopp, A., Lehesranta, S., Vatén, A., Help, H., El-Showk, S., Scheres, B., et al. (2011). Phloem-transported cytokinin regulates polar auxin transport and maintains vascular pattern in the root meristem. *Curr. Biol.* 21, 927–932. doi: 10.1016/j.cub.2011.04.049

Blilou, I., Xu, J., Wildwater, M., Willemsen, V., Paponov, I., Frimi, J., et al. (2005). The PIN auxin efflux facilitator network controls growth and patterning in *Arabidopsis* roots. *Nature* 433, 39–44. doi: 10.1038/nature03184

Bloch, D., Puli, M. R., Mosquna, A., and Yalovsky, S. (2019). Abiotic stress modulates root patterning via ABA-regulated microRNA expression in the endodermis initials. *Dev. Camb.* 146:dev177097. doi: 10.1242/dev.177097

Brumos, J., Robles, L. M., Yun, J., Vu, T. C., Jackson, S., Alonso, J. M., et al. (2018). Local auxin biosynthesis is a key regulator of plant development. *Dev. Cell* 47, 306.e5–318.e5. doi: 10.1016/j.devcel.2018.09.022

Brunoud, G., Wells, D. M., Oliva, M., Larrieu, A., Mirabet, V., Burrow, A. H., et al. (2012). A novel sensor to map auxin response and distribution at high spatio-temporal resolution. *Nature* 482, 103–106. doi: 10.1038/nature10791

Cajero Sánchez, W., García-Ponce, B., Sánchez, M., de la, P., Álvarez-Buylla, E. R., and Garay-Arroyo, A. (2018). Identifying the transition to the maturation zone in three ecotypes of *Arabidopsis thaliana* roots. *Commun. Integr. Biol.* 11:e1395993. doi: 10.1080/19420889.2017.1395993

Cao, X. F., Linstead, P., Berger, F., Kieber, J., and Dolan, L. (1999). Differential ethylene sensitivity of epidermal cells is involved in the establishment of cell pattern in the *Arabidopsis* root. *Physiol. Plant.* 106, 311–317. doi: 10.1034/j.1399-3054.1999.106308.x

Carol, R. J., and Dolan, L. (2002). Building a hair: tip growth in *Arabidopsis thaliana* root hairs. *Philos. Trans. R. Soc. Lond. B Biol. Sci.* 357, 815–821. doi: 10.1098/rstb.2002.1092

Chae, H. S., Faure, F., and Kieber, J. J. (2003). The eto1, eto2, and eto3 mutations and cytokinin treatment increase ethylene biosynthesis in *Arabidopsis* by increasing the stability of ACS protein. *Plant Cell* 15, 545–559. doi: 10.1105/tpc.006882

Chaiwanon, J., Wang, W., Zhu, J. Y., Oh, E., and Wang, Z. Y. (2016). Information integration and communication in plant growth regulation. *Cell* 164, 1257–1268. doi: 10.1016/j.cell.2016.01.044

Chaiwanon, J., and Wang, Z.-Y. (2015). Spatiotemporal brassinosteroid signaling and antagonism with auxin pattern stem cell dynamics in *Arabidopsis* roots. *Curr. Biol.* 25, 1031–1042. doi: 10.1016/j.cub.2015.02.046

Chen, Q., Sun, J., Zhai, Q., Zhou, W., Qi, L., Xu, L., et al. (2011). The basic helix-loop-helix transcription factor myc2 directly represses plethora

expression during jasmonate-mediated modulation of the root stem cell niche in *Arabidopsis*. *Plant Cell* 23, 3335–3352. doi: 10.1105/tpc.111.089870

Cheng, Y., Zhu, W., Chen, Y., Ito, S., Asami, T., and Wang, X. (2014). Brassinosteroids control root epidermal cell fate via direct regulation of a MYB-bHLH-WD40 complex by GSK3-like kinases. *eLife* 2014:2525. doi: 10.7554/eLife.02525

Cosgrove, D. J. (2005). Growth of the plant cell wall. *Nat. Rev. Mol. Cell Biol.* 6, 850–861. doi: 10.1038/nrm1746

Dastidar, M. G., Scarpa, A., Mägele, I., Ruiz-Duarte, P., von Born, P., Bald, L., et al. (2019). ARF5/MONOPTEROS directly regulates miR390 expression in the *Arabidopsis thaliana* primary root meristem. *Plant Direct* 3:e00116. doi: 10.1002/pld3.116

De Rybel, B., Audenaert, D., Xuan, W., Overvoorde, P., Strader, L. C., Kepinski, S., et al. (2012). A role for the root cap in root branching revealed by the non-auxin probe naxillin. *Nat. Chem. Biol.* 8, 798–805. doi: 10.1038/nchembio.1044

Del Campillo, E., Abdel-Aziz, A., Crawford, D., and Patterson, S. E. (2004). Root cap specific expression of an endo-β-1,4-D-glucanase (cellulase): a new marker to study root development in *Arabidopsis*. *Plant Mol. Biol.* 56, 309–323. doi: 10.1007/s11103-004-3380-3

Dello Ioio, R., Galinha, C., Fletcher, A. G., Grigg, S. P., Molnar, A., Willemsen, V., et al. (2012). A PHABULOSA/cytokinin feedback loop controls root growth in *Arabidopsis*. *Curr. Biol.* 22, 1699–1704. doi: 10.1016/j.cub.2012.07.005

Dello Ioio, R., Linhares, F. S., and Sabatini, S. (2008a). Emerging role of cytokinin as a regulator of cellular differentiation. *Curr. Opin. Plant Biol.* 11, 23–27. doi: 10.1016/j.pbi.2007.10.006

Dello Ioio, R., Nakamura, K., Moubayidin, L., Perilli, S., Taniguchi, M., Morita, M. T., et al. (2008b). A genetic framework for the control of cell division and differentiation in the root meristem. *Science* 322, 1380–1384. doi: 10.1126/science.1164147

Dello Ioio, R., Linhares, F. S., Scacchi, E., Casamitjana-Martinez, E., Heidstra, R., Costantino, P., et al. (2007). Cytokinins determine *Arabidopsis* root-meristem size by controlling cell differentiation. *Curr. Biol.* 17, 678–682. doi: 10.1016/j.cub.2007.02.047

Di Mambro, R., De Ruvo, M., Pacifici, E., Salvi, E., Sozzani, R., Benfey, P. N., et al. (2017). Auxin minimum triggers the developmental switch from cell division to cell differentiation in the *Arabidopsis* root. *Proc. Natl. Acad. Sci. U. S. A.* 114, E7641–E7649. doi: 10.1073/pnas.1705833114

Di Mambro, R., Svolacchia, N., Dello Ioio, R., Pierdonati, E., Salvi, E., Pedrazzini, E., et al. (2019). The lateral root cap acts as an auxin sink that controls meristem size. *Curr. Biol.* 29, 1199.e4–1205.e4. doi: 10.1016/j.cub.2019.02.022

Dietrich, D. (2018). Hydrotropism: how roots search for water. *J. Exp. Bot.* 11 69, 2759–2771. doi: 10.1093/jxb/ery034

Dietrich, D., Pang, L., Kobayashi, A., Fozard, J. A., Boudolf, V., Bhosale, R., et al. (2017). Root hydrotropism is controlled via a cortex-specific growth mechanism. *Nat. Plants* 3:17057. doi: 10.1038/nplants.2017.57

Ding, Z., and Friml, J. (2010). Auxin regulates distal stem cell differentiation in *Arabidopsis* roots. *Proc. Natl. Acad. Sci. U. S. A.* 107, 12046–12051. doi: 10.1073/pnas.1000672107

Dolan, L. (2001). The role of ethylene in root hair growth in *Arabidopsis*. *J. Plant Nutr. Soil Sci.* 164, 141–145. doi: 10.1002/1522-2624(200104)164:2<141::aid-jpln141>3.0.co;2-z

Dolan, L., and Davies, J. (2004). Cell expansion in roots. *Curr. Opin. Plant Biol.* 7, 33–39. doi: 10.1016/j.pbi.2003.11.006

Dolan, L., Janmaat, K., Willemsen, V., Linstead, P., Poethig, S., Roberts, K., et al. (1993). Cellular organisation of the *Arabidopsis thaliana* root. *Dev. Camb. Engl.* 119, 71–84.

Dombrecht, B., Gang, P. X., Sprague, S. J., Kirkegaard, J. A., Ross, J. J., Reid, J. B., et al. (2007). MYC2 differentially modulates diverse jasmonate-dependent functions in *Arabidopsis*. *Plant Cell* 19, 2225–2245. doi: 10.1105/tpc.106.048017

Drisch, R. C., and Stahl, Y. (2015). Function and regulation of transcription factors involved in root apical meristem and stem cell maintenance. *Front. Plant Sci.* 6:505. doi: 10.3389/fpls.2015.00505

Dubreuil, C., Jin, X., Grönlund, A., and Fischer, U. (2018). A local auxin gradient regulates root cap self-renewal and size homeostasis. *Curr. Biol.* 28, 2581.e3–2587.e3. doi: 10.1016/j.cub.2018.05.090

Fendrych, M., Van Hautegem, T., Van Durme, M., Olvera-Carrillo, Y., Huysmans, M., Karimi, M., et al. (2014). Programmed cell death controlled by ANAC033/SOMBRERO determines root cap organ size in *Arabidopsis*. *Curr. Biol.* 24, 931–940. doi: 10.1016/j.cub.2014.03.025

Feng, Y., Xu, P., Li, B., Li, P., Wen, X., An, F., et al. (2017). Ethylene promotes root hair growth through coordinated EIN3/EIL1 and RHD6/RSL1 activity in *Arabidopsis*. *Proc. Natl. Acad. Sci. U. S. A.* 114, 13834–13839. doi: 10.1073/pnas.1711723115

Feraru, E., Feraru, M. I., Barbez, E., Waidmann, S., Sun, L., Gaidora, A., et al. (2019). PILS6 is a temperature-sensitive regulator of nuclear auxin input and organ growth in *Arabidopsis thaliana*. *Proc. Natl. Acad. Sci. U. S. A.* 116, 3893–3898. doi: 10.1073/pnas.1814015116

Feraru, E., and Friml, J. (2008). PIN polar targeting. *Plant Physiol.* 147, 1553–1559. doi: 10.1104/pp.108.121756

Fridman, Y., Elkouby, L., Holland, N., Vragović, K., Elbaum, R., and Savaldi-Goldstein, S. (2014). Root growth is modulated by differential hormonal sensitivity in neighboring cells. *Genes Dev.* 28, 912–920. doi: 10.1101/gad.239335.114

Friml, J., Benková, E., Blilou, I., Wisniewska, J., Hamann, T., Ljung, K., et al. (2002). AtPIN4 mediates sink-driven auxin gradients and root patterning in *Arabidopsis*. *Cell* 108, 661–673. doi: 10.1016/S0092-8674(02)00656-6

Friml, J., Yang, X., Michniewicz, M., Weijers, D., Quint, A., Tietz, O., et al. (2004). A PINOID-dependent binary switch in apical-basal PIN polar targeting directs auxin efflux. *Science* 306, 862–865. doi: 10.1126/science.1100618

Fu, X., and Harberd, N. P. (2003). Auxin promotes *Arabidopsis* root growth by modulating gibberellin response. *Nature* 421, 740–743. doi: 10.1038/nature01387

Galinha, C., Hofhuis, H., Luijten, M., Willemsen, V., Blilou, I., Heidstra, R., et al. (2007). PLETHORA proteins as dose-dependent master regulators of *Arabidopsis* root development. *Nature* 449, 1053–1057. doi: 10.1038/nature06206

Garay-Arroyo, A., Ortiz-Moreno, E., De La Paz Sánchez, M., Murphy, A. S., García-Ponce, B., Marsch-Martínez, N., et al. (2013). The MADS transcription factor XAL2/AGL14 modulates auxin transport during *Arabidopsis* root development by regulating PIN expression. *EMBO J.* 32, 2884–2895. doi: 10.1038/emboj.2013.216

García-Gómez, M. L., Azpeitia, E., and Álvarez-Buylla, E. R. (2017). A dynamic genetic-hormonal regulatory network model explains multiple cellular behaviors of the root apical meristem of *Arabidopsis* thalian. *PLoS Comput. Biol.* 13:e1005488. doi: 10.1371/journal.pcbi.1005488

González-García, M. P., Vilarrasa-Blasi, J., Zhiponova, M., Divol, F., Mora-García, S., Russinova, E., et al. (2011). Brassinosteroids control meristem size by promoting cell cycle progression in *Arabidopsis* roots. *Development* 138, 849–859. doi: 10.1242/dev.057331

Gray, W. M. (2004). Hormonal regulation of plant growth and development. *PLoS Biol.* 2:e311. doi: 10.1371/journal.pbio.0020311

Griffiths, J., Murase, K., Rieu, I., Zentella, R., Zhang, Z.-L., Powers, S. J., et al. (2006). Genetic characterization and functional analysis of the GID1 gibberellin receptors in *Arabidopsis*. *Plant Cell* 18, 3399–3414. doi: 10.1105/tpc.106.047415

Hacham, Y., Holland, N., Butterfield, C., Ubeda-Tomas, S., Bennett, M. J., Chory, J., et al. (2011). Brassinosteroid perception in the epidermis controls root meristem size. *Development* 138, 839–848. doi: 10.1242/dev.061804

He, J., Duan, Y., Hua, D., Fan, G., Wang, L., Liu, Y., et al. (2012). DEXH box RNA helicase-mediated mitochondrial reactive oxygen species production in *Arabidopsis* mediates crosstalk between abscisic acid and auxin signaling. *Plant Cell* 24, 1815–1833. doi: 10.1105/tpc.112.098707

He, J. X., Gendron, J. M., Sun, Y., Gampala, S. S. L., Gendron, N., Sun, C. Q., et al. (2005). BZR1 is a transcriptional repressor with dual roles in brassinosteroid homeostasis and growth responses. *Science* 307, 1634–1638. doi: 10.1126/science.1107580

Hodge, A. (2009). Root decisions. *Plant Cell Environ.* 32, 628–640. doi: 10.1111/j.1365-3040.2008.01891.x

Hong, J. H., Chu, H., Zhang, C., Ghosh, D., Gong, X., and Xu, J. (2015). A quantitative analysis of stem cell homeostasis in the *Arabidopsis* columella root cap. *Front. Plant Sci.* 6:206. doi: 10.3389/fpls.2015.00206

Huysmans, M., Buono, R. A., Skorzinski, N., Radio, M. C., De Winter, F., Parizot, B., et al. (2018). NAC transcription factors ANAC087 and ANAC046 control distinct aspects of programmed cell death in the *Arabidopsis* columella and lateral root cap. *Plant Cell* 30, 2197–2213. doi: 10.1105/tpc.18.00293

Ishida, T., Adachi, S., Yoshimura, M., Shimizu, K., Umeda, M., and Sugimoto, K. (2010). Auxin modulates the transition from the mitotic cycle to the endocycle in *Arabidopsis*. *Development* 137, 63–71. doi: 10.1242/dev.035840

Ishida, T., Kurata, T., Okada, K., and Wada, T. (2008). A genetic regulatory network in the development of trichomes and root hairs. *Annu. Rev. Plant Biol.* 59, 365–386. doi: 10.1146/annurev.arplant.59.032607.092949

Ivanov, V. B., and Dubrovsky, J. G. (2013). Longitudinal zonation pattern in plant roots: conflicts and solutions. *Trends Plant Sci.* 18, 237–243. doi: 10.1016/j.tplants.2012.10.002

Jang, G., Yoon, Y., and Choi, Y. D. (2019). Jasmonic acid modulates xylem development by controlling expression of PIN-FORMED 7. *Plant Signal. Behav.* 14:1637664. doi: 10.1080/15592324.2019.1637664

Jung, J. K. H., and McCouch, S. (2013). Getting to the roots of it: genetic and hormonal control of root architecture. *Front. Plant Sci.* 4:186. doi: 10.3389/fpls.2013.00186

Kang, Y. H., Breda, A., and Hardtke, C. S. (2017). Brassinosteroid signaling directs formative cell divisions and protophloem differentiation in *Arabidopsis* root meristems. *Dev. Camb.* 144, 272–280. doi: 10.1242/dev.145623

Knox, K., Grierson, C. S., and Leyser, O. (2003). AXR3 and SHY2 interact to regulate root hair development. *Development* 130, 5769–5777. doi: 10.1242/dev.00659

Kondo, Y., Tamaki, T., and Fukuda, H. (2014). Regulation of xylem cell fate. *Front. Plant Sci.* 5:315. doi: 10.3389/fpls.2014.00315

Kong, X., Liu, G., Liu, J., and Ding, Z. (2018). The root transition zone: a hot spot for signal crosstalk. *Trends in Plant Sci.* 23, 403–409. doi: 10.1016/j.tplants.2018.02.004

Konishi, M., Donner, T. J., Scarpella, E., and Yanagisawa, S. (2015). MONOPTEROS directly activates the auxin-inducible promoter of the Dof5.8 transcription factor gene in *Arabidopsis thaliana* leaf provascular cells. *J. Exp. Bot.* 66, 283–291. doi: 10.1093/jxb/eru418

Kuderová, A., Urbánková, I., Válková, M., Malbeck, J., Brzobohatý, B., Némethová, D., et al. (2008). Effects of conditional IPT-dependent cytokinin overproduction on root architecture of *Arabidopsis* seedlings. *Plant Cell Physiol.* 49, 570–582. doi: 10.1093/pcp/pcn029

Kumar, N., and Iyer-Pascuzzi, A. S. (2020). Shedding the last layer: mechanisms of root cap cell release. *Plants* 9:308. doi: 10.3390/plants9030308

Kumpf, R. P., and Nowack, M. K. (2015). The root cap: a short story of life and death. *J. Exp. Bot.* 66, 5651–5662. doi: 10.1093/jxb/erv295

Le, J., Vandenbussche, F., Van Der Straeten, D., and Verbelen, J. P. (2001). In the early response of *Arabidopsis* roots to ethylene, cell elongation is up- and down-regulated and uncoupled from differentiation. *Plant Physiol.* 125, 519–522. doi: 10.1104/pp.125.2.519

Lee, H. S., Kim, Y., Pham, G., Kim, J. W., Song, J. H., Lee, Y., et al. (2015). Brassinazole resistant 1 (BZR1)-dependent brassinosteroid signalling pathway leads to ectopic activation of quiescent cell division and suppresses columella stem cell differentiation. *J. Exp. Bot.* 66, 4835–4849. doi: 10.1093/jxb/erv316

Lee, R. D.-W., and Cho, H.-T. (2013). Auxin, the organizer of the hormonal/environmental signals for root hair growth. *Front. Plant Sci.* 4:448. doi: 10.3389/fpls.2013.00448

Li, T., Lei, W., He, R., Tang, X., Han, J., Zou, L., et al. (2020). Brassinosteroids regulate root meristem development by mediating BIN2-UPB1 module in *Arabidopsis*. *PLoS Genet.* 16:e1008883. doi: 10.1371/journal.pgen.1008883

Li, X., Chen, L., Forde, B. G., and Davies, W. J. (2017). Abscisic acid regulates root elongation through the activities of auxin and ethylene in *Arabidopsis thaliana*. *Front. Plant Sci.* 8:1493. doi: 10.3389/fpls.2017.01493

Libault, M., Brechenmacher, L., Cheng, J., Xu, D., and Stacey, G. (2010). Root hair systems biology. *Trends Plant Sci.* 15, 641–650. doi: 10.1016/j.tplants.2010.08.010

Mähönen, A. P., Tusscher, K. T., Siligato, R., Smetana, O., Díaz-Triviño, S., Salojärvi, J., et al. (2014). PLETHORA gradient formation mechanism separates auxin responses. *Nature* 515, 125–129. doi: 10.1038/nature13663

Marín-de la Rosa, N., Pfeiffer, A., Hill, K., Locascio, A., Bhalerao, R. P., Miskolczi, P., et al. (2015). Genome wide binding site analysis reveals transcriptional coactivation of cytokinin-responsive genes by DELLA proteins. *PLoS Genet.* 11:e1005337. doi: 10.1371/journal.pgen.1005337

Masucci, J. D., and Schiefelbein, J. W. (1996). Hormones act downstream of TTG and GL2 to promote root hair outgrowth during epidermis development in the *Arabidopsis* root. *Plant Cell* 8, 1505–1517. doi: 10.1105/tpc.8.9.1505

Medford, J. I., Horgan, R., El-Sawi, Z., and Klee, H. J. (1989). Alterations of endogenous cytokinins in transgenic plants using a chimeric isopentenyl transferase gene. *Plant Cell* 1, 403–413. doi: 10.1105/tpc.1.4.403

Méndez-Bravo, A., Ruiz-Herrera, L. F., Cruz-Ramírez, A., Guzman, P., Martínez-Trujillo, M., Ortiz-Castro, R., et al. (2019). CONSTITUTIVE TRIPLE RESPONSE1 and PIN2 act in a coordinate manner to support the indeterminate root growth and meristem cell proliferating activity in *Arabidopsis* seedlings. *Plant Sci.* 280, 175–186. doi: 10.1016/j.plantsci.2018.11.019

Michniewicz, M., Zago, M. K., Abas, L., Weijers, D., Schweighofer, A., Meskiene, I., et al. (2007). Antagonistic Regulation of PIN phosphorylation by PP2A and PINOID directs auxin flux. *Cell* 130, 1044–1056. doi: 10.1016/j.cell.2007.07.033

Miyawaki, K., Matsumoto-Kitano, M., and Kakimoto, T. (2004). Expression of cytokinin biosynthetic isopentenyltransferase genes in *Arabidopsis*: tissue specificity and regulation by auxin, cytokinin, and nitrate. *Plant J.* 37, 128–138. doi: 10.1046/j.1365-313X.2003.01945.x

Montesinos, J. C., Abuzeineh, A., Kopf, A., Juanes-Garcia, A., Ötvös, K., Petrášek, J., et al. (2020). Phytohormone cytokinin guides microtubule dynamics during cell progression from proliferative to differentiated stage. *EMBO J.* 39:e104238. doi: 10.15252/embj.2019104238

Moubayidin, L., DiMambro, R., Sozzani, R., Pacifici, E., Salvi, E., Terpstra, I., et al. (2013). Spatial coordination between stem cell activity and cell differentiation in the root meristem. *Dev. Cell* 26, 405–415. doi: 10.1016/j.devcel.2013.06.025

Moubayidin, L., Perilli, S., Dello Ioio, R., Di Mambro, R., Costantino, P., and Sabatini, S. (2010). The rate of cell differentiation controls the *Arabidopsis* root meristem growth phase. *Curr. Biol.* 20, 1138–1143. doi: 10.1016/j.cub.2010.05.035

Moubayidin, L., Salvi, E., Giustini, L., Terpstra, I., Heidstra, R., Costantino, P., et al. (2016). A Scarecrow-based regulatory circuit controls *Arabidopsis thaliana* meristem size from the root endodermis. *Planta* 243, 1159–1168. doi: 10.1007/s00425-016-2471-0

Mravec, J., Skčpa, P., Bailly, A., Hoyerová, K., Křeček, P., Bielach, A., et al. (2009). Subcellular homeostasis of phytohormone auxin is mediated by the ER-localized PIN5 transporter. *Nature* 459, 1136–1140. doi: 10.1038/nature08066

Müssig, C., Shin, G. H., and Altmann, T. (2003). Brassinosteroids promote root growth in *Arabidopsis*. *Plant Physiol.* 133, 1261–1271. doi: 10.1104/pp.103.028662

Okamoto, T., Tsurumi, S., Shibasaki, K., Obana, Y., Takaji, H., Oono, Y., et al. (2008). Genetic dissection of hormonal responses in the roots of *Arabidopsis* grown under continuous mechanical impedance. *Plant Physiol.* 146, 1651–1662. doi: 10.1104/pp.107.115519

Pacifici, E., Di Mambro, R., Dello Ioio, R., Costantino, P., and Sabatini, S. (2018). Acidic cell elongation drives cell differentiation in the *Arabidopsis* root. *EMBO J.* 37:e99134. doi: 10.15252/embj.201899134

Pasternak, T., Groot, E. P., Kazantsev, F. V., Teale, W., Omelyanchuk, N., Kovrizhnykh, V., et al. (2019). Salicylic acid affects root meristem patterning via auxin distribution in a concentration-dependent manner. *Plant Physiol.* 180, 1725–1739. doi: 10.1104/pp.19.00130

Pasternak, T., Rudas, V., Potters, G., and Jansen, M. A. K. (2005). Morphogenic effects of abiotic stress: reorientation of growth in *Arabidopsis thaliana* seedlings. *Environ. Exp. Bot.* 53, 299–314. doi: 10.1016/j.envexpbot.2004.04.009

Petersson, S. V., Johansson, A. I., Kowalczyk, M., Makoveychuk, A., Wang, J. Y., Moritz, T., et al. (2009). An auxin gradient and maximum in the *arabidopsis* root apex shown by high-resolution cell-specific analysis of IAA distribution and synthesis. *Plant Cell* 21, 1659–1668. doi: 10.1105/tpc.109.066480

Petrášek, J., and Friml, J. (2009). Auxin transport routes in plant development. *Development* 136, 2675–2688. doi: 10.1242/dev.030353

Pi, L., Aichinger, E., van der Graaff, E., Llavata-Peris, C. I., Weijers, D., Hennig, L., et al. (2015). Organizer-derived WOX5 signal maintains root columella stem cells through chromatin-mediated repression of CDF4 expression. *Dev. Cell* 33, 576–588. doi: 10.1016/j.devcel.2015.04.024

Promchuea, S., Zhu, Y., Chen, Z., Zhang, J., and Gong, Z. (2017). ARF2 coordinates with PLETHORAs and PINs to orchestrate ABA-mediated root meristem activity in *Arabidopsis*. *J. Integr. Plant Biol.* 59, 30–43. doi: 10.1111/jipb.12506

Qin, H., He, L., and Huang, R. (2019). The coordination of ethylene and other hormones in primary root development. *Front. Plant. Sci.* 10:874. doi: 10.3389/fpls.2019.00874

Rahman, A., Hosokawa, S., Oono, Y., Amakawa, T., Goto, N., and Tsurumi, S. (2002). Auxin and ethylene response interactions during *Arabidopsis* root hair development dissected by auxin influx modulators. *Plant Physiol.* 130, 1908–1917. doi: 10.1104/pp.010546

Rahman, A., Tsurumi, S., Amakawa, T., Soga, K., Hoson, T., Goto, N., et al. (2000). Involvement of ethylene and gibberellin signalings in chromosaponin I-induced cell division and cell elongation in the roots of *Arabidopsis* seedlings. *Plant Cell Physiol.* 41, 1–9. doi: 10.1093/pcp/41.1.1

Ramachandran, P., Augstein, F., Nguyen, V., and Carlsbecker, A. (2020). Coping with water limitation: hormones that modify plant root xylem development. *Front. Plant. Sci.* 11:570. doi: 10.3389/fpls.2020.00570

Ramachandran, P., Wang, G., Augstein, F., de Vries, J., and Carlsbecker, A. (2018). Continuous root xylem formation and vascular acclimation to water deficit involves endodermal ABA signalling via miR165. *Development* 145:dev159202. doi: 10.1242/DEV.159202

Richards, S., Wink, R. H., and Simon, R. (2015). Mathematical modelling of WOX5 - and CLE40 -mediated columella stem cell homeostasis in *Arabidopsis*. *EXBOTJ* 66, 5375–5384. doi: 10.1093/jxb/erv257

Rizza, A., Walia, A., Lanquar, V., Frommer, W. B., and Jones, A. M. (2017). In vivo gibberellin gradients visualized in rapidly elongating tissues. *Nat. Plants* 3, 803–813. doi: 10.1038/s41477-017-0021-9

Rizza, A., Walia, A., Tang, B., and Jones, A. M. (2019). Visualizing cellular gibberellin levels using the nlsGPS1 förster resonance energy transfer (FRET) biosensor. *J. Vis. Exp.* 2019, 1–9. doi: 10.3791/58739

Ruyter-Spira, C., Kohlen, W., Charnikhova, T., van Zeijl, A., van Bezouwen, L., de Ruijter, N., et al. (2011). Physiological effects of the synthetic strigolactone analog GR24 on root system architecture in *Arabidopsis*: another belowground role for strigolactones? *Plant Physiol.* 155, 721–734. doi: 10.1104/pp.110.166645

Rùžièka, K., Ljung, K., Vanneste, S., Podhorská, R., Beeckman, T., Friml, J., et al. (2007). Ethylene regulates root growth through effects on auxin biosynthesis and transport-dependent auxin distribution. *Plant Cell* 19, 2197–2212. doi: 10.1105/tpc.107.052126

Růzička, K., Šimášková, M., Duclercq, J., Petrášek, J., Zažímalová, E., Simon, S., et al. (2009). Cytokinin regulates root meristem activity via modulation of the polar auxin transport. *Proc. Natl. Acad. Sci. U. S. A.* 106, 4284–4289. doi: 10.1073/pnas.0900060106

Sabatini, S. (2003). SCARECROW is involved in positioning the stem cell niche in the Arabidopsis root meristem. *Genes Dev.* 17, 354–358. doi: 10.1101/gad.252503

Salazar-Henao, J. E., Vélez-Bermúdez, I. C., and Schmidt, W. (2016). The regulation and plasticity of root hair patterning and morphogenesis. *Development* 143, 1848–1858. doi: 10.1242/dev.132845

Salvi, E., Rutten, J. P., Di Mambro, R., Polverari, L., Licursi, V., Negri, R., et al. (2020). A self-organized PLT/Auxin/ARR-B network controls the dynamics of root zonation development in *Arabidopsis thaliana*. *Dev. Cell* 53, 431.e23–443.e23. doi: 10.1016/j.devcel.2020.04.004

Sánchez-Calderón, L., Ibarra-Cortes, M. E., and Zepeda-Jazo, I. (2013). *"Root Development and Abiotic Stress Adaptation," in Abiotic Stress - Plant Responses and Applications in Agriculture*. London: IntechOpen, doi: 10.5772/55043

Santuari, L., Sanchez-Perez, G. F., Luijten, M., Rutjens, B., Terpstra, I., Berke, L., et al. (2016). The PLETHORA gene regulatory network guides growth and cell differentiation in *Arabidopsis* roots. *Plant Cell* 28, 2937–2951. doi: 10.1105/tpc.16.00656

Sarkar, A. K., Luijten, M., Miyashima, S., Lenhard, M., Hashimoto, T., Nakajima, K., et al. (2007). Conserved factors regulate signalling in *Arabidopsis thaliana* shoot and root stem cell organizers. *Nature* 446, 811–814. doi: 10.1038/nature05703

Scheres, B., and Krizek, B. A. (2018). Coordination of growth in root and shoot apices by AIL/PLT transcription factors. *Curr. Opin. Plant Biol.* 41, 95–101. doi: 10.1016/j.pbi.2017.10.002

Scheres, B., and Wolkenfelt, H. (1998). The *Arabidopsis* root as a model to study plant development. *Plant Physiol. Biochem.* 36, 21–32. doi: 10.1016/S0981-9428(98)80088-0

Schiefelbein, J., Kwak, S. H., Wieckowski, Y., Barron, C., and Bruex, A. (2009). The gene regulatory network for root epidermal cell-type pattern formation in *Arabidopsis*. *J. Exp. Bot.* 60, 1515–1521. doi: 10.1093/jxb/ern339

Shani, E., Weinstain, R., Zhang, Y., Castillejo, C., Kaiserli, E., Chory, J., et al. (2013). Gibberellins accumulate in the elongating endodermal cells of *Arabidopsis* root. *Proc. Natl. Acad. Sci. U. S. A.* 110, 4834–4839. doi: 10.1073/pnas.1300436110

Shibata, M., and Sugimoto, K. (2019). A gene regulatory network for root hair development. *J. Plant Res.* 132, 301–309. doi: 10.1007/s10265-019-01100-2

Shimotohno, A., Heidstra, R., Blilou, I., and Scheres, B. (2018). Root stem cell niche organizer specification by molecular convergence of PLETHORA and SCARECROW transcription factor modules. *Genes Dev.* 32, 1085–1100. doi: 10.1101/gad.314096.118

Smet, W., and De Rybel, B. (2016). Genetic and hormonal control of vascular tissue proliferation. *Curr. Opin. Plant Biol.* 29, 50–56. doi: 10.1016/j.pbi.2015.11.004

Somssich, M., Khan, G. A., and Staffan, S. P. (2016). Cell wall heterogeneity in root development of *arabidopsis*. *Front. Plant. Sci.* 7:1242. doi: 10.3389/fpls.2016.01242

Stahl, Y., Wink, R. H., Ingram, G. C., and Simon, R. (2009). A signaling module controlling the stem cell niche in *Arabidopsis* root meristems. *Curr. Biol.* 19, 909–914. doi: 10.1016/j.cub.2009.03.060

Stepanova, A. N., Hoyt, J. M., Hamilton, A. A., and Alonso, J. M. (2005). A link between ethylene and auxin uncovered by the characterization of two root-specific ethylene-insensitive mutants in *Arabidopsis*. *Plant Cell* 17, 2230–2242. doi: 10.1105/tpc.105.033365

Stepanova, A. N., Robertson-Hoyt, J., Yun, J., Benavente, L. M., Xie, D. Y., Doležal, K., et al. (2008). TAA1-mediated auxin biosynthesis is essential for hormone crosstalk and plant development. *Cell* 133, 177–191. doi: 10.1016/j.cell.2008.01.047

Stepanova, A. N., Yun, J., Likhacheva, A. V., and Alonso, J. M. (2007). Multilevel interactions between ethylene and auxin in *Arabidopsis* roots. *Plant Cell* 19, 2169–2185. doi: 10.1105/tpc.107.052068

Street, I. H., Aman, S., Zubo, Y., Ramzan, A., Wang, X., Shakeel, S. N., et al. (2015). Ethylene inhibits cell proliferation of the *Arabidopsis* root meristem. *Plant Physiol.* 169, 338–350. doi: 10.1104/pp.15.00415

Street, I. H., Mathews, D. E., Yamburkenko, M. V., Sorooshzadeh, A., John, R. T., Swarup, R., et al. (2016). Cytokinin acts through the auxin influx carrier AUX1 to regulate cell elongation in the root. *Development* 143, 3982–3993. doi: 10.1242/dev.132035

Sun, Y., Fan, X. Y., Cao, D. M., Tang, W., He, K., Zhu, J. Y., et al. (2010). Integration of brassinosteroid signal transduction with the transcription network for plant growth regulation in *Arabidopsis*. *Dev. Cell* 19, 765–777. doi: 10.1016/j.devcel.2010.10.010

Swarup, R., Friml, J., Marchant, A., Ljung, K., Sandberg, G., Palme, K., et al. (2001). Localization of the auxin permease AUX1 suggests two functionally distinct hormone transport pathways operate in the *Arabidopsis* root apex. *Genes Dev.* 15, 2648–2653. doi: 10.1101/gad.210501

Swarup, R., Perry, P., Hagenbeek, D., Van Der Straeten, D., Beemster, G. T. S., Sandberg, G., et al. (2007). Ethylene upregulates auxin biosynthesis in *Arabidopsis* seedlings to enhance inhibition of root cell elongation. *Plant Cell* 19, 2186–2196. doi: 10.1105/tpc.107.052100

Takahashi, N., Kajihara, T., Okamura, C., Kim, Y., Katagiri, Y., Okushima, Y., et al. (2013). Cytokinins control endocycle onset by promoting the expression of an APC/C activator in *Arabidopsis* roots. *Curr. Biol.* 23, 1812–1817. doi: 10.1016/j.cub.2013.07.051

Takatsuka, H., Higaki, T., and Umeda, M. (2018). Actin reorganization triggers rapid cell elongation in roots. *Plant Physiol.* 178, 1130–1141. doi: 10.1104/pp.18.00557

Takatsuka, H., and Umeda, M. (2014). Hormonal control of cell division and elongation along differentiation trajectories in roots. *J. Exp. Bot.* 65, 2633–2643. doi: 10.1093/jxb/ert485

Takatsuka, H., and Umeda, M. (2019). ABA inhibits root cell elongation through repressing the cytokinin signaling. *Plant Signal. Behav.* 14:e1578632. doi: 10.1080/15592324.2019.1578632

Tanimoto, E. (2005). Regulation of root growth by plant hormones - roles for auxin and gibberellin. *Crit. Rev. Plant Sci.* 24, 249–265. doi: 10.1080/07352680500196108

Tanimoto, M., Roberts, K., and Dolan, L. (1995). Ethylene is a positive regulator of root hair development in *Arabidopsis thaliana*: root hair development in *A. thaliana*. *Plant J.* 8, 943–948. doi: 10.1046/j.1365-313X.1995.8060943.x

Tapia-López, R., García-Ponce, B., Dubrovsky, J. G., Garay-Arroyo, A., Pérez-Ruíz, R. V., Kim, S.-H., et al. (2008). An AGAMOUS-related MADS-box gene, XAL1

(AGL12), regulates root meristem cell proliferation and flowering transition in *Arabidopsis*. *Plant Physiol.* 146, 1182–1192. doi: 10.1104/pp.107.108647

Tian, H., Wabnik, K., Niu, T., Li, H., Yu, Q., Pollmann, S., et al. (2014). WOX5–IAA17 feedback circuit-mediated cellular auxin response is crucial for the patterning of root stem cell niches in *Arabidopsis*. *Mol. Plant* 7, 277–289. doi: 10.1093/mp/sst118

Tsugeki, R., and Fedoroff, N. V. (1999). Genetic ablation of root cap cells in *Arabidopsis*. *Proc. Natl. Acad. Sci. U. S. A.* 96, 12941–12946. doi: 10.1073/pnas.96.22.12941

Ubeda-Tomás, S., Federici, F., Casimiro, I., Beemster, G. T. S., Bhalerao, R., Swarup, R., et al. (2009). Gibberellin signaling in the endodermis controls *Arabidopsis* root meristem size. *Curr. Biol.* 19, 1194–1199. doi: 10.1016/j.cub.2009.06.023

Ubeda-Tomás, S., Swarup, R., Coates, J., Swarup, K., Laplaze, L., Beemster, G. T. S., et al. (2008). Root growth in *Arabidopsis* requires gibberellin/DELLA signalling in the endodermis. *Nat. Cell Biol.* 10, 625–628. doi: 10.1038/ncb1726

Van den Berg, C., Willemsen, V., Hage, W., Weisbeek, P., and Scheres, B. (1995). Cell fate in the *Arabidopsis* root meristem determined by directional signalling. *Nature* 378, 62–65. doi: 10.1038/378062a0

Van Den Berg, C., Willemsen, V., Hendriks, G., Weisbeek, P., and Scheres, B. (1997). Short-range control of cell differentiation in the *Arabidopsis* root meristem. *Nature* 390, 287–289. doi: 10.1038/36856

Vaseva, I. I., Qudeimat, E., Potuschak, T., Du, Y., Genschik, P., Vandenbussche, F., et al. (2018). The plant hormone ethylene restricts *Arabidopsis* growth via the epidermis. *Proc. Natl. Acad. Sci. U.S.A.* 115, E4130–E4139. doi: 10.1073/pnas.1717649115

Vaughan-Hirsch, J., Goodall, B., and Bishopp, A. (2018). North, East, South, West: mapping vascular tissues onto the *Arabidopsis* root. *Curr. Opin. Plant Biol.* 41, 16–22. doi: 10.1016/j.pbi.2017.07.011

Vázquez-Chimalhua, E., Ruíz-Herrera, L. F., Barrera-Ortiz, S., Valencia-Cantero, E., and López-Bucio, J. (2019). The bacterial volatile dimethyl-hexa-decylamine reveals an antagonistic interaction between jasmonic acid and cytokinin in controlling primary root growth of *Arabidopsis* seedlings. *Protoplasma* 256, 643–654. doi: 10.1007/s00709-018-1327-9

Verbelen, J. P., De Cnodder, T., Le, J., Vissenberg, K., and Baluška, F. (2006). The root apex of *Arabidopsis thaliana* consists of four distinct zones of growth activities: meristematic zone, transition zone, fast elongation zone and growth terminating zone. *Plant Signal. Behav.* 1, 296–304. doi: 10.4161/psb.1.6.3511

Vieten, A., Vanneste, S., Wiśniewska, J., Benková, E., Benjamins, R., Beeckman, T., et al. (2005). Functional redundancy of PIN proteins is accompanied by auxin-dependent cross-regulation of PIN expression. *Development* 132, 4521–4531. doi: 10.1242/dev.02027

Vissenberg, K., Claeijs, N., Balcerowicz, D., and Schoenaers, S. (2020). Hormonal regulation of root hair growth and responses to the environment in *Arabidopsis*. *J. Exp. Bot.* 71, 2412–2427. doi: 10.1093/jxb/eraa048

Vragoviæ, K., Selaa, A., Friedlander-Shani, L., Fridman, Y., Hacham, Y., Holland, N., et al. (2015). Translatome analyses capture of opposing tissuespecific brassinosteroid signals orchestrating root meristem differentiation. *Proc. Natl. Acad. Sci. U. S. A.* 112, 923–928. doi: 10.1073/pnas.1417947112

Waidmann, S., Sarkel, E., and Kleine-Vehn, J. (2020). Same same, but different: growth responses of primary and lateral roots. *J. Exp. Bot.* 71, 2397–2411. doi: 10.1093/jxb/eraa027

Wang, J. W., Wang, L. J., Mao, Y. B., Cai, W. J., Xue, H. W., and Chen, X. Y. (2005). Control of root cap formation by MicroRNA-targeted auxin response factors in *Arabidopsis*. *Plant Cell* 17, 2204–2216. doi: 10.1105/tpc.105.033076

Wang, Y. H., and Irving, H. R. (2011). Developing a model of plant hormone interactions. *Plant Signal. Behav.* 6, 494–500. doi: 10.4161/psb.6.4.14558

Wein, A., Le Gac, A. L., and Laux, T. (2020). Stem cell ageing of the root apical meristem of *Arabidopsis thaliana*. *Mech. Ageing Dev.* 190:111313. doi: 10.1016/j.mad.2020.111313

Wen, F., Curlango-Rivera, G., and Hawes, M. C. (2007). Proteins among the polysaccharides: a new perspective on root cap Slime. *Plant Signal. Behav.* 2, 410–412. doi: 10.4161/psb.2.5.4344

Werner, T., Motyka, V., Laucou, V., Smets, R., Van Onckelen, H., and Schmülling, T. (2003). The plant cell cytokinin-deficient transgenic *Arabidopsis* plants show multiple developmental alterations indicating opposite functions of cytokinins in the regulation of shoot and root meristem activity. *Plant Cell* 15, 2532–2550. doi: 10.1105/tpc.014928

Willemsen, V., Bauch, M., Bennett, T., Campilho, A., Wolkenfelt, H., Xu, J., et al. (2008). The NAC domain transcription factors FEZ and SOMBRERO control the orientation of cell division plane in *Arabidopsis* root stem cells. *Dev. Cell* 15, 913–922. doi: 10.1016/j.devcel.2008.09.019

Wu, Y., and Cosgrove, D. J. (2000). Adaptation of roots to low water potentials by changes in cell wall extensibility and cell wall proteins. *J. Exp. Bot.* 51, 1543–1553. doi: 10.1093/jexbot/51.350.1543

Xie, Q., Essemine, J., Pang, X., Chen, H., and Cai, W. (2020). Exogenous application of abscisic acid to shoots promotes primary root cell division and elongation. *Plant Sci.* 292:110385. doi: 10.1016/j.plantsci.2019.110385

Xuan, W., Audenaert, D., Parizot, B., Möller, B. K., Njo, M. F., De Rybel, B., et al. (2015). Root cap-derived auxin pre-patterns the longitudinal axis of the *Arabidopsis* root. *Curr. Biol.* 25, 1381–1388. doi: 10.1016/j.cub.2015.03.046

Xuan, W., Band, L. R., Kumpf, R. P., Van Damme, D., Parizot, B., De Rop, G., et al. (2016). Cyclic programmed cell death stimulates hormone signaling and root development in *Arabidopsis*. *Science* 351, 384–387. doi: 10.1126/science.aad2776

Yang, L., Zhang, J., He, J., Qin, Y., Hua, D., Duan, Y., et al. (2014). ABA-mediated ROS in mitochondria regulate root meristem activity by controlling PLETHORA expression in *Arabidopsis*. *PLoS Genet.* 10:e1004791. doi: 10.1371/journal.pgen.1004791

Yin, Y., Vafeados, D., Tao, Y., Yoshida, S., Asami, T., and Chory, J. (2005). A new class of transcription factors mediates brassinosteroid-regulated gene expression in *Arabidopsis*. *Cell* 120, 249–259. doi: 10.1016/j.cell.2004.11.044

Zdarska, M., Cuyacot, A. R., Tarr, P. T., Yamoune, A., Szmitkowska, A., Hrdinová, V., et al. (2019). ETR1 integrates response to ethylene and cytokinins into a single multistep phosphorelay pathway to control root growth. *Mol. Plant* 12, 1338–1352. doi: 10.1016/j.molp.2019.05.012

Zhang, H., Han, W., De Smet, I., Talboys, P., Loya, R., Hassan, A., et al. (2010). ABA promotes quiescence of the quiescent centre and suppresses stem cell differentiation in the *Arabidopsis* primary root meristem. *Plant J.* 64, 764–774. doi: 10.1111/j.1365-313X.2010.04367.x

Zhang, S., Huang, L., Yan, A., Liu, Y., Liu, B., Yu, C., et al. (2016). Multiple phytohormones promote root hair elongation by regulating a similar set of genes in the root epidermis in *Arabidopsis*. *J. Exp. Bot.* 67, 6363–6372. doi: 10.1093/jxb/erw400

Zhu, C., Gan, L., Shen, Z., and Xia, K. (2006). Interactions between jasmonates and ethylene in the regulation of root hair development in *Arabidopsis*. *J. Exp. Bot.* 57, 1299–1308. doi: 10.1093/jxb/erj103

Zhu, Z., An, F., Feng, Y., Li, P., Xue, L. Mu, A., et al. (2011). Derepression of ethylene-stabilized transcription factors (EIN3/EIL1) mediates jasmonate and ethylene signaling synergy in *Arabidopsis*. *Proc. Natl. Acad. Sci. U. S. A.* 108, 12539–12544. doi: 10.1073/pnas.1103959108

Conflict of Interest: The authors declare that the research was conducted in the absence of any commercial or financial relationships that could be construed as a potential conflict of interest.

frontiers in Plant Science

REVIEW
published: 27 April 2021
doi: 10.3389/fpls.2021.660274

Reactive Oxygen Species Link Gene Regulatory Networks During *Arabidopsis* Root Development

*Kosuke Mase and Hironaka Tsukagoshi**

Faculty of Agriculture, Meijo University, Nagoya, Japan

Plant development under altered nutritional status and environmental conditions and during attack from invaders is highly regulated by plant hormones at the molecular level by various signaling pathways. Previously, reactive oxygen species (ROS) were believed to be harmful as they cause oxidative damage to cells; however, in the last decade, the essential role of ROS as signaling molecules regulating plant growth has been revealed. Plant roots accumulate relatively high levels of ROS, and thus, maintaining ROS homeostasis, which has been shown to regulate the balance between cell proliferation and differentiation at the root tip, is important for proper root growth. However, when the balance is disturbed, plants are unable to respond to the changes in the surrounding conditions and cannot grow and survive. Moreover, ROS control cell expansion and cell differentiation processes such as root hair formation and lateral root development. In these processes, the transcription factor-mediated gene expression network is important downstream of ROS. Although ROS can independently regulate root growth to some extent, a complex crosstalk occurs between ROS and other signaling molecules. Hormone signals are known to regulate root growth, and ROS are thought to merge with these signals. In fact, the crosstalk between ROS and these hormones has been elucidated, and the central transcription factors that act as a hub between these signals have been identified. In addition, ROS are known to act as important signaling factors in plant immune responses; however, how they also regulate plant growth is not clear. Recent studies have strongly indicated that ROS link these two events. In this review, we describe and discuss the role of ROS signaling in root development, with a particular focus on transcriptional regulation. We also summarize the crosstalk with other signals and discuss the importance of ROS as signaling molecules for plant root development.

Keywords: reactive oxygen species, *Arabidopsis thaliana*, transcription factor, primary root development, stem cell niche, lateral root development, root hair development, crosstalk

OPEN ACCESS

Edited by:
Ramiro Esteban Rodriguez, CONICET Instituto de Biología Molecular y Celular de Rosario, Argentina

Reviewed by:
Ana María Laxalt, National University of Mar del Plata, Argentina
Keith Lindsey, Durham University, United Kingdom

***Correspondence:**
Hironaka Tsukagoshi
thiro@meijo-u.ac.jp

Specialty section:
This article was submitted to Plant Development and EvoDevo, a section of the journal Frontiers in Plant Science

Received: *29 January 2021*
Accepted: *22 March 2021*
Published: *27 April 2021*

Citation:
Mase K and Tsukagoshi H (2021) Reactive Oxygen Species Link Gene Regulatory Networks During Arabidopsis Root Development. Front. Plant Sci. 12:660274. doi: 10.3389/fpls.2021.660274

Abbreviations: ABA, abscisic acid; ARFs, auxin response factors; bHLH, basic helix-loop-helix; BRs, brassinosteroids; CASPs, Casparian strip domain proteins; DSBs, double-strand breaks; ERF, ethylene response factor; FLS2, *FLAGELLIN SENSING 2*; LR, lateral root; LRP, LR primordium; MAMPs, microbe-associated molecular patterns; NPR1, NON-EXPRESSOR OF PR GENES 1. PLT, PLETHORA; PSK5, PHYTOSULFOKINE 5; QC, quiescent center; RBOH proteins, RESPIRATORY BURST OXIDASE HOMOLOG proteins; RCS, reactive carbonyl species; RGF1, root meristem growth factor 1; *RHD6*, *ROOT HAIR DEFECTIVE 6*; RITF1, RGF1 INDUCIBLE TRANSCRIPTION FACTOR 1; ROPs, Rho-type GTPases of plants; ROS, reactive oxygen species; RSL4, ROOT HAIR DEFECTIVE SIX-LIKE 4; SA, salicylic acid; SCN, stem cell niche; SCR, SCARECROW; SHR, SHORT ROOT; SKP2B, S-phase kinase-associated protein 2; SOD, superoxide dismutase; SOG1, SUPPRESSOR OF GAMMA RESPONSE 1; VLCFAs, very-long chain fatty acids; WOX5, WUSCHEL-related homeobox 5.

INTRODUCTION

Oxygen (O_2) is a stable molecule that is required for the survival of aerobic organisms on Earth. However, during various *in vivo* processes, especially respiration, it can change into high-energy molecules called reactive oxygen species (ROS; superoxide, O_2^-; hydrogen peroxide, H_2O_2; hydroxyl radical, $^{\cdot}OH$; and singlet oxygen, $^1O_2$). In general, high levels of ROS are known to be cytotoxic because their oxidative properties in living cells cause damage to DNA, lipids, and proteins.

In plants, ROS are produced as a by-product of normal aerobic metabolism processes such as electron transport chains or redox reactions in chloroplasts or mitochondria (Hossain et al., 2015). Even other cellular compartments such as peroxisomes and microsomes generate ROS (Hossain et al., 2015). NADPH oxidases (RESPIRATORY BURST OXIDASE HOMOLOG proteins, also called RBOH proteins), which are known as O_2^- generators, function in fundamental respiration processes such as photosynthetic electron transport chains and mitochondrial respiratory electron transport chains as well as play a role in catalyzing ROS on the plasma membrane (Chapman et al., 2019; Kaya et al., 2019). O_2^-, a precursor of various ROS, is converted to H_2O_2 spontaneously or enzymatically *via* superoxide dismutase (SOD; Wang Y. et al., 2018), oxalate oxidase (Caliskan and Cuming, 1998), or diamine oxidase (Federico and Angelini, 1986). ROS are generated both inside and outside cells, although their lifespan is very short. Among ROS, H_2O_2 is the most stable (half-life, more than 1 ms), is considered an important redox signaling molecule (Mhamdi and Van Breusegem, 2018), and is spontaneously metabolized to H_2O and O_2 by class III peroxidases (Smirnoff and Arnaud, 2019). $^{\cdot}OH$ possesses the highest oxidizing power and is unstable (half-life, 1 ns; Mittler, 2017; Mhamdi and Van Breusegem, 2018). $^1O_2$ is usually formed in chloroplast photosystem II (Dmitrieva et al., 2020). Although ROS are cytotoxic, previous studies have shown that plants utilize them as signaling molecules to develop organs and respond to stress by regulating gene expression.

Plants are constantly subjected to various abiotic and biotic stresses such as salt, drought, and pathogen attack, which significantly increase ROS levels, leading to redox imbalance in their life cycle (Hasanuzzaman et al., 2020). Plants also accumulate massive amounts of ROS for protection against pathogen attack, which involves cell death of plant cells themselves (Qi et al., 2017). The excess accumulation of ROS might damage their organs and could occasionally lead to dysfunction or death. However, appropriate ROS levels act as signaling molecules for organ development and in response to biotic or abiotic stress. In fact, plant root tips constantly accumulate ROS levels that are not found in normal leaves (Dunand et al., 2007). In the process of evolution, plants have established an elaborate system for controlling oxidative stress and using ROS as signaling molecules. Herein, we introduce the important role of ROS homeostasis, focusing on plant roots.

Roots play critical roles in plants. They structurally support the plant and provide water and nutrients for survival. Furthermore, roots act as sensors for detecting alterations in the surrounding environment, such as drought and salt stress and presence of microorganisms. Roots also maintain growth in the direction of gravity with cell proliferation and differentiation in the root tip. In addition, lateral roots and root hairs facilitate the expansion of the surface and rhizosphere. Plant roots can be distinguished into different zones from the root tip to the base along the longitudinal axis based on their characteristics: the meristematic, elongation, and maturation zones (Petricka et al., 2012).

Root growth occurs by the repeated cell division in the meristematic zone. A quiescent center (QC) is located in the apical meristem, which hardly divides, but is surrounded by a stem cell niche (SCN). The major genetic regulators of root growth include the AP-2 transcription factor PLETHORAs (PLTs; Aida et al., 2004), the GRAS family transcription factor SHORT ROOT (SHR; Benfey et al., 1993; Helariutta et al., 2000), SCARECROW (SCR; Di Laurenzio et al., 1996; Sabatini et al., 2003), and the homeodomain transcription factor WUSCHEL-related homeobox 5 (WOX5; Sarkar et al., 2007). Both PLT1 and PLT2 are required for distal cell division and stem cell maintenance (Aida et al., 2004), and redox balance has been reported to affect PLT functions (Licausi et al., 2013). SHR is first expressed in the stele (Benfey et al., 1993; Helariutta et al., 2000) and then moves into the cells, including the QC and endodermis (Nakajima et al., 2001). SCR, which is one of the downstream SHR transcription factors, plays a role in radial patterning and acts cell-autonomously for the distal specification of the QC interacting with SHR at the protein level (Di Laurenzio et al., 1996; Nakajima et al., 2001; Sabatini et al., 2003; Levesque et al., 2006) in a parallel pathway to PLT-related network (Aida et al., 2004). SCR–SHR regulates asymmetric cell division at the SCN and determines the identity of the endodermis and cortex cells by regulating the expression of cell cycle-related genes (Nakajima et al., 2001; Sozzani et al., 2010). WOX5, which is expressed at the QC, acts non-cell-autonomously to prevent stem cell differentiation downstream of SHR and SCR, but not of PLT proteins (Sarkar et al., 2007). In addition to these transcription factors, many other factors generate complex gene networks and systems for the maintenance of the SCN (Iyer-Pascuzzi and Benfey, 2009; Petricka et al., 2012). Thus, a gene regulatory network controlled by several key transcription factors ensures proper root development by controlling cell patterning in the SCN.

In the elongation zone, cells stop proliferating and rapidly begin to elongate along the longitudinal axis with cell wall loosening. The primary plant cell wall is composed of several polysaccharides such as cellulose, hemicelluloses, and pectins (Gorshkova et al., 2013). Although cell wall enzymes generate and modify cell wall components, ROS are also important for cell wall remodeling (hardening or loosening). Many studies have shown that ROS generated in the apoplast *via* NADPH oxidases in the plasma membrane are involved in controlling cell wall rigidity (Kärkönen and Kuchitsu, 2015). As mentioned above, extracellular O_2^- is spontaneously or enzymatically converted to H_2O_2 and then to $^{\cdot}OH$. The release of these reactive oxygen radicals can enzyme-independently oxidize cell wall polysaccharides *via* electron transfer (Kärkönen and Kuchitsu, 2015; Somssich et al., 2016). Especially, $^{\cdot}OH$ cleaves pectin and/or hemicellulose resulting in the loosening of the cell wall

in the elongation zone (Chen and Schopfer, 1999). Conversely, the accumulation of apoplastic H_2O_2 and ROS scavengers such as ascorbic acid can inhibit cell wall elongation (Somssich et al., 2016). Thus, during cell wall remodeling, apoplastic ROS homeostasis helps cells in the elongation zone to control vertical growth.

In the maturation zone, cell maturation involves finely differentiated organs such as the Casparian strip, root hair, and lateral root. The Casparian strip acts as a diffusion barrier in the root endodermal cell layers of vascular plants and helps to protect against pathogen attack and to conduct selective nutrient uptake (Barberon, 2017; Nakamura and Grebe, 2018). The establishment of the Casparian strip in *Arabidopsis* roots requires localized ROS production. Several NADPH oxidases—mainly RBOHF and RBOHD—and peroxidases produce ROS in the extracellular matrix through the action of localized Casparian strip domain proteins (CASPs), which act as scaffolds on the root endodermal plasma membrane (Fujita et al., 2020). During Casparian strip formation, localized ROS production facilitates oxidative polymerization of monolignols to form lignin macromolecules (Liu, 2012). Casparian strip formation is initiated by the binding of the vasculature-derived peptide, Casparian strip integrity factor (CIFs), and its receptor, SCHENGEN3 (SGN3), which colocalizes on the endodermis with SGN1 kinase (Fujita et al., 2020), followed by the expression of transcription factors such as MYB36 (Kamiya et al., 2015), MYB41 (Kosma et al., 2014), and MYB15 (Chezem et al., 2017), which regulate Casparian strip formation, suberization, and lignification, respectively, by regulating downstream gene expression (Fujita et al., 2020). In particular, MYB36 directly and positively regulates the expression of genes required for Casparian strip formation, such as *CASP1*, *PEROXIDASE 64* (*PER64*), and *Enhanced Suberin 1* (*ESB1*; Kamiya et al., 2015). Thus, under these signaling pathways, local ROS accumulation around the root endodermal cells contributes to lignification, which acts as a diffusion barrier. Conversely, root hair and lateral root play important roles in the expansion of the rhizosphere. ROS are also involved as signaling molecules in this process.

Although ROS are known to regulate various aspects of root development, they themselves do not control root growth. This process is controlled by a very complex signal network, which especially involves interaction with plant hormones. Auxin, which is one of the critical plant hormones, has physiological activity and significantly affects several plant development processes such as cell proliferation and elongation. In the root, auxin accumulates at high concentration in the apical meristem and forms a gradient that decreases toward the basal meristem according to polar transport, which is mainly regulated by auxin influx and efflux carriers—AUX and PINs—respectively (Armengot et al., 2016). In addition, cytokinin, which is an antagonist hormone of auxin, is important and affects plant development along with auxin activity. Morphological formation has been shown to be controlled by auxin and cytokinin signaling; moreover, redox balance is known to play an important role in hormonal activity (Tognetti et al., 2017). Other hormones such as brassinosteroids (BRs), abscisic acid (ABA), and salicylic acid (SA) are also involved in ROS signaling (Overmyer et al., 2003; Lv et al., 2018; Planas-Riverola et al., 2019). In the crosstalk between ROS and plant hormones, various key transcription factors and downstream secondary messengers have been found to play important roles.

To prove that ROS act as signaling molecules, as described above, it is important to detect ROS at the cellular level. Therefore, accurate and specific tools for detecting each ROS are required. For instance, nitroblue tetrazolium (NBT) and diaminobenzidine (DAB) are widely used for the classical staining methods. NBT can be used to detect or quantify O_2^- by observing blue deposits under a bright field or by formazan extraction (Driever et al., 2009; Bournonville and Díaz-Ricci, 2011). DAB reacts with H_2O_2 to form brown polymerization products (Driever et al., 2009). Since DAB staining is performed under relatively low pH conditions (pH < 3.6), care should be taken to avoid ROS production under these experimental conditions rather than DAB staining itself (Swanson et al., 2011). DAB shows relatively low specificity for ROS. Both staining methods can detect ROS at the tissue level, but they cause cell death. To measure the real-time behavior of ROS, more accurate and live-cell methods using fluorescent probes such as dihydroethidium (DHE), hydroxyphenyl fluorescein (HPF), 2′-7′-dichlorodihydrofluorescein diacetate (DCFH-DA), H_2O_2-3′-O-acetyl-6′-O-pentafluorobenzenesulfonyl-2′-7′-difluorofluorescein-Ac (H_2O_2-BES-Ac), and peroxy orange 1 (PO1) have been developed. DHE produces red fluorescence and is used to detect O_2^- (Benov et al., 1998; Kalyanaraman et al., 2012). HPF can detect highly reactive oxygen species such as $^{\cdot}OH$ and $ONOO^-$, whereas it barely reacts with O_2^-, H_2O_2, and $^1O_2$ (Setsukinai et al., 2003). DCFH-DA is frequently used to detect H_2O_2. A specific indicator for H_2O_2, H_2O_2-BES-Ac is useful for measuring intracellular H_2O_2 (Maeda et al., 2004; Maeda, 2008). PO1 produces intracellular fluorescence in response to H_2O_2 (Chang et al., 2004; Miller et al., 2005; Dickinson et al., 2010). However, because aromatic boronate-based indicators can react with $ONOO^-$ faster than with H_2O_2, they may reduce the specificity for H_2O_2 detection (Ortega-Villasante et al., 2018). Furthermore, it is also possible to perform spatial detection of ROS by double staining with different ROS-specific probes with different fluorescence wavelength, for example DHE and BES-H_2O_2-Ac (Tsukagoshi et al., 2010). Additionally, promoter reporter constructs such as *pZat12:Luciferase* and *pWRKY40:Luciferase*, carrying the promoters of ROS-responsive genes, are utilized for live imaging in *Arabidopsis* for detecting the alterations in ROS levels indirectly through gene expression (Miller et al., 2009; Devireddy et al., 2018). Furthermore, HyPer, a transgenic fluorescent indicator, can be used for detecting intracellular H_2O_2 (Belousov et al., 2006). HyPer consists of a circularly permuted yellow fluorescent protein (cpYFP) inserted into OxyR-RD, which is the regulatory domain of an *Escherichia coli* peroxide sensor. Notably, the fluorescence of HyPer is pH dependent (Belousov et al., 2006; Swanson et al., 2011). Using these methods, it is possible to visualize the speed of spread and spatiotemporal regulation of ROS signaling in a live plant (Hernández-Barrera et al., 2015; Fichman et al., 2019). Many studies related to ROS require different methods for detecting and quantifying their levels at the scale of cells, tissues,

and organs. These methods of ROS detection have led to the discovery of changes in ROS levels related to root growth and crosstalk with other signals.

Since many recent studies have revealed the molecular mechanisms regulated by ROS, we focused on the functions of ROS as signaling molecules in root development and on the crosstalk with other signals such as phytohormones and biotic stresses in *Arabidopsis thaliana*. In particular, we describe the regulation of gene expression by transcription factors, which act as key regulators of signal transduction.

ROS ACT AS SIGNALING MOLECULES FOR REGULATING ROOT GROWTH

The gradient distribution of ROS regulates the transition of cells from proliferation to differentiation at the root tip. O_2^- accumulates in the meristematic zone, whereas H_2O_2 mainly accumulates in the elongation zone (Dunand et al., 2007). During ROS signaling, transcriptional control is one of the key regulators of root development. For maintaining the ROS balance between the meristematic and elongation zones, *UPBEAT1* (*UPB1*), which is a basic helix-loop-helix (bHLH) transcription factor (Tsukagoshi et al., 2010), plays a key role in the transcriptional regulation of ROS. UPB1 regulates ROS (H_2O_2 and O_2^-) homeostasis by repressing the expression of class III peroxidases in the elongation zone (Tsukagoshi et al., 2010). The changes in the spatial distribution of ROS alter the size of the meristematic zone. The *upb1-1* mutant has a larger meristematic zone than that of the wild type owing to the increase in the number of cells, which accumulates O_2^-, because the expression of UPB1-targeted peroxidases is not suppressed by UPB1. Thus, the root length of the *upb1-1* mutant is longer than that of the wild type. In contrast, the *UPB1* overexpression line has a reduced level of O_2^- in the meristematic zone; thus, the size of the meristematic zone and the length of the root are smaller and shorter, respectively, than those of the wild type. These results indicate that the spatial distribution of at least two ROS, O_2^- and H_2O_2, is critical for determining the cell status between proliferation and differentiation at the root tip (Tsukagoshi et al., 2010).

Root meristem growth factor 1 (RGF1) also controls root meristem size through ROS signaling (Matsuzaki et al., 2010; Yamada et al., 2020). RGF1 is an essential peptide hormone that controls the size of the meristematic zone, both as an intrinsic and extrinsic signal (Matsuzaki et al., 2010; Meng et al., 2012; Whitford et al., 2012; Yamada et al., 2020). Exogenous RGF1 treatment increases the size of the meristematic zone, whereas the *rgf1/2/3* triple mutant has a smaller meristematic zone (Matsuzaki et al., 2010). The H_2O_2 levels decreased and O_2^- levels increased in the meristematic and elongation zones 24 h after treatment with the RGF1 peptide. In the RGF1 receptor mutant *rgfr1/2/3*, the levels of H_2O_2 and O_2^- in the meristematic zone remained unchanged after RGF1 peptide treatment compared with those in the wild type. These data indicate that the RGF1-receptor pathway controls the distribution of ROS during the development of the root meristem (Yamada et al., 2020). In addition, *RGF1 INDUCIBLE TRANSCRIPTION FACTOR 1* (*RITF1*) was identified as a downstream factor in the RGF1–ROS signaling pathway (Yamada et al., 2020). The root meristem size was smaller and root growth rate was lower in the *ritf1* mutant than in the wild type. Furthermore, after RGF1 treatment, O_2^- accumulation was lower in the *ritf1* mutant than in the wild type (Yamada et al., 2020). In addition, ROS signals modulated by RITF1 regulate the stability of the PLT2 protein, which is one of the key transcription factors for stem cell maintenance (Aida et al., 2004). PLT2 has previously been shown to be regulated by oxidative posttranslational modifications (Shaikhali et al., 2008; Dietz et al., 2010; Licausi et al., 2011, 2013; Waszczak et al., 2014). Moreover, transcriptome analysis did not reveal significant changes in *UPB1* expression upon RGF1 treatment (Yamada et al., 2020). After RGF1 treatment, the expression of five peroxidase genes was elevated, but they were not the targets of UPB1, suggesting that RGF1 regulates meristem size independently of UPB1 (Yamada et al., 2020). Therefore, *RITF1*, induced by the RGF1 peptide, which is secreted from the QC and columella stem cells, regulates PLT2 stability and distribution at the root tip and, thus, controls the meristem size under ROS signaling (Yamada et al., 2020). These data suggest that the RGF1–RITF1–ROS signaling pathway plays a crucial role in the maintenance of the root SCN by regulating PLT stability and distribution. Furthermore, the RGF1 regulatory pathway is independent of the auxin regulatory pathway for PLT (Matsuzaki et al., 2010).

MYB30, in addition to regulating the meristematic zone, is one of the key transcriptional regulators under ROS signaling and has been reported to regulate root cell elongation (Mabuchi et al., 2018). Among the upregulated transcription factors in the "ROS-map," which is a time-course microarray analysis of *Arabidopsis* root tips treated with H_2O_2, *MYB30* showed the most prominent expression induction by H_2O_2 in both the meristematic and elongation zones (Mabuchi et al., 2018). MYB30 regulates root growth in response to H_2O_2 at the level of cellular elongation in the root tip by upregulating the expression of *LTPG1*, *LTPG2*, and *LTP5* (Mabuchi et al., 2018). *LTPG*s and *LTP* encode lipid transfer proteins that are thought to be the transporter of very-long chain fatty acids (VLCFAs). In fact, root growth inhibition in *ltpg1/2* double mutants showed weak but significant insensitivity to exogenous H_2O_2 treatment. This indicates that VLCFA transport to the outside of cells needs to be controlled under ROS signaling for root elongation. Interestingly, MYB30 and its target genes function in not only ROS-dependent root developmental processes in the root tip, but also in plant immune responses toward bacterial elicitors in aerial tissues (Raffaele et al., 2008; Mabuchi et al., 2018). Therefore, the MYB30 regulatory network activated in response to H_2O_2 treatment is involved in maintaining the balance between root growth and defense (Mabuchi et al., 2018). In addition, the use of the "ROS-map" revealed another early ROS-responsible transcription factor, *ANAC032*, which is NAC [NAM, no apical meristem; ATAF1/2, *Arabidopsis* transcription activation factor; and CUC2, CUP-shaped cotyledon2 (Souer et al., 1996; Aida et al., 1997; Duval et al., 2002)], as a root growth regulator (Maki et al., 2019). Interestingly, ANAC032 is an upstream transcription

factor of the MYB30 regulatory network (Maki et al., 2019). Previous studies suggested that ANAC032 plays important roles in response to abiotic stresses such as high-intensity light, salinity, and oxidation (Mahmood et al., 2016) and is a key mediator between SA- and jasmonic acid-dependent defense signaling (Devi Allu et al., 2016). In the root, ANAC032 plays a dominant role in the transition zone, but not in the apical meristematic zone, and negatively regulates root growth (Maki et al., 2019). These findings suggest that ANAC032 and MYB30 transcriptional cascades are the key regulators of root cell elongation under ROS signaling.

ROS IN ROOT STEM CELL IDENTITY AND CELL CYCLE PROGRESSION

In the apical meristem, which accumulates mainly O_2^-, several systems of SCN maintenance and cell cycle regulation by ROS are available. The *Arabidopsis* prohibitin protein PHB3 regulates the root SCN by restricting the spatial expression of the ethylene response factor (ERF) transcription factors *ERF115*, *ERF114*, and *ERF109* (Kong et al., 2018). The *phb3* mutant accumulated more ROS, leading to an increase in the expression of *ERF115*, *ERF114*, and *ERF109*, which was independent of cell death signaling (Heyman et al., 2013; Kong et al., 2018). In the *phb3* mutant, both the QC-specific transcription factor, *WOX5*, and the QC-specific marker QC184 were strongly downregulated. Furthermore, *PLT1*, *PLT2*, and *SCR*, which are the root SCN-defining transcription factors, were downregulated in the *phb3* mutant. However, the expression of *SHR* was not affected in *phb3*. Interestingly, ERF115, ERF114, and ERF109 directly regulate the expression of peptide hormone precursors, PHYTOSULFOKINE5 (PSK5) and PSK2, which produce sulfonated pentapeptide hormones that regulate cellular dedifferentiation and proliferation (Matsubayashi et al., 1999; Kutschmar et al., 2009; Kong et al., 2018), in parallel with the PLT pathway. In addition, ERF115 controls cell division at the QC and replenishes stem cells by regulating the expression of *PSK5* (Heyman et al., 2013). Thus, the transcriptional network of ERFs controlled through alterations in ROS distribution regulated by PHB3 is essential to maintain root SCN identity and, thus, root development.

The *A. thaliana* P-loop NTPase encoded by APP1 controls ROS homeostasis in the mitochondria of the root apical meristem cells and affects SCN identity (Del Pozo, 2016; Yu et al., 2016). The loss of *APP1* lowers the concentration of O_2^- by upregulating *PER11* and *PER55*, which belong to class III peroxidase family (Yu et al., 2016). In contrast, *APP1* overexpression, as well as elevated ROS levels, promotes cell division at the QC and distal stem cell (DSC) differentiation in the root. In the *app1* mutant, the expression levels of transcription factors such as *WOX5*, *PLT1*, *PLT2*, and *UPB1* and of several cell cycle-related genes were not altered; however, the expression of *SHR* and *SCR* was transcriptionally and translationally reduced (Yu et al., 2016). Therefore, APP1-regulated ROS signaling might regulate cell division at the QC and DSC identity by controlling SHR and SCR functions.

Reactive oxygen species levels also influence cell cycle progression at the transcriptional level. Exogenous H_2O_2 treatment affects the expression of G_1–S and G_2–M transition-related genes in the meristematic zone (Tsukagoshi, 2012). Repression of cell cycle-related genes by H_2O_2 reduces the meristem size, resulting in root growth inhibition. This also supports the role of ROS as signaling molecules that regulate gene expression. In addition, treatment with zeocin, an inducer of DNA double-strand breaks (DSBs), led to the accumulation of H_2O_2 in the elongation zone (Chen and Umeda, 2015). DSBs control the coordinated expression of cell cycle-related genes. In plants, DNA lesions such as DSBs or DNA single-strand breaks are sensed by ataxia telangiectasia-mutated (ATM) and ATR and Rad3-related (ATR), respectively (Riballo et al., 2004; Shiotani and Zou, 2009). The downstream transcription factor of these signaling pathways, SUPPRESSOR OF GAMMA RESPONSE 1 (SOG1), governs multiple responses to DNA damage (Yoshiyama et al., 2009, 2013). In the *sog1* mutant, zeocin treatment-induced H_2O_2 hardly accumulated in the elongation zone (Chen and Umeda, 2015). SOG1 directly regulates the expression of *FMO1*, which encodes a flavin-containing monooxygenase, and changes in the distribution of H_2O_2 upon DNA damage (Chen and Umeda, 2015). Furthermore, SOG1 has been shown to induce directly the expression of *SIAMESE/SIAMESE-RELATED* (*SIM*/*SMR*), *SMR5*, and *SMR7*, which act as cyclin-dependent kinase inhibitors in response to oxidative stress-induced DNA damage (Yi et al., 2014). These data suggest that the SOG1-regulated network plays a central role in the response to DNA damage to facilitate cell cycle progression.

Thus, ROS are considered as one of the important regulators of root meristem activity and cell proliferation by regulating gene expression of key transcription factors for SCN maintenance, such as *PLT*s, *SCR*–*SHR*, and ERFs, as well as cell cycle-related genes.

ROS IN LATERAL ROOT DEVELOPMENT

Reactive oxygen species also play an important role in lateral root (LR) development. In the maturation zone, LRs develop from a limited number of pericycle cells called founder cells (Dolan et al., 1993; Casimiro et al., 2003) in the primary root. Founder cells, in response to auxin accumulation at specific sites, undergo anticlinal cell divisions to form an LR primordium (LRP; Malamy and Benfey, 1997; Dubrovsky et al., 2008). Molecular evidence that ROS are involved in LR development was obtained by cell sorting and transcriptomic analysis of S-phase kinase-associated protein 2 (SKP2B)-expressing cells. *SKP2B* encodes an F-box ubiquitin ligase that regulates the division of founder cells (Manzano et al., 2012). Cell sorting was used to identify genes co-expressed with SKP2B-GFP-expressing cells to analyze genes that are specifically expressed during LR development (Manzano et al., 2014), since *SKP2B* is expressed in all stages of the LRP (Manzano et al., 2012). From these cell sorting transcriptomic data sets, numerous genes involved in redox activity (ROS signaling) were identified (Manzano et al., 2012, 2014). Several peroxidase genes were found to be significantly

downregulated in *UPB1*-overexpressing plants (Tsukagoshi et al., 2010; Manzano et al., 2014). *UPB1* is expressed in the early stage of LRP development, although its expression seems to be restricted to the peripheral cells of the primordium, and ROS highly accumulate in the emerging LR (Manzano et al., 2014). The *upb1-1* mutant showed a higher number of emerged and mature LRs than those in wild-type plants. In contrast, roots of *UPB1*-overexpressing plants had significantly reduced number of later stages of LRP (Manzano et al., 2014). Thus, ROS signaling involving UPB1-regulated peroxidase genes is important for LR development, especially during LR emergence. In addition, the expression of *UPB1* in the peripheral cells of LRP suggests its role in cell differentiation by repressing peroxidase genes, as noted in the root tip (Tsukagoshi et al., 2010; Manzano et al., 2014).

A new role for MYB36 in LRP development has been revealed (Fernández-Marcos et al., 2017). MYB36 is known to regulate directly and positively the formation of Casparian strips through the expression of *CASP1*, *PER64*, and *ESB1* (Kamiya et al., 2015; Liberman et al., 2015). During LRP development, MYB36 maintains the ROS balance at the LRP boundary in the pericycle cells, which is required for the transition from flat- to dome-shaped primordia by controlling a set of peroxidase genes, *PER9* and *PER64*, and perhaps other peroxidases (Fernández-Marcos et al., 2017). The *myb36* mutant contained more LRP cells along the innermost cell layer than in the wild type; therefore, the lack of *MYB36* produces a flat LRP phenotype. This phenotype is complemented by treatment with potassium iodide, which is a scavenger of H_2O_2 (Fernández-Marcos et al., 2017). Furthermore, UPB1 is involved in the regulation of ROS under iron homeostasis. This regulation also controls LR development (Ravet et al., 2009; Briat et al., 2010; Reyt et al., 2015). These results strongly suggest that ROS homeostasis regulated by peroxidases is important for LR development. Peroxidases might be involved in the regulation of cell wall loosening for facilitating the emergence of LRP from overlay cells in the primary root or the reduction of auxin activity by oxidizing IAA (Lagrimini et al., 1997). However, the function of peroxidase genes co-expressing with SKP2B during LR formation is independent of auxin (Manzano et al., 2014).

Respiratory burst oxidase homolog (NADPH oxidase protein)-mediated ROS production also facilitates LR emergence (Orman-Ligeza et al., 2016). AtrbohD and AtrbohF negatively modulate lateral root development by controlling the local generation of superoxide (Orman-Ligeza et al., 2016). The LR density is increased in the double mutants *atrbohD1/F1* and *atrbohD2/F2*, which leads to the production of O_2^-, but not of H_2O_2, in the maturation zone of the primary root (Li et al., 2015). Thus, the regulation of ROS spatiotemporal accumulation patterns plays a critical role in LR emergence.

Recently, evidence of molecular linkage between auxin and ROS has been reported. Auxin induces H_2O_2 accumulation and initiates LR formation (Ma et al., 2014). Auxin upregulates the expression of *RBOH* genes through the transcription factor ROOT HAIR DEFECTIVE SIX-LIKE4 (RSL4; Mangano et al., 2017). Interestingly, *RSL4* is directly regulated by auxin response factors (ARFs; Mangano et al., 2017). Furthermore, a feed-forward regulation among auxin, ROS, and LR development has been recently reported. H_2O_2 produced by RBOH, whose expression is induced by RSL4, promotes IAA14 degradation through its downstream product, reactive carbonyl species (RCS; Biswas et al., 2019). These results indicate that a clear molecular interaction exists between ROS and auxin signals that regulate LR development.

ROS IN ROOT HAIR DEVELOPMENT

Reactive oxygen species are also involved in the regulation of polar growth, such as in pollen tube and root hair development. Root hairs develop from root epidermal cells and attain a tubular protruding structure in a polar growth manner. In the *Arabidopsis* root, which belongs to type III root hair formation pattern (Datta et al., 2011), the epidermal cells are arranged in files of non-hair cells (N) and hair cells (H; Duckett et al., 1994; Galway et al., 1994). *SCRAMBLED* (*SCM*), a leucine-rich repeat receptor-like kinase, regulates the expression of transcription factors that define the cell fate (Kwak et al., 2005). The molecular mechanisms regulated by transcription factors of N or H cell fate have been extensively studied in *Arabidopsis* (Shibata and Sugimoto, 2019). In N cells, the protein complex of the R2R3-type MYB transcription factor *WEREWOLF* (*WER*; Lee and Schiefelbein, 1999), a bHLH-type transcription factor *GLABLA3* (*GL3*) or its homolog *ENHANCER OF GLABLA3* (*EGL3*; Bernhardt et al., 2003), and the WD repeat protein *TRANSPARENT TESTA GLABLA1* (*TTG1*; Galway et al., 1994) play an important role in suppressing root hair development, thereby enhancing the expression of the homeodomain transcription factor *GLABRA2* (*GL2*), which functions as a negative regulator of root hair differentiation (Di Cristina et al., 1996; Masucci and Schiefelbein, 1996). Conversely, the mobile R3-type MYB transcription factor, *CAPRICE* (*CPC*), plays a key role (Wada et al., 1997) in the development of root hair in H cells. CPC protein moves from N cells to neighboring H cells and binds with GL3/EGL3-TTG1 to form an inactive complex followed by root hair formation through the inhibition of *GL2* expression (Wada et al., 2002; Kurata et al., 2005). Furthermore, several CPC-related R3 Myb proteins, *TRIPTYCON* (*TRY*: Schellmann et al., 2002) and *ENHANCER OF TRY AND CPC1* (*ETC1*; Simon et al., 2007), have been shown to have partially redundant functions (Kirik et al., 2004; Serna, 2008; Tominaga-Wada et al., 2017; Zhou et al., 2020). CPC and its homologs are also required for the induction of the bHLH transcription factor, *ROOT HAIR DEFECTIVE 6* (*RHD6*), which plays key roles in the determination of root hair identity (Masucci and Schiefelbein, 1994; Menand et al., 2007; Shibata and Sugimoto, 2019). The bHLH transcription factor RSL4 regulates root hair growth under the RHD6 regulatory network (Datta et al., 2015; Shibata and Sugimoto, 2019).

Root hair development can be divided into two main stages: root hair initiation and tip growth (Grierson et al., 2014). Rho-type GTPases of plants (ROPs) are required as determinants of the root hair initiation site (Molendijk et al., 2001; Jones et al., 2002; Denninger et al., 2019). ROP guanine nucleotide exchange factor 3 (RopGEF3) recruits ROPs to the future site

of hair formation. Before a cell begins to bulge, RopGEF4 is recruited for the positive regulation of tip growth (Denninger et al., 2019). ROOT HAIR DEFECTIVE 2 (RHD2), known as NADPH oxidase or respiratory burst oxidase homolog C (RBOHC), modulates root hair budding (Monshausen et al., 2007; Takeda et al., 2008). The *rhd2* mutant has shorter root hair than the wild type because of the decreased ROS accumulation in the root hair tips. Although RBOHC is the main RBOH in root hair development, RBOHH and RBOHJ are important ROS-producing enzymes in this process (Foreman et al., 2003; Monshausen et al., 2007; Mangano et al., 2017). Of these RBOHs, *RBOHC* and *RBOHJ* are transcriptionally regulated by RSL4 for root tip growth (Mangano et al., 2017). In addition, RSL4 directly regulates the expression of several peroxidase genes (Mangano et al., 2017). ROS accumulation at the root hair tip activates Ca^{2+}-permeable channels, which have not yet been identified; this promotes Ca^{2+} influx into the cytoplasm (Foreman et al., 2003; Wu et al., 2010) and modulates cell wall stiffness during rapid hair elongation (Mendrinna and Persson, 2015). The Ca^{2+} gradient observed in wild-type root hair is a continuous gradient in the cytosol, with the highest concentration close to the tip apex (Monshausen et al., 2007; Mendrinna and Persson, 2015). In addition, high levels of cytoplasmic Ca^{2+} trigger ROS production by RBOHs, thereby completing a positive feedback loop during root hair elongation (Takeda et al., 2008). Conversely, PHYTOCHROME AND FLOWERING TIME1 (PFT1)/MED15 subunit of the mediator complex also plays critical roles in root hair morphogenesis (Sundaravelpandian et al., 2013a,b). PFT1 controls the distribution of ROS by activating the gene expression of H_2O_2-generating class III peroxidases (Sundaravelpandian et al., 2013a). The *pft1-1* mutant failed to initiate root hair formation and had shorter roots because of reduced expression of PFT1-regulated peroxidase genes (Sundaravelpandian et al., 2013a). Furthermore, inhibition of NADPH oxidase activity by treatment with diphenyleneiodonium also caused defective root hair development by decreasing ROS accumulation at the tip of root hair (Foreman et al., 2003; Lohar et al., 2007). These results suggest the importance of accurate ROS homeostasis at the root hair tips for root hair formation.

Although flavonol levels are low in the epidermis, ROS accumulate in the epidermis. A flavonoid-deficient mutant, *transparent testa 4* (*tt4*), showed increased root hair number and ROS levels in H cells. The *tt4* mutants treated with potassium iodide showed reduced root hair number and ROS accumulation. These results indicate that flavonols act as antioxidants in H cells to control root hair development by modulating ROS accumulation (Gayomba and Muday, 2020).

The relationship between root development and ROS described so far is shown in **Figure 1**.

CROSSTALK BETWEEN ROS AND OTHER MOLECULES

The root growth control mechanism involves many plant hormones. In this section, we discuss the interaction of ROS with several other hormone signaling pathways involved in root development, reiterating that ROS act as signaling molecules. When considering signal transduction, determining how each signal interacts is important. In this regard, the crosstalk between ROS and all plant hormones needs to be discussed for understanding the entire complex signal network for root development. However, some of the crosstalks have not been well elucidated at the molecular level, and all of them cannot be discussed at once. In recent years, numerous studies have investigated the crosstalk between ROS and plant hormones during root development. Therefore, we have elaborated on the crosstalks between several important molecules and ROS, which seem to be important for root development.

Even though several studies indicate the molecular linkage between auxin and ROS, the connection between these two signals needs to be further investigated. Although we have already mentioned the molecular linkage between ROS and auxin signaling in LR development, several studies have indicated the independence of these two signals. Thus, we need to elucidate how the distribution of auxin is regulated by ROS, and how ROS regulate the stability of auxin signal regulators at the molecular level. A recent study provided evidence for the relationship between auxin distribution and ROS action in the root tip. The exogenous application of H_2O_2 led to auxin accumulation in the root apical meristem, along with a decrease in the abundance of PIN auxin efflux carriers (Zwiewka et al., 2019). In particular, H_2O_2 interferes with the intracellular trafficking of PIN2, leading to the decrease in PIN2 protein levels in the plasma membrane of root epidermal cells (Zwiewka et al., 2019). This affects root meristem size by altering the auxin maxima. However, this alteration in PIN2 trafficking is an early event in response to oxidative stress. Studies need to assess the long-term responses for revealing the entire crosstalk between ROS and auxin distribution. With regard to protein degradation, RCS, which is a downstream target of ROS in auxin signaling (please also see section "ROS in Lateral Root Development"), regulates IAA14 protein stability (Biswas et al., 2019). However, the mechanism by which RCS controls IAA stability has not yet been studied (Biswas et al., 2019). Determining whether TIR1 or E3 ligase in the SCF–TIR1 complex is activated by ROS or RCS is important to better understand the molecular mechanism that regulates the ROS–RCS–auxin signal at the posttranscriptional level.

The crosstalk between cytokinin and ROS is also important because cytokinins are closely associated with auxin for regulating root growth. The overproduction of endogenous cytokinin by the overexpression of the cytokinin biosynthetic gene, *ADENOSINE PHOSPHATE-ISOPENTENYL TRANSFERASE 8* (*AtIPT8*), in *Arabidopsis* roots does not affect ROS levels under normal conditions. However, *AtIPT8* overexpressors accumulate more ROS than the wild type after NaCl treatment. Under these conditions, *AtIPT8* overexpressors showed a short root phenotype. Moreover, several NADPH oxidases, which are known as ROS-producing enzymes, are upregulated after NaCl treatment in *AtIPT8* overexpressors. Conversely, ROS scavenging-related genes were downregulated after NaCl treatment in the *AtIPT8* overexpressors (Wang et al., 2015). According to that study, although only cytokinin overproduction cannot lead to the accumulation of ROS in the

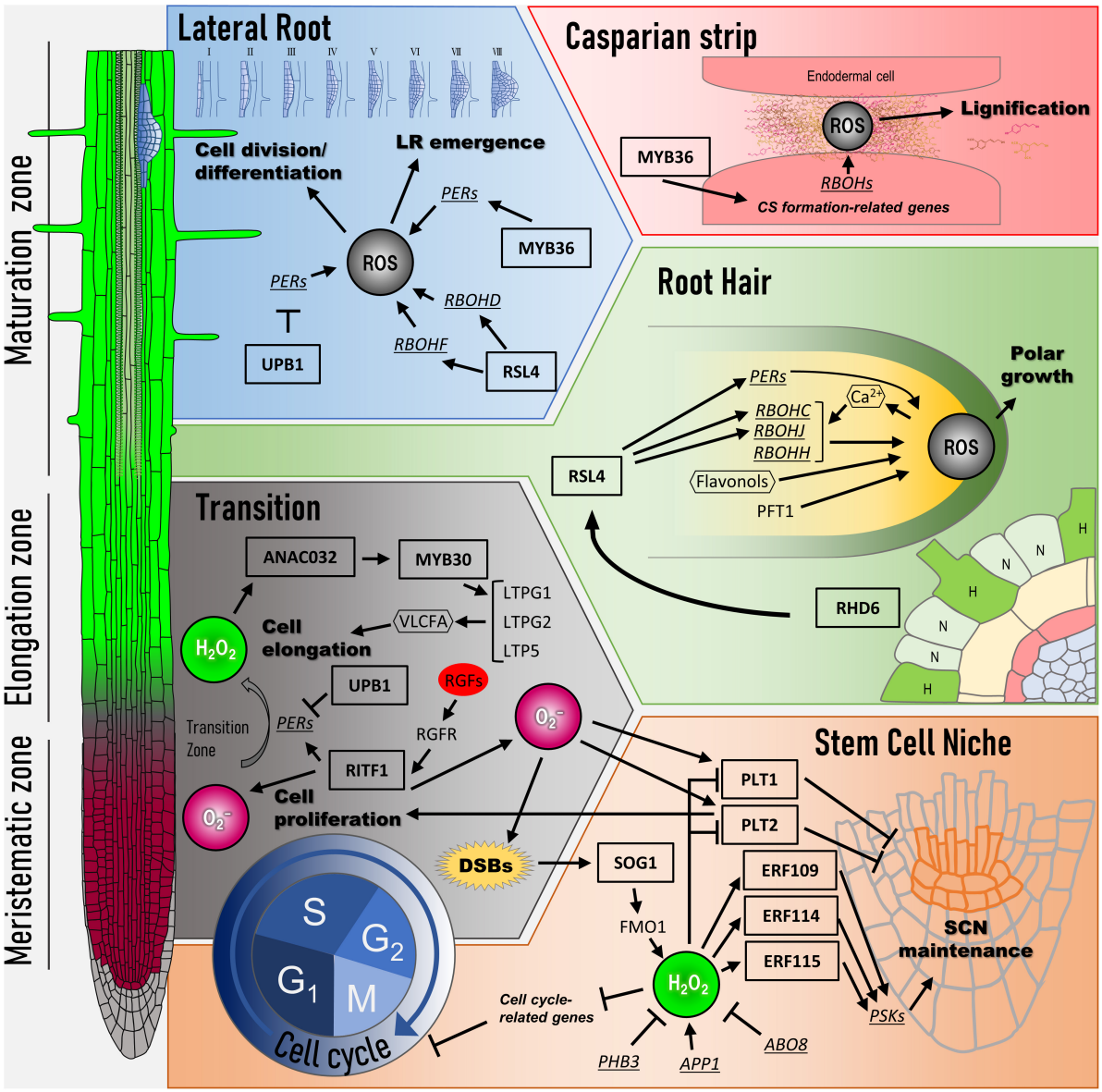

FIGURE 1 | Transcriptional network of ROS signaling for root development. At the left side, three regions in *Arabidopsis* root are shown (meristematic zone, elongation zone, and maturation zone). Color gradient in the primary root indicates the distribution of ROS (red: O_2^- and green: H_2O_2). Cell cycle: ROS regulates the expression of G_1–S as well as G_2–M transition-related genes. SOG1, a key transcription factor, is activated in response to DNA damage such as double-strand breaks (DSBs). SOG1 directly induces the expression of FMO1, which encodes flavin-containing monooxygenase. H_2O_2 level modulated by FMO1 influences the expressions of cell cycle-related genes. Stem cell niche: H_2O_2 level is lowered by ABO8, PHB, and RITF1 signaling pathways, whereas APP1 signaling pathway leads to its accumulation. H_2O_2 regulates the expression of *ERF109*, *ERF114*, and *ERF115* and represses PLT activity for SCN maintenance. RITF1 signaling pathway positively regulates PLT activity through O_2^- accumulation. Transition: ROS spatial distribution between O_2^- and H_2O_2 decides the transition from cell proliferation to cell elongation. UPB1, a key transcription factor, changes ROS spatial distribution by regulating the expression of peroxidases (PERs). RITF1 also controls the meristem size under ROS signaling through PLT2 protein stability. In the elongation zone, ANAC032 and MYB30 regulate the expression of cell elongation-related genes in response to H_2O_2. Root hair: Whether epidermal cells can form root hair is determined by gene network (H, hair cells; N, non-hair cells). The RHD6 gene regulatory network begins to bulge at the root hair initiation site in H cells. RSL4, which is under the RHD6 gene regulatory network, controls the expression of *RBOHC*/*RHD2*, *RBOHJ*, and several *PERs* for the root tip growth. A positive feedback loop is formed during hair elongation among Ca^{2+}-permeable channels and RBOHs *via* ROS. In addition, ROS distribution in the root hair tip is controlled by PFT1, which regulates the expression of *PERs*. Flavonols contribute to the development of root hair as antioxidants, which modulate ROS accumulation. Lateral root: Lateral root (LR) development is initiated from pericycle cells called founder cells. UPB1 controls LR emergence by regulating the expression of *PERs* at the peripheral cells of LRP. RSL4 regulates the expression of *RBOHs*, followed by ROS production, for facilitating LR emergence. MYB36 in LR development maintains ROS balance at the LRP boundary in the pericycle cells to allow their transition from flat to dome-shaped primordia. Casparian strip: In the endodermal cells, localized ROS in apoplasts induced by RBOHD and RBOHF are utilized for the lignification for the Casparian strip formation. Arrows indicate positive regulation, and blunted lines indicate negative regulation. Ovals, rectangles, and hexagons indicate signal molecules such as plant hormones, transcription factors, and secondary messenger molecules, respectively. PER, peroxidases; DSB, double-strand breaks; SCN, stem cell niche; LR, lateral root; CS, Casparian strip.

roots, cytokinins might enhance the salinity stress that inhibits root growth by modulating ROS accumulation. However, a study on root phototropism elucidated the relationship between cytokinins, ROS, and flavonols. In that study, flavonols were found to be regulators of root phototropism by transcriptomic and metabolomic profile analysis (Silva-Navas et al., 2016). In fact, flavonols accumulate in the transition zone at the root tip and reduce cell proliferation by scavenging superoxide anions (Silva-Navas et al., 2016). Cytokinins induce flavonol biosynthesis through SHORT HYPOCOTYL 2 (SHY2), which is a transcription factor limiting meristem size under cytokinin signaling (Dello Ioio et al., 2008). Even though this result indicates that ROS levels are not directly controlled by cytokinins, ROS downstream of cytokinins might control the transition between cell proliferation and differentiation. Interestingly, H_2O_2 accumulation regulated by UPB1 also controls flavonol content at the root tip (Silva-Navas et al., 2016). These results indicate the existence of a complex crosstalk between cytokinins and ROS signaling during the regulation of plant root growth.

In addition to auxin and cytokinin, BRs are important plant hormones that regulate many aspects of plant growth and development. The molecular mechanism between UPB1 and BR that regulates root growth has recently been elucidated. In the BR signaling pathway, the phosphorylation of signal component proteins is crucial. BR signals are perceived by the receptor kinase BRASSINOSTEROID-INSENSITIVE 1 (BRI1). BRI1 interacts with coreceptors, BRI1-ASSOCIATED RECEPTOR KINASE 1 (BAK1) and SOMATIC EMBRYOGENESISRECEPTOR KINASEs (SERKs), to transmit the signals downstream by protein phosphorylation (Shang et al., 2016; Wang H. et al., 2018). One of the BRI1 downstream kinases, BRASSINOSTEROID INSENSITIVE 2 (BIN2), interacts with UPB1 and phosphorylates UPB1 (Li et al., 2020). Phosphorylated UPB1 interacts with other BR signal-related bHLH proteins, paclobutrazol-resistant proteins 2 and 3 (PRE2/3), and controls downstream gene expression. Moreover, a transcription factor involving BR signaling, BRI1-EMS-SUPRESSOR 1 (BES1), directly regulates *UPB1* expression (Li et al., 2020). Because of these transcriptional regulation and protein interactions, root growth, especially root meristem development, is regulated. These results strongly indicate that two signaling pathways between ROS and BR are connected through UPB1–BIN2 interactions.

Abscisic acid is known to be the key regulator of both abiotic and biotic stresses (Nakashima et al., 2014). As for root growth, ABA affects auxin distribution and PLT protein stability through the production of ROS in the mitochondria of the root tips (Yang et al., 2014). A mutant, *aba-overly sensitive 8-1* (*abo8-1*), exhibits retarded growth and hypersensitivity to ABA. *ABO8*, which encodes pentatricopeptide repeat protein, is highly expressed in the root tips and LRP and regulates the splicing of mitochondrial complex I NAD4 intron 3. The *abo8-1* mutant shows excessive accumulation of ROS because of the incomplete mitochondrial electron transport chain of complex I. High accumulation of ROS in *abo8-1* reduces the expression of *PLT* genes and root meristem activity, thereby altering auxin distribution (Yang et al., 2014). These results suggest that appropriate ROS levels in the mitochondria are crucial mediators of root SCN maintenance and root growth through auxin distribution. This also indicates the existence of a crosstalk among ROS–ABA–auxin for the regulation of root meristem size. Moreover, the MYB30 regulatory gene network for root elongation is regulated by ABA. ABA induces *MYB30* expression in the root, but ROS accumulation levels after ABA treatment in the roots are not altered in both wild type and *myb30* mutants (Sakaoka et al., 2018). These results indicate that MYB30 acts as a hub between ROS and ABA signaling to regulate root cell elongation.

Reactive oxygen species are also known as signaling molecules in plant immune responses. In the aerial part, ROS are rapidly produced and accumulated by pathogen attack, which is called oxidative burst (Peleg-Grossman et al., 2012). This leads to defense against the attacking pathogens as well as the modification of the cell wall to become stiffened (Denness et al., 2011). The burst is induced by microbe-associated molecular patterns (MAMPs; Albert, 2013). Exogenous treatment with Flg22, which is one of the MAMPs, increases ROS levels, followed by a decrease in root development (Gómez-Gómez et al., 1999). This phenomenon indicates a molecular linkage between ROS and biotic stresses. MYB30 is known to activate the hyperresponse after the oxidative burst (Raffaele et al., 2008). Flg22 treatment shortened mature cell length in the wild-type root, but this phenotype was alleviated in *myb30* mutants (Mabuchi et al., 2018). Moreover, H_2O_2 levels increased upon Flg22 treatment in both wild type and *myb30* mutants to the same extent (Mabuchi et al., 2018), indicating that MYB30 regulates root length by increasing ROS levels caused by Flg22 treatment, not because of ROS biosynthesis but because of a defect in signaling downstream of ROS biosynthesis. Indeed, the expression levels of *MYB30* and several target genes such as *LTPG2* and *LTP5* were induced by Flg22 treatment (Mabuchi et al., 2018). *FLAGELLIN SENSING 2* (*FLS2*), which is a receptor kinase of Flg22, is expressed in the vasculature of the root elongation zone (Gómez-Gómez et al., 1999; Beck et al., 2014) and is upregulated in almost all cell files by Flg22 and H_2O_2 treatments (Beck et al., 2014). Moreover, *the fls2* mutant showed insensitivity to Flg22 treatment, which regulated root elongation. These results provide excellent evidence that ROS and MYB30 induced by ROS are important for the connection between root growth and biotic stresses such as plant immune response.

With regard to plant immune responses, SA is a crucial signaling molecule (Zhou and Zhang, 2020), and SA is related with ROS in various stress responses (Herrera-Vásquez et al., 2015). SA signals are received by the receptor proteins NON-EXPRESSOR OF PR GENES 1 (NPR1) and its paralogs NPR3 and NPR4 (Ding et al., 2018), which regulate the expression of downstream SA-dependent genes. Similar to that in shoot parts, SA treatment leads to the accumulation of ROS in the root tip through the upregulation of the gene expression of *RBOHD* and *RBOHF*, and the ROS control cell activity at the QC through PLTs and WOX5 regulation (Wang et al., 2021). However, the upregulation of *RBOHD* and *RBOHF* in root tips by SA treatment is not observed in the *npr1* mutant and *npr3/4* double mutants. This indicates that the regulation of the expression

of *RBOHD* and *RBOHF* by SA is NPR dependent. Therefore, a part of the ROS accumulation upon SA treatment related to SCN maintenance is regulated by the SA–NPR regulatory system. Auxin and ethylene are also involved in this regulation *via* PLT and ERFs (Kong et al., 2018; Wang et al., 2021). Although these studies focused on SCN maintenance, considering that Flg22 activates SA signals is important, because SA as well as Flg22 may regulate cell elongation by interacting with ROS signaling.

DISCUSSION

In this review, we introduce and discuss the functions of ROS as a root growth regulator. Modifying biological substances by the chemical activity of ROS itself is important, but ROS are known to play a more important role as a signaling molecule through gene expression regulation in a broad range of aspects of root development and stress responses (**Figure 2**). Indeed, ROS regulate the proliferation of cells, determination of cell identity, differentiation of root cells, and adaptation to even more biotic and abiotic stress. Considering the function of ROS, elucidation of all aspects of ROS signaling would provide information regarding the control of root development and stress response. For this, the perception of ROS signals, that is, the starting point of signal transduction, needs to be determined. Many studies have indicated that ROS are generated by NADPH oxidases localized on the plasma membrane. However, ROS such as superoxide and hydrogen peroxide are produced in the apoplast. Because of the chemical features of ROS, they cannot permeate the plasma membrane. For signal transduction with gene expression regulation, ROS generated by NADPH oxidase should be transported into cells. Although H_2O_2 is known to be transported from the apoplast to the cytosol *via* aquaporins (Waszczak et al., 2018), H_2O_2 sensors on the plasma membrane were not identified for a long time. Recently, an LRR receptor kinase, hydrogen peroxide-induced Ca^{2+} 1 (HPCA1), was identified as a H_2O_2 sensor that regulates Ca^{2+} channels on the plasma membrane (Wu et al., 2020). HPCA1 activates Ca^{2+} channels upon binding to H_2O_2 and regulates stomatal closure (Wu et al., 2020). To our knowledge, this was the first report of a cell surface sensor for H_2O_2 in plants. In this case, H_2O_2 transduces the signal *via* Ca^{2+} influx, followed by an increase in Ca^{2+} concentration in the cell. However, H_2O_2 does not act as the primary signal for regulating gene expression. Although whether HPCA1 is a H_2O_2 signal receptor for root development is not known, HPCA1 can be used to explore how H_2O_2 signals are transduced from the outside of cells. If HPCA1 or its homologs function in the roots to activate Ca^{2+} channels, the role of Ca^{2+} in root hair development could be elucidated. Furthermore, whether any H_2O_2 sensor other than HPCA1 is present in plant cells is not yet known. Identification of such a sensor or receptors would lead to the elucidation of the ROS regulatory gene expression network; nonetheless, the function of some transcription factors in yeast and bacteria has been shown to be modulated in the presence of H_2O_2 to modulate their function (Zheng et al., 1998).

In addition to the perception of ROS signals in a cell, cell-to-cell ROS signal transduction is also important for understanding

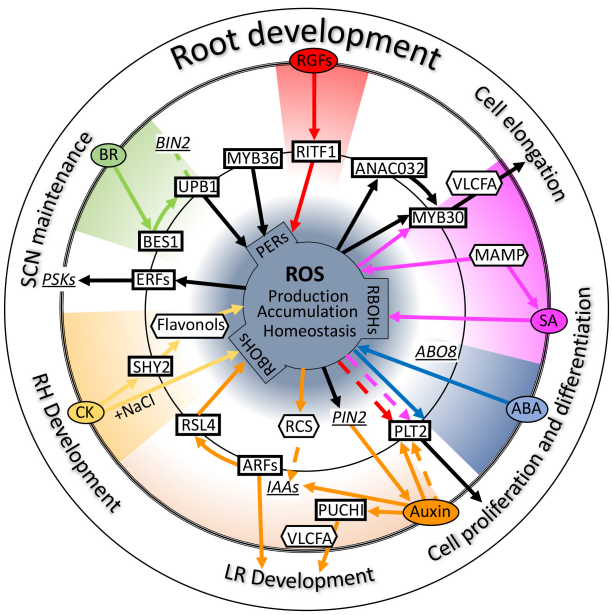

FIGURE 2 | Crosstalk between reactive oxygen species (ROS) and plant hormones. Schematic diagram of the crosstalk of several hormones and ROS signals centered on some key transcription factors involved in root development. Ovals, rectangles, and hexagons indicate signal molecules such as plant hormones, transcription factors, and secondary messenger molecules, respectively. Underlined italicized letter indicate genes involved in these signals as important intermediators. Solid lines refer to "transcriptional regulation," and dotted lines indicate "regulation at the protein level." Black lines indicate direct regulation by ROS or regulation of ROS homeostasis. Colored lines indicate each signal transduction. Please see the main text for further details. Auxin (orange); ABA, abscisic acid (blue); BR, brassinosteroid (green); CK, cytokinin (yellow); SA, salicylic acid (purple); RGFs, root meristem growth factors (red); PERs, peroxidases; PSKs, phytosulfokines; RCS, reactive carbonyl species; LR, lateral root; RH, root hair; SCN, stem cell niche.

ROS function. ROS and Ca^{2+} induced by local stress have been shown to activate a calcium-dependent autopropagating wave of ROS. The ROS wave spreads to the entire plant and causes ROS-specific responses in distant organs (Suzuki et al., 2013). In this case, ROS itself and several secondary signal molecules such as calcium ions and plasma membrane-electric potential form rapid and distant waves together (Gilroy et al., 2014). This wave is triggered by abiotic stresses such as heat and light (Suzuki et al., 2013). Whether the ROS wave also regulates plant root development is not yet known. According to the evidence of the crosstalk of ROS with other hormone signaling pathways, a regulatory mechanism that transduces the ROS signal to the adjacent cells might exist to regulate cell differentiation by the ROS wave. If appropriate ROS fluorescent markers are available that respond rapidly and ROS-specifically, such as R2D2 for auxin indicator (Liao et al., 2015), ROS wave for root development can be elucidated using live imaging.

We also discussed the crosstalk between ROS and several other molecules, mainly plant hormones involved in root development. In several cases, secondary molecules that connect ROS and hormone signals are important, for example, RCS in auxin, flavonols in cytokinin, and calcium ions in root hair development

and ROS wave. These secondary molecules play important roles as hubs in the signal crosstalk. Other secondary molecules involved between ROS and root development include VLCFA. *MYB30* overexpression upregulates VLCFA synthesis genes in the leaves and roots (Raffaele et al., 2008; Mabuchi et al., 2018). This indicates that VLCFA is induced by H_2O_2 because *MYB30* is an H_2O_2-inducible gene. In fact, in the wild-type root, the expression of VLCFA synthesis genes was upregulated upon H_2O_2 treatment (Mabuchi et al., 2018). Independent of these studies, VLCFA has been shown to be an important regulator of lateral root emergence (Trinh et al., 2019). VLCFA synthetic genes are expressed by the AP2 family transcription factor, PUCHI, in developing LRP, and mutants of these genes show lateral root defects (Trinh et al., 2019). This result indicates that VLCFA acts as a regulator of lateral root development. Considering the accumulation pattern of ROS in the LRP, a large amount of ROS accumulated in the LR (Manzano et al., 2012). These two studies strongly indicate the possibility that VLCFA acts as a secondary molecule for LR development under ROS signaling. In addition, auxin leads to the accumulation of ROS (Gayomba and Muday, 2020) and is presumed to accumulate in the LRP, causing the accumulation of ROS. This possibility needs to be confirmed experimentally, but the molecular relationship among auxin–ROS–VLCFA is considerably interesting for lateral root development.

Another interesting secondary molecule under ROS signaling is microRNA. Several studies have identified many microRNAs, including microRNA160, 165/166, and 393A, which respond to several abiotic stresses such as oxidative, cold, salt, and UV-B (Iyer et al., 2012; Barciszewska-Pacak et al., 2015). According to the functions of microRNA160, which targets ARF10, ARF16, and ARF17 (Khan et al., 2011), and microRNA393A, which targets TIR1 and AFB2 (Iglesias et al., 2014), ROS-responsive microRNAs can act as secondary molecules connecting ROS and auxin signals. microRNA165/166 suppresses class III homeodomain leucine zipper (HD-ZIP III), primarily PHABULOSA (PHB), which regulates protoxylem differentiation (Carlsbecker et al., 2010). Moreover, microRNA165/166 functions non-cell-autonomously in the root (Carlsbecker et al., 2010; Miyashima et al., 2011). According to their nature, microRNAs that respond to ROS may play a role as secondary molecules for cell–cell communication in root development and stress responses.

Although, in this review, we only focused on ROS function in root development, they may also be important for all aspects of plant growth. ROS play a pivotal role in plant root development and are the connection hub of other signaling pathways. Moreover, the participation of secondary molecules downstream of ROS has also been shown to be important for ROS signal transduction. However, many missing links exist in ROS signaling. With the development of latest technology, further research can be performed to reveal the mode of signal transduction at the single-cell level by using single-cell omics. In addition, the dynamics of inter- and intracellular ROS would be revealed by live imaging performed using super-resolution microscopes. These findings suggest that new technologies for plant growth control can be developed by targeting relatively common molecules such as ROS.

AUTHOR CONTRIBUTIONS

HT revised, guided, and improved the manuscript. Both authors carefully revised and edited the manuscript, replotted the figures, and drafted the manuscript.

FUNDING

This work was supported by the JSPS KAKENHI Grant Numbers 20H05426 and 19H03251 to HT.

ACKNOWLEDGMENTS

We would like to thank Editage (www.editage.com) for English language editing.

REFERENCES

Aida, M., Beis, D., Heidstra, R., Willemsen, V., Blilou, I., Galinha, C., et al. (2004). The PLETHORA genes mediate patterning of the *Arabidopsis* root stem cell niche. *Cell* 119, 109–120. doi: 10.1016/j.cell.2004.09.018

Aida, M., Ishida, T., Fukaki, H., Fujisawa, H., and Tasaka, M. (1997). Genes involved in organ separation in *Arabidopsis*: an analysis of the cup-shaped cotyledon mutant. *Plant Cell* 9, 841–857. doi: 10.1105/tpc.9.6.841

Albert, M. (2013). Peptides as triggers of plant defence. *J. Exp. Bot.* 64, 5269–5279. doi: 10.1093/jxb/ert275

Armengot, L., Marquès-Bueno, M. M., and Jaillais, Y. (2016). Regulation of polar auxin transport by protein and lipid kinases. *J. Exp. Bot.* 67, 4015–4037. doi: 10.1093/jxb/erw216

Barberon, M. (2017). The endodermis as a checkpoint for nutrients. *New Phytol.* 213, 1604–1610. doi: 10.1111/nph.14140

Barciszewska-Pacak, M., Milanowska, K., Knop, K., Bielewicz, D., Nuc, P., Plewka, P., et al. (2015). *Arabidopsis* microRNA expression regulation in a wide range of abiotic stress responses. *Front. Plant Sci.* 6:410. doi: 10.3389/fpls.2015.00410

Beck, M., Wyrsch, I., Strutt, J., Wimalasekera, R., Webb, A., Boller, T., et al. (2014). Expression patterns of flagellin sensing 2 map to bacterial entry sites in plant shoots and roots. *J. Exp. Bot.* 65, 6487–6498. doi: 10.1093/jxb/eru366

Belousov, V. V., Fradkov, A. F., Lukyanov, K. A., Staroverov, D. B., Shakhbazov, K. S., Terskikh, A. B., et al. (2006). Genetically encoded fluorescent indicator for intracellular hydrogen peroxide. *Nat. Methods* 3, 281–286. doi: 10.1038/nmeth866

Benfey, P. N., Linstead, P. J., Roberts, K., Schiefelbein, J. W., Hauser, M. T., and Aeschbacher, R. A. (1993). Root development in *Arabidopsis*: four mutants with dramatically altered root morphogenesis. *Development* 119, 57–70.

Benov, L., Sztejnberg, L., and Fridovich, I. (1998). Critical evaluation of the use of hydroethidine as a measure of superoxide anion radical. *Free Radic. Biol. Med.* 25, 826–831. doi: 10.1016/s0891-5849(98)00163-4

Bernhardt, C., Lee, M. M., Gonzalez, A., Zhang, F., Lloyd, A., and Schiefelbein, J. (2003). The bHLH genes GLABRA3 (GL3) and ENHANCER OF GLABRA3 (EGL3) specify epidermal cell fate in the *Arabidopsis* root. *Development* 130, 6431–6439. doi: 10.1242/dev.00880

Biswas, M. S., Fukaki, H., Mori, I. C., Nakahara, K., and Mano, J. (2019). Reactive oxygen species and reactive carbonyl species constitute a feed-forward loop in

auxin signaling for lateral root formation. *Plant J.* 100, 536–548. doi: 10.1111/tpj.14456

Bournonville, C. F. G., and Díaz-Ricci, J. C. (2011). Quantitative determination of superoxide in plant leaves using a modified NBT staining method. *Phytochem. Anal.* 22, 268–271. doi: 10.1002/pca.1275

Briat, J.-F., Ravet, K., Arnaud, N., Duc, C., Boucherez, J., Touraine, B., et al. (2010). New insights into ferritin synthesis and function highlight a link between iron homeostasis and oxidative stress in plants. *Ann. Bot.* 105, 811–822. doi: 10.1093/aob/mcp128

Caliskan, M., and Cuming, A. C. (1998). Spatial specificity of H_2O_2-generating oxalate oxidase gene expression during wheat embryo germination. *Plant J.* 15, 165–171. doi: 10.1046/j.1365-313x.1998.00191.x

Carlsbecker, A., Lee, J.-Y., Roberts, C. J., Dettmer, J., Lehesranta, S., Zhou, J., et al. (2010). Cell signaling by microRNA165/6 directs gene dose-dependent root cell fate. *Nature* 465, 316–321. doi: 10.1038/nature08977

Casimiro, I., Beeckman, T., Graham, N., Bhalerao, R., Zhang, H., Casero, P., et al. (2003). Dissecting *Arabidopsis* lateral root development. *Trends Plant Sci.* 8, 165–171. doi: 10.1016/s1360-1385(03)00051-7

Chang, M. C. Y., Pralle, A., Isacoff, E. Y., and Chang, C. J. (2004). A selective, cell-permeable optical probe for hydrogen peroxide in living cells. *J. Am. Chem. Soc.* 126, 15392–15393. doi: 10.1021/ja0441716

Chapman, J. M., Muhlemann, J. K., Gayomba, S. R., and Muday, G. K. (2019). RBOH-dependent ROS synthesis and ROS scavenging by plant specialized metabolites to modulate plant development and stress responses. *Chem. Res. Toxicol.* 32, 370–396. doi: 10.1021/acs.chemrestox.9b00028

Chen, P., and Umeda, M. (2015). DNA double-strand breaks induce the expression of flavin-containing monooxygenase and reduce root meristem size in *Arabidopsis thaliana*. *Genes Cells* 20, 636–646. doi: 10.1111/gtc.12255

Chen, S., and Schopfer, P. (1999). Hydroxyl-radical production in physiological reactions. A novel function of peroxidase. *Eur. J. Biochem.* 20, 726–735. doi: 10.1046/j.1432-1327.1999.00199.x

Chezem, W. R., Memon, A., Li, F.-S., Weng, J.-K., and Clay, N. K. (2017). SG2-type R2R3-MYB transcription factor MYB15 controls defense-induced lignification and basal immunity in *Arabidopsis*. *Plant Cell* 29, 1907–1926. doi: 10.1105/tpc.16.00954

Datta, S., Kim, C. M., Pernas, M., Pires, N. D., Proust, H., Tam, T., et al. (2011). Root hairs: development, growth and evolution at the plant-soil interface. *Plant Soil* 346, 1–14. doi: 10.1007/s11104-011-0845-4

Datta, S., Prescott, H., and Dolan, L. (2015). Intensity of a pulse of RSL4 transcription factor synthesis determines *Arabidopsis* root hair cell size. *Nat. Plants* 1:15138.

Del Pozo, J. C. (2016). Reactive oxygen species: from harmful molecules to fine-tuning regulators of stem cell niche maintenance. *PLoS Genet.* 12:e1006251. doi: 10.1371/journal.pgen.1006251

Dello Ioio, R., Nakamura, K., Moubayidin, L., Perilli, S., Taniguchi, M., Morita, M. T., et al. (2008). A genetic framework for the control of cell division and differentiation in the root meristem. *Science* 322, 1380–1384. doi: 10.1126/science.1164147

Denness, L., McKenna, J. F., Segonzac, C., Wormit, A., Madhou, P., Bennett, M., et al. (2011). Cell wall damage-induced lignin biosynthesis is regulated by a reactive oxygen species- and jasmonic acid-dependent process in *Arabidopsis*. *Plant Physiol.* 156, 1364–1374. doi: 10.1104/pp.111.175737

Denninger, P., Reichelt, A., Schmidt, V. A. F., Mehlhorn, D. G., Asseck, L. Y., Stanley, C. E., et al. (2019). Distinct RopGEFs successively drive polarization and outgrowth of root hairs. *Curr. Biol.* 29, 1854–1865. doi: 10.1016/j.cub.2019.04.059

Devi Allu, A., Brotman, Y., Xue, G.-P., and Balazadeh, S. (2016). Transcription factor ANAC032 modulates JA/SA signalling in response to *Pseudomonas* syringae infection. *EMBO Rep*. 17, 1578–1589. doi: 10.15252/embr.201642197

Devireddy, A. R., Zandalinas, S. I., Gómez-Cadenas, A., Blumwald, E., and Mittler, R. (2018). Coordinating the overall stomatal response of plants: rapid leaf-to-leaf communication during light stress. *Sci. Signal.* 11:eaam9514. doi: 10.1126/scisignal.aam9514

Di Cristina, M., Sessa, G., Dolan, L., Linstead, P., Baima, S., Ruberti, I., et al. (1996). The *Arabidopsis* Athb-10 (GLABRA2) is an HD-Zip protein required for regulation of root hair development. *Plant J.* 10, 393–402. doi: 10.1046/j.1365-313x.1996.10030393.x

Di Laurenzio, L., Wysocka-Diller, J., Malamy, J. E., Pysh, L., Helariutta, Y., Freshour, G., et al. (1996). The SCARECROW gene regulates an asymmetric cell division that is essential for generating the radial organization of the *Arabidopsis* root. *Cell* 86, 423–433. doi: 10.1016/s0092-8674(00)80115-4

Dickinson, B. C., Huynh, C., and Chang, C. J. (2010). A palette of fluorescent probes with varying emission colors for imaging hydrogen peroxide signaling in living cells. *J. Am. Chem. Soc.* 132, 5906–5915. doi: 10.1021/ja1014103

Dietz, K.-J., Vogel, M. O., and Viehhauser, A. (2010). AP2/EREBP transcription factors are part of gene regulatory networks and integrate metabolic, hormonal and environmental signals in stress acclimation and retrograde signalling. *Protoplasma* 245, 3–14. doi: 10.1007/s00709-010-0142-8

Ding, Y., Sun, T., Ao, K., Peng, Y., Zhang, Y., Li, X., et al. (2018). Opposite roles of salicylic acid receptors NPR1 and NPR3/4 in transcriptional regulation of plant immunity. *Cell* 173, 1454–1467. doi: 10.1016/j.cell.2018.03.044

Dmitrieva, V. A., Tyutereva, E. V., and Voitsekhovskaja, O. V. (2020). Singlet oxygen in plants: generation, detection, and signaling roles. *Int. J. Mol. Sci.* 21:3237. doi: 10.3390/ijms21093237

Dolan, L., Janmaat, K., Willemsen, V., Linstead, P., Poethig, S., Roberts, K., et al. (1993). Cellular organization of the *Arabidopsis thaliana* root. *Development* 119, 71–84.

Driever, S. M., Fryer, M. J., Mullineaux, P. M., and Baker, N. R. (2009). Imaging of reactive oxygen species in vivo. *Methods Mol. Biol.* 479, 109–116.

Dubrovsky, J. G., Sauer, M., Napsucialy-Mendivil, S., Ivanchenko, M. G., Friml, J., Shishkova, S., et al. (2008). Auxin acts as a local morphogenetic trigger to specify lateral root founder cells. *Proc. Natl. Acad. Sci. U.S.A.* 105, 8790–8794. doi: 10.1073/pnas.0712307105

Duckett, C. M., Grierson, C., Linstead, P., Schneider, K., Lawson, E., Dean, C., et al. (1994). Clonal relationships and cell patterning in the root epidermis of *Arabidopsis*. *Development* 120, 2465–2474.

Dunand, C., Crèvecoeur, M., and Penel, C. (2007). Distribution of superoxide and hydrogen peroxide in *Arabidopsis* root and their influence on root development: possible interaction with peroxidases. *New Phytol.* 174, 332–341. doi: 10.1111/j.1469-8137.2007.01995.x

Duval, M., Hsieh, T.-F., Kim, S. Y., and Thomas, T. L. (2002). Molecular characterization of AtNAM: a member of the *Arabidopsis* NAC domain superfamily. *Plant Mol. Biol.* 50, 237–248.

Federico, R., and Angelini, R. (1986). Occurrence of diamine oxidase in the apoplast of pea epicotyls. *Planta* 167, 300–302. doi: 10.1007/bf00391430

Fernández-Marcos, M., Desvoyes, B., Manzano, C., Liberman, L. M., Benfey, P. N., Del Pozo, J. C., et al. (2017). Control of *Arabidopsis* lateral root primordium boundaries by MYB36. *New Phytol.* 213, 105–112. doi: 10.1111/nph.14304

Fichman, Y., Miller, G., and Mittler, R. (2019). Whole-plant live imaging of reactive oxygen species. *Mol. Plant* 12, 1203–1210. doi: 10.1016/j.molp.2019.06.003

Foreman, J., Demidchik, V., Bothwell, J. H. F., Mylona, P., Miedema, H., Torres, M. A., et al. (2003). Reactive oxygen species produced by NADPH oxidase regulate plant cell growth. *Nature* 422, 442–446. doi: 10.1038/nature01485

Fujita, S., De Bellis, D., Edel, K. H., Köster, P., Andersen, T. G., Schmid-Sieger, E., et al. (2020). SCHENGEN receptor module drives localized ROS production and lignification in plant roots. *EMBO J.* 39:e103894.

Galway, M. E., Masucci, J. D., Lloyd, A. M., Walbot, V., Davis, R. W., and Schiefelbein, J. W. (1994). The TTG gene is required to specify epidermal cell fate and cell patterning in the *Arabidopsis* root. *Dev. Biol.* 166, 740–754. doi: 10.1006/dbio.1994.1352

Gayomba, S. R., and Muday, G. K. (2020). Flavonols regulate root hair development by modulating accumulation of reactive oxygen species in the root epidermis. *Development* 147:dev185819. doi: 10.1242/dev.185819

Gilroy, S., Suzuki, N., Miller, G., Choi, W.-G., Toyota, M., Devireddy, A. R., et al. (2014). A tidal wave of signals: calcium and ROS at the forefront of rapid systemic signaling. *Trends Plant Sci.* 19, 623–630. doi: 10.1016/j.tplants.2014.06.013

Gómez-Gómez, L., Felix, G., and Boller, T. (1999). A single locus determines sensitivity to bacterial flagellin in *Arabidopsis thaliana*. *Plant J.* 18, 277–284. doi: 10.1046/j.1365-313x.1999.00451.x

Gorshkova, T. A., Kozlova, L. V., and Mikshina, P. V. (2013). Spatial structure of plant cell wall polysaccharides and its functional significance. *Biochemistry* 78, 836–853. doi: 10.1134/s0006297913070146

Grierson, C., Nielsen, E., Ketelaarc, T., and Schiefelbein, J. (2014). Root hairs. *Arabidopsis Book* 12:e0172.

Hasanuzzaman, M., Bhuyan, M. H. M. B., Parvin, K., Bhuiyan, T. F., Anee, T. I., Nahar, K., et al. (2020). Regulation of ROS metabolism in plants under environmental stress: a review of recent experimental evidence. *Int. J. Mol. Sci.* 21:8695. doi: 10.3390/ijms21228695

Helariutta, Y., Fukaki, H., Wysocka-Diller, J., Nakajima, K., Jung, J., Sena, G., et al. (2000). The SHORT-ROOT gene controls radial patterning of the *Arabidopsis* root through radial signaling. *Cell* 101, 555–567. doi: 10.1016/s0092-8674(00)80865-x

Hernández-Barrera, A., Velarde-Buendía, A., Zepeda, I., Sanchez, F., Quinto, C., Sánchez-Lopez, R., et al. (2015). Hyper, a hydrogen peroxide sensor, indicates the sensitivity of the *Arabidopsis* root elongation zone to aluminum treatment. *Sensors* 15, 855–867. doi: 10.3390/s150100855

Herrera-Vásquez, A., Salinas, P., and Holuigue, L. (2015). Salicylic acid and reactive oxygen species interplay in the transcriptional control of defense genes expression. *Front. Plant Sci.* 6:171. doi: 10.3389/fpls.2015.00171

Heyman, J., Cools, T., Vandenbussche, F., Heyndrickx, K. S., Van Leene, J., Vercauteren, I., et al. (2013). ERF115 controls root quiescent center cell division and stem cell replenishment. *Science* 342, 860–863. doi: 10.1126/science.1240667

Hossain, M. A., Bhattacharjee, S., Armin, S.-M., Qian, P., Xin, W., Li, H.-Y., et al. (2015). Hydrogen peroxide priming modulates abiotic oxidative stress tolerance: insights from ROS detoxification and scavenging. *Front. Plant Sci.* 6:420. doi: 10.3389/fpls.2015.00420

Iglesias, M. J., Terrile, M. C., Windels, D., Lombardo, M. C., Bartoli, C. G., Vazquez, F., et al. (2014). MiR393 regulation of auxin signaling and redox-related components during acclimation to salinity in *Arabidopsis*. *PLoS One* 9:e107678. doi: 10.1371/journal.pone.0107678

Iyer, N. J., Jia, X., Sunkar, R., Tang, G., and Mahalingam, R. (2012). microRNAs responsive to ozone-induced oxidative stress in *Arabidopsis thaliana*. *Plant Signal. Behav.* 7, 484–491. doi: 10.4161/psb.19337

Iyer-Pascuzzi, A. S., and Benfey, P. N. (2009). Transcriptional networks in root cell fate specification. *Biochem. Biophys. Acta* 1789, 315–325. doi: 10.1016/j.bbagrm.2008.09.006

Jones, M. A., Shen, J.-J., Fu, Y., Li, H., Yang, Z., and Grierson, C. S. (2002). The *Arabidopsis* Rop2 GTPase is a positive regulator of both root hair initiation and tip growth. *Plant Cell* 14, 763–776. doi: 10.1105/tpc.010359

Kalyanaraman, B., Darley-Usmar, V., Davies, K. J. A., Dennery, P. A., Forman, H. J., Grisham, M. B., et al. (2012). Measuring reactive oxygen and nitrogen species with fluorescent probes: challenges and limitations. *Free Radic. Biol. Med.* 52, 1–6. doi: 10.1016/j.freeradbiomed.2011.09.030

Kamiya, T., Borghi, M., Wang, P., Danku, J. M. C., Kalmbach, L., Hosmani, P. S., et al. (2015). The MYB36 transcription factor orchestrates Casparian strip formation. *Proc. Natl. Acad. Sci. U.S.A.* 112, 10533–10538. doi: 10.1073/pnas.1507691112

Kärkönen, A., and Kuchitsu, K. (2015). Reactive oxygen species in cell wall metabolism and development in plants. *Phytochemistry* 112, 22–32. doi: 10.1016/j.phytochem.2014.09.016

Kaya, H., Takeda, S., Kobayashi, M. J., Kimura, S., Iizuka, A., Imai, A., et al. (2019). Comparative analysis of the reactive oxygen species-producing enzymatic activity of *Arabidopsis* NADPH oxidases. *Plant J.* 98, 291–300. doi: 10.1111/tpj.14212

Khan, G. A., Declerck, M., Sorin, C., Hartmann, C., Crespi, M., and Lelandais-Brière, C. (2011). MicroRNAs as regulators of root development and architecture. *Plant Mol. Biol.* 77, 47–58. doi: 10.1007/s11103-011-9793-x

Kirik, V., Simon, M., Huelskamp, M., and Schiefelbein, J. (2004). The ENHANCER OF TRY AND CPC1 gene acts redundantly with TRIPTYCHON and CAPRICE in trichome and root hair cell patterning in *Arabidopsis*. *Dev. Biol.* 268, 506–513. doi: 10.1016/j.ydbio.2003.12.037

Kong, X., Tian, H., Yu, Q., Zhang, F., Wang, R., Gao, S., et al. (2018). PHB3 maintains root stem cell niche identity through ROS-responsive AP2/ERF transcription factors in *Arabidopsis*. *Cell Rep.* 22, 1350–1363. doi: 10.1016/j.celrep.2017.12.105

Kosma, D. K., Murmu, J., Razeq, M. F., Santos, P., Bourgault, R., Molina, I., et al. (2014). AtMYB41 activates ectopic suberin synthesis and assembly in multiple plant species and cell types. *Plant J.* 80, 216–229. doi: 10.1111/tpj.12624

Kurata, T., Ishida, T., Kawabata-Awai, C., Noguchi, M., Hattori, S., Sano, R., et al. (2005). Cell-to-cell movement of the CAPRICE protein in *Arabidopsis* root epidermal cell differentiation. *Development* 132, 5387–5398. doi: 10.1242/dev.02139

Kutschmar, A., Rzewuski, G., Stührwohldt, N., Beemster, G. T. S., Inzé, D., and Sauter, M. (2009). PSK-α promotes root growth in *Arabidopsis*. *New Phytol.* 181, 820–831. doi: 10.1111/j.1469-8137.2008.02710.x

Kwak, S.-H., Shen, R., and Schiefelbein, J. (2005). Positional signaling mediated by a receptor-like kinase in *Arabidopsis*. *Science* 307, 1111–1113. doi: 10.1126/science.1105373

Lagrimini, L. M., Joly, R. J., Dunlap, J. R., and Liu, T. T. (1997). The consequence of peroxidase overexpression in transgenic plants on root growth and development. *Plant Mol. Biol.* 33, 887–895.

Lee, M. M., and Schiefelbein, J. (1999). WEREWOLF, a MYB-related protein in *Arabidopsis*, is a position-dependent regulator of epidermal cell patterning. *Cell* 99, 473–483. doi: 10.1016/s0092-8674(00)81536-6

Levesque, M. P., Vernoux, T., Busch, W., Cui, H., Wang, J. Y., Blilou, I., et al. (2006). Whole-genome analysis of the SHORT-ROOT developmental pathway in *Arabidopsis*. *PLoS Biol.* 4:e143. doi: 10.1371/journal.pbio.0040143

Li, N., Sun, L., Zhang, L., Song, Y., Hu, P., Li, C., et al. (2015). AtrbohD and AtrbohF negatively regulate lateral root development by changing the localized accumulation of superoxide in primary roots of *Arabidopsis*. *Planta* 241, 591–602. doi: 10.1007/s00425-014-2204-1

Li, T., Lei, W., He, R., Tang, X., Han, J., Zou, L., et al. (2020). Brassinosteroids regulate root meristem development by mediating BIN2-UPB1 module in Arabidopsis. *PLoS Genet.* 16:e1008883. doi: 10.1371/journal.pgen.1008883

Liao, C.-Y., Smet, W., Brunoud, G., Yoshida, S., Vernoux, T., and Weijers, D. (2015). Reporters for sensitive and quantitative measurement of auxin response. *Nat. Methods* 12, 207–210. doi: 10.1038/nmeth.3279

Liberman, L. M., Sparks, E. E., Moreno-Risueno, M. A., Petricka, J. J., and Benfey, P. N. (2015). MYB36 regulates the transition from proliferation to differentiation in the *Arabidopsis* root. *Proc. Natl. Acad. Sci. U.S.A.* 112, 12099–12104. doi: 10.1073/pnas.1515576112

Licausi, F., Kosmacz, M., Weits, D. A., Giuntoli, B., Giorgi, F. M., Voesenek, L. A. C. J., et al. (2011). Oxygen sensing in plants is mediated by an N-end rule pathway for protein destabilization. *Nature* 479, 419–422. doi: 10.1038/nature10536

Licausi, F., Ohme-Takagi, M., and Perata, P. (2013). APETALA2/Ethylene responsive factor (AP2/ERF) transcription factors: mediators of stress responses and developmental programs. *New Phytol.* 199, 639–649. doi: 10.1111/nph.12291

Liu, C.-J. (2012). Deciphering the enigma of lignification: precursor transport, oxidation, and the topochemistry of lignin assembly. *Mol. Plant* 5, 304–317. doi: 10.1093/mp/ssr121

Lohar, D. P., Haridas, S., Gantt, J. S., and VandenBosch, K. A. (2007). A transient decrease in reactive oxygen species in roots leads to root hair deformation in the legume-rhizobia symbiosis. *New Phytol.* 173, 39–49. doi: 10.1111/j.1469-8137.2006.01901.x

Lv, B., Tian, H., Zhang, F., Liu, J., Lu, S., Bai, M., et al. (2018). Brassinosteroids regulate root growth by controlling reactive oxygen species homeostasis and dual effect on ethylene synthesis in *Arabidopsis*. *PLoS Genet.* 14:e1007144. doi: 10.1371/journal.pgen.1007144

Ma, F., Wang, L., Li, J., Samma, M. K., Xie, Y., Wang, R., et al. (2014). Interaction between HY1 and H2O2 in auxin-induced lateral root formation in *Arabidopsis*. *Plant Mol. Biol.* 85, 49–61. doi: 10.1007/s11103-013-0168-3

Mabuchi, K., Maki, H., Itaya, T., Suzuki, T., Nomoto, M., Sakaoka, S., et al. (2018). MYB30 links ROS signaling, root cell elongation, and plant immune resposes. *Proc. Natl. Acad. Sci. U.S.A.* 115, E4710–E4719. doi: 10.1073/pnas.1804233115

Maeda, H. (2008). Which are you watching, an individual reactive oxygen species or total oxidative stress? *Ann. N. Y. Acad. Sci.* 1130, 149–156. doi: 10.1196/annals.1430.012

Maeda, H., Fukuyasu, Y., Yoshida, S., Fukuda, M., Saeki, K., Matsuno, H., et al. (2004). Fluorescent probes for hydrogen peroxide based on a non-oxidative mechanism. *Angew. Chem. Int. Ed. Engl.* 43, 2389–2391. doi: 10.1002/anie.200452381

Mahmood, K., Xu, Z., El-Kereamy, A., Casaretto, J. A., and Rothstein, S. J. (2016). The *Arabidopsis* transcription factor ANAC032 represses anthocyanin biosynthesis in response to high sucrose and oxidative and abiotic stresses. *Front. Plant Sci.* 7:1548. doi: 10.3389/fpls.2016.01548

Maki, H., Sakaoka, S., Itaya, T., Suzuki, T., Mabuchi, K., Amabe, T., et al. (2019). ANAC032 regulates root growth through the MYB30 gene regulatory network. *Sci. Rep.* 9:11358. doi: 10.1038/s41598-019-47822-0

Malamy, J. E., and Benfey, P. N. (1997). Organization and cell differentiation in lateral roots of *Arabidopsis thaliana*. *Development* 124, 33–44.

Mangano, S., Denita-Juarez, S. P., Choi, H.-S., Marzol, E., Hwang, Y., Ranocha, P., et al. (2017). Molecular link between auxin and ROS-mediated polar growth. *Proc. Natl. Acad. Sci. U.S.A.* 114, 5289–5294. doi: 10.1073/pnas.1701536114

Manzano, C., Pallero-Baena, M., Casimiro, I., De Rybel, B., Orman-Ligeza, B., Van Isterdael, G., et al. (2014). The emerging role of reactive oxygen species signaling during lateral root development. *Plant Physiol.* 165, 1105–1119. doi: 10.1104/pp.114.238873

Manzano, C., Ramirez-Parra, E., Casimiro, I., Otero, S., Desvoyes, B., De Rybel, B., et al. (2012). Auxin and epigenetic regulation of SKP2B, an F-box that represses lateral root formation. *Plant Physiol.* 160, 749–762. doi: 10.1104/pp.112.198341

Masucci, J. D., and Schiefelbein, J. W. (1994). The rhd6 mutation of *Arabidopsis thaliana* alters root-hair initiation through an auxin- and ethylene-associated process. *Plant Physiol.* 106, 1335–1346. doi: 10.1104/pp.106.4.1335

Masucci, J. D., and Schiefelbein, J. W. (1996). Hormones act downstream of TTG and GL2 to promote root hair outgrowth during epidermis development in the *Arabidopsis* root. *Plant Cell* 8, 1505–1517. doi: 10.2307/3870246

Matsubayashi, Y., Morita, A., Matsunaga, E., Furuya, A., Hanai, N., and Sakagami, Y. (1999). Physiological relationships between auxin, cytokinin, and a peptide growth factor, phytosulfokine-α, in stimulation of asparagus cell proliferation. *Planta* 207, 559–565. doi: 10.1007/s004250050518

Matsuzaki, Y., Ogawa-Ohnishi, M., Mori, A., and Matsubayashi, Y. (2010). Secreted peptide signals required for maintenance of root stem cell niche in *Arabidopsis*. *Science* 329, 1065–1067. doi: 10.1126/science.1191132

Menand, B., Yi, K., Jouannic, S., Hoffmann, L., Ryan, E., Linstead, P., et al. (2007). An ancient mechanism controls the development of cells with a rooting function in land plants. *Science* 316, 1477–1480. doi: 10.1126/science.1142618

Mendrinna, A., and Persson, S. (2015). Root hair growth: it's a one way street. *F1000Prime Rep.* 7:23.

Meng, L., Buchanan, B. B., Feldman, L. J., and Luan, S. (2012). CLE-like (CLEL) peptides control the pattern of root growth and lateral root development in *Arabidopsis*. *Proc. Natl. Acad. Sci. U.S.A.* 109, 1760–1765. doi: 10.1073/pnas.1119864109

Mhamdi, A., and Van Breusegem, F. (2018). Reactive oxygen species in plant development. *Development* 145:dev164376. doi: 10.1242/dev.164376

Miller, E. W., Albers, A. E., Pralle, A., Isacoff, E. Y., and Chang, C. J. (2005). Boronate-based fluorescent probes for imaging cellular hydrogen peroxide. *J. Am. Chem. Soc.* 127, 16652–16659. doi: 10.1021/ja054474f

Miller, G., Schlauch, K., Tam, R., Cortes, D., Torres, M. A., Shulaev, V., et al. (2009). The plant NADPH oxidase RBOHD mediates rapid systemic signaling in response to diverse stimuli. *Sci. Signal.* 2:ra45. doi: 10.1126/scisignal.2000448

Mittler, R. (2017). ROS are good. *Trends Plant Sci.* 22, 11–19. doi: 10.1016/j.tplants.2016.08.002

Miyashima, S., Koi, S., Hashimoto, T., and Nakajima, K. (2011). Non-cell-autonomous microRNA165 acts in a dose-dependent manner to regulate multiple differentiation status in the *Arabidopsis* root. *Development* 138, 2303–2313. doi: 10.1242/dev.060491

Molendijk, A. J., Bischoff, F., Rajendrakumar, C. S., Friml, J., Braun, M., Gilroy, S., et al. (2001). *Arabidopsis thaliana* Rop GTPases are localized to tips of root hairs and control polar growth. *EMBO J.* 20, 2779–2788. doi: 10.1093/emboj/20.11.2779

Monshausen, G. B., Bibikova, T. N., Messerli, M. A., Shi, C., and Gilroy, S. (2007). Oscillations in extracellular pH and reactive oxygen species modulate tip growth of *Arabidopsis* root hairs. *Proc. Natl. Acad. Sci. U.S.A.* 104, 20996–21001. doi: 10.1073/pnas.0708586104

Nakajima, K., Sena, G., Nawy, T., and Benfey, P. N. (2001). Intercellular movement of the putative transcription factor SHR in root patterning. *Nature* 413, 307–311. doi: 10.1038/35095061

Nakamura, M., and Grebe, M. (2018). Outer, inner and planar polarity in the *Arabidopsis* root. *Curr. Opin. Plant Biol.* 41, 46–53. doi: 10.1016/j.pbi.2017.08.002

Nakashima, K., Yamaguchi-Shinozaki, K., and Shinozaki, K. (2014). The transcriptional regulatory network in the drought response and its crosstalk in abiotic stress responses including drought, cold, and heat. *Front. Plant Sci.* 5:170. doi: 10.3389/fpls.2014.00170

Orman-Ligeza, B., Parizot, B., De Rycke, R., Fernandez, A., Himschoot, E., Van Breusegem, F., et al. (2016). RBOH-mediated ROS production facilitates lateral root emergence in *Arabidopsis*. *Development* 143, 3328–3339. doi: 10.1242/dev.136465

Ortega-Villasante, C., Burén, S., Blázquez-Castro, A., Barón-Sola, Á, and Hernández, L. E. (2018). Fluorescent in vivo imaging of reactive oxygen species and redox potential in plants. *Free Radic. Biol. Med.* 122, 202–220. doi: 10.1016/j.freeradbiomed.2018.04.005

Overmyer, K., Brosché, M., and Kangasjärvi, J. (2003). Reactive oxygen species and hormonal control of cell death. *Trends Plant Sci.* 8, 335–342. doi: 10.1016/s1360-1385(03)00135-3

Peleg-Grossman, S., Melamed-Book, N., and Levine, A. (2012). ROS production during symbiotic infection suppresses pathogenesis-related gene expression. *Plant Signal. Behav.* 7, 409–415. doi: 10.4161/psb.19217

Petricka, J. J., Winter, C. M., and Benfey, P. N. (2012). Control of *Arabidopsis* root development. *Annu. Rev. Plant Biol.* 63, 563–590.

Planas-Riverola, A., Gupta, A., Betegón-Putze, I., Bosch, N., Ibañes, M., and Caño-Delgado, A. I. (2019). Brassinosteroid signaling in plant development and adaptation to stress. *Development* 146:dev151894. doi: 10.1242/dev.151894

Qi, J., Wang, J., Gong, Z., and Zhou, J. M. (2017). Apoplastic ROS signaling in plant immunity. *Curr. Opin. Plant Biol.* 38, 92–100. doi: 10.1016/j.pbi.2017.04.022

Raffaele, S., Vailleau, F., Léger, A., Joubès, J., Miersch, O., Huard, C., et al. (2008). A MYB transcription factor regulates very-long-chain fatty acid biosynthesis for activation of the hypersensitive cell death response in *Arabidopsis*. *Plant Cell* 20, 752–767. doi: 10.1105/tpc.107.054858

Ravet, K., Touraine, B., Boucherez, J., Briat, J.-F., Gaymard, F., and Cellier, F. (2009). Ferritins control interaction between iron homeostasis and oxidative stress in *Arabidopsis*. *Plant J.* 57, 400–412. doi: 10.1111/j.1365-313x.2008.03698.x

Reyt, G., Boudouf, S., Boucherez, J., Gaymard, F., and Briat, J.-F. (2015). Iron- and ferritin-dependent reactive oxygen species distribution: impact on *Arabidopsis* root system architecture. *Mol. Plant* 8, 439–453. doi: 10.1016/j.molp.2014.11.014

Riballo, E., Kühne, M., Rief, N., Doherty, A., Smith, G. C. M., Recio, M.-J., et al. (2004). A pathway of double-strand break rejoining dependent upon ATM, Artemis, and proteins locating to gamma-H2AX foci. *Mol. Cell* 16, 715–724. doi: 10.1016/j.molcel.2004.10.029

Sabatini, S., Heidstra, R., Wildwater, M., and Scheres, B. (2003). SCARECROW is involved in positioning the stem cell niche in the *Arabidopsis* root meristem. *Genes Dev.* 17, 354–358. doi: 10.1101/gad.252503

Sakaoka, S., Mabuchi, K., Morikami, A., and Tsukagoshi, H. (2018). MYB30 regulates root cell elongation under abscisic acid signaling. *Commun. Integr. Biol.* 11:e1526604. doi: 10.1080/19420889.2018.1526604

Sarkar, A. K., Luijten, M., Miyashima, S., Lenhard, M., Hashimoto, T., Nakajima, K., et al. (2007). Conserved factors regulate signalling in *Arabidopsis thaliana* shoot and root stem cell organizers. *Nature* 446, 811–814. doi: 10.1038/nature05703

Schellmann, S., Schnittger, A., Kirik, V., Wada, T., Okada, K., Beermann, A., et al. (2002). TRIPTYCHON and CAPRICE mediate lateral inhibition during trichome and root hair patterning in *Arabidopsis*. *EMBO J.* 21, 5036–5046. doi: 10.1093/emboj/cdf524

Serna, L. (2008). CAPRICE positively regulates stomatal formation in the *Arabidopsis* hypocotyl. *Plant Signal. Behav.* 3, 1077–1082. doi: 10.4161/psb.3.12.6254

Setsukinai, K., Urano, Y., Kakinuma, K., Majima, H. J., and Nagano, T. (2003). Development of novel fluorescence probes that can reliably detect reactive oxygen species and distinguish specific species. *J. Biol. Chem.* 278, 3170–3175. doi: 10.1074/jbc.m209264200

Shaikhali, J., Heiber, I., Seidel, T., Ströher, E., Hiltscher, H., Birkmann, S., et al. (2008). The redox-sensitive transcription factor Rap2.4a controls nuclear expression of 2-Cys peroxiredoxin A and other chloroplast antioxidant enzymes. *BMC Plant Biol.* 8:48. doi: 10.1186/1471-2229-8-48

Shang, Y., Dai, C., Lee, M. M., Kwak, J. M., and Nam, K. H. (2016). BRI1-associated receptor kinase 1 regulates guard cell ABA signaling mediated by open stomata 1 in *Arabidopsis*. *Mol. Plant* 9, 447–460. doi: 10.1016/j.molp.2015.12.014

Shibata, M., and Sugimoto, K. (2019). A gene regulatory network for root hair development. *J. Plant Res.* 132, 301–309. doi: 10.1007/s10265-019-01100-2

Shiotani, B., and Zou, L. (2009). Single-stranded DNA orchestrates an ATM-to-ATR switch at DNA breaks. *Mol. Cell* 33, 547–558. doi: 10.1016/j.molcel.2009.01.024

Silva-Navas, J., Moreno-Risueno, M. A., Manzano, C., Téllez-Robledo, B., Navarro-Neila, S., Carrasco, V., et al. (2016). Flavonols mediate root phototropism and growth through regulation of proliferation-to-differentiation transition. *Plant Cell* 28, 1372–1387. doi: 10.1105/tpc.15.00857

Simon, M., Lee, M. M., Lin, Y., Gish, L., and Schiefelbein, J. (2007). Distinct and overlapping roles of single-repeat MYB genes in root epidermal patterning. *Dev. Biol.* 311, 566–578. doi: 10.1016/j.ydbio.2007.09.001

Smirnoff, N., and Arnaud, D. (2019). Hydrogen peroxide metabolism and functions in plants. *New Phytol.* 211, 1197–1214. doi: 10.1111/nph.15488

Somssich, M., Khan, G. A., and Persson, S. (2016). Cell wall heterogeneity in root development of *Arabidopsis*. *Front. Plant Sci.* 7:1242. doi: 10.3389/fpls.2016.01242

Souer, E., van Houwelingen, A., Kloos, D., Mol, J., and Koes, R. (1996). The no apical meristem gene of Petunia is required for pattern formation in embryos and flowers and is expressed at meristem and primordia boundaries. *Cell* 85, 159–170. doi: 10.1016/s0092-8674(00)81093-4

Sozzani, R., Cui, H., Moreno-Risueno, M. A., Busch, W., Van Norman, J. M., Vernoux, T., et al. (2010). Spatiotemporal regulation of cell-cycle genes by SHORTROOT links patterning and growth. *Nature* 466, 128–132. doi: 10.1038/nature09143

Sundaravelpandian, K., Chandrika, N. N. P., and Schmidt, W. (2013a). PFT1, a transcriptional mediator complex subunit, controls root hair differentiation through reactive oxygen species (ROS) distribution in *Arabidopsis*. *New Phytol.* 197, 151–161. doi: 10.1111/nph.12000

Sundaravelpandian, K., Chandrika, N. N. P., Tsai, Y.-H., and Schmidt, W. (2013b). PFT1-controlled ROS balance is critical for multiple stages of root hair development. *Plant Signal. Behav.* 8:e24066. doi: 10.4161/psb.24066

Suzuki, N., Miller, G., Salazar, C., Mondal, H. A., Shulaev, E., Cortes, D. F., et al. (2013). Temporal-spatial interaction between reactive oxygen species and abscisic acid regulates rapid systemic acclimation in plants. *Plant Cell* 25, 3553–3569. doi: 10.1105/tpc.113.114595

Swanson, S. J., Choi, W.-G., Chanoca, A., and Gilroy, S. (2011). In vivo imaging of Ca2+, pH, and reactive oxygen species using fluorescent probes in plants. *Annu. Rev. Plant Biol.* 62, 273–297. doi: 10.1146/annurev-arplant-042110-103832

Takeda, S., Gapper, C., Kaya, H., Bell, E., Kuchitsu, K., and Dolan, L. (2008). Local positive feedback regulation determines cell shape in root hair cells. *Science* 319, 1241–1244. doi: 10.1126/science.1152505

Tognetti, V. B., Bielach, A., and Hrtyan, M. (2017). Redox regulation at the site of primary growth: auxin, cytokinin and ROS crosstalk. *Plant Cell Environ.* 40, 2586–2605. doi: 10.1111/pce.13021

Tominaga-Wada, R., Kurata, T., and Wada, T. (2017). Localization of ENHANCER OF TRY AND CPC1 protein in *Arabidopsis* root epidermis. *Plant Physiol.* 214, 48–52. doi: 10.1016/j.jplph.2017.04.001

Trinh, D.-C., Lavenus, J., Goh, T., Boutté, Y., Drogue, Q., Vaissayre, V., et al. (2019). PUCHI regulates very long chain fatty acid biosynthesis during lateral root and callus formation. *Proc. Natl. Acad. Sci. U.S.A.* 116, 14325–14330. doi: 10.1073/pnas.1906300116

Tsukagoshi, H. (2012). Defective root growth triggered by oxidative stress is controlled through the expression of cell cycle-related genes. *Plant Sci.* 197, 30–39. doi: 10.1016/j.plantsci.2012.08.011

Tsukagoshi, H., Busch, W., and Benfey, P. N. (2010). Transcriptional regulation of ROS controls transition from proliferation to differentiation in the root. *Cell* 143, 606–616. doi: 10.1016/j.cell.2010.10.020

Wada, T., Kurata, T., Tominaga, R., Koshino-Kimura, Y., Tachibana, T., Goto, K., et al. (2002). Role of positive regulator of root hair development, CAPRICE, in *Arabidopsis* rot epidermal cell differentiation. *Development* 129, 5409–5419. doi: 10.1242/dev.00111

Wada, T., Tachibana, T., Shimura, Y., and Okada, K. (1997). Epidermal cell differentiation in Arabidopsis determined by a Myb homolog, CPC. *Science* 277, 1113–1116. doi: 10.1126/science.277.5329.1113

Wang, H., Tang, J., Liu, J., Hu, J., Liu, J., Chen, Y., et al. (2018). Abscisic acid signaling inhibits brassinosteroid signaling through dampening the dephosphorylation of BIN2 by ABI1 and ABI2. *Mol. Plant* 11, 315–325. doi: 10.1016/j.molp.2017.12.013

Wang, Y., Branicky, R., Noë, A., and Hekimi, S. (2018). Superoxide dismutases: dual roles in controlling ROS damage and regulating ROS signaling. *J. Cell Biol.* 217, 1915–1928. doi: 10.1083/jcb.201708007

Wang, Y., Shen, W., Chan, Z., and Wu, Y. (2015). Endogenous cytokinin overproduction modulates ROS homeostasis and decreases salt stress resistance in *Arabidopsis thaliana*. *Front. Plant Sci.* 6:1004. doi: 10.3389/fpls.2015.01004

Wang, Z., Rong, D., Chen, D., Xiao, Y., Liu, R., Wu, S., et al. (2021). Salicylic acid promotes quiescent center cell division through ROS accumulation and down-regulation of PLT1, PLT2, and WOX5. *J. Integr. Plant Biol.* 63, 583–596. doi: 10.1111/jipb.13020

Waszczak, C., Akter, S., Eeckhout, D., Persiau, G., Wahni, K., Bodra, N., et al. (2014). Sulfenome mining in *Arabidopsis thaliana*. *Proc. Natl. Acad. Sci. U.S.A.* 111, 11545–11550. doi: 10.1073/pnas.1411607111

Waszczak, C., Carmody, M., and Kangasjärvi, J. (2018). Reactive oxygen species in plant signaling. *Annu. Rev. Plant Biol.* 69, 209–236.

Whitford, R., Fernandez, A., Tejos, R., Pérez, A. C., Kleine-Vehn, J., Vanneste, S., et al. (2012). GOLVEN secretory peptides regulate auxin carrier turnover during plant gravitropic responses. *Dev. Cell* 22, 678–685. doi: 10.1016/j.devcel.2012.02.002

Wu, F., Chi, Y., Jiang, Z., Xu, Y., Xie, L., Huang, F., et al. (2020). Hydrogen peroxide sensor HPCA1 is an LRR receptor kinase in *Arabidopsis*. *Nature* 578, 577–581. doi: 10.1038/s41586-020-2032-3

Wu, J., Shang, Z., Wu, J., Jiang, X., Moschou, P. N., Sun, W., et al. (2010). Spermidine oxidase-derived H_2O_2 regulates pollen plasma membrane hyperpolarization-activated Ca (2+) -permeable channels and pollen tube growth. *Plant J.* 63, 1042–1053. doi: 10.1111/j.1365-313x.2010.04301.x

Yamada, M., Han, X., and Benfey, P. N. (2020). RGF1 controls root meristem size through ROS signaling. *Nature* 577, 85–88. doi: 10.1038/s41586-019-1819-6

Yang, L., Zhang, J., He, J., Qin, Y., Hua, D., Duan, Y., et al. (2014). ABA-mediated ROS in mitochondria regulate root meristem activity by controlling PLETHORA expression in *Arabidopsis*. *PLoS Genet.* 10:e1004791. doi: 10.1371/journal.pgen.1004791

Yi, D., Alvim Kamei, C. L., Cools, T., Vanderauwera, S., Takahashi, N., Okushima, Y., et al. (2014). The *Arabidopsis* SIAMESE-RELATED cyclin-dependent kinase inhibitors SMR5 and SMR7 regulate the DNA damage checkpoint in response to reactive oxygen species. *Plant Cell* 26, 296–309. doi: 10.1105/tpc.113.118943

Yoshiyama, K. O., Kobayashi, J., Ogita, N., Ueda, M., Kimura, S., Maki, H., et al. (2013). ATM-mediated phosphorylation of SOG1 is essential for the DNA damage response in *Arabidopsis*. *EMBO Rep.* 14, 817–822. doi: 10.1038/embor.2013.112

Yoshiyama, K., Conklin, P. A., Huefner, N. D., and Britt, A. B. (2009). Suppressor of gamma response 1 (SOG1) encodes a putative transcription factor governing multiple responses to DNA damage. *Proc. Natl. Acad. Sci. U.S.A.* 106, 12843–12848. doi: 10.1073/pnas.0810304106

Yu, Q., Tian, H., Yue, K., Liu, J., Zhang, B., Li, X., et al. (2016). A P-Loop NTPase regulates quiescent center cell division and distal stem cell identity through the regulation of ROS homeostasis in *Arabidopsis* root. *PLoS Genet.* 12:e1006175. doi: 10.1371/journal.pgen.1006175

Zheng, M., Åslund, F., and Storz, G. (1998). Activation of the OxyR transcription factor by reversible disulfide bond formation. *Science* 279, 1718–1722. doi: 10.1126/science.279.5357.1718

Zhou, J.-M., and Zhang, Y. (2020). Plant immunity: danger perception and signaling. *Cell* 181, 978–989. doi: 10.1016/j.cell.2020.04.028

Zhou, X., Xiang, Y., Li, C., and Yu, G. (2020). Modulatory role of reactive oxygen species in root development in model plant of *Arabidopsis thaliana*. *Front. Plant Sci.* 11:485932. doi: 10.3389/fpls.2020.485932

Zwiewka, M., Bielach, A., Tamizhselvan, P., Madhavan, S., Ryad, E. E., Tan, S., et al. (2019). Root adaptation to H_2O_2-induced oxidative stress by ARF-GEF BEN1- and cytoskeleton-mediated PIN2 trafficking. *Plant Cell Physiol.* 60, 255–273. doi: 10.1093/pcp/pcz001

Conflict of Interest: The authors declare that the research was conducted in the absence of any commercial or financial relationships that could be construed as a potential conflict of interest.

frontiers in Plant Science

REVIEW
published: 04 May 2021
doi: 10.3389/fpls.2021.661361

Unraveling Root Development Through Single-Cell Omics and Reconstruction of Gene Regulatory Networks

*Laura Serrano-Ron, Javier Cabrera, Pablo Perez-Garcia and Miguel A. Moreno-Risueno**

Centro de Biotecnología y Genómica de Plantas (Universidad Politécnica de Madrid–Instituto Nacional de Investigación y Tecnología Agraria y Alimentaria), Campus de Montegancedo, Pozuelo de Alarcón, Madrid, Spain

Over the last decades, research on postembryonic root development has been facilitated by "omics" technologies. Among these technologies, microarrays first, and RNA sequencing (RNA-seq) later, have provided transcriptional information on the underlying molecular processes establishing the basis of System Biology studies in roots. Cell fate specification and development have been widely studied in the primary root, which involved the identification of many cell type transcriptomes and the reconstruction of gene regulatory networks (GRN). The study of lateral root (LR) development has not been an exception. However, the molecular mechanisms regulating cell fate specification during LR formation remain largely unexplored. Recently, single-cell RNA-seq (scRNA-seq) studies have addressed the specification of tissues from stem cells in the primary root. scRNA-seq studies are anticipated to be a useful approach to decipher cell fate specification and patterning during LR formation. In this review, we address the different scRNA-seq strategies used both in plants and animals and how we could take advantage of scRNA-seq to unravel new regulatory mechanisms and reconstruct GRN. In addition, we discuss how to integrate scRNA-seq results with previous RNA-seq datasets and GRN. We also address relevant findings obtained through single-cell based studies and how LR developmental studies could be facilitated by scRNA-seq approaches and subsequent GRN inference. The use of single-cell approaches to investigate LR formation could help to decipher fundamental biological mechanisms such as cell memory, synchronization, polarization, or pluripotency.

Keywords: single-cell RNA-seq, gene regulatory networks, root development, organogenesis, cell fate

OPEN ACCESS

Edited by:
Svetlana Shishkova, National Autonomous University of Mexico, Mexico

Reviewed by:
Josh T. Cuperus, University of Washington, United States
Margaret Bezrutczyk, Lawrence Berkeley National Laboratory, United States

****Correspondence:***
Miguel A. Moreno-Risueno
miguelangel.moreno@upm.es

Specialty section:
This article was submitted to Plant Development and EvoDevo, a section of the journal Frontiers in Plant Science

Received: *30 January 2021*
Accepted: *25 March 2021*
Published: *04 May 2021*

Citation:
Serrano-Ron L, Cabrera J, Perez-Garcia P and Moreno-Risueno MA (2021) Unraveling Root Development Through Single-Cell Omics and Reconstruction of Gene Regulatory Networks. Front. Plant Sci. 12:661361. doi: 10.3389/fpls.2021.661361

INTRODUCTION

Cells are the units of all biological systems. However, the functionality of cells in multicellular organisms requires their specification into tissues and cell types, and thus cells acquire different identities. It is anticipated that the analysis of multicellular organisms at the single-cell level will greatly facilitate the understanding of the mechanisms that govern specific biological processes (Macosko et al., 2015; Ziegenhain et al., 2017).

Cell identity can be understood as the integration of factors such as morphology, phenotype and function (which are related to the present), lineage (related to the past), and molecular state (which determines the future) (Morris, 2019). Usually, cell types are classified by features such as morphology, location, and molecular profile. The recent development of single-cell omics methods comes as a useful approach to discern cell types based on their molecular fingerprints. Furthermore, the use of these methods have facilitated the ability to gain new insights and obtain results that were thought to be unattainable a few years ago such as the generation of a cell atlas of the whole planarian (Plass et al., 2018), the discovery of new types of human blood cells (Villani et al., 2017), or unraveling neuron programming from embryonic stem cells (Velasco et al., 2017). In this review, we summarize single-cell RNA-sequencing (scRNA-seq) strategies as well as the use of these datasets to reconstruct predictive Gene Regulatory Networks (GRN). In addition, we discuss the integration of scRNA-seq results with already available RNA-seq datasets and GRN. We also review recent advances eased by these technologies in various organisms. Finally, we propose that scRNA-seq approaches can facilitate the identification of unknown regulatory mechanism during lateral root formation and propose possible single-cell omics experiments that can address remaining biological questions in the field.

SINGLE-CELL OMICS APPROACHES

Single-cell omics technologies allow us to study multicellular organisms in an unbiased manner. As each cell is analyzed separately from the rest, specific molecular marks can be used to associate cells with existing molecular patterns, thus defining cell populations without previous assumptions. In contrast, approaches based on biomarkers or microdissection assign cells to predefined populations, which can potentially cause inaccurate results by mixing different types of cells. Single-cell omics technologies use different isolation methods and various types of data can be obtained: transcriptomic, proteomic, metabolomic, epigenetic data, and others.

Isolation of Cells

An initial isolation step is required in any type of single-cell experiment. This has been specially challenging in plants as the cell wall prevents cell separation. Plant cells can be physically isolated through micromanipulators and micropipettes, or through laser microdissection. While these methods can be used in single-cell experiments, their low throughput and experimental difficulty have reduced their use; although these methods are considered to be precise and a labeling step could not be required (Thakare et al., 2014; Anjam et al., 2016; Zeb et al., 2019). For single-cell omics analyses, the plant cell wall is normally enzymatically digested allowing cell disaggregation to generate protoplasts (Birnbaum et al., 2005). As protoplasting facilitates high throughput processing in subsequent single-cell isolation methods, it has become one of the preferred techniques to disaggregate plant cells (Prakadan et al., 2017; Mincarelli et al., 2018). Protoplasting can generate a stress response in cells, thereby it can potentially alter their transcriptomes. However, it has been shown that changes in gene expression induced by the protoplasting procedure are reduced. Moreover, genes induced by protoplasting have been identified, so they can be easily ruled out from subsequent analyses (Birnbaum, 2003; Villarino et al., 2016).

As an alternative to protoplasting, nuclei isolation has been used in single cell experiments. Nuclei isolation has become the preferred isolation technique in animals for single-cell transposase-accessible chromatin sequencing (scATAC-seq) and SCI- seq. In scATAC-seq library adaptors are inserted into open chromatin regions to determine chromatin accessibility, while in SCI- seq, nucleosomes bound to genomic DNA are removed to generate uniformly distributed sequence reads followed by an assessment of copy-number variants (Vitak et al., 2017). Nuclei isolation for single-cell experiments can be achieved by enzymatic digestion of the cell membrane and subsequent centrifugation (Habib et al., 2016). The main advantages of single-nucleus- over single-cell isolation in single-cell experiments are the higher representation of rare cell types and the apparently lack of induced stress response genes (Wu et al., 2019). Nuclei isolation for single-cell experiments in plants is in the process of being implemented, while previously microarray and RNA-seq of plant nuclei were successfully performed using Isolation of Nuclei in Tagged Cell Types (INTACT) (Deal and Henikoff, 2010; Reynoso et al., 2018). In this method, nuclei of the desired cell type are labeled through the transgenic expression of a tagged protein, which can be later used for affinity purification. INTACT could be used in plant single-cell experiments as an alternative to protoplasting.

Once cells or nuclei are disaggregated, the main isolation methods prior to single-cell experiments are the following (**Figure 1A**):

- **FACS-Based Cell Isolation.** Fluorescence-Activated Cell Sorting (FACS) is a well-known method that utilizes flow cytometry to profile fluorescently marked cells. After fluorescence detection, individual cells are sorted and deposited into microtiter plates (Ramsköld et al., 2012; Jaitin et al., 2014). This approach is broadly used as it is compatible with different workflows and has the ability to automatically select the desired cells based on fluorescence and other cell characteristics. The main drawbacks concern cell damage, the large amount of initial material and the cost (Zeb et al., 2019).

- **Microfluidic Structures Cell Isolation.** These approaches are based on microfluidic devices, which typically are valves, droplets, and nanowells (Prakadan et al., 2017). Valves-based systems rely on microchannels made of an elastic membrane that can be deflected by applying pressure to block the flow and confine individual cells (Hong and Quake, 2003). Droplet-based systems make use of aqueous droplets in inert carrier oil. Individual cells are captured in droplets because they are loaded at low densities to obtain, at most, a single element per drop. In addition, one barcoded bead and lysis buffer are included in each droplet (Klein et al., 2015;

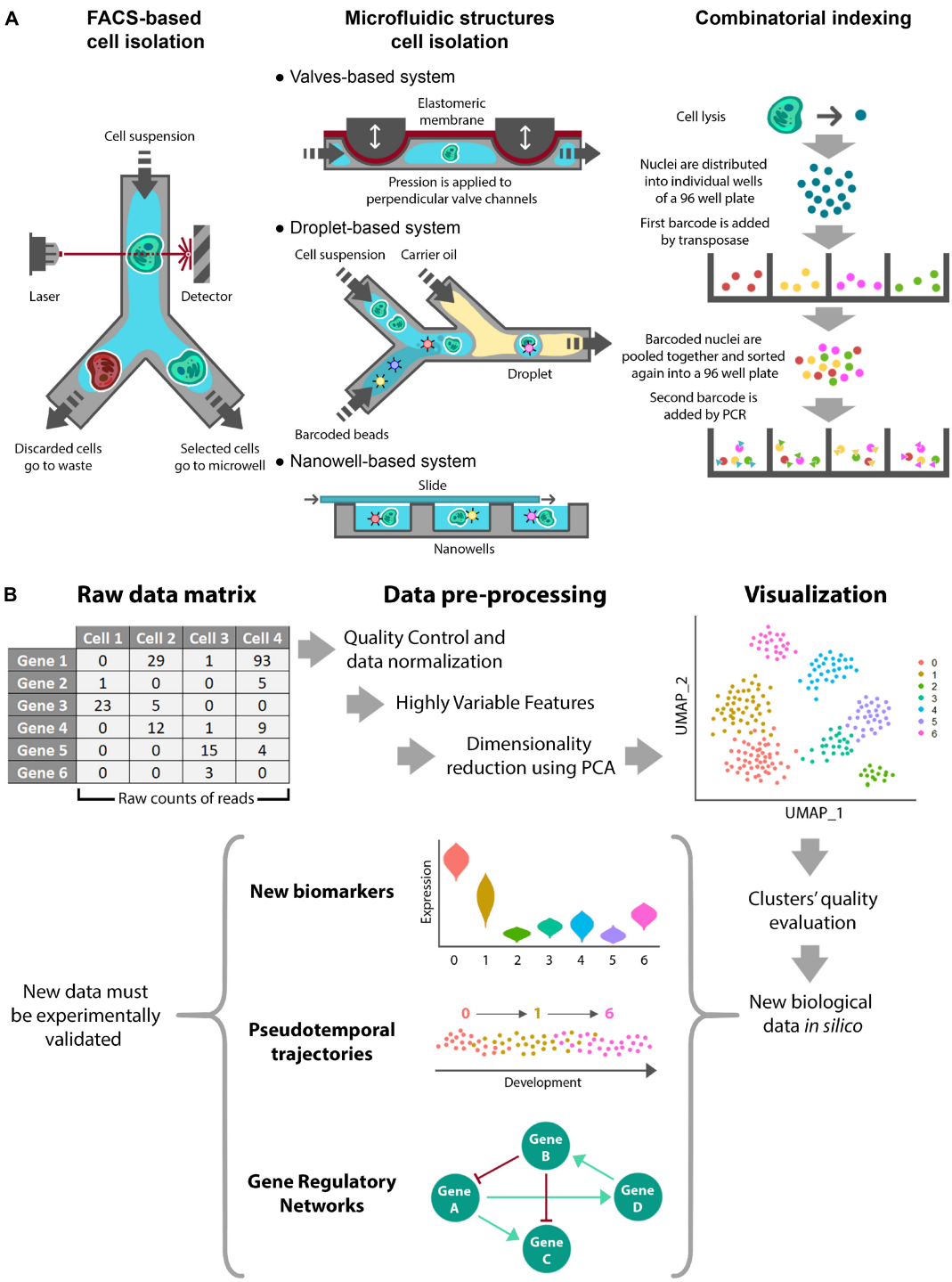

FIGURE 1 | Single-cell Omics experimental procedures. Schematic representation of a single-cell omics experiment showing **(A)** the different available methods for cell isolation and **(B)** a standardized workflow for *in silico* processing of RNA sequencing data.

Macosko et al., 2015). Finally, nanowell-based methods use cells at low concentration to encapsulate individual cells. In this case, roofless nanolitre-scale wells are filled with the cell suspension by gravity and then sealed on the top with a slide (Gierahn et al., 2017; Prakadan et al., 2017). In comparison with the FACS/plates-based method, these approaches can reduce the reagent cost per cell and maximize throughput due to the small size of the microfluidic devices. As cell isolation

and DNA amplification are integrated in these methods, they are time and cost effective. In contrast, the main disadvantages of these methods are higher rates of cell damage and lower purity of the selected cells (Prakadan et al., 2017; Zeb et al., 2019). In occasions, these methods have been associated to lower depth of sequencing.

- **Combinatorial Indexing.** These methods are used to label and classify isolated nuclei. SCI-seq was the first single-cell whole-genome sequencing method using a combinatorial indexing strategy (Vitak et al., 2017). Combinatorial indexing normally uses a two-step barcoding workflow to label cell nuclei and DNA molecules. First, nuclei are isolated in several small pools, each one receiving a primary transposase-based barcode. After adding the first barcode, nuclei are mixed together and sorted again into small pools, when a second barcode is added by PCR to each pool. This way, each nucleus receives a unique combination of barcodes that identifies it (Vitak et al., 2017; Mincarelli et al., 2018). This method comes as an alternative to physical compartmentalization, eliminating the requirement for custom equipment. An additional advantage is its high throughput. On the contrary, shallowness of subsequent sequencing can be mentioned as its main drawback (Mincarelli et al., 2018).

Molecular Profiling

The available single-cell methods enable the measurement of a catalog of cell parameters. Most single-cell approaches have addressed the identity of the cell (Stuart and Satija, 2019), which included the analysis of particular aspects of the transcriptome (Picelli et al., 2013; Macosko et al., 2015), genome (Navin et al., 2011; Vitak et al., 2017), epigenome (Gomez et al., 2013; Buenrostro et al., 2015; Lake et al., 2018), and proteome (Darmanis et al., 2016; Stoeckius et al., 2017). The specific methods available for each one of these modalities are reviewed in Stuart and Satija (2019).

More recently, efforts have focused on simultaneously analyzing several of the transcriptome, genome, epigenome, or proteome parameters for each single cell. This is known as multimodal profiling and anticipates a more profound understanding of the biology of the cell. Examples of these types of analyses are scG&T-seq (simultaneous measurement of genomic DNA and mRNA) and scM&T-seq (simultaneous measurement of DNA methylation and mRNA). Other cases of multimodal profiling are the cell lineage tracing methods scGESTALT, ScarTrace, and LINNAEUS. These methods infer lineage relationships between groups of cells based on shared DNA mutations, simultaneously analyzing the clonal history of the cell and its transcriptomic identity (Macaulay et al., 2015; Angermueller et al., 2016; Alemany et al., 2018; Raj et al., 2018; Spanjaard et al., 2018; Stuart and Satija, 2019).

Data Processing and *in silico* Analysis

Once data are obtained and quantified, they are arranged in a matrix containing the extracted biological features per cell (**Figure 1B**). As the most commonly used analysis is scRNA-seq, we will focus on this type of data. scRNA-seq data are presented as a digital gene expression matrix of read counts per gene (in rows) and per cell (in columns). Many studies analyze these data using Seurat, which is used as an R package. Seurat aims to dissect heterogeneity from single-cell transcriptomic measurements integrating diverse types of single-cell data. The specific data processing workflow is comprehensively explained at the command level in the Seurat developers' website[1] (Butler et al., 2018; Stuart et al., 2019). The workflow involves the following steps (**Figure 1B**):

- **Quality Control and Normalization.** This first step selects the cells that will be used for subsequent analyses. This is performed through different quality control filters. Although Seurat pipeline is originally designed for animal tissues, similar quality controls can be used in plants such as the number of unique genes or molecules per cell and/or the percentage of reads that map to the mitochondrial genome (mitochondrial reads are expected to remain constant). Typical desired values for a cell are between 200 and 2,500 unique feature counts/cell and between 1 and 5% of mitochondrial counts/cell. In addition, quality controls in plants can be extended to chloroplast/plastid-derived counts (Shulse et al., 2019), which are expected to remain constant in an organ- or tissue- dependent manner. Next, selected cells are processed in order to normalize counts through different algorithms. Several of these algorithms involve regression analysis and removal of unwanted sources of variation.

- **Identification of Highly Variable Features.** Most variable features, i.e., genes with most different expression values among the normalized dataset, are used to perform dimensionality reduction and clustering. The statistical methods that can be used for normalization in Seurat are the natural logarithmic or centered logarithmic transformation of the count ratio and the scaled non-logarithmic transformation of the count ratio. To select the top variable features, Seurat assigns a dispersion value for each gene. This dispersion value can be the standard deviation, the expected variance fitted by a polynomial regression or the z-score. Finally, the genes with the highest dispersion values are selected. In addition, several statistical methods have been developed to obtain the differentially expressed genes from scRNA-seq experiments. The majority of these algorithms (SCDE, MAST, SigEMD, DEsingle, SINCERA, DESeq2, edgeR) are implemented for R and (D3E) for python (Wang et al., 2019; Hoffman et al., 2020).

- **Linear Dimensional Reduction and Determination of the Dimensionality of the Dataset.** After scaling the data (linear transformation), a principal component analysis (PCA) is performed using the most variable features previously determined. The primary sources of heterogeneity in the dataset (genes and cells) can then be explored using various methods. This information helps to assess the number of principal components that should be considered to accurately represent the dataset.

[1] https://satijalab.org/

- **Clustering and Visualization.** Cells are clustered using the selected principal components of the PCA. As 5–10 principal components are normally used for clustering in Seurat, the resulting clusters cannot be easily represented by PCA plotting, so they are normally visualized by non-linear dimensional reduction methods, such as t-distributed Stochastic Neighborhood Embedding (tSNE) or Uniform Manifold Approximation and Projection (UMAP) (Maaten and Hinton, 2008; McInnes et al., 2018). These methods preserve local similarities while they represent data/cells in a non-linear way that better captures clustering as compared with PCA plotting. Next, differentially expressed genes among clusters can be identified. These genes have enriched expression in specific clusters and represent biomarkers. The following step usually consists of assigning specific cell type identities to the clusters. To do so, a typical approach is examining the expression of known cell type markers (Denyer et al., 2019; Ryu et al., 2019). A complementary option to identify cell types or assign identity to clusters is through the Index of Cell Identity (ICI) method (Efroni et al., 2015). The ICI method computes a score for each cell based on libraries of gene expression profiles for known cell types. The resulting score gives the relative contribution of each known cell type to the identity of the cell, thus facilitating its identification. An additional advantage of the ICI method is that cells with mixed identities can be categorized.

Pseudotemporal and Network Analyses

scRNA-seq data can be used to reconstruct GRN as well as to perform the so called pseudotime analyses. Pseudotime studies aim to order cells along a one-dimensional axis that represents a continuous process such as differentiation or development. These methods assign a relative time to the cells to compute their order. Even though development or differentiation processes imply differences in gene expression profiles, progression can occur at different speeds depending on each cell. Thus, cell transcriptomics are analyzed as state-dependent instead of as time-dependent features (Rich-Griffin et al., 2020). Most commonly used methods include Monocle (Trapnell et al., 2014), Wishbone (Setty et al., 2016), Diffusion (Haghverdi et al., 2016), and Velocyto (La Manno et al., 2018). In addition, as Velocyto is based on the measurement of intronic RNA reads (defined as RNA velocity), it can infer the future transcriptional state of cells. This addresses some of the problems found in the other methods such as rooting and branching of the trajectories (La Manno et al., 2018; Stuart et al., 2019). However, the lower abundance of intronic reads detected in plants can hinder the annotation of gene splicing rates, thus potentially rendering less reliable results for Velocyto in plants (Li et al., 2016; Jean-Baptiste et al., 2019).

Development of microarray and RNA-seq technologies have greatly contributed to the generation of a large amount of expression data, facilitating the identification of molecular mechanisms regulating cell-type-specific gene expression during development or stress (Brady et al., 2007; Dinneny et al., 2008). In parallel, bioinformatics methods were developed to infer genetic interactions using sequenced transcriptomes, thus making GRN reconstruction possible. GRN represent gene regulatory dependencies which are mathematically inferred from transcriptomic data. In GRN, the nodes represent the genes, and the edges the positive or negative regulatory connections among them (Blencowe et al., 2019; Haque et al., 2019). GRN can also be inferred from protein-protein interaction experiments (e.g., pull-down, yeast two-hybrid, or bimolecular fluorescence complementation) or from protein-DNA interaction experiments, such as yeast one-hybrid or ChIP-sequencing assays (de Matos Simoes et al., 2013). Particularly, GRN inferred from yeast one- and two-hybrid approaches have greatly contributed to our understanding of development and stress in Arabidopsis. These GRN have provided new insights into secondary cell wall gene regulation under abiotic stress (Taylor-Teeples et al., 2014), showed coordinated transcriptional regulation of enzymes involved in nitrogen metabolism (Gaudinier et al., 2018) and identified upstream regulation of AUXIN RESPONSE FACTORS to modulate auxin signaling throughout development (Truskina et al., 2020).

GRN inference algorithms have been classified into three major groups (Haque et al., 2019). The first group of methods uses linear and non-linear statistic correlation to measure the dependency between genes based on their expression patterns. These methods assume that the presence or absence of co-expressed transcripts reflects gene regulations. An improvement of this type of methods assumes that gene expression is deterministically controlled by upstream regulators. Based on this assumption, one of these methods, GENIST, first clusters putative regulated genes using gene expression data to subsequently model expression of each gene over time as a probabilistic function of itself and its putative upstream regulators, thus defining regulatory interactions (de Luis Balaguer et al., 2017). Secondly, probabilistic graphical models include other variables such as space. Thus, these methods are useful to reconstruct GRNs using samples collected from different cell types. At last, machine learning supervised and unsupervised methods have been used as an alternative to the previous methods. In the case of machine learning supervised methods, the algorithm is initially fed with previously demonstrated gene regulatory interactions (Haque et al., 2019). Machine learning analyses offer us algorithms not only for GRN inference but also for feature extraction across multi-dimensional datasets allowing integration of heterogeneous data from various high-throughput experimental techniques. As a result of GRN reconstruction, the relationships between genes can be established as direct or indirect (if one gene regulates another through an undefined intermediary) and signed (if the regulation determines activation –positive- or repression –negative of the downstream gene) or unsigned (if the type of regulation is unknown).

In plant biology, many GRN have been generated from RNA-seq experiments and these GRN have been proven to be useful to comprehend specific molecular processes (Haque et al., 2019). For example, a GRN predicting regulation of stem cells at the root apical meristem led to the identification of *TESMIN LIKE CXC2* as a master regulator of stem cell division (Clark et al., 2019). Similarly, the role of *PERIANTHIA*

as regulator of the quiescent center was predicted by a GRN and further validated experimentally (de Luis Balaguer et al., 2017). GRN elucidated from RNA-seq experiments have also provided new insights into seed development (Ni et al., 2016).

GRN can also be generated from scRNA-seq data (Pratapa et al., 2020), which raises new challenges. For instance, GRN derived from scRNA-seq might be devoid of certain interactions related to the less abundant transcripts (as a consequence of lower depth of sequencing of scRNA-seq as compared with RNAseq). In contrast, GRN derived from scRNA-seq can identify TF-gene interactions at the single-cell level within a cell type or a tissue, therefore providing higher spatial resolution (Hu et al., 2020). Inferring GRN from scRNA-seq also represents a computational challenge as the transcriptomes of thousands of cells must be statistically analyzed and integrated to connect putative regulators (normally transcription factors) with downstream genes. Different methods to infer GRN from scRNA-seq have been developed (Pratapa et al., 2020). To improve reliability of the results, some methods such as GENIE3 initially feed the algorithm with specific information about the potential nodes or hubs (i.e., transcriptional regulators), which may regulate other genes (Huynh-Thu et al., 2010). Other methods such as SCODE or SINCERITIES require a time-course structure. In those cases, in which temporality of the dataset is not defined, pseudotime inference can be used to feed these methods with a relative time. Moreover, GENIE3, which reconstructs GRN from regression analyses of gene expression patterns using tree-based ensemble methods, also emerges as an alternative approach when temporal information is not available. Notably, GENIE3, has become one of the top performers when evaluated as benchmarking algorithm in DREAM4 (Marbach et al., 2012) and BEELINE (Pratapa et al., 2020). Furthermore Pratapa et al. (2020), shows that techniques that do not require pseudotime-ordered cells recover gene interactions more accurately.

Single-cell GRN inference methods have also been implemented to cope with problems intrinsic to scRNA-seq data, including those which are consequential to the so-called dropout effect. The dropout effect occurs when transcripts that are present in some cells show, however, zero reads in other cells; as this hampers the statistical analysis (Qiu, 2020). Moreover, scRNAseq data is affected by the variation in sequencing depth among cells and heterogeneity due to cell specialization or the cell cycle stage. Altogether, these issues affect GRN reconstruction from scRNA-seq and require specific methodology (Pratapa et al., 2020).

Once a GRN is generated from scRNA-seq data, analysis and mining of the network is greatly facilitated by software such as Cytoscape (Shannon, 2003). Cytoscape can be used to visualize and dissect the network as it can extract genes of interest and their neighbors, hubs (nodes highly connected), or filter specific relationships. In addition, Cytoscape integrates gene and pathway annotation, as well as expression patterns from external databases. The integration of this information into the network enables further analyses such as functional enrichment (based on gene ontology categories) or dissection of molecular pathways.

To facilitate a more profound understanding of the molecular processes related to development or stress, we propose that RNA-seq and GRN data are integrated with the new profiles and GRN obtained by scRNA-seq. However, many GRN were inferred for whole organs or sorted cells based on marker expression and lack single cell resolution. To address this issue, several deconvoluting methods can be used to infer (sub-)cell types or clusters of cells with specific transcriptomic signatures from tissues or bulk cells that have been sequenced by RNA-seq (Sun et al., 2019; Avila Cobos et al., 2020). scRNA-seq and deconvoluted RNA-seq data can then be systematically compared through the analysis of gene expression patterns, differentially expressed genes and reconstructed GRN using each dataset as input. Furthermore, scRNA-seq and deconvoluted RNA-seq datasets could be combined to reconstruct an integrated GRN. As an example of the potential of these approaches, a GRN reconstructed for trichoblast differentiation using scRNA-seq data and compared with a known GRN for root hair formation has further contributed to understanding this developmental process identifying new regulators (Denyer et al., 2019).

With the exception of the GRN reconstructed for trichoblast differentiation (Denyer et al., 2019), plant GRN do not normally integrate scRNA-seq data. Thus, current GRN do not consider developmental trajectories or intermediate transcriptomic states of cells, and thus this regulation has remained unexplored so far. With the use of scRNA-seq technology, intermediate transcriptomic states and cell trajectories can be integrated into GRN to gain further insight into the underlying molecular processes (Pratapa et al., 2020). GRN obtained through a cell lineage trajectory could increase the reliability of the network, as changes in gene relationships would be monitored with a higher resolution, which includes regulation of intermediate developmental stages. In this way, the molecular pathways regulating the developmental transitions or differentiation of the different cell linages of the primary root meristem could be more precisely defined.

Experimental Validation

Single-cell omics analyses generate a huge amount of information such as cell trajectories, new types of cells (previously undetermined or misclassified), differentially expressed genes, and biomarkers. As these findings are typically based on statistical correlative analyses, they need to be experimentally assessed so their functional relevance can be determined.

A commonly used validation method to investigate expression patterns inferred from scRNA-seq analysis is to generate transcriptional reporters. In this approach, the promoter of a biomarker gene is transcriptionally fused to the *uidA* gene or a fluorescent protein coding sequence. Then, the reporter activity can be visualized under a (fluorescent) microscope to confirm expression of the biomarker gene in the cell type of interest (Reece-Hoyes and Walhout, 2018) or associated to a specific molecular process. Another option is performing fluorescence *in situ* hybridization (FISH) or colorimetric *in situ* hybridization (CISH) using the mRNA sequence of the biomarker as a probe (Femino et al., 1998; Marcino, 2013). Finally, functional validation of differentially expressed genes and cell type function can be investigated through loss-of-function

mutants or overexpression lines (Capecchi, 1989; Visscher et al., 2015; Hahn et al., 2017).

The gene regulations established in a GRN can also be validated by perturbation experiments. These experiments are based on creating mutations in transcription factors or hubs of the network (for instance using the CRISPR/CAS9 technology). Subsequently, sc-RNAseq is performed in these mutants and the GRN is reconstructed again to test the edges and/or sign of the regulatory predictions of the initial GRN (Fiers et al., 2018).

UNRAVELING THE HETEROGENEITY AND TEMPORALITY OF TRANSCRIPTOMIC CHANGES

A major strength of scRNA-seq is the identification of scarce or new cell variants as well as of intermediate states of known cell types. The identification of these new types of cells suggests that formative or differentiation pathways are continuous dynamic processes, rather than a succession of homogeneous stages as previously profiled by microarrays or RNA-seq data using fluorescent markers that categorized cells into predefined cell types (Brady et al., 2007; Li et al., 2016).

The international consortium of the Human Cell Atlas Project aims to describe all the cell types in the human body in terms of their molecular signatures (Regev et al., 2017[2]). Contributions to this project have found new cell types in the different organs or tissues of the human body, e.g., retina (Lukowski et al., 2019), liver (Aizarani et al., 2019), or lungs (Braga et al., 2019). The generation of a Plant Cell Atlas Project has been proposed. The Plant Cell Atlas Project initiative will profile plants through scRNA-seq, proteomics and imaging, while all these datasets will be integrated using machine-learning algorithms. This initiative will likely accelerate discoveries in the field of plant science (Rhee et al., 2019).

Some scRNA-seq studies have been performed in plants, such as in the moss *Physcomitrella patens* (Kubo et al., 2019), maize (Nelms and Walbot, 2019; Satterlee et al., 2020; Bezrutczyk et al., 2021; Xu et al., 2021), rice (Liu et al., 2021) and the model plant *Arabidopsis thaliana* (Denyer et al., 2019; Jean-Baptiste et al., 2019; Ryu et al., 2019; Shulse et al., 2019; Zhang et al., 2019; Kim et al., 2021). The Arabidopsis root constitutes a model for stem cell and post-embryonic development. scRNA-seq of the Arabidopsis root has identified intermediate cellular states during cell differentiation. In these studies, not only cells from the main tissues were detected but also less-abundant cells such as the quiescent center and protoxylem cells. The information provided by these studies was thought to facilitate the future characterization of regulators involved in cell fate specification during root differentiation. As an initial approximation, matching pairs of transcriptional factors and their binding *cis* elements in the promoters of putatively downstream genes was carried out (Jean-Baptiste et al., 2019).

scRNA-seq studies in roots have also provided new insights into postembryonic development. Critical bifurcation points during cell differentiation have been identified by the use of pseudo-temporal trajectories (Jean-Baptiste et al., 2019). In addition, the sequential regulation of transcription factors to drive cell differentiation was proposed (Denyer et al., 2019). Detailed investigation of epidermal cells offers a good example of the possibilities of scRNA-seq techniques to comprehensively study cell differentiation. The trajectory from meristematic epidermal cells to fully differentiated root hair- or non-hair cells was traced. This approach resulted in the identification of an intermediate unknown identity for epidermal cells, which presented both hair- and non-hair-cell marker genes. This existence of this intermediate cell identity suggested that specification of epidermal cell fate would require a late decision in development. Further transcriptional information obtained from mutants impaired in specific types of epidermal cells identified the main regulators of epidermis differentiation and cell fate specification (Ryu et al., 2019). In addition, developmental trajectories of endodermis cells were investigated using scRNA-seq (Shulse et al., 2019).

scRNA-seq was used to study the regenerative capacity of root cells after excision of the root tip. After excision, the remaining cells undergo changes in cell identity that lead to the formation of a new functional meristem. Changes in cell identity during meristem regeneration are fast and organized. scRNA-seq studies showed the existence of predominant transitions in cell identity during the regeneration process, and identified the transcriptional changes associated with those transitions (Efroni et al., 2016). In agreement with the idea that some changes in cell identity are most likely to occur than others, ablation of single cells in roots specifically triggers the division of the adjacent cells on the external side. Subsequently, the daughter cells replace the damaged ones (Marhava et al., 2019). The use of scRNA-seq or other single-cell omics approaches could contribute to a better understanding of the regeneration processes of excised organs or ablated cells.

scRNA-seq not just limited to development or regeneration studies. Signaling and response to environmental changes may be interpreted differently by each cell. This hypothesis has been supported by scRNA-seq studies in the Arabidopsis root (Jean-Baptiste et al., 2019; Shulse et al., 2019). Although it is known that the heat response is not uniform across cells, scRNA-seq has shown that all cells belonging to the same cell type show unique and specific transcriptomic differences upon heat treatment (as compared with other cell types) (Jean-Baptiste et al., 2019). A cell-type specific response to heat is in agreement with previous research showing cell-type specific responses to other stresses (Dinneny et al., 2008), and demonstrates the versatility of single-cell approaches.

In addition to scRNA-seq techniques, other single-cell oriented studies or at cell resolution have been shown to be useful to unravel biological processes. For instance, analysis of the epigenetic state of single stomatal guard cells deciphered the specific role of H3K27me3 epigenetic mark during differentiation (Lee et al., 2019). Moreover, confocal laser microscopy techniques in roots allowed the investigation of biological processes with single-cell resolution (González-García et al., 2015; Long et al., 2017). A different example of a study performed

[2]www.humancellatlas.org

with cell resolution was measuring the pace of the circadian clock in individual cells. This study concluded the existence of at least two main types of rhythms, one consisting of waves moving shootward and another moving rootward. This work shows a requirement for cell-to-cell communication in order to synchronize the clock and the subsequent outputs (Gould et al., 2018).

All these studies in plants demonstrate the existence of specific regulation in single cells. Therefore, a more extensive use of single cell-omics approaches could greatly contribute to a better understanding of the molecular processes taking place in individual cells, including how cells coordinate and facilitate functionality in a multicellular organism.

FILLING GAPS IN ROOT DEVELOPMENT: A CASE FOR THE INVESTIGATION OF LATERAL ROOT FORMATION

Although RNA-seq of sorted cell types, derived GRN and scRNA-seq have been used to study plant development, lateral root formation remains largely unexplored by these approaches (Lavenus et al., 2015; Voß et al., 2015). Lateral roots appear as repeated units along the primary root axis, however formation of lateral roots involves various pre-patterning and developmental stages (Malamy and Benfey, 1997; Lavenus et al., 2013). We will revise these developmental stages discussing how single-cell omics approaches might contribute to their molecular dissection (**Figure 2**).

Lateral Root Pre-patterning Is Mediated by the Root Clock

Although lateral root formation is a plastic developmental process, the locations (prebranch sites) where these new organs form are defined by a time-dependent mechanism known as the Root Clock. The Root Clock was identified using the synthetic auxin-response promoter *DR5:Luciferase*, which rhythmically pulses in a region of the root tip known as the Oscillation Zone (OZ). Further transcriptomic analyses of this region showed changes in the expression of thousands of genes that fluctuated in or out of phase with DR5 (De Smet et al., 2007; Moreno-Risueno et al., 2010). It was later observed that auxin accumulation in the epidermis following programmed cell death of the root cap, as well as auxin signaling throughout the OZ contributed to the Root Clock pulses and affected subsequent prebranch site formation (De Rybel et al., 2010; Xuan et al., 2015, 2016). However, if auxin accumulates in the internal tissues of the OZ (other than the epidermis) is unresolved. The core oscillator of the Root Clock has been recently identified, demonstrating that negative auxin signaling regulation is critical for the Root Clock oscillations and establishes the periodicity of the system (Perianez-Rodriguez et al., 2021). In addition it was shown that the Root Clock oscillator can be entrained by external cues that lead to the periodic accumulation of auxin in the OZ such as during the gravitropic response. Even though the OZ is characterized by activity of the *DR5:Luciferase* marker, it remains unclear if the OZ can be understood as a homogeneous region with similar responses in all its constituent cells. Time-course scRNA-seq of the OZ might unravel the contribution of the different cell types to the oscillations, the molecular bases of cell synchrony during an oscillation, and if cell responses in the OZ are homogenous.

Pre-branch Site Formation Involves an Unknown Cell Memory Mechanism

During root growth, new cells exit the meristem as they enlarge and differentiate. Thus the root longitudinal axis can be understood as developmental time: the older and more differentiated a cell is, the further away it will be from the meristem (Fisher and Sozzani, 2016; Perez-Garcia and Moreno-Risueno, 2018). Although all cells move across the OZ during root growth, only cells exposed to the peak of the in-phase oscillations become prebranch sites and show permanent activity of *DR5:Luciferase* (Moreno-Risueno et al., 2010; Xuan et al., 2015, 2016). Due to the dynamism of the Root Clock oscillations, cells enter and exit the OZ at different stages of the oscillations. This generated the hypothesis of whether cells get primed and are specified as prebranch sites depending on the phase of the oscillation (Traas and Vernoux, 2010). This hypothesis is in agreement with multilevel computational simulations of prebranch priming in the OZ, which shows that only reduced clusters of cells are exposed to maxima of the in-phase oscillations when they leave the OZ (Perianez-Rodriguez et al., 2021). Even though vesicular trafficking and cell wall remodeling affecting pectin esterification status have been shown to mediate Root Clock function leading to prebranch site specification (Wachsman et al., 2020) the molecular nature of the priming signal and its subsequent memorization by cells remains unresolved. Detailed single-cell omics studies of the OZ might help to understand cell memory and thus the molecular mechanism leading to prebranch site specification.

Founder Cell Specification and Polarization Cues Have Not Been Identified

Primed xylem pole pericycle (XPP) cells, i.e., those in prebranch sites, are specified as lateral root founder cells (FC) in the differentiation zone. FC are cells which are able to initiate lateral root organogenesis, thus FC specification involves the acquisition of pluripotency. Next in the lateral root formation process, the nuclei of two adjacent FC migrate toward each other and FC divide asymmetrically to generate two morphological and presumably functionally different daughter cells. To date, the signal that triggers the specification of XPP cells into pluripotent FC is unknown. A number of regulators and molecular processes have been described to be part of this process and/or regulate FC division leading to lateral root initiation (Okushima et al., 2007; De Smet et al., 2008, 2010; De Rybel et al., 2010; Van Damme et al., 2011; Goh et al., 2012; Cho et al., 2013; Vermeer et al., 2014; Xuan et al., 2015; Murphy et al., 2016; Roberts et al., 2016; Ramakrishna et al., 2019; Trinh et al., 2019; Vilches Barro et al., 2019; Fernandez et al., 2020; Singh et al., 2020). In addition,

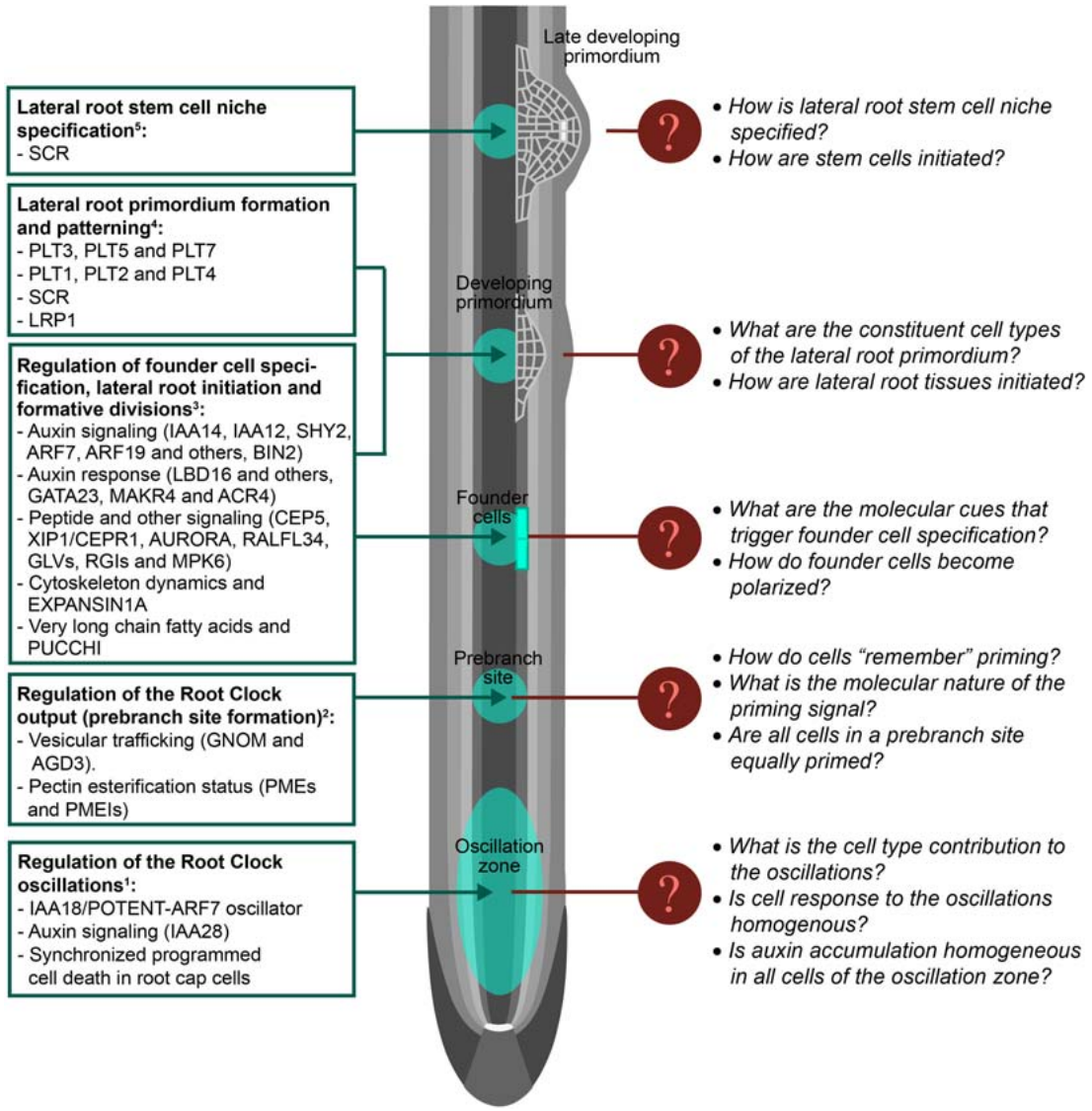

FIGURE 2 | Filling the gaps in lateral root development. Schematic representation of an Arabidopsis primary root on which lateral root development stages are shown. Known regulation of lateral root formation is shown on the left. Note that regulators are indicated by abbreviated names. Unknown regulation or missing features of lateral root formation are indicated for specific developmental stages. Tissue layers are represented in gray. The quiescent center is represented in white: [1]Please see references (De Smet et al., 2007; De Rybel et al., 2010; Moreno-Risueno et al., 2010; Xuan et al., 2015, 2016; Perianez-Rodriguez et al., 2021); [2](Wachsman et al., 2020); [3](Malamy and Benfey, 1997; Okushima et al., 2007; De Smet et al., 2008, 2010; De Rybel et al., 2010; Van Damme et al., 2011; Goh et al., 2012; Cho et al., 2013; Vermeer et al., 2014; Lavenus et al., 2015; Voß et al., 2015; Xuan et al., 2015; Murphy et al., 2016; Roberts et al., 2016; Ramakrishna et al., 2019; Trinh et al., 2019; Vilches Barro et al., 2019; Fernandez et al., 2020; Singh et al., 2020); [4](Malamy and Benfey, 1997; Goh et al., 2016; Du and Scheres, 2017; Singh et al., 2020); [5](Goh et al., 2016).

several of these regulators have been shown to control subsequent formative divisions. As mutants for these regulators still have FC and their expression is not restricted to FC (Motte et al., 2019), it is unlikely that these regulators are the determinants of FC specification. The use of scRNA-seq in cells marked as prebranch sites and/or FC using available fluorescent reporters (Wachsman et al., 2020; Perianez-Rodriguez et al., 2021) could lead to unravel the molecular cues or determinants of FC specification. In addition, the signal that triggers FC polarization (if other than auxin) as well as the subsequent signaling cascade is unknown. The study of FC transcriptomes or proteomes with single-cell resolution could facilitate the identification of this putative signal and the subsequent polarization mechanism.

Lateral Root Formation Requires Regulation of Cell Identity Transitions

After the first asymmetric division of FC, non-deterministic cell divisions take place to form the lateral root primordium (LRP) (De Smet et al., 2008; von Wangenheim et al., 2016). The tissues

surrounding the LRP need to adapt to the new growing mass of cells causing opposing mechanical forces which play a role in determining the LRP shape (Lucas et al., 2013; Vermeer et al., 2014). However, the LRP is not a homogeneous mass of cells. A careful characterization of LRP formation in Arabidopsis has led to the classification of developmental stages which associate with specific marker expression and growth domains (Malamy and Benfey, 1997). These results suggest the early formation of tissues and specific regulation of cell fate in the LRP. More recently, it has been shown that meristem maintenance regulators of the primary root are expressed in specific subsets of cells of the LRP as well as their role in LRP patterning (Goh et al., 2016; Du and Scheres, 2017). These findings indicate the existence of distinctive cell identities in the LRP and a requirement for regulation of cell fate. A detailed single-cell transcriptional map during LRP formation and GRN reconstruction would reveal the ontogeny of the LRP, the constituent cell types or tissues, and how these would be initiated to eventually form a new lateral root.

Establishment of a New Stem Cell Niche in the Lateral Root Primordium

PLETHORA (PLT) 3, PLT5, PLT7, and SCARECROW (SCR) factors are broadly expressed at the initial stages of LRP formation. Later on, PLT3, PLT5, and PLT7 activate PLT1, PLT2, and PLT4 in the central part of the LRP (Du and Scheres, 2017). SCR also shows enriched expression in the central part of the LRP after stage III/IV of development (Malamy and Benfey, 1997; Goh et al., 2016). This more restricted expression pattern of SCR, PLT1, PLT2, and PLT4 is coincident with activation of the quiescent center regulator WUSCHEL RELATED HOMEOBOX 5 (WOX5) and the establishment of an auxin maximum (Goh et al., 2016; Du and Scheres, 2017). Intriguingly, this process resembles regeneration of the primary root stem cell niche. Following quiescent center ablation, the combined action of the primary root meristem maintenance regulators (PLT1, PLT2, SCR, and SHORT-ROOT-SHR) leads to the confined expression of WOX5 and to the establishment of a new auxin maximum, which associates with stem cell niche re-specification (Xu et al., 2006). Resection of the root meristem leads to an embryo-like program of development in which expression of PLT1, PLT2, SCR, and SHR is re-organized preceding stem cell niche specification (Sena et al., 2009; Efroni et al., 2016). Given the similarities of these regenerative processes with lateral root formation, it is tempting to speculate that similar developmental mechanisms might exist. The use of scRNA-seq followed by the reconstruction of GRN might shed light into regulation of the developmental transitions leading to the establishment of a new stem cell niche during lateral root formation.

CONCLUDING REMARKS

Single-cell omics technologies have been developed over the last few years, and more recently they have been implemented for plants. Notably, these technologies have facilitated the acquisition of results with unprecedented resolution for both animals and plants. The ability of the single-cell approaches (particularly of scRNA-Seq) to profile cell states has improved our understanding of cell functionality in multicellular organisms. With the use of scRNA-seq technology, new transcriptomic states and cell-types have been identified. Most of the new transcriptomic states have been interpreted as intermediate cell identities defining cell trajectories associated with development or differentiation. Single-cell datasets have also been used to identify gene regulatory interactions and different algorithms have been developed or implemented to generate GRN from scRNA-seq data. The integration of the new scRNA-seq and GRN with previous transcriptomic and GRN data has not been systematically explored, while such an approach could facilitate the identification of unknown regulatory mechanism. In addition, the integration of single-cell omics datasets with other heterogeneous data such as imaging or genetics (as proposed in the Plant Cell Atlas Project) could help to gain new insights into plant biology and development, likely contributing to unravel fundamental questions such as cell memory, synchronization, polarization, and pluripotency.

AUTHOR CONTRIBUTIONS

MM-R, LS-R, JC, and PP-G: conceptualization. LS-R, JC, and PP-G: methodology and writing-original draft. MM-R: resources, writing-review, editing, and supervision. MM-R and PP-G: funding acquisition. All authors contributed to the article and approved the submitted version.

FUNDING

This work was funded by Ministerio de Economía y Competitividad (MINECO) and Ministerio de Ciencia e Innovación of Spain and ERDF (grants BFU2016-80315-P and PID2019-111523GB-I00 to MM-R), by Comunidad de Madrid (CM) and Universidad Politécnica de Madrid (UPM, grant APOYO_JOVENES_2Y36R7_20_TRG6W7 to PP-G), and by the "Severo Ochoa Program for Centres of Excellence in R&D" from the Agencia Estatal de Investigacion of Spain [SEV-2016-0672 (2017–2021)] to MM-R and PP-G through CBGP. LS-R was supported by FPI contract BES-2017-080155 from MINECO, PP-G by Programa Atraccion Talento from CM (2017-T2/BIO-3453), and JC by a Juan de la Cierva Contract FJCI-2016-28607 from MINECO.

REFERENCES

Aizarani, N., Saviano, A., Mailly, L., Durand, S., Herman, J. S., Pessaux, P., et al. (2019). A human liver cell atlas reveals heterogeneity and epithelial progenitors. *Nature* 572, 199–204. doi: 10.1038/s41586-019-1373-2

Alemany, A., Florescu, M., Baron, C. S., Peterson-Maduro, J., and Van Oudenaarden, A. (2018). Whole-organism clone tracing using single-cell sequencing. *Nature* 556, 108–112. doi: 10.1038/nature25969

Angermueller, C., Clark, S. J., Lee, H. J., Macaulay, I. C., Teng, M. J., Hu, T. X., et al. (2016). Parallel single-cell sequencing links transcriptional and

epigenetic heterogeneity. *Nat. Methods* 13, 229–232. doi: 10.1038/nmeth.3728

Anjam, M. S., Ludwig, Y., Hochholdinger, F., Miyaura, C., Inada, M., Siddique, S., et al. (2016). An improved procedure for isolation of high-quality RNA from nematode-infected *Arabidopsis* roots through laser capture microdissection. *Plant Methods* 12:25.

Avila Cobos, F., Alquicira-Hernandez, J., Powell, J. E., Mestdagh, P., and De Preter, K. (2020). Benchmarking of cell type deconvolution pipelines for transcriptomics data. *Nat. Commun.* 11:5650.

Bezrutczyk, M., Zöllner, N. R., Kruse, C. P. S., Hartwig, T., Lautwein, T., Köhrer, K., et al. (2021). Evidence for phloem loading via the abaxial bundle sheath cells in maize leaves. *Plant Cell* koaa055.

Birnbaum, K. (2003). A gene expression map of the *Arabidopsis* root. *Science* 302, 1956–1960. doi: 10.1126/science.1090022

Birnbaum, K., Jung, J. W., Wang, J. Y., Lambert, G. M., Hirst, J. A., Galbraith, D. W., et al. (2005). Cell type–specific expression profiling in plants via cell sorting of protoplasts from fluorescent reporter lines. *Nat. Methods* 2, 615–619. doi: 10.1038/nmeth0805-615

Blencowe, M., Arneson, D., Ding, J., Chen, Y.-W., Saleem, Z., and Yang, X. (2019). Network modeling of single-cell omics data: challenges, opportunities, and progresses. *Emerg. Top. Life Sci.* 3, 379–398. doi: 10.1042/etls20180176

Brady, S. M., Orlando, D. A., Lee, J. Y., Wang, J. Y., Koch, J., Dinneny, J. R., et al. (2007). A high-resolution root spatiotemporal map reveals dominant expression patterns. *Science* 318, 801–806. doi: 10.1126/science.1146265

Braga, F.a.V, Kar, G., Berg, M., Carpaij, O. A., Polanski, K., Simon, L. M., et al. (2019). A cellular census of human lungs identifies novel cell states in health and in asthma. *Nat. Med.* 25, 1153–1163.

Buenrostro, J. D., Wu, B., Litzenburger, U. M., Ruff, D., Gonzales, M. L., Snyder, M. P., et al. (2015). Single-cell chromatin accessibility reveals principles of regulatory variation. *Nature* 523, 486–490. doi: 10.1038/nature14590

Butler, A., Hoffman, P., Smibert, P., Papalexi, E., and Satija, R. (2018). Integrating single-cell transcriptomic data across different conditions, technologies, and species. *Nat. Biotechnol.* 36, 411–420. doi: 10.1038/nbt.4096

Capecchi, M. R. (1989). Altering the genome by homologous recombination. *Science* 244, 1288–1292. doi: 10.1126/science.2660260

Cho, H., Ryu, H., Rho, S., Hill, K., Smith, S., Audenaert, D., et al. (2013). A secreted peptide acts on BIN2-mediated phosphorylation of ARFs to potentiate auxin response during lateral root development. *Nat. Cell Biol.* 16, 66–76. doi: 10.1038/ncb2893

Clark, N. M., Buckner, E., Fisher, A. P., Nelson, E. C., Nguyen, T. T., Simmons, A. R., et al. (2019). Stem-cell-ubiquitous genes spatiotemporally coordinate division through regulation of stem-cell-specific gene networks. *Nat. Commun.* 10:5574.

Darmanis, S., Gallant, C. J., Marinescu, V. D., Niklasson, M., Segerman, A., Flamourakis, G., et al. (2016). Simultaneous multiplexed measurement of RNA and proteins in single cells. *Cell Rep.* 14, 380–389. doi: 10.1016/j.celrep.2015.12.021

de Luis Balaguer, M. A., Fisher, A. P., Clark, N. M., Fernandez-Espinosa, M. G., Möller, B. K., Weijers, D., et al. (2017). Predicting gene regulatory networks by combining spatial and temporal gene expression data in *Arabidopsis* root stem cells. *Proc. Natl. Acad. Sci. U.S.A.* 114, E7632–E7640.

de Matos Simoes, R., Dehmer, M., and Emmert-Streib, F. (2013). Interfacing cellular networks of S. cerevisiae and E. coli: connecting dynamic and genetic information. *BMC Genomics* 14:324. doi: 10.1186/1471-2164-14-324

De Rybel, B., Vassileva, V., Parizot, B., Demeulenaere, M., Grunewald, W., Audenaert, D., et al. (2010). A novel aux/IAA28 signaling cascade activates GATA23-dependent specification of lateral root founder cell identity. *Curr. Biol.* 20, 1697–1706. doi: 10.1016/j.cub.2010.09.007

De Smet, I., Lau, S., Voss, U., Vanneste, S., Benjamins, R., Rademacher, E. H., et al. (2010). Bimodular auxin response controls organogenesis in *Arabidopsis*. *Proc. Natl. Acad. Sci. U.S.A.* 107, 2705–2710. doi: 10.1073/pnas.0915001107

De Smet, I., Tetsumura, T., De Rybel, B., Dit Frey, N. F., Laplaze, L., Casimiro, I., et al. (2007). Auxin-dependent regulation of lateral root positioning in the basal meristem of *Arabidopsis*. *Development* 134, 681–690. doi: 10.1242/dev.02753

De Smet, I., Vassileva, V., De Rybel, B., Levesque, M. P., Grunewald, W., Van Damme, D., et al. (2008). Receptor-like kinase ACR4 restricts formative cell divisions in the *Arabidopsis* root. *Science* 322, 594–597. doi: 10.1126/science.1160158

Deal, R. B., and Henikoff, S. (2010). A simple method for gene expression and chromatin profiling of individual cell types within a tissue. *Dev. Cell* 18, 1030–1040. doi: 10.1016/j.devcel.2010.05.013

Denyer, T., Ma, X., Klesen, S., Scacchi, E., Nieselt, K., and Timmermans, M. C. (2019). Spatiotemporal developmental trajectories in the *Arabidopsis* root revealed using high-throughput single-cell RNA sequencing. *Dev. Cell* 48, 840–852.e845.

Dinneny, J. R., Long, T. A., Wang, J. Y., Jung, J. W., Mace, D., Pointer, S., et al. (2008). Cell identity mediates the response of *Arabidopsis* roots to abiotic stress. *Science* 320, 942–945. doi: 10.1126/science.1153795

Du, Y., and Scheres, B. (2017). PLETHORA transcription factors orchestrate de novo organ patterning during *Arabidopsis* lateral root outgrowth. *Proc. Natl. Acad. Sci. U.S.A.* 114, 11709–11714. doi: 10.1073/pnas.1714410114

Efroni, I., Ip, P.-L., Nawy, T., Mello, A., and Birnbaum, K. D. (2015). Quantification of cell identity from single-cell gene expression profiles. *Genome Biol.* 16, 1–12.

Efroni, I., Mello, A., Nawy, T., Ip, P.-L., Rahni, R., Delrose, N., et al. (2016). Root regeneration triggers an embryo-like sequence guided by hormonal interactions. *Cell* 165, 1721–1733. doi: 10.1016/j.cell.2016.04.046

Femino, A. M., Fay, F. S., Fogarty, K., and Singer, R. H. (1998). Visualization of single RNA transcripts in situ. *Science* 280, 585–590. doi: 10.1126/science.280.5363.585

Fernandez, A. I., Vangheluwe, N., Xu, K., Jourquin, J., Claus, L.a.N, Morales-Herrera, S., et al. (2020). GOLVEN peptide signalling through RGI receptors and MPK6 restricts asymmetric cell division during lateral root initiation. *Nat. Plants* 6, 533–543. doi: 10.1038/s41477-020-0645-z

Fiers, M. W. E. J., Minnoye, L., Aibar, S., Bravo González-Blas, C., Kalender Atak, Z., and Aerts, S. (2018). Mapping gene regulatory networks from single-cell omics data. *Brief. Funct. Genom.* 17, 246–254. doi: 10.1093/bfgp/elx046

Fisher, A. P., and Sozzani, R. (2016). Uncovering the networks involved in stem cell maintenance and asymmetric cell division in the *Arabidopsis* root. *Curr. Opin. Plant Biol.* 29, 38–43. doi: 10.1016/j.pbi.2015.11.002

Gaudinier, A., Rodriguez-Medina, J., Zhang, L., Olson, A., Liseron-Monfils, C., Bågman, A.-M., et al. (2018). Transcriptional regulation of nitrogen-associated metabolism and growth. *Nature* 563, 259–264. doi: 10.1038/s41586-018-0656-3

Gierahn, T. M., Wadsworth, M. H. II, Hughes, T. K., Bryson, B. D., Butler, A., Satija, R., et al. (2017). Seq-Well: portable, low-cost RNA sequencing of single cells at high throughput. *Nat. Methods* 14, 395–398. doi: 10.1038/nmeth.4179

Goh, T., Joi, S., Mimura, T., and Fukaki, H. (2012). The establishment of asymmetry in *Arabidopsis* lateral root founder cells is regulated by LBD16/ASL18 and related LBD/ASL proteins. *Development* 139, 883–893. doi: 10.1242/dev.071928

Goh, T., Toyokura, K., Wells, D. M., Swarup, K., Yamamoto, M., Mimura, T., et al. (2016). Quiescent center initiation in the*Arabidopsis*lateral root primordia is dependent on theSCARECROWtranscription factor. *Development* 143, 3363–3371. doi: 10.1242/dev.135319

Gomez, D., Shankman, L. S., Nguyen, A. T., and Owens, G. K. (2013). Detection of histone modifications at specific gene loci in single cells in histological sections. *Nat. methods* 10, 171–177. doi: 10.1038/nmeth.2332

González-García, M.-P., Pavelescu, I., Canela, A., Sevillano, X., Leehy, K. A., Nelson, A. D., et al. (2015). Single-cell telomere-length quantification couples telomere length to meristem activity and stem cell development in *Arabidopsis*. *Cell Rep.* 11, 977–989. doi: 10.1016/j.celrep.2015.04.013

Gould, P. D., Domijan, M., Greenwood, M., Tokuda, I. T., Rees, H., Kozma-Bognar, L., et al. (2018). Coordination of robust single cell rhythms in the *Arabidopsis* circadian clock via spatial waves of gene expression. *Elife* 7:e31700.

Habib, N., Li, Y., Heidenreich, M., Swiech, L., Avraham-Davidi, I., Trombetta, J. J., et al. (2016). Div-Seq: single-nucleus RNA-Seq reveals dynamics of rare adult newborn neurons. *Science* 353, 925–928. doi: 10.1126/science.aad7038

Haghverdi, L., Büttner, M., Wolf, F. A., Buettner, F., and Theis, F. J. (2016). Diffusion pseudotime robustly reconstructs lineage branching. *Nat. Methods* 13, 845. doi: 10.1038/nmeth.3971

Hahn, F., Eisenhut, M., Mantegazza, O., and Weber, A. P. (2017). Generation of targeted knockout mutants in *Arabidopsis thaliana* using CRISPR/Cas9. *Bio Protoc.* 7:e2384.

Haque, S., Ahmad, J. S., Clark, N. M., Williams, C. M., and Sozzani, R. (2019). Computational prediction of gene regulatory networks in plant growth and development. *Curr. Opin. Plant Biol.* 47, 96–105. doi: 10.1016/j.pbi.2018.10.005

Hoffman, J. A., Papas, B. N., Trotter, K. W., and Archer, T. K. (2020). Single-cell RNA sequencing reveals a heterogeneous response to Glucocorticoids in breast cancer cells. *Commun. Biol.* 3:126.

Hong, J. W., and Quake, S. R. (2003). Integrated nanoliter systems. *Nat. Biotechnol.* 21, 1179–1183. doi: 10.1038/nbt871

Hu, X., Hu, Y., Wu, F., Leung, R. W. T., and Qin, J. (2020). Integration of single-cell multi-omics for gene regulatory network inference. *Comput. Struct. Biotechnol. J.* 18, 1925–1938. doi: 10.1016/j.csbj.2020.06.033

Huynh-Thu, V. A., Isalan, M., Irrthum, A., Wehenkel, L., and Geurts, P. (2010). Inferring regulatory networks from expression data using tree-based methods. *PLoS One* 5:e12776. doi: 10.1371/journal.pone.0012776

Jaitin, D. A., Kenigsberg, E., Keren-Shaul, H., Elefant, N., Paul, F., Zaretsky, I., et al. (2014). Massively parallel single-cell RNA-seq for marker-free decomposition of tissues into cell types. *Science* 343, 776–779. doi: 10.1126/science.1247651

Jean-Baptiste, K., Mcfaline-Figueroa, J. L., Alexandre, C. M., Dorrity, M. W., Saunders, L., Bubb, K. L., et al. (2019). Dynamics of gene expression in single root cells of *Arabidopsis thaliana*. *Plant Cell* 31, 993–1011. doi: 10.1105/tpc.18.00785

Kim, J.-Y., Symeonidi, E., Pang, T. Y., Denyer, T., Weidauer, D., Bezrutczyk, M., et al. (2021). Distinct identities of leaf phloem cells revealed by single cell transcriptomics. *Plant Cell* koaa060.

Klein, A. M., Mazutis, L., Akartuna, I., Tallapragada, N., Veres, A., Li, V., et al. (2015). Droplet barcoding for single-cell transcriptomics applied to embryonic stem cells. *Cell* 161, 1187–1201. doi: 10.1016/j.cell.2015.04.044

Kubo, M., Nishiyama, T., Tamada, Y., Sano, R., Ishikawa, M., Murata, T., et al. (2019). Single-cell transcriptome analysis of Physcomitrella leaf cells during reprogramming using microcapillary manipulation. *Nucleic Acids Res.* 47, 4539–4553.

La Manno, G., Soldatov, R., Zeisel, A., Braun, E., Hochgerner, H., Petukhov, V., et al. (2018). RNA velocity of single cells. *Nature* 560, 494–498.

Lake, B. B., Chen, S., Sos, B. C., Fan, J., Kaeser, G. E., Yung, Y. C., et al. (2018). Integrative single-cell analysis of transcriptional and epigenetic states in the human adult brain. *Nat. Biotechnol.* 36, 70–80. doi: 10.1038/nbt.4038

Lavenus, J., Goh, T., Guyomarc'h, S., Hill, K., Lucas, M., Voß, U., et al. (2015). Inference of the *Arabidopsis* lateral root gene regulatory network suggests a bifurcation mechanism that defines primordia flanking and central zones. *Plant Cell* 27, 1368–1388. doi: 10.1105/tpc.114.132993

Lavenus, J., Goh, T., Roberts, I., Guyomarc'h, S., Lucas, M., De Smet, I., et al. (2013). Lateral root development in *Arabidopsis*: fifty shades of auxin. *Trends Plant Sci.* 18, 450–458. doi: 10.1016/j.tplants.2013.04.006

Lee, L. R., Wengier, D. L., and Bergmann, D. C. (2019). Cell-type–specific transcriptome and histone modification dynamics during cellular reprogramming in the *Arabidopsis* stomatal lineage. *Proc. Natl. Acad. Sci. U.S.A.* 116, 21914–21924. doi: 10.1073/pnas.1911400116

Li, S., Yamada, M., Han, X., Ohler, U., and Benfey, P. N. (2016). High-Resolution expression map of the *Arabidopsis* root reveals alternative splicing and lincRNA regulation. *Devel. Cell* 39, 508–522. doi: 10.1016/j.devcel.2016.10.012

Liu, Q., Liang, Z., Feng, D., Jiang, S., Wang, Y., Du, Z., et al. (2021). Transcriptional landscape of rice roots at the single-cell resolution. *Mol. Plant* 14, 384–394. doi: 10.1016/j.molp.2020.12.014

Long, Y., Stahl, Y., Weidtkamp-Peters, S., Postma, M., Zhou, W., Goedhart, J., et al. (2017). In vivo FRET–FLIM reveals cell-type-specific protein interactions in *Arabidopsis* roots. *Nature* 548, 97–102. doi: 10.1038/nature23317

Lucas, M., Kenobi, K., Von Wangenheim, D., Voβ, U., Swarup, K., De Smet, I., et al. (2013). Lateral root morphogenesis is dependent on the mechanical properties of the overlaying tissues. *Proc. Natl. Acad. Sci. U.S.A.* 110, 5229–5234. doi: 10.1073/pnas.1210807110

Lukowski, S. W., Lo, C. Y., Sharov, A. A., Nguyen, Q., Fang, L., Hung, S. S., et al. (2019). A single-cell transcriptome atlas of the adult human retina. *EMBO J.* 38:e100811.

Maaten, L. V. D., and Hinton, G. (2008). Visualizing data using t-SNE. *J. Mach. Learn. Res.* 9, 2579–2605.

Macaulay, I. C., Haerty, W., Kumar, P., Li, Y. I., Hu, T. X., Teng, M. J., et al. (2015). G&T-seq: parallel sequencing of single-cell genomes and transcriptomes. *Nat. Methods* 12, 519–522.

Macosko, E. Z., Basu, A., Satija, R., Nemesh, J., Shekhar, K., Goldman, M., et al. (2015). Highly parallel genome-wide expression profiling of individual cells using nanoliter droplets. *Cell* 161, 1202–1214. doi: 10.1016/j.cell.2015.05.002

Malamy, J. E., and Benfey, P. N. (1997). Organization and cell differentiation in lateral roots of *Arabidopsis thaliana*. *Development* 124, 33–44.

Marbach, D., Costello, J. C., Küffner, R., Vega, N. M., Prill, R. J., Camacho, D. M., et al. (2012). Wisdom of crowds for robust gene network inference. *Nat. Methods* 9, 796–804. doi: 10.1038/nmeth.2016

Marcino, J. (2013). A comparison of two methods for colorimetric in situ hybridization using paraffin-embedded tissue sections and digoxigenin-labeled hybridization probes. *J. Aquat. Anim. Health* 25, 119–124. doi: 10.1080/08997659.2013.781552

Marhava, P., Hoermayer, L., Yoshida, S., Marhavý, P., Benková, E., and Friml, J. (2019). Re-activation of stem cell pathways for pattern restoration in plant wound healing. *Cell* 177,957–969.e913.

McInnes, L., Healy, J., and Melville, J. (2018). Umap: uniform manifold approximation and projection for dimension reduction. *arXiv* [preprint] arXiv:1802.03426.

Mincarelli, L., Lister, A., Lipscombe, J., and Macaulay, I. C. (2018). Defining cell identity with single-cell omics. *Proteomics* 18:1700312. doi: 10.1002/pmic.201700312

Moreno-Risueno, M. A., Van Norman, J. M., Moreno, A., Zhang, J., Ahnert, S. E., and Benfey, P. N. (2010). Oscillating gene expression determines competence for periodic *Arabidopsis* root branching. *Science* 329, 1306–1311. doi: 10.1126/science.1191937

Morris, S. A. (2019). The evolving concept of cell identity in the single cell era. *Development* 146:dev169748. doi: 10.1242/dev.169748

Motte, H., Vanneste, S., and Beeckman, T. (2019). Molecular and environmental regulation of root development. *Annu. Rev. Plant Biol.* 70, 465–488. doi: 10.1146/annurev-arplant-050718-100423

Murphy, E., Vu, L. D., Van Den Broeck, L., Lin, Z., Ramakrishna, P., Van De Cotte, B., et al. (2016). RALFL34 regulates formative cell divisions in *Arabidopsis* pericycle during lateral root initiation. *J. Exp. Bot.* 67, 4863–4875. doi: 10.1093/jxb/erw281

Navin, N., Kendall, J., Troge, J., Andrews, P., Rodgers, L., Mcindoo, J., et al. (2011). Tumour evolution inferred by single-cell sequencing. *Nature* 472:90. doi: 10.1038/nature09807

Nelms, B., and Walbot, V. (2019). Defining the developmental program leading to meiosis in maize. *Science* 364, 52–56. doi: 10.1126/science.aav6428

Ni, Y., Aghamirzaie, D., Elmarakeby, H., Collakova, E., Li, S., Grene, R., et al. (2016). A machine learning approach to predict gene regulatory networks in seed development in *Arabidopsis*. *Front. Plant Sci.* 7:1936. doi: 10.3389/fpls.2016.01936

Okushima, Y., Fukaki, H., Onoda, M., Theologis, A., and Tasaka, M. (2007). ARF7 and ARF19 regulate lateral root formation via direct activation of LBD/ASL genes in *Arabidopsis*. *Plant Cell* 19, 118–130. doi: 10.1105/tpc.106.047761

Perez-Garcia, P., and Moreno-Risueno, M. A. (2018). Stem cells and plant regeneration. *Dev. Biol.* 442, 3–12.

Perianez-Rodriguez, J., Rodriguez, M., Marconi, M., Bustillo-Avendaño, E., Wachsman, G., Sanchez-Corrionero, A., et al. (2021). An auxin-regulable oscillatory circuit drives the root clock in *Arabidopsis*. *Sci. Adv.* 7:eabd4722. doi: 10.1126/sciadv.abd4722

Picelli, S., Björklund, ÅK., Faridani, O. R., Sagasser, S., Winberg, G., and Sandberg, R. (2013). Smart-seq2 for sensitive full-length transcriptome profiling in single cells. *Nat. Methods* 10, 1096–1098. doi: 10.1038/nmeth.2639

Plass, M., Solana, J., Wolf, F. A., Ayoub, S., Misios, A., Glažar, P., et al. (2018). Cell type atlas and lineage tree of a whole complex animal by single-cell transcriptomics. *Science* 360:eaaq1723. doi: 10.1126/science.aaq1723

Prakadan, S. M., Shalek, A. K., and Weitz, D. A. (2017). Scaling by shrinking: empowering single-cell'omics' with microfluidic devices. *Nat. Rev. Genet.* 18, 345–361. doi: 10.1038/nrg.2017.15

Pratapa, A., Jalihal, A. P., Law, J. N., Bharadwaj, A., and Murali, T. (2020). Benchmarking algorithms for gene regulatory network inference from single-cell transcriptomic data. *Nat. Methods* 17, 147–154. doi: 10.1038/s41592-019-0690-6

Qiu, P. (2020). Embracing the dropouts in single-cell RNA-seq analysis. *Nat. Commun.* 11:1169.

Raj, B., Wagner, D. E., Mckenna, A., Pandey, S., Klein, A. M., Shendure, J., et al. (2018). Simultaneous single-cell profiling of lineages and cell types in the vertebrate brain. *Nat. Biotechnol.* 36, 442–450. doi: 10.1038/nbt.4103

Ramakrishna, P., Ruiz Duarte, P., Rance, G. A., Schubert, M., Vordermaier, V., Vu, L. D., et al. (2019). EXPANSIN A1-mediated radial swelling of pericycle cells positions anticlinal cell divisions during lateral root initiation. *Proc. Natl. Acad. Sci. U.S.A.* 116, 8597–8602. doi: 10.1073/pnas.1820882116

Ramsköld, D., Luo, S., Wang, Y.-C., Li, R., Deng, Q., Faridani, O. R., et al. (2012). Full-length mRNA-Seq from single-cell levels of RNA and individual circulating tumor cells. *Nat. Biotechnol.* 30, 777–782. doi: 10.1038/nbt.2282

Reece-Hoyes, J. S., and Walhout, A. J. (2018). Gateway recombinational cloning. *Cold Spring Harb. Protoc.* 2018:pdb.top094912. doi: 10.1101/pdb.top094912

Regev, A., Teichmann, S. A., Lander, E. S., Amit, I., Benoist, C., Birney, E., et al. (2017). Science forum: the human cell atlas. *Elife* 6:e27041.

Reynoso, M., Pauluzzi, G., Cabanlit, S., Velasco, J., Bazin, J., Deal, R., et al. (2018). Isolation of nuclei in tagged cell types (INTACT), RNA extraction and ribosomal RNA degradation to prepare material for RNA-Seq. *Bio Protoc.* 8:e2458.

Rhee, S. Y., Birnbaum, K. D., and Ehrhardt, D. W. (2019). Towards building a plant cell atlas. *Trends Plant Sci.* 24, 303–310. doi: 10.1016/j.tplants.2019.01.006

Rich-Griffin, C., Stechemesser, A., Finch, J., Lucas, E., Ott, S., and Schäfer, P. (2020). Single-cell transcriptomics: a high-resolution avenue for plant functional genomics. *Trends Plant Sci.* 25, 186–197. doi: 10.1016/j.tplants.2019.10.008

Roberts, I., Smith, S., Stes, E., De Rybel, B., Staes, A., Van De Cotte, B., et al. (2016). CEP5 and XIP1/CEPR1 regulate lateral root initiation in *Arabidopsis*. *J. Exp. Bot.* 67, 4889–4899. doi: 10.1093/jxb/erw231

Ryu, K. H., Huang, L., Kang, H. M., and Schiefelbein, J. (2019). Single-cell RNA sequencing resolves molecular relationships among individual plant cells. *Plant Physiol.* 179, 1444–1456. doi: 10.1104/pp.18.01482

Satterlee, J. W., Strable, J., and Scanlon, M. J. (2020). Plant stem-cell organization and differentiation at single-cell resolution. *Proc. Natl. Acad. Sci. U.S.A.* 117, 33689–33699. doi: 10.1073/pnas.2018788117

Sena, G., Wang, X., Liu, H.-Y., Hofhuis, H., and Birnbaum, K. D. (2009). Organ regeneration does not require a functional stem cell niche in plants. *Nature* 457, 1150–1153. doi: 10.1038/nature07597

Setty, M., Tadmor, M. D., Reich-Zeliger, S., Angel, O., Salame, T. M., Kathail, P., et al. (2016). Wishbone identifies bifurcating developmental trajectories from single-cell data. *Nat. Biotechnol.* 34, 637–645. doi: 10.1038/nbt.3569

Shannon, P. (2003). Cytoscape: a software environment for integrated models of biomolecular interaction networks. *Genome Res.* 13, 2498–2504. doi: 10.1101/gr.1239303

Shulse, C. N., Cole, B. J., Ciobanu, D., Lin, J., Yoshinaga, Y., Gouran, M., et al. (2019). High-throughput single-cell transcriptome profiling of plant cell types. *Cell Rep.* 27, 2241–2247.e2244.

Singh, S., Yadav, S., Singh, A., Mahima, M., Singh, A., Gautam, V., et al. (2020). Auxin signaling modulates LATERAL ROOT PRIMORDIUM 1 (LRP1) expression during lateral root development in *Arabidopsis*. *Plant J.* 101, 87–100. doi: 10.1111/tpj.14520

Spanjaard, B., Hu, B., Mitic, N., Olivares-Chauvet, P., Janjuha, S., Ninov, N., et al. (2018). Simultaneous lineage tracing and cell-type identification using CRISPR–Cas9-induced genetic scars. *Nat. Biotechnol.* 36, 469–473. doi: 10.1038/nbt.4124

Stoeckius, M., Hafemeister, C., Stephenson, W., Houck-Loomis, B., Chattopadhyay, P. K., Swerdlow, H., et al. (2017). Simultaneous epitope and transcriptome measurement in single cells. *Nat. Methods* 14:865. doi: 10.1038/nmeth.4380

Stuart, T., Butler, A., Hoffman, P., Hafemeister, C., Papalexi, E., Mauck Iii, W. M., et al. (2019). Comprehensive integration of single-cell data. *Cell* 177, 1888–1902.e1821.

Stuart, T., and Satija, R. (2019). Integrative single-cell analysis. *Nat. Rev. Genet.* 20, 257–272. doi: 10.1038/s41576-019-0093-7

Sun, X., Sun, S., and Yang, S. (2019). An efficient and flexible method for deconvoluting bulk RNA-seq data with single-cell RNA-seq data. *Cells* 8:1161. doi: 10.3390/cells8101161

Taylor-Teeples, M., Lin, L., De Lucas, M., Turco, G., Toal, T. W., Gaudinier, A., et al. (2014). An *Arabidopsis* gene regulatory network for secondary cell wall synthesis. *Nature* 517, 571–575.

Thakare, D., Yang, R., Steffen, J. G., Zhan, J., Wang, D., Clark, R. M., et al. (2014). RNA-Seq analysis of laser-capture microdissected cells of the developing central starchy endosperm of maize. *Genomics Data* 2, 242–245. doi: 10.1016/j.gdata.2014.07.003

Traas, J., and Vernoux, T. (2010). Oscillating roots. *Science* 329, 1290–1291. doi: 10.1126/science.1195572

Trapnell, C., Cacchiarelli, D., Grimsby, J., Pokharel, P., Li, S., Morse, M., et al. (2014). The dynamics and regulators of cell fate decisions are revealed by pseudotemporal ordering of single cells. *Nat. Biotechnol.* 32:381. doi: 10.1038/nbt.2859

Trinh, D.-C., Lavenus, J., Goh, T., Boutté, Y., Drogue, Q., Vaissayre, V., et al. (2019). PUCHI regulates very long chain fatty acid biosynthesis during lateral root and callus formation. *Proc. Natl. Acad. Sci. U.S.A.* 116, 14325–14330. doi: 10.1073/pnas.1906300116

Truskina, J., Han, J., Chrysanthou, E., Galvan-Ampudia, C. S., Lainé, S., Brunoud, G., et al. (2020). A network of transcriptional repressors modulates auxin responses. *Nature* 589, 116–119. doi: 10.1038/s41586-020-2940-2

Van Damme, D., De Rybel, B., Gudesblat, G., Demidov, D., Grunewald, W., De Smet, I., et al. (2011). *Arabidopsis* α aurora kinases function in formative cell division plane orientation. *Plant Cell* 23, 4013–4024. doi: 10.1105/tpc.111.089565

Velasco, S., Ibrahim, M. M., Kakumanu, A., Garipler, G., Aydin, B., Al-Sayegh, M. A., et al. (2017). A multi-step transcriptional and chromatin state cascade underlies motor neuron programming from embryonic stem cells. *Cell Stem Cell* 20, 205–217.e208.

Vermeer, J. E. M., Von Wangenheim, D., Barberon, M., Lee, Y., Stelzer, E. H. K., Maizel, A., et al. (2014). A spatial accommodation by neighboring cells is required for organ initiation in *Arabidopsis*. *Science* 343, 178–183. doi: 10.1126/science.1245871

Vilches Barro, A., Stöckle, D., Thellmann, M., Ruiz-Duarte, P., Bald, L., Louveaux, M., et al. (2019). Cytoskeleton dynamics are necessary for early events of lateral root initiation in *Arabidopsis*. *Current Biology* 29, 2443–2454.e2445.

Villani, A.-C., Satija, R., Reynolds, G., Sarkizova, S., Shekhar, K., Fletcher, J., et al. (2017). Single-cell RNA-seq reveals new types of human blood dendritic cells, monocytes, and progenitors. *Science* 356:eaah4573. doi: 10.1126/science.aah4573

Villarino, G. H., Hu, Q., Manrique, S., Flores-Vergara, M., Sehra, B., Robles, L., et al. (2016). Transcriptomic signature of the SHATTERPROOF2 expression domain reveals the meristematic nature of *Arabidopsis* gynoecial medial domain. *Plant Physiol.* 171, 42–61. doi: 10.1104/pp.15.01845

Visscher, A. M., Belfield, E. J., Vlad, D., Irani, N., Moore, I., and Harberd, N. P. (2015). Overexpressing the multiple-stress responsive gene At1g74450 reduces plant height and male fertility in *Arabidopsis thaliana*. *PLoS One* 10:e0140368. doi: 10.1371/journal.pone.0140368

Vitak, S. A., Torkenczy, K. A., Rosenkrantz, J. L., Fields, A. J., Christiansen, L., Wong, M. H., et al. (2017). Sequencing thousands of single-cell genomes with combinatorial indexing. *Nat. Methods* 14, 302–308. doi: 10.1038/nmeth.4154

von Wangenheim, D., Fangerau, J., Schmitz, A., Smith, R. S., Leitte, H., Stelzer, E. H., et al. (2016). Rules and self-organizing properties of post-embryonic plant organ cell division patterns. *Curr. Biol.* 26, 439–449. doi: 10.1016/j.cub.2015.12.047

Voß, U., Wilson, M. H., Kenobi, K., Gould, P. D., Robertson, F. C., Peer, W. A., et al. (2015). The circadian clock rephases during lateral root organ initiation in *Arabidopsis thaliana*. *Nat. Commun.* 6:7641.

Wachsman, G., Zhang, J., Moreno-Risueno, M. A., Anderson, C. T., and Benfey, P. N. (2020). Cell wall remodeling and vesicle trafficking mediate the root clock in *Arabidopsis*. *Science* 370, 819–823. doi: 10.1126/science.abb7250

Wang, T., Li, B., Nelson, C. E., and Nabavi, S. (2019). Comparative analysis of differential gene expression analysis tools for single-cell RNA sequencing data. *BMC Bioinformatics* 20:40. doi: 10.1186/s12859-019-2599-6

Wu, H., Kirita, Y., Donnelly, E. L., and Humphreys, B. D. (2019). Advantages of single-nucleus over single-cell RNA sequencing of adult kidney: rare cell types and novel cell states revealed in fibrosis. *J. Am. Soc. Nephrol.* 30, 23–32. doi: 10.1681/asn.2018090912

Xu, J., Hofhuis, H., Heidstra, R., Sauer, M., Friml, J., and Scheres, B. (2006). A molecular framework for plant regeneration. *Science* 311, 385–388. doi: 10.1126/science.1121790

Xu, X., Crow, M., Rice, B. R., Li, F., Harris, B., Liu, L., et al. (2021). Single-cell RNA sequencing of developing maize ears facilitates functional analysis and trait candidate gene discovery. *Dev. Cell* 56, 557–568.e556.

Xuan, W., Audenaert, D., Parizot, B., Möller, B. K., Njo, M. F., De Rybel, B., et al. (2015). Root cap-derived auxin pre-patterns the longitudinal axis of the *Arabidopsis* root. *Curr. Biol.* 25, 1381–1388. doi: 10.1016/j.cub.2015.03.046

Xuan, W., Band, L. R., Kumpf, R. P., Van Damme, D., Parizot, B., De Rop, G., et al. (2016). Cyclic programmed cell death stimulates hormone signaling and root development in *Arabidopsis*. *Science* 351, 384–387. doi: 10.1126/science.aad2776

Zeb, Q., Wang, C., Shafiq, S., and Liu, L. (2019). "An overview of single-cell isolation techniques," in *Single-Cell Omics*, eds D. Barh and V. Azevedo (Amsterdam: Elsevier), 101–135. doi: 10.1016/b978-0-12-814919-5.00006-3

Zhang, T.-Q., Xu, Z.-G., Shang, G.-D., and Wang, J.-W. (2019). A single-cell RNA sequencing profiles the developmental landscape of *Arabidopsis* root. *Mol. Plant* 12, 648–660. doi: 10.1016/j.molp.2019.04.004

Ziegenhain, C., Vieth, B., Parekh, S., Reinius, B., Guillaumet-Adkins, A., Smets, M., et al. (2017). Comparative analysis of single-cell RNA sequencing methods. *Mol. Cell* 65, 631–643.e634.

Conflict of Interest: The authors declare that the research was conducted in the absence of any commercial or financial relationships that could be construed as a potential conflict of interest.

frontiers in Plant Science

ORIGINAL RESEARCH
published: 14 May 2021
doi: 10.3389/fpls.2021.646736

PIP2, An Auxin Induced Plant Peptide Hormone Regulates Root and Hypocotyl Elongation in *Arabidopsis*

Saddam Hussain[1,2†], Wei Wang[2†], Sajjad Ahmed[2], Xutong Wang[2], Adnan[2], Yuxin Cheng[2], Chen Wang[2], Yating Wang[2], Na Zhang[2], Hainan Tian[2], Siyu Chen[2], Xiaojun Hu[1], Tianya Wang[2] and Shucai Wang[1,2]*

[1]Laboratory of Plant Molecular Genetics & Crop Gene Editing, School of Life Sciences, Linyi University, Linyi, China, [2]Key Laboratory of Molecular Epigenetics of MOE, Northeast Normal University, Changchun, China

OPEN ACCESS

Edited by:
Ling Huang,
Salk Institute for Biological Studies,
United States

Reviewed by:
Dior Rose Kelley,
Iowa State University, United States
Wei Zhang,
Shandong University, China

***Correspondence:**
Shucai Wang
wangshucai@yahoo.com

[†]These authors have contributed equally to this work

Specialty section:
This article was submitted to Plant Development and EvoDevo, a section of the journal Frontiers in Plant Science

Received: 28 December 2020
Accepted: 29 March 2021
Published: 14 May 2021

Citation:
Hussain S, Wang W, Ahmed S, Wang X, Adnan, Cheng Y, Wang C, Wang Y, Zhang N, Tian H, Chen S, Hu X, Wang T and Wang S (2021) PIP2, An Auxin Induced Plant Peptide Hormone Regulates Root and Hypocotyl Elongation in Arabidopsis. Front. Plant Sci. 12:646736. doi: 10.3389/fpls.2021.646736

Auxin is one of the traditional plant hormones, whereas peptide hormones are peptides with hormone activities. Both auxin and plant peptide hormones regulate multiple aspects of plant growth and development, and there are cross-talks between auxin and plant peptide hormones. PAMP-INDUCED SECRETED PEPTIDES (PIPs) and PIP-LIKEs (PIPLs) are a new family of plant peptide hormone, and PIPL3/TARGET OF LBD SIXTEEN 2 (TOLS2) has been shown to regulate lateral root formation in *Arabidopsis*. We report here the identification of *PIP2* as an auxin response gene, and we found it plays a role in regulating root and hypocotyl development in *Arabidopsis*. By using quantitative RT-PCR, we found that the expression of *PIP2* but not *PIP1* and *PIP3* was induced by auxin, and auxin induced expression of *PIP2* was reduced in *nph4-1* and *arf19-4*, the lost-of-function mutants of *Auxin Response Factor 7* (*ARF7*) and *ARF19*, respectively. By generating and characterizing overexpressing transgenic lines and gene edited mutants for *PIP2*, we found that root length in the *PIP2* overexpression plant seedlings was slightly shorter when compared with that in the Col wild type plants, but root length of the *pip2* mutant seedlings remained largely unchanged. For comparison, we also generated overexpressing transgenic lines and gene edited mutants for *PIP3*, as well as *pip2 pip3* double mutants. Surprisingly, we found that root length in the *PIP3* overexpression plant seedlings is shorter than that of the *PIP2* overexpression plant seedlings, and the *pip3* mutant seedlings also produced short roots. However, root length in the *pip2 pip3* double mutant seedlings is largely similar to that in the *pip3* single mutant seedlings. On the other hand, hypocotyl elongation assays indicate that only the *35S:PIP2* transgenic plant seedlings produced longer hypocotyls when compared with the Col wild type seedlings. Further analysis indicates that PIP2 promotes cell division as well as cell elongation in hypocotyls. Taken together, our results suggest that *PIP2* is an auxin response gene, and PIP2 plays a role in regulating root and hypocotyl elongation in *Arabidopsis* likely *via* regulating cell division and cell elongation.

Keywords: auxin, peptide hormone, PIP2, PIP3, root elongation, *Arabidopsis*

INTRODUCTION

The plant hormone auxin regulates multiple aspects of plant growth and development largely by activating the expression of auxin response genes (Davies, 1995; Chapman and Estelle, 2009). The activation of auxin response genes is mainly regulated by the TRANSPORT INHIBITOR RESPONSE 1 (TIR1) auxin receptor (Dharmasiri et al., 2005; Kepinski and Leyser, 2005), and two different families of transcription factors, i.e., the AUXIN RESPONSE FACTOR (ARF) family and the AUXIN (Aux)/INDOLE-3-ACETIC ACID (IAA) protein family (Guilfoyle et al., 1998; Reed, 2001; Guilfoyle and Hagen, 2007). Five of the ARFs, including ARF5, ARF6, ARF7, ARF8, and ARF19 function as transcription activators and are able to activate the expression of auxin response genes (Tiwari et al., 2003; Wang et al., 2005). However, when the level of cellular auxin is low, Aux/IAA proteins, the transcription repressors in auxin signaling (Tiwari et al., 2004), can form dimmers with ARF activators and inhibit their activities (Tiwari et al., 2003). When the level of cellular auxin is elevated, auxin are able to bind and activate the TIR1 auxin receptor, leading to degradation of Aux/IAA proteins *via* 26S proteasome, therefore release the inhibition of Aux/IAA proteins on ARF activators, resulting in activation of auxin response genes (Guilfoyle and Hagen, 2007; Tan et al., 2007; Hayashi, 2012).

So far several different gene families such as *Aux/IAAs*, *GRETCHEN HAGENs* (*GH3s*), and *SMALL AUXIN-UP RNAs* (*SAURs*; Hagen and Guilfoyle, 2002), and some other genes such as *ASYMMETRIC LEAVES2-LIKE/LATERAL ORGAN BOUNDARIES DOMAIN* (*ASL/LBD*), *PACLOBUTRAZOL RESISTANCE 6* (*PRE6*) and *LATERAL ROOT PRIMORDIUM1* (*LRP1*; Lee et al., 2009; Coudert et al., 2013; Zheng et al., 2017; Singh et al., 2020), have been identified as auxin response genes. However, considering that auxin is involved in the regulation of almost all the aspects of plant growth and development, large numbers of auxin response genes should still remain unidentified (Kieffer et al., 2010). On the other hand, exploration of the functions of the auxin response genes is still on going, as an example, the *SAURs* were identified as an auxin response gene family about 25 years ago (Gil et al., 1994), yet it is only in recent years that SAURs have been identified to regulate several different aspects of plant growth and development, such as cell expansion (Spartz et al., 2012; Kong et al., 2013; Qiu, et al., 2020), pollen tube growth (He et al., 2018), apical hook development (Kathare et al., 2018), hypocotyl and stamen filament elongation (Chae et al., 2012), and leaf senescence (Hou et al., 2013; Wen et al., 2020).

Peptide hormones are peptides with hormone activities in animal, bacteria and yeast (Edlund and Jessell, 1999). The first plant peptide hormone, systemin, was identified about 30 years ago (Pearce et al., 1991), and more than 20 different types of plant peptide hormones have been identified since then (Hirakawa et al., 2017; Hirakawa and Sawa, 2019). Plant peptide hormones are also involved in the regulation of different aspects of plant growth and development. As examples, CLAVATA3/ENDOSPERM SURROUNDING REGIONs (CLEs) regulate the maintains of shoot and root apical meristem (Kinoshita et al., 2007; Jun et al., 2010; Katsir et al., 2011; Guo et al., 2015), POLARIS (PLS), AUXIN-RESPONSICE ENDOFENOUS POLYPEPTIDE 1(AREP1) and GROWTH FACTOR/CLE LIKE/GOLVEN (RGF/CLEL/GLV) regulate root growth (Casson et al., 2002; Matsuzaki et al., 2010; Meng et al., 2012a; Fernandez et al., 2013; Yang et al., 2014), RGF/CLEL/GLV regulates lateral root formation (Matsuzaki et al., 2010; Meng et al., 2012a; Fernandez et al., 2013), PLS regulates vascular development (Casson et al., 2002), EPIDERMAL PATTERNING FACTORs (EPFs) regulate stomata development (Hara et al., 2007; Hunt and Gray, 2009; Sugano et al., 2010), DEVIL (DVL1) and ROTUNDIFOLIA4 (ROT4) regulate leaf and fruit development (Narita et al., 2004; Wen et al., 2004), and INFLORESCENCE DEFICIENT IN ABSCISSION LIKEs (IDLs) regulate floral organ abscission (Butenko et al., 2003; Cho et al., 2008; Stenvik et al., 2008).

At least some of the aspects of plant growth and development are regulate by both auxin response genes and plant peptide hormones. For example, both the plant peptide hormones PLS, AREP1 and RGF/CLEL/GLV and some Aux/IAA proteins such as IAA9 are able to regulate root growth (Casson et al., 2002; Matsuzaki et al., 2010; Meng et al., 2012a; Fernandez et al., 2013; Yang et al., 2014), and auxin is involved in CLE regulated vascular proliferation (Whitford et al., 2008). Some other experiments have also indicated that there are cross-talk between auxin and some of plant peptide hormones. For example, the expression of *PLS*, *AREP1* and *RGF/CLEL/GLV* genes are induced by auxin, whereas PLS and RGF/CLEL/GLV peptides are able to regulate auxin transport (Casson et al., 2002; Chilley et al., 2006; Meng et al., 2012b; Whitford et al., 2012; Yang et al., 2014).

PAMP-INDUCED SECRETED PEPTIDES (PIPs) and PIP-LIKEs (PIPLs) are a new family of plant peptide hormone identified in *Arabidopsis* in recent years (Hou et al., 2014; Vie et al., 2015). Both PIP and PIPL propeptides have an N-terminal signal peptide and a C-terminal SGPS motif, which is part of the biologically active peptides, with an exception of PIP2 and PIP3 prepropeptides, which have two SGPS motifs (Hou et al., 2014; Vie et al., 2015). The PIP peptides including PIP1, PIP2 and PIP3 have been shown to modulate immunity (Hou et al., 2014; Najafi et al., 2020), and the expression of several *PIPs* and *PIPLs* family genes is induced by biotic and/or abiotic stresses (Hou et al., 2014; Vie et al., 2015). On the other hand, it has been reported that the PIPL3/TARGET OF LBD SIXTEEN 2(TOLS2) is able to regulate lateral root formation (Toyokura, et al., 2019). Here, we report the identification of *PIP2* as an auxin response gene, and we found that PIP2 is involved in the regulation of root and hypocotyl development in *Arabidopsis*.

MATERIALS AND METHODS

Plant Materials and Growth Conditions

The Columbia-0 (Col) ecotype *Arabidopsis* (*Arabidopsis thaliana*) was used as wild type for plant transformation and auxin response analysis of the *PIP* genes, and as a control for root length, hypocotyl length, cell number and cell length analysis. The *nph4-1* and *arf19-4* mutants are in the Col wild type

background (Harper et al., 2000; Wang et al., 2005). The *35S:PIP2* and *35S:PIP3* overexpress plants were generated by transforming Col wild type plants, and the *pip2* and *pip3* single and the *pip2 pip3* double mutants were obtained by editing *PIP2* and *PIP3* genes in the Col wild type plants *via* CRISPR/Cas9 gene editing techniques.

For plant transformation, the Col wild type seeds were sown directly into the soil pots and grown in a growth chamber. To obtain seedlings for auxin treatment and phenotypic analysis, seeds of the Col wild type, the *nph4-1*, *arf19-4*, *pip2*, *pip3*, and *pip2 pip3* mutants, and the *35S:PIP2* and *35S:PIP3* overexpress plants were surface sterilized with 25% (v/v) bleach for 10 min, washed with sterile deionized water for four times, and then sown on 1/2 Murashige and Skoog (MS) petri plates, containing vitamins (Plant Media), 1% (w/v) sucrose, pH 5.8, and solidified with 0.6% (w/v) phytoagar (Plant Media). The plates were then kept in 4°C for 2 days, and then moved to a growth chamber.

The growth condition in the growth chamber was set as 23°C temperature, 60% relative humidity conditions, and photon density set at ~120 μmol m^{-2} s^{-1} under a 16 h light/8 h dark photoperiod unless indicated otherwise.

Auxin Treatment, RNA Isolation, and Quantitative RT-PCR

To examine the expression of *PIP2* and *PIP3* in response to auxin, 10-day-old Col wild type seedlings were transferred to petri plates containing 10 μM IAA and shaked on a shaker in dark for 4 h. To examine auxin regulated epression of *PIP2* and *IAA19* in *nph4-1* and *arf19-4* mutants, 10-day-old Col wild type, and *nph4-1* and *arf19-4* mutant seedlings were treated with 10 μM IAA for 4 h. Seedlings were collected, total RNA was isolated, cDNA was synthesized as described previously (Wang et al., 2015a), and used to detect the expression of *PIP2*, *PIP3* and *IAA19* with a process described previously (Wang et al., 2015b), and the expression of *ACTIN2* (*ACT2*) gene was used as an internal control. The primers used for quantitative RT-PCR (qRT-PCR) analysis of *IAA19* and *ACT2* have been described previously (Liu et al., 2015; Wang et al., 2015a,b), and analyzed by using delta delta method (ΔΔCt). The primers used for qRT-PCR analysis of *PIP2* and *PIP3* were 5'-GGAGAAGTTCGTGGCTAGTTTAT-3' and 5'-CTTCC TGTCCACGACCTTATG-3', 5'-AGAGAACCTCGTGGCTAAG T-3' and 5'-GGGACCTGAATGCTTACCATATT-3' respectively.

Constructs

To generate *pPZP-35S:PIP2* and *pPZP-35S:PIP3* constructs for plant transformation, the full length open-reading frame (ORF) sequences of *PIP2* and *PIP3* were amplified and inserted, respectively into the *pUC19* vector with an N-terminal HA tag using NdeI and SacI restriction sites (Tiwari et al., 2004; Tian et al., 2015). The *35S:PIP2* and *35S:PIP3* fragments in the *pUC19-35S:PIP2* and *pUC19-35S:PIP3* constructs were then digested with Pst1 and Sac1 enzymes and sub-cloned into the binary vector *pPZP211* (Hajdukiewicz et al., 1994). The primers used to amplify *PIP2* were 5'-CAACATATGATGATGAACAAA AACGTTCTG-3' and 5'-CAAGAGCTCTTAGTGGCCCGGTCC G-3', to amplify *PIP3* were, 5'-CAACATATGATGATGAACA AAGTTGTTTTGG-3', and, 5'-CAAGAGCTCTTAGTGACCG GGTCCACTC-3'.

To generate CRISPR/Cas9 constructs for gene editing of *PIP2* and *PIP3*, exon sequences of *PIP2* and *PIP3* were evaluated on CRISPRscan[1] for potential target sequences. Target specificity was then assessed on Cas-OFFinder.[2] The cas9 targeted sequences selected for *PIP2* were 5'-GTTCTTCATGTTGATTGGTT (CGG)-3' and 5'-GCTTGGTCTAACAAAGACCG(AGG)-3', for *PIP3* were 5'-GTGGTGGAGGCTCGTCCTTT(GGG)-3' and 5'-GAAGGCTGAAGAGAACCTCG(TGG)-3'. The target sequences were inserted into the *pHEE-FT* vector (Cheng et al., 2019). The primer used to generate CRISPR/Cas9 constructs for editing *PIP2* were DT1-BsF (*PIP2*), 5'-ATATATGGTCTCGATTGTT CTTCATGTTGATTGGTTGTT-3', DT1-F0 (*PIP2*), 5'- TGTTC TTCATGTTGATTGGTTGTTTTAGAGCTAGAAATAGC-3', DT 2-R0 (*PIP2*), 5'-AACCGGTCTTTGTTAGACCAAGCAATCTCT TAGTCGACTCTAC-3, DT2-BsR (*PIP2*), 5'- ATTATTGGTCT CGAAACCGGTCTTTGTTAGACCAAGCAA-3'; for editing *PIP3* were DT1-BsF (*PIP3*), 5'-ATATATGGTCTCGATTGTGG TGGAGGCTCGTCCTTTGTT-3',

DT1-F0 (*PIP3*), 5'-TGTGGTGGAGGCTCGTCCTTTGTTT TAGAGCTAGAAATAGC-3',

DT2-R0 (*PIP3*), 5'-AACCGAGGTTCTCTTCAGCCTTCAA TCTCTTAGTCGACTCTAC-3', DT2-BsR (*PIP3*), 5'-ATTATTG GTCTCGAAACCGAGGTTCTCTTCAGCCTTCAA-3'; for editing both *PIP2* and *PIP3* were DT1-BsF (*PIP2&PIP3*), 5'-ATATAT GGTCTCGATTGTGGTGGAGGCTCGTCCTTTGTT-3',

DT1-F0 (*PIP2&PIP3*), 5'-TGTGGTGGAGGCTCGTCCTTT GTTTTAGAGCTAGAAATAGC-3', DT2-R0 (*PIP2&PIP3*), 5' AACAACCAATCAACATGAAGAACAATCTCTTAGTCGACT CTAC-3',

DT2-BsR (*PIP2&PIP3*), 5'-ATTATTGGTCTCGAAACAACC AATCAACATGAAGAACAA -3'. *U6-26-IDF* and *U6-29-IDR* primers used for colony PCR and sequencing of the CRISPR/ Cas9 constructs have been described previously (Chen et al., 2019a).

Plants Transformation, Transgenic Plants Selection, and Cas9-Free Mutant Isolation

To generate overexpress plants and *Cas9* free mutants, about 1-month-old Col wild type plants with several mature flowers were transformed with *pPZP211-35S:PIP2, pPZP211-35S:PIP3*, and the CRISPR/Cas9 constructs respectively, *via Agrobacterium tumefaciens* (GV3101) mediated floral dip method (Clough and Bent, 1998).

The *35S:PIP2* and *35S:PIP3* overexpression plants were selected as described previously (Wang et al., 2020). Multiple homozygous lines were obtained and two lines with high expression levels of *PIP2* and *PIP3*, respectively were used for the experiments.

Gene edited mutants were selected by germinating the T1 seeds on 1/2 MS plates containing 50 μg/ml Kanamycin and 100 μg/ml Carbenicillin, examining gene editing status in the

[1]http://www.crisprscan.org/?page=sequence
[2]http://www.rgenome.net/cas-offinder/

early flowering plants by amplifying and sequencing the genomic sequence *PIP2* and *PIP3*, respectively, and then selecting homozygous mutants from normal flowering T2 plants. The absent of T-DNA insertion in the homozygous mutants were confirmed by PCR amplification of *Cas9* gene fragment as described previously (Cheng et al., 2019).

DNA Isolation and PCR

To check the editing status of *PIP2* and *PIP3*, DNA was isolated from the leaves of T1 or T2 transgenic plants. The extracted DNA was used as a template for PCR amplification using genomic primers specific to *PIP2* and *PIP3*, respectively. To obtain Cas9 free mutant plants, DNA was isolated from the leaves of T2 progeny of the edited T1 plants, and used as template for PCR amplification using *Cas9* specific primer. The primers used for PCR amplification of *Cas9* gene have been described previously (Chen et al., 2019a).

Primary Root Length Assays

Primary root length of the Col wild type, the *35S:PIP2* and *35S:PIP3* transgenic plant seedlings, and the *pip2*, *pip3*, *pip2 pip3* mutant seedlings were assayed as described previously (Wang et al., 2019). For each line, 21–25 seedlings were used for the experiments.

Hypocotyl Length Assays

Seeds of the Col wild type, the *35S:PIP2* and *35S:PIP3* transgenic plants, and the *pip2*, *pip3*, and *pip2 pip3* mutants were sterilized and sown on 1/2 MS plates, kept at 4°C in the dark for 2 days, and then moved to a growth room with dim light (~60 μmol m^{-2} s^{-1}). Four-day-old seedlings were used for hypocotyl length assays as reported previously (Wang et al., 2007; Gao et al., 2008). Pictures were taken by using a Nikon digital camera, and the hypocotyl length was calculated by using Image J software. For each line, 29–42 seedlings were used for the experiments.

Hypocotyl Cell Number and Cell Length Assays

Hypocotyl cell number and cell length were measured as described previously with some modifications (Scheres et al., 1994; Wang et al., 2007; Gao et al., 2008; Qu et al., 2017). In brief, 4-day-old dim light-grown seedlings of the Col wild type, the *35S:PIP2* and *35S:PIP3* transgenic plants, and the *pip2*, *pip3*, and *pip2 pip3* mutants were mounted in a film of water on a glass slide and covered with a cover slip to prevent dehydration. Cell number was counted under an OLYMPUS BX53 microscope, at the distance between the top of the root hairs around the collet, and the base of the "V" made by the petioles of the cotyledon (Scheres et al., 1994). The second row cells from the top to the base of the hypocotyls epidermis in longitudinal direction were used for cell length measurement (Qu et al., 2017). Pictures were taken under an OLYMPUS BX53 microscope, and cell length was measured by using Image J. For each line, 22–29 seedlings were used for the experiments.

RESULTS

PIP2 Is an Auxin Response Genes

It has been previously reported that the expression of some plant peptide hormone genes including *PLS* and *RGF*/*CLEL*/*CLV* was regulated by auxin (Casson et al., 2002; Chilley et al., 2006; Meng et al., 2012b; Whitford et al., 2012; Guo et al., 2015). The *PIPLs* peptide hormone gene *PIPL3* has recently been shown to regulate lateral root initiation in *Arabidopsis*, a process controlled by auxin (Toyokura et al., 2019), inducing a cross talk between PIP peptide hormone and auxin.

To examine if PIP peptide hormones may be involved in the regulation of auxin regulated plant growth and development. We first examined the expression of *PIP* genes including *PIP1*, *PIP2*, and *PIP3* in response to auxin. Seedlings of the Col wild type *Arabidopsis* were treated with IAA for 4 h and qRT-PCR was used to examine the expression of the *PIP* genes. As shown in **Figure 1A**, the expression level of *PIP2* increased about 10 folds in response to auxin treatment, whereas the expression level of *PIP1* and *PIP3* remained largely unchanged, suggest that *PIP2* is an auxin response gene, but *PIP1* and *PIP3* are not.

It has been shown that five of the ARFs, including ARF5, ARF6, ARF7, ARF8, and ARF19 are activators that positively regulating the expression of some auxin response genes (Tiwari et al., 2003; Wang et al., 2005), to examine if they may involve in the regulation of *PIP2*, we examine auxin response of *PIP2* in *nph4-1/arf7* and *arf19-4*, two ARF activator gene mutants in hand by using qRT-PCR. We found that the auxin response of *PIP2* was decreased in both *nph4-1* and *arf19-4* mutants (**Figure 1B**), suggest that ARF7 and ARF19 may regulate the expression of *PIP2*. To our surprise, we found that the basal expression level of *PIP2*, i.e., in the absence of auxin was increased about 4-fold in the *nph4-1* mutant (**Figure 1B**). As a control, auxin response of *IAA19* was reduced in the *nhp4-1* and *arf19* mutants, but their basal expression levels remained largely unchanged in both mutants (**Figure 1C**), a result similar as reported previously (Wang et al., 2005).

Generation of *PIP2* Gene Mutants by CRISPR-Cas9 Gene Editing

To examine the functions of PIP2, we generated plants overexpressing *PIP2*, and gene edited mutants of *PIP2* gene *via* CRISPR/Cas9 mediated gene editing. Overexpression plants were generated by transforming Col wild type *Arabidopsis* with *pPZP211-35S:PIP2* construct, selecting homozygous plants in T3 generation, and examining the expression level of *PIP2* in the homozygous transgenic plants (**Figure 2A**). We also generated *PIP3* overexpression plants (**Figure 2B**), in order to compare the functions of auxin responsive and non-responsive *PIP* genes. Two independent lines with similar expression levels of *PIP* genes were selected for further experiments.

Gene edited mutants of *PIP2* gene was generated by transforming Col wild type *Arabidopsis* with *PIP2* targeting CRISPR/Cas9 construct generated by using a *pHEE-FT* vector (Cheng et al., 2019), checking gene editing status in early

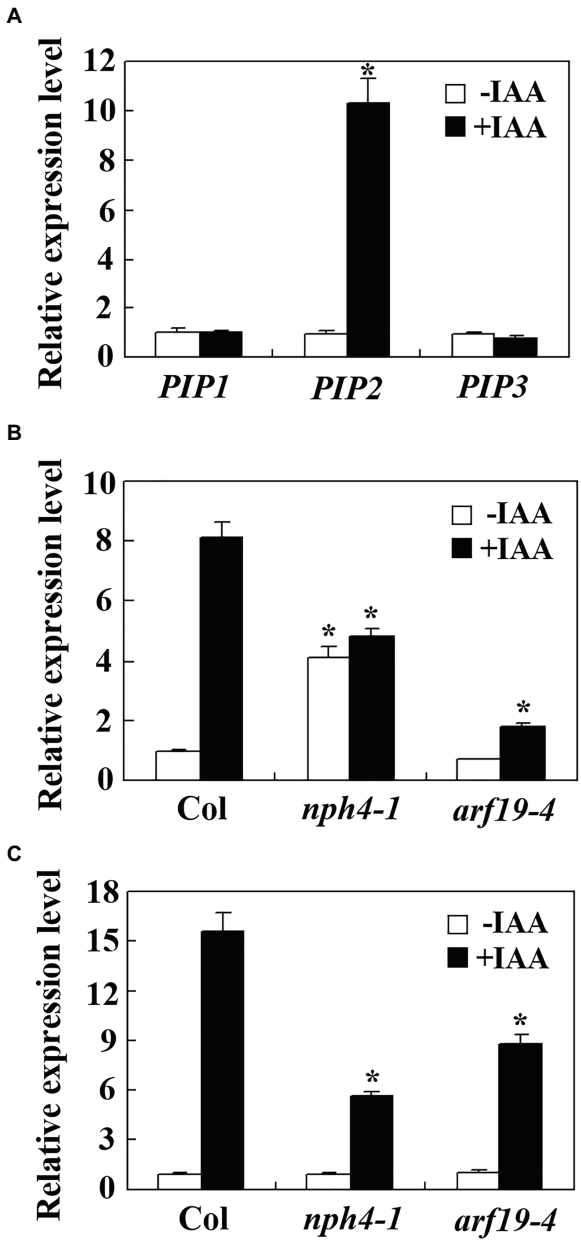

FIGURE 1 | *PIP2* is an auxin response gene. **(A)** Expression of PAMP-INDUCED SECRETED PEPTIDES (*PIPs*) in response to auxin treatment. Ten-days-old Col wild type seedlings were treated with 10 μM INDOLE-3-ACETIC ACID (IAA) for 4 h, total RNA was isolated and quantitative RT-PCR (qRT-PCR) was used to examine the expression of *PIPs*. Expression of *ACTIN2* (*ACT2*) was used as an inner control, and the expression level of corresponding *PIP* genes in the control seedlings was set as 1. Data represent mean ± SD of three repeats. *significantly different from absent of IAA (student's *t* test, $p < 0.001$). Expression of *PIP2* **(B)** and *IAA19* **(C)** in the *nph4-1* and *arf19-4* mutants in response to auxin treatment. Ten-day-old Col wild type, *nph4-1* and *arf19-4* mutant seedlings were treated with 10 μM IAA for 4 h. Total RNA was isolated and qRT-PCR was used to examine the expression of *PIP2* or *IAA19*. Expression of *ACT2* was used as an inner control, and the expression level of *PIP2* or *IAA19* in control seedlings of the Col wild type was set as 1. Data represent mean ± SD of three repeats. *significantly different from the corresponding expression level in the Col wild type seedlings (student's *t*-test, $p < 0.001$). The experiments were repeated three times with similar results.

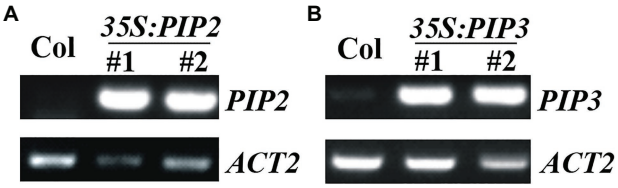

FIGURE 2 | Expression of *PIP2* and *PIP3* in the *35S:PIP2* and *35S:PIP3* transgenic plants. **(A)** Expression of *PIP2* in the *35S:PIP2* transgenic plants. **(B)** Expression of *PIP3* in the *35S:PIP3* transgenic plants. Total RNA was isolated from 10-day-old homozygous transgenic plants and RT-PCR was used to examine the expression of *PIP2* or *PIP3*. Expression of *ACT2* was used as a control.

flowering T1 plants, selecting Cas9-free homozygous mutants in normal flowering T2 generations. For comparison, we generated gene edited mutant for *PIP3* gene by transforming Col wild type *Arabidopsis* with *PIP3* targeting CRISPR/Cas9 construct, as well as mutants with both *PIP2* and *PIP3* genes were edited by transforming Col wild type *Arabidopsis* with CRISPR/Cas9 construct targeting both *PIP2* and *PIP3*.

Two independent single mutants for *PIP2* and *PIP3* genes respectively, i.e., *pip2-c1*, *pip2-c2*, *pip3-c1*, and *pip3-c2*, and two independent double mutants, i.e., *pip2 pip3-c1*, *pip2 pip3-c2* were obtained and used for the experiments. In the *pip2* mutants, either a single nucleotide insertion or a small fragment deletion was occurred (**Figure 3A**). For both the *pip3* mutants, a small fragment deletion was occurred (**Figure 3B**). Whereas in the *pip2 pip3* double mutants, a single nucleotide insertion was occurred for *PIP2* (**Figure 3A**), and either a single nucleotide insertion or a small fragment deletion was occurred for *PIP3* (**Figure 3B**). All the nucleotide insertion or small fragment deletion led to amino substitution and premature stop of the ORF, as a result, the predicated amino acid sequences for *PIP2* and *PIP3* genes in the single and double mutants leak the amino acids of the mature PIP2 and PIP3 peptides (**Figure 4**).

PIP2 and PIP3 Affect Root Elongation in *Arabidopsis* Seedlings

As regulating root elongation is one of the characterized functions of auxin (Rehman et al., 2007), we examine the possible roles of PIP2 in root elongation by using the overexpression plants and gene edited mutants generated. Sterilized seeds of the Col wild type, the *35S:PIP2* transgenic plants and the *pip2* mutants were plated on 1/2 MS plates, and grown vertically for root elongation observation. As shown in **Figure 5A**, the *35S:PIP2* transgenic plant seedlings produced short roots when compared with the Col wild type seedlings, whereas that in the *pip2* mutant seedlings remained largely unchanged. Quantitative analysis showed that the root length of the *35S:PIP2* transgenic plant seedlings were about 90% of the Col wild type (**Figure 5B**). On the other hand, the transgenic plant seedlings expressing *PIP3*, the non-auxin responsive *PIP* gene, produced much shorter roots when compared with that in the Col wild type seedlings, and the root length in the

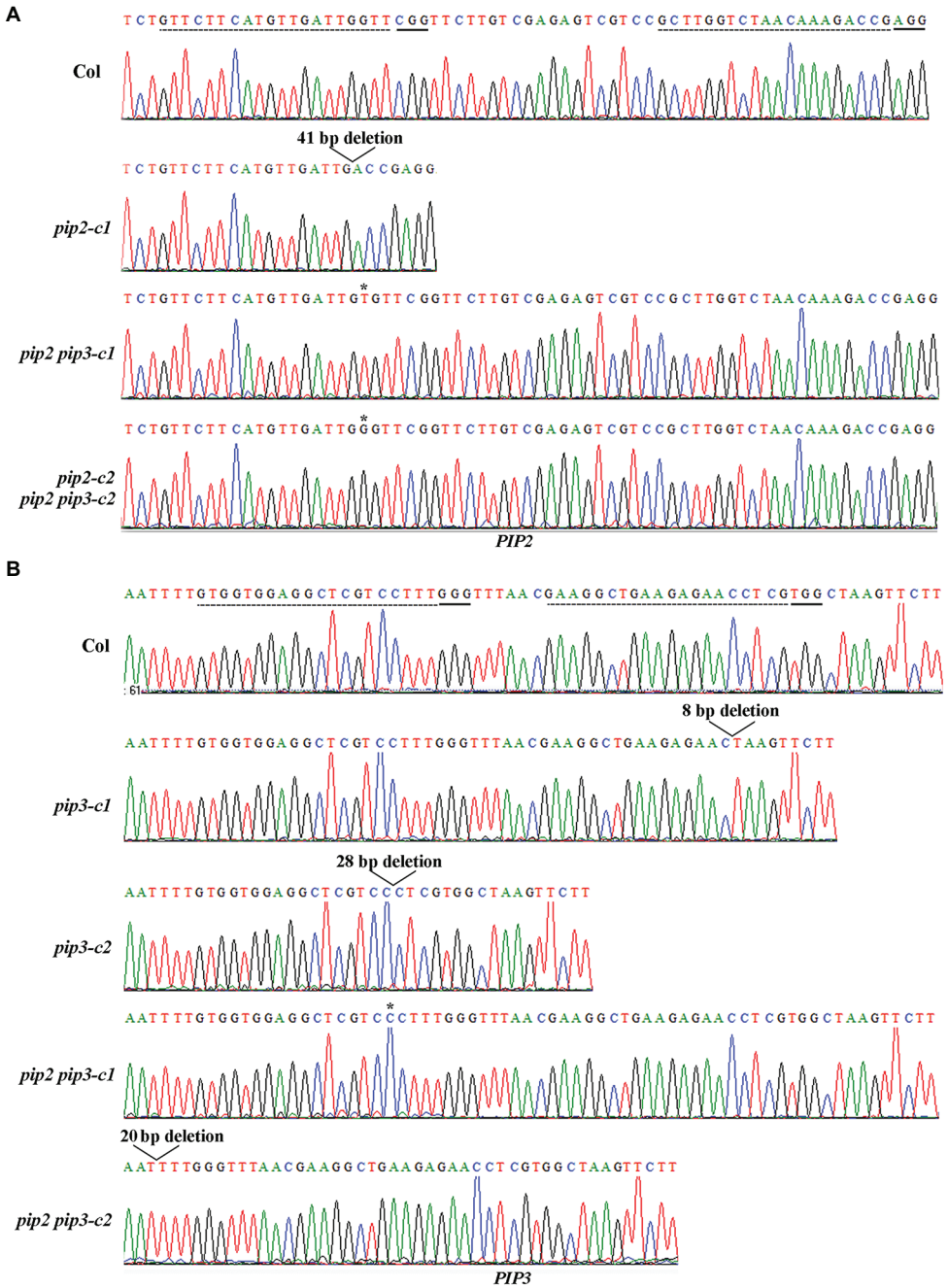

FIGURE 3 | Generation of the *pip2*, *pip3*, and *pip2 pip3* mutants by CRISPR/Cas9 gene editing. **(A)** Editing status of *PIP2* in the *pip2* and *pip2 pip3* mutants. **(B)** Editing status of *PIP3* in the *pip3* and *pip2 pip3* mutants. DNA was isolated from leaves collected from early bolting T1 plants or normal bolting T2 plants, and PCR was used to amplify the coding sequence of *PIP2* and/or *PIP3*. The PCR products were recovered and sequenced, and sequencing results were compared with genome sequence of *PIP2* or *PIP3* to check the editing status. Dash lines indicate the target sequences, and solid lines indicate the PAM sites.

pip3 mutant seedlings was also reduced (**Figure 5A**). The root length in both the *35S:PIP3* transgenic plant seedlings and the *pip3* mutant seedlings was about 60% of the Col wild type seedlings (**Figure 5B**). We also found that root length in the *pip2 pip3* double mutant seedlings is largely similar to that in the *pip3* single mutant seedlings (**Figure 5**).

PIP2 Affects Hypocotyl Elongation

Having shown that PIP2 is involved in the regulation of root elongation, we want further examine the cellular basis of PIP2 in regulating root elongation, i.e., if PIP2 may affects cell division and cell elongation. Considering that cell division and cell elongation in root may vary at different development stages,

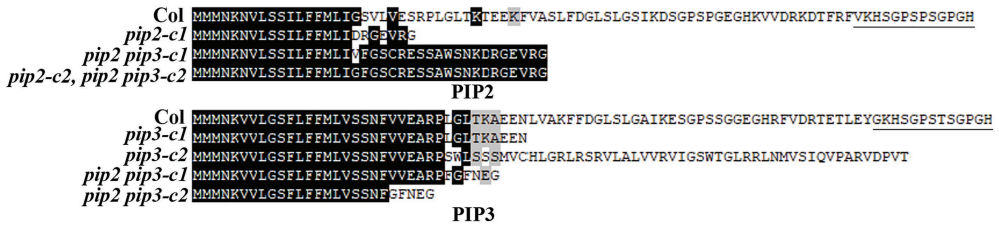

FIGURE 4 | Amino acid alignment of PIP2 and PIP3 in the Col wild type and the *pip2*, *pip3* and *pip2 pip3* mutants. The open-reading frame (ORF) of *PIP2* and *PIP3* sequences in the *pip2* and *pip2 pip3* mutants were identified by using ORFfinder (https://www.ncbi.nlm.nih.gov/orffinder/), and corresponding amino acid sequences were used for alignment with the amino acid sequences of PIP2 and PIP3, respectively. Under lines indicate the mature PIP2 and PIP3 peptides.

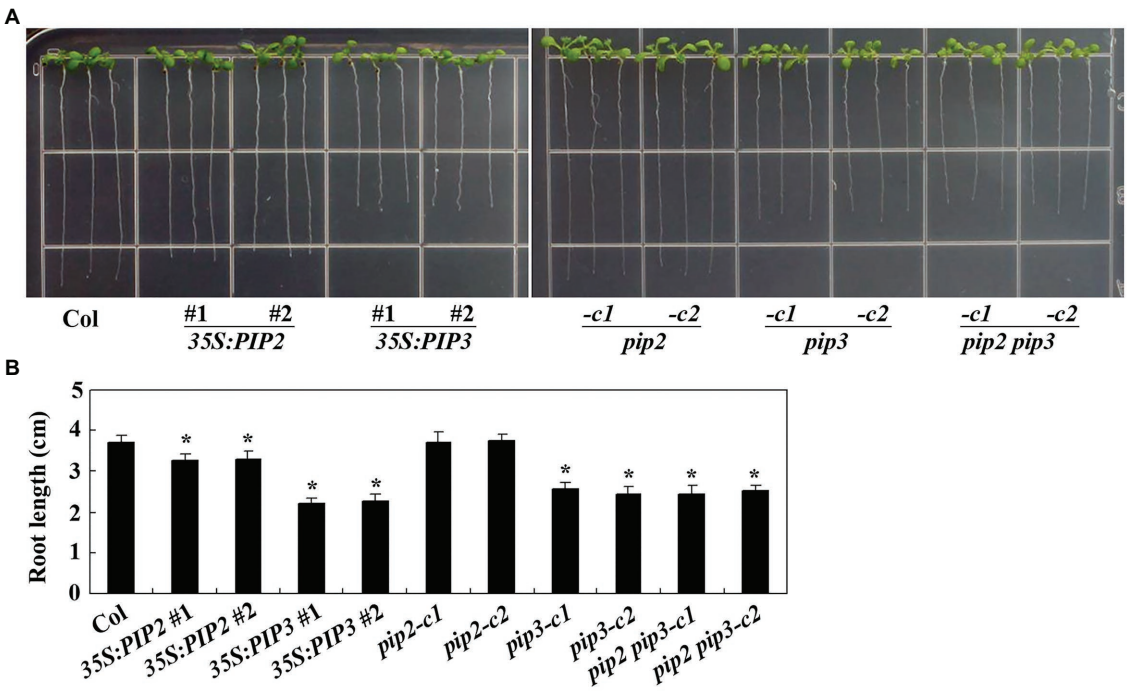

FIGURE 5 | PIP2 and PIP3 affect root elongation. **(A)** Root elongation in seedlings of the Col wild type, the *35S:PIP2* and *35S:PIP3* transgenic plants, and the *pip2*, *pip3* and *pip2 pip3* mutants. Seeds were sterilized and plated on 1/2 Murashige and Skoog (MS) plates, kept at 4°C and in darkness for 2 days before transferred to a growth room and grown vertically for 8 days. Pictures were taken by using a digital camera. **(B)** Root length in seedlings of the Col wild type, the *35S:PIP2* and *35S:PIP3* transgenic plants, and the *pip2*, *pip3*, and *pip2 pip3* mutants. Root length of 8-day-old seedlings was measured. Data represent the mean ± SD of 21–25 seedlings. *significantly different from that of the Col wild type seedlings (student's *t*-test, $p < 0.001$). The experiments were repeated three times with similar results.

we sought to examine cell division and cell elongation of epidermis cells in hypocotyls, where the number of epidermis cells is pre-determined during embryogenesis (Gendreau et al., 1997), and has been shown to be a reliable and robust system for simultaneously detect defects in cell division and cell elongation (Ullah et al., 2001, 2003; Gao et al., 2008).

To examine the effects of PIP2 in cell division and cell elongation, we first examined hypocotyl elongation in the Col wild type, the *35S:PIP2* transgenic plant and the *pip2* mutant seedlings. Sterilized seeds the Col wild type, the *35S:PIP2* transgenic plants and the *pip2* mutants were plated on 1/2 MS plates grown vertically under dim light for hypocotyl length assays. We found that, unlike that observed in root elongation, seedlings of the *35S:PIP2* transgenic plant produced longer hypocotyls (**Figure 6A**), i.e., an ~15% longer compared with the Col wild type seedlings (**Figure 6B**), whereas that in the *pip2* mutant seedlings remained similar to the Col wild type (**Figure 6**). On the other hand, although root length was affected in both the *35S:PIP3* transgenic plant and the *pip3* mutant seedlings (**Figure 6**), the hypocotyl length in the seedlings of these plants is largely unaffected, and the hypocotyl length in the *pip2 pip3* double mutants is also indistinguishable from the Col wild type seedlings (**Figure 6**).

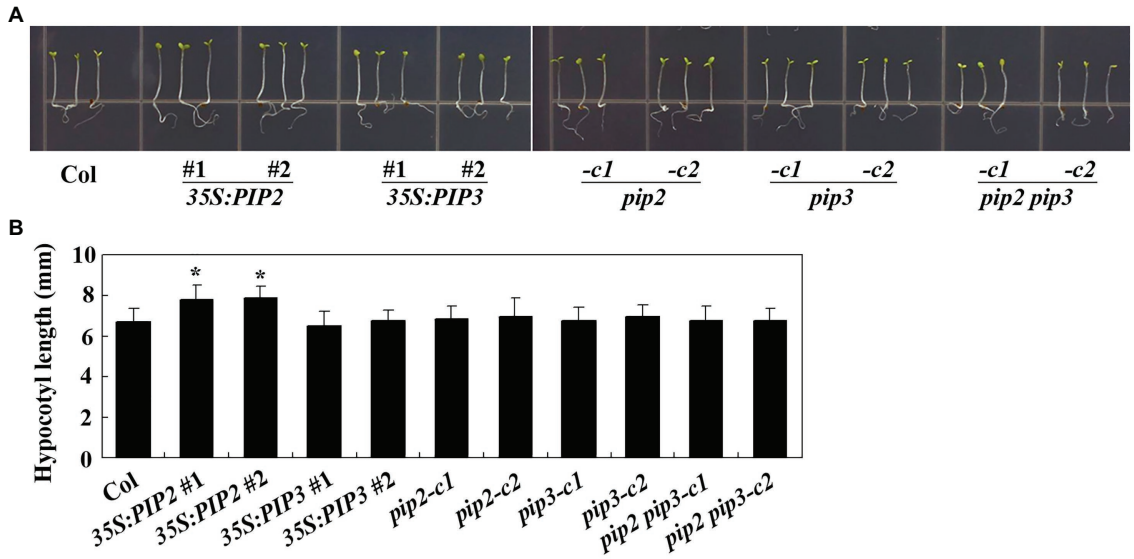

FIGURE 6 | PIP2 affects hypocotyl elongation. **(A)** Hypocotyl elongation in seedlings of the Col wild type, the *35S:PIP2* and *35S:PIP3* transgenic plants, and the *pip2*, *pip3*, and *pip2 pip3* mutants. Seeds were sterilized and plated on 1/2 MS plates, kept at 4°C and in darkness for 2 days before transferred to a growth room and grown under dim light. Pictures were taken 4 days after the transfer by using a digital camera. **(B)** Hypocotyl length in seedlings of the Col wild type, the *35S:PIP2* and *35S:PIP3* transgenic plants, and the *pip2*, *pip3*, and *pip2 pip3* mutants. Hypocotyl length of 4-day-old seedlings grown under dim light were measured. Data represent the mean ± SD of 29–42 seedlings. *significantly different from that of the Col wild type seedlings (student's *t*-test, $p < 0.001$). The experiments were repeated three times with similar results.

PIP2 Affects Cell Division and Elongation in Hypocotyls

We then examined cell division and cell elongation of epidermis cells in hypocotyls of dim light grown seedlings of the Col wild type, the *35S:PIP2* transgenic plants and the *pip2* mutants. As shown in **Figure 7A**, the overall morphology of the epidermis cells in the *35S:PIP2* transgenic plants and the *pip2* mutant seedlings are largely indistinguishable from that in the Col wild type plants. However, quantitative analysis shows that the hypocotyls of the *35S:PIP2* transgenic plants produced more epidermis cells, i.e., ~36 cells in a single cell file in the *35S:PIP2* transgenic plant seedlings compared to ~30 cells in the Col wild type seedlings (**Figure 7B**). In addition, epidermis cell length in the hypocotyls of the *35S:PIP2* transgenic plant seedlings was also increased, i.e., ~150 μM in the *35S:PIP2* transgenic plant seedlings compared to ~120 in the Col wild type seedlings. Consistent with hypocotyl length, no changes in epidermis cell number and cell length were observed in hypocotyls of the *35S:PIP3* transgenic plant seedlings, the *pip2* and the *pip2* single and the *pip2 pip3* double mutant seedlings (**Figure 7**).

DISCUSSION

Accumulated experiment evidence suggest that there are cross talks between the plant hormone auxin and the plant peptide hormones. It has been shown that auxin is able to regulated the expression of some plant peptide hormone genes (Casson et al., 2002; Chilley et al., 2006; Meng et al., 2012b; Whitford et al., 2012; Yang et al., 2014), and some plant peptide hormones are able to regulate auxin transport (Casson et al., 2002; Chilley et al., 2006; Meng et al., 2012b; Whitford et al., 2012; Yang et al., 2014). Consistent with the presence of cross talks between plant hormones and plant peptide hormones, some plant peptide hormones and auxin response genes have been shown to be able to regulate the same specific aspects of plant growth and development (Casson et al., 2002; Matsuzaki et al., 2010; Meng et al., 2012a; Fernandez et al., 2013; Yang et al., 2014).

PIPL3, a member of the PIPs and PIPLs, a plant peptide hormone family identified in recent years (Hou et al., 2014; Vie et al., 2015), has recently shown to regulate lateral root formation (Toyokura, et al., 2019). In the *gLBD16-SRDX* transgenic plants, the expression of the *TOLS2pro:GUS* reporter is induced by auxin (Toyokura, et al., 2019), indicating a cross talk between PIPL3 and auxin. At least two pieces of evidence suggest that there is also cross talk between PIP2 and auxin. One is that the expression of *PIP2* was induced by auxin, and auxin induced expression of *PIP2* was reduced in ARF activator gene mutants *nph4-1* and *arf19-4* (**Figure 1**). Another is that both root elongation and hypocotyl elongation, two of many aspects of plant growth and development regulated by auxin (Chapman and Estelle, 2009), are affected in the *PIP2* overexpression plant seedlings (**Figures 5, 6**). Yet it is possible that the *PIPs* and/or *PIPLs* whose expression is not regulated by auxin may also have cross talks with auxin, as root elongation was affected in the *PIP3* overexpression plant and *pip3* mutant seedlings (**Figure 5**). Generation of overexpressing plants and/or gene edited mutants for *PIP2* and *PIP3* in auxin signaling

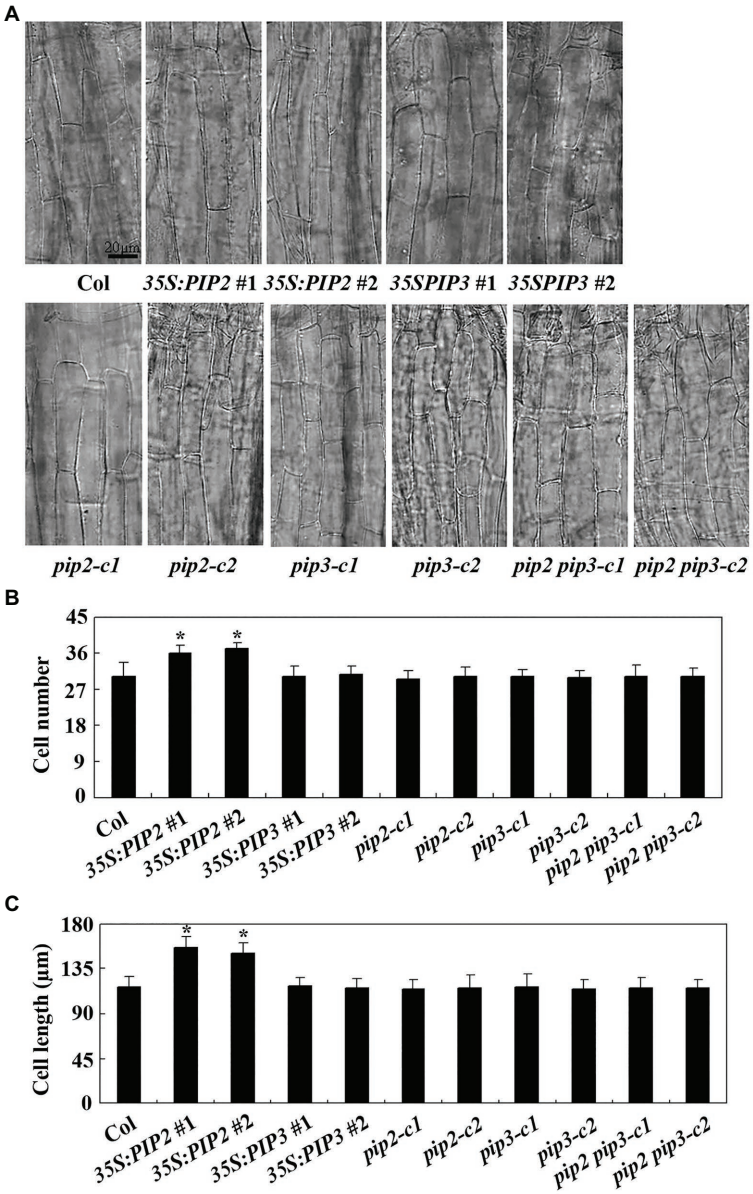

FIGURE 7 | PIP2 affects cell prolification and cell elongation in hypocotyls. **(A)** Hypocotyl cells in seedlings of the Col wild type, the *35S:PIP2* and *35S:PIP3* transgenic plants, and the *pip2*, *pip3*, and *pip2 pip3* mutants. Four-day-old dim light-grown seedlings were fixed and pictures were taken under an OLYMPUS BX53 microscope. **(B)** Number of hypocotyl cell in seedlings of the Col wild type, the *35S:PIP2* and *35S:PIP3* transgenic plants, and the *pip2*, *pip3* and *pip2 pip3* mutants. Cell number of a single cell line of the 4-day-old seedlings grown under dim light was counted under an OLYMPUS BX53 microscope. Data represent the mean ± SD of 10–12 seedlings. *significantly different from that of the Col wild type seedlings (student's *t*-test, $p < 0.001$). The experiments were repeated three times with similar results. **(C)** Hypocotyl cell length in seedlings of the Col wild type, the *35S:PIP2* and *35S:PIP3* transgenic plants, and the *pip2*, *pip3*, and *pip2 pip3* mutants. Length of the second row cells from the top to the base of the hypocotyls epidermis in longitudinal direction were was measured by using Image J. Data represent the mean ± SD of 22–29 seedlings. *significantly different from that of the Col wild type seedlings (student's *t*-test, $p < 0.001$). The experiments were repeated three times with similar results.

mutants may able to examine directly if there is cross talk between PIPs/PIPLs and auxin in regulating root and hypocotyl elongation.

Different from that of *PIP2*, the expression levels of *PIP1* and *PIP3* remind largely unchanged in response to auxin treatment (**Figure 1**), suggest that other signaling pathways may also regulate the expression of *PIPs*. As a matter of fact, previously reports showed that the expression of several genes of the *PIPs* and *PIPLs* family is induced by biotic and/or abiotic stress (Hou et al., 2014; Vie et al., 2015), suggest that other plant hormones such salicylic acid and abscisc acid may regulate the expression of *PIPs* and/or *PIPLs*. Available evidence suggest that PIP1 and PIP2 play an important role in regulating plant response to biotic stresses (Hou et al., 2014; Vie et al., 2015),

eventhough the expression of both *PIP2* and *PIP3* was not affected by ABA treatment (Vie et al., 2015), considering that the expression of *PIP2* and *PIP3* was affected by salt and cold (Vie et al., 2015), it is very likely that PIP2 and PIP3 may also involve in the regulation of plant response to abiotic stresses.

To our surprise, we found that root length was reduced in both *PIP3* overexpression plant and *pip3* mutant seedlings (**Figure 5**), indicating that right amount of PIP3 peptides may be critical for proper root elongation. We also found that both root length and hypocotyl length in the *pip3* single and the *pip2 pip3* double mutants are indistinguishable (**Figures 5, 6**), suggest that they may not have redundant functions in regulating root and hypocotyl elongation. However, considering that there are three *PIP* and eight *PIPL* genes in *Arabidopsis* (Hou et al., 2014; Vie et al., 2015; Toyokura, et al., 2019), we could not rule out the possibility that PIP and/or PIPL peptide hormones may function redundantly to regulate plant growth and development. It is possible that PIP2 and PIP3 may have different functions and/or functional mechanisms in regulating plant growth and development. As a matter of fact, it has been shown that PIP2 and PIP3 regulate plant biotic response in different ways, PIP2 regulates antipathogen activity by regulating the expression of some PTI-related genes, *WRKY* genes, *flg22-induced receptor-like kinase 1* (*FRK1*) and the SAR marker gene *PR-1* (Chen et al., 2019b), whereas PIP3 regulates immunity by regulating the biosynthesis and signaling of SA and JA in *Arabidopsis* (Najafi et al., 2020). On the other hand, both PIP2 and PIP3 contain two conserved SGPS motifs (Vie et al., 2015), and may able to produce two mature peptides, which may have different functions. As an example, CLAVATA3/ESR-RELATED 18 (CLE18) produces two peptides, one functions as an inhibitor of tracheal element differentiation and root growth (Ito et al., 2006), whereas the other promotes root growth (Meng et al., 2012a).

By examining cell numbers and cell length in hypocotyls, we found that PIP2 may regulate cell division as well as cell elongation (**Figure 7**), therefore to regulate root and hypocotyl elongation. However, further efforts are required to explore the functional mechanism of PIP2 in regulating root and hypocotyl elongation. First, it will be of interest to identify the receptors of PIP2. Both PIP1 and PIP2 regulate plant immunity, and RECEPTOR-LIKE KINASE 7 (RLK7) has been identified as a receptor of PIP1 (Hou et al., 2014). Interestingly, RLK7 is also a receptor of TOLS2/PIPL3, (Toyokura, et al., 2019), therefore it is worthwhile to examine if RLK7 may serve as a receptor of PIP2. Second, it will be of interest to examine how the expression of *PIP2* is regulated. The expression level of *PIP2* was increased in response to auxin treatment, and auxin induced expression of *PIP2* was reduced in the *nph4-1* and *arf19-4* mutants (**Figure 1**). Considering that ARF activators are responsible for the activation of auxin response genes (Tiwari et al., 2003; Wang et al., 2005), these results suggest that ARF activators may regulate the expression of *PIP2*, yet more experiments are required to examine if ARF activators may directly regulate the expression of *PIP2*. Considering that *TOLS2*/*PIPL3* is a direct target of LBD16, and TOLS2/PIPL3 functions through an auxin-SLR/IAA14-ARF7/19-LBD16-TOLS2/PIPL3-RLK7-PUCHI pathway to regulate lateral root founder cell formation (Toyokura, et al., 2019), it is also possible that *PIP2* is directly regulated by LBD16 or some other regulator downstream of ARF7/ARF19. Third, identification of PIP2 regulated genes may also help reveal the functional mechanisms of PIP2. It has been reported that among the four auxin-induced LR-related reporter genes (De Rybel et al., 2010), only two were induced by TOLS2/PIPL3, suggest that TOLS2/PIPL3 may induce gene expression in a pathway independent of auxin signaling (Toyokura, et al., 2019), but this cannot rule out the possibility that TOLS2/PIPL3 may play a feedback regulating role in auxin signaling. This may be also the case of PIP2. Last but not least, our genetic evidence suggest that PIP2 play a different role in regulating root and hypocotyl elongation, i.e., inhibit root elongation (**Figure 5**), but promote hypocotyl elongation (**Figure 6**), which may cause by different sensitivities of different parts of the plant in response to the peptides produced by overexpressing *PIP2*. Considering that PIPs/PIPLs are peptide hormone, and similar to overexpress *PIP1* and *PIP2* genes in plants, exogenous application of synthetic PIP1 and PIP2 peptides are able to enhanced immune responses in *Arabidopsis* (Hou et al., 2014), it is still worthwhile to example if exogenous application synthetic PIP2 and PIP3 peptides may able to, and how to regulate plant growth and development.

Nevertheless, our results show that *PIP2* is an auxin response gene, and that PIP2 may regulate root and hypocotyl elongation *via* regulating cell division and cell elongation.

DATA AVAILABILITY STATEMENT

The original contributions presented in the study are included in the article/supplementary material, further inquiries can be directed to the corresponding author.

AUTHOR CONTRIBUTIONS

SW conceived the study. SH, WW, and SW designed the experiments and drafted the manuscript. SH, WW, SA, XW, Adnan, YC, CW, YW, NZ, HT, and SC did the experiments. XH, WW, TW, and SW analyzed the data. All authors contributed to the article and approved the submitted version.

FUNDING

This research was supported by the National Natural Science Foundation of China (32071938), the National Key R&D Program of China (2016YFD0101900) and a startup funding from Linyi University (LYDX2019BS039). The funders had no role in study design, data collection and analysis, decision to publish, or preparation of the manuscript.

REFERENCES

Butenko, M. A., Patterson, S. E., Grini, P. E., Stenvik, G. E., Amundsen, S. S., Mandal, A., et al. (2003). Inflorescence deficient in abscission controls floral organ abscission in Arabidopsis and identifies a novel family of putative ligands in plants. *Plant Cell* 15, 2296–2307. doi: 10.1105/tpc.014365

Casson, S. A., Chilley, P. M., Topping, J. F., Evans, I. M., Souter, M. A., and Lindsey, K. (2002). The POLARIS gene of Arabidopsis encodes a predicted peptide required for correct root growth and leaf vascular patterning. *Plant Cell* 14, 1705–1721. doi: 10.1105/tpc.002618

Chae, K., Isaacs, C. G., Reeves, P. H., Maloney, G. S., Muday, G. K., Nagpal, P., et al. (2012). Arabidopsis SMALL AUXIN UP RNA63 promotes hypocotyl and stamen filament elongation. *Plant J.* 71, 684–697. doi: 10.1111/j.1365-313X.2012.05024.x

Chapman, E. J., and Estelle, M. (2009). Mechanism of auxin-regulated gene expression in plants. *Annu. Rew. Genet.* 43, 265–285. doi: 10.1146/annurev-genet-102108-134148

Chen, Y. L., Fan, K. T., Hung, S. C., and Chen, Y. R. (2019b). The role of peptides cleaved from protein precursors in eliciting plant stress reactions. *New Phytol.* 225, 2267–2282. doi: 10.1111/nph.16241

Chen, S., Zhang, N., Zhang, Q., Zhou, G., Tian, H., Hussain, S., et al. (2019a). Genome editing to integrate seed size and abiotic stress tolerance traits in *Arabidopsis* reveals a role for *DPA4* and *SOD7* in the regulation of inflorescence architecture. *Int. J. Mol. Sci.* 20:2695. doi: 10.3390/ijms20112695

Cheng, Y., Zhang, N., Hussain, S., Ahmed, S., Yang, W., and Wang, S. (2019). Integration of a FT expression cassette into CRISPR/Cas9 construct enables fast generation and easy identification of transgene-free mutants in *Arabidopsis*. *PLoS One* 14:e0218583. doi: 10.1371/journal.pone.0218583

Chilley, P. M., Casson, S. A., Tarkowski, P., Hawkins, N., Wang, K. L., Hussey, P. J., et al. (2006). The POLARIS peptide of Arabidopsis regulates auxin transport and root growth via effects on ethylene signaling. *Plant Cell* 18, 3058–3072. doi: 10.1105/tpc.106.040790

Cho, S. K., Larue, C. T., Chevalier, D., Wang, H., Jinn, T. L., Zhang, S., et al. (2008). Regulation of floral organ abscission in *Arabidopsis thaliana*. *Proc. Natl. Acad. Sci. U. S. A.* 105, 15629–15634. doi: 10.1073/pnas.0805539105

Clough, S. J., and Bent, A. F. (1998). Floral dip: a simplified method for agrobacterium-mediated transformation of *Arabidopsis thaliana*. *Plant J.* 16, 735–743. doi: 10.1046/j.1365-313x.1998.00343.x

Coudert, Y., Dievart, A., Droc, G., and Gantet, P. (2013). ASL/LBD phylogeny suggests that genetic mechanisms of root initiation downstream of auxin are distinct in lycophytes and euphyllophytes. *Mol. Biol. Evol.* 30, 569–572. doi: 10.1093/molbev/mss250

Davies, P. J. (1995). *Plant Hormones: Physiology, Biochemistry and Molecular Biology*. Dordrecht: Kluwer.

De Rybel, B., Vassileva, V., Parizot, B., Demeulenaere, M., Grunewald, W., Audenaert, D., et al. (2010). A novel aux/IAA28 signaling cascade activates GATA23-dependent specification of lateral root founder cell identity. *Curr. Biol.* 20, 1697–1706. doi: 10.1016/j.cub.2010.09.007

Dharmasiri, N., Dharmasiri, S., and Estelle, M. (2005). The F-box protein TIR1 is an auxin receptor. *Nature* 435, 441–445. doi: 10.1038/nature03543

Edlund, T., and Jessell, T. M. (1999). Progression from extrinsic to intrinsic signaling in cell fate specification: a view from the nervous system. *Cell* 96, 211–224. doi: 10.1016/S0092-8674(00)80561-9

Fernandez, A., Drozdzecki, A., Hoogewijs, K., Nguyen, A., Beeckman, T., Madder, A., et al. (2013). Transcriptional and functional classification of the GOLVEN/ROOT GROWTH FACTOR/CLE-like signaling peptides reveals their role in lateral root and hair formation. *Plant Physiol.* 161, 954–970. doi: 10.1104/pp.112.206029

Gao, Y., Wang, S., Asami, T., and Chen, J.-G. (2008). Loss-of-function mutations in the *Arabidopsis* heterotrimeric G-protein alpha subunit enhance the developmental defects of brassinosteroid signaling and biosynthesis mutants. *Plant Cell Physiol.* 49, 1013–1024. doi: 10.1093/pcp/pcn078

Gendreau, E., Traas, J., Desnos, T., Grandjean, O., Caboche, M., and Höfte, H. (1997). Cellular basis of hypocotyl growth in *Arabidopsis thaliana*. *Plant Physiol.* 114, 295–305. doi: 10.1104/pp.114.1.295

Gil, P., Liu, Y., Orbović, V., Verkamp, E., Poff, K. L., and Green, P. J. (1994). Characterization of the auxin-inducible SAUR-AC1 gene for use as a molecular genetic tool in Arabidopsis. *Plant Physiol.* 104, 777–784. doi: 10.1104/pp.104.2.777

Guilfoyle, T. J., and Hagen, G. (2007). Auxin response factors. *Curr. Opin. Plant Biol.* 10, 453–460. doi: 10.1016/j.pbi.2007.08.014

Guilfoyle, T. J., Ulmasov, T., and Hagen, G. (1998). The ARF family of transcription factors and their role in plant hormone-responsive transcription. *Cell. Mol. Life Sci.* 54, 619–627. doi: 10.1007/s000180050190

Guo, H., Zhang, W., Tian, H., Zheng, K., Dai, X., Liu, S., et al. (2015). An auxin responsive CLE gene regulates shoot apical meristem development in Arabidopsis. *Front. Plant Sci.* 6:295. doi: 10.3389/fpls.2015.00295

Hagen, G., and Guilfoyle, T. J. (2002). Auxin-responsive gene expression: genes, promoters, and regulatory factors. *Plant Mol. Biol.* 49, 373–485. doi: 10.1023/A:1015207114117

Hajdukiewicz, P., Svab, Z., and Maliga, P. (1994). The small, versatile pPZP family of agrobacterium binary vectors for plant transformation. *Plant Mol. Biol.* 25, 989–994. doi: 10.1007/BF00014672

Hara, K., Kajita, R., Torii, K. U., Bergmann, D. C., and Kakimoto, T. (2007). The secretory peptide gene EPF1 enforces the stomatal one-cell-spacing rule. *Genes Dev.* 21, 1720–1725. doi: 10.1101/gad.1550707

Harper, R. M., Stowe-Evans, E. L., Luesse, D. R., Muto, H., Tatematsu, K., Watahiki, M. K., et al. (2000). The NPH4 locus encodes the auxin response factor ARF7, a conditional regulator of differential growth in aerial Arabidopsis tissue. *Plant Cell* 12, 757–770. doi: 10.1105/tpc.12.5.757

Hayashi, K.-I. (2012). The interaction and integration of auxin signaling components. *Plant Cell Physiol.* 53, 965–975. doi: 10.1093/pcp/pcs035

He, S. L., Hsieh, H. L., and anf Jauh, G. Y., (2018). SMALL AUXIN UP RNA62/75 are required for the translation of transcripts essential for pollen tube growth. *Plant Physiol.* 178, 626–640. doi: 10.1104/pp.18.00257

Hirakawa, Y., and Sawa, S. (2019). Diverse function of plant peptide hormones in local signaling and development. *Curr. Opin. Plant Biol.* 51, 81–87. doi: 10.1016/j.pbi.2019.04.005

Hirakawa, Y., Torii, K. U., and Uchida, N. (2017). Mechanisms and strategies shaping plant peptide hormones. *Plant Cell Physiol.* 58, 1313–1318. doi: 10.1093/pcp/pcx069

Hou, S., Wang, X., Chen, D., Yang, X., Wang, M., Turrà, D., et al. (2014). The secreted peptide PIP1 amplifies immunity through receptor-like kinase 7. *PLoS Pathog.* 10:e1004331. doi: 10.1371/journal.ppat.1004331

Hou, K., Wu, W., and Gan, S. S. (2013). SAUR36, a small auxin up RNA gene, is involved in the promotion of leaf senescence in Arabidopsis. *Plant Physiol.* 161, 1002–1009. doi: 10.1104/pp.112.212787

Hunt, L., and Gray, J. E. (2009). The signaling peptide EPF2 controls asymmetric cell divisions during stomatal development. *Curr. Biol.* 19, 864–869. doi: 10.1016/j.cub.2009.03.069

Ito, Y., Nakanomyo, I., Motose, H., Iwamoto, K., Sawa, S., Dohmae, N., et al. (2006). Dodeca-CLE peptides as suppressors of plant stem cell differentiation. *Science* 313, 842–845. doi: 10.1126/science.1128436

Jun, J., Fiume, E., Roeder, A. H., Meng, L., Sharma, V. K., Osmont, K. S., et al. (2010). Comprehensive analysis of CLE polypeptide signaling gene expression and overexpression activity in Arabidopsis. *Plant Physiol.* 154, 1721–1736. doi: 10.1104/pp.110.163683

Kathare, P. K., Dharmasiri, S., and Dharmasiri, N. (2018). SAUR53 regulates organ elongation and apical hook development in Arabidopsis. *Plant Signal. Behav.* 13:e1514896. doi: 10.1080/15592324.2018.1514896

Katsir, L., Davies, K. A., Bergmann, D. C., and Laux, T. (2011). Peptide signaling in plant development. *Curr. Biol.* 21, 356–364. doi: 10.1016/j.cub.2011.03.012

Kepinski, S., and Leyser, O. (2005). The Arabidopsis F-box protein TIR1 is an auxin receptor. *Nature* 435, 446–451. doi: 10.1038/nature03542

Kieffer, M., Neve, J., and Kepinski, S. (2010). Defining auxin response contexts in plant development. *Curr. Opin. Plant Biol.* 13, 12–20. doi: 10.1016/j.pbi.2009.10.006

Kinoshita, A., Nakamura, Y., Sasaki, E., Kyozuka, J., Fukuda, H., and Sawa, S. (2007). Gain-of-function phenotypes of chemically synthetic CLAVATA3/ESR-related (CLE) peptides in *Arabidopsis thaliana* and *Oryza sativa*. *Plant Cell Physiol.* 48, 1821–1825. doi: 10.1093/pcp/pcm154

Kong, Y., Zhu, Y., Gao, C., She, W., Lin, W., Chen, Y., et al. (2013). Tissue-specific expression of SMALL AUXIN UP RNA41 differentially regulates cell expansion and root meristem patterning in Arabidopsis. *Plant Cell Physiol.* 54, 609–621. doi: 10.1093/pcp/pct028

Lee, H. W., Kim, N. Y., Lee, D. J., and Kim, J. (2009). LBD18/ASL20 regulates lateral root formation in combination with LBD16/ASL18 downstream of

ARF7 and ARF19 in Arabidopsis. *Plant Physiol.* 151, 1377–1389. doi: 10.1104/pp.109.143685

Liu, S., Hu, Q., Luo, S., Li, Q., Yang, X., Wang, X., et al. (2015). Expression of wild-type *PtrIAA14.1*, a poplar aux/IAA gene causes morphological changes in *Arabidopsis*. *Front. Plant Sci.* 6:388. doi: 10.3389/fpls.2015.00388

Matsuzaki, Y., Ogawa-Ohnishi, M., Mori, A., and Matsubayashi, Y. (2010). Secreted peptide signals required for maintenance of root stem cell niche in Arabidopsis. *Science* 329, 1065–1067. doi: 10.1126/science.1191132

Meng, L., Buchanan, B. B., Feldman, L. J., and Luan, S. (2012a). CLE-like (CLEL) peptides control the pattern of root growth and lateral root development in Arabidopsis. *Proc. Natl. Acad. Sci. U. S. A.* 109, 1760–1765. doi: 10.1073/pnas.1119864109

Meng, L., Buchanan, B. B., Feldman, L. J., and Luan, S. (2012b). A putative nuclear CLE-like (CLEL) peptide precursor regulates root growth in Arabidopsis. *Mol. Plant* 5, 955–957. doi: 10.1093/mp/sss060

Najafi, J., Brembu, T., Vie, A. K., Viste, R., Winge, P., Somssich, I. E., et al. (2020). PAMP-INDUCED SECRETED PEPTIDE 3 modulates immunity in Arabidopsis. *J. Exp. Bot.* 71, 850–864. doi: 10.1093/jxb/erz482

Narita, N. N., Moore, S., Horiguchi, G., Kubo, M., Demura, T., Fukuda, H., et al. (2004). Overexpression of a novel small peptide ROTUNDIFOLIA4 decreases cell proliferation and alters leaf shape in *Arabidopsis thaliana*. *Plant J.* 38, 699–713. doi: 10.1111/j.1365-313X.2004.02078.x

Pearce, G., Strydom, D., Johnson, S., and Ryan, C. A. (1991). A polypeptide from tomato leaves induces wound-inducible proteinase inhibitor proteins. *Science* 253, 895–898. doi: 10.1126/science.253.5022.895

Qiu, T., Qi, M., Ding, X., Zheng, Y., Zhou, T., Chen, Y., et al. (2020). The SAUR41 subfamily of SMALL AUXIN UP RNA genes is abscisic acid inducible to modulate cell expansion and salt tolerance in *Arabidopsis thaliana* seedlings. *Ann. Bot.* 125, 805–819. doi: 10.1093/aob/mcz160

Qu, X., Zhao, Z., and Tian, Z. (2017). *ERECTA* regulates cell elongation by activating auxin biosynthesis in *Arabidopsis thaliana*. *Front. Plant Sci.* 8:1688. doi: 10.3389/fpls.2017.01688

Reed, J. W. (2001). Roles and activities of aux/IAA proteins in Arabidopsis. *Trends Plant Sci.* 6, 420–425. doi: 10.1016/S1360-1385(01)02042-8

Rehman, A., Bannigan, A., Sulaman, W., Pechter, P., Blancaflor, E. B., and Baskin, T. I. (2007). Auxin, actin and growth of the *Arabidopsis thaliana* primary root. *Plant J.* 50, 514–528. doi: 10.1111/j.1365-313X.2007.03068.x

Scheres, B., Wolkenfelt, H., Willemsen, V., Terlouw, M., Lawson, E., Dean, C., et al. (1994). Embryonic origin of the *Arabidopsis* primary root and root meristem initials. *Development* 120, 2475–2487.

Singh, S., Yadav, S., Singh, A., Mahima, M., Singh, A., Gautam, V., et al. (2020). Auxin signaling modulates LATERAL ROOT PRIMORDIUM1 (LRP1) expression during lateral root development in Arabidopsis. *Plant J.* 101, 87–100. doi: 10.1111/tpj.14520

Spartz, A. K., Lee, S. H., Wenger, J. P., Gonzalez, N., Itoh, H., Inzé, D., et al. (2012). The SAUR19 subfamily of SMALL AUXIN UP RNA genes promote cell expansion. *Plant J.* 70, 978–990. doi: 10.1111/j.1365-313X.2012.04946.x

Stenvik, G. E., Tandstad, N. M., Guo, Y., Shi, C. L., Kristiansen, W., Holmgren, A., et al. (2008). The EPIP peptide of INFLORESCENCE DEFICIENT IN ABSCISSION is sufficient to induce abscission in Arabidopsis through the receptor-like kinases HAESA and HAESA-LIKE2. *Plant Cell* 20, 1805–1817. doi: 10.1105/tpc.108.059139

Sugano, S. S., Shimada, T., Imai, Y., Okawa, K., Tamai, A., Mori, M., et al. (2010). Stomagen positively regulates stomatal density in Arabidopsis. *Nature* 463, 241–244. doi: 10.1038/nature08682

Tan, X., Calderon-Villalobos, L. I. A., Sharon, M., Zheng, C., Robinson, C. V., Estelle, M., et al. (2007). Mechanism of auxin perception by the TIR1 ubiquitun ligase. *Nature* 446, 640–645. doi: 10.1038/nature05731

Tian, H., Guo, H., Dai, X., Cheng, Y., Zheng, K., Wang, X., et al. (2015). An ABA down-regulated bHLH transcription repressor gene, *bHLH129* regulates root elongation and ABA response when overexpressed in *Arabidopsis*. *Sci. Rep.* 5:17587. doi: 10.1038/srep17587

Tiwari, S. B., Hagen, G., and Guilfoyle, T. (2003). The roles of auxin response factor domains in auxin-responsive transcription. *Plant Cell* 15, 533–543. doi: 10.1105/tpc.008417

Tiwari, S. B., Hagen, G., and Guilfoyle, T. J. (2004). Aux/IAA proteins contain a potent transcriptional repression domain. *Plant Cell* 16, 533–543. doi: 10.1105/tpc.017384

Toyokura, K., Goh, T., Shinohara, H., Shinoda, A., Kondo, Y., Okamoto, Y., et al. (2019). Lateral inhibition by a peptide hormone-receptor cascade during Arabidopsis lateral root founder cell formation. *Dev. Cell* 48, 64–75. doi: 10.1016/j.devcel.2018.11.031

Ullah, H., Chen, J. G., Temple, B., Boyes, D. C., Alonso, J. M., Davis, K. R., et al. (2003). The beta-subunit of the Arabidopsis G protein negatively regulates auxin-induced cell division and affects multiple developmental processes. *Plant Cell* 15, 393–409. doi: 10.1105/tpc.006148

Ullah, H., Chen, J. G., Young, J. C., Im, K. H., Sussman, M. R., and Jones, A. M. (2001). Modulation of cell proliferation by heterotrimeric G protein in Arabidopsis. *Science* 292, 2066–2069. doi: 10.1126/science.1059040

Vie, A. K., Najafi, J., Liu, B., Winge, P., Butenko, M. A., Hornslien, K. S., et al. (2015). The IDA/IDA-LIKE and PIP/PIP-LIKE gene families in Arabidopsis: phylogenetic relationship, expression patterns, and transcriptional effect of the PIPL3 peptide. *J. Exp. Bot.* 66, 5351–5365. doi: 10.1093/jxb/erv285

Wang, S., Chang, Y., Guo, J., and Chen, J.-G. (2007). *Arabidopsis* ovate family protein 1 is a transcriptional repressor that suppresses cell elongation. *Plant J.* 50, 858–872. doi: 10.1111/j.1365-313X.2007.03096.x

Wang, X., Liu, S., Tian, H., Wang, S., and Chen, J.-G. (2015b). The small ethylene response factor ERF96 is involved in the regulation of the abscisic acid response in *Arabidopsis*. *Front. Plant Sci.* 6:1064. doi: 10.3389/fpls.2015.01064

Wang, S., Tiwari, S. B., Hagen, G., and Guilfoyle, T. J. (2005). AUXIN RESPONSE FACTOR7 restores the expression of auxin-responsive genes in mutant *Arabidopsis* leaf mesophyll protoplasts. *Plant Cell* 17, 1979–1993. doi: 10.1105/tpc.105.031096

Wang, X., Wang, X., Hu, Q., Dai, X., Tian, H., Zheng, K., et al. (2015a). Characterization of an activation-tagged mutant uncovers a role of *GLABRA2* in anthocyanin biosynthesis in *Arabidopsis*. *Plant J.* 83, 300–311. doi: 10.1111/tpj.12887

Wang, W., Wang, X., Wang, X., Ahmed, S., Hussain, S., Zhang, N., et al. (2019). Integration of *RACK1* and ethylene signaling regulates plant growth and development in *Arabidopsis*. *Plant Sci.* 280, 31–40. doi: 10.1016/j.plantsci.2018.11.009

Wang, X., Wang, W., Wang, Y., Zhou, G., Liu, S., Li, D., et al. (2020). AIW1 and AIW2, two ABA-induced WD40 repeat-containing transcription repressors function redundantly to regulate ABA and salt responses in *Arabidopsis*. *J. Plant Interact.* 15, 196–206. doi: 10.1080/17429145.2020.1778110

Wen, J., Lease, K. A., and Walker, J. C. (2004). DVL, a novel class of small polypeptides: overexpression alters Arabidopsis development. *Plant J.* 37, 668–677. doi: 10.1111/j.1365-313X.2003.01994.x

Wen, Z., Mei, Y., Zhou, J., Cui, Y., Wang, D., and Wang, N. N. (2020). SAUR49 can positively regulate leaf senescence by suppressing SSPP in Arabidopsis. *Plant Cell Physiol.* 61, 644–658. doi: 10.1093/pcp/pcz231

Whitford, R., Fernandez, A., De Groodt, R., Orteqa, E., and Hilson, P. (2008). Plant CLE peptides from two distinct functional classes synergistically induce division of vascular cells. *Proc. Natl. Acad. Sci. U.S.A.* 105, 18625–19630. doi: 10.1073/pnas.0809395105

Whitford, R., Fernandez, A., Tejos, R., Pérez, A. C., Kleine-Vehn, J., Vanneste, S., et al. (2012). GOLVEN secretory peptides regulate auxin carrier turnover during plant gravitropic responses. *Dev. Cell* 22, 678–685. doi: 10.1016/j.devcel.2012.02.002

Yang, F., Song, Y., Yang, H., Liu, Z., Zhu, G., and Yang, Y. (2014). An auxin-responsive endogenous peptide regulates root development in Arabidopsis. *J. Integr. Plant Biol.* 56, 635–647. doi: 10.1111/jipb.12178

Zheng, K., Wang, Y., Zhang, N., Jia, Q., Wang, X., Hou, C., et al. (2017). Involvement of PACLOBUTRAZOL RESISTANCE6/KIDARI, an atypical bHLH transcription factor, in auxin responses in *Arabidopsis*. *Front. Plant Sci.* 8:1813. doi: 10.3389/fpls.2017.01813

Conflict of Interest: The authors declare that the research was conducted in the absence of any commercial or financial relationships that could be construed as a potential conflict of interest.

frontiers in Plant Science

REVIEW
published: 17 May 2021
doi: 10.3389/fpls.2021.674010

Arabinogalactan Proteins in Plant Roots – An Update on Possible Functions

*Dagmar Hromadová†, Aleš Soukup† and Edita Tylová**

Department of Experimental Plant Biology, Faculty of Science, Charles University, Prague, Czechia

Responsiveness to environmental conditions and developmental plasticity of root systems are crucial determinants of plant fitness. These processes are interconnected at a cellular level with cell wall properties and cell surface signaling, which involve arabinogalactan proteins (AGPs) as essential components. AGPs are cell-wall localized glycoproteins, often GPI-anchored, which participate in root functions at many levels. They are involved in cell expansion and differentiation, regulation of root growth, interactions with other organisms, and environmental response. Due to the complexity of cell wall functional and regulatory networks, and despite the large amount of experimental data, the exact molecular mechanisms of AGP-action are still largely unknown. This dynamically evolving field of root biology is summarized in the present review.

Keywords: AGP, arabinogalactan proteins, root growth, root hairs, interactions, fasciclin-like, GPI anchor

OPEN ACCESS

Edited by:
Svetlana Shishkova, National Autonomous University of Mexico, Mexico

Reviewed by:
Azeddine Driouich, Université de Rouen, France
Juan M. Losada, Institute of Subtropical and Mediterranean Horticulture La Mayora, Spain
Birgit Classen, University of Kiel, Germany
Silvia Vieira Coimbra, University of Porto, Portugal

***Correspondence:**
Edita Tylová
edmunz@natur.cuni.cz

†These authors share first authorship

Specialty section:
This article was submitted to Plant Development and EvoDevo, a section of the journal Frontiers in Plant Science

Received: *28 February 2021*
Accepted: *19 April 2021*
Published: *17 May 2021*

Citation:
Hromadová D, Soukup A and Tylová E (2021) Arabinogalactan Proteins in Plant Roots – An Update on Possible Functions. Front. Plant Sci. 12:674010. doi: 10.3389/fpls.2021.674010

INTRODUCTION

Plants are sessile organisms with cells surrounded by cell walls which mediate interactions with surrounding environment. Communication across the cell wall and related cell surface signaling is an essential, complex, and largely unexplored aspect of plant biology (Seifert and Blaukopf, 2010; Duman et al., 2020; Rui and Dinneny, 2020). The deposition and remodeling of the cell wall enables growth and development of plant organs, and cell-wall derived signals mediate responses to internal and external factors (Voxeur and Hofte, 2016; Gigli-Bisceglia et al., 2020).

Arabinogalactan proteins (AGPs) are ubiquitous in the cell wall and in extracellular exudates (Showalter, 2001). They take part in the regulatory and functional continuum of the plasmalemma, cell wall, and environment (Ellis et al., 2010). AGPs occur in all plant organs (Clarke et al., 1979; Fincher et al., 1983; Nguema-Ona et al., 2012; He et al., 2019) but molecular mechanisms of their function remain rather puzzling. They are involved in the regulation of plant growth and development, affect cell wall properties, structure, and architecture (Seifert, 2018, 2021; Tucker et al., 2018), play a role in stem development and differentiation (Ito et al., 2005; MacMillan et al., 2010; Liu et al., 2020), root growth and differentiation (Dolan et al., 1995; Bossy et al., 2009; Nguema-Ona et al., 2012), sexual reproduction (Cheung et al., 1995; Cheung and Wu, 1999; Nguema-Ona et al., 2012; Pereira et al., 2015; Su and Higashiyama, 2018), embryogenesis (Kreuger and van Holst, 1993; Yu and Zhao, 2012; Perez-Perez et al., 2018), fruit ripening (Leszczuk et al., 2020a,b), response to abiotic and biotic stress factors (Mareri et al., 2018; Seifert, 2021), and interactions with microorganisms (Nguema-Ona et al., 2013; Rashid, 2016).

The root system, not covered by a protective cuticle, is constantly interacting with the rhizosphere. It secretes protective mucilage and other compounds, interchanges signaling molecules with soil organisms, and adjusts root development according to the heterogeneous distribution of soil resources with an amazing degree of plasticity. Roots thus present a unique system to evaluate different aspects of AGP functions in the cell wall and extracellular spaces (**Figure 1**). In roots, AGPs are important regulators of elongation and differentiation of cells (Shi et al., 2003), including root hairs (Kirchner et al., 2018; Borassi et al., 2020). They represent important components of root exudates, aid in the formation of a rhizosheath (Galloway et al., 2020), modulate response to root pathogens and parasites (Gaspar et al., 2004; Bozbuga et al., 2018), and are involved in the establishment of root symbioses with beneficial microorganisms (Brewin, 2004). AGPs even form major components of the glue-like adhesive nanoparticles secreted by the roots of climbing plants (Huang et al., 2016). In this review we summarize selected aspects of AGP action related to root development and function (**Figure 1**), updating previous excellent reviews (Nguema-Ona et al., 2012, 2013) and covering recent advances in this field of root biology. Available AGP mutants with phenotypic manifestations in roots are summarized (**Table 1**).

ARABINOGALACTAN PROTEINS

Structural proteins are a minor but essential component of the primary cell wall (Rui and Dinneny, 2020) and include proline-rich proteins (PRPs), glycine-rich proteins (GRPs), extensins (EXTs), and AGPs. AGPs are present in vascular plants, bryophytes (Bartels et al., 2017; Johnson et al., 2017; Ma et al., 2017; Classen et al., 2019) and green algae (Palacio-Lopez et al., 2019; Přerovská et al., 2021). AGPs or AGP-like proteins have also been detected in brown algae (Herve et al., 2016) and cyanobacteria (Jackson et al., 2012) opening discussion on their evolutionary origin (Knox, 2016).

Arabinogalactan proteins have the most extensive glycosylation of Pro/Hyp-rich glycoproteins. Their carbohydrate moiety forms 90 to 99% of their molecular mass, combining galactose and arabinose as major sugars with fucose, rhamnose, and glucuronic acid as minor sugars (Fincher et al., 1983; Ellis et al., 2010; Showalter and Basu, 2016; Silva J. et al., 2020). AGPs form a complex family (Showalter, 2001). Their classification has been modified several times over the last decades. Most recently they have been divided into several groups according to their molecular structure: classical AGP, AG peptides, Lys-rich AGPs, chimeric AGPs including FLAs (FASCICLIN-LIKE AGPs), ENODLs (EARLY NODULIN-LIKE AGPs), XYLPs (XYLOGEN-LIKE AGPs), other chimeric AGPs, and HAEs (AGP-EXT hybrids) (Showalter, 2001; Pereira et al., 2015; Mareri et al., 2018; He et al., 2019; Silva J. et al., 2020). Classical AGPs are characterized by the presence of an N-terminal signal sequence, which targets the protein to the endoplasmic reticulum (ER) and secretory pathway, a middle PAST-rich domain (rich in Pro, Ala, Ser, and Thr), and a C-terminal sequence, which is cleaved during the establishment of the GPI (glycosylphosphatidylinositol) anchor in the ER (Schultz et al., 1998). AG-peptides are short classical AGPs with only 10–15 amino acids. Fasciclin-like (FLA) AGPs are also similar to classical AGPs, but possess one or two fasciclin-like domains (FAS) in their protein core (He et al., 2019). Lys-rich AGPs contain a Lys-rich domain between PAST domain and C-terminus, ENODLs contain plastocyanin-like domains, XYLPs contain non-specific lipid transfer protein domains, and HAEs combine modules characteristic for AGPs and EXTs. For further details of classification see recent reviews (Ma et al., 2017; Silva J. et al., 2020).

Proposed mechanisms of AGP functions vary among groups or may be combined within a single protein. Crosslinking of glycoproteins, such as EXTs and AGPs, by cell wall peroxidases might reinforce the cell wall (Bradley et al., 1992; Kjellbom et al., 1997). AGPs are covalently linked to pectins or hemicelluloses (Immerzeel et al., 2006; Tan et al., 2013) and their action as "pectin plasticizers" was hypothesized (Lamport et al., 2006; Corral-Martinez et al., 2019). Another putative mechanism is an enzymatic release of mobile oligosaccharides from AGP glycan side chains that may act as signaling molecules possibly recognized by plasma membrane receptors (Showalter, 2001; Van Hengel and Roberts, 2002; Zagorchev et al., 2014; Silva J. et al., 2020). In spite of studies linking activity of plant chitinases with AGPs action in developmental processes (van Hengel et al., 2001; Dos Santos et al., 2006; Zielinski et al., 2021), this mechanism needs to be proven and membrane receptors recognizing AGP-borne oligosaccharide fragments are not yet characterized. AGPs crosslinked with other cell-wall polysaccharides, especially pectins, can also modulate the plasma membrane-cell wall continuum and cell to cell adhesion (Schultz et al., 1998; Showalter, 2001). FLAs can be involved in crosslinking and cell wall adhesion through the interactions of their FLA domains in the protein core – a mechanism proposed based on their similarity with animal fasciclins and their homophilic interactions, which influence developmental processes (Snow et al., 1989; Elkins et al., 1990). The crosslinking with pectins through PAC (Proline-rich Arabinogalactan protein and Conserved Cysteines) domain is another putative mechanism. This type of interaction was documented for AtAGP31 (Hijazi et al., 2014). The protein even interacted with itself through PAC domain *in vitro* (Hijazi et al., 2014).

Arabinogalactan proteins are often attached to the outer side of the plasma membrane by a GPI-anchor. GPI-anchored proteins act as signal transductors that may enable the targeting of partner receptor-like kinases or modulate ligand recognition specificity as co-receptors (Yeats et al., 2018; Zhou, 2019). A proposed function of AGPs may be related to the cleavage of GPI-anchors, which may generate intracellular messengers or extracellular signals to neighboring cells (Schultz et al., 1998; Showalter, 2001). However, this remains to be conclusively proven. The cleavage of the anchor may also release the plasma membrane from the cell wall matrix, influencing membrane dynamics, including the trafficking of membrane receptors between the plasmalemma and inner compartments (Seifert, 2020). AGPs might act as a cargo linkage/receptor during the

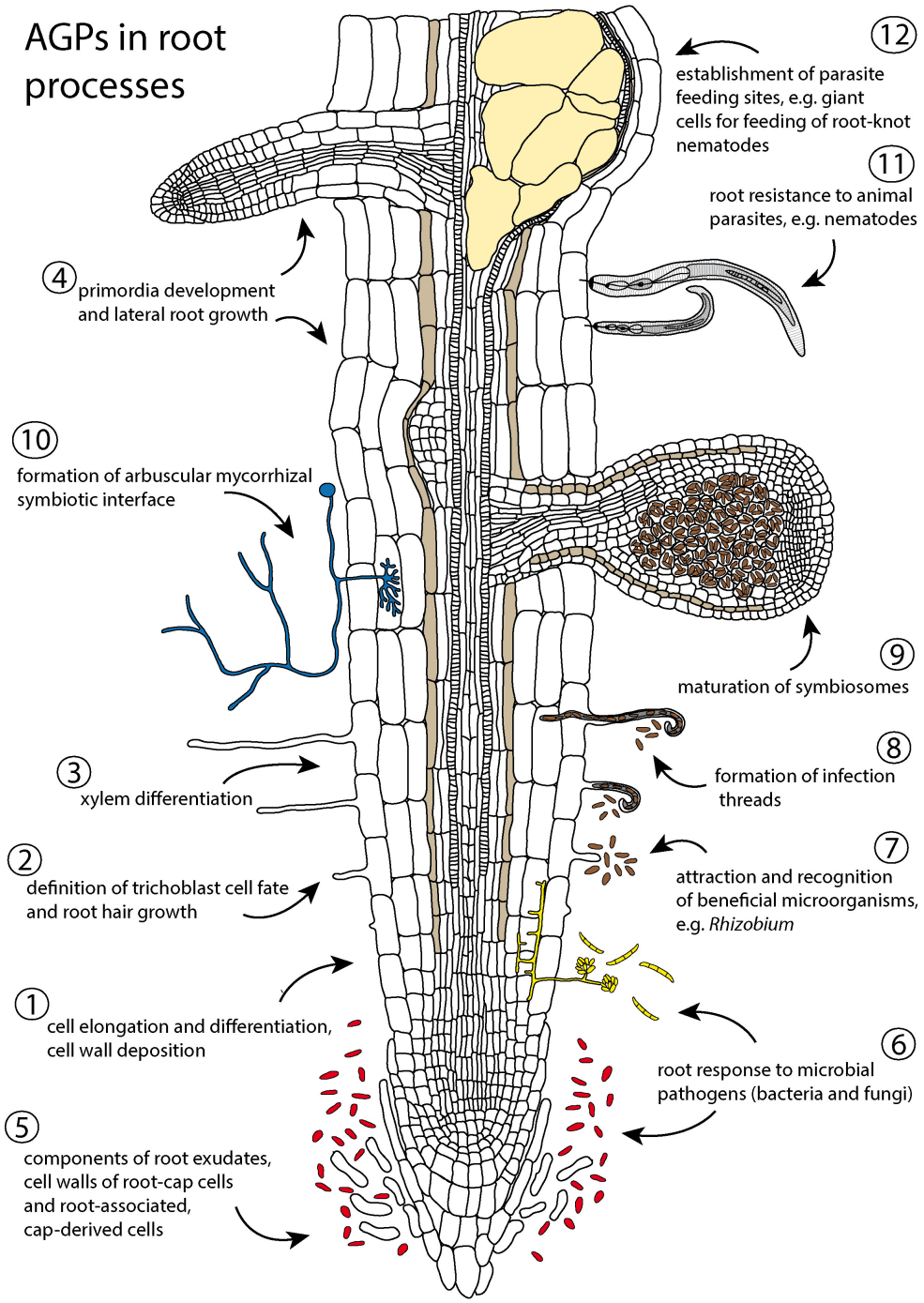

FIGURE 1 | Schematic summary of the involvement of arabinogalactan proteins (AGPs) in root processes. (1–4) AGPs modulate cell wall properties and regulate developmental events in roots: (1) cell division, cell expansion and cell wall deposition (Shi et al., 2003; Yang et al., 2007; Zhang et al., 2011; Seifert, 2018, 2021; Tucker et al., 2018), (2) trichoblast definition and root hair growth (Šamaj et al., 1999; Lin et al., 2011; Marzec et al., 2015; Kirchner et al., 2018; Borassi et al., 2020), (3) xylem differentiation (Dolan et al., 1995; Bossy et al., 2009), and (4) early events of lateral root development (Yang et al., 2007; Johnson et al., 2011; Zhang et al., 2011). (5–12) AGPs are components of root exudates and cell walls of root cap cells and root-associated, cap-derived cells (border cells and border-like cells) and participate in responses to biotic and abiotic environmental factors: (5–6) help to protect roots against abiotic stress (e.g., drought, toxicity) and microbial pathogens (Cannesan et al., 2012; Koroney et al., 2016; Marquez et al., 2018; Driouich et al., 2019; Galloway et al., 2020), (7–10) participate in establishment of mutualistic interaction with N-fixing microorganisms (Berry et al., 2002; Brewin, 2004; Brewin et al., 2008; Tsyganova et al., 2009, 2019; Nguema-Ona et al., 2013), arbuscular fungi (Gollotte et al., 1995; Balestrini and Lanfranco, 2006; Schultz and Harrison, 2008) and beneficial endophytes (Basińska-Barczak et al., 2020; Nivedita et al., 2020), and (11–12) affect root susceptibility to parasites (Beneventi et al., 2013; Bozbuga et al., 2018).

TABLE 1 | Mutants with modulated expression of *AGP* genes showing phenotypic manifestations in root system.

Gene, locus identifier	Species	Mutant	Gene modulation	Phenotypic manifestations in root system	Important effects in other plant organs
AGP mutants with observed root phenotypes					
AtFLA1, At5g55730	*A. thaliana*	*fla1*	Knock-out T-DNA	*fla1*:higher number of lateral roots, longer primary roots, altered pericycle cell division on callus inducing medium (Johnson et al., 2011)	*fla1*:reduced shoot regeneration from root explants *in vitro*, no shoot phenotype under normal growth conditions (Johnson et al., 2011)
AtFLA3, At2g24450	*A. thaliana*	*fla3*	Knock-down (RNAi)	*fla3*:no root phenotype observed (Li et al., 2010)	*fla3*:shorter siliques, less seeds, abnormal non-viable pollen grains (Li et al., 2010)
		FLA3-ox	Overexpression	*FLA3*-ox: enhanced primary root growth, formation of abnormal root cap cells (Li et al., 2010)	*FLA3*-ox: larger leaves, reduced female fertility, very short siliques, less seeds (Li et al., 2010)
SOS5/AtFLA4, At3g46550	*A. thaliana*	*sos5/atfla4*	EMS mutag.	*sos5/atfla4*: defective cell expansion, reduced root growth under salinity, altered cell wall structure (Shi et al., 2003), recovered by external ABA (Seifert et al., 2014; Xue and Seifert, 2015)	*sos5/atfla4*: slightly larger leaves, longer petioles, shorter siliques (Shi et al., 2003)
AtAGP8, At2g45470	*A. thaliana*	*agp8*	Knock-out (T-DNA)	*agp8*: increased susceptibility to root-knot nematodes (Bozbuga et al., 2018)	*agp8*: not analyzed
AtAGP14, At5g56540	*A. thaliana*	*agp14*	Knock-out (T-DNA)	*agp14*: longer root hairs in control and low-Pi conditions (Lin et al., 2011)	*agp14*:not analyzed
AtAGP15, At5g11740	*A. thaliana*	*agp15*	Knock-out (T-DNA)	*agp15*: contiguous root hair formation milder then *atagp21* (Borassi et al., 2020)	*agp15*: not analyzed
AtAGP17, At2g23130	*A. thaliana*	*rat1/agp17*	Knock-down (T-DNA)	*rat1/agp17*: roots resistant to *Agrobacterium* transformation (Nam et al., 1999; Gaspar et al., 2004)	*rat1/agp17*: not analyzed
AtAGP18, At4g37450,	*A. thaliana*	*agp18*	Knock-down (RNAi)	*agp18*: no root phenotype observed (Acosta-García and Vielle-Calzada, 2004)	*agp18*: higher seed abortion (Acosta-García and Vielle-Calzada, 2004)
		AGP18-ox	Overexpression	*AGP18*-ox: shorter primary roots, lower number of lateral roots (Zhang et al., 2011)	*AGP18*-ox: abnormal survival of megaspores (Demesa-Arevalo and Vielle-Calzada, 2013), smaller rosettes with multiple branches, less viable seeds, short siliques (Zhang et al., 2011)
AtAGP19, At1g68725	*A. thaliana*	*agp19*	Knock-out (T-DNA)	*agp19*: reduced lateral root number, smaller vascular cylinder of primary root (Yang et al., 2007; Zhang et al., 2011)	*agp19*: reduced cell division and expansion in shoot, shorter siliques, less seeds (Yang et al., 2007)
AtAGP21, At1g55330	*A. thaliana*	*agp21*	Knock-out (T-DNA)	*agp21*: contiguous root hair formation (Borassi et al., 2020)	*agp21*: not analyzed
AtAGP30, At2g33790	*A. thaliana*	*agp30*	Transposon insertion	*agp30*: inhibited initiation of adventitious roots from a callus culture, faster germination, lower sensitivity to external ABA (Van Hengel and Roberts, 2003)	*agp30*: not analyzed
		AGP30-ox	Overexpression	*AGP30-ox*: not analyzed	*AGP30-ox*: inhibited shoot development (Van Hengel and Roberts, 2003)
BcFLA1	*Brassica carinata*	*bcfla1*	Knock-down (CRISPR)	*bcfla1*: reduced root-hair length in Pi-deficient conditions (Kirchner et al., 2018)	*bcfla1*: not analyzed

EMS-mutag, selected from ethane-methyl-sulfonate mutagenized population; HSR, high sugar response; MUR, murus; RAT, resistant to agrobacterium transformation; SOS, Salt Overly Sensitive; T-DNA, T-DNA insertion.

endocytosis of extracellular material (Wang et al., 2019). The function of AGPs is likely related to the general adhesive properties of their peripheral carbohydrate moieties, which are Ca^{2+} and pH-dependent (Tan et al., 2018). AGPs are putative calcium capacitors (Lamport and Varnai, 2013; Lopez-Hernandez et al., 2020), which bind Ca^{2+} in a reversible and pH-dependent manner and thus enable Ca^{2+} oscillations and signal transduction (Lamport and Varnai, 2013; Lamport et al., 2018). *Arabidopsis thaliana* mutants with compromised glucuronidation of arabinogalactans and AGPs have reduced Ca^{2+}-binding capacity, disrupted calcium wave propagation in roots, and show serious growth defects (Lopez-Hernandez et al., 2020). The complexity of putative functions and available study tools still did not provide consistent insight into physiological aspects of this protein family.

AGPS IN PLANT ROOTS

Arabinogalactan proteins are abundant throughout the plant body, including the roots. Su and Higashiyama (2018) summarized expression data for 130 of 151 *AtAGP* genes (including all subgroups; classical AGPs, AG peptides, FLA, XYPL, PAG, etc.) and many of them were expressed in roots. In *Populus trichocarpa*, 18 of 35 identified *PtrFLA* genes were analyzed by qRT-PCR and all of them were expressed in roots (Zang et al., 2015). In *Triticum aestivum*, all 34 identified *TaFLA* genes were expressed mostly in seeds and roots (Faik et al., 2006). In *Oryza sativa*, 10 of the 69 identified *OsAGPs* were abundantly expressed in roots (Ma and Zhao, 2010). AGP epitopes, localized via an immuno-histochemical approach, appeared differentially in various root tissues: pericycle sectors according to vascular tissue context (Knox et al., 1989; Casero et al., 1998), developing vascular tissues, trichoblasts, atrichoblasts, growing root hairs, root caps, and border cells, for review see Showalter (2001) and Nguema-Ona et al. (2012).

Early experiments with β-Glc-Yariv reagent, which interacts with AGPs, precipitates them from solution and disrupts their activity (Yariv et al., 1967; McCartney et al., 2003), indicated a significant role for AGPs in root growth. The β-Glc-Y-enriched medium strongly reduced growth of both the root and the shoot, but the compound itself accumulated only in root. Shoot growth inhibition thus seems to be a secondary effect of the affected root system (Willats and Knox, 1996). The impaired cell elongation of the cortical cells and the bulging of the rhizodermal cells within the elongation and differentiation zones are the primary effects of the treatment (Willats and Knox, 1996; Ding and Zhu, 1997). The ability of β-Glc-Yariv to trigger cell bulging and disorganization of cortical microtubules in roots of *A. thaliana* was later confirmed by Nguema-Ona et al. (2007). Although not specific for a particular AGP, β-Glc-Yariv highlighted the importance of AGPs in root growth and cell differentiation.

A more focused classification of functional mechanisms comes from the study of particular mutants. Disturbances of polysaccharide metabolism and AGP carbohydrate moieties were associated with reduced primary root growth in *reb1/rhd1* (*root epidermal bulger 1/root hair defective 1*), a galactose biosynthesis mutant of *A. thaliana* (see below) (Baskin et al., 1992; Nguema-Ona et al., 2006). Its phenotype can be suppressed by supplementing growth media with 10 mM galactose, which recovered root cell expansion and anisotropic growth of control (Nguema-Ona et al., 2006). Other evidence supporting the role of AGPs and their sugar moieties in root elongation came from the *mur1* (*murus 1*) mutant of *A. thaliana* with reduced fucosylation (see below), which induces a significant reduction of root elongation, and more interestingly, earlier and more frequent lateral root development (Van Hengel and Roberts, 2002). Developing primordia of *mur1* do not label for fucose-containing epitopes (Freshour et al., 2003). Unfortunately, neither of those experiment identified affected phase of lateral root development.

The protein SOS5/AtFLA4 (SALT OVERLY SENSITIVE 5/FLA ARABINOGALACTAN PROTEIN 4) is one of the best characterized AGP members. *A. thaliana sos5/fla4* mutant, with point mutation in the FAS domain of AtFLA4, displays reduced root growth under high salinity. This phenotype is caused by defected cell expansion (for more details see below) (Shi et al., 2003) and can be suppressed by external ABA application (Seifert et al., 2014). Another non-classical AGP influencing root growth and development is AtAGP30, which is not anchored by GPI into plasma membrane. The *atagp30* mutant of *A. thaliana* fails to initiate adventitious roots from a callus culture, but growth of already established roots, lateral roots and root hairs are apparently unaffected (Van Hengel and Roberts, 2003; Van Hengel et al., 2004). *AtAGP30* transcription starts in the primary root with germination, occurs mostly in the root tip and decreases as tissue differentiate (Van Hengel and Roberts, 2003; Van Hengel et al., 2004). Interestingly, its ectopic overexpression is detrimental for shoot development and stable overexpression transformants are not viable (Van Hengel and Roberts, 2003). A recent study linked AtAGP30 with restriction of cadmium (Cd) entrance and root tip tolerance to this stressor (Jing et al., 2019). It seems that the ability to maintain *AtAGP30* expression under Cd stress is proportional to the level of Cd tolerance (Jing et al., 2019). Unfortunately, it is a pure speculation whether for example Cd retention in the cell wall or membrane protection due to AtAGP30 presence is involved.

AGP presence during lateral root development was indicated by positive antibody labeling in e.g., *Musa* spp. (Wu et al., 2017) or *Solanum lycopersicum* (Sala et al., 2017). However, there are not many reports connecting AGPs with lateral root development. Mutant *atfla1* of *A. thaliana* produces a higher number of lateral roots compared to the wild type, which suggests the role of AtFLA1 in early events of lateral root development (Johnson et al., 2011). The phase of lateral root primordia development (initiation, development and outgrowth) which is affected in *atfla1* and can cause the observed phenotype has not been defined. However, peculiar differences in pericycle division of *atfla1* on callus inducing medium hint at initiation and/or starting divisions. *AtFLA1* expression is not root-specific but was detected in the elongation zone of primary roots, and in the meristem and vasculature of lateral roots (Johnson et al., 2011). Cell division as well as cell expansion were affected also in *atagp19* mutant (Yang et al., 2007; Zhang et al., 2011) resulting

in plants with fewer lateral roots, and a smaller vascular cylinder of the primary root due to the lower number of procambial cells. Unfortunately, this is mentioned without any details (Yang et al., 2007), only later commented by Zhang et al. (2011). AtAGP19 along with AtAGP17 and AtAGP18 are members of a subfamily of lysine-rich classical AGPs. AGP19 is abundant in the central cylinder of roots (Yang et al., 2007, 2011). Interestingly, decreasing the arabinogalactosylation of AGPs reduces primary root growth (Gille et al., 2013), but induces longer lateral roots in *A. thaliana* (Ogawa-Ohnishi and Matsubayashi, 2015). It is possible that altered carbohydrate side chains of AGPs modify their ability to crosslink *in muro* resulting in changes to cell wall mechanical properties that manifests during cell expansion and organ growth.

Several other AGPs are linked with root growth. *AtFLA3* is barely expressed in the mature roots of wild-type *A. thaliana*, but its ectopic overexpression stimulates primary root growth and triggers the formation of abnormal root cap cells (Li et al., 2010). In contrast, ectopic overexpression of *AtAGP18* significantly inhibits root growth (Zhang et al., 2011). AtAGP18 regulates megaspore development (Demesa-Arevalo and Vielle-Calzada, 2013) but it is expressed also in roots, mostly in vascular tissues (Yang and Showalter, 2007), and its expression is under the control of ABA (Zhang et al., 2011). The AtAGP18-RNAi silenced lines have a high rate of seed abortion. Root growth phenotype was not observed in the same study but it was not analyzed in details (Acosta-García and Vielle-Calzada, 2004). AtAGP18 would therefore be an interesting candidate for future root-focused studies.

ROOT HAIRS

Several pieces of evidence implicate some AGPs in the regulation of root hair initiation and growth. Aberrant root-hair development in *atagp21* is connected with contiguous root hair formation and high root hair density (Borassi et al., 2020). AtAGP21 is a part of the brassinosteroid regulatory circuits upstream of GL2 (GLABRA2), RHD6 (ROOT HAIR DEFECTIVE 6) and other downstream transcription factors determining the development of epidermal cells into root hairs. AtAGP21 itself is positively regulated by the BZR1 transcription factor and acts as a suppressor of GL2 (Borassi et al., 2020). A root-hair phenotype similar to *atagp21* also occurs in other *A. thaliana* mutants with altered AGP content, such as O-glycosylation, fucosylation, or arabinosylation of AGPs, e.g., *atagp15*, *hpgt* (Ogawa-Ohnishi and Matsubayashi, 2015; Borassi et al., 2020). The *hpgt1-1 hpgt2-1 hpgt3-1* triple-mutant is defective in O-glycosylation of AGPs due to the disruption of hydroxyproline galactosyltransferase 1–3 and forms longer and more dense root hairs compared to wild-type plants (Ogawa-Ohnishi and Matsubayashi, 2015). O-glycosylation of AtAGP21 is essential for its function, particularly secretion and cellular targeting (Borassi et al., 2020). Contiguous root hair development can also be triggered by β-Glc-Y (α-Man-Y has no effect) crosslinking AGPs and limiting their action in the cell wall, providing additional evidence for the role of AGPs in determining rhizodermal-cell fate in *A. thaliana* (Borassi et al., 2020). Another piece of evidence linking AGPs and root hair growth is a long-hair phenotype of *agp14* mutant of *A. thaliana* (Lin et al., 2011) and a short-hair phenotype of higher-order *glcat14* (β-*glucuronosyl-transferases 14A-C*) mutants of *A. thaliana* with increased AGP contents (Zhang et al., 2020).

The role of AGPs in the determination of rhizodermal-cell fate is further supported by studies on other plant species. In *Zea mays* and *Hordeum vulgare*, specific AGP epitopes were detected on the surface of trichoblasts and root hairs, which differed from those of atrichoblasts (Šamaj et al., 1999; Marzec et al., 2015). Moreover, epitopes detected by LM2, LM14, and MAC207 antibodies, which are normally present at the surface of trichoblasts in *H. vulgare*, were absent in the rhizodermis of barley *root-hairless mutant 1* (Marzec et al., 2015). In *Brassica carinata*, downregulation of *BcFLA1*, encoding a FLA AGP, via CRISPR/Cas9 significantly reduced root-hair length in phosphate-deficient conditions (Kirchner et al., 2018). *BcFLA1* expression was enhanced by Pi deficiency, specifically in the low-P efficient cultivar of *B. carinata*. This cultivar is efficient in Pi uptake and increases the length of root hairs in Pi-deficient conditions considerably (Kirchner et al., 2018).

Interestingly, extensin related modifications of O-glycosylation did affect the root hair growth but not cell fate (Velasquez et al., 2015). Proline-rich extensin-like receptor kinase 13 (PERK13) was shown to provide negative control of root hair growth. *A. thaliana* mutant *rhs10/perk13* (*root hair specific 10/proline-rich extensin-like receptor kinase 13*) has longer root hairs. PERK13 has AGP motifs in its extracellular domain, which may be important for its regulatory function (Hwang et al., 2016). It is proposed that AGP motifs sense the cell-wall integrity, triggering down-stream signal transduction (Cho, 2016). These results taken together indicate that AGPs might affect root hair formation via sensing or modification of cell wall properties, and can participate in signaling pathways controlling root-hair cell fate by an interaction with other proteins or cell wall components, e.g., receptor-like kinases or pectins.

ROOT CELL EXPANSION, DIFFERENTIATION, AND CELL-WALL PROPERTIES

As for other plant organs, the growth of roots is determined by cell division, elongation, and differentiation, which are tightly connected with cell wall characteristics. Cell wall composition and mechanical properties are developmentally regulated and respond to environmental factors (Cosgrove, 2005; Caffall and Mohnen, 2009; Somssich et al., 2016; Rui and Dinneny, 2020). Localization of GPI-anchored AGPs on the outer surface of the plasma membrane and their linkage to other cell wall components make them putative linkers of protoplast and the cell wall. β-D-glucosyl units of "active Yariv" reagent (Yariv et al., 1967) bind and precipitate AGPs, disrupting their action. Such treatment, similar to anti-AGP antibodies, induces rearrangement of microtubule cortical arrays in rhizodermal cells within minutes (Nguema-Ona et al., 2007) and stimulates an

intense swelling of epidermal cells in the elongation zone in the longer term in *A. thaliana* (Ding and Zhu, 1997; Nguema-Ona et al., 2007). The impaired cell elongation was also observed in cell suspension cultures of *Daucus carota* (Willats and Knox, 1996).

A similar effect of AGPs on cell volume expansion is induced if the AGP glycosylation machinery is affected. Mutations in AGP-specific O-galactosyltransferases lead to defects in cell expansion. The *galt2 galt5* (*hydroxyproline-O-galactosyltransferase 2,5*) mutant of *A. thaliana* has two disrupted AGP-specific galactosyltransferases, which are important for binding the galactose to the protein backbone and initializing O-glycosylation (Basu et al., 2013, 2015). Together with the lower glycosylation status of AGPs, the mutant displays reduced seed-coat cellulose content, swollen root-tip cells, and other root growth defects, e.g., inhibition of root growth, reduction of root hair length and density (Basu et al., 2015). Shorter roots were observed also in the quintuple mutant *galt2 galt3 galt4 galt5 galt6*, but surprisingly this mutant formed longer root hairs compared to wild type (Zhang et al., 2021). All these observations highlight the importance of O-glycosylation in cell growth and cell wall deposition (Basu et al., 2015; Showalter and Basu, 2016). In addition, the disruption of two Golgi-localized exo-β-1,3-galactosidases of glycoside hydroxylase family 43 (GH3) in the *gh43* mutant of *A. thaliana* increases the content of cell-wall bound AGPs and triggers serious defects in root cell expansion and adhesion, e.g., root epidermal cell swelling and loss of anisotropic growth (Nibbering et al., 2020). These exo-β-1,3-galactosidases are putatively involved in the processing of AGPs during their maturation in the Golgi, regulating the length of the β-1,3-galactan backbone of AGPs, and altering the affinity of mature AGPs to other cell wall components (Nibbering et al., 2020).

The connection between AGP glycosylation and regulation of root cell expansion and cell wall properties is highlighted in other studies, where galactosylation and fucosylation are modified, affecting AGPs along with pectins and hemicelluloses. The *A. thaliana* mutant *mur1* with a disrupted GDP-D-mannose-4,6-dehydratase enzyme of the GDP-L-fucose biosynthetic pathway contains less L-fucose in cell walls (Reiter et al., 1993; Bonin et al., 1997). L-fucose is a minor component of AGPs (Silva J. et al., 2020) as well as xyloglucans (Somssich et al., 2016). The L-fucose deficient mutant shows reduced root elongation by more than half compared to the wild type, and swollen root tips. Root growth inhibition is caused by a significant reduction in cell elongation, while the activity of root apical meristem is normal (Bonin et al., 1997; Van Hengel and Roberts, 2002). Alteration of root cell anisotropic growth occurs also in the *reb1/rhd1* mutant (Baskin et al., 1992). Reduced root elongation and bulging trichoblasts observed in this mutant (Baskin et al., 1992; Andème-Onzighi et al., 2002) seem related to altered galactosylation of cell-wall xyloglucans (Nguema-Ona et al., 2006). The mutant has defective UDP D-galactose 4-epimerase enzyme (Seifert et al., 2002) and makes structurally different cell wall xyloglucans, which are devoid of galactose and fucose residues (Nguema-Ona et al., 2006). There is also an obvious link to AGPs and cytoskeletal structures, as the trichoblasts of *reb1/rhd1* have disorganized microtubules and lack AGPs detectable by JIM14 and LM2 antibodies (Andème-Onzighi et al., 2002). However, the functional link is currently not known.

Mutant *dim/dwf1 (diminuto/dwarf1)* of *A. thaliana* in the brassinosteroid biosynthesis gene DIM/DWF1 (Klahre et al., 1998) is strongly affected in cell elongation and has reduced cellulose and lignin content (Hossain et al., 2012). The *dim/dwf1* phenotype correlates with the amount of AGPs in the tissue, highlighting the role of AGPs in cell expansion (Takahashi et al., 1995) and implicating them in an executive part of the brassinosteroid signaling circuit (Jia et al., 2020).

Stress-Enhanced Developmental Response

Arabinogalactan protein-related growth defects often manifest strongly in the presence of high salinity or other stress factors, and are linked to cell wall integrity, maintenance, and adjustment of mechanical properties (Rui and Dinneny, 2020). Synthesis of L-arabinose, which is incorporated into AGPs, EXTs and some cell wall polysaccharides, depend on the *MUR4/HSR8* (*MURUS4/HIGH SUGAR RESPONSE 8*) Golgi-localized UDP-D-xylose 4-epimerase. Plants of *mur4/hsr8* show a significant reduction of L-arabinose (Reiter et al., 1997; Burget and Reiter, 1999; Burget et al., 2003) and a strong short-root phenotype under salinity, but not in either standard or osmotic stress (mannitol treatment) growth conditions (Zhao et al., 2019). Analysis of *mur4/hsr8* mutant indicates defective cell wall structure but not signaling. This phenotype results in decreased root elongation and also cell-cell adhesion, resulting in epidermal discontinuity and bursting of cells (Zhao et al., 2019). Described defects were rescued by exogenous arabinose, but not glucose or xylose, confirming UDP-Ara biosynthesis consequence and affecting the level of AGP staining in roots (Zhao et al., 2019). Other enzymes affecting cell-wall AGPs are FUT4 and FUT6 (α-1,2-fucosyltransferases 4, 6), which are responsible for their fucosylation. Double mutant of *A. thaliana fut4 fut6* has lower content of fucose and xylose in AGP extracts and short-root phenotype under conditions of salt stress (Tryfona et al., 2014).

The role of AGPs as pectin plasticizers and regulators of cell-wall extensibility under salt stress was proposed rather early (Zhu et al., 1993; Lamport et al., 2006; Olmos et al., 2017). Interestingly, AGPs isolated from roots (and other organs) of the seagrass *Zostera marina* reportedly had specific characteristics, distinguishing them from the AGPs of land plants (high degree of branching, high content of terminal α-L-arabinose), which might enhance the salt tolerance of this marine species (Pfeifer et al., 2020). In *Urochloa decumbens*, AGP epitopes accumulated in root cell walls of after aluminum treatment to maintain cell wall flexibility and increase the high-aluminum tolerance of this tropical grass (Silva T.F. et al., 2020). A recently proposed alternative model of AGP action under salinity stress is their function as carriers, binding Na^+ ions and transferring them into the vacuole via vesicle trafficking (Olmos et al., 2017).

One of the best characterized AGPs in the context of salinity is SOS5/FLA4. The salt-sensitive mutant *sos5/fla4* of *A. thaliana* has swollen root-tip cells due to abnormal cell expansion occurring under salt stress (Shi et al., 2003). Cell walls of *sos5/fla4* have

an altered structure. The pectin-rich middle lamella, essential for intercellular adhesion, is reduced and primary cell walls are thinner and less organized compared to the wild type (Shi et al., 2003). Interestingly, the hypertensive *sos5/fla4* root phenotype under salt stress is milder in ABA-oversensitive mutants and suppressible by exogenous application of ABA (Seifert et al., 2014; Acet and Kadioglu, 2020). The protein might act synergistically with ABA as a putative modulator of ABA signaling upstream of cell wall biosynthesis (Seifert et al., 2014) and independent of the RBOHD and RBOHF (RESPIRATORY BURST OXIDASE HOMOLOG D,F) NADH oxidases (Xue and Seifert, 2015) of the ABA-signaling pathway controlling root growth (Jiao et al., 2013).

Interaction between ABA and SOS5/FLA4 modulates the content of H_2O_2 under salt stress (Acet and Kadioglu, 2020), indicating a more significant signaling rather than structural role for SOS5/FLA4. This is consistent with an identical phenotype reported previously for two AGP-specific galactosyltransferases (GALT2 and GALT5), fasciclin-like AGP (SOS5/FLA4) and two leucine rich repeat receptor kinases (FEI1 and FEI2) (Shi et al., 2003; Xu et al., 2008; Basu et al., 2015), which placed those components into a single regulatory pathway (Basu et al., 2016) and derived speculation that SOS5/FLA4 might act as a sensor of conditions in the apoplast via FEI kinases (Turupcu et al., 2018; Seifert, 2021). SOS5/FLA4 tagged with GFP was detected on the plasma membrane, soluble in the apoplast, and in endosomes (Xue et al., 2017). Its C-terminal fasciclin 1 domain (Fas1-2) is essential for its function, possibly involved in molecular interactions. The N-terminal Fas1 domain (Fas1-1) stabilizes proteins in the plasma-membrane (Xue et al., 2017), and it is a putative negative regulator of Fas1-2 binding to FEI1 kinase, which might augment the regulation of root growth according to environmental conditions (Turupcu et al., 2018; Seifert, 2021).

The roles of other individual AGPs and their subtypes still remain to be elucidated, but there is extensive experimental evidence (often coming from organs other than roots) which supports their role in cell wall biochemistry, deposition, and signaling. Modulation of *EgrFLA1,2,3* expression levels in *Eucalyptus grandis* (MacMillan et al., 2010, 2015), *PtFLA6* in *Populus* (Wang et al., 2015), *AtFLA11*, *AtFLA12*, and *AtFLA16* in *A. thaliana* (MacMillan et al., 2010; Liu et al., 2020) altered stem cell-wall polysaccharide composition, cell-wall thickness, and stem mechanical properties. *GhAGP3* and *GhAGP4* are specifically expressed during the transition between cell elongation to the secondary cell wall deposition in developing cotton (*Gossypium hirsutum)* fibers, highlighting their roles during secondary cell wall formation (Liu et al., 2008). In *Physcomitrella patens*, application of AGP binding β-Glc-Yariv or the downregulation of *AGP1* reduced the expansion of the protonema apical cell (Lee et al., 2005).

ROOT INTERACTIONS WITH OTHER ORGANISMS

Roots provide an interface for interaction with rhizosphere biota. AGPs, putative environment-cell-wall-protoplast signal transductors (Seifert and Roberts, 2007), are important components of root exudates and root cell walls, especially in the root-cap and root-associated, cap-derived cells (Vicré et al., 2005; Cannesan et al., 2012; Koroney et al., 2016; Swamy et al., 2016; Driouich et al., 2019) and aid in the formation of the rhizosheath (Galloway et al., 2020). As such, they are likely mediators of root-microorganism interactions, participating in the attraction, recognition, and colonization of roots by beneficial microorganisms as well as in root responses to microbial pathogens (Nguema-Ona et al., 2012, 2013, 2014; Mareri et al., 2018) and parasites (Bozbuga et al., 2018).

Mutualistic Interactions

AGPs and chimeric arabinogalactan protein-extensins (AGPEs) take part in the mutual interactions between roots and microorganisms. AGP-epitopes were found at arbuscular mycorrhiza symbiotic interfaces (Gollotte et al., 1995; Balestrini and Lanfranco, 2006). The involvement of MtAMA1 (ARBUSCULAR MYCORRHIZA AGP 1) in arbuscular mycorrhiza is indicated by the specific expression of the *MtAMA1* gene exclusively in arbuscule containing cortical cells of *Medicago truncatula* (Schultz and Harrison, 2008). Its mode of operation in the plant-fungi interface is still unknown, but signaling feedback from the cell wall might be anticipated. The authors speculate about a possible coreceptor on the plasma membrane or a mobile signaling molecule after its release from plasma membrane by the cleavage of the GPI anchor (Schultz and Harrison, 2008). Interestingly, two AGP-like (AGL) proteins were identified in the genome of *Glomus intraradices*, with a specific structure not found in plants or non-mycorrhizal fungi. These GiAGLs contain repeat domains that can form polyproline II helices with positively and negatively charged faces. The authors suggest their role in the interaction with host cell wall surface (Schultz and Harrison, 2008). Unfortunately, there are few recent references on this particular topic.

A symbiont as a source of AGPs at the host interface was recorded also from free-living cyanobacteria *Nostoc*, containing a putative AGP peptide genes (classical AGP, AG peptide, and FLA class) and cell surface epitopes responsive to AGP antibodies were detected at the *Nostoc-Gunnera* interface (Jackson et al., 2012). Their discovery suggests that the role of AGPs in the host-symbiont interface might develop from rather ancient cell surface interaction processes and AGP role might evolutionarily originate from very early symbioses (Jackson et al., 2012).

Interaction via AGPs during symbiotic infection by nitrogen-fixing rhizobia has been repeatedly proven, for review see Brewin (2004), Brewin et al. (2008), Nguema-Ona et al. (2013), Rashid (2016). Formation of new lateral root organs - nodules colonized by rhizobia, is a tightly orchestrated process, which is mainly initiated by microbial entry via an infection thread (Coba de la Pena et al., 2017; Ferguson et al., 2019). Rhizobia traveling through infection threads are embedded in a matrix containing AGPEs and other glycoproteins (Rathbun et al., 2002; Brewin, 2004; Reguera et al., 2010). Abnormal infection thread development in *Pisum sativum* mutants (*sym33; sym 40*) is associated with disrupted targeting of AGPEs (MAC265 antibody) exocytosis and authors speculate that this might be

correlated with inefficient symbiosome formation in mutants (Tsyganova et al., 2009). Cell wall remodeling that takes place during onset of the symbiosome (Coba de la Pena et al., 2017; Tsyganova et al., 2019) is the potentially affected process. AGPs (localized with JIM1 antibody) are present in the nodule membranes during the maturation of symbiosomes in *Pisum* (Tsyganova et al., 2019). Their significance is still unclear but their presence was not observed in nodules of the *sym31* mutant (Tsyganova et al., 2019) with undifferentiated bacterioids and symbiosome membranes staying in the juvenile state (Borisov et al., 1997). This indicates that AGPs play a role in symbiosome maturation and ontogeny (Tsyganova et al., 2019). AGPs are abundant also in the actinorhizal nodules of *Alnus*, especially during early nodulation stages (Berry et al., 2002).

In addition, *AGP*-encoding genes are upregulated in *Oryza sativa* roots upon colonization by *Piriformospora indica* (Nivedita et al., 2020), a beneficial growth-promoting fungal endophyte that improves salt-stress tolerance in many plant species (Waller et al., 2005; Trivedi et al., 2013). In *Triticum aestivum*, AGP-epitopes (detected by JIM14) occur abundantly in roots infected by *Trichoderma* ssp., a beneficial fungal antagonist of phytopathogens (Basińska-Barczak et al., 2020). These recent observations indicate that AGPs may also promote root interaction with beneficial endophytes.

Response to Pathogens and Parasites

Analyzing the role of AGPs in root response to pathogens, a suppressive role to early infection by microbial pathogens was demonstrated by AGPs extracted from border cells (BC) of *Pisum sativum* and border-like cells (BLC) of *Brassica napus* (Cannesan et al., 2012). AGPs from BL and BLC attracted zoospores of oomycete *Aphanomyces euteiches* and induced their encystment (loss of the motility due to loss of the flagella). The attraction was far more efficient for *P. sativum* extract in agreement with the fact that *A. euteiches* is the pathogen of *P. sativum* not *B. napus*. Root exudates, but not extracted AGPs, then strongly stimulated their germination (Cannesan et al., 2012). Root-associated, cap-derived cells (BC and BLC) thus act as a blind target, trapping the pathogen (extracellular root trap) and preventing its contact with the root proper (Hawes et al., 2000; Driouich et al., 2019; Ropitaux et al., 2020).

There is also substantial evidence that the composition of AGPs in roots or root exudates changes in response to pathogens or parasites. In *Solanum tuberosum*, AGPs (detected with LM2 and JIM15 antibodies) were upregulated in root exudates in response to elicitors derived from *Pectobacterium atrosepticum*, the pathogen causing soft rot disease in potato (Koroney et al., 2016). In *Musa* spp. roots, AGPs were upregulated by *Fusarium oxysporum* f. sp. *cubense* infection (Wu et al., 2017). Changes in AGP levels occurred in the roots of *A. thaliana* infected by *Plasmodiophora brassiace*, which caused clubroot disease. In this case, AGPs were mostly downregulated, but FLA5 was upregulated together with many cell-wall-modifying enzymes, alpha-expansins in particular (Irani et al., 2018). In the roots of *Glycine max*, repression of *FLA* encoding genes was induced by the fungal pathogen *Macrophomina phaseolina* (Marquez et al., 2018) trying to seize root tissues. Besides microbial pathogens, animal parasites induce changes in root AGP levels as well. In roots of a resistant cultivar of *Glycine max*, the upregulation of *FLAs* is triggered by the attack of root-knot nematodes (Beneventi et al., 2013).

Fluctuation of AGP levels occurs also during the attack of parasitic plant species of *Cuscuta* genus on the host-plant stems. Epidermal contact of *Cuscuta reflexa* stimulates the secretion of AGPs by the host plant, *Lycopersicon esculentum,* to enhance its adhesion to the host stem in the early phase of interaction (Albert et al., 2006). Downregulation of *attAGP* (*attachment AGP)* expression decreased the attachment capability of the parasite (Albert et al., 2006). The presence of AGPs in attachment "cement" was recorded on the surface (holdfast epidermal cells) of *C. campestris and C. japonica* stems (Hozumi et al., 2017) supporting the role of AGPs in parasite-host attachment. Accumulation of AGPs in the tip of developing haustoria appear after penetration of the host stem (Hozumi et al., 2017; Shimizu and Aoki, 2019) and expression analysis of *Cuscuta* developing haustoria identified them as FLAs. On the contrary, the later intrusive growth of *Cuscuta* haustorium triggers the depletion of AGPs in stem tissues facing the attack, which was shown for *Pelargonium zonale* penetrated by *C. reflexa* (Striberny and Krause, 2015). In Orobanchaceae root parasites, AGPs accumulate in the hyaline body, a specialized parenchymatous central core of the parasitic haustorium. The functional significance of this accumulation is, however, unclear (Pielach et al., 2014).

Mechanisms of AGP action in root biotic interaction are still unresolved and puzzling. Several mechanisms were proposed, including the recognition and attachment of microbes, formation of a protective biofilm against degradation of cell wall by pathogenic organisms, or antimicrobial action, for review see Nguema-Ona et al. (2013) and Mareri et al. (2018). In addition, the significance of AGPs in response to pathogens is frequently inconclusive. They may act together with EXTs to modify the cell wall cross-linking in response to pathogens, for review see Rashid (2016). In some studies, EXTs seemed more important. Among others, EXTs rather than AGPs correlated with the resistance to *F. oxysporum* f. sp. *cubense,* in spite of the pathogen-induced changes in AGP levels in *Musa* spp. cultivars (Wu et al., 2017). β-Glc-Y reagent failed to affect the interaction with *Pectobacterium atrosepticum*, although AGPs were upregulated in response to this pathogen in *Solanum tuberosum* roots. Root exudate pre-incubated with β-Glc-Y promoted the growth of the pathogen in a very similar way as non-incubated one (Koroney et al., 2016). Higher levels of AGPs and also EXTs were detected in roots of a *Benincasa hispida* cultivar resistant to *F. oxysporum* f. sp. *Benincaseae* (Xie et al., 2011). Various studies indicate that other cell-wall glycoproteins (EXTs or AGPEs), are at least equally important and change their levels in roots in response to pathogens or symbionts (Shailasree et al., 2004; Plancot et al., 2013; Wu et al., 2017; Castilleux et al., 2020).

Further and more conclusive functional characterization of AGPs roles in root-pathogen interactions thus requires direct evidence based e.g., on modulation of *AGP*-genes expression and analyses of induced phenotypes. There are only few studies revealing the role of individual AGPs in this process. *A. thaliana*

rat1/agp17 (resistant to Agrobacterium transformation 1) mutant, defective in arabinogalactan protein AtAGP17, is resistant to *Agrobacterium* transformations of root segments (Nam et al., 1999; Gaspar et al., 2004). In spite of the difficulties with *AtAGP17* transcript detection in roots (Gaspar et al., 2004; Yang et al., 2007, 2011), the protein seems highly abundant in root tissues (Yang et al., 2011). It affects the attachment of *Agrobacterium* to the root surface and modulates the systemic acquired resistance, which allows for successful infection (Gaspar et al., 2004). Two other AGPs, *AtAGP12*, and *AtAGP24,* enhanced their expression in the roots of *A. thaliana* after infection of *Plectosphaerella cucumerina*, a necrotrophic fungal pathogen. AtAGP24-GFP localized in close proximity to plasma membrane and the overexpression of *AtAGP24* strongly increased the susceptibility to *P. cucumerina*, which is evidence for its involvement in the pathogen response (Dobon et al., 2015).

There is also direct evidence of the involvement of a particular *AGP* gene in root defense against animal parasites. The knock-out of *AtAGP8* gene in *A. thaliana* leads to a significantly increased susceptibility toward root-knot nematode *Meloidogyne incognita* (Bozbuga et al., 2018). The susceptibility seems related to the cell wall composition and resistance of root tissue to form specific feeding sites, giant cells. These hypertrophied multinucleate cells re-differentiate from a small number of root cells being pierced by a nematode stylet. Their cells walls contain AGPs and are enriched with highly methyl-esterified homogalacturonans, xyloglucans and arabinans, allowing for plasticity and cell expansion (Bozbuga et al., 2018). Increased susceptibility to root cyst nematode was also observed in *reb1/rhd1* mutant (Baum et al., 2000; Wubben et al., 2004) with lower AGP levels in roots (Ding and Zhu, 1997). Besides the *atagp8* and *reb1/rhd1* mutants, increased susceptibility to nematodes was found in two rhamnogalacturonan I pectin deficient mutants of *A. thaliana* (*arabinan deficient 1,2*), while mutants with suppressed mannan and galactan epitopes (*mannan synthesis-related 1* and β-*galactosidase 5*) were more resistant (Gantulga et al., 2008; Harholt et al., 2012; Wang et al., 2013; Bozbuga et al., 2018).

CONCLUSION

Cell-wall localized AGPs work as modulators of cell expansion and differentiation, signal transductors on the cell surface, and effectors of responses to environmental conditions and other organisms. In roots, the multifaceted roles of AGPs are emphasized due to the requirement for high growth plasticity and constant exchange of signals with the environment. The data gained from observing plants with altered expression of *AGPs* or carbohydrate composition of cell wall, immunohistochemical studies, and structural analyses clearly link AGPs and their glycosylation status with cell wall properties, cell expansion and organ growth.

Despite the obvious significance of AGPs, we still have limited information about the roles of individual AGPs in roots and the whole plant. Abundance of AGPs, the complexity of their functions, and their obvious redundancy make this issue challenging. A detailed focus on loss-of-function mutants can move us ahead in understanding the mechanisms of AGP action in roots. Characterization of AGP mutants were summarized in this review alongside other studies on cell wall chemistry to provide an overview of the current state of this topic.

AUTHOR CONTRIBUTIONS

DH performed the literature survey, drafted and wrote the manuscript. ET performed the literature survey, drafted and wrote the manuscript, and made the figure and table. AS conceptualized and finalized the manuscript. All authors contributed to the article and approved the submitted version.

ACKNOWLEDGMENTS

The authors thank Lena M. Hunt M.Sc. for English language correction.

REFERENCES

Acet, T., and Kadioglu, A. (2020). SOS5 gene-abscisic acid crosstalk and their interaction with antioxidant system in *Arabidopsis thaliana* under salt stress. *Physiol. Mol. Biol. Plants* 26, 1831–1845. doi: 10.1007/s12298-020-00873-4

Acosta-García, G., and Vielle-Calzada, J.-P. (2004). A classical arabinogalactan protein is essential for the initiation of female gametogenesis in *Arabidopsis*. *Plant Cell* 16, 2614–2628. doi: 10.1105/tpc.104.024588

Albert, M., Belastegui-Macadam, X., and Kaldenhoff, R. (2006). An attack of the plant parasite *Cuscuta reflexa* induces the expression of attAGP, an attachment protein of the host tomato. *Plant J.* 48, 548–556. doi: 10.1111/j.1365-313X.2006.02897.x

Andème-Onzighi, C., Sivaguru, M., Judy-March, J., Baskin, T. I., and Driouich, A. (2002). The reb1-1 mutation of *Arabidopsis* alters the morphology of trichoblasts, the expression of arabinogalactan-proteins and the organization of cortical microtubules. *Planta* 215, 949–958. doi: 10.1007/s00425-002-0836-z

Balestrini, R., and Lanfranco, L. (2006). Fungal and plant gene expression in arbuscular mycorrhizal symbiosis. *Mycorrhiza* 16, 509–524. doi: 10.1007/s00572-006-0069-2

Bartels, D., Baumann, A., Maeder, M., Geske, T., Heise, E. M., von Schwartzenberg, K., et al. (2017). Evolution of plant cell wall: arabinogalactan-proteins from three moss genera show structural differences compared to seed plants. *Carbohydr. Polym.* 163, 227–235. doi: 10.1016/j.carbpol.2017.01.043

Basińska-Barczak, A., Błaszczyk, L., and Szentner, K. (2020). Plant cell wall changes in common wheat roots as a result of their interaction with beneficial fungi of *Trichoderma*. *Cells* 9:2319. doi: 10.3390/cells9102319

Baskin, T. I., Betzner, A. S., Hoggart, R., Cork, A., and Williamson, R. (1992). Root morphology mutants in *Arabidopsis thaliana*. *Funct. Plant Biol.* 19, 427–437. doi: 10.1071/PP9920427

Basu, D., Liang, Y., Liu, X., Himmeldirk, K., Faik, A., Kieliszewski, M., et al. (2013). Functional identification of a hydroxyproline-o-galactosyltransferase specific for arabinogalactan protein biosynthesis in *Arabidopsis*. *J. Biol. Chem.* 288, 10132–10143. doi: 10.1074/jbc.M112.432609

Basu, D., Tian, L., Debrosse, T., Poirier, E., Emch, K., Herock, H., et al. (2016). Glycosylation of a fasciclin-like arabinogalactan-protein (SOS5) mediates root growth and seed mucilage adherence via a cell wall receptor-like kinase (FEI1/FEI2) pathway in *Arabidopsis*. *PLoS One* 11:e0145092. doi: 10.1371/journal.pone.0145092

Basu, D., Wang, W., Ma, S., DeBrosse, T., Poirier, E., Emch, K., et al. (2015). Two hydroxyproline galactosyltransferases, GALT5 and GALT2, function in arabinogalactan-protein glycosylation, growth and development in *Arabidopsis*. *PLoS One* 10:e0125624. doi: 10.1371/journal.pone.0125624

Baum, T., Wubben, M. K. II, Su, H., and Rodermel, S. (2000). A screen for *Arabidopsis thaliana* mutants with altered susceptibility to *Heterodera schachtii*. *J. Nematol.* 32:166.

Beneventi, M. A., da Silva, O. B., de Sá, M. E. L., Firmino, A. A. P., de Amorim, R. M. S., Albuquerque, ÉV. S., et al. (2013). Transcription profile of soybean-root-knot nematode interaction reveals a key role of phythormones in the resistance reaction. *BMC Genomics* 14:322. doi: 10.1186/1471-2164-14-322

Berry, A. M., Rasmussen, U., Bateman, K., Huss-Danell, K., Lindwall, S., and Bergman, B. (2002). Arabinogalactan proteins are expressed at the symbiotic interface in root nodules of *Alnus* spp. *New Phytol.* 155, 469–479. doi: 10.1046/j.1469-8137.2002.00466.x

Bonin, C. P., Potter, I., Vanzin, G. F., and Reiter, W.-D. (1997). The MUR1 gene of *Arabidopsis thaliana* encodes an isoform of GDP-D-mannose-4, 6-dehydratase, catalyzing the first step in the de novo synthesis of GDP-L-fucose. *Proc. Natl. Acad. Sci.* 94, 2085–2090. doi: 10.1073/pnas.94.5.2085

Borassi, C., Gloazzo Dorosz, J., Ricardi, M. M., Carignani Sardoy, M., Pol Fachin, L., Marzol, E., et al. (2020). A cell surface arabinogalactan-peptide influences root hair cell fate. *New Phytol.* 227, 732–743. doi: 10.1111/nph.16487

Borisov, A. Y., Rozov, S., Tsyganov, V., Morzhina, E., Lebsky, V., and Tikhonovich, I. (1997). Sequential functioning of Sym-13 and Sym-31, two genes affecting symbiosome development in root nodules of pea (*Pisum sativum* L.). *Mol. Gen. Genet.* 254, 592–598. doi: 10.1007/s004380050456

Bossy, A., Blaschek, W., and Classen, B. (2009). Characterization and immunolocalization of arabinogalactan-proteins in roots of *Echinacea purpurea*. *Planta Med.* 75, 1526–1533. doi: 10.1055/s-0029-1185801

Bozbuga, R., Lilley, C. J., Knox, J. P., and Urwin, P. E. (2018). Host-specific signatures of the cell wall changes induced by the plant parasitic nematode, *Meloidogyne incognita*. *Sci. Rep.* 8:17302. doi: 10.1038/s41598-018-35529-7

Bradley, D. J., Kjellbom, P., and Lamb, C. J. (1992). Elicitor-and wound-induced oxidative cross-linking of a proline-rich plant cell wall protein: a novel, rapid defense response. *Cell* 70, 21–30. doi: 10.1016/0092-8674(92)90530-P

Brewin, N. J. (2004). Plant cell wall remodelling in the *Rhizobium*–legume symbiosis. *Crit. Rev. Plant Sci.* 23, 293–316. doi: 10.1080/07352680490480734

Brewin, N., Khodorenko, A., Tsyganov, V., Borisov, A., Tikhonovich, I., and Rathbun, E. (2008). "Legume AGP-extensins in *Rhizobium* infection," in *Biological Nitrogen Fixation: Towards Poverty Alleviation Through Sustainable Agriculture*, eds F. Dakora, S. Chimphango, A. Valentine, C. Elmerich, and N. WE (Dordrecht: Springer), 185–187. doi: 10.1007/978-1-4020-8252-8_70

Burget, E. G., and Reiter, W.-D. (1999). The mur4 mutant of *Arabidopsis* is partially defective in the de novo synthesis of uridine diphosphol-arabinose. *Plant Physiol.* 121, 383–390. doi: 10.1104/pp.121.2.383

Burget, E. G., Verma, R., Mølhøj, M., and Reiter, W.-D. (2003). The biosynthesis of L-arabinose in plants: molecular cloning and characterization of a Golgi-localized UDP-D-xylose 4-epimerase encoded by the MUR4 gene of *Arabidopsis*. *Plant Cell* 15, 523–531. doi: 10.1105/tpc.008425

Caffall, K. H., and Mohnen, D. (2009). The structure, function, and biosynthesis of plant cell wall pectic polysaccharides. *Carbohydr. Res.* 344, 1879–1900. doi: 10.1016/j.carres.2009.05.021

Cannesan, M. A., Durand, C., Burel, C., Gangneux, C., Lerouge, P., Ishii, T., et al. (2012). Effect of arabinogalactan proteins from the root caps of pea and *Brassica napus* on *Aphanomyces euteiches* zoospore chemotaxis and germination. *Plant Physiol.* 159, 1658–1670. doi: 10.1104/pp.112.198507

Casero, P. J., Casimiro, I., and Knox, J. P. (1998). Occurrence of cell surface arabinogalactan-protein and extensin epitopes in relation to pericycle and vascular tissue development in the root apex of four species. *Planta* 204, 252–259. doi: 10.1007/s004250050254

Castilleux, R., Plancot, B., Gugi, B., Attard, A., Loutelier-Bourhis, C., Lefranc, B., et al. (2020). Extensin arabinosylation is involved in root response to elicitors and limits oomycete colonization. *Ann. Bot.* 125, 751–763. doi: 10.1093/aob/mcz068

Cheung, A. Y., Wang, H., and Wu, H.-M. (1995). A floral transmitting tissue-specific glycoprotein attracts pollen tubes and stimulates their growth. *Cell* 82, 383–393. doi: 10.1016/0092-8674(95)90427-1

Cheung, A., and Wu, H.-M. (1999). Arabinogalactan proteins in plant sexual reproduction. *Protoplasma* 208, 87–98. doi: 10.1007/BF01279078

Cho, H.-T. (2016). Arabinogalactan protein motif-containing receptor-like kinases are likely to play the negative feedback factor to maintain proper root hair length. *Plant Signal. Behav.* 11, 2007–2022. doi: 10.1080/15592324.2016.1226454

Clarke, A., Anderson, R., and Stone, B. (1979). Form and function of arabinogalactans and arabinogalactan-proteins. *Phytochemistry* 18, 521–540. doi: 10.1016/S0031-9422(00)84255-7

Classen, B., Baumann, A., and Utermoehlen, J. (2019). Arabinogalactan-proteins in spore-producing land plants. *Carbohydr. Polym.* 210, 215–224. doi: 10.1016/j.carbpol.2019.01.077

Coba de la Pena, T., Fedorova, E., Pueyo, J. J., and Lucas, M. M. (2017). The symbiosome: legume and *Rhizobia* co-evolution toward a nitrogen-fixing organelle? *Front. Plant Sci.* 8:2229. doi: 10.3389/fpls.2017.02229

Corral-Martinez, P., Driouich, A., and Segui-Simarro, J. M. (2019). Dynamic changes in arabinogalactan-protein, pectin, xyloglucan and xylan composition of the cell wall during microspore embryogenesis in *Brassica napus*. *Front. Plant Sci.* 10:332. doi: 10.3389/fpls.2019.00332

Cosgrove, D. J. (2005). Growth of the plant cell wall. *Nat. Rev. Mol. Cell Biol.* 6, 850–861. doi: 10.1038/nrm1746

Demesa-Arevalo, E., and Vielle-Calzada, J. P. (2013). The classical arabinogalactan protein AGP18 mediates megaspore selection in *Arabidopsis*. *Plant Cell* 25, 1274–1287. doi: 10.1105/tpc.112.106237

Ding, L., and Zhu, J.-K. (1997). A role for arabinogalactan-proteins in root epidermal cell expansion. *Planta* 203, 289–294. doi: 10.1007/s004250050194

Dobon, A., Canet, J. V., Garcia-Andrade, J., Angulo, C., Neumetzler, L., Persson, S., et al. (2015). Novel disease susceptibility factors for fungal necrotrophic pathogens in *Arabidopsis*. *PLoS Pathog.* 11:e1004800. doi: 10.1371/journal.ppat.1004800

Dolan, L., Linstead, P., and Roberts, K. (1995). An AGP epitope distinguishes a central metaxylem initial from other vascular initials in the *Arabidopsis* root. *Protoplasma* 189, 149–155. doi: 10.1007/bf01280168

Dos Santos, A. L. W., Wiethölter, N., El Gueddari, N. E., and Moerschbacher, B. M. (2006). Protein expression during seed development in *Araucaria angustifolia*: transient accumulation of class IV chitinases and arabinogalactan proteins. *Physiol. Plant.* 127, 138–148. doi: 10.1111/j.1399-3054.2005.00637.x

Driouich, A., Smith, C., Ropitaux, M., Chambard, M., Boulogne, I., Bernard, S., et al. (2019). Root extracellular traps versus neutrophil extracellular traps in host defence, a case of functional convergence? *Biol. Rev. Camb. Philos. Soc.* 94, 1685–1700. doi: 10.1111/brv.12522

Duman, Z., Eliyahu, A., Abu-Abied, M., and Sadot, E. (2020). The contribution of cell wall remodeling and signaling to lateral organs formation. *Isr. J. Plant Sci.* 67, 110–127. doi: 10.1163/22238980-20191115

Elkins, T., Zinn, K., McAllister, L., HoffMann, F. M., and Goodman, C. S. (1990). Genetic analysis of a *Drosophila* neural cell adhesion molecule: interaction of fasciclin I and Abelson tyrosine kinase mutations. *Cell* 60, 565–575. doi: 10.1016/0092-8674(90)90660-7

Ellis, M., Egelund, J., Schultz, C. J., and Bacic, A. (2010). Arabinogalactan-proteins: key regulators at the cell surface? *Plant Physiol.* 153, 403–419. doi: 10.1104/pp.110.156000

Faik, A., Abouzouhair, J., and Sarhan, F. (2006). Putative fasciclin-like arabinogalactan-proteins (FLA) in wheat (*Triticum aestivum*) and rice (*Oryza sativa*): identification and bioinformatic analyses. *Mol. Genet. Genomics* 276, 478–494. doi: 10.1007/s00438-006-0159-z

Ferguson, B. J., Mens, C., Hastwell, A. H., Zhang, M., Su, H., Jones, C. H., et al. (2019). Legume nodulation: the host controls the party. *Plant Cell Environ.* 42, 41–51. doi: 10.1111/pce.13348

Fincher, G. B., Stone, B. A., and Clarke, A. E. (1983). Arabinogalactan-proteins: structure, biosynthesis, and function. *Annu. Rev. Plant Physiol.* 34, 47–70. doi: 10.1146/annurev.pp.34.060183.000403

Freshour, G., Bonin, C. P., Reiter, W.-D., Albersheim, P., Darvill, A. G., and Hahn, M. G. (2003). Distribution of fucose-containing xyloglucans in cell walls of the *mur1* mutant of *Arabidopsis*. *Plant Physiol.* 131, 1602–1612. doi: 10.1104/pp.102.016444

Galloway, A. F., Akhtar, J., Marcus, S. E., Fletcher, N., Field, K., and Knox, P. (2020). Cereal root exudates contain highly structurally complex polysaccharides with soil-binding properties. *Plant J.* 103, 1666–1678. doi: 10.1111/tpj.14852

Gantulga, D., Turan, Y., Bevan, D. R., and Esen, A. (2008). The *Arabidopsis* At1g45130 and At3g52840 genes encode beta-galactosidases with activity toward cell wall polysaccharides. *Phytochemistry* 69, 1661–1670. doi: 10.1016/j.phytochem.2008.01.023

Gaspar, Y. M., Nam, J., Schultz, C. J., Lee, L.-Y., Gilson, P. R., Gelvin, S. B., et al. (2004). Characterization of the *Arabidopsis* lysine-rich arabinogalactan-protein AtAGP17 mutant (rat1) that results in a decreased efficiency of *Agrobacterium* transformation. *Plant Physiol.* 135, 2162–2171. doi: 10.1104/pp.104.045542

Gigli-Bisceglia, N., Engelsdorf, T., and Hamann, T. (2020). Plant cell wall integrity maintenance in model plants and crop species-relevant cell wall components and underlying guiding principles. *Cell. Mol. Life Sci.* 77, 2049–2077. doi: 10.1007/s00018-019-03388-8

Gille, S., Sharma, V., Baidoo, E. E., Keasling, J. D., Scheller, H. V., and Pauly, M. (2013). Arabinosylation of a Yariv-precipitable cell wall polymer impacts plant growth as exemplified by the *Arabidopsis* glycosyltransferase mutant *ray1*. *Mol. Plant* 6, 1369–1372. doi: 10.1093/mp/sst029

Gollotte, A., Gianinazzi-Pearson, V., and Gianinazzi, S. (1995). Immunodetection of infection thread glycoprotein and arabinogalactan protein in wild type *Pisum sativum* (L.) or an isogenic mycorrhiza-resistant mutant interacting with *Glomus mosseae*. *Symbiosis* 18, 69–85.

Harholt, J., Jensen, J. K., Verhertbruggen, Y., Sogaard, C., Bernard, S., Nafisi, M., et al. (2012). ARAD proteins associated with pectic Arabinan biosynthesis form complexes when transiently overexpressed in planta. *Planta* 236, 115–128. doi: 10.1007/s00425-012-1592-3

Hawes, M. C., Gunawardena, U., Miyasaka, S., and Zhao, X. (2000). The role of root border cells in plant defense. *Trends Plant Sci.* 5, 128–133. doi: 10.1016/S1360-1385(00)01556-9

He, J., Zhao, H., Cheng, Z., Ke, Y., Liu, J., and Ma, H. (2019). Evolution analysis of the fasciclin-like arabinogalactan proteins in plants shows variable fasciclin-AGP domain constitutions. *Int. J. Mol. Sci.* 20:1945. doi: 10.3390/ijms20081945

Herve, C., Simeon, A., Jam, M., Cassin, A., Johnson, K. L., Salmean, A. A., et al. (2016). Arabinogalactan proteins have deep roots in eukaryotes: identification of genes and epitopes in brown algae and their role in *Fucus serratus* embryo development. *New Phytol.* 209, 1428–1441. doi: 10.1111/nph.13786

Hijazi, M., Roujol, D., Nguyen-Kim, H., Del Rocio Cisneros Castillo, L., Saland, E., Jamet, E., et al. (2014). Arabinogalactan protein 31 (AGP31), a putative network-forming protein in *Arabidopsis thaliana* cell walls? *Ann. Bot.* 114, 1087–1097. doi: 10.1093/aob/mcu038

Hossain, Z., McGarvey, B., Amyot, L., Gruber, M., Jung, J., and Hannoufa, A. (2012). DIMINUTO 1 affects the lignin profile and secondary cell wall formation in *Arabidopsis*. *Planta* 235, 485–498. doi: 10.1007/s00425-011-1519-4

Hozumi, A., Bera, S., Fujiwara, D., Obayashi, T., Yokoyama, R., Nishitani, K., et al. (2017). Arabinogalactan proteins accumulate in the cell walls of searching hyphae of the stem parasitic plants, *Cuscuta campestris* and *Cuscuta japonica*. *Plant Cell Physiol.* 58, 1868–1877. doi: 10.1093/pcp/pcx121

Huang, Y., Wang, Y., Tan, L., Sun, L., Petrosino, J., Cui, M.-Z., et al. (2016). Nanospherical arabinogalactan proteins are a key component of the high-strength adhesive secreted by English ivy. *Proc. Natl. Acad. Sci. U.S.A.* 113, E3193–E3202. doi: 10.1073/pnas.1600406113

Hwang, Y., Lee, H., Lee, Y. S., and Cho, H. T. (2016). Cell wall-associated ROOT HAIR SPECIFIC 10, a proline-rich receptor-like kinase, is a negative modulator of *Arabidopsis* root hair growth. *J. Exp. Bot.* 67, 2007–2022. doi: 10.1093/jxb/erw031

Immerzeel, P., Eppink, M. M., de Vries, S. C., Schols, H. A., and Voragen, A. G. J. (2006). Carrot arabinogalactan proteins are interlinked with pectins. *Physiol. Plant.* 128, 18–28. doi: 10.1111/j.1399-3054.2006.00712.x

Irani, S., Trost, B., Waldner, M., Nayidu, N., Tu, J., Kusalik, A. J., et al. (2018). Transcriptome analysis of response to *Plasmodiophora brassicae* infection in the *Arabidopsis* shoot and root. *BMC Genomics* 19:23. doi: 10.1186/s12864-017-4426-7

Ito, S., Suzuki, Y., Miyamoto, K., Ueda, J., and Yamaguchi, I. (2005). AtFLA11, a fasciclin-like arabinogalactan-protein, specifically localized in screlenchyma cells. *Biosci. Biotech. Biochem.* 69, 1963–1969. doi: 10.1271/bbb.69.1963

Jackson, O., Taylor, O., Adams, D. G., and Knox, J. P. (2012). Arabinogalactan proteins occur in the free-living cyanobacterium genus *Nostoc* and in plant–*Nostoc* symbioses. *Mol. Plant Microbe Interact.* 25, 1338–1349. doi: 10.1094/MPMI-04-12-0095-R

Jia, Z., Giehl, R. F. H., and von Wiren, N. (2020). The root foraging response under low nitrogen depends on DWARF1-mediated brassinosteroid biosynthesis. *Plant Physiol.* 183, 998–1010. doi: 10.1104/pp.20.00440

Jiao, Y., Sun, L., Song, Y., Wang, L., Liu, L., Zhang, L., et al. (2013). AtrbohD and AtrbohF positively regulate abscisic acid-inhibited primary root growth by affecting Ca2+ signalling and auxin response of roots in *Arabidopsis*. *J. Exp. Bot.* 64, 4183–4192. doi: 10.1093/jxb/ert228

Jing, Y., Shi, L., Li, X., Zheng, H., and He, L. (2019). AGP30: Cd tolerance related gene associate with mitochondrial pyruvate carrier 1. *Plant Signal. Behav.* 14:1629269. doi: 10.1080/15592324.2019.1629269

Johnson, K. L., Cassin, A. M., Lonsdale, A., Wong, G. K., Soltis, D. E., Miles, N. W., et al. (2017). Insights into the evolution of hydroxyproline-rich glycoproteins from 1000 plant transcriptomes. *Plant Physiol.* 174, 904–921. doi: 10.1104/pp.17.00295

Johnson, K. L., Kibble, N. A., Bacic, A., and Schultz, C. J. (2011). A fasciclin-like arabinogalactan-protein (FLA) mutant of *Arabidopsis thaliana*, *fla1*, shows defects in shoot regeneration. *PLoS One* 6:e25154. doi: 10.1371/journal.pone.0025154

Kirchner, T. W., Niehaus, M., Rossig, K. L., Lauterbach, T., Herde, M., Kuster, H., et al. (2018). Molecular background of Pi deficiency-induced root hair growth in *Brassica carinata* – a fasciclin-like arabinogalactan protein is involved. *Front. Plant Sci.* 9:1372. doi: 10.3389/fpls.2018.01372

Kjellbom, P., Snogerup, L., Stöhr, C., Reuzeau, C., McCabe, P. F., and Pennell, R. I. (1997). Oxidative cross-linking of plasma membrane arabinogalactan proteins. *Plant J.* 12, 1189–1196. doi: 10.1046/j.1365-313X.1997.12051189.x

Klahre, U., Noguchi, T., Fujioka, S., Takatsuto, S., Yokota, T., Nomura, T., et al. (1998). The *Arabidopsis* DIMINUTO/DWARF1 gene encodes a protein involved in steroid synthesis. *Plant Cell* 10, 1677–1690. doi: 10.1105/tpc.10.10.1677

Knox, J. P., Day, S., and Roberts, K. (1989). A set of cell surface glycoproteins forms an early marker of cell position, but not cell type, in the root apical meristem of *Daucus carota* L. *Development* 106, 47–56.

Knox, P. (2016). Delving in the deep for the origin of plant cell surface proteoglycans. *New Phytol.* 209, 1341–1343. doi: 10.1111/nph.13862

Koroney, A. S., Plasson, C., Pawlak, B., Sidikou, R., Driouich, A., Menu-Bouaouiche, L., et al. (2016). Root exudate of *Solanum tuberosum* is enriched in galactose-containing molecules and impacts the growth of *Pectobacterium atrosepticum*. *Ann. Bot.* 118, 797–808. doi: 10.1093/aob/mcw128

Kreuger, M., and van Holst, G.-J. (1993). Arabinogalactan proteins are essential in somatic embryogenesis of *Daucus carota* L. *Planta* 189, 243–248. doi: 10.1007/BF00195083

Lamport, D. T., and Varnai, P. (2013). Periplasmic arabinogalactan glycoproteins act as a calcium capacitor that regulates plant growth and development. *New Phytol.* 197, 58–64. doi: 10.1111/nph.12005

Lamport, D. T., Kieliszewski, M. J., and Showalter, A. M. (2006). Salt stress upregulates periplasmic arabinogalactan proteins: using salt stress to analyse AGP function. *New Phytol.* 169, 479–492. doi: 10.1111/j.1469-8137.2005.01591.x

Lamport, D. T., Tan, L., Held, M. A., and Kieliszewski, M. J. (2018). Pollen tube growth and guidance: Occam's razor sharpened on a molecular arabinogalactan glycoprotein Rosetta stone. *New Phytol.* 217, 491–500. doi: 10.1111/nph.14845

Lee, K. J., Sakata, Y., Mau, S.-L., Pettolino, F., Bacic, A., Quatrano, R. S., et al. (2005). Arabinogalactan proteins are required for apical cell extension in the moss *Physcomitrella patens*. *Plant Cell* 17, 3051–3065. doi: 10.1105/tpc.105.034413

Leszczuk, A., Cybulska, J., Skrzypek, T., and Zdunek, A. (2020a). Properties of arabinogalactan proteins (AGPs) in apple (*Malus* x *Domestica*) fruit at different stages of ripening. *Biology* 9:225. doi: 10.3390/biology9080225

Leszczuk, A., Kalaitzis, P., Blazakis, K. N., and Zdunek, A. (2020b). The role of arabinogalactan proteins (AGPs) in fruit ripening-a review. *Hortic. Res.* 7:176. doi: 10.1038/s41438-020-00397-8

Li, J., Yu, M., Geng, L. L., and Zhao, J. (2010). The fasciclin-like arabinogalactan protein gene, *FLA3*, is involved in microspore development of *Arabidopsis*. *Plant J.* 64, 482–497. doi: 10.1111/j.1365-313X.2010.04344.x

Lin, W. D., Liao, Y. Y., Yang, T. J., Pan, C. Y., Buckhout, T. J., and Schmidt, W. (2011). Coexpression-based clustering of *Arabidopsis* root genes predicts functional modules in early phosphate deficiency signaling. *Plant Physiol.* 155, 1383–1402. doi: 10.1104/pp.110.166520

Liu, D., Tu, L., Li, Y., Wang, L., Zhu, L., and Zhang, X. (2008). Genes encoding fasciclin-like arabinogalactan proteins are specifically expressed during cotton fiber development. *Plant Mol. Biol. Rep.* 26, 98–113. doi: 10.1007/s11105-008-0026-7

Liu, E., MacMillan, C. P., Shafee, T., Ma, Y., Ratcliffe, J., van de Meene, A., et al. (2020). Fasciclin-like arabinogalactan-protein 16 (FLA16) is required for stem development in *Arabidopsis*. *Front. Plant Sci.* 11:615392. doi: 10.3389/fpls.2020.615392

Lopez-Hernandez, F., Tryfona, T., Rizza, A., Yu, X. L., Harris, M. O. B., Webb, A. A. R., et al. (2020). Calcium binding by arabinogalactan polysaccharides is important for normal plant development. *Plant Cell* 32, 3346–3369. doi: 10.1105/tpc.20.00027

Ma, H., and Zhao, J. (2010). Genome-wide identification, classification, and expression analysis of the arabinogalactan protein gene family in rice (*Oryza sativa* L.). *J. Exp. Bot.* 61, 2647–2668. doi: 10.1093/jxb/erq104

Ma, Y., Yan, C., Li, H., Wu, W., Liu, Y., Wang, Y., et al. (2017). Bioinformatics prediction and evolution analysis of arabinogalactan proteins in the plant kingdom. *Front. Plant Sci.* 8:66. doi: 10.3389/fpls.2017.00066

MacMillan, C. P., Mansfield, S. D., Stachurski, Z. H., Evans, R., and Southerton, S. G. (2010). Fasciclin-like arabinogalactan proteins: specialization for stem biomechanics and cell wall architecture in *Arabidopsis* and *Eucalyptus*. *Plant J.* 62, 689–703. doi: 10.1111/j.1365-313X.2010.04181.x

MacMillan, C. P., Taylor, L., Bi, Y., Southerton, S. G., Evans, R., and Spokevicius, A. (2015). The fasciclin-like arabinogalactan protein family of *Eucalyptus grandis* contains members that impact wood biology and biomechanics. *New Phytol.* 206, 1314–1327. doi: 10.1111/nph.13320

Mareri, L., Romi, M., and Cai, G. (2018). Arabinogalactan proteins: actors or spectators during abiotic and biotic stress in plants? *Plant Biosyst.* 153, 173–185. doi: 10.1080/11263504.2018.1473525

Marquez, N., Giachero, M. L., Gallou, A., Debat, H. J., Cranenbrouck, S., Di Rienzo, J. A., et al. (2018). Transcriptional changes in mycorrhizal and nonmycorrhizal soybean plants upon infection with the fungal pathogen *Macrophomina phaseolina*. *Mol. Plant Microbe Interact.* 31, 842–855. doi: 10.1094/MPMI-11-17-0282-R

Marzec, M., Szarejko, I., and Melzer, M. (2015). Arabinogalactan proteins are involved in root hair development in barley. *J. Exp. Bot.* 66, 1245–1257. doi: 10.1093/jxb/eru475

McCartney, L., Steele-King, C. G., Jordan, E., and Knox, J. P. (2003). Cell wall pectic (1→4)−β−d-galactan marks the acceleration of cell elongation in the *Arabidopsis* seedling root meristem. *Plant J.* 33, 447–454. doi: 10.1046/j.1365-313X.2003.01640.x

Nam, J., Mysore, K., Zheng, C., Knue, M., Matthysse, A., and Gelvin, S. (1999). Identification of T-DNA tagged *Arabidopsis* mutants that are resistant to transformation by *Agrobacterium*. *Mol. Gen. Genet.* 261, 429–438. doi: 10.1007/s004380050985

Nguema-Ona, E., Andème-Onzighi, C., Aboughe-Angone, S., Bardor, M., Ishii, T., Lerouge, P., et al. (2006). The *reb1-1* mutation of *Arabidopsis*. Effect on the structure and localization of galactose-containing cell wall polysaccharides. *Plant Physiol.* 140, 1406–1417. doi: 10.1104/pp.105.074997

Nguema-Ona, E., Bannigan, A., Chevalier, L., Baskin, T. I, and Driouich, A. (2007). Disruption of arabinogalactan proteins disorganizes cortical microtubules in the root of *Arabidopsis thaliana*. *Plant J.* 52, 240–251. doi: 10.1111/j.1365-313X.2007.03224.x

Nguema-Ona, E., Coimbra, S., Vicré-Gibouin, M., Mollet, J.-C., and Driouich, A. (2012). Arabinogalactan proteins in root and pollen-tube cells: distribution and functional aspects. *Ann. Bot.* 110, 383–404. doi: 10.1093/aob/mcs143

Nguema-Ona, E., Vicre-Gibouin, M., Cannesan, M. A., and Driouich, A. (2013). Arabinogalactan proteins in root-microbe interactions. *Trends Plant Sci.* 18, 440–449. doi: 10.1016/j.tplants.2013.03.006

Nguema-Ona, E., Vicre-Gibouin, M., Gotte, M., Plancot, B., Lerouge, P., Bardor, M., et al. (2014). Cell wall O-glycoproteins and N-glycoproteins: aspects of biosynthesis and function. *Front. Plant Sci.* 5:499. doi: 10.3389/fpls.2014.00499

Nibbering, P., Petersen, B. L., Motawia, M. S., Jorgensen, B., Ulvskov, P., and Niittyla, T. (2020). Golgi-localized exo-beta1,3-galactosidases involved in cell expansion and root growth in *Arabidopsis*. *J. Biol. Chem.* 295, 10581–10592. doi: 10.1074/jbc.RA120.013878

Nivedita, Gazara, R. K., Khan, S., Iqrar, S., Ashrafi, K., and Abdin, M. Z. (2020). Comparative transcriptome profiling of rice colonized with beneficial endophyte, *Piriformospora indica*, under high salinity environment. *Mol. Biol. Rep.* 47, 7655–7673. doi: 10.1007/s11033-020-05839-z

Ogawa-Ohnishi, M., and Matsubayashi, Y. (2015). Identification of three potent hydroxyproline O-galactosyltransferases in *Arabidopsis*. *Plant J.* 81, 736–746. doi: 10.1111/tpj.12764

Olmos, E., Garcia De La Garma, J., Gomez-Jimenez, M. C., and Fernandez-Garcia, N. (2017). Arabinogalactan proteins are involved in salt-adaptation and vesicle trafficking in tobacco by-2 cell cultures. *Front. Plant Sci.* 8:1092. doi: 10.3389/fpls.2017.01092

Palacio-Lopez, K., Tinaz, B., Holzinger, A., and Domozych, D. S. (2019). Arabinogalactan proteins and the extracellular matrix of Charophytes: a sticky business. *Front. Plant Sci.* 10:447. doi: 10.3389/fpls.2019.00447

Pereira, A. M., Pereira, L. G., and Coimbra, S. (2015). Arabinogalactan proteins: rising attention from plant biologists. *Plant Reprod.* 28, 1–15. doi: 10.1007/s00497-015-0254-6

Perez-Perez, Y., Carneros, E., Berenguer, E., Solis, M. T., Barany, I., Pintos, B., et al. (2018). Pectin de-methylesterification and AGP increase promote cell wall remodeling and are required during somatic embryogenesis of *Quercus suber*. *Front. Plant Sci.* 9:1915. doi: 10.3389/fpls.2018.01915

Pfeifer, L., Shafee, T., Johnson, K. L., Bacic, A., and Classen, B. (2020). Arabinogalactan-proteins of *Zostera marina* L. contain unique glycan structures and provide insight into adaption processes to saline environments. *Sci. Rep.* 10:8232. doi: 10.1038/s41598-020-65135-5

Pielach, A., Leroux, O., Domozych, D. S., Knox, J. P., and Popper, Z. A. (2014). Arabinogalactan protein-rich cell walls, paramural deposits and ergastic globules define the hyaline bodies of rhinanthoid Orobanchaceae haustoria. *Ann. Bot.* 114, 1359–1373. doi: 10.1093/aob/mcu121

Plancot, B., Santaella, C., Jaber, R., Kiefer-Meyer, M. C., Follet-Gueye, M. L., Leprince, J., et al. (2013). Deciphering the responses of root border-like cells of *Arabidopsis* and flax to pathogen-derived elicitors. *Plant Physiol.* 163, 1584–1597. doi: 10.1104/pp.113.222356

Přerovská, T., Henke, S., Bleha, R., Spiwok, V., Gillarová, S., Yvin, J. C., et al. (2021). Arabinogalactan-like glycoproteins from *Ulva lactuca* (Chlorophyta) show unique features compared to land plants AGPs. *J. Phycol.* 57, 619–635. doi: 10.1111/jpy.13121

Rashid, A. (2016). Defense responses of plant cell wall non-catalytic proteins against pathogens. *Physiol. Mol. Plant Pathol.* 94, 38–46. doi: 10.1016/j.pmpp.2016.03.009

Rathbun, E. A., Naldrett, M. J., and Brewin, N. J. (2002). Identification of a family of extensin-like glycoproteins in the lumen of *Rhizobium*-induced infection threads in pea root nodules. *Mol. Plant Microbe Interact.* 15, 350–359. doi: 10.1094/MPMI.2002.15.4.350

Reguera, M., Abreu, I., Brewin, N. J., Bonilla, I., and Bolanos, L. (2010). Borate promotes the formation of a complex between legume AGP-extensin and Rhamnogalacturonan II and enhances production of *Rhizobium* capsular polysaccharide during infection thread development in *Pisum sativum* symbiotic root nodules. *Plant Cell Environ.* 33, 2112–2120. doi: 10.1111/j.1365-3040.2010.02209.x

Reiter, W. D., Chapple, C., and Somerville, C. R. (1997). Mutants of *Arabidopsis thaliana* with altered cell wall polysaccharide composition. *Plant J.* 12, 335–345. doi: 10.1046/j.1365-313X.1997.12020335.x

Reiter, W.-D., Chapple, C. C., and Somerville, C. R. (1993). Altered growth and cell walls in a fucose-deficient mutant of *Arabidopsis*. *Science* 261, 1032–1035. doi: 10.1126/science.261.5124.1032

Ropitaux, M., Bernard, S., Schapman, D., Follet-Gueye, M. L., Vicre, M., Boulogne, I., et al. (2020). Root border cells and mucilage secretions of soybean, *Glycine max* (Merr) L.: Characterization and role in interactions with the oomycete *Phytophthora parasitica*. *Cells* 9:2215. doi: 10.3390/cells9102215

Rui, Y., and Dinneny, J. R. (2020). A wall with integrity: surveillance and maintenance of the plant cell wall under stress. *New Phytol.* 225, 1428–1439. doi: 10.1111/nph.16166

Sala, K., Malarz, K., Barlow, P. W., and Kurczynska, E. U. (2017). Distribution of some pectic and arabinogalactan protein epitopes during *Solanum lycopersicum* (L.) adventitious root development. *BMC Plant Biol.* 17:25. doi: 10.1186/s12870-016-0949-3

Šamaj, J., Braun, M., Baluška, F., Ensikat, H.-J., Tsumuraya, Y., and Volkmann, D. (1999). Specific localization of arabinogalactan-protein epitopes at the surface

of maize root hairs. *Plant Cell Physiol.* 40, 874–883. doi: 10.1093/oxfordjournals.pcp.a029617

Schultz, C. J., and Harrison, M. J. (2008). Novel plant and fungal AGP-like proteins in the *Medicago truncatula-Glomus intraradices* arbuscular mycorrhizal symbiosis. *Mycorrhiza* 18, 403–412. doi: 10.1007/s00572-008-0194-1

Schultz, C., Gilson, P., Oxley, D., Youl, J., and Bacic, A. (1998). GPI-anchors on arabinogalactan-proteins: implications for signalling in plants. *Trends Plant Sci.* 3, 426–431. doi: 10.1016/S1360-1385(98)01328-4

Seifert, G. J. (2018). Fascinating fasciclins: a surprisingly widespread family of proteins that mediate interactions between the cell exterior and the cell surface. *Int. J. Mol. Sci.* 19:1628. doi: 10.3390/ijms19061628

Seifert, G. J. (2020). On the potential function of type II arabinogalactan O-glycosylation in regulating the fate of plant secretory proteins. *Front. Plant Sci.* 11:563735. doi: 10.3389/fpls.2020.563735

Seifert, G. J. (2021). The FLA4-FEI pathway: a unique and mysterious signaling module related to cell wall structure and stress signaling. *Genes* 12:145. doi: 10.3390/genes12020145

Seifert, G. J., and Blaukopf, C. (2010). Irritable walls: the plant extracellular matrix and signaling. *Plant Physiol.* 153, 467–478. doi: 10.1104/pp.110.153940

Seifert, G. J., and Roberts, K. (2007). The biology of arabinogalactan proteins. *Annu. Rev. Plant Biol.* 58, 137–161. doi: 10.1146/annurev.arplant.58.032806.103801

Seifert, G. J., Barber, C., Wells, B., Dolan, L., and Roberts, K. (2002). Galactose biosynthesis in *Arabidopsis*: genetic evidence for substrate channeling from UDP-D-galactose into cell wall polymers. *Curr. Biol.* 12, 1840–1845. doi: 10.1016/S0960-9822(02)01260-5

Seifert, G. J., Xue, H., and Acet, T. (2014). The *Arabidopsis thaliana FASCICLIN LIKE ARABINOGALACTAN PROTEIN 4* gene acts synergistically with abscisic acid signalling to control root growth. *Ann. Bot.* 114, 1125–1133. doi: 10.1093/aob/mcu010

Shailasree, S., Kini, K. R., Deepak, S., Kumudini, B. S., and Shetty, H. S. (2004). Accumulation of hydroxyproline-rich glycoproteins in pearl millet seedlings in response to *Sclerospora graminicola* infection. *Plant Sci.* 167, 1227–1234. doi: 10.1016/j.plantsci.2004.06.012

Shi, H., Kim, Y., Guo, Y., Stevenson, B., and Zhu, J.-K. (2003). The *Arabidopsis* SOS5 locus encodes a putative cell surface adhesion protein and is required for normal cell expansion. *Plant Cell* 15, 19–32. doi: 10.1105/tpc.007872

Shimizu, K., and Aoki, K. (2019). Development of parasitic organs of a stem holoparasitic plant in genus *Cuscuta*. *Front. Plant Sci.* 10:1435. doi: 10.3389/fpls.2019.01435

Showalter, A. (2001). Arabinogalactan-proteins: structure, expression and function. *Cell. Mol. Life Sci.* 58, 1399–1417. doi: 10.1007/PL00000784

Showalter, A. M., and Basu, D. (2016). Glycosylation of arabinogalactan-proteins essential for development in *Arabidopsis*. *Commun. Integr. Biol.* 9:e0125624. doi: 10.1080/19420889.2016.1177687

Silva, J., Ferraz, R., Dupree, P., Showalter, A. M., and Coimbra, S. (2020). Three decades of advances in arabinogalactan-protein biosynthesis. *Front. Plant Sci.* 11:610377. doi: 10.3389/fpls.2020.610377

Silva, T. F., Ferreira, B. G., Dos Santos Isaias, R. M., Alexandre, S. S., and Franca, M. G. C. (2020). Immunocytochemistry and density functional theory evidence the competition of aluminum and calcium for pectin binding in *Urochloa decumbens* roots. *Plant Physiol. Biochem.* 153, 64–71. doi: 10.1016/j.plaphy.2020.05.015

Snow, P. M., Bieber, A. J., and Goodman, C. S. (1989). Fasciclin III: a novel homophilic adhesion molecule in *Drosophila*. *Cell* 59, 313–323. doi: 10.1016/0092-8674(89)90293-6

Somssich, M., Khan, G. A., and Persson, S. (2016). Cell wall heterogeneity in root development of *Arabidopsis*. *Front. Plant Sci.* 7:1242. doi: 10.3389/fpls.2016.01242

Striberny, B., and Krause, K. (2015). Cell wall glycoproteins at interaction sites between parasitic giant dodder (*Cuscuta reflexa*) and its host *Pelargonium zonale*. *Plant Signal. Behav.* 10:e1086858. doi: 10.1080/15592324.2015.1086858

Su, S., and Higashiyama, T. (2018). Arabinogalactan proteins and their sugar chains: functions in plant reproduction, research methods, and biosynthesis. *Plant Reprod.* 31, 67–75. doi: 10.1007/s00497-018-0329-2

Swamy, M. K., Akhtar, M. S., and Sinniah, U. R. (2016). "Root exudates and their molecular interactions with rhizospheric microbes," in *Plant, Soil and Microbes*, eds K. R. Hakeem and M. S. Akhtar (Cham: Springer), 59–77. doi: 10.1007/978-3-319-29573-2_4

Takahashi, T., Gasch, A., Nishizawa, N., and Chua, N.-H. (1995). The DIMINUTO gene of *Arabidopsis* is involved in regulating cell elongation. *Genes Dev.* 9, 97–107. doi: 10.1101/gad.9.1.97

Tan, L., Eberhard, S., Pattathil, S., Warder, C., Glushka, J., Yuan, C., et al. (2013). An *Arabidopsis* cell wall proteoglycan consists of pectin and arabinoxylan covalently linked to an arabinogalactan protein. *Plant Cell* 25, 270–287. doi: 10.1105/tpc.112.107334

Tan, L., Tees, D., Qian, J., Kareem, S., and Kieliszewski, M. J. (2018). Intermolecular interactions between glycomodules of plant cell wall arabinogalactan-proteins and extensins. *Cell Surf.* 1, 25–33. doi: 10.1016/j.tcsw.2018.03.001

Trivedi, D. K., Bhatt, H., Pal, R. K., Tuteja, R., Garg, B., Johri, A. K., et al. (2013). Structure of RNA-interacting cyclophilin A-like protein from *Piriformospora indica* that provides salinity-stress tolerance in plants. *Sci. Rep.* 3:3001. doi: 10.1038/srep03001

Tryfona, T., Theys, T. E., Wagner, T., Stott, K., Keegstra, K., and Dupree, P. (2014). Characterisation of FUT4 and FUT6 α-(1→2)-fucosyltransferases reveals that absence of root arabinogalactan fucosylation increases *Arabidopsis* root growth salt sensitivity. *PLoS One* 9:e93291. doi: 10.1371/journal.pone.0093291

Tsyganova, A. V., Seliverstova, E. V., Brewin, N. J., and Tsyganov, V. E. (2019). Comparative analysis of remodelling of the plant-microbe interface in *Pisum sativum* and *Medicago truncatula* symbiotic nodules. *Protoplasma* 256, 983–996. doi: 10.1007/s00709-019-01355-5

Tsyganova, A. V., Tsyganov, V. E., Findlay, K. C., Borisov, A. Y., Tikhonovich, I. A., and Brewin, N. J. (2009). Distribution of legume arabinogalactan protein-extensin (AGPE) glycoproteins in symbiotically defective pea mutants with abnormal infection threads. *Cell Tissue Biol.* 3, 93–102. doi: 10.1134/s1990519x09010131

Tucker, M. R., Lou, H., Aubert, M. K., Wilkinson, L. G., Little, A., Houston, K., et al. (2018). Exploring the role of cell wall-related genes and polysaccharides during plant development. *Plants* 7:42. doi: 10.3390/plants7020042

Turupcu, A., Almohamed, W., Oostenbrink, C., and Seifert, G. J. (2018). A speculation on the tandem fasciclin 1 repeat of FLA4 proteins in angiosperms. *Plant Signal. Behav.* 13:e1507403. doi: 10.1080/15592324.2018.1507403

Van Hengel, A. J., and Roberts, K. (2002). Fucosylated arabinogalactan-proteins are required for full root cell elongation in *Arabidopsis*. *Plant J.* 32, 105–113. doi: 10.1046/j.1365-313X.2002.01406.x

Van Hengel, A. J., and Roberts, K. (2003). AtAGP30, an arabinogalactan-protein in the cell walls of the primary root, plays a role in root regeneration and seed germination. *Plant J.* 36, 256–270. doi: 10.1046/j.1365-313X.2003.01874.x

Van Hengel, A. J., Barber, C., and Roberts, K. (2004). The expression patterns of arabinogalactan-protein *AtAGP30* and *GLABRA2* reveal a role for abscisic acid in the early stages of root epidermal patterning. *Plant J.* 39, 70–83. doi: 10.1111/j.1365-313X.2004.02104.x

van Hengel, A. J., Tadesse, Z., Immerzeel, P., Schols, H., Van Kammen, A., and de Vries, S. C. (2001). N-acetylglucosamine and glucosamine-containing arabinogalactan proteins control somatic embryogenesis. *Plant Physiol.* 125, 1880–1890. doi: 10.1104/pp.125.4.1880

Velasquez, S. M., Marzol, E., Borassi, C., Pol-Fachin, L., Ricardi, M. M., Mangano, S., et al. (2015). Low sugar is not always good: impact of specific O-glycan defects on tip growth in *Arabidopsis*. *Plant Physiol.* 168, 808–813. doi: 10.1104/pp.114.255521

Vicré, M., Santaella, C., Blanchet, S., Gateau, A., and Driouich, A. (2005). Root border-like cells of *Arabidopsis*. Microscopical characterization and role in the interaction with rhizobacteria. *Plant Physiol.* 138, 998–1008. doi: 10.1104/pp.104.051813

Voxeur, A., and Hofte, H. (2016). Cell wall integrity signaling in plants: "to grow or not to grow that's the question". *Glycobiology* 26, 950–960. doi: 10.1093/glycob/cww029

Waller, F., Achatz, B., Baltruschat, H., Fodor, J., Becker, K., Fischer, M., et al. (2005). The endophytic fungus *Piriformospora indica* reprograms barley to salt-stress tolerance, disease resistance, and higher yield. *Proc. Natl. Acad. Sci. U.S.A.* 102, 13386–13391. doi: 10.1073/pnas.0504423102

Wang, H., Jiang, C., Wang, C., Yang, Y., Yang, L., Gao, X., et al. (2015). Antisense expression of the fasciclin-like arabinogalactan protein *FLA6* gene in *Populus* inhibits expression of its homologous genes and alters stem biomechanics and

cell wall composition in transgenic trees. *J. Exp. Bot.* 66, 1291–1302. doi: 10.1093/jxb/eru479

Wang, L., Cheng, M., Yang, Q., Li, J., Wang, X., Zhou, Q., et al. (2019). Arabinogalactan protein-rare earth element complexes activate plant endocytosis. *Proc. Natl. Acad. Sci. U.S.A.* 116, 14349–14357. doi: 10.1073/pnas.1902532116

Wang, Y., Mortimer, J. C., Davis, J., Dupree, P., and Keegstra, K. (2013). Identification of an additional protein involved in mannan biosynthesis. *Plant J.* 73, 105–117. doi: 10.1111/tpj.12019

Willats, W. G., and Knox, J. P. (1996). A role for arabinogalactan-proteins in plant cell expansion: evidence from studies on the interaction of β−glucosyl Yariv reagent with seedlings of *Arabidopsis thaliana*. *Plant J.* 9, 919–925. doi: 10.1046/j.1365-313X.1996.9060919.x

Wu, Y., Fan, W., Li, X., Chen, H., Takac, T., Samajova, O., et al. (2017). Expression and distribution of extensins and AGPs in susceptible and resistant banana cultivars in response to wounding and *Fusarium oxysporum*. *Sci. Rep.* 7:42400. doi: 10.1038/srep42400

Wubben, M. J. II, Rodermel, S. R., and Baum, T. J. (2004). Mutation of a UDP-glucose-4-epimerase alters nematode susceptibility and ethylene responses in *Arabidopsis* roots. *Plant J.* 40, 712–724. doi: 10.1111/j.1365-313X.2004.02257.x

Xie, D., Ma, L., Samaj, J., and Xu, C. (2011). Immunohistochemical analysis of cell wall hydroxyproline-rich glycoproteins in the roots of resistant and susceptible wax gourd cultivars in response to *Fusarium oxysporum* f. sp. *Benincasae* infection and fusaric acid treatment. *Plant Cell Rep*. 30, 1555–1569. doi: 10.1007/s00299-011-1069-z

Xu, S. L., Rahman, A., Baskin, T. I., and Kieber, J. J. (2008). Two leucine-rich repeat receptor kinases mediate signaling, linking cell wall biosynthesis and ACC synthase in *Arabidopsis*. *Plant Cell* 20, 3065–3079. doi: 10.1105/tpc.108.063354

Xue, H., and Seifert, G. J. (2015). Fasciclin like arabinogalactan protein 4 and respiratory burst oxidase homolog D and F independently modulate abscisic acid signaling. *Plant Signal. Behav.* 10:e989064. doi: 10.4161/15592324.2014.989064

Xue, H., Veit, C., Abas, L., Tryfona, T., Maresch, D., Ricardi, M. M., et al. (2017). *Arabidopsis thaliana* FLA4 functions as a glycan-stabilized soluble factor via its carboxy-proximal Fasciclin 1 domain. *Plant J.* 91, 613–630. doi: 10.1111/tpj.13591

Yang, J., and Showalter, A. M. (2007). Expression and localization of AtAGP18, a lysine-rich arabinogalactan-protein in *Arabidopsis*. *Planta* 226, 169–179. doi: 10.1007/s00425-007-0478-2

Yang, J., Sardar, H. S., McGovern, K. R., Zhang, Y., and Showalter, A. M. (2007). A lysine-rich arabinogalactan protein in *Arabidopsis* is essential for plant growth and development, including cell division and expansion. *Plant J.* 49, 629–640. doi: 10.1111/j.1365-313X.2006.02985.x

Yang, J., Zhang, Y., Liang, Y., and Showalter, A. M. (2011). Expression analyses of AtAGP17 and AtAGP19, two lysine-rich arabinogalactan proteins, in *Arabidopsis*. *Plant Biol.* 13, 431–438. doi: 10.1111/j.1438-8677.2010.00407.x

Yariv, J., Lis, H., and Katchalski, E. (1967). Precipitation of Arabic acid and some seed polysaccharides by glycosylphenylazo dyes. *Biochem. J.* 105, 1C–2C. doi: 10.1042/bj1050001c

Yeats, T. H., Bacic, A., and Johnson, K. L. (2018). Plant glycosylphosphatidylinositol anchored proteins at the plasma membrane-cell wall nexus. *J. Int. Plant Biol.* 60, 649–669. doi: 10.1111/jipb.12659

Yu, M., and Zhao, J. (2012). The cytological changes of tobacco zygote and proembryo cells induced by beta-glucosyl Yariv reagent suggest the involvement of arabinogalactan proteins in cell division and cell plate formation. *BMC Plant Biol*. 12:126. doi: 10.1186/1471-2229-12-126

Zagorchev, L., Kamenova, P., and Odjakova, M. (2014). The role of plant cell wall proteins in response to salt stress. *Sci. World J.* 2014:764089. doi: 10.1155/2014/764089

Zang, L., Zheng, T., Chu, Y., Ding, C., Zhang, W., Huang, Q., et al. (2015). Genome-wide analysis of the fasciclin-like arabinogalactan protein gene family reveals differential expression patterns, localization, and salt stress response in *Populus*. *Front. Plant Sci.* 6:1140. doi: 10.3389/fpls.2015.01140

Zhang, Y., Held, M. A., and Showalter, A. M. (2020). Elucidating the roles of three beta-glucuronosyltransferases (GLCATs) acting on arabinogalactan-proteins using a CRISPR-Cas9 multiplexing approach in *Arabidopsis*. *BMC Plant Biol.* 20:221. doi: 10.1186/s12870-020-02420-5

Zhang, Y., Held, M. A., Kaur, D., and Showalter, A. M. (2021). CRISPR-Cas9 multiplex genome editing of the hydroxyproline-O-galactosyltransferase gene family alters arabinogalactan-protein glycosylation and function in *Arabidopsis*. *BMC Plant Biol*. 21:16. doi: 10.1186/s12870-020-02791-9

Zhang, Y., Yang, J., and Showalter, A. M. (2011). AtAGP18 is localized at the plasma membrane and functions in plant growth and development. *Planta* 233, 675–683. doi: 10.1007/s00425-010-1331-6

Zhao, C., Zayed, O., Zeng, F., Liu, C., Zhang, L., Zhu, P., et al. (2019). Arabinose biosynthesis is critical for salt stress tolerance in *Arabidopsis*. *New Phytol.* 224, 274–290. doi: 10.1111/nph.15867

Zhou, K. (2019). Glycosylphosphatidylinositol-anchored proteins in *Arabidopsis* and one of their common roles in signaling transduction. *Front. Plant Sci.* 10:1022. doi: 10.3389/fpls.2019.01022

Zhu, J. K., Shi, J., Singh, U., Wyatt, S. E., Bressan, R. A., Hasegawa, P. M., et al. (1993). Enrichment of vitronectin-and fibronectin-like proteins in NaCl-adapted plant cells and evidence for their involvement in plasma membrane–cell wall adhesion. *Plant J.* 3, 637–646. doi: 10.1111/j.1365-313X.1993.00637.x

Zielinski, K., Dubas, E., Gersi, Z., Krzewska, M., Janas, A., Nowicka, A., et al. (2021). Beta-1,3-Glucanases and chitinases participate in the stress-related defence mechanisms that are possibly connected with modulation of arabinogalactan proteins (AGP) required for the androgenesis initiation in rye (*Secale cereale* L.). *Plant Sci.* 302:110700.

Conflict of Interest: The authors declare that the research was conducted in the absence of any commercial or financial relationships that could be construed as a potential conflict of interest.

frontiers in Plant Science

ORIGINAL RESEARCH
published: 25 May 2021
doi: 10.3389/fpls.2021.661352

Interaction of OsRopGEF3 Protein With OsRac3 to Regulate Root Hair Elongation and Reactive Oxygen Species Formation in Rice (*Oryza sativa*)

Eui-Jung Kim[1], Woo-Jong Hong[1], Win Tun[1], Gynheung An[1], Sun-Tae Kim[2], Yu-Jin Kim[3] and Ki-Hong Jung[1]**

[1] Graduate School of Biotechnology and Crop Biotech Institute, Kyung Hee University, Yongin, South Korea, [2] Department of Plant Bioscience, Pusan National University, Miryang, South Korea, [3] Department of Life Science and Environmental Biochemistry, and Life and Industry Convergence Research Institute, Pusan National University, Miryang, South Korea

Root hairs are tip-growing cells that emerge from the root epidermis and play a role in water and nutrient uptake. One of the key signaling steps for polar cell elongation is the formation of Rho-GTP by accelerating the intrinsic exchange activity of the Rho-of-plant (ROP) or the Rac GTPase protein; this step is activated through the interaction with the plant Rho guanine nucleotide exchange factor (RopGEFs). The molecular players involved in root hair growth in rice are largely unknown. Here, we performed the functional analysis of *OsRopGEF3*, which is highly expressed in the root hair tissues among the *OsRopGEF* family genes in rice. To reveal the role of OsRopGEF3, we analyzed the phenotype of loss-of-function mutants of *OsRopGEF3,* which were generated using the CRISPR-Cas9 system. The mutants had reduced root hair length and increased root hair width. In addition, we confirmed that reactive oxygen species (ROS) were highly reduced in the root hairs of the *osropgef3* mutant. The pairwise yeast two-hybrid experiments between OsRopGEF3 and OsROP/Rac proteins in rice revealed that the OsRopGEF3 protein interacts with OsRac3. This interaction and colocalization at the same subcellular organelles were again verified in tobacco leaf cells and rice root protoplasts via bimolecular functional complementation (BiFC) assay. Furthermore, among the three respiratory burst oxidase homolog (OsRBOH) genes that are highly expressed in rice root hair cells, we found that OsRBOH5 can interact with OsRac3. Our results demonstrate an interaction network model wherein OsRopGEF3 converts the GDP of OsRac3 into GTP, and OsRac3-GTP then interacts with the N-terminal of OsRBOH5 to produce ROS, thereby suggesting OsRopGEF3 as a key regulating factor in rice root hair growth.

Keywords: ***Oryza sativa*, OsRopGEF3, OsRac3, OsRBOH5, reactive oxygen species, root hair**

OPEN ACCESS

Edited by:
Ramiro Esteban Rodriguez, Consejo Nacional de Investigaciones Científicas y Técnicas (CONICET), Instituto de Biología Molecular y Celular de Rosario (IBR), Argentina

Reviewed by:
Katarzyna Retzer, Academy of Sciences of the Czech Republic, Czechia
Cecilia Borassi, Consejo Nacional de Investigaciones Científicas y Técnicas (CONICET), Instituto de Investigaciones Bioquímicas de Buenos Aires (IIBBA), Argentina

***Correspondence:**
Yu-Jin Kim
yjkim2020@pusan.ac.kr
Ki-Hong Jung
khjung2010@khu.ac.kr

Specialty section:
This article was submitted to Plant Development and EvoDevo, a section of the journal Frontiers in Plant Science

Received: *30 January 2021*
Accepted: *14 April 2021*
Published: *25 May 2021*

Citation:
Kim E-J, Hong W-J, Tun W, An G, Kim S-T, Kim Y-J and Jung K-H (2021) Interaction of OsRopGEF3 Protein With OsRac3 to Regulate Root Hair Elongation and Reactive Oxygen Species Formation in Rice (Oryza sativa). Front. Plant Sci. 12:661352. doi: 10.3389/fpls.2021.661352

INTRODUCTION

Root hairs are specialized cells formed by the expansion of epidermis cells located on the root's outermost layer. They play an important role in supporting plant growth-like hormone response or absorbing water and nutrients (Gilroy and Jones, 2000; Vissenberg et al., 2020). The pattern of root hair cells (termed trichoblasts) and non-hair cells (atrichoblasts) is determined by their fate in the meristematic zone; the length of the root hair increases in the elongation zone of the root, while its growth stops in the maturation zone (Dolan et al., 1993; Duckett et al., 1994; Bibikova and Gilroy, 2002). Root hairs develop in a polarized manner from trichoblasts. Root hair growth involves cell wall and cytoskeleton reorganization, which is regulated by signaling molecules such as reactive oxygen species (ROS) and calcium gradients (Lin et al., 2015; Mangano et al., 2017).

Molecular genetic studies in *Arabidopsis thaliana* have identified key genes regulating root hair development. These include several transcription factors affecting the growth of root hair length, such as ROOT HAIR DEFECTIVE SIX-LIKE (RSL) transcription factor and R2R3 class MYB transcription factor (Slabaugh et al., 2011; Datta et al., 2015). Auxin response factor 5 (ARF5) regulates the expression of RSL4, and RSL2/RSL4 binds to the root hair-specific *cis*-element (RHEs) present in the promoters of RBOHC and RBOHH to produce ROS (Mangano et al., 2017). RBOHC and RBOHH loss-of-function mutants show reduced root hair length and ROS at the apical tip. ROS at the tip of the root hairs regulates the activity of calcium ion channels (Foreman et al., 2003; Carol et al., 2005; Jones et al., 2007), thereby regulating the activity of enzymes involved in cell wall expansion (Bosch and Hepler, 2005; Palin and Geitmann, 2012). Similarly, RSL and RBOH have been found in rice (*Oryza sativa*). OsRSL class II subfamily binds with rice root hairless 1 (OsRHL1) to regulate root hair growth (Moon et al., 2019b). Furthermore, auxin-responsive OsRBOH3 gene regulates root hair development (Wang et al., 2018).

In coordination with ROS, calcium, and cytoskeleton, a small GTP-binding protein, namely, ROP Rho-related GTPases from plants (ROP/Rac), acts as a molecular switch that cycles between an active (GTP-bound) and an inactive (GDP-bound) conformation (Cherfils and Chardin, 1999; Yang, 2002; Berken et al., 2005). Active ROP/Rac binds to the N-terminus of RBOH, after which the exposed EF-hand motif of RBOH (Wong et al., 2007) can bind with calcium ions. Disruption of ROP affects apical actin dynamics, calcium signaling, and ROS production, and constitutive activations also alter tip growth, resulting in wavy or swollen root hair tips (Molendijk et al., 2001; Bloch et al., 2005).

Recently, the molecular player targeting ROPs to the polarized tip membrane was identified as ROP-guanine nucleotide exchange factor (RopGEF), which converts inactive ROP to active ROP. Among the 14 RopGEF genes in *Arabidopsis* (Gu et al., 2006), AtRopGEF3 regulates the initiation and bulging of root hair through physical interaction with AtROP2, while RopGEF4 regulates subsequent growth of root hair tips (Denninger et al., 2019), indicating the subfunctionalization of different RopGEF members. The molecular function of RopGEF and ROP/Rac in root hair growth of other plants is less known. There are 11 *OsRopGEFs* and 7 *OsRac* genes in rice (Miki et al., 2005; Kim et al., 2020). The functions of control grain size, RNA silencing, apoptosis regulation, and gene expression in OsRacs have been studied (Kawasaki et al., 1999; Miki and Shimamoto, 2004; Zhang et al., 2019). Phylogenetic analysis and expression profiles suggest different features of ROP between *Arabidopsis* and rice (Kim et al., 2020). However, it has not been elucidated how OsRopGEF and OsRac regulate root hair development in rice, a model crop plant.

In this study, we aim to elucidate the function of OsRopGEF3 in rice root hair growth. First, we identified how OsRopGEF3 affects root hair development in rice. Using the CRISPR-Cas9 gene editing system, we found that the loss-of-function mutant of OsRopGEF3 showed an abnormal root hair phenotype, with ROS reduction. Furthermore, the OsRopGEF3 protein localizes at the plasma membrane (PM)-associated cytoplasm within rice root hair cells. Through yeast two-hybrid (Y2H) and bimolecular fluorescence complementation (BiFC) analyses, we found that OsRopGEF3 interacts with OsRac3. Finally, we identified that the N-terminal of OsRBOH5 interacts with OsRac3. We also describe and discuss the mechanism of rice root hair development associated with OsRopGEF3, OsRac3, and OsRBOH5.

MATERIALS AND METHODS

Multiple Sequence Alignment, Meta-Expression Analysis, and Domain Analysis

To perform a phylogenetic analysis of the OsRac family, protein sequences were collected from the rice genome annotation project[1] (Moon et al., 2020). Multiple amino acid sequences were aligned using ClustalW, and phylogenetic analysis was performed using MEGA-X under neighbor-joining methods. Using a publicly available rice Affymetrix microarray data in the National Center for Biotechnology Information Gene Expression Omnibus (NCBI GEO datasets), we normalized the signal intensity with the R language and then transformed them into log2 values. The normalized data, with averaged Affymetrix anatomical meta-expression data, were used for heatmap construction. The TMHMM[2] and Pfam[3] databases were used for domain analysis.

Plant Growth, Nucleic Acid Extraction, and RT-qPCR

To grow rice (*O. sativa japonica* cv. Dongjin), the seeds were sterilized with 50% of sodium hypochlorite for 30 min, washed with distilled water for three times, and then germinated on Murashige and Skoog (MS) media under controlled conditions in 7 days (28/25°C day/night, 8-h photoperiod, and 78% relative humidity). The seedlings were grown in the growth

[1]http://rice.plantbiology.msu.edu/

[2]http://www.cbs.dtu.dk/services/TMHMM/

[3]https://pfam.xfam.org/

chamber or greenhouse for 1 month and then transferred to a paddy field of Kyung Hee University. The tobacco plants (*Nicotiana benthamiana*) were grown in chambers at controlled conditions (25°C day/night, 16-h photoperiod, and 50% relative humidity) in 3–4 weeks.

Various rice tissues were immediately frozen in liquid nitrogen and ground with Tissue-Lyser II (Qiagen, Hilden, Germany) or mortar and pestle (CoorsTek 60310). The leaf tissues were sampled from 1-month-old plants for mutant analysis, and six other tissues were sampled for real-time quantitative PCR (RT-qPCR) (shoots and roots from 1-week-old plants, leaves and young panicles from 1-month-old plants, developing seeds 5–10 days after pollination, and root hairs from seedling roots 3 days after germination). DNA was extracted using the cetyltrimethylammonium bromide (CTAB)-chloroform method, and the sequence genotype was analyzed in Macrogen Corp.[4]using BigDye Terminator v3.1 cycle sequencing kit (Applied Biosystems). Total RNA was extracted with a TRIzol buffer and purified with an RNeasy plant mini kit (Qiagen); complementary DNA (cDNA) was synthesized using SuPrimeScript RT premix (GeNet Bio). To identify the tissue specific expression by RT-qPCR, we used the Roter-Gene Q instrument system (Qiagen, Hilden, Germany) and the internal control for rice ubiquitin 5 (*OsUbi5*, LOC_Os01g22490), as previously reported (Kim et al., 2019). RT-qPCR was performed with three independent biological replicates. Relative transcript levels and fold change were calculated by previously reported methods (Schmittgen and Livak, 2008). All RT-qPCR primers used in our experiments are listed in **Supplementary Table 1**.

Vector Construction

To design the guide RNA for CRISPR-Cas9 vector cloning, we selected two target regions using the CRISPRdirect software (Naito et al., 2015). For CRISPR-Cas9 vector cloning, we synthesized oligo dimers with annealed primers and ligated the dimers with the pRGEB32 binary vector (Xie et al., 2015). To clone the *OsRopGEF3* promoter, the pOsRopGEF3:OsRopGEF3-GFP plasmid was generated; the 2000 base-pair upstream from the start codon and the open reading frame (ORF) of *OsRopGEF3* genes were amplified by PCR and cloned into the binary vector pGA3427, which includes the enhanced green fluorescent protein (eGFP) sequence. To clone the beta-glucuronidase (GUS) fusion vector (*pOsRopGEF3: GUS*), the 2000 upstream sequence from the stop codon was amplified and ligated into a BamH1-treated pGA3519 vector. Ligated vectors were transformed into *Escherichia coli*, *TOP10*. The confirmed plasmid was then transformed into *Agrobacterium tumefaciens*, *LBA4404*. The transgenic rice plants were generated via *Agrobacterium*-mediated cocultivation of the rice callus (Lee et al., 1999). All of the cloning primers we have used in our experiments are listed in **Supplementary Table 1**. For the protoplast experiments, the ORFs of *OsRopGEF3*, *OsRac3*, and *OsRBOH5* were each ligated into the Sma1-treated pGA3574 vector, which was tagged with eGFP, mCherry, and N- and C-terminal fragments of Venus.

[4]https://dna.macrogen.com

Morphological Analysis

To minimize the transformation side effects, at least three generations after the tissue culture of plants were used for all root hair measurements. All root hairs were measured from the primary roots of rice 3 days after germination (DAG). The root hair lengths and widths were quantified 2–8 mm from the root apex. The length was measured only when the starting point of the root hairs was visible from the root, and the width was measured at the center of the root hair. BX61 (Olympus, Tokyo, Japan) and SZX61 (Olympus, Tokyo, Japan) microscopes were used for plant photography, and the root hair lengths and widths were measured using Image J software (Schneider et al., 2012). Data were observed in 10 seedlings each for the control and mutant plants and presented as means and standard deviation.

Histochemical Assay

For GUS staining, transgenic plants were mixed with GUS staining solution and vacuumed for 30 min. After that, samples were incubated for 24 h at 37°C in dark conditions (Moon et al., 2019a). Chlorophyll was gradually removed by 70% and absolute ethanol. For ROS detection, the primary roots from three DAG plants were collected and mixed with 10 μM 2′, 7′-dichlorodihydrofluorescein diacetate (CM-H2DCFDA) (Invitrogen) or 1 mg/ml 3,3′-diaminobenzidine (DAB) solution. Next, the samples were vacuumed for 15 min in dark conditions, followed by incubation for 30 min for CM-H2DCFDA staining and 3 h for DAB staining at room temperature in dark conditions. After staining, the primary roots were washed three times with 1% phosphate-buffered saline (PBS). Root hairs were observed under a BX61 microscope (Olympus) and a laser scanning confocal microscope LSM 510 (Carl Zeiss, Jena, Germany). GFP intensity was calculated using ZEN Blue software.

Y2H Analysis

The full-length coding sequence (CDS) of OsRopGEF3 and the N-terminus region of OsRBOH5 were fused into a pGADT7 vector, and the full CDS of OsRac3 was fused with the pGBKT7 vector. Each construct was transformed into the AH109 strain and plated on SM media lacking leucine, tryptophan, histidine, and alanine and incubated for 3 days at 30°C as previously reported (Fields and Song, 1989). The primer sequences used in Y2H analysis are listed in **Supplementary Table 1**.

Subcellular Localization Analysis

The ORFs of OsRopGEF3 and OsRac3 were amplified from the root hair cDNA and cloned into a pGREEN vector fused with GFP. For BiFC, Venus fluorescence protein, which emits a bright yellow signal, was used for complementation. OsRopGEF3 was fused with the N-terminus of Venus, and OsRac3 was fused with the C-terminus of Venus.

The constructs were transfected into the *A. tumefaciens* strain GV3101 and infiltrated in tobacco leaf as described previously (Sparkes et al., 2006). All constructs used for tobacco infiltration were expressed under the control of the Cauliflower mosaic virus (CaMV) 35S promoter. After 72 h of infiltration, GFP fluorescence was observed by a confocal laser scanning

microscope (Zeiss LSM 510, Jena, Germany) with 500–530 nm for emission and 488 nm for excitation. YFP fluorescence was detected at 530–560 nm for emission and 500–530 nm for excitation. FM4-64 (Thermo Fisher Scientific) was used as a PM marker and observed with red fluorescence protein (RFP) channel in a 558-nm microscope. The empty GFP protein was used as a control (**Supplementary Figure 2**).

For protoplast transformation, OC cells isolated from rice root cells were cultured in R2S media for at least 1 month. The protoplasts were then extracted using cellulase and macerozyme

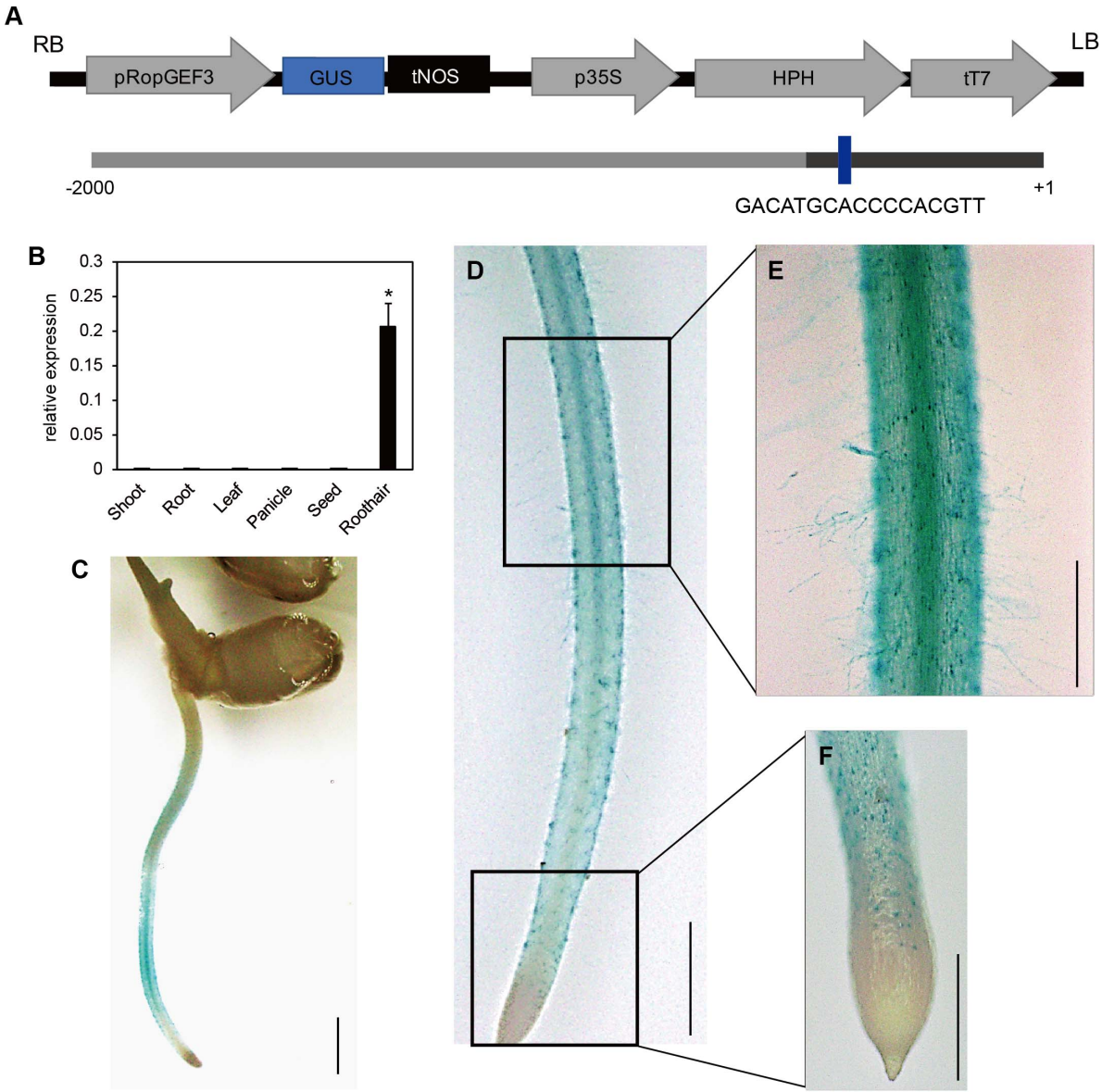

FIGURE 1 | Expression pattern of *OsRopGEF3*. **(A)** The pGA3519 vector map used for histochemical GUS assay of OsRopGEF3 genes. The pGA3519 vector contains a sequence of hygromycin-resistance genes. LB, left border of the vector; RB, right border of the vector; pOsRopGEF3, promoter sequence of *OsRopGEF3*; GUS, beta-glucuronidase; tNOS, NOS terminator; p35S, 35S promoter; HPH, Hygromycin-B-phosphotransferase gene; tT7, T7 terminator. The following shows the promoter region of OsRopGEF3. The dark bar represents the 5′-untranslated region (UTR). The RHE cis-element region is present in the promoter of OsRopGEF3. + 1 means the first base of the start codon, and -2,000 means 2,000 base pairs upstream from it. **(B)** The real-time quantitative PCR (RT-qPCR) analysis of OsRopGEF3 from diverse rice tissues. Rice ubiquitin 5 gene (*OsUBI5*; LOC_Os01g22490) was used as an internal expression control. *X*-axis, the sample name used for analysis; *Y*-axis, the relative expression level of OsRopGEF3. The error bar indicates standard errors in three biological replicates. Significant differences are indicated by asterisks, $*p < 0.01$. The data were analyzed using one-way ANOVA with repeated measurements using Tukey's pairwise comparison test. **(C–F)** Histochemical GUS assay of transgenic lines. The 2,000 base-pair upstream region from the start codon of OsRopGEF3 genes cloned and ligated to the pGA3519 vector. **(C)** The picture of whole plants, bars = 3 mm. **(D)** The entire root from the apical tip to the maturation zone, bars = 2 mm. **(E)** The root hairs and the elongation zone of root, and **(F)** the apical tip and meristematic zone of the root, bars = 500 μm.

r-10 (Yakult) as previously reported (Cho et al., 2016; Wong et al., 2018). The construct was transformed using PEG-mediated protoplast transfection. After transformation, the protoplasts were incubated for > 16 h in dark conditions. All the primers used in our experiments are listed in **Supplementary Table 1**.

RESULTS

Identification of Root Hair-Specific Genes Expressed in Rice

The meta-analysis of public microarray data based on the National Center for Biotechnology Information Gene Expression Omnibus (NCBI GEO)[5] datasets indicated that *OsRopGEF1*, *OsRopGEF3*, and *OsRopGEF11* of the *OsRopGEF* family genes are highly expressed in the root hair tissue (Kim et al., 2020). Among them, *OsRopGEF3* is also strongly expressed in reproductive tissues, such as anthers and pollen, and has high sequence similarity to pollen specific *OsRopGEF* genes. Based on the expression pattern and sequence similarity analyses, we assumed that OsRopGEF3 might have a more important function for root hair elongation than the others because pollen tubes and root hairs share tip-focused growth. RT-qPCR and histochemical assay using GUS proteins have verified the expression patterns of *OsRopGEF3* (**Figure 1**). *OsRopGEF3* was expressed more in

[5]https://www.ncbi.nlm.nih.gov/geo/

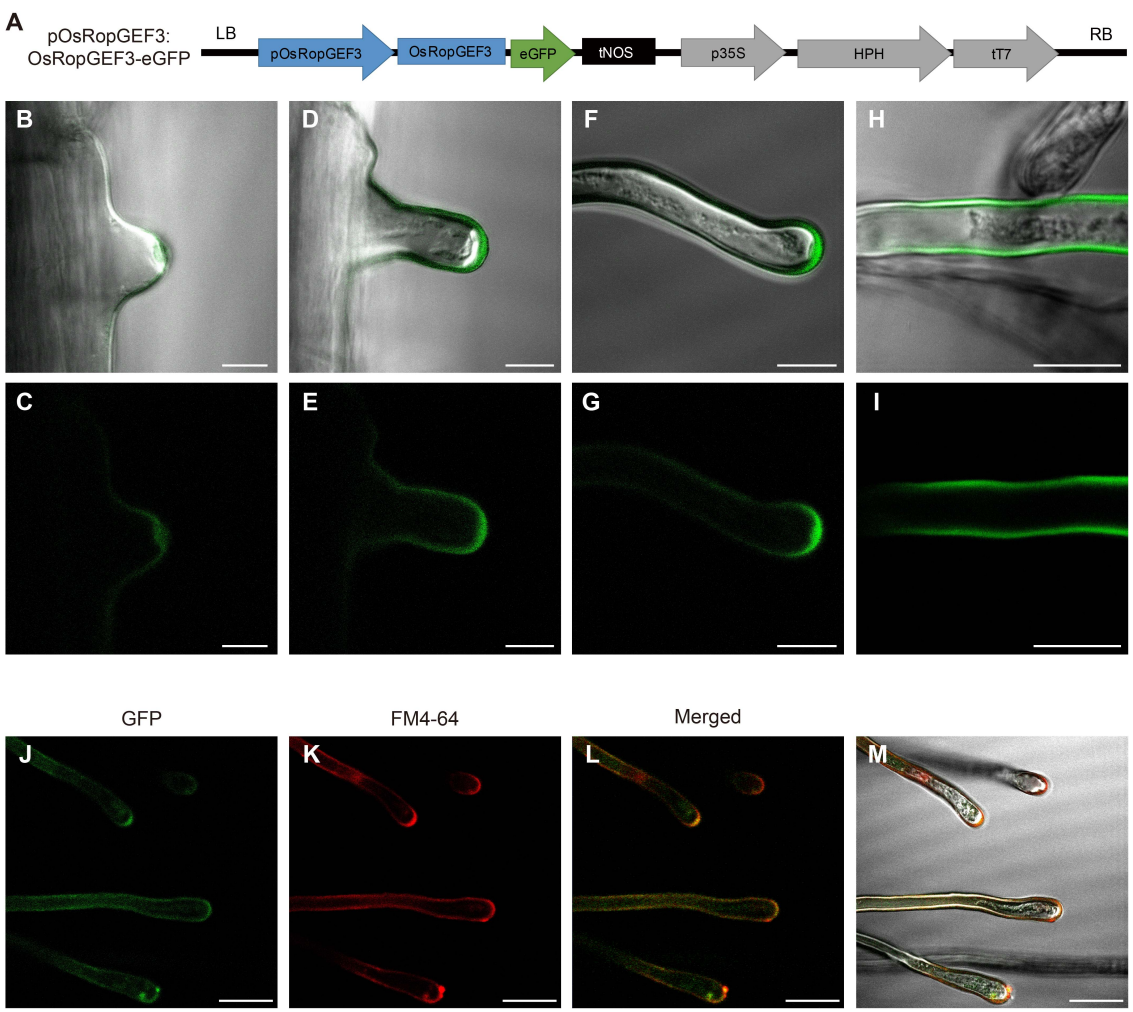

FIGURE 2 | Subcellular localization of OsRopGEF3 in the growing root hairs in rice. **(A)** The pGA3427 vector map used for gain-of-function and fluorescent tagging of OsRopGEF3 genes. OsRopGEF3 native promoter, 2,000 base pairs upstream from the start codon, allowed it to be overexpressed only on the root hairs and tagged with an eGFP (pOsRopGEF3:OsRopGEF3-eGFP). The pGA3427 vector contains a sequence of hygromycin-resistance genes. LB, left border of the vector; RB, right border of the vector; pOsRopGEF3, promoter sequence of *OsRopGEF3*; eGFP, enhance green fluorescence protein; tNOS, NOS terminator; p35S, 35S promoter; HPH, hygromycin-B-phosphotransferase gene; tT7, T7 terminator. **(B–I)** The confocal images of rice root hair in transgenic lines (pOsRopGEF3:OsRopGEF3-eGFP). As root hairs gradually grow, the subcellular localization of OsRopGEF3 protein was detected by fluorescence. **(B,C)** The apical tip part of the initiation states, **(D–G)** the apical tip part of the elongation states, **(H,I)** fully grown root hairs, and **(J–M)** representative confocal images of the root hair in transgenic line stained with FM4-64 dye. FM4-64 was checked on the RFP channel. Bars = 10 μm **(B–I)** and 20 μm **(J–M)**.

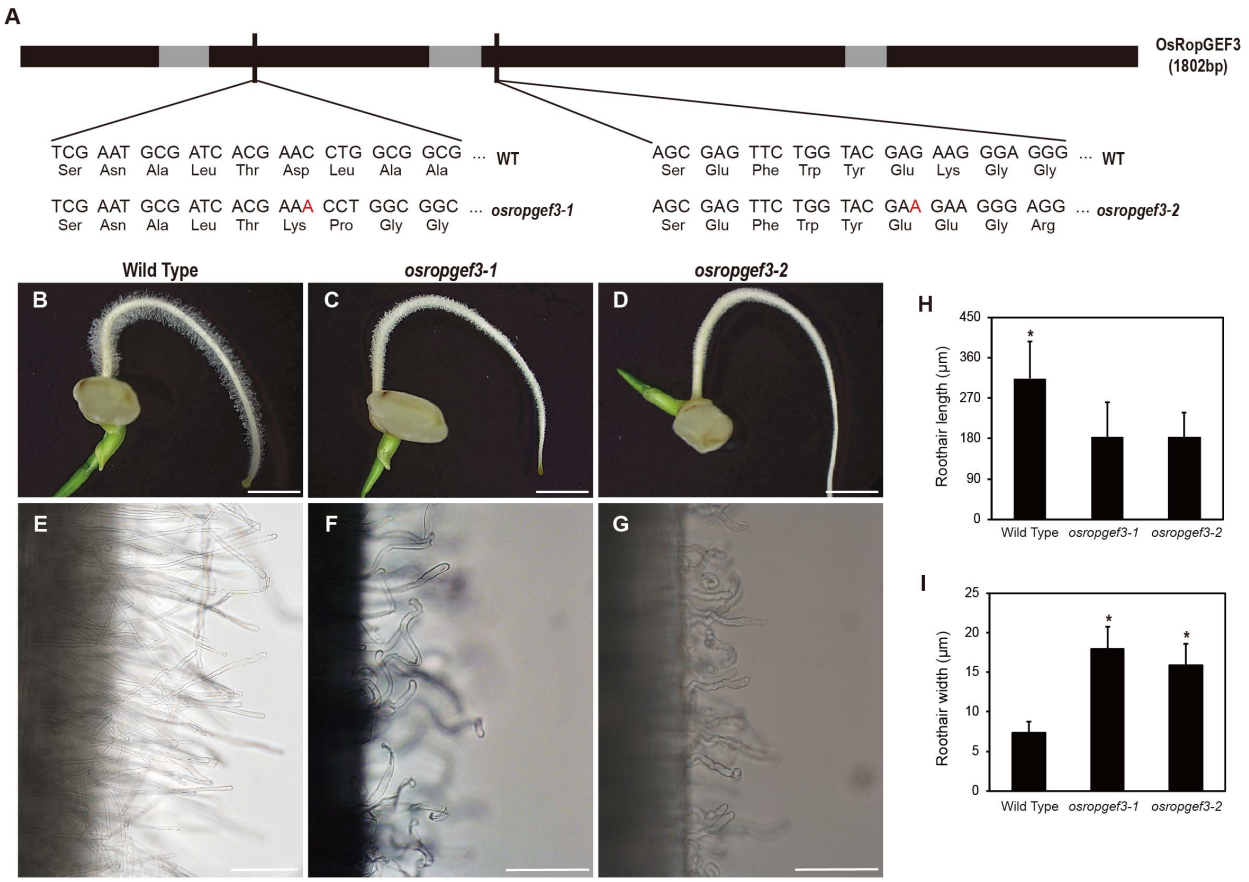

FIGURE 3 | The functional analysis of OsRopGEF3 genes using loss-of-function on rice root hairs. **(A)** The black bar represents the exon, the gray bar represents the intron, and the thin black bar represents the gRNA target point for the mutant line. *OsRopGEF3* genomic DNA has 1802 base pairs. The first loss-of-function mutant (*osropgef3-1*) designated the front of the second exon as the gRNA target site, and the second mutant (*osropgef3-2*) designed the target in the third exon. In both mutant lines, one base (adenine) was inserted, and subsequently, both amino acid sequences were broken, and there was no stop codon produced. **(B–G)** Phenotypic analysis in 3 days after germination loss-of-function transgenic plants. Bars = 3 mm **(B–D)** and 100 μm **(E–G)**. **(H,I)** The root hair length and width comparison between the wild-type and *osropgef3* mutant. The length and width of the root hairs were quantified 2–8 mm from the root apex. The average was calculated by measuring at least 100 root hairs per plant. Error bars represent standard errors in six biological replicates. Significant differences are indicated by asterisks, $^*p < 0.05$. The data were analyzed using Student's *t*-test.

root hair tissues than in other tissues (**Figure 1B**). In addition, RHE lies upstream of OsROPGEF3 (**Figure 1A**), indicating possible gene expression regulated by RSL in a root hair-specific manner. In rice seedlings at three DAG, the GUS signal of *OsRopGEF3* was strongly observed in the root hair tissues and elongation zone of the root, where the root hairs usually start to grow (**Figures 1C,D**). GUS signals are mainly observed in the trichoblast cells of the meristematic zone and the root hairs in the elongation zone (**Figures 1E,F**).

OsRopGEF3 Protein Is Mainly Localized in the PM of Rice Root Hairs

To identify the subcellular localization of the OsRopGEF3 protein, we generate gain-of-function transgenic lines that express OsRopGEF3 protein fused with GFP under the native promoter (*pOsRopGEF3:OsRopGEF3-GFP*) in a wild-type (*O. sativa japonica* cv. Dongjin) background (**Figure 2A**). The OsRopGEF3 tagged with GFP protein localizes strongly at root hairs. When the development of root hair cells initiates, the GFP signal is mainly clustered and located in the cytoplasm of the tip region (**Figures 2B,C**). In the growing root hairs, the GFP signal was spread near the PM but was mainly located at the apical tip region (**Figures 2D,E**). The signal is getting stronger as the root hairs keep growing (**Figures 2F,G**). When the root hairs were fully grown, the fluorescent signals were distributed throughout the PM (**Figures 2H,I**). To verify this localization pattern, we stained the root hairs with FM4-64 dye, which has been used to track the PM. As a result, it was confirmed that the GFP signal appears PM-related in the root hairs through colocalization with FM4-64 signals (**Figures 2J–M**). It was colocalized in the PM, strongly observed in the root hair tip, and identified in the root hair body. However, when predicting protein domains through transmembrane helices hidden Markov models (TMHMM) and Pfam databases (hidden Markov models), no transmembrane domain was observed in

OsRopGEF3 (**Supplementary Figure 1**). Of the 514 total amino acids in OsRopGEF3, S71 to K416 were aligned to the plant-specific ROP nucleotide exchanger (PRONE) domain.

Abnormal Root Hair Phenotypes in the Loss-of-Function Mutant of OsRopGEF3

To know the functional roles of the gene, we generated the loss-of-function mutants of *OsRopGEF3* via targeted mutagenesis using the CRISPR-Cas9 system. We then identified two homozygous lines carrying mutations in different exon regions. The second and third exon of the *OsRopGEF3* were targeted for gene editing, and corresponding mutants are named, *osropgef3-1* and *osropgef3-2* (**Figure 3A**). The *osropgef3-1* line has one base (adenine) insertion in the second exon, and the *osropgef3-2* line has one base (adenine) insertion in the third exon. Both lines have abnormal protein sequences, which change the ORFs but do not create a stop codon. All loss-of-function mutant lines produce defective root hair development phenotypes. Differences in root hair development between mutant and wild types can be clearly distinguished from three DAG (**Figures 3B–D**). Phenotypic differences were the greatest in plants on 3–5 DAG. To compare the phenotypes in detail, we measured the length and width of root hairs between the wild-type and *osropgef3* mutants at three DAG. On average, wild-type root hairs were 290 μm long and 7 μm thick (**Figures 3H,I**). In contrast to wild-type root hairs, the length of the root hairs of *osropgef3-1* and *osropgef3-2* decreased by 180 μm, while the width increased up to 16–18 μm and showed a wavy phenotype (**Figures 3E–I**), clearly presenting defects in root hair elongation.

OsRopGEF3 Is Involved in ROS Generation

To check the intracellular levels of ROS generation in root hair cells, primary roots were stained with CM-H2DCFDA and DAB at three DAG (**Figure 4**). After CM-H2DCFDA staining, the wild-type plants were strongly stained throughout the roots

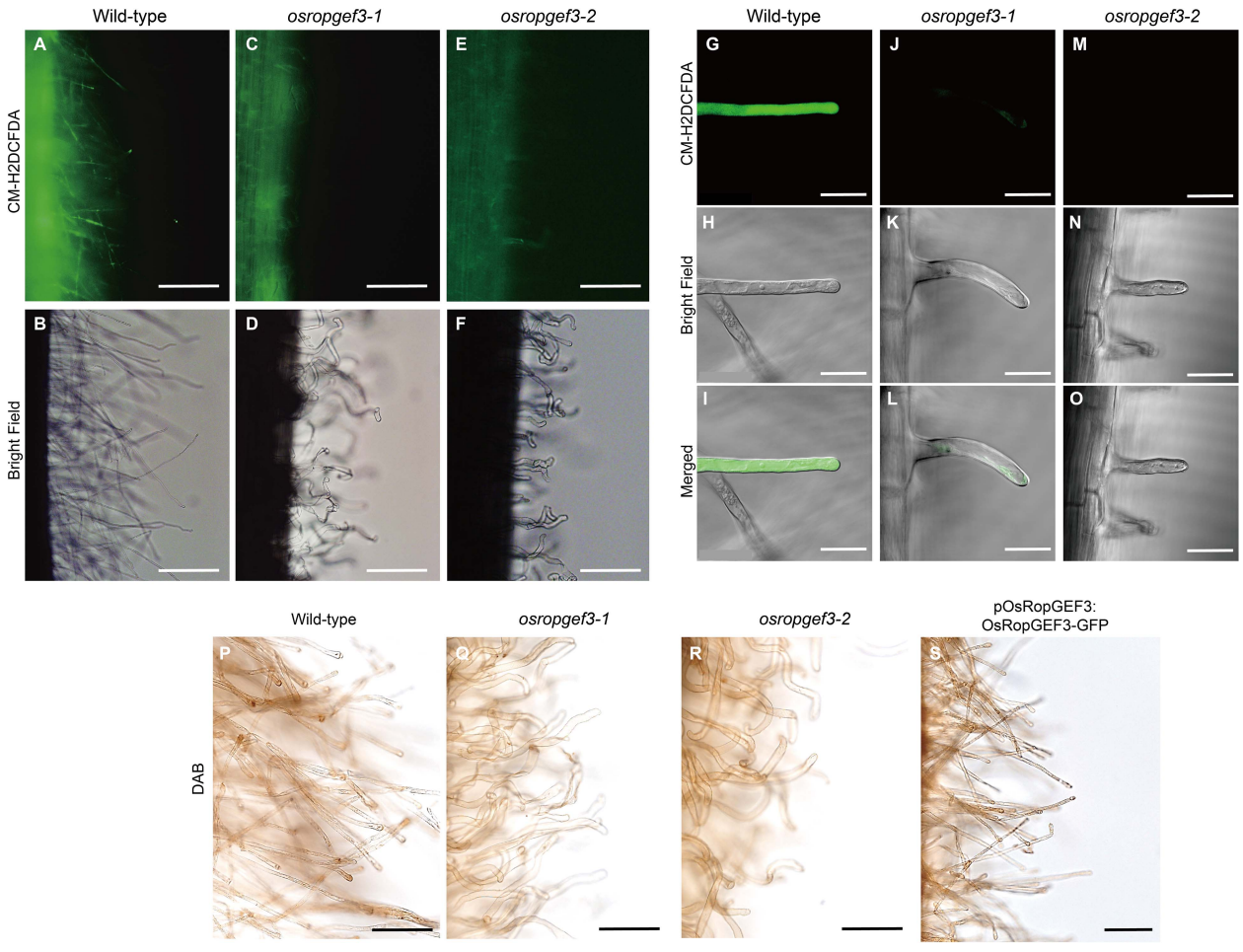

FIGURE 4 | The difference in reactive oxygen species (ROS) in the root hairs of wild-type, *osropgef3* mutants, and gain-of-function line. Representative confocal images of the wild-type and OsRopGEF3 mutant root hairs. **(A–F)** Hydrogen peroxide staining using CM-H2DCFDA dye in three DAG rice roots. Bars = 100 μm. **(G–O)** Zoom photo of CM-H2DCFDA staining using a confocal microscope. Bars = 20 μm. **(P–S)** 3,3′-Diaminobenzidine (DAB) staining in wild-type, two loss-of-function homozygous mutants, and gain-of-function lines (pOsRopGEF3:OsRopGEF3-GFP) in the primary root of three DAG rice plants. Bars = 50 μm.

(**Figures 4A,B**). However, the roots of *osropgef3-1* and *osropgef3-2* mutants were less stained, with negligible staining in the root hairs (**Figures 4C–F**). We then observed the root hairs using a confocal microscope to detect differences in ROS levels. Using the same fluorescence intensity, ROS was detected throughout the entire root hairs of the wild-type plants, but *osropgef3* mutants had weak signals in the apex or were not stained at all (**Figures 4G–O**). The GFP intensity of the root hair apex was approximately 3,500 for the wild-type plants and 0–500 for the mutants (**Supplementary Figure 2**). Next, to confirm the variation in ROS intensity in the OsRopGEF3 gain-of-function transgenic line (*pOsRopGEF3:OsRopGEF3-GFP*), we used DAB dye for staining. CM-H2DCFDA dye could not be used because this transgenic line was tagged with GFP. The wild-type root hairs were strongly stained at the apex region (**Figure 4P**), whereas *osropgef3* root hairs were weakly stained (**Figures 4Q,R**). The gain-of-function line showed staining similar to the wild-type plants (**Figure 4S**). These results demonstrate that *OsRopGEF3* plays a role in ROS production in root hairs.

OsRopGEF3 and OsRac3 Interact in the PM

To find the functional interaction partner for OsRopGEF3 among the OsRac family members in the rice genome, we first analyzed the expression patterns of the entire *OsRac* genes. Heatmap expression data based on the public Affymetrix microarray data consisting of various rice tissues and organs were generated and integrated into a phylogenetic tree (**Figure 5A**). The meta-expression analysis suggests some candidate OsRac that have

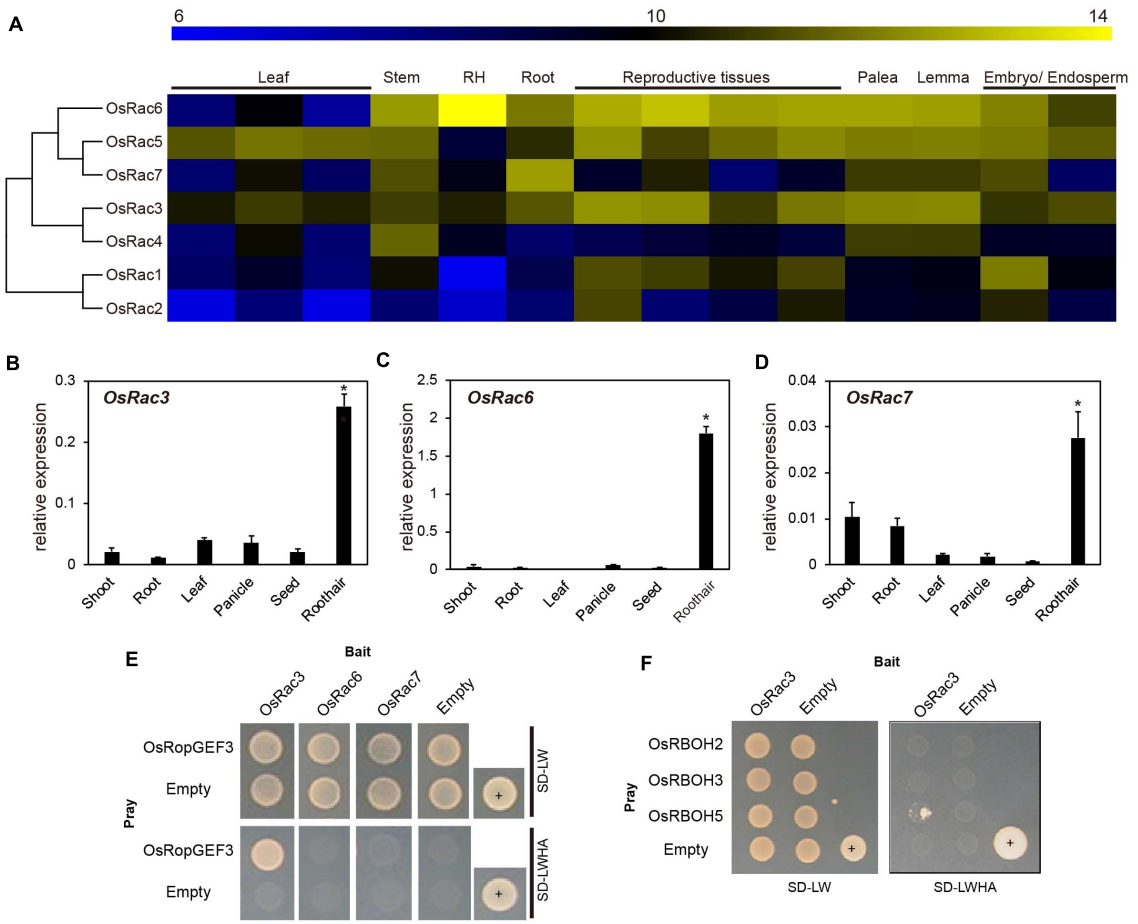

FIGURE 5 | Expression pattern of OsRac and identification of the interacting proteins using yeast two-hybrid analysis. **(A)** Microarray meta-expression analysis and phylogenetic tree of seven *OsRac* genes. The phylogenetic tree was constructed by neighbor-joining methods. In the heatmap, the yellow color indicates a high expression, and the blue color indicates a low expression. Numeric values indicate an average of the normalized log2 intensity of microarray data. Leaf includes the leaf blade, leaf sheath, flag leaf, and reproductive tissues including the anther, carpel, ovary, and pistil. RH, root hair. **(B–D)** Expression verification of *OsRac* using real-time quantitative PCR (RT-qPCR). Rice ubiquitin 5 (LOC_Os01g22490) was used as an internal control. *X*-axis, the sample name used for analysis; *Y*-axis, the relative expression level of the *OsRac3*, *OsRac6*, and *OsRac7*. The error bar indicates standard errors in three biological replicates. Significant differences are indicated by asterisks, $^*p < 0.01$. The data were analyzed using one-way ANOVA with repeated measurements using Tukey's pairwise comparison test. **(E)** The interaction between OsRopGEF3 and three OsRac (OsRac3, OsRac6, and OsRac7) evaluated using the yeast two-hybrid system. **(F)** Identification of the interaction between OsRac3 and three OsRBOH that have highly specific expression in root hair tissues. SD-LW, synthetic defined media without Leu and Trp; SD-LWHA, synthetic defined media without Leu, Trp, His, Ala; + , positive control; empty vector of pGADT7 and pGBKT7 used as a negative control.

the potential to interact with OsRopGEF3 in root hairs. Of the seven *OsRac* genes, *OsRac6* has the highest expression in the root hair tissue, followed by *OsRac3*. *OsRac4* and *OsRac7* have weak expression in root hair. However, none of the *OsRac* genes showed strong expression only in the root hairs. Besides root hairs, *OsRac6* was also highly expressed in the stem, root, palea, lemma, embryo, endosperm, and all reproductive tissues. *OsRac3* was evenly expressed in all analyzed tissues and organs, and *OsRac4* was expressed in the stem, palea, and lemma. RT-qPCR results for six tissues, i.e., shoot, root, leaf, panicle, seed, and root hair, tended to be similar to meta-expression data patterns (**Figures 5B–D**). As expected, three genes, *OsRac3*, *OsRac6*, and *OsRac7*, showed a significant level of expression in root hairs. In particular, *OsRac6* showed the highest expression in root hair tissues. The expression of the remaining genes, i.e., *OsRac1*, *OsRac2*, *OsRac4*, and *OsRac5*, was negligible in the root hairs (**Supplementary Figure 3**).

Using Y2H, we confirmed the interaction between OsRopGEF3 and these three OsRac proteins (**Figure 5E**). The full CDS of each protein was fused with the prey and bait domain. As a result, OsRac3 interacted with OsRopGEF3. However, although OsRac6 was most strongly expressed in root hairs, it did not show any interaction with OsRopGEF3. The interaction between OsRopGEF3 and OsRac3 has also been verified in tobacco leaf cells. The empty GFP vector was used as a positive control (**Supplementary Figure 4**). As shown in **Figure 6**, when expressed individually, OsRopGEF3 was located near the PM (**Figures 6A–D**), and OsRac3 was located in the PM and the cytoplasm (**Figures 6E–H**). FM4-64 dye was used as a PM marker. When 1 M NaCl treatment was used to cause plasmolysis, the GFP signals were merged well with FM4-64 (**Supplementary Figure 5**). Next, the interaction of these two proteins was verified within tobacco cells using BiFC. Similar to the Y2H results, we confirmed that OsRopGEF3 and OsRac3 bind near the PM (**Figures 6I–L**). Interestingly, OsRac3 was spread out in the cytoplasm when expressed alone, but with its binding partner OsRopGEF3, it was also localized near the PM. Intracellular colocalization of the proteins was confirmed through the rice root protoplast system. OsRopGEF3 was mainly located in the PM, whereas OsRac3 was located in the PM and the cytoplasm (**Figures 7A–C**). Next, the interaction of the two proteins was verified through BiFC in rice root cells. The Venus signal was observed in the PM, as shown by the BiFC results in tobacco (**Figures 7D–F**). Although we did not confirm the exact

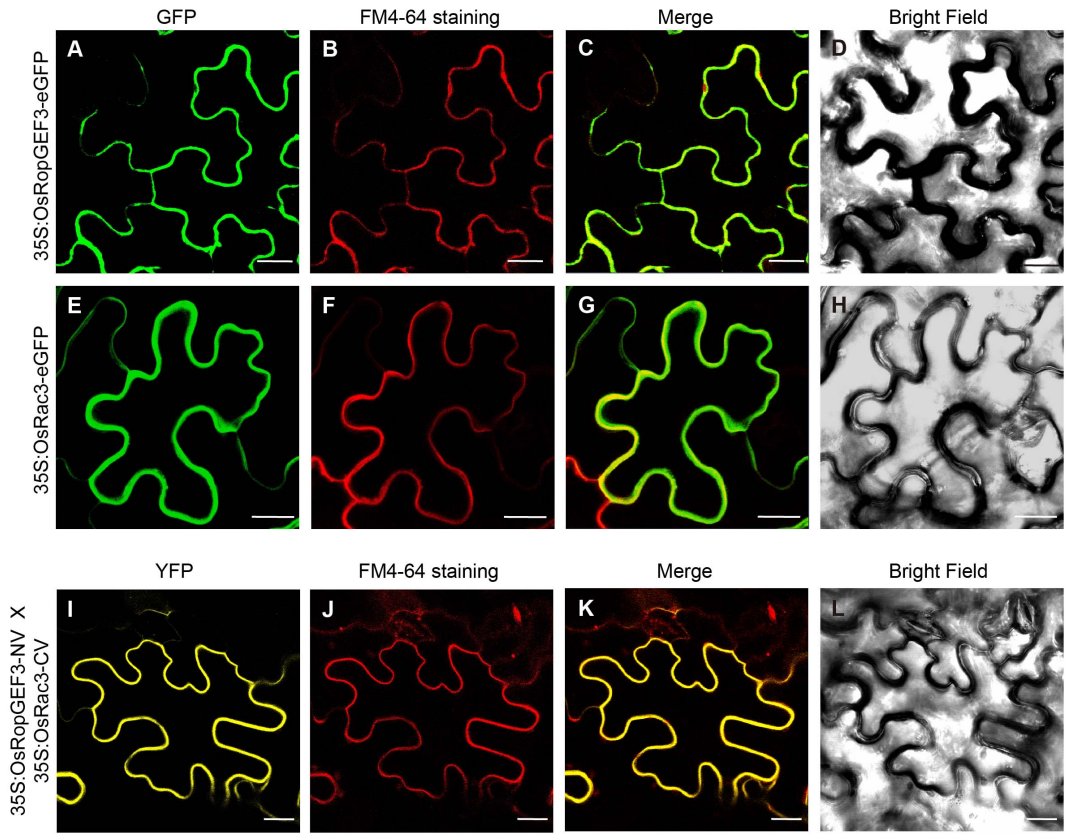

FIGURE 6 | Subcellular localization and BiFC of OsRopGEF3 and OsRac3 in tobacco leaf cells. **(A–H)** Subcellular localization of OsRopGEF3 and OsRac3. These proteins were tagged with enhanced green fluorescent protein (eGFP) and transiently expressed individually in tobacco (*Nicotiana benthamiana*) leaf cells using a 35S promoter. The cells were stained with FM4-64 dye to confirm PM localization. FM4-64 is detected as red fluorescence protein (RFP) signals. **(I–L)** BiFC visualization of OsRopGEF3 and OsRac3. OsRopGEF3 was tagged with the N-terminus of the Venus protein, and OsRac3 was tagged with the C-terminus. Both constructs were coexpressed inside the cells and were stained with FM4-64 dye to confirm their localization. BiFC signals were detected as YFP signals. Bars = 20 μm.

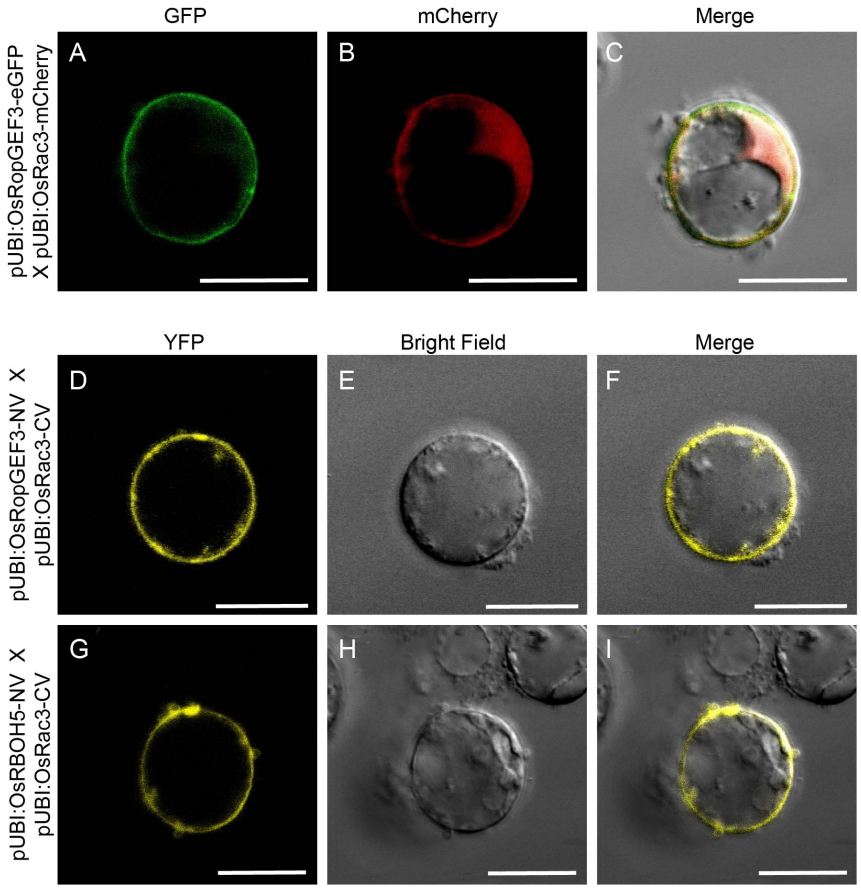

FIGURE 7 | Colocalization and BiFC visualization in rice root protoplasts. **(A–C)** Subcellular localization of OsRopGEF3 and OsRac3. The complete ORF OsRopGEF3 was combined with eGFP, whereas that of OsRac3 was combined with mCherry. These constructs were coexpressed in root protoplasts. **(D–F)** Fill-length OsRopGEF3 and OsRac3 proteins were individually fused with the N- and C-terminals of Venus protein. **(G–I)** The N-terminal protein region of OsRBOH5 was fused with the N-terminal of Venus protein and cotransfected with OsRac3-CV. Each construct was expressed using a maize Ubi (ZmUbi) promoter. The protoplasts were observed under a laser scanning confocal microscope. Bars = 10 μm.

position of the two proteins in the rice root hair cells, our data suggest that the two proteins were colocalized in the root cells and interacted in the PM.

OsRac3 Interacts With the N-Terminus of OsRBOH5

Significant ROS decrease in the *osropgef3* root hairs may be due to the functional failure of OsRac3. ROP/Rac binds to multiple proteins and is involved in various mechanisms. Among these roles, ROP/Rac has been reported to bind to RBOH, which produces ROS inside plant cells. Three RBOH genes are highly expressed in the root hairs of rice: *OsRBOH2*, *OsRBOH3*, and *OsRBOH5* (Kim et al., 2019). Accordingly, we aimed to detect OsRBOH, an interaction partner of OsRac3, using Y2H. The full CDS of OsRac3 and N-terminal region of OsRBOH were combined with the prey and bait domain. As a result, OsRac3 weakly interacted with the N-terminus of OsRBOH5 in the yeast system (**Figure 5F**). Furthermore, to confirm their interaction inside the rice cells, BiFC was performed in root protoplast cells. When both constructs were coexpressed within the protoplast, a strong clear signal was observed in the PM (**Figures 7G–I**). These results indicate that OsRac3 interacts with the N-terminus of OsRBOH5 in the PM of rice root cells.

DISCUSSION

In this study, we confirmed that *OsRopGEF3*, among the OsRopGEF family members, plays a key role in root hair development. When homozygous loss-of-function mutants were generated for *OsRopGEF3* using the CRISPR-Cas9 system, *osropgef3-1* and *osropgef3-2* showed abnormal phenotypes with root hair length decrease, root hair width increase, and wavy phenotype. Of the phenotypes in *osropgef3*, increased root hair width and wavy phenotype are assumed to be related to *OsRac3*. Previous studies have shown that changes in the activity of ROP/Rac induce abnormal phenotypes in root hairs. Supercentipede 1 (SCN1) is a RhoGTPase GDP dissociation inhibitor (RhoGDI) that negatively regulates ROP/Rac activity. The homozygous loss-of-function mutant of *SCN1* has a

branched root hair phenotype (Parker et al., 2000), suggesting that the phenotypic change is due to abnormal ROP activity. Furthermore, mutations in both tip growth defective 1 (TIP1) and pluripetala (PLP) genes (*plp-3 tip1-4*) resulted in decreased root hair length and multiple root hair axes. These phenotypes are due to cytoplasmic accumulation and instability of ROP2 in the root hair apex. Interestingly, the single mutant of the PLP gene shows significantly reduced cytoplasmic ROS and abnormal actin dynamics (Chai et al., 2016). Swollen root hairs were mainly observed for the mutant of the TIP1 gene, a palmitoyl transferase (Hemsley et al., 2005). The loss-of-function mutants for both TIP1 and root hair defective 1 (RHD1) genes had huge swollen root hairs (Parker et al., 2000). It is predicted that the mutant has defective protein palmitoylation and cell wall synthesis and is related to ROP/Rac because palmitoylation of AtROP7, AtROP8, and AtROP10 is required for their proper functioning in the cells (Lavy et al., 2002).

Although ROP/Rac has an important function in root hair elongation, RopGEF is also essential because ROP/Rac cannot function normally without RopGEF. Since the GFP signal was observed in the gain-of-function line (*pOsRopGEF3:OsRopGEF3-GFP*), there is no doubt about the overexpression of this gene. However, this transgenic line showed no significant differences in the length and width of the root hair compared with those of the wild-type plant. This result suggests that OsRopGEF3 and OsRac3 proteins cannot work alone in root hair development. In *osropgef3*, OsRac3 cannot be activated to its GTP-binding form because OsRopGEF3 is absent, thereby affecting various downstream events involved in root hair development in the mutant. However, even in the presence of excessive OsRopGEF3, no phenotypic changes occurred in *osropgef3* due to the limited amount of OsRac3.

Another consideration is the subcellular localization of OsRopGEF3. According to protein domain analysis, OsRopGEF3 does not have a transmembrane domain. Nevertheless, the reason for its location in the PM is expected to be due to its interaction with other transmembrane proteins. RopGEF proteins have preserved serine residues in the C-terminus and have self-inhibition mechanisms involving interaction with the plant-specific ROP nucleotide exchanger (PRONE) domain of receptor-like kinase (RLK) (Fodor-Dunai et al., 2011; Craddock et al., 2012). Since a PRONE domain exists in OsRopGEF3, it is predicted that OsRopGEF3 might interact with root hair RLK. In the BiFC analysis of OsRopGEF3 with OsRac3 in tobacco leaf cells and rice root protoplasts, the YFP signal was located in the PM. These results indicate that OsRopGEF3 can also attach to RLK during its interaction with OsRac3 or does not bind directly but forms complex with other proteins (Akamatsu et al., 2015). Although OsRac3 is localized at the membrane near the cytoplasm when it is expressed alone, the BiFC signal is a

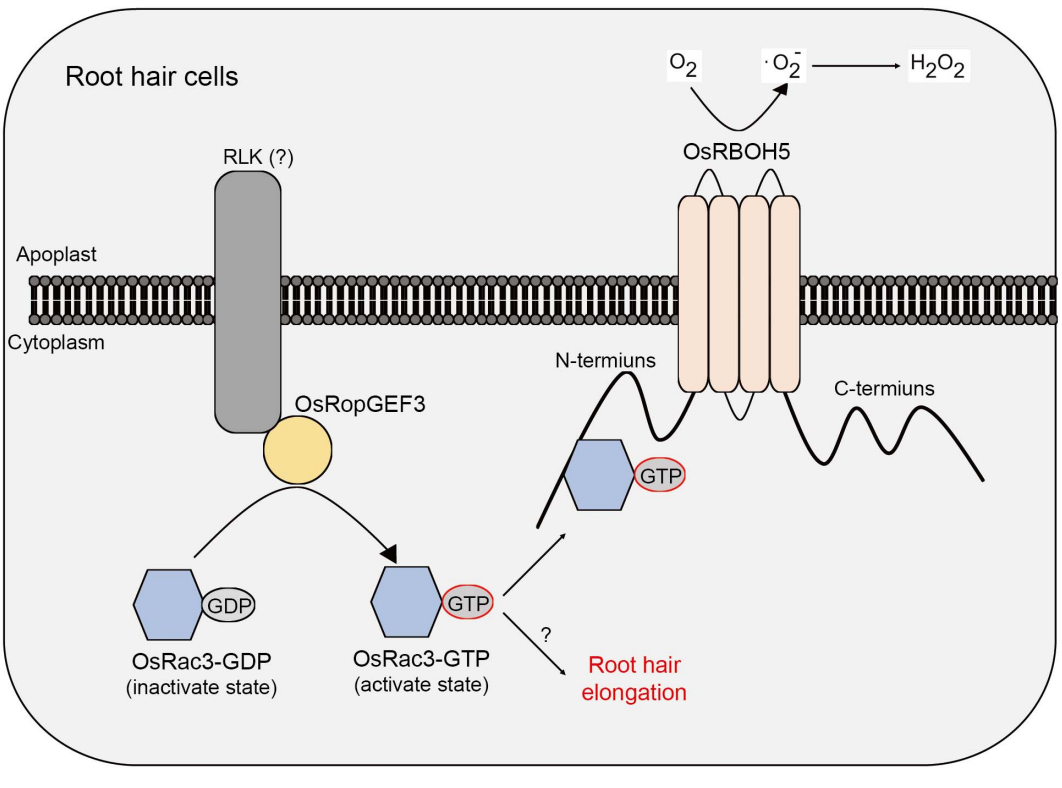

FIGURE 8 | Models of OsRopGEF, OsRac, and OsRBOH proteins inside the rice root hair cells. Based on the PM, the upper part is the apoplast and the lower part is the cytoplasm. OsRopGEF3 localizes to the PM. However, since OsRopGEF3 does not have a transmembrane domain, it is expected to interact with RLK using the PRONE domain. OsRopGEF3 interacts with OsRac3 near the PM to change GDP to GTP. OsRac3-GTP was bound to the N-terminal of OsRBOH5 and resulted in ROS generation in the apoplast. Furthermore, OsRac3 can regulate root hair elongation. However, the specific pathway remains unknown.

meaningful demonstration of the interaction of OsRopGEF3 and OsRac3. However, our results do not provide direct evidence of colocalization or interaction between OsRopGEF3 and OsRac3 inside rice root hairs, thereby warranting further investigation.

Overall, this research aimed to emphasize the relationship of OsRopGEF3–OsRac3–OsRBOH5. The *osropgef3* mutant has significantly reduced ROS in its root hairs, and OsRac3 interacts with OsRBOH5. Based on previous studies, it is known that the activation of ROS in root hairs is mainly regulated by root hair defective-six like (RSL) and root hair-defective (RHD), which are induced by auxin treatment. It is well known that the RSL transcription factor upregulates RBOH, which produces ROS, and is involved in root hair growth (Mangano et al., 2017). However, the OsRBOH5 gene did not show any expression change in root hair tissues in response to the exogenous auxin treatment (Kim et al., 2019). Due to the lack of functional analysis of OsRac3 and OsRBOH5, our results cannot clearly demonstrate the relationship between ROS and root hair development in rice. However, this suggests that OsRBOH5 may not be affected by the transcription factor RSL and may function differently from the Auxin-IAA-RSL-RBOH mechanism. A functional study of OsRBOH5 will be needed to see if ROS produced by OsRBOH5 can affect root hair growth.

CONCLUSION

This study demonstrates a correlation between RopGEF and ROP/Rac protein in rice root hair cells. Through a meta-expression analysis based on public microarray data, RT-qPCR, and GUS reporter system, it was demonstrated that *OsRopGEF3* is highly expressed in rice root hairs. Gain-of-function mutants tagged with fluorescent protein revealed that OsRopGEF3 was mainly located in the apical dome of the growing root hairs. In addition, the loss-of-function mutants, which were generated using the CRISPR/Cas9 system, showed a short and thick root hair phenotype. Furthermore, through Y2H and BiFC experiments, OsRac3 protein was identified as an interacting partner of OsRopGEF3. OsRac3 protein interacts with the N-terminus domain of OsRBOH5. Our results indicate that OsRopGEF3 interacts with OsRac3 protein and then exchanges GDP with GTP to activate OsRac3 in rice root hair cells. Furthermore, the activated form of OsRac3 protein interacts with OsRBOH5 to produce ROS (**Figure 8**).

DATA AVAILABILITY STATEMENT

The datasets presented in this study can be found in online repositories. The names of the repository/repositories and accession number(s) can be found in the article/**Supplementary Material**.

AUTHOR CONTRIBUTIONS

E-JK, Y-JK, and K-HJ conceived and designed the experiments, analyzed the data, and wrote the manuscript. E-JK, W-JH, and WT contributed to the experiments. GA and S-TK contributed to manuscript revision. All authors contributed to the article and approved the submitted version.

FUNDING

This work was supported by grants from the New Breeding Technology Center Program (PJ01492703 to K-HJ), the Rural Development Administration, Republic of Korea and the National Research Foundation (NRF), and Ministry of Education, Science and Technology (2021R1A2C2010448 to J-KH, 2019R1C1C1002636 and 2021R1A4A2001968 to Y-JK).

SUPPLEMENTARY MATERIAL

The Supplementary Material for this article can be found online at: https://www.frontiersin.org/articles/10.3389/fpls.2021.661352/full#supplementary-material

Supplementary Figure 1 | Transmembrane domain analysis of *OsRopGEF3*, *OsRac3*, and *OsRBOH5*.

Supplementary Figure 2 | Fluorescence intensity comparison of ROS staining.

Supplementary Figure 3 | Identification of OsRac gene expression using qRT-PCR.

Supplementary Figure 4 | Induction of plasmolysis in tobacco leaf epidermal cells by treatment with 1M NaCl. OsRopGEF3-eGFP and OsRac3-eGFP were individually transiently expressed in cells.

Supplementary Figure 5 | Transient expression pattern of p35S-eGFP (empty vector) in tobacco leaf cells.

Supplementary Table 1 | Primer sequences used in this study.

REFERENCES

Akamatsu, A., Uno, K., Kato, M., Wong, H. L., Shimamoto, K., and Kawano, Y. (2015). New insights into the dimerization of small GTPase Rac/ROP guanine nucleotide exchange factors in rice. *Plant Signal Behav.* 10:e1044702. doi: 10.1080/15592324.2015.1044702

Berken, A., Thomas, C., and Wittinghofer, A. (2005). A new family of RhoGEFs activates the Rop molecular switch in plants. *Nature* 436, 1176–1180. doi: 10.1038/nature03883

Bibikova, T., and Gilroy, S. (2002). Root hair development. *J. Plant Growth Regul.* 21, 383–415.

Bloch, D., Lavy, M., Efrat, Y., Efroni, I., Bracha-Drori, K., Abu-Abied, M., et al. (2005). Ectopic expression of an activated RAC in Arabidopsis disrupts membrane cycling. *Mol. Biol. Cell* 16, 1913–1927. doi: 10.1091/mbc.e04-07-0562

Bosch, M., and Hepler, P. K. (2005). Pectin methylesterases and pectin dynamics in pollen tubes. *Plant Cell* 17, 3219–3226. doi: 10.1105/tpc.105.037473

Carol, R. J., Takeda, S., Linstead, P., Durrant, M. C., Kakesova, H., Derbyshire, P., et al. (2005). A RhoGDP dissociation inhibitor spatially regulates growth in root hair cells. *Nature* 438, 1013–1016. doi: 10.1038/nature04198

Chai, S., Ge, F. R., Feng, Q. N., Li, S., and Zhang, Y. (2016). PLURIPETALA mediates ROP 2 localization and stability in parallel to SCN 1 but synergistically with TIP 1 in root hairs. *Plant J.* 86, 413–425. doi: 10.1111/tpj.13179

Cherfils, J., and Chardin, P. (1999). GEFs: structural basis for their activation of small GTP-binding proteins. *Trends Biochem. Sci.* 24, 306–311. doi: 10.1016/s0968-0004(99)01429-2

Cho, L. H., Yoon, J., Pasriga, R., and An, G. (2016). Homodimerization of Ehd1 is required to induce flowering in rice. *Plant Physiol.* 170, 2159–2171. doi: 10.1104/pp.15.01723

Craddock, C., Lavagi, I., and Yang, Z. (2012). New insights into Rho signaling from plant ROP/Rac GTPases. *Trends Cell Biol.* 22, 492–501. doi: 10.1016/j.tcb.2012.05.002

Datta, S., Prescott, H., and Dolan, L. (2015). Intensity of a pulse of RSL4 transcription factor synthesis determines Arabidopsis root hair cell size. *Nat. Plants* 1:15138.

Denninger, P., Reichelt, A., Schmidt, V. A., Mehlhorn, D. G., Asseck, L. Y., Stanley, C. E., et al. (2019). Distinct ROPGEFs successively drive polarization and outgrowth of root hairs. *Curr. Biol.* 29, 1854.–1865.

Dolan, L., Janmaat, K., Willemsen, V., Linstead, P., Poethig, S., Roberts, K., et al. (1993). Cellular organisation of the Arabidopsis thaliana root. *Development* 119, 71–84. doi: 10.1242/dev.119.1.71

Duckett, C., Grierson, C., Linstead, P., Schneider, K., Lawson, E., Dean, C., et al. (1994). Clonal relationships and cell patterning in the root epidermis of Arabidopsis. *Development* 120, 2465–2474. doi: 10.1242/dev.120.9.2465

Fields, S., and Song, O. (1989). A novel genetic system to detect protein–protein interactions. *Nature* 340, 245–246. doi: 10.1038/340245a0

Fodor-Dunai, C., Fricke, I., Potocký, M., Dorjgotov, D., Domoki, M., Jurca, M. E., et al. (2011). The phosphomimetic mutation of an evolutionarily conserved serine residue affects the signaling properties of Rho of plants (ROPs). *Plant J.* 66, 669–679. doi: 10.1111/j.1365-313x.2011.04528.x

Foreman, J., Demidchik, V., Bothwell, J. H., Mylona, P., Miedema, H., Torres, M. A., et al. (2003). Reactive oxygen species produced by NADPH oxidase regulate plant cell growth. *Nature* 422, 442–446. doi: 10.1038/nature01485

Gilroy, S., and Jones, D. L. (2000). Through form to function: root hair development and nutrient uptake. *Trends Plant Sci.* 5, 56–60. doi: 10.1016/s1360-1385(99)01551-4

Gu, Y., Li, S., Lord, E. M., and Yang, Z. (2006). Members of a novel class of Arabidopsis Rho guanine nucleotide exchange factors control Rho GTPase-dependent polar growth. *Plant Cell* 18, 366–381. doi: 10.1105/tpc.105.036434

Hemsley, P. A., Kemp, A. C., and Grierson, C. S. (2005). The TIP GROWTH DEFECTIVE1 S-acyl transferase regulates plant cell growth in Arabidopsis. *Plant Cell* 17, 2554–2563. doi: 10.1105/tpc.105.031237

Jones, M. A., Raymond, M. J., Yang, Z., and Smirnoff, N. (2007). NADPH oxidase-dependent reactive oxygen species formation required for root hair growth depends on ROP GTPase. *J. Exp. Bot.* 58, 1261–1270. doi: 10.1093/jxb/erl279

Kawasaki, T., Henmi, K., Ono, E., Hatakeyama, S., Iwano, M., Satoh, H., et al. (1999). The small GTP-binding protein rac is a regulator of cell death in plants. *Proc. Natl. Acad. Sci. U S A.* 96, 10922–10926. doi: 10.1073/pnas.96.19.10922

Kim, E., Kim, Y., Hong, W., Lee, C., Jeon, J., and Jung, K. (2019). genome-wide analysis of root hair preferred RBOH genes suggests that three RBOH genes are associated with auxin-mediated root hair development in rice. *J. Plant Biol.* 62, 229–238. doi: 10.1007/s12374-019-0006-5

Kim, E., Park, S., Hong, W., Silva, J., Liang, W., Zhang, D., et al. (2020). Genome-wide analysis of RopGEF gene family to identify genes contributing to pollen tube growth in rice (Oryza sativa). *BMC Plant Biol.* 20, 1–15. doi: 10.1186/s12870-020-2298-5

Lavy, M., Bracha-Drori, K., Sternberg, H., and Yalovsky, S. (2002). A cell-specific, prenylation-independent mechanism regulates targeting of type II RACs. *Plant Cell* 14, 2431–2450. doi: 10.1105/tpc.005561

Lee, S., Jeon, J., Jung, K., and An, G. (1999). Binary vectors for efficient transformation of rice. *J. Plant Biol.* 42, 310–316. doi: 10.1007/bf03030346

Lin, Q., Ohashi, Y., Kato, M., Tsuge, T., Gu, H., Qu, L. J., et al. (2015). GLABRA2 directly suppresses basic helix-loop-helix transcription factor genes with diverse functions in root hair development. *Plant Cell* 27, 2894–2906.

Mangano, S., Denita-Juarez, S. P., Choi, H. S., Marzol, E., Hwang, Y., Ranocha, P., et al. (2017). Molecular link between auxin and ROS-mediated polar growth. *Proc. Natl. Acad. Sci. U S A.* 114, 5289–5294. doi: 10.1073/pnas.1701536114

Miki, D., and Shimamoto, K. (2004). Simple RNAi vectors for stable and transient suppression of gene function in rice. *Plant Cell Physiol.* 45, 490–495. doi: 10.1093/pcp/pch048

Miki, D., Itoh, R., and Shimamoto, K. (2005). RNA silencing of single and multiple members in a gene family of rice. *Plant Physiol.* 138, 1903–1913. doi: 10.1104/pp.105.063933

Molendijk, A. J., Bischoff, F., Rajendrakumar, C. S., Friml, J., Braun, M., Gilroy, S., et al. (2001). Arabidopsis thaliana Rop GTPases are localized to tips of root hairs and control polar growth. *EMBO J.* 20, 2779–2788. doi: 10.1093/emboj/20.11.2779

Moon, S., Chandran, A. K. N., Kim, Y., Gho, Y., Hong, W., An, G., et al. (2019a). Rice RHC encoding a putative cellulase is essential for normal root hair elongation. *J. Plant Biol.* 62, 82–91. doi: 10.1007/s12374-018-0393-z

Moon, S., Cho, L. H., Kim, Y. J., Gho, Y. S., Jeong, H. Y., Hong, W. J., et al. (2019b). RSL Class II transcription factors guide the nuclear localization of RHL1 to regulate root hair development. *Plant Physiol.* 179, 558–568. doi: 10.1104/pp.18.01002

Moon, S., Hong, W., Kim, Y., Chandran, A. K. N., Gho, Y., Yoo, Y., et al. (2020). Comparative transcriptome analysis reveals gene regulatory mechanism of UDT1 on anther development. *J. Plant Biol.* 63, 289–296. doi: 10.1007/s12374-020-09250-w

Naito, Y., Hino, K., Bono, H., and Ui-Tei, K. (2015). CRISPRdirect: software for designing CRISPR/Cas guide RNA with reduced off-target sites. *Bioinformatics* 31, 1120–1123. doi: 10.1093/bioinformatics/btu743

Palin, R., and Geitmann, A. (2012). The role of pectin in plant morphogenesis. *Biosystems* 109, 397–402. doi: 10.1016/j.biosystems.2012.04.006

Parker, J. S., Cavell, A. C., Dolan, L., Roberts, K., and Grierson, C. S. (2000). Genetic interactions during root hair morphogenesis in Arabidopsis. *Plant Cell* 12, 1961–1974. doi: 10.2307/3871206

Schmittgen, T. D., and Livak, K. J. (2008). Analyzing real-time PCR data by the comparative C T method. *Nat. Protoc.* 3:1101. doi: 10.1038/nprot.2008.73

Schneider, C. A., Rasband, W. S., and Eliceiri, K. W. (2012). NIH image to ImageJ: 25 years of image analysis. *Nat. Methods* 9, 671–675. doi: 10.1038/nmeth.2089

Slabaugh, E., Held, M., and Brandizzi, F. (2011). Control of root hair development in Arabidopsis thaliana by an endoplasmic reticulum anchored member of the R2R3-MYB transcription factor family. *Plant J.* 67, 395–405. doi: 10.1111/j.1365-313x.2011.04602.x

Sparkes, I. A., Runions, J., Kearns, A., and Hawes, C. (2006). Rapid, transient expression of fluorescent fusion proteins in tobacco plants and generation of stably transformed plants. *Nat. Protoc.* 1:2019. doi: 10.1038/nprot.2006.286

Vissenberg, K., Claeijs, N., Balcerowicz, D., and Schoenaers, S. (2020). Hormonal regulation of root hair growth and responses to the environment in Arabidopsis. *J. Exp. Bot.* 71, 2412–2427. doi: 10.1093/jxb/eraa048

Wang, S., Zhu, X., Lin, J., Zheng, W., Zhang, B., Zhou, J., et al. (2018). OsNOX3, encoding a NADPH oxidase, regulates root hair initiation and elongation in rice. *Biol. Plant* 62, 732–740. doi: 10.1007/s10535-018-0714-3

Wong, H. L., Akamatsu, A., Wang, Q., Higuchi, M., Matsuda, T., Okuda, J., et al. (2018). In vivo monitoring of plant small GTPase activation using a Förster resonance energy transfer biosensor. *Plant Methods* 14, 1–14.

Wong, H. L., Pinontoan, R., Hayashi, K., Tabata, R., Yaeno, T., Hasegawa, K., et al. (2007). Regulation of rice NADPH oxidase by binding of Rac GTPase to its N-terminal extension. *Plant Cell* 19, 4022–4034. doi: 10.1105/tpc.107.055624

Xie, K., Minkenberg, B., and Yang, Y. (2015). Boosting CRISPR/Cas9 multiplex editing capability with the endogenous tRNA-processing system. *Proc. Natl. Acad. Sci. U S A.* 112, 3570–3575. doi: 10.1073/pnas.1420294112

Yang, Z. (2002). Small GTPases: versatile signaling switches in plants. *Plant Cell* 14, S375–S388.

Zhang, Y., Xiong, Y., Liu, R., Xue, H. W., and Yang, Z. (2019). The Rho-family GTPase OsRac1 controls rice grain size and yield by regulating cell division. *Proc. Natl. Acad. Sci. U S A.* 116, 16121–16126. doi: 10.1073/pnas.1902321116

Conflict of Interest: The authors declare that the research was conducted in the absence of any commercial or financial relationships that could be construed as a potential conflict of interest.

frontiers in Plant Science

ORIGINAL RESEARCH
published: 04 June 2021
doi: 10.3389/fpls.2021.669143

PagERF16 of *Populus* Promotes Lateral Root Proliferation and Sensitizes to Salt Stress

Shengji Wang[1†], *Juanjuan Huang*[1†], *Xingdou Wang*[1], *Yan Fan*[1], *Qiang Liu*[2] and *Youzhi Han*[1*]

[1] College of Forestry, Shanxi Agricultural University, Jinzhong, China, [2] College of Forestry, Hebei Agricultural University, Baoding, China

The aggravation of soil salinization limits the growth and development of plants. The AP2/ERF transcription factors (TFs) have been identified and play essential roles in plant development and stress response processes. In this study, the function of *PagERF16* was detected using the overexpressing (OX) and RNAi transgenic poplar 84K hybrids. Plant growth, stomatal conductance, antioxidant enzymes activity, and *PagERF16* co-expressed *TFs* were analyzed using morphological, physiological, and molecular methods. OX showed a more robust lateral root system with a bigger diameter and volume compared to the wild-type plants (WT). Physiological parameters indicated the bigger stomatal aperture and lower stomatal density of OX along with the lower Catalase (CAT) activity and higher malondialdehyde (MDA) content contributed to the salt sensitivity. The plant height and rooting rate of OX and RNAi were significantly worse compared to WT. Other than that, the morphology and physiology of RNAi plants were similar to WTs, suggesting that the function of *PagERF16* may be redundant with other TFs. Our results indicate that when *PagERF16* expression is either too high or too low, poplar growth and rooting is negatively affected. In addition, a downstream target TF, NAC45, involved in Auxin biosynthesis, was identified and *PagERF16* could directly bind to its promoter to negatively regulate its expression. These results shed new light on the function of ERF TFs in plant root growth and salt stress tolerance.

Keywords: salt sensitivity, *PagERF16*, lateral root growth, transgenics, poplar

OPEN ACCESS

Edited by:
Ramiro Esteban Rodriguez, CONICET Instituto de Biología Molecular y Celular de Rosario (IBR), Argentina

Reviewed by:
Joanna Kacprzyk, University College Dublin, Ireland
Rita María Ulloa De La Serna, University of Buenos Aires, Argentina

***Correspondence:**
Youzhi Han
hanyouzhi@sxau.edu.cn

[†]*These authors have contributed equally to this work*

Specialty section:
This article was submitted to Plant Development and EvoDevo, a section of the journal Frontiers in Plant Science

Received: *22 February 2021*
Accepted: *19 April 2021*
Published: *04 June 2021*

Citation:
Wang S, Huang J, Wang X, Fan Y, Liu Q and Han Y (2021) PagERF16 of Populus Promotes Lateral Root Proliferation and Sensitizes to Salt Stress. Front. Plant Sci. 12:669143. doi: 10.3389/fpls.2021.669143

INTRODUCTION

Abiotic stresses, such as extreme temperatures, drought, and soil salinity, are identified to be major adverse environmental conditions that plants often encounter (Zhu, 2016; Gong et al., 2020; Ritonga and Chen, 2020). These stressors often limit the geographic distribution of plant species, affect their growth and development, and reduce biomaterial and bioenergy production (Zhu, 2016; Li et al., 2019). For salt stress, it is important to distinguish primary stress signals from secondary signals that are caused by excess salt. The primary signal is hyperosmotic stress, while the secondary effects of salt stress include oxidative stress, damage to cellular components, and metabolic dysfunction. Although some cellular responses result from primary stress signals, others arise primarily from secondary signals (Zhu, 2002, 2016). Plants dehydrate during hyperosmotic conditions, whereupon they close their stomata to avoid further water loss, while simultaneously experiencing a stress-induced reduction in growth (Jung et al., 2017). As is well-known, roots are

identified as the first organs to sense soil moisture conditions, and a robust root system is key to improve plant growth and stress tolerance under an osmotic environment (Matsuo et al., 2008; Uga et al., 2013). However, the genetic and regulatory mechanisms that confer root-mediated salt stress tolerance still remain poorly understood.

Several plant mechanisms that respond to salt stress are regulated by a subset of salt stress-responsive transcription factors (TFs) (Zhu, 2002; Chinnusamy et al., 2004; Song et al., 2016; Chen et al., 2019). Members of the AP2/ERF, MYB, bZIP, and NAC TF families are identified to play key roles in regulating plant salt tolerance mechanisms as salt stress induces or inhibits their expression; this regulation is followed by the activation of downstream salt-correlated genes that are required for plant growth and development (Nakashima et al., 2014; Lee et al., 2016). The differential expression of these *TFs* typically results from changes in the levels of specific epigenetic modifications on the genes for these TFs through stress signal transduction (Jaenisch and Bird, 2003; Kouzarides, 2007). The overexpression of salt stress-related TFs can enhance plant stress tolerance. For example, overexpression of the TF *DREB1A* in transgenic *Arabidopsis* and rice has activated the expression of many stress tolerant genes, which in turn increased plant tolerance to drought, salt, and freezing (Liu et al., 1998; Gilmour et al., 2000; Datta et al., 2012). Expression of the *BplMYB46* is seen to improve salt and osmotic tolerance in *Betula platyphylla* by affecting the expression of genes which include *SOD*, *POD*, and *P5CS* (Guo et al., 2017). It has been shown that a rice stress-responsive TF encoded by the rice *NAC1* gene (*SNAC1*) plays an essential role in drought stress tolerance. Plants expressing *SNAC1* have displayed significantly enhanced tolerance to drought and salinity in multiple generations, and they were found to contain higher levels of water and chlorophyll in their leaves, compared to the wild types (Saad et al., 2013). *NAC45* from poplar is induced by salt stress and hypersensitizes to salt stress (Zhang et al., 2015). Moreover, *ATAF2* as the homologous gene of *NAC45* negatively regulates plant abiotic stress defense and is involved in the auxin biosynthesis pathways by inducing the expression of *NIT2* (Delessert et al., 2005; Huh et al., 2012; Wang and Culver, 2012; Zhang et al., 2015).

Members of the AP2/ERF family, which contain the conserved AP2 domain, are especially spread in plants and are classified into ten subgroups (Nakano et al., 2006). AP2/ERF TFs regulating plant growth, root development, and stress tolerance have been revealed. In *Arabidopsis thaliana*, *PUCHI*, which encodes a AP2/EREBP TF, contributes to lateral root formation and morphogenesis (Hirota et al., 2007). Overexpression of the *A. thaliana HARDY* gene improved rice water use efficiency with enhanced root strength, branching, and cortical cells under drought and salt conditions (Karaba et al., 2007). Both the *ERF3* and *AP37* rice genes play positive roles in promoting crown root development, and the overexpressed plants display significant grain yield increase under the previously recorded drought conditions (Oh et al., 2009; Zhao et al., 2015). Additionally, the overexpression of *OsERF71* and *OsERF137* provides drought resistance and increased grain yield by altering the root structure of rice (Ambavaram et al., 2014; Lee et al., 2016). In *Populus*, *PtaERF003* was determined to have a positive effect on both adventitious and lateral root proliferation (Trupiano et al., 2013).

In this study, we detected the function of *PagERF16*, an ERF TF gene, with molecular biology and physiology indexes using overexpressing (OX) and RNAi transgenic poplar 84K hybrids (*Populus alba* × *P. glandulosa*). OX plants displayed salt hypersensitivity characteristics and a robust lateral root system compared to wild-type (WT) plants. By cross-referencing RNA-seq data, a putative target, *NAC45*, was identified. Yeast one hybrid assay and RT-qPCR indicated that *PagERF16* negatively regulated the expression of *NAC45* by binding to the DRE motif in its promoter. This will provide a theoretical basis for the study of ERF TFs in poplar growth and salt sensitivity.

MATERIALS AND METHODS

Plant Materials and Growth Conditions

Poplar 84K was used for all experiments. To examine the spatiotemporal expression of *PagERF16*, 1-month-old clonally propagated seedlings grown in a chamber (21–25°C, 16-h light/8-h dark cycle with supplemental light of ∼300 $\mu Em^{-2}s^{-1}$, three-band linear fluorescent lamp T5 28W 6400K, and 60–80 % humidity) with 1/2 Murashige and Skoog (MS) plant medium were treated with 100 mM NaCl solution for 24 and 48 h. The roots, stems, mature leaves (second), and shoots were excised from the plants, immediately frozen in liquid nitrogen, and stored at −80°C until use (Li et al., 2012; Lin et al., 2013; He et al., 2019).

Total RNA Extraction

Total RNA from the collected poplar 84K materials was extracted using a RNAprep Pure Plant Kit (TIANGEN, Beijing, China) as previously described (Yao et al., 2016; Li et al., 2019). RNA quality and quantity were measured using a Bio-Spectrometer fluorescence photometer (Eppendorf, Hauppauge, NY, USA). The extracted RNA was then used for RT-qPCR, gene cloning, and RNA-seq.

RT-qPCR Analysis

RT-qPCR was performed as previously described, and cDNAs were synthesized using a Fast Quant RT Kit (TIANGEN), according to the manufacturer's instructions (Wang et al., 2014; Yao et al., 2016). RT-qPCR was performed using TB Green Premix Ex Taq ^{TM} II (TaKaRa, Dalian, China) on an Agilent Mx3000P Real-Time PCR System (Li et al., 2012, 2019). The primers, developed using Primer Premier v6.0 software (PREMIER Biosoft, Palo Alto, CA, USA), were listed in **Supplementary Table 1** (He et al., 2019). *Actin* and *EF1* was used as the housekeeping reference gene. PCR amplification in the logarithmic phase for each DNA sample was analyzed (Li et al., 2019).

Generation of Transgenic Poplar

The coding region of *PagERF16* was amplified from poplar 84K and inserted into a pART-CAM vector under the control of the cauliflower mosaic virus (CaMV) 35S promoter at the XhoI and XbaI sites after sequence confirmation to generate

an overexpression (OX) construct (Gang et al., 2019; He et al., 2019). RNAi construct was designed for the downregulation of *PagERF16*. Specific sequence of *PagERF16* were amplified using primers *PagERF16-RNAi_1* and cloned into pKANNIBAL vector at the XhoI and XbaI sites to form RNAi transgene fragments. After sequencing, the RNAi transgene fragments were subcloned into pRAT27 vector with primes *PagERF16-RNAi_2* at the XhoI and XbaI sites to obtain RNAi construct (Li et al., 2019). OX and RNAi constructs were then introduced into an *Agrobacterium tumefaciens* strain *GV3101* for poplar 84K transformation as previously described (He et al., 2018). The expression of *PagERF16* in transgenic (OX and RNAi) and WT plants was determined using PCR and RT-qPCR of leaf tissues as described above (He et al., 2019; Li et al., 2019). The primers used for vector construction, PCR, and RT-qPCR were summarized in **Supplementary Table 1**.

Phylogenetic Analysis

Multiple sequence alignments were performed using Clustal X1.83 as previously described (Wang et al., 2019). An unrooted phylogenetic tree was constructed using MEGA 7.0.21 with the neighbor-joining method and 1,000 bootstrap replicates (Kumar et al., 2016).

Morphological and Physiological Measurements

To confirm salt stress tolerance, shoots cut from 1-month-old OX, RNAi, and WT plants were sub-cultured on 1/2 MS medium containing 50 mM NaCl for 30 d (Yao et al., 2016). In each experiment, six plants per transgenic line and six WT plants were used. Three OX or RNAi lines served as three biological repeats, respectively. Mature leaf (second) and root images were taken using an Epson Expression 10,000 XL desktop scanner and further analyzed using the WinRHIZO system (Regent Instruments, Quebec, Canada) to obtain measurements such as the average root diameter, tips, surface area, volume, total length, leaf area, and aspect ratio (Liu et al., 2015, 2019). The color of leaf was detected using the WR SERIES COLORIMETER (FRU, Shenzhen, China) with the LAB methods according to the manufacturer's instruction.

The leaf (second) relative water content (RWC) was calculated as (FW-DW)/(TW-DW) × 100. The leaf was detached and weighted to obtain the fresh weight (FW). The leaf was placed in water for 24 h and was weighted to get the turgid weight (TW). The leaf was dried to a constant weight at 65°C and was used as the dry weight (DW) (Wang et al., 2016).

Peroxidase (POD), superoxide dismutase (SOD), Catalase (CAT) activity, malondialdehyde (MDA) content, and relative electrical conductance was measured as previously described (Yao et al., 2016; Wang et al., 2017; He et al., 2018).

Stomatal density and size were detected with leaves floated on stomatal opening buffer (containing 10 mM CaCl2, 50 mM KCl, and 5 mM MES, pH 6.15) for 3 h in the light to preopen stomata. Lower epidermal strips were collected for measurement of stomatal apertures using an Olympus BH-2 light microscope (Wang et al., 2020).

RNA-Seq Analysis

Leaves (second) from 1-month-old OX and WT plants were used for RNA-seq. WT plants were treated with 100 mM NaCl solution (WT_S) for 24 h. A total of nine libraries, three independent transgenic lines (OX-12, OX-16, and OX-19) under normal growth conditions (materials from six plants pooled per line), three samples from the WT, and three samples from WT_S (materials pooled from six plants for each) were sequenced using IIlumina Novaseq 6,000 with the 2 × 150 bp paired reads by Majorbio (Majorbio Bio-pharm Technology, Shanghai, China). Raw data about 4.0 GB per sample was obtained and clean reads were mapped to the *P. trichocarpa* genome v.4.0 using TopHat2 (Kim et al., 2013). Gene expression was reported as transcripts per million reads (TPM). Differentially expressed genes (DEGs) between OX and WT, as well as between WT and WT_S, were identified using DESeq2 with a $\log_2$fold-change ($|\log_2 FC|$) ≥ 1 and an adjusted P-value < 0.05 as cutoffs (Love et al., 2014; Schurch et al., 2016). The data were analyzed on the free online platform Majorbio Cloud (www.majorbio.com).

Motif Discovery

Conserved motifs of proteins were detected using the program MEME version 5.0.2 (Bailey et al., 2009). MEME was run with the following parameters: any number of repetitions, a maximum number of 6 motifs, and between 6 and 50 residues for optimum motif widths. Promoter sequences (2 kb upstream of the translation start site) were blasted and obtained from the Phytozome v12.1 database. The cis-elements prediction and location in promoters were performed using the PlantCARE (http://bioinformatics.psb.ugent.be/webtools/plantcare/html/).

Yeast One-Hybrid Assays

The yeast one-hybrid assay was performed to verify the physical interactions between *PagERF16* and the promoter of downstream target genes (Luo et al., 2020). The promoter sequence (−525 bp to −197 bp upstream of the translation start site) of *NAC45* containing DRE cis-element was amplified using primers *Promoter-NAC45* from 84K poplar and cloned into the pAbAi vector. The CDS of *PagERF16* were cloned using primers *AD-PagERF16* and inserted into the pGADT7 vector (Clontech, CA, USA). The primers used were listed in **Supplementary Table 1**. The *pGADT7-Rec-53* and *p53-AbAi* were used as positive control and *pGADT7-ERF16* and *pAbAi* served as the negative control. The recombinant plasmids were transformed into yeast *Y1H* Gold strains and plated on the SD/-Leu medium containing either 0 or 200 ng/ml Aureobasidin A (AbA).

Statistical Analysis

One-way analysis of variance was used to detect the significance of the differences among morphology and physiology indexes using OriginPro 2016 (Northampton, MA, USA). A Tukey test was performed to determine significant differences by a p-value cutoff value of 0.05. t-test was used to analyze gene expression differences between transgenic and WT plants.

RESULTS

PagERF16 Is a Salt Stress Related Transcription Activator

The study has indicated that 25 *ERF* TF genes, including *ERF16*, were up- or downregulated when *Populus* was exposed to NaCl, KCl, $CdCl_2$, and PEG 6,000 solutions (Yao et al., 2019). To elucidate the potential function of *PagERF16* in poplar 84K salt tolerance and growth, the spatiotemporal expression pattern was analyzed using RT-qPCR with primers *PagERF16-RT* under 100 mM NaCl treatment (**Supplementary Table 1**). When subjected to salt stress, *PagERF16* in roots was determined to be sensitive to salt stress, whose transcript levels decreased to significantly lower level at 48 h (**Figure 1A**). However, expression of *PagERF16* in shoots and leaves was found to be highly induced at 24 or 48 h, respectively (**Figure 1A**). On the other hand, the expression of *PagERF16* in stems showed no significant change. These results suggested that *PagERF16* may function in roots development and be suppressed by salt stress at least in roots.

To detect the feasible molecular structure of *PagERF16*, the cDNA was cloned from poplar 84K using PCR with *PagERF16-CAM* primers (**Supplementary Table 1**). The coding sequence (CDS) of *PagERF16* was 408 bp encoding 106 amino acid residues. Motif discovery analysis showed that *PagERF16* has a conserved AP2 domain located in amino acid sequences 3–52 (**Figure 1B**). A phylogenetic tree with homologous proteins from other plant species was constructed, and *PagERF16* was roughly homologous with *NtERF16* of *Nicotiana tabacum* and *AtERF16* of *Arabidopsis thaliana* (**Figure 1C**). Multiple alignment of the amino acid sequences indicated that *PagERF16* shared common conserved domains with *PtERF16* of *P. trichocarpa* and *PeERF16* of *P. euphratica* (**Figure 1D**).

PagERF16 Overexpressing Poplar Is Sensitive to Salt Stress

To investigate the biological functions of *PagERF16*, transgenic poplar 84K overexpressing (OX) or downregulating (RNAi) *PagERF16* were generated under the control of a CaMV 35S promoter. The transgenic lines were verified using PCR with *PagERF16-T1* primers, which were composed of a forward primer from the promoter of CaMV 35S and a reverse primer from *PagERF16* (**Supplementary Table 1**; **Supplementary Figure 1A**). In total, 19 OX and nine RNAi transgenic lines were obtained in this study (**Supplementary Figures 1A,B**). RT-qPCR using the leaf tissues was used to cross-verify the transgenic plants at a transcript level. Three OX and three RNAi transgenic lines (OX-12, OX-16, OX-19, RNAi-1, RNAi-4, and RNAi-5) with the highest and lowest *PagERF16* transcript level were selected for further analysis (**Supplementary Figures 1C,D**). The expression of *PagERF16* in selected OX was significantly higher than WT while that in RNAi was only 0.6 times to WT. The indistinctive expression between the RNAi and WT may be one of the reasons contributing to the phenotypic similarity between RNAi and WT.

Under normal growth condition (NC, 0 mM NaCl), the plant height of OX was shorter than that of WT and RNAi (**Figures 2A,G**). However, an obvious difference was found that the lateral roots of OX were thicker and stronger compared to

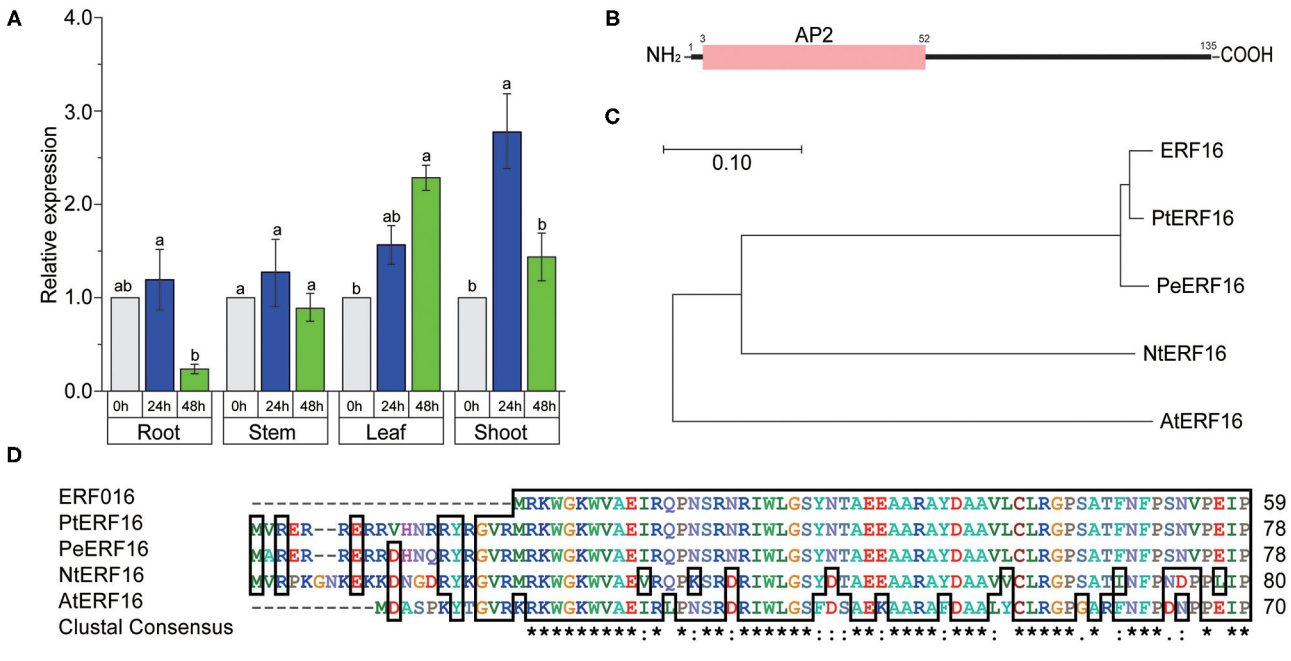

FIGURE 1 | Spatio-temporal expression pattern and sequence alignment of *PagERF16*. **(A)** Relative expression of *PagERF16* in roots, stems, leaves, and shoots, respectively, under 100 mM NaCl. Different lowercases above the bar chart indicate significant differences among samples ($p \leq 0.05$). **(B)** AP2 conserved domain architecture of PagERF16 of poplar. **(C)** Phylogenetic analysis of PagERF16 homologs in *P. trichocarpa*, *P. euphratica*, *Nicotianu tabacum,* and *Arabidopsis thaliana*. **(D)** Multiple sequence alignment of PagERF16 amino acid sequence of *Populus trichocarpa*, *P. euphratica*, *Nicotianu tabacum,* and *Arabidopsis thaliana*.

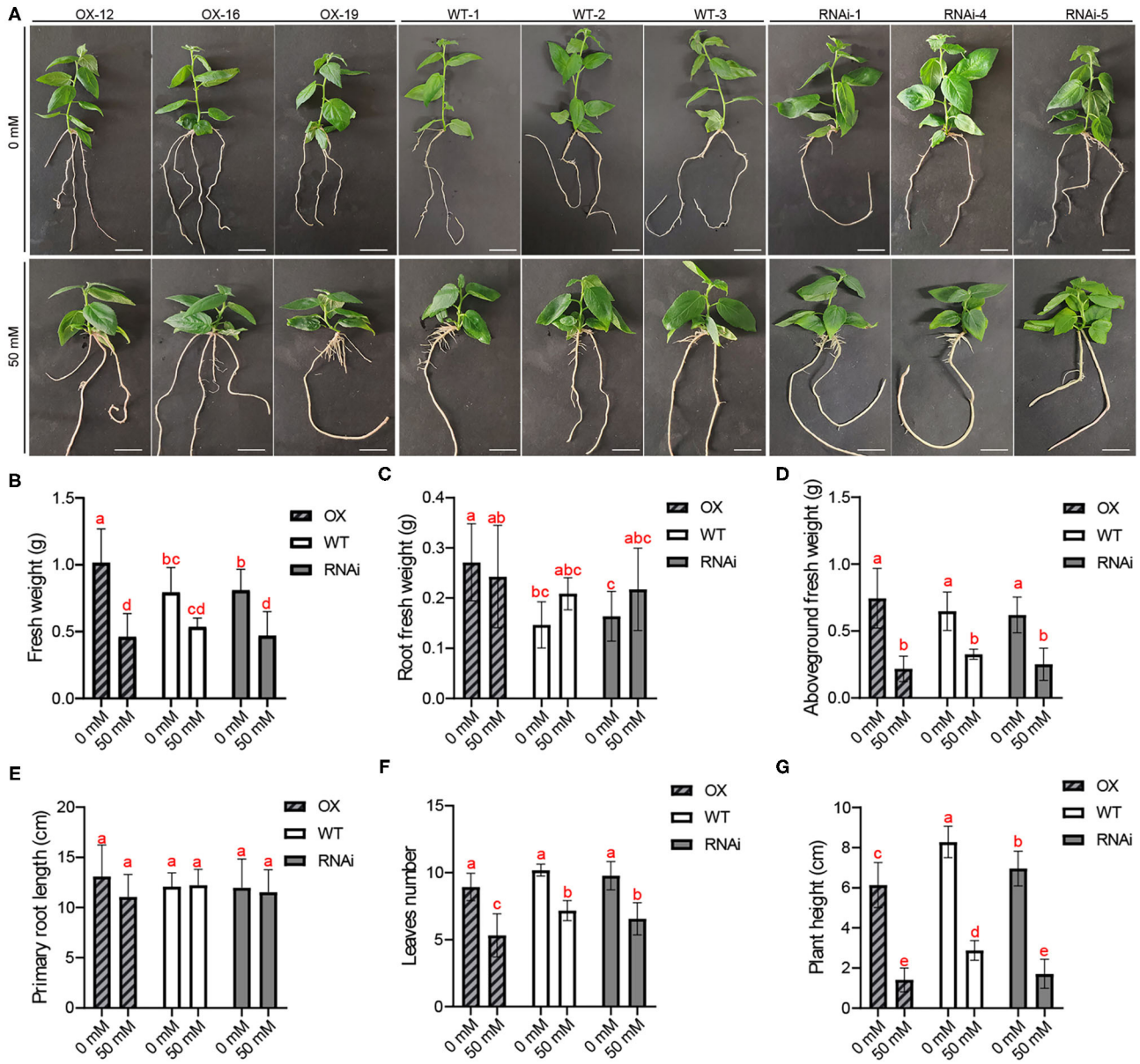

FIGURE 2 | PagERF16 was sensitive to salt stress. **(A)** Morphology of the OX, RNAi, and WT grown on medium containing 50 mM NaCl for 30 d. Bars, 2 cm. **(B)** Fresh weight of whole plant. **(C)** Root fresh weight. **(D)** Fresh weight of aboveground tissues. **(E)** Length of primary root. **(F)** Numbers of leaves per plant. **(G)** Height of plant. The plot represents the mean ± SD of six plants per line. Three OX and RNAi lines serve as three biological repeats, respectively. Different lowercases indicate significant differences among samples ($p \leq 0.05$).

the WT and RNAi (**Figure 2A**). The root fresh weight of OX was much bigger than that of WT and RNAi while the primary root length was similar (**Figures 2C,E**). The fresh weight of the aboveground tissues among the OX, RNAi, and WT had no significant differences (**Figure 2D**). These results indicated that the robust lateral roots of OX made a major contribution to the bigger fresh weight of OX (**Figure 2B**). The numbers of leaves per plant was similar among the different genotypes (**Figure 2F**). The morphology of RNAi plants was relatively similar to the WT, although WT plants were higher (**Figure 2**). In addition, we found that the leaf color was different among OX, RNAi, and WT, but the difference could not be well-distinguished in a picture (**Figure 2A**). We quantify the color of leaf using LAB method in the following experiments.

When sub-cultured under salt stress (50 mM NaCl) conditions for 30 d, the plant height of transgenic and WT plants decreased but the roots thickened to different degrees (**Figure 2**). The fresh weight and aboveground fresh weight were similar among OX, RNAi, and WT, but the reduction of OX compared to that under normal condition was biggest (**Figures 2B,D**). The root

fresh weight of OX was relatively reduced to that under normal condition while WT and RNAi were increased (**Figure 2C**). We also found that the salt stress did not significantly inhibit the elongation of primary roots but decreased the number of leaves, especially in OX (**Figures 2E,F**). Above all, the overexpression of *PagERF16* made poplar sensitive to salt stress.

PagERF16 Enhances Lateral Root Growth

To verify the effect of *PagERF16* on the lateral root system, the roots of OX, RNAi, and NT were scanned and analyzed using WinRHIZO software. Under normal condition, total root length and tips showed no significant difference among OX, RNAi, and WT (**Figures 3A,E**), but the root average diameter and volume of OX was much bigger than those of WT and RNAi (**Figures 3B,D**). The surface area of OX was significantly bigger than that of RNAi, although both showed no difference to WT (**Figure 3C**). Individual statistical analysis of roots with Diameter > 1.0 was made and it was found that the length, surface area, and volume of OX were significantly bigger than those of WT and RNAi (**Figures 3F–H**). All above parameters of RNAi were similar to those of WT.

When exposed to salt stress, the total root length and tips of all genotypes were reduced but diameter, surface area, and volume were increased (**Figure 3**). The root length and tips of OX and RNAi were smaller than those of WT, indicating that salt stress inhibited OX and RNAi lateral root elongation and numbers to a much deeper degree (**Figures 3A,E**). The root length and tips of RNAi was similar to those of OX. The diameter and volume of OX were bigger than those of RNAi, suggesting that although the salt stress increased the diameter and volume of RNAi, the diameter increment caused by the expression of *PagERF16* to OX still cannot be ignored (**Figures 3B,D**). The diameter and volume of RNAi were similar to those of WT while surface area was smaller. Parameters of roots with Diameter > 1.0 were not significantly different between WT and OX or WT and RNAi, but those of OX were much bigger than those of RNAi (**Figures 3F–H**).

In addition, the rooting rate of sub-cultured shoots were monitored. Under normal condition, the initial rooting time and rooting rate of OX was worse than that of WT, while RNAi only showed a difference from WT in rooting time. Nevertheless, the rooting rate and rooting time of WT were much better than those of OX and RNAi after being treated with salt stress, especially OX. Overexpressing of *PagERF16* significantly reduced the rooting rate of poplar and postponed rooting time, which may be the reason that primary root length of OX was not elongated compared to WT (**Figure 3I**). All of these findings indicated that *PagERF16* functioned in poplar root growth, especially in lateral root proliferation.

PagERF16 Reduces Stomatal Density and Increases Stomatal Width

Under normal growth conditions, the plant height of OX was smaller than that of WT (**Figure 2G**), but the parameters of leaf, including leaf area, length, and width, were bigger (**Figures 4A–C**). RNAi showed similar leaf phenotype with OX that was bigger than WT. The leaf aspect ratio of these three genotypes was not different (**Figure 4D**). These results indicated that *PagERF16* could affect the size of leaves but not the shape characteristics. After being treated with salt stress, the leaf size of OX and RNAi was significantly decreased, especially the OX, while WT showed no change (**Figures 4A–C**). The leaf aspect ratio of these three genotypes increased to different degrees, suggesting that salt stress induced the leaf shape to become slenderer (**Figure 4D**). In addition, the leaf color of OX was more yellowish green compared to WT and the difference decreased after being treated with salt stress (**Supplementary Table 2**).

To investigate whether changes of leaf phenotype contributed to salt stress tolerance of poplar, the leaf RWC and electrical conductance were measured. Results showed that both of these two indexes were not significantly changed among the three genotypes with/without salt stress treatment (**Figures 4E,F**). What caught our attention was that the stomatal density and size was different among transgenic plants and WT (**Figures 4G–J**). The stomatal density of OX decreased but the width increased compared to the WT. However, the leaf characteristics of RNAi were similar to WT.

PagERF16 Inhibits Antioxidant Enzymes Synthesis

When plants encounter a severe environment, antioxidant enzymes will increase to reduce the contents of reactive oxygen species (ROS). ROS accumulation is an important messenger in stomatal movement (opening and closure), leading to reduced water loss (Zhang et al., 2020). To detect the function of *PagERF16* in stomatal movement and ROS accumulation, we analyzed the activity of antioxidant enzymes. Under normal conditions, the POD and SOD activities and MDA content of OX were similar to those of WT but significantly lower than those of RNAi (**Figures 5A,B,D**). The CAT activity of these three genotypes showed no difference (**Figure 5C**). These indicated that repressing *PagERF16* increased the antioxidant enzymes synthesis of poplar. When treated with salt stress, POD and SOD activities and MDA content were all induced and OX had more POD and MDA than WT and RNAi. The CAT activity was inhibited by salt stress.

The transcript level of genes relevant to ROS accumulation was also explored in this study. Results showed that the OX plants had relatively higher expression levels in all of these nine genes (**Figures 5E–M**). Expression of *POD2* and *POD3* were significantly induced in OX compared to WT while suppressed in RNAi (**Figures 5F,G**). Moreover, *SOD1*, *SOD2*, and *P5CS1* were downregulated in RNAi (**Figures 5H,I,M**). Expression of *POD1*, *SOD3*, *APX1*, and *APX2* were not different from each other among the three genotypes (**Figures 5E,J–L**). These indicated that overexpressing *PagERF16* could up-regulate genes involved in POD metabolism process to modulate poplar salt stress tolerance, while repressing *PagERF16* inhibited the synthesis of POD, SOD, and P5CS1 proteins.

PagERF16 Negatively Regulates the Expression of *NAC45*

To unravel the regulatory function of *PagERF16*, leaf transcriptomes were analyzed in WT and OX plants using

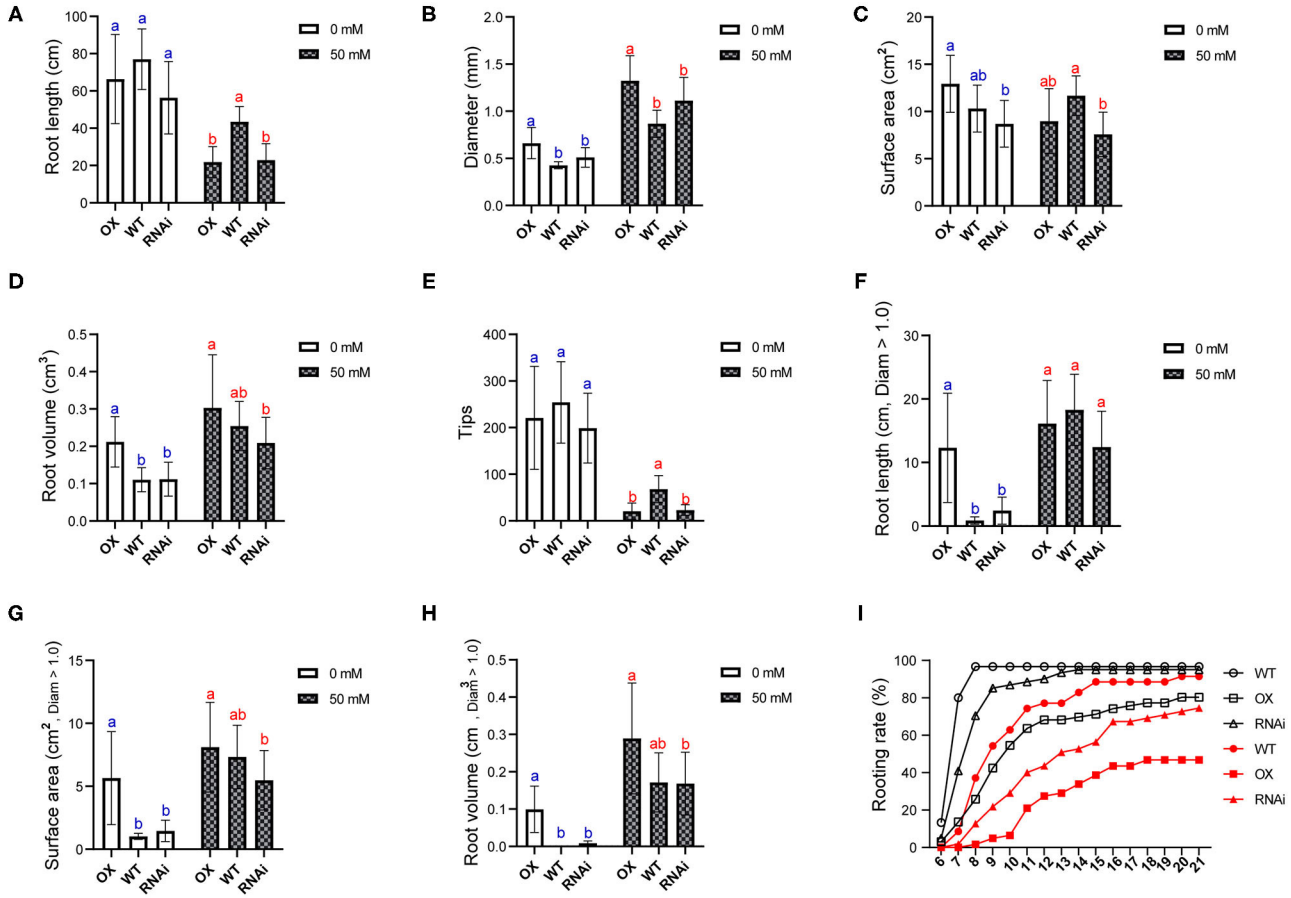

FIGURE 3 | PagERF16 promoted lateral root proliferation by increasing the diameter and volume. **(A)** Total length of root. **(B)** Average diameter of root. **(C)** Total surface area of root. **(D)** Total volume of root. **(E)** Tips of root system. **(F–H)** Represent the length, surface area, and volume of roots with diameter >1.0 mm, respectively. The plot represents the mean ± SD of six plants per line. Three OX or RNAi lines serve as three biological repeats. Different lowercases indicate significant differences among genotypes under the control (blue) or salt stress (red) conditions ($p \leq 0.05$). **(I)** Rooting rate of 60 shoots per genotype (OX, RNAi, and WT) sub-cultured on medium without (black) or with 50 mM NaCl (red).

RNA-seq. DEGs in WT_S vs WT and in OX vs WT were selected using $|\log_2 FC| \geq 1$ and adjusted p-value ≤ 0.05 cutoffs (**Supplementary Tables 3**, **4**). In total, 1,175 DEGs were identified for WT_S with 1.9 times more up- than downregulated genes (766 and 409, respectively, **Supplementary Figure 2A**). A much smaller amount of DEGs were identified for OX, which showed a converse distribution with 3.6 times more down- than upregulated genes (226 and 62, respectively). The TFs of the DEGs were identified using PlantTFDB 4.0 with Hmmscan (E-value < 1.0E-5) methods and were annotated using BLAST (E-value < 1.0E-5). The TFs for WT_S mainly belonged to NAC, ERF, MYB-related, and WRKY TF families (**Supplementary Figure 2B**), whereas TFs for OX were enriched in WRKY and MYB-related TF families (**Supplementary Figure 2C**). In total, seven common TFs were identified for WT_S and OX plants, more than half of which (WRKY24, WRKY33, WRKY40, and WRKY41) belonged to WRKY family in prediction. There was also one NAC (NAC45), one bZIP TF (bZIP14), and one GRAS (SCARECROW-like5, **Supplementary Table 5**). Expression pattern showed that all of the genes were down-regulated in OX (**Figure 6A**). To identify target TFs that may be related to *ERF16*, a correlation analysis was performed, using Spearman method. Only *bZIP14* was directly correlated with *PagERF16* and the remaining five TFs related to each other filled in another network (**Figure 6B**).

To reveal the regulation relationship between *PagERF16* and the five-TFs network, *cis*-elements in the promoter regions of the inferred targets were detected using the PlantCARE programme. We found that *NAC45* contained a DRE motif which could be bound to PagERF16 (Cheng et al., 2019). Yeast one-hybrid assays showed that PagERF16 could directly bind to the promoter (−525 to −197 bp upstream of the translation start site) of *NAC45* containing the DRE motif (**Figures 6C,D**). In addition, RT-qPCR cross-validated that *NAC45* was highly induced in RNAi plants (**Figure 6E**). However, the expression of *NAC45* in OX showed no significant difference to WT. These suggested that repressing *PagERF16* could induce the expression of *NAC45*, but

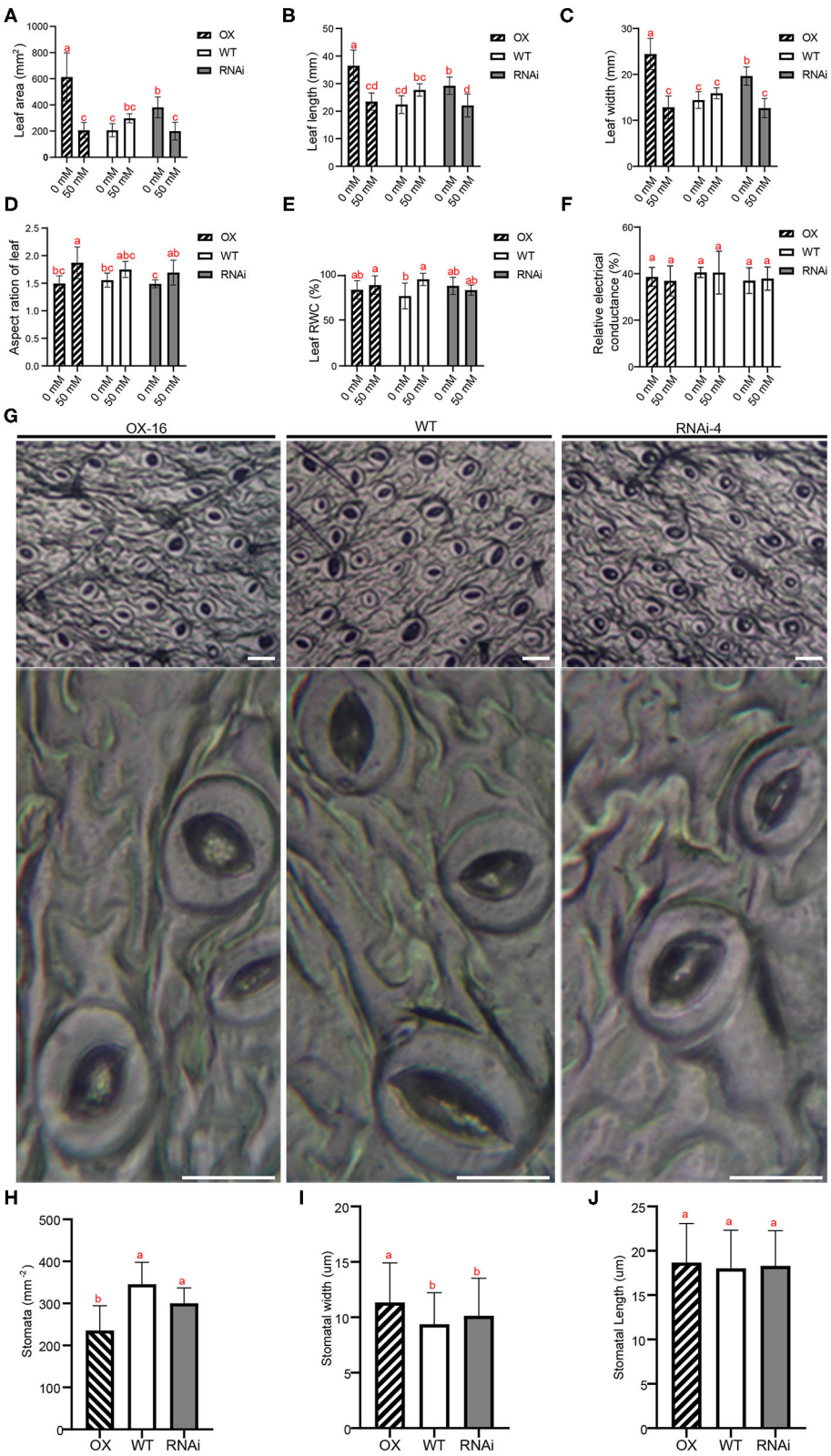

FIGURE 4 | PagERF16 decreased stomatal density and increased stomatal width. **(A–D)** Represent area, length, width, and aspect ratio of the second mature leaf. **(E)** Relative water content of the second mature leaf. **(F)** Relative electrical conductance of the second leaf. **(G)** Scanning electron micrograph of the abaxial leaf epidermis. Bars, 20 μm. **(H–J)** show the stomatal density, width, and length. The plot represents the mean ± SD of six plants per line. Three OX or RNAi lines serve as three biological repeats. Different lowercases indicate significant differences among samples ($p \leq 0.05$).

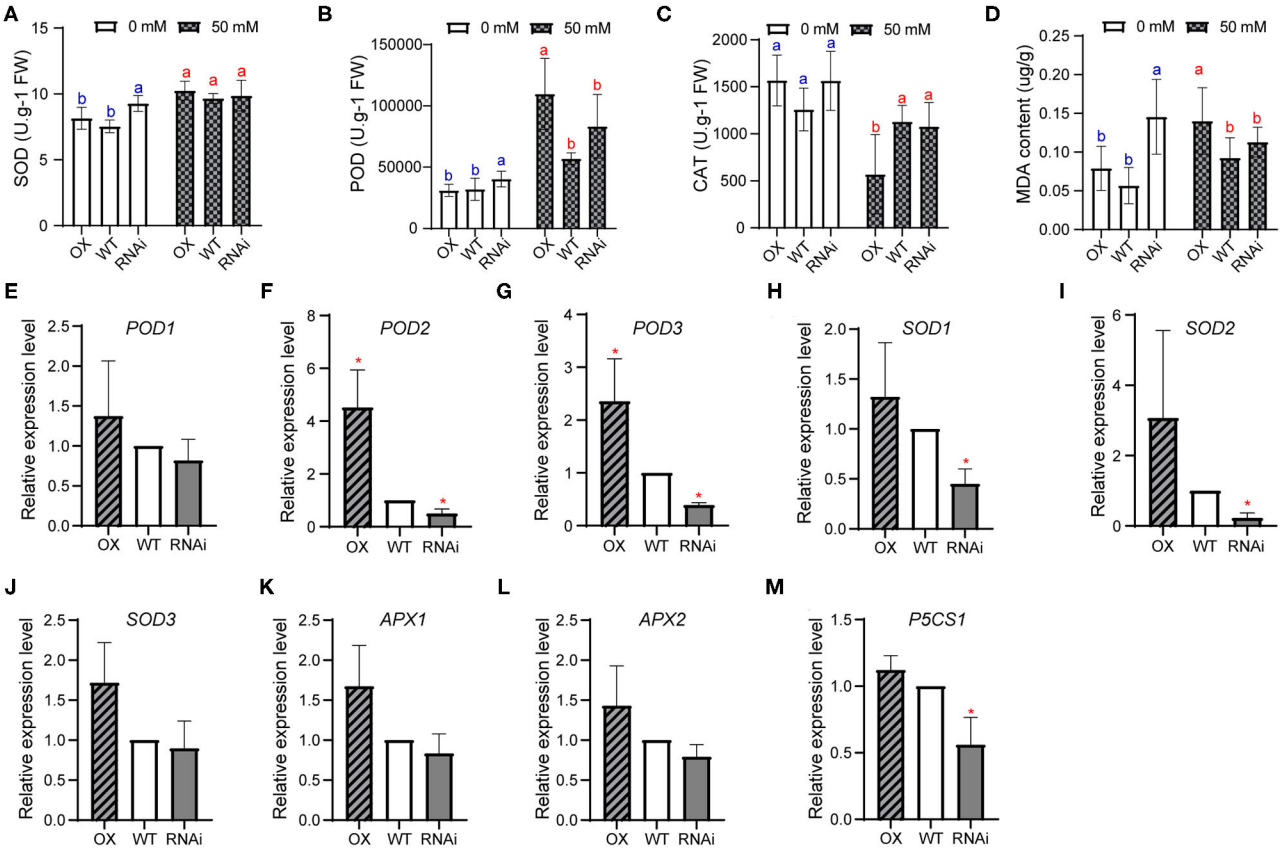

FIGURE 5 | PagERF16 modulated the physiology and gene expression relevant to antioxidant enzymes. **(A–D)** Superoxide dismutase (SOD), peroxidase (POD), catalase (CAT), and MDA contents. The plot represents the mean ± SD of six plants per line. Three OX or RNAi lines serve as three biological repeats. Different lowercases indicate significant differences among samples ($p \leq 0.05$). **(E–M)** Expression of *POD1*, *POD2*, *POD3*, *SOD1*, *SOD2*, *SOD3*, *APX1*, *APX2*, and *P5CS1* in transgenic and WT plants. The plot represents the mean ± SD of three repeats. Asterisks denote significant differences between transgenic and WT: $^*p \leq 0.05$.

PagERF16 overexpression had an insignificant effect on *NAC45* (**Figures 6A,E**).

DISCUSSION

PagERF16 Is a Salt-Stress-Related Transcription Activator

AtERF16 belongs to subgroup II of the ERF TF family, members of which contain CMII-1, CMII-2, and CMII-3, the three conserved motifs in the C-terminal region adjacent to the AP2/ERF domain (Nakano et al., 2006). ERF in this subfamily most likely acts as a transcriptional activator through binding to the GCC-box or DRE (dehydration responsive element) promoter element and may be involved in the regulation of gene expression by biotic or abiotic stress factors and by components of stress signal transduction pathways. Expression of *AtERF014* was determined to be induced by *Pseudomonas syringae* pv. *tomato* (*Pst*) and *Botrytis cinerea* (*Bc*). *AtERF014*-overexpressing plants displayed increased *Pst* resistance but decreased *Bc* resistance, whereas *AtERF014*-RNAi plants exhibited decreased *Pst* resistance but increased *Bc* resistance (Zhang et al., 2016). Additionally, ERFs in subgroup II were also involved in plant secondary metabolism and the growth/development process. AtERF19 plays a primary role in plant growth and development and causes an increased tolerance to water deprivation, strengthening their chances of reproductive success (Scarpeci et al., 2017). Previous studies suggest that *ERF16* is located in the nucleus of the poplar cell and could specifically bind to the DRE motif to regulate abiotic stress of transgenic plants (Cheng et al., 2019). However, the function and molecular mechanism of *ERF16* in poplar root growth and salt stress tolerance remain to be clarified. In order to evaluate the function of *PagERF16* in ligneous plants, the gene was cloned from 84K poplar and was roughly homologous with *AtERF16*, suggesting that it may play a role in poplar growth and stress tolerance (**Figures 1C,D**). *PagERF16* transcript levels in roots were sensitive to salt stress that decreased significantly after being exposed to NaCl but induced in leaves (**Figure 1A**). Similar results were obtained in previous studies, in which the spatiotemporal expression pattern of *ERF16* was reported and possible functions involved in salt stress were inferred (Cheng et al., 2019; Yao et al., 2019). This suggests that *PagERF16* may have a function in the root tissues that affects the salt sensitivity of poplars. The induced expression of *PagERF16* in leaves maybe related to the stomatal density

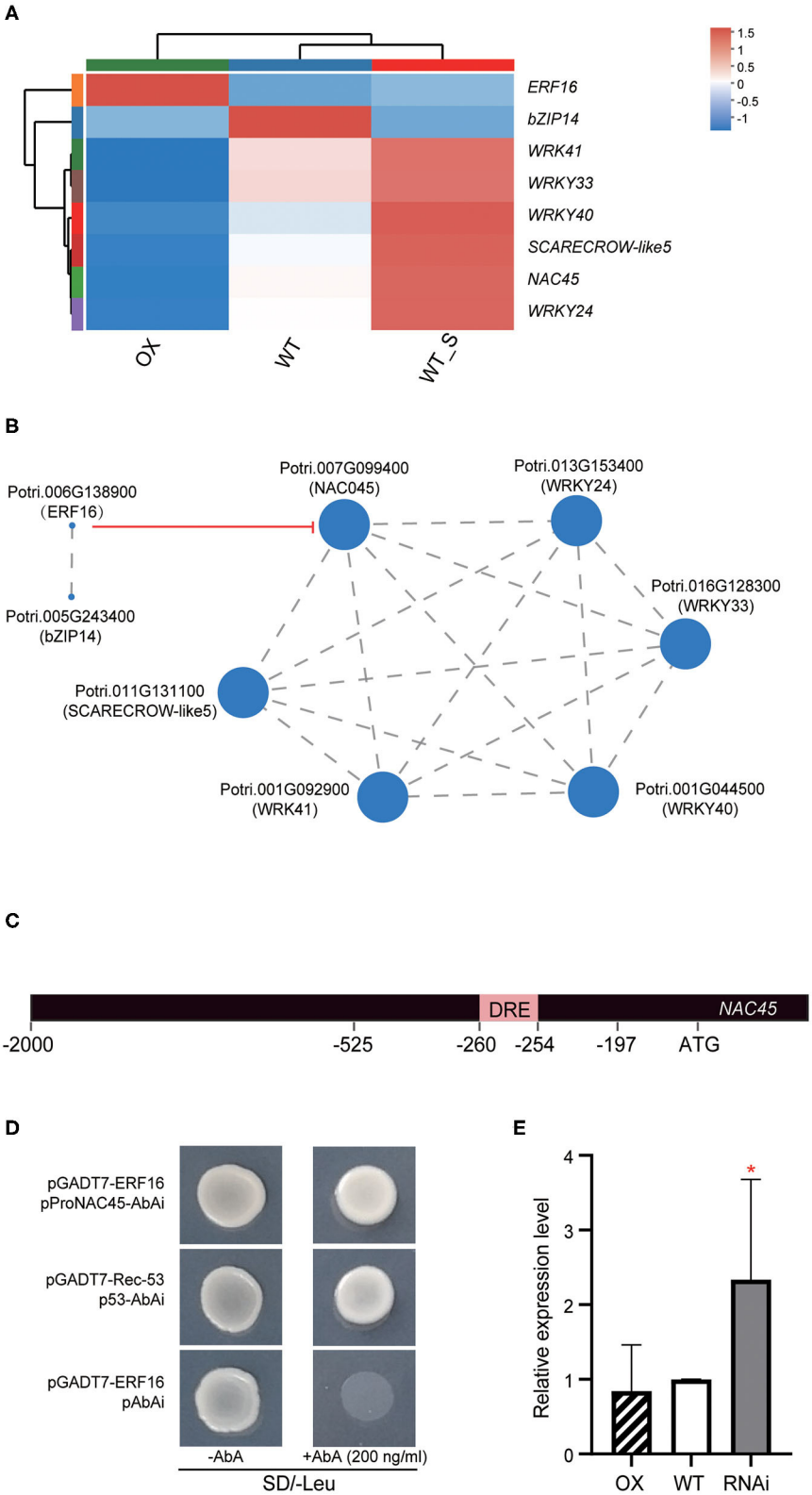

FIGURE 6 | PagERF16 negatively regulated the expression of NAC45. **(A)** Expression pattern of differentially expressed TFs related to salt stress and PagERF16. WT_S, WT treated with 100 NaCl for 48 h. Red denotes high expression and blue indicates low expression. **(B)** Correlation analysis of co-expressed TFs using

(Continued)

FIGURE 6 | Spearman methods. Each node (Node) in the Figure represents a gene, and the wiring between nodes represents the correlation of gene expression. The larger the node, the more the number of expression correlations between this gene and other genes. Red line indicates PagERF16 negatively regulated the expression of NAC45. **(C)** Promoter structure of *NAC45*. **(D)** *PagERF16* directedly binding to the promoter of *NAC45* revealed by yeast one hybrid assay. The pGADT7-Rec-53 and p53-AbAi were used as positive control and pGADT7-ERF16 and pAbAi served as the negative control. The yeast Y1H Gold strains and plated on the SD/-Leu medium containing either 0 or 200 ng/ml AbA. **(E)** Relative expression level of *NAC45* in OX, RNAi, and WT. The plot represents the mean ± SD of three repeats. Asterisks denote significant differences between transgenic and WT: $*p \leq 0.05$.

reduction and stomatal width increase, which modulate plant adaptation to salt stress (**Figures 4H,I**).

PagERF16 Promotes Lateral Root Proliferation

Members of ERF family are involved in regulating lateral rooting. Overexpressed *PtAIL1* is able to grow more adventitious roots, whereas RNA interference mediated the downexpression of *PtAIL1* expression, which leads to a delay in adventitious root formation (Rigal et al., 2012). PtaERF003 function is linked to the auxin signal transduction pathway and has a positive effect on lateral root proliferation in poplars (Trupiano et al., 2013). In this study, 1-month-old OX plants with overexpressed *PagERF16* had robust lateral roots with bigger root diameter and fresh weight than WT (**Figures 1**, **2**). We also found that overexpressing *PagERF16* could reduce the rooting rate of poplar and postpone rooting time, which led to no change in the length of primary root (**Figure 3**). All of these resulted in the lateral root proliferation and thickening of OX. Meanwhile, the repressing transgenic plants using RNAi showed similar phenotypes and physiological characteristics to the wild type suggesting that function of *PagERF16* may be redundant with other TFs, for example *PtERF194* (Potri.018G038100). *PagERF16* was highly homologous with *PtERF194* and both of them hit the same ortholog *AtERF016* in *Arabidopsis* (Yao et al., 2019). The plant height and rooting rate of RNAi were also significantly decreased compared to those of WT (**Figures 2G**, **3I**) suggesting that *PagERF16* expression level must be tightly regulated, since too high or too low levels negatively affect the rooting rate.

PagERF16 Hypersensitizes to Salt Stress

Overexpression of *ERFs* can also negatively affect plant growth and often result in dwarf plants, which was somewhat consistent with our results (Zhang et al., 2009; Lee et al., 2016; Kudo et al., 2017; Wessels et al., 2019). The plant height of OX was shorter than WT plants, but the leaves were larger (**Figures 1**, **4**). Under salt stress conditions, plants could close their stomata to decrease water loss from leaves. In this study, the stomatal width (aperture) of OX was bigger than that of WT, which explained why it was sensitive to salt stress to a degree (**Figures 4G,I**). The other factor that regulates stomatal conductance is stomatal density; regulation of stomatal density is a long-term response (Wang et al., 2016). Under stress conditions, stomatal density responses differ depending on the stress intensity and species. Reduced stomatal density due to drought stress is present in wheat and umbu trees (Quarrie and Jones, 1977; Silva et al., 2009). However, an increase in stomatal density was detected in rice during moderate drought, but there was a decrease in severe drought (Xu and Zhou, 2008). Reducing stomatal density may lead to a decrease in cumulative photosynthetic activity and increase in stress threat. We think the reduction of stomatal density decreased photosynthesis and contributed to the salt sensitivity of OX under 50 mM NaCl conditions (**Figures 4G,H**).

Movement of stomata is induced by many factors, including ROS, ABA, and salt stress, and plays important roles in plant abiotic stress endurance (Wang et al., 2016). Under drought conditions, ROS accumulate rapidly to control the stomatal movement as a second messenger, while antioxidant enzymes will increase to reduce the content of ROS. In addition, MDA content is related to membrane lipid peroxidation and the higher MDA content represents more membrane damage. In our present study, the POD activity of OX was similar to that of WT under normal growth conditions but was higher when exposed to salt stress (**Figure 5**). The MDA content showed similar trends with POD activity. However, CAT activity of OX was significantly lower than that of WT. These indicated that the lower CAT activity and higher MDA content contributed to the salt sensitivity of OX. Expression of genes relevant to ROS scavenging showed that the transcript level of *POD2* and *POD3* were higher in OX, yet could not enhance poplar salt tolerance. The decreased expression of *POD2*, *POD3*, *SOD2*, and *P5CS1* of RNAi indicated that the repression of PagERF16 could inhibit their expression, which may contribute to the decrease of plant height and rooting rate.

The fact that *PagERF16* regulated both salt stress sensitivity and lateral root proliferation suggested that the influence of *PagERF16* on these two biological processes was interlinked. The transcriptome analyses offer insight into the possible mechanisms for how *PagERF16* might modulate the lateral root systems to affect salt sensitivity of poplar plants. Combined with Yeast one-hybrid assays, we found that PagERF16 could directly bind to the promoter of *NAC45* through the DRE motif to participate in the regulation of the five-TFs network (**Figures 6C,D**). Studies have indicated that *NAC45* is homologous with *ATAF2* of *Arabidopsis*, which is involved in auxin biosynthesis by binding to the promoter of *NIT2* and acts as a negative regulator during the plant stress response process (Delessert et al., 2005; Huh et al., 2012; Wang and Culver, 2012; Zhang et al., 2015). The *ERF16-NAC45* interaction suggested that *PagERF16* may participate in the auxin biosynthesis pathway, but whether it promotes lateral root proliferation through the *ERF16-NAC45* interaction remains to be studied. RT-qPCR showed that *PagERF16* induced the expression of *NAC45* in RNAi plants (**Figure 6E**). NAC45 is a negative regulator during plant stress response process; the induced *NAC45* could make RNAi poplar sensitive to salt stress. On the contrary, *PagERF16*

was sensitive to salt stress and the repressed *PagERF16* would make the RNAi poplar more tolerant to salt stress. The opposite effect of induced-*NAC45* and repressed-*PagERF16* in RNAi may be another reason why the phenotype of RNAi was mostly similar to that of WT. However, the expression of *NAC45* in OX was lightly affected by *PagERF16*, indicating that the interaction relationship between *PagERF16* and *NAC45* may not function directly in regulating salt tolerance or sensitivity of poplar.

DATA AVAILABILITY STATEMENT

The datasets presented in this study can be found in online repositories. The names of the repository/repositories and accession number(s) can be found at: https://www.ncbi.nlm.nih.gov/, PRJNA716488.

AUTHOR CONTRIBUTIONS

SW and YH planned and designed the research and wrote the manuscript. JH, QL, XW, and YF performed experiments and analyzed data. All authors contributed to the article and approved the submitted version.

FUNDING

Funding for this work was provided by the National Natural Science Foundation of China (31800564, 31700534) and the University Science and Technology Innovation Project of Shanxi Province (2019L0392).

ACKNOWLEDGMENTS

We gratefully acknowledge the staff and students at Shanxi Agricultural University and those who assisted in materials collection and methodology: Lin Wang, Weifeng Wang, and Yu Xian.

SUPPLEMENTARY MATERIAL

The Supplementary Material for this article can be found online at: https://www.frontiersin.org/articles/10.3389/fpls.2021.669143/full#supplementary-material

Supplementary Figure 1 | The transgenic lines were verified using PCR and RT-qPCR. **(A,B)** Respectively represent overexpressed and RNAi lines verified using PCR with primers composed of a forward primer from the promoter of *CaMV 35S* and a reverse primer from *PagERF16*. M, DNA marker 2000; WT, wild-type control. **(C,D)** Shows the relative expression of *PagERF16* in OX or RNAi lines. OX-12, OX-16, and OX-19 marked with red tags and RNAi-1, RNAi-4, and RNAi-5 with blue were selected for further analysis. **(E)** Shoots were sub-cultured on medium without (0 mM) or with 50 mM NaCl. Bars, 1 cm.

Supplementary Figure 2 | Identification of differentially expressed TFs coexisted between OX and WT_S. **(A)** Statistics of DEGs in OX and WT_S compared to WT plants. **(B,C)** Statistics of TF family of DEGs for WT_S and OX.

Supplementary Table 1 | Primer sequences used in this study.

Supplementary Table 2 | Statistic analysis of leaf color of OX, RNAi, and WT using LAB methods. $0 < \Delta L$, white; $0 > \Delta L$, black; $0 < \Delta A$, red; $0 > \Delta A$, green; $0 < \Delta B$, yellow; $0 > \Delta B$, blue. ΔE, color difference, $\Delta E^* = [(\Delta L^*)^2 + (\Delta A^*)^2 + (\Delta B^*)^2]^{1/2}$, $1 < \Delta E \leq 2$, not significant; $2 < \Delta E$, the difference is visible.

Supplementary Table 3 | DEGs in WT_S vs. WT.

Supplementary Table 4 | DEGs in OX vs. WT.

Supplementary Table 5 | Expression and gene annotation of TFs.

REFERENCES

Ambavaram, M. M., Basu, S., Krishnan, A., Ramegowda, V., Batlang, U., Rahman, L., et al. (2014). Coordinated regulation of photosynthesis in rice increases yield and tolerance to environmental stress. *Nat. Commun.* 5:5302. doi: 10.1038/ncomms6302

Bailey, T. L., Boden, M., Buske, F. A., Frith, M., Grant, C. E., Clementi, L., et al. (2009). MEME SUITE: tools for motif discovery and searching. *Nucleic Acids Res.* 37, W202–W208. doi: 10.1093/nar/gkp335

Chen, S., Lin, X., Zhang, D. W., Li, Q., Zhao, X. Y., and Chen, S. (2019). Genome-wide analysis of NAC gene family in *Betula pendula*. *Forests* 10:741. doi: 10.3390/f10090741

Cheng, Z., Zhang, X., Zhao, K., Yao, W., Li, R., Zhou, B., et al. (2019). Over-expression of ERF38 gene enhances salt and osmotic tolerance in transgenic poplar. *Front. Plant Sci.* 10:1375. doi: 10.3389/fpls.2019.01375

Chinnusamy, V., Schumaker, K., and Zhu, J. K. (2004). Molecular genetic perspectives on cross-talk and specificity in abiotic stress signalling in plants. *J. Exp. Bot.* 55, 225–236. doi: 10.1093/jxb/erh005

Datta, K., Baisakh, N., Ganguly, M., Krishnan, S., Yamaguchi Shinozaki, K., and Datta, S. K. (2012). Overexpression of Arabidopsis and rice stress genes' inducible transcription factor confers drought and salinity tolerance to rice. *Plant Biotechnol. J.* 10, 579–586. doi: 10.1111/j.1467-7652.2012.00688.x

Delessert, C., Kazan, K., Wilson, I. W., Van Der Straeten, D., Manners, J., Dennis, E. S., et al. (2005). The transcription factor ATAF2 represses the expression of pathogenesis-related genes in Arabidopsis. *Plant J.* 43, 745–757. doi: 10.1111/j.1365-313X.2005.02488.x

Gang, H. X., Li, R. H., Zhao, Y. M., Liu, G. F., Chen, S., and Jiang, J. (2019). Loss of GLK1 transcription factor function reveals new insights in chlorophyll biosynthesis and chloroplast development. *J. Exp. Bot.* 70, 3125–3138. doi: 10.1093/jxb/erz128

Gilmour, S. J., Sebolt, A. M., Salazar, M. P., Everard, J. D., and Thomashow, M. F. (2000). Overexpression of the Arabidopsis CBF3 transcriptional activator mimics multiple biochemical changes associated with cold acclimation. *Plant Physiol.* 124, 1854–1865. doi: 10.1104/pp.124.4.1854

Gong, Z., Xiong, L., Shi, H., Yang, S., Herrera-Estrella, L. R., Xu, G., et al. (2020). Plant abiotic stress response and nutrient use efficiency. *Sci. China Life Sci.* 63, 635–674. doi: 10.1007/s11427-020-1683-x

Guo, H., Wang, Y., Wang, L., Hu, P., Wang, Y., Jia, Y., et al. (2017). Expression of the MYB transcription factor gene BplMYB46 affects abiotic stress tolerance and secondary cell wall deposition in Betula platyphylla. *Plant Biotechnol. J.* 15, 107–121. doi: 10.1111/pbi.12595

He, F., Li, H. G., Wang, J. J., Su, Y., Wang, H. L., Feng, C. H., et al. (2019). PeSTZ1, a C2H2-type zinc finger transcription factor from Populus euphratica, enhances freezing tolerance through modulation of ROS scavenging by directly regulating PeAPX2. *Plant Biotechnol. J.* 17, 2169–2183. doi: 10.1111/pbi.13130

He, F., Wang, H. L., Li, H. G., Su, Y., Li, S., Yang, Y., et al. (2018). PeCHYR1, a ubiquitin E3 ligase from Populus euphratica, enhances drought tolerance via ABA-induced stomatal closure by ROS production in Populus. *Plant Biotechnol. J.* 16, 1514–1528. doi: 10.1111/pbi.12893

Hirota, A., Kato, T., Fukaki, H., Aida, M., and Tasaka, M. (2007). The auxin-regulated AP2/EREBP gene PUCHI is required for morphogenesis in the

early lateral root primordium of Arabidopsis. *Plant Cell* 19, 2156–2168. doi: 10.1105/tpc.107.050674

Huh, S. U., Lee, S. B., Kim, H. H., and Paek, K. H. (2012). ATAF2, a NAC transcription factor, binds to the promoter and regulates NIT2 gene expression involved in auxin biosynthesis. *Mol. Cells* 34, 305–313. doi: 10.1007/s10059-012-0122-2

Jaenisch, R., and Bird, A. (2003). Epigenetic regulation of gene expression: how the genome integrates intrinsic and environmental signals. *Nat. Genet.* 33(Suppl.), 245–254. doi: 10.1038/ng1089

Jung, H., Chung, P. J., Park, S. H., Redillas, M., Kim, Y. S., Suh, J. W., et al. (2017). Overexpression of OsERF48 causes regulation of OsCML16, a calmodulin-like protein gene that enhances root growth and drought tolerance. *Plant Biotechnol. J.* 15, 1295–1308. doi: 10.1111/pbi.12716

Karaba, A., Dixit, S., Greco, R., Aharoni, A., Trijatmiko, K. R., Marsch-Martinez, N., et al. (2007). Improvement of water use efficiency in rice by expression of HARDY, an Arabidopsis drought and salt tolerance gene. *Proc. Natl. Acad. Sci. U.S.A.* 104, 15270–15275. doi: 10.1073/pnas.0707294104

Kim, D., Pertea, G., Trapnell, C., Pimentel, H., Kelley, R., and Salzberg, S. L. (2013). TopHat2: accurate alignment of transcriptomes in the presence of insertions, deletions and gene fusions. *Genome Biol.* 14:R36. doi: 10.1186/gb-2013-14-4-r36

Kouzarides, T. (2007). Chromatin modifications and their function. *Cell* 128, 693–705. doi: 10.1016/j.cell.2007.02.005

Kudo, M., Kidokoro, S., Yoshida, T., Mizoi, J., Todaka, D., Fernie, A. R., et al. (2017). Double overexpression of DREB and PIF transcription factors improves drought stress tolerance and cell elongation in transgenic plants. *Plant Biotechnol. J.* 15, 458–471. doi: 10.1111/pbi.12644

Kumar, S., Stecher, G., and Tamura, K. (2016). MEGA7: molecular evolutionary genetics analysis version 7.0 for bigger datasets. *Mol. Biol. Evol.* 33, 1870–1874. doi: 10.1093/molbev/msw054

Lee, D. K., Jung, H., Jang, G., Jeong, J. S., Kim, Y. S., Ha, S. H., et al. (2016). Overexpression of the OsERF71 transcription factor alters rice root structure and drought resistance. *Plant Physiol.* 172, 575–588. doi: 10.1104/pp.16.00379

Li, Q., Lin, Y. C., Sun, Y. H., Song, J., Chen, H., Zhang, X. H., et al. (2012). Splice variant of the SND1 transcription factor is a dominant negative of SND1 members and their regulation in Populus trichocarpa. *Proc. Natl. Acad. Sci. U.S.A.* 109, 14699–14704. doi: 10.1073/pnas.1212977109

Li, S., Lin, Y. J., Wang, P., Zhang, B., Li, M., Chen, S., et al. (2019). The AREB1 transcription factor influences histone acetylation to regulate drought responses and tolerance in populus trichocarpa. *Plant Cell* 31, 663–686. doi: 10.1105/tpc.18.00437

Lin, Y. C., Li, W., Sun, Y. H., Kumari, S., Wei, H., Li, Q., et al. (2013). SND1 transcription factor-directed quantitative functional hierarchical genetic regulatory network in wood formation in Populus trichocarpa. *Plant Cell* 25, 4324–4341. doi: 10.1105/tpc.113.117697

Liu, B., Li, H., Zhu, B., Koide, R. T., Eissenstat, D. M., and Guo, D. (2015). Complementarity in nutrient foraging strategies of absorptive fine roots and arbuscular mycorrhizal fungi across 14 coexisting subtropical tree species. *New Phytol.* 208, 125–136. doi: 10.1111/nph.13434

Liu, B., Li, L., Rengel, Z., Tian, J., Li, H., and Lu, M. (2019). Roots and arbuscular mycorrhizal fungi are independent in nutrient foraging across subtropical tree species. *Plant Soil* 442, 97–112. doi: 10.1007/s11104-019-04161-3

Liu, Q., Kasuga, M., Sakuma, Y., Abe, H., Miura, S., Yamaguchi-Shinozaki, K., et al. (1998). Two transcription factors, DREB1 and DREB2, with an EREBP/AP2 DNA binding domain separate two cellular signal transduction pathways in drought- and low-temperature-responsive gene expression, respectively, in Arabidopsis. *Plant Cell* 10, 1391–1406. doi: 10.1105/tpc.10.8.1391

Love, M. I., Huber, W., and Anders, S. (2014). Moderated estimation of fold change and dispersion for RNA-seq data with DESeq2. *Genome Biol.* 15:550. doi: 10.1186/s13059-014-0550-8

Luo, X., Dai, Y., Zheng, C., Yang, Y., Chen, W., Wang, Q., et al. (2020). The ABI4-RbohD/VTC2 regulatory module promotes Reactive Oxygen Species (ROS) accumulation to decrease seed germination under salinity stress. *New Phytol.* 229, 950–962. doi: 10.1111/nph.16921

Matsuo, N., Ozawa, K., and Mochizuki, T. (2008). Genotypic differences in root hydraulic conductance of rice (Oryza sativa L.) in response to water regimes. *Plant Soil* 316, 25–34. doi: 10.1007/s11104-008-9755-5

Nakano, T., Suzuki, K., Fujimura, T., and Shinshi, H. (2006). Genome-wide analysis of the ERF gene family in Arabidopsis and rice. *Plant Physiol.* 140, 411–432. doi: 10.1104/pp.105.073783

Nakashima, K., Yamaguchi-Shinozaki, K., and Shinozaki, K. (2014). The transcriptional regulatory network in the drought response and its crosstalk in abiotic stress responses including drought, cold, and heat. *Front. Plant Sci.* 5:170. doi: 10.3389/fpls.2014.00170

Oh, S.-J., Kim, Y. S., Kwon, C.-W., Park, H. K., Jeong, J. S., and Kim, J.-K. (2009). Overexpression of the transcription factor AP37 in rice improves grain yield under drought conditions. *Plant Physiol.* 150, 1368–1379. doi: 10.1104/pp.109.137554

Quarrie, S. A., and Jones, H. G. (1977). Effects of abscisic acid and water stress on development and morphology of wheat. *J. Exp. Bot.* 28, 192–203. doi: 10.1093/jxb/28.1.192

Rigal, A., Yordanov, Y. S., Perrone, I., Karlberg, A., Tisserant, E., Bellini, C., et al. (2012). The AINTEGUMENTA LIKE1 homeotic transcription factor PtAIL1 controls the formation of adventitious root primordia in poplar. *Plant Physiol.* 160, 1996–2006. doi: 10.1104/pp.112.204453

Ritonga, F. N., and Chen, S. (2020). Physiological and molecular mechanism involved in cold stress tolerance in plants. *Plants (Basel)* 9:560. doi: 10.3390/plants9050560

Saad, A. S., Li, X., Li, H. P., Huang, T., Gao, C. S., Guo, M. W., et al. (2013). A rice stress-responsive NAC gene enhances tolerance of transgenic wheat to drought and salt stresses. *Plant Sci.* 203–204, 33–40. doi: 10.1016/j.plantsci.2012.12.016

Scarpeci, T. E., Frea, V. S., Zanor, M. I., and Valle, E. M. (2017). Overexpression of AtERF019 delays plant growth and senescence, and improves drought tolerance in Arabidopsis. *J. Exp. Bot.* 68, 673–685. doi: 10.1093/jxb/erw429

Schurch, N. J., Schofield, P., Gierlinski, M., Cole, C., Sherstnev, A., Singh, V., et al. (2016). How many biological replicates are needed in an RNA-seq experiment and which differential expression tool should you use? *RNA* 22, 839–851. doi: 10.1261/rna.053959.115

Silva, E. C., Nogueira, R. J. M. C., Vale, F. H. A., Araújo, F. P.,d., and Pimenta, M. A. (2009). Stomatal changes induced by intermittent drought in four umbu tree genotypes. *Br. J. Plant Physiol.* 21, 33–42. doi: 10.1590/S1677-04202009000100005

Song, L., Huang, S. C., Wise, A., Castanon, R., Nery, J. R., Chen, H., et al. (2016). A transcription factor hierarchy defines an environmental stress response network. *Science* 354:aag1550. doi: 10.1126/science.aag1550

Trupiano, D., Yordanov, Y., Regan, S., Meilan, R., Tschaplinski, T., Scippa, G. S., et al. (2013). Identification, characterization of an AP2/ERF transcription factor that promotes adventitious, lateral root formation in Populus. *Planta* 238, 271–282. doi: 10.1007/s00425-013-1890-4

Uga, Y., Sugimoto, K., Ogawa, S., Rane, J., Ishitani, M., Hara, N., et al. (2013). Control of root system architecture by DEEPER ROOTING 1 increases rice yield under drought conditions. *Nat. Genet.* 45, 1097–1102. doi: 10.1038/ng.2725

Wang, C., Liu, S., Dong, Y., Zhao, Y., Geng, A., Xia, X., et al. (2016). PdEPF1regulates water-use efficiency and drought tolerance by modulating stomatal density in poplar. *Plant Biotechnol. J.* 14, 849–860. doi: 10.1111/pbi.12434

Wang, L., Li, Z., Lu, M., and Wang, Y. (2017). ThNAC13, a NAC transcription factor from tamarix hispida, confers salt, and osmotic stress tolerance to transgenic tamarix and *Arabidopsis*. *Front. Plant Sci.* 8:635. doi: 10.3389/fpls.2017.00635

Wang, N., Liu, W., Yu, L., Guo, Z., Chen, Z., Jiang, S., et al. (2020). HEAT SHOCK FACTOR A8a modulates flavonoid synthesis and drought tolerance. *Plant Physiol.* 184, 1273–1290. doi: 10.1104/pp.20.01106

Wang, S., Huang, J., Wang, X., Dang, H., Jiang, T., and Han, Y. (2019). Expression analysis of the NAC transcription factor family of populus in response to salt stress. *Forests* 10:688. doi: 10.3390/f10080688

Wang, S., Wang, J., Yao, W., Zhou, B., Li, R., and Jiang, T. (2014). Expression patterns of WRKY genes in di-haploid Populus simonii x P. nigra in response to salinity stress revealed by quantitative real-time PCR and RNA sequencing. *Plant Cell Rep.* 33, 1687–1696. doi: 10.1007/s00299-014-1647-y

Wang, X., and Culver, J. N. (2012). DNA binding specificity of ATAF2, a NAC domain transcription factor targeted for degradation by Tobacco mosaic virus. *BMC Plant Biol.* 12:157. doi: 10.1186/1471-2229-12-157

Wessels, B., Seyfferth, C., Escamez, S., Vain, T., Antos, K., Vahala, J., et al. (2019). An AP2/ERF transcription factor ERF139 coordinates xylem cell expansion and secondary cell wall deposition. *New Phytol.* 224, 1585–1599. doi: 10.1111/nph.15960

Xu, Z., and Zhou, G. (2008). Responses of leaf stomatal density to water status and its relationship with photosynthesis in a grass. *J. Exp. Bot.* 59, 3317–3325. doi: 10.1093/jxb/ern185

Yao, W., Wang, S., Zhou, B., and Jiang, T. (2016). Transgenic poplar overexpressing the endogenous transcription factor ERF76 gene improves salinity tolerance. *Tree Physiol.* 36, 896–908. doi: 10.1093/treephys/tpw004

Yao, W., Zhou, B., Zhang, X., Zhao, K., Cheng, Z., and Jiang, T. (2019). Transcriptome analysis of transcription factor genes under multiple abiotic stresses in Populus simonii × P.nigra. *Gene* 707, 189–197. doi: 10.1016/j.gene.2019.04.071

Zhang, G., Chen, M., Li, L., Xu, Z., Chen, X., Guo, J., et al. (2009). Overexpression of the soybean GmERF3 gene, an AP2/ERF type transcription factor for increased tolerances to salt, drought, and diseases in transgenic tobacco. *J. Exp. Bot.* 60, 3781–3796. doi: 10.1093/jxb/erp214

Zhang, H., Hong, Y., Huang, L., Li, D., and Song, F. (2016). Arabidopsis AtERF014 acts as a dual regulator that differentially modulates immunity against Pseudomonas syringae pv. tomato and Botrytis cinerea. *Sci. Rep.* 6:30251. doi: 10.1038/srep30251

Zhang, X., Lu, X., Duan, H., Lian, C., Xia, X., and Yin, W. (2015). Cloning and functional analysis of PeNAC045 from Populus euphratica. *J. Beijing For. Univ.* 37, 1–10. doi: 10.13332/j.1000-1522.20150066

Zhang, Y., Zhou, Y., Zhang, D., Tang, X., Li, Z., Shen, C., et al. (2020). PtrWRKY75 overexpression reduces stomatal aperture and improves drought tolerance by salicylic acid-induced reactive oxygen species accumulation in poplar. *Environ. Exp. Bot.* 176:104117. doi: 10.1016/j.envexpbot.2020.104117

Zhao, Y., Cheng, S., Song, Y., Huang, Y., Zhou, S., Liu, X., et al. (2015). The interaction between Rice ERF3 and WOX11 promotes crown root development by regulating gene expression involved in cytokinin signaling. *Plant Cell* 27, 2469–2483. doi: 10.1105/tpc.15.00227

Zhu, J. K. (2002). Salt and drought stress signal transduction in plants. *Annu. Rev. Plant Biol.* 53, 247–273. doi: 10.1146/annurev.arplant.53.091401.143329

Zhu, J. K. (2016). Abiotic stress signaling and responses in plants. *Cell* 167, 313–324. doi: 10.1016/j.cell.2016.08.029

Conflict of Interest: The authors declare that the research was conducted in the absence of any commercial or financial relationships that could be construed as a potential conflict of interest.

frontiers in Plant Science

SYSTEMATIC REVIEW
published: 04 October 2021
doi: 10.3389/fpls.2021.735514

Early "Rootprints" of Plant Terrestrialization: Selaginella Root Development Sheds Light on Root Evolution in Vascular Plants

*Tao Fang[1,2], Hans Motte[1,2], Boris Parizot[1,2] and Tom Beeckman[1,2]**

[1]Department of Plant Biotechnology and Bioinformatics, Ghent University, Ghent, Belgium, [2]VIB Center for Plant Systems Biology, Ghent, Belgium

Roots provide multiple key functions for plants, including anchorage and capturing of water and nutrients. Evolutionarily, roots represent a crucial innovation that enabled plants to migrate from aquatic to terrestrial environment and to grow in height. Based on fossil evidence, roots evolved at least twice independently, once in the lycophyte clade and once in the euphyllophyte (ferns and seed plants) clade. In lycophytes, roots originated in a stepwise manner. Despite their pivotal position in root evolution, it remains unclear how root development is controlled in lycophytes. Getting more insight into lycophyte root development might shed light on how genetic players controlling the root meristem and root developmental processes have evolved. Unfortunately, genetic studies in lycophytes are lagging behind, lacking advanced biotechnological tools, partially caused by the limited economic value of this clade. The technology of RNA sequencing (RNA-seq) at least enabled transcriptome studies, which could enhance the understanding or discovery of genes involved in the root development of this sister group of euphyllophytes. Here, we provide an overview of the current knowledge on root evolution followed by a survey of root developmental events and how these are genetically and hormonally controlled, starting from insights obtained in the model seed plant Arabidopsis and where possible making a comparison with lycophyte root development. Second, we suggest possible key genetic regulators in root development of lycophytes mainly based on their expression profiles in *Selaginella moellendorffii* and phylogenetics. Finally, we point out challenges and possible future directions for research on root evolution.

Keywords: root branching, *Selaginella moellendorffii*, evolution, lycophyte, root meristem

OPEN ACCESS

Edited by:
Raffaele Dello Ioio, Sapienza University of Rome, Italy

Reviewed by:
Elena Salvi, University of Cambridge, United Kingdom
Keiko Sakakibara, Rikkyo University, Japan

****Correspondence:***
Tom Beeckman
tom.beeckman@psb.vib-ugent.be

Specialty section:
This article was submitted to Plant Development and EvoDevo, a section of the journal Frontiers in Plant Science

Received: *02 July 2021*
Accepted: *10 September 2021*
Published: *04 October 2021*

Citation:
Fang T, Motte H, Parizot B and Beeckman T (2021) Early "Rootprints" of Plant Terrestrialization: Selaginella Root Development Sheds Light on Root Evolution in Vascular Plants. Front. Plant Sci. 12:735514. doi: 10.3389/fpls.2021.735514

INTRODUCTION

Whereas filamentous rhizoids fulfilled the "rooting" function of the first land plants (Jones and Dolan, 2012), true roots with a fully integrated vascular system developed in Early Devonian times and provided a much better ability to anchor large plants and absorb water and nutrients. Therefore, roots were an important innovation for successful colonization of land.

In (extant) seed plants, a typical root system is composed of an embryonic primary root and postembryonic adventitious and lateral roots (Motte and Beeckman, 2019; Motte et al., 2020; **Figure 1A**). Crucial for their continuous growth is the development and maintenance of a root meristem, a tissue consisting of continuously dividing cells representing a source of cells to build the tissues of the main root. In seed plants, the root apical meristem (RAM) of the primary root is formed during embryo development while lateral root (LR) meristems are formed *de novo* in existing root tissues (Trinh et al., 2018). Both the development and maintenance of these meristems are controlled by a complex signaling network, including hormones, especially auxins, and transcription factors (TFs; Motte et al., 2019).

In extant non-seed vascular plants, different root systems can be found. In leptosporangiate ferns (e.g., *Ceratopteris richardii*), roots are shoot-borne and can form LRs, but in a rigid pattern (Hou et al., 2004; Hou and Blancaflor, 2018). In lycophytes, the first lineage where roots arose, and including the emerging model organism *Selaginella moellendorffii* (Chang et al., 2016), the embryonic root is short-lived, and the majority of the rooting system, consisting of root-bearing rhizophores and roots, is formed postembryonically (Mello et al., 2019). The rhizophore in Selaginella is a unique kind of root-bearing (from which roots develop) organ, a positive gravitropic leafless cylinder without typical root traits such as a root cap (RC) and root hairs (Nageli and Leitgeb, 1868; Mello et al., 2019). The transition from the rhizophore to the root is hallmarked by the appearance of these root traits (Lu and Jernstedt, 1996; Dolzblasz et al., 2018). Roots in Selaginella do not branch laterally, but at the tip (termed dichotomous root branching; Fang et al., 2019; Motte and Beeckman, 2019; Motte et al., 2020). Interestingly, fossil evidence reveals that there have been multiple origins for both the lateral and dichotomous branching patterns in root evolution (Hetherington et al., 2020), while dichotomous root branching seems to be conserved throughout lycophyte evolution (Hetherington and Dolan, 2017).

Intriguingly, the transition from rootless plants to the first root-bearing organisms did not require extra gene families, which suggests that the exploitation of existing genetic programs was sufficient for the generation of roots (Ferrari et al., 2020). Consistently, the number of TF families increased before but not during plant terrestrialization (Catarino et al., 2016). Although expansions of gene families is considered to underpin the evolution of gene function and biological innovations (Panchy et al., 2016), genomic analyses revealed that only limited expansions occurred at the divergence between the lycophyte and euphyllophyte clades (One Thousand Plant Transcriptomes Initiative et al., 2019; Wong et al., 2020). Thus, it seems that early root evolution might have adopted the functional co-option (new use of existing traits) of genes that duplicated in a large scale before emergence of vascular plants. Further on, root evolution has to be considered as an ongoing selective process instead of a sudden appearance, which is supported by anatomical (Fujinami et al., 2017) and fossil (Hetherington and Dolan, 2018b) evidence showing that roots gradually evolved multiple times to acquire traits in a stepwise manner within the lycophyte lineage. Moreover, paleobotanical evidence indicates that roots evolved at least twice, independently once in lycophytes and once in euphyllophytes (Raven and Edwards, 2001; Friedman et al., 2004; **Figure 1**). Nevertheless, gene expression programs seem to be conserved between these two lineages, suggesting the existence of an ancient root developmental program from the common ancestor of the vascular plants, or parallel recruitment of largely the same program to enable root development (Huang and Schiefelbein, 2015).

In this review, we first provide an overview of the current view on root evolution followed by an overview of the development, morphology, and anatomy of lycophyte roots (focusing on Selaginella). Furthermore, we survey the importance of auxins in root development of mainly Selaginella and speculate on the possible role of TFs for which evidence could be found in the conservation of their sequences and reported gene expression data in *S. moellendorffii*.

ROOT EVOLUTION

Land colonization by plants happened around 470 million years ago and is a milestone in plant evolution. It is generally believed that a bryophyte-like common ancestor of vascular plants developed rhizoids for rooting from the bottom surface of axes over 400 million years ago. Supportive for this, the extinct vascular lineage origin-spanning species, such as *Aglaophyton majus* and *Rhynia gwynne-vaughanii*, also developed bryophyte-like rhizoid-based rooting systems. Similar rooting systems were still preserved in the extinct early Devonian lycophytes, e.g., *Nothia aphylla*, which also lacked specialized rooting axes, i.e., sporophytic terminal axial organs performing rooting functions (Hetherington and Dolan, 2018a, 2019; Hetherington, 2019).

Roots evolved in a stepwise manner during lycophyte evolution. For example, a specialized rooting axe, with a continuous epidermal surface rather than a RC, was found in the extinct lycophyte *Asteroxylon mackiei* (Hetherington and Dolan, 2018b). This rooting organ deviates from the currently known roots of extant vascular plants that have a RC surrounding the RAM and indicates that roots did not appear from the start in their present form. Indeed, similarities with modern roots could be identified in less old fossilized lycophyte root meristems, dating back to over 300 million years ago, which showed a generally similar cellular organization with extant lycophyte root meristems (Hetherington et al., 2016).

Phylogenetic analyses considering fossil taxa demonstrated that roots evolved at least twice in vascular plants (Friedman et al., 2004; Hetherington and Dolan, 2018b, 2019), once in the lycophytes and once in the euphyllophytes, a sister clade of the lycophytes within the vascular plants. Euphyllophyte roots are anatomically similar to lycophyte roots, where an apical meristem provides cells for a multilayered main root with a central vasculature and typical root traits such as the RC and root hairs (Bierhorst, 1971). A characteristic generally interpreted as a sign of the dual origin is the different root branching strategy that is found in the extant vascular plants: (endogenous) LR branching in euphyllophytes and dichotomous (isotomous) root branching in lycophytes (Motte and Beeckman, 2019;

Motte et al., 2020). However, recent paleobotanical evidence showed a different trajectory of euphyllophyte root evolution: (1) Dichotomous root branching was common in many early euphyllophyte groups during Devonian and Carboniferous periods; (2) LR branching evolved multiple times in at least three main euphyllophyte lineages independently: possibly first in the lignophytes (seed plants and progymnosperms, an extinct paraphyletic assemblage from which the seed plants evolved, including Archaeopteridales and Aneurophytales), second in Equisetopsida and third in ferns, including Marattiales and Leptosporangiate ferns (Hetherington et al., 2020). In contrast to the evolution of euphyllophyte root branching, root dichotomy seems to be conserved throughout lycophyte evolution (Hetherington and Dolan, 2017; Hetherington et al., 2020).

The living lycophytes consist of the orders Lycopodiales, Selaginellales, and Isoetales (PPG I, 2016). A first Selaginella genome was sequenced in *S. moellendorffii* (Banks et al., 2011) giving rise to multiple transcriptomic studies with root samples (Motte et al., 2020). Moreover, transient transfection of *S. moellendorffii* root protoplasts was used to test functioning of transcriptional responses (Mello et al., 2019). Thus, newly valuable omics resources and an expanded molecular toolbox advocate this species as an emerging representative in lycophyte (root) research. However, though genomes of several other Selaginella species have been sequenced (Ge et al., 2016; VanBuren et al., 2018; Xu et al., 2018), genomic resources of the other orders, i.e., Lycopodiales and Isoetales, still remain limited (Motte et al., 2020). In addition, the current molecular toolbox still needs to be much expanded. One of the greatest challenges in lycophyte research is to establish a (stable) transformation system, which would allow decent investigations into gene function using transgenics.

RAM ORGANIZATION

The RAM is crucial for plant roots as it forms a growing tip that supplies the root with new cells. To ensure this, it harbors one or more initials or stem cells, which do not differentiate but keep dividing to produce different cell types and to replenish

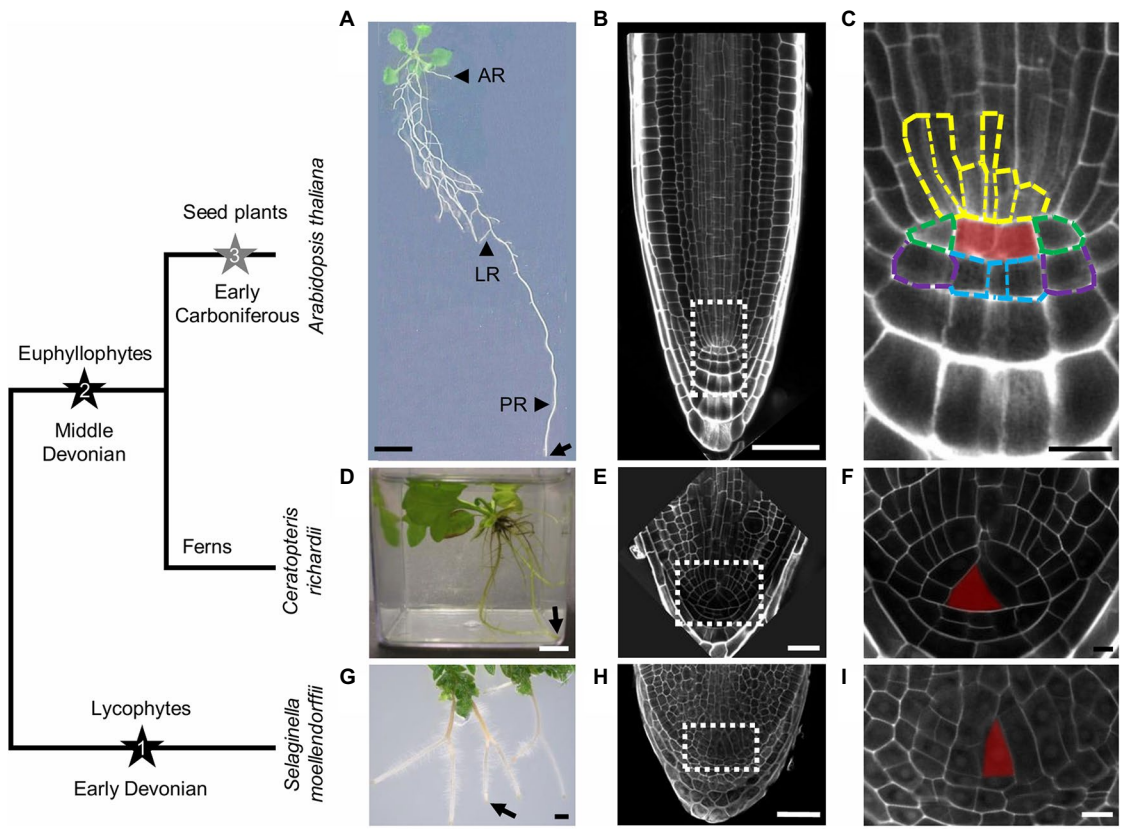

FIGURE 1 | Simplified cladogram with images of rooting system and root meristem of the major groups of vascular plants. Black stars indicate the first two (1 and 2) valid independent root origins. It is currently unclear whether root evolution in seed plants can be seen as the third independent event (3), indicated by a gray star. **(A,D,G)** Rooting systems of *Arabidopsis thaliana* **(A)**, *Ceratopteris richardii* **(D)**, and *Selaginella moellendorffii* **(G)**. **(A)** In *A. thaliana*, adventitious roots (AR) and lateral roots (LR) arise from hypocotyl and primary root (PR), respectively. **(B,E,H)** Root meristems of *A. thaliana* **(B)**, *C. richardii* **(E)**, and *S. moellendorffii* **(H)**, which are magnifications of the root tips indicated by the arrows in **(A,D,G)**. **(C,F,I)** are magnifications as indicated by the dashed rectangles in **(B,E,H)**. **(C)** The quiescent center (red overlay) regulates or organizes the surrounding stem cells (initials) indicated by dashed outlines in different colors: vasculature initials (yellow), columella initials (blue), lateral root cap/epidermis initials (purple), and endodermis/cortex initials (green). In *C. richardii* **(F)** and *S. moellendorffii* **(I)**, the central apical cell or initial cell (red overlay) presumably organizes itself and is the sole root stem cell. Scale bars: 1 cm **(A,D,G)**, 50 μm **(B,E,H)**, and 10 μm **(C,F,I)**.

the stem cell pool in the root. In Arabidopsis, the RAM contains a region of mitotically almost inactive cells, the quiescent center (QC), which is surrounded by different stem cells, including the initials for the vasculature, columella, lateral root cap/epidermis, and endodermis/cortex (Dolan et al., 1993; Motte et al., 2019; **Figures 1B,C**). The QC and the stem cells compose the root stem cell niche (SCN), in which the QC is important to maintain the identity of the stem cells (van den Berg et al., 1997; Sabatini et al., 2003).

Unlike Arabidopsis RAMs, the Selaginella RAM does not possess a QC but presumably only one stem cell called the initial cell (IC; **Figures 1H,I**). However, it is unknown how the identity of this initial cell is determined. The IC is presumably tetrahedral and probably cuts off daughter cells from four sides as the source of cells for the whole root (Imaichi and Kato, 1989; **Figure 1I**). Interestingly, the Selaginella RAM organization is quite similar to the organization of the fern RAM (**Figures 1E,F**). In some leptosporangiate ferns, the IC is also tetrahedral and divides a fixed number of times in a cyclic order at the three proximal sides, producing as such a fixed number of merophytes (packets of cells which are clonally related), which are stacked to form a root (Gunning et al., 1978; Hou and Blancaflor, 2018; **Figure 1F**). For instance, in the root apex of the fern *Azolla pinnata*, the IC divides 43 times to produce 12 successive merophytes, representing determinate root growth (Piekarska-Stachowiak and Nakielski, 2013). In addition, RC cells are produced from the IC distal face (Hou and Hill, 2004). A similar easy traceable cell division pattern is not obvious in Selaginella, and it is currently not entirely clear how a root in this plant is constructed.

Intriguingly, some other lycophytes, including *Lycopodium clavatum* and *Lycopodium diphasiastrum*, possess roots with a QC-like region, which contain cells with a slightly higher frequency of mitotic cell division than QC cells in the Arabidopsis root (Fujinami et al., 2017). In contrast, the lycophytes *Lycopodium obscurum* and Isoetaceae have no QC or QC-like region, but tiers of ICs from which different cell layers are derived (Yi and Kato, 2001; Fujinami et al., 2017). Such anatomic disparity of RAM organization in the extant lycophytes supports the idea that roots even evolved multiple times within this lineage.

ROOT BRANCHING

One of the advantages of seed plants during the colonization of land is their LR branching pattern, which is plastic and adaptable toward different conditions (Motte and Beeckman, 2019). In Arabidopsis, LR formation is well studied spatially and chronologically (Banda et al., 2019). LR formation in this species is initiated by nuclear migration and asymmetric divisions of two adjacent pericycle founder cells (Malamy and Benfey, 1997; Casimiro et al., 2001; Goh et al., 2012a); after initiation and a series of anticlinal and periclinal cell divisions, a new LR primordium is gradually formed, and a new SCN installed (Goh et al., 2016; Torres-Martinez et al., 2019; **Figure 2A**).

Lycophyte roots do not branch laterally like seed plants (Fang et al., 2019), possibly due to the lack of pluripotency of the pericycle cells. Instead, lycophyte roots branch dichotomously, and hence, two branches are formed at the root tip after bifurcation of the root meristem (Troll, 1937; Hetherington and Dolan, 2017; Fang et al., 2019). In Selaginella, formation of two ICs results in two new young root primordia (Otreba and Gola, 2011; **Figures 2B,C**). The primordia develop with continuity of vascular tissues and procambium preserved in both apices (**Figure 2C**). Until this phase, the branching is still well hidden inside the parent root tip (Otreba and Gola, 2011). After emergence from the parent root tip, the two new apices do not branch immediately and harbor only one IC in each RAM. Each RAM develops and will bifurcate again, a process that can be repeated several times as the root grows.

It is currently unknown which events are taking place to prepare Selaginella roots for branching. In addition, how two new ICs appear is still not clear: They are considered to emerge either after inactivation of the original IC (Imaichi and Kato, 1989; Otreba and Gola, 2011), or alternatively, a second IC might be derived from the original IC (Barlow and Lück, 2004). Investigation into the early branching events is required to answer this fundamental question. To our knowledge, only two papers described RAM bifurcation initiation in other lycophytes. In Isoetes, prior to branching, the apical meristem broadens and through a specific cell division pattern two rows of small and narrow non-meristematic cells are produced in the center of the meristem separating two groups of initials (Yi and Kato, 2001). In Lycopodium, a representative of the lycophytes having roots with a QC-like region as mentioned higher, dichotomous branching occurs by the appearance of actively dividing cells in the quiescent tissue. As a result, the parental meristem divides into two daughter meristems (Fujinami et al., 2021). The different bifurcation mechanisms within the lycophytes are probably reflecting the different RAM organization resulting from the gradual evolution of roots within this lineage.

AUXIN CONTROL

Hormones play major roles in the control of root development and especially auxins are essential for RAM maintenance and LR formation, which is well-documented for Arabidopsis. To our knowledge, lycophyte root responses toward hormones have only been studied in Selaginellaceae, and mainly toward auxins.

Auxins, early characterized as "root forming hormones of plants" (Went, 1929), have long been known to regulate the development and maintenance of root meristems in plants. In particular auxin transport and, as a result, auxin gradients with increasing level toward the root tip is of utmost importance for this control. Arabidopsis root tips show an "inverted fountain" of auxin movement: auxin flows from the transition zone between meristem and elongation zone in a rootward direction and is then inverted in the RC through the epidermis and flows back to the transition zone. Both AUXIN1/LIKE-AUX1 (AUX/LAX) auxin influx carriers and PIN-FORMED (PIN) efflux carriers are important in this process (Trewavas, 1986; Gaillochet and Lohmann, 2015), which results in an auxin gradient with a maximum at the QC. This is crucial for the

positioning of the QC and the surrounding stem cells (Sabatini et al., 1999; Shimotohno and Scheres, 2019). Similarly, auxin maxima and auxin signaling are crucial at different steps during LR formation (Cavallari et al., 2021).

Auxin biosynthesis, signaling, transport, and conjugation all predated evolution of vascular plants (Bowman et al., 2021). However, it is currently unknown whether auxin is also involved in the IC maintenance of the lycophyte RAM. In any case, auxin is, just as in other plants, rootwardly transported in Selaginella roots (Wochok and Sussex, 1974). Disturbance of this transport affects both root growth and meristem organization, whereas increase of auxin levels affects root growth, advocating for a role of an auxin gradient in the root meristem organization (Fang et al., 2019). Supportive for this, key components of auxin transport, e.g., AUX/LAXs and PINs, have also been identified in *S. moellendorffii* (Banks et al., 2011).

Moreover, exogenously applied auxins promote initiation of roots in Selaginella, whereas inhibitors of auxin transport prevent this initiation. The auxin indole-3-acetic acid (IAA; Williams, 1937) and auxin precursor indole-3-butyric acid (IBA; Webster, 1969) are even able to change the shoot fate to root fate of the angle meristem, located in the angles of shoot branches in many Selaginella species and giving rise to new shoots or rhizophores (Jernstedt et al., 1992; Banks, 2009). Likewise, the synthetic auxin 2,4-dichlorophenoxyacetic acid (2,4-D) promotes the root fate in the dorsal angle meristems (Mello et al., 2019). In contrast, an auxin transport inhibitor, 2,3,5-triiodobenzoic acid (TIBA), changes the angle meristems toward development of leafy shoots (Wochok and Sussex, 1975; Mello et al., 2019).

Other examples in Selaginella support a possible role of auxin in the root meristem development. Root-to-shoot conversion can be suppressed by the use of 1-naphthaleneacetic acid (NAA) in *Selaginella willdenowii* (Wochok and Sussex, 1976), and IBA can be used to initiate root cultures in *Selaginella microphylla* (Jha et al., 2013). On the other hand, IBA might also induce root to shoot conversion, indicating that not only auxin as such, but also a controlled balance of auxin levels, gradients, or signaling is possibly required during RAM establishment.

Furthermore, auxins also affect the dichotomous root branching in Selaginella. Different auxins promote proliferation

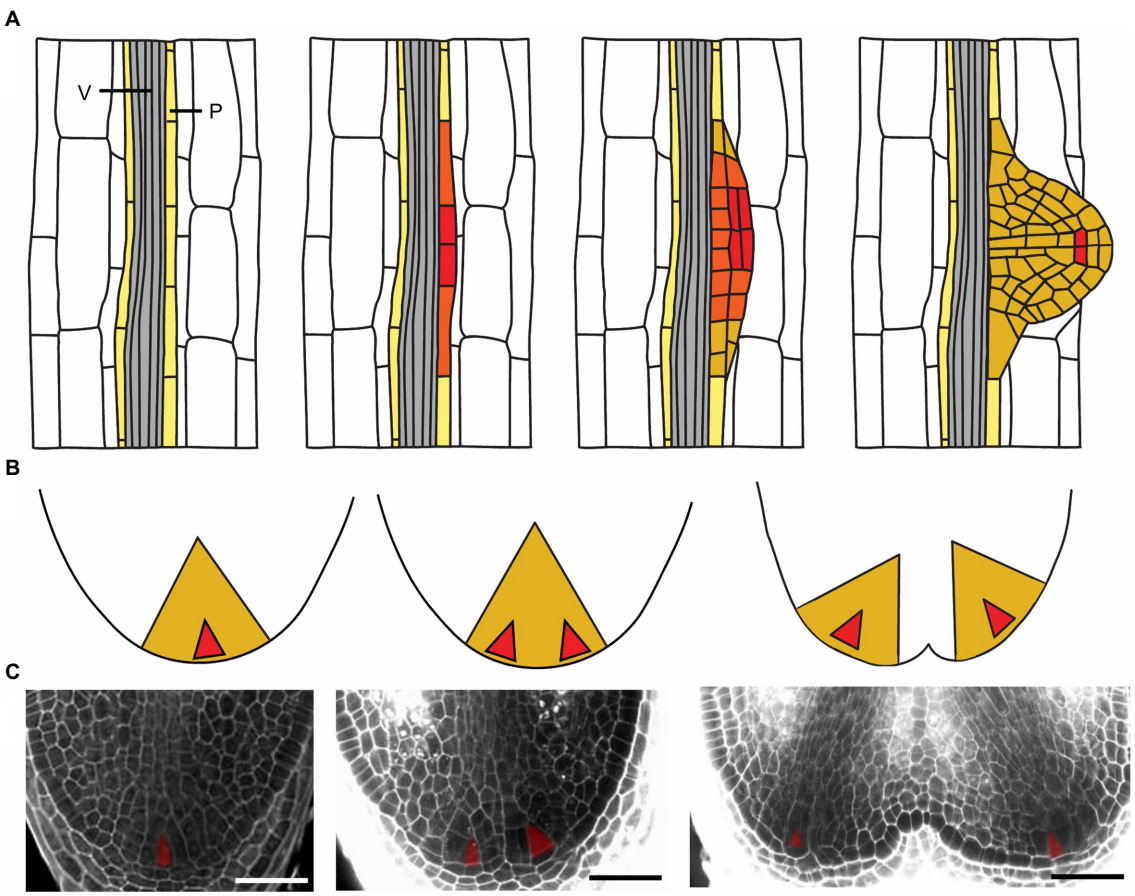

FIGURE 2 | Root branching processes in Arabidopsis and Selaginella. **(A)** Scheme of LR development in Arabidopsis. An LR initiates in the xylem-pole pericycle cells (P, light yellow). After a series of anticlinal and periclinal cell divisions, an LR primordium is developed. Gray indicates vascular tissue (V). **(B,C)** Scheme and images of dichotomous root branching in *S. moellendorffii*. Shortly after the meristem starts to bifurcate, two young root primordia are formed with apical cells installed. The meristems further develop into more mature primordia. The color gradient, red–orange–dark yellow, respectively, indicates high–medium–low levels of stem cell-ness in all the root meristems. Scale bars: 50 μm.

activity in root tips, whereas high concentrations of the polar auxin transporter inhibitor, naphthylphthalamic acid (NPA), stop growth and branching (Fang et al., 2019), or result in callus-like tissue at the root tip (Sanders and Langdale, 2013). It is important to note though that auxins do not directly induce root branching in *S. moellendorffii*, suggesting that the branching initiation itself depends on an auxin-independent process (Fang et al., 2019).

COMPARATIVE GENOMICS AND TRANSCRIPTOMICS TO GET INSIGHTS INTO LYCOPHYTE ROOT DEVELOPMENT

Most of our current knowledge about genetic players in development of the primary root and LR is obtained from Arabidopsis research, which revealed a core set of TFs at a cellular level (recently reviewed by Motte et al., 2019 and Shimotohno and Scheres, 2019). Yet mechanisms controlling RAM activities remain elusive in lycophytes, and data that could highlight possible players are mainly restricted to comparative genomics or gene expression data.

Recently, multiple tools to analyze gene expression data from *S. moellendorffii* and to perform comparative studies with other plant species have become available such as the recently designed Co-expression Network Toolkit (CoNekT; Proost and Mutwil, 2018), in which Ferrari et al. (2020) integrated different publicly available *S. moellendorffii* RNA-seq datasets. Additionally, Ferrari et al. (2020) designed the Selaginella eFP Browser, which provides color-coding pictographic representations for the gene expression level in different organs or tissues (Winter et al., 2007). As auxins seem to play a role in RAM establishment and maintenance of vascular plants, we surveyed the representative gene families that are, respectively, crucial in auxin biosynthesis, signaling, transport, and metabolism as well as important transcriptional regulators and highlight their possible role in Selaginella root development mainly based on phylogenetic and transcriptomic studies.

Auxin Biosynthesis

TRYPTOPHAN AMINOTRANSFERASE (TAA) and YUCCA FLAVIN-DEPENDENT MONOOXYGENASE (YUC/YUCCA) gene families play a crucial role in auxin biosynthesis in plants (Mashiguchi et al., 2011). Members regulate plant root development, as reviewed by Olatunji et al. (2017). TAA proteins likely originated during chlorophyte evolution (Mutte, 2020), whereas the origin of YUCs is unclear. An ancient divergence into the clades YUC and sYUC occurred during charophyte evolution, while the sYUC clade disappeared in Arabidopsis (Mutte, 2020). Furthermore, *YUC* genes belong to a deeply conserved auxin-dependent gene set with similar regulation patterns shared by all land plants (Mutte et al., 2018).

In Arabidopsis, the highest auxin synthesis rate of the root is detected in the RAM (Ljung et al., 2005). Specifically, auxin is locally produced in the QC, which is required for RAM maintenance (Casanova-Saez and Voss, 2019). Mutations in the *TAA* genes *TAA1* and *TAA1-RELATED2* (*TAR2*) result in reduced root meristematic activity (Stepanova et al., 2008), whereas most *YUC* mutants do not even form a root meristem (Cheng et al., 2007), demonstrating their importance in RAM maintenance and establishment. Additionally, some *YUC* genes are also expressed at early stages during LR formation (Hentrich et al., 2013; Cai et al., 2014; Tang et al., 2017), suggesting a possible role during LR development as well.

Selaginella moellendorffii has one *TAA* homologue, which does not have specific or high expression in the root or RAM (Ferrari et al., 2020), suggesting a possibly limited role in lycophyte root development. Interestingly, an auxin biosynthesis inhibitor that competitively inhibits YUC enzymes reduces root growth in *S. moellendorffii* (Kaneko et al., 2020). Additionally, transcripts of two *sYUC* genes accumulate substantially in the *S. moellendorffii* root and one of them is also highly expressed in the RAM (**Table 1**). On the contrary, transcripts of the three homologues from the YUC clade only have low abundance. Thus, in particular, auxin biosynthesis *via* sYUC homologues might be important in the establishment or maintenance of the root meristem of lycophytes.

Auxin Signaling

The core components of auxin signaling are TRANSPORT INHIBITOR RESPONSE 1/AUXIN SIGNALING F-BOX (TIR1/AFB) auxin receptors, AUXIN/INDOLE-3-ACETIC ACID (Aux/IAA) transcriptional repressors, and AUXIN RESPONSE FACTOR (ARF) TFs (Perrot-Rechenmann, 2014; Leyser, 2018). Auxin binds TIR1/AFB-Aux/IAA co-receptors, which leads to degradation of the Aux/IAAs and release of ARF TFs that regulate auxin responsive genes (Gray et al., 2001; Dharmasiri et al., 2005; Tan et al., 2007; Dos Santos Maraschin et al., 2009; Korasick et al., 2014; Israeli et al., 2020). Such a complete auxin response system is present in all land plants, but increased in complexity during evolution (Bowman et al., 2021). Phylogenetic analysis shows that the *Aux/IAA* gene family diverged into canonical and noncanonical *Aux/IAAs*. The latter do not bind to TIR1/AFB and cannot form a co-receptor. The ARF family split into class A, B. and C ARF subfamilies (Mutte et al., 2018), with class A ARFs being transcriptional activators, whereas the B or C classes are repressors.

In Arabidopsis, various Aux/IAA-ARF modules, involving canonical Aux/IAAs and all ARF classes, are involved in LR formation, embryonic RAM initiation, or RAM maintenance (Dello Ioio et al., 2008; Ding and Friml, 2010; Goh et al., 2012b; Palovaara et al., 2016; Promchuea et al., 2017; Du and Scheres, 2018). Interestingly, also the noncanonical IAA33 controls root stem cell identity *via* interaction with ARF10 and ARF16 (Lv et al., 2020), belonging to the class C. The orthologue of ARF16 also seems to be involved in RAM initiation in the conifer *Pinus pinaster* (de Vega-Bartol et al., 2013).

In *S. moellendorffii*, one *TIR1* homologue is highly expressed in the root and two homologues of *IAA33* show high expression in the RAM (**Table 1**), but none of the *ARF* homologues show specific or high expression in the root or RAM (Ferrari et al., 2020). Thus, it seems possible that noncanonical *IAAs* play a role in the meristem, whereas the role of *ARF* genes may be limited.

TABLE 1 | Specific and high root and root apical meristem (RAM) expression of the auxin-related gene family members in *S. moellendorffii*.

Gene family	Clade	Function	Gene ID	Arabidopsis homologue name	SRE	HRE	S RAM E	H RAM E
YUC	sYUC	Auxin biosynthesis	Smo113792	N/A		+		
YUC	sYUC	Auxin biosynthesis	Smo422043	N/A		+		+
TIR1/AFB	TIR1/AFB	Auxin receptor	Smo170974	TIR1, AFB1-5		+		
Aux/IAA	ncIAA	Auxin signaling	Smo415204	IAA33				+
Aux/IAA	ncIAA	Auxin signaling	Smo417391	IAA33				+
PIN	Lyco	Auxin transport	Smo119024	N/A	+			+

+: specific root/RAM expression [SRE / S RAM E, specific measure (SPM) > 0.85]. SPM was calculated in the CoNekT (Proost and Mutwil, 2018; Ferrari et al., 2020) using the Tissue Specificity (root) or Condition Specificity (RAM) method. High root/RAM expression (HRE / H RAM E): shown red color based on absolute value in Selaginella eFP Browser (Winter et al., 2007; Ferrari et al., 2020). Published phylogenetic trees were prioritized for homologue inference, and OrthoFinder (v1.1.8 in CoNekT) was alternatively used to also identify robust homologues within the same orthogroup (Emms and Kelly, 2015, 2019). N/A, not available.

Mello et al. (2019) further demonstrated that the transcriptional auxin responses function in *S. moellendorffii*, using auxin-treated root protoplasts transfected with a DR5 auxin response marker.

Auxin Transport

Polar auxin transport is believed to be a key part of a molecular toolkit used by the early streptophytes toward a better adaptation to land conditions (Bennett et al., 2014; Bennett, 2015). PIN proteins that are auxin efflux transporters direct polar auxin transport to regulate development of the RAM and the LR meristem, which has been intensively studied in Arabidopsis (Motte et al., 2019). A duplication occurred within the lycophytes, producing two PIN subclades (Lyco PIN1 and Lyco PIN2), which are sister to all the euphyllophyte subclades: Eu1-3 (Bennett et al., 2014; Bennett, 2015). The protein sequences of the lycophyte and euphyllophyte clades are similar, but differences exist. For instance, PIN2 has a particular hydrophilic loop domain that originated during seed plant evolution and that is crucial to mediate fast gravitropic response of the root for good adaptation to dry land (Zhang et al., 2019).

In Arabidopsis, PIN1 and PIN3 play key roles in RAM establishment and LR initiation (Friml et al., 2003; Marhavy et al., 2013; Chen et al., 2015). In addition, expression of PIN proteins is induced by auxins in the root (Vieten et al., 2005). Intriguingly, in contrast to seed plants, the fern Azolla does not show an increased RAM size when treated with auxins, nor an induction of *PIN* expression (de Vries et al., 2016), which suggests a different mechanism in the control of meristem size compared to Arabidopsis.

In *S. moellendorffii*, representative PINs failed to replace the fast root gravitropism of *AtPIN2* (Zhang et al., 2019). Particularly PINV may play an important role in generation of the root meristem, as *PINV* is specifically expressed in the *S. moellendorffii* root and the transcripts accumulate at a high level in the RAM (**Table 1**). In the gametophyte-dominant bryophyte Physcomitrella, PINs also drive meristem function as auxin transport facilitators (Bennett et al., 2014). Intriguingly, a recent study utilized extensive cross-species functional complementation experiments with *PIN* genes from different streptophyte lineages, showing that the shoot/root development function, e.g., establishment of auxin maxima at the root tip, actually originated in land plants (Zhang et al., 2020).

Auxin Metabolism

The GRETCHEN HAGEN3 (GH3) enzyme family conjugate compounds including auxin to amino acids, in order to control auxin homeostasis, which has an important role in plant development such as root growth (Casanova-Sáez et al., 2021). Phylogenetically, GH3s are classified into three groups: I–III (Chiu et al., 2018).

In Arabidopsis, a group II member GH3.17 is involved in the formation of auxin minima, which regulates RAM size (Di Mambro et al., 2017). In addition, the other group II genes regulate LR formation with a possible involvement in root pre-patterning by controlling levels of IBA-derived auxin in the RC (Xuan et al., 2015).

In *S. moellendorffii*, GH3s, especially the group II, play a predominant role in auxin homeostasis (Kaneko et al., 2020). However, the only homologue of Arabidopsis group II genes does not show specific or high expression in the root or RAM (Ferrari et al., 2020).

Developmental Genes

Gene families, such as AINTEGUMENTA (ANT), GRAS [for GIBBERELLIC ACID INSENSITIVE (GAI), REPRESSOR OF GA1 (RGA), and SCARECROW (SCR)], and WUSCHEL (WUS)-LIKE HOMEOBOX (WOX), contain genes that play diverse roles in plant signaling and development. Some of these gene family members are important root stem cell regulators (Motte et al., 2020). In Arabidopsis, *PLETHORA* genes, which are ANT gene family members, control QC specification and stem cell activity, with a concentration gradient closely associated with auxin maxima (Aida et al., 2004). The GRAS member SHORTROOT (SHR) is expressed in the root vascular tissue and moves to the QC, initial of cortex and endodermis, as well as endodermis in Arabidopsis (Helariutta et al., 2000; Nakajima et al., 2001; Cui et al., 2007; Augstein and Carlsbecker, 2018). In these cells, another GRAS family member SCR forms a heterodimer with SHR (Hirano et al., 2017; Hakoshima, 2018), playing a key role in root stem cell control. In addition, SCARECROW-LIKE 23 (SCL23), which is encoded by the closest homologue of *SCR*, acts redundantly with SCR in the SCN (Long et al., 2015). The WOX family member *WOX5* is expressed in the QC and the WOX TF moves to the adjacent stem cells, preventing

TABLE 2 | Specific and high root and RAM expression of the developmental genes in *S. moellendorffii*.

Gene family	Clade	Gene ID	Arabidopsis homologue name	SRE	HRE	S RAM E	H RAM E
ANT	euANT	Smo96572	ANT, AIL1				+
GRAS	SCR	Smo84762	SCR, SCL23		+		+
GRAS	SHR	Smo12696	SHR, SCL29/32	++			
GRAS	SHR	Smo53339	SHR, SCL29/32		+		
GRAS	SHR	Smo64241	SHR, SCL29/32		+		
GRAS	SHR	Smo90295	SHR, SCL29/32		+		
WOX	T1WOX	Smo4561	WOX10/13/14	+		+	+

+: specific root/RAM expression [SRE / S RAM E, specific measure (SPM) > 0.85]; ++: exclusive expression (SPM = 1). SPM calculated in the CoNekT (Proost and Mutwil, 2018; Ferrari et al., 2020) using the Tissue Specificity (root) or Condition Specificity (RAM) method. High root/RAM expression (HRE / H RAM E): shown red color based on absolute value in Selaginella eFP Browser (Winter et al., 2007; Ferrari et al., 2020). Published phylogenetic trees were prioritized for homologue inference, and OrthoFinder (v1.1.8 in CoNekT) was alternatively used to also identify robust homologues within the same orthogroup (Emms and Kelly, 2015, 2019). N/A, not available.

them from differentiation in the SCN (Sarkar et al., 2007; Kong et al., 2015). Moreover, *WOX13* is expressed in RAM stem cells, suggesting possible importance in root meristem formation (Deveaux et al., 2008).

The above-mentioned TFs also interact with each other during the regulation of meristem activity. For example, PLTs constrain the expression domain of WOX5 in the SCN, in which they maintain the QC and regulate the fate of columella stem cells (Burkart et al., 2019). SCR physically interacts with PLT, as well as TEOSINTE-BRANCHED1/CYCLOIDEA/PCF20 (TCP20), which induces *WOX5* expression to specify the SCN (Shimotohno et al., 2018). In turn, *WOX5* interacts with *SHR/SCR* and auxin pathways to maintain the SCN, preserving the QC identity (Sarkar et al., 2007).

These key regulators also function in the LR meristem formation: *PLT3*, *PLT5*, and *PLT7* are expressed early in the stage I primordium where the by them controlled asymmetric cell division occurs afterward to give rise to the stage II primordium. In addition, *PLT1*, *PLT2*, and *PLT4* are expressed later during LR outgrowth (Du and Scheres, 2017). SHR is crucial for LR development, including initiation and the control of asymmetric divisions of cortex/endodermis initials (Lucas et al., 2011). Besides, SHR activates *SCR* expression, which is the key for LR QC formation (Goh et al., 2016). Similarly as in the primary root, *WOX5* is during LR formation induced by a joint activity of PLTs, TCP20, and SCR (Shimotohno et al., 2018). Moreover, *WOX13* is not only expressed at the early stage of LR development, but also expressed during LR emergence (Deveaux et al., 2008). To investigate the possible significance in lycophyte root development, we next survey these gene families and highlight their possible roles in the lycophyte *S. moellendorffii*.

ANT

Based on a recently updated phylogenetic study, the ANT family can be divided into three clades: preANT, basalANT, and euANT; divergence of the ancestral preANT into two land plant-specific clades (basalANT and euANT) is hypothesized to be involved in plant terrestrialization (Dipp-Alvarez and Cruz-Ramirez, 2019). The most recently diverged euANT lineage, which has been intensively studied in Arabidopsis, includes members such as PLTs and ANT. Within the euANT lineage, two major sister clades can be found: one including AtANT and AINTEGUMENTA-like1 (AtAIL1), and the other including all the PLTs of Arabidopsis (Kim et al., 2005; Floyd and Bowman, 2007; Dipp-Alvarez and Cruz-Ramirez, 2019).

In *S. moellendorffii*, five genes were retrieved in this family: two in the euANT lineage and the other three in the basalANT lineage (Dipp-Alvarez and Cruz-Ramirez, 2019). All lycophyte euANT members fall within the ANT/AIL1 clade. Still, their motifs also overlap with the Arabidopsis PLT-specific motifs (Motte et al., 2020). One of the *S. moellendorffii* euANT homologues has a high expression in the RAM (**Table 2**), which may point to a possible role in the lycophyte RAM. Thus, it could be that the euANT TFs have conserved roles in RAMs of land plants.

GRAS

GIBBERELLIC ACID INSENSITIVE (GAI), REPRESSOR OF GA1 (RGA), and SCARECROW (SCR) genes are believed to be incorporated into the common ancestor of Zygnematophyceae (the likely sister group to land plants) and land plants, *via* horizontal gene transfer from soil bacteria, to regulate processes from development to defense against various stresses during early land colonization. *GRAS* genes also expanded in the common ancestor, which is believed to be relevant for the evolution and radiation of land plants after divergence (Cheng et al., 2019). Ancient diversification of *GRAS* genes into different major clades occurred before divergence of the moss and vascular plants (Engstrom, 2011). Among the clades, *SHR* and *SCR* are representatives from the two clades of SHR and SCR, respectively (Bolle, 2004, 2016).

Interestingly, the *S. moellendorffii* genome contains, relatively to its genome size, more *GRAS* genes than Arabidopsis (Song et al., 2014). In *S. moellendorffii*, five genes were retrieved belonging to the SHR clade, and two genes for the SCR clade (Wang et al., 2016; Zhang et al., 2018). All but one Selaginella *SHR* gene have either high root expression, or have exclusive root expression (**Table 2**), suggesting a possible role of this clade in lycophyte root development. In addition, one homologue of *SCR* and *SCL23*, from the SCR clade, is

highly expressed in the root and more specifically, in the RAM as well (**Table 2**). Thus, the expression of multiple *SHR* and *SCR* homologues is associated with the root meristem, and the SHR-SCR function might possibly be (partially) conserved in vascular plants.

WOX

WUSCHEL-LIKE HOMEOBOX can be divided into three superclades, which were recently termed Type 1 (T1WOX, the WOX10/13/14 clade), Type 2 (T2WOX, the WOX8/9 and WOX11/12 clades), and Type 3 (T3WOX, the WUS, WOX1/6, WOX2, WOX3, WOX4 and WOX5/7 clades) (Wu et al., 2019).

In the fern *C. richardii*, T2*WOX* genes, *WOXA* and *WOXB* are, respectively, expressed in the root mother cells and throughout the root meristem; the T3*WOX* member *WUSCHEL-LIKE* (*WUL*) is expressed in the root tips, whereas the T1*WOX* members *WOX13A* and *WOX13B* do not have specific root expression (Nardmann and Werr, 2012). In *S. moellendorffii*, eight *WOX* genes can be retrieved (Nardmann et al., 2009). Only one Selaginella *WOX* gene has specific and high expression in the RAM (**Table 2**), implying a possible role in the lycophyte root meristem. This *WOX* gene is a T1WOX member, lacking the canonical WUS-box, a conserved motif shared within the WUS subclade that is, at least in angiosperms, required for stem cell regulation and repressive transcriptional activities (Dolzblasz et al., 2016; Zhou et al., 2018). Thus, this T1WOX member, if having a function in stem cell specification, probably works *via* a different mechanism.

DISCUSSION AND CONCLUSION

Fossil records of extinct lycophytes argue that true roots were absent in the ancient lycophyte trees and that a modified shoot system was co-opted to execute root functions (Kenrick, 2013). During early root evolution, lycophyte roots acquired root traits in a stepwise manner (Hetherington and Dolan, 2018b, 2019). Consistently, different extant lycophyte species have various types of RAM organization (Fujinami et al., 2017, 2020). Thus, it is conceivable that multiple root origins occurred during lycophyte evolution. Interestingly, branching of the root system in different patterns predated root evolution (Hao et al., 2010; Matsunaga and Tomescu, 2016; Rothwell and Tomescu, 2018), but the dichotomous branching pattern was preserved in the extant lycophyte roots. Insights in the dynamics of lycophyte RAM organization and initiation of root branching still await breakthroughs in molecular technologies and application of advanced imaging methods, e.g., live imaging.

How the evolution of plant growth hormones has been associated with root evolution is largely elusive. In the case of auxin, emergence of the core components mediating the response clearly predated lycophyte evolution (Bowman et al., 2021). In contrast to seed plants, auxins cannot induce root branching in non-seed vascular plants (Hou and Hill, 2004; Fang et al., 2019). To better understand hormonal pathways controlling development of lycophyte root meristems, the effect of more hormones, for example cytokinin, ethylene, and abscisic acid, should be experimentally tested and physiologically and genetically evaluated.

It is intriguing that lycophytes utilized the same set of probably only slightly expanded gene families for root evolution (One Thousand Plant Transcriptomes Initiative et al., 2019; Ferrari et al., 2020). Consistently, the majority of TF families evolved before land colonization of plants (Catarino et al., 2016). Thus, it is plausible that the rootless common ancestor of vascular plants co-opted the present genetic material for root evolution. Supportive for this, important developmental gene families, which are reviewed here, might play central roles in root meristem maintenance of lycophytes.

As gene families evolved and expanded (One Thousand Plant Transcriptomes Initiative et al., 2019; Wong et al., 2020), functional divergence will have occurred. Here, we mainly used *S. moellendorffii* expression data to predict the function, as stable transformation is currently unavailable in lycophyte research, obstructing functional investigation. We fully realize that the expression data alone do not legitimate to conclude on functional conservation or divergence of lycophyte genes. More experimental approaches, such as *in situ* hybridization, cross-species functional complementation and sequence domain analysis, may help to better understand root-function evolution of the gene families. We hope that our study is able to motivate the community to collect more such early "rootprints" of lycophytes, which would allow us to see clearer evolutionary trajectories of the root in vascular plants.

DATA AVAILABILITY STATEMENT

The original contributions presented in the study are included in the article, further inquiries can be directed to the corresponding author.

AUTHOR CONTRIBUTIONS

TF conceptualized the manuscript. TF, HM and TB wrote the manuscript. HM made the figures. All authors contributed to the article and approved the submitted version.

FUNDING

This study was financially supported by the Fonds voor Wetenschappelijk Onderzoek – Vlaanderen (FWO)-projects G027313N and G028421N. TF was financially supported by China Scholarship Council (CSC) and Lotus Unlimited Project in the Erasmus Mundus program of the European Union.

ACKNOWLEDGMENTS

We thank Davy Opdenacker, Ward Poelmans, and Wouter Smet for sharing images.

REFERENCES

Aida, M., Beis, D., Heidstra, R., Willemsen, V., Blilou, I., Galinha, C., et al. (2004). The *PLETHORA* genes mediate patterning of the *Arabidopsis* root stem cell niche. *Cell* 119, 109–120. doi: 10.1016/j.cell.2004.09.018

Augstein, F., and Carlsbecker, A. (2018). Getting to the roots: a developmental genetic view of root anatomy and function from Arabidopsis to lycophytes. *Front. Plant Sci.* 9:1410. doi: 10.3389/fpls.2018.01410

Banda, J., Bellande, K., von Wangenheim, D., Goh, T., Guyomarc'h, S., Laplaze, L., et al. (2019). Lateral root formation in *Arabidopsis*: A well-ordered LRexit. *Trends Plant Sci.* 24, 826–839. doi: 10.1016/j.tplants.2019.06.015

Banks, J. A. (2009). Selaginella and 400 million years of separation. *Annu. Rev. Plant Biol.* 60, 223–238. doi: 10.1146/annurev.arplant.59.032607.092851

Banks, J. A., Nishiyama, T., Hasebe, M., Bowman, J. L., Gribskov, M., dePamphilis, C., et al. (2011). The Selaginella genome identifies genetic changes associated with the evolution of vascular plants. *Science* 332, 960–963. doi: 10.1126/science.1203810

Barlow, P. W., and Lück, J. (2004). Deterministic cellular descendance and its relationship to the branching of plant organ axes. *Protoplasma* 224, 129–143. doi: 10.1007/s00709-004-0063-5

Bennett, T. (2015). PIN proteins and the evolution of plant development. *Trends Plant Sci.* 20, 498–507. doi: 10.1016/j.tplants.2015.05.005

Bennett, T., Brockington, S. F., Rothfels, C., Graham, S. W., Stevenson, D., Kutchan, T., et al. (2014). Paralogous radiations of PIN proteins with multiple origins of noncanonical PIN structure. *Mol. Biol. Evol.* 31, 2042–2060. doi: 10.1093/molbev/msu147

Bierhorst, D. W. (1971). *Morphology of Vascular Plants.* New York: Macmillan.

Bolle, C. (2004). The role of GRAS proteins in plant signal transduction and development. *Planta* 218, 683–692. doi: 10.1007/s00425-004-1203-z

Bolle, C. (2016). "Structure and evolution of plant GRAS family proteins," in *Plant Transcription Factors: Evolutionary, Structural and Functional Aspects*. ed. D. H. Gonzalez (Cambridge, MA: Academic Press), 153–161.

Bowman, J. L., Flores Sandoval, E., and Kato, H. (2021). On the evolutionary origins of land plant auxin biology. *Cold Spring Harb. Perspect. Biol.* 13:a040048. doi: 10.1101/cshperspect.a040048

Burkart, R. C., Strotmann, V. I., Kirschner, G. K., Akinci, A., Czempik, L., Maizel, A., et al. (2019). PLETHORA and WOX5 interaction and subnuclear localisation regulates Arabidopsis root stem cell maintenance. BioRxiv [Preprint]. doi: 10.1101/818187

Cai, X. T., Xu, P., Zhao, P. X., Liu, R., Yu, L. H., and Xiang, C. B. (2014). *Arabidopsis* ERF109 mediates cross-talk between jasmonic acid and auxin biosynthesis during lateral root formation. *Nat. Commun.* 5:5833. doi: 10.1038/ncomms6833

Casanova-Sáez, R., Mateo-Bonmatí, E., and Ljung, K. (2021). Auxin metabolism in plants. *Cold Spring Harb. Perspect. Biol.* 13:a039867. doi: 10.1101/cshperspect.a039867

Casanova-Saez, R., and Voss, U. (2019). Auxin metabolism controls developmental decisions in land plants. *Trends Plant Sci.* 24, 741–754. doi: 10.1016/j.tplants.2019.05.006

Casimiro, I., Marchant, A., Bhalerao, R. P., Beeckman, T., Dhooge, S., Swarup, R., et al. (2001). Auxin transport promotes *Arabidopsis* lateral root initiation. *Plant Cell* 13, 843–852. doi: 10.1105/tpc.13.4.843

Catarino, B., Hetherington, A. J., Emms, D. M., Kelly, S., and Dolan, L. (2016). The stepwise increase in the number of transcription factor families in the Precambrian predated the diversification of plants on land. *Mol. Biol. Evol.* 33, 2815–2819. doi: 10.1093/molbev/msw155

Cavallari, N., Artner, C., and Benkova, E. (2021). Auxin-regulated lateral root organogenesis. *Cold Spring Harb. Perspect. Biol.* 13:a039941. doi: 10.1101/cshperspect.a039941

Chang, C., Bowman, J. L., and Meyerowitz, E. M. (2016). Field guide to plant model systems. *Cell* 167, 325–339. doi: 10.1016/j.cell.2016.08.031

Chen, Q., Liu, Y., Maere, S., Lee, E., Van Isterdael, G., Xie, Z., et al. (2015). A coherent transcriptional feed-forward motif model for mediating auxin-sensitive *PIN3* expression during lateral root development. *Nat. Commun.* 6:8821. doi: 10.1038/ncomms9821

Cheng, Y., Dai, X., and Zhao, Y. (2007). Auxin biosynthesis by the YUCCA flavin monooxygenases controls the formation of floral organs and vascular tissues in *Arabidopsis*. *Genes Dev.* 20, 1790–1799. doi: 10.1101/gad.1415106

Cheng, S., Xian, W., Fu, Y., Marin, B., Keller, J., Wu, T., et al. (2019). Genomes of subaerial Zygnematophyceae provide insights into land plant evolution. *Cell* 179, 1057–1067. doi: 10.1016/j.cell.2019.10.019

Chiu, L.-W., Heckert, M. J., You, Y., Albanese, N., Fenwick, T., Siehl, D. L., et al. (2018). Members of the GH3 family of proteins conjugate 2,4-D and dicamba with aspartate and glutamate. *Plant Cell Physiol.* 59, 2366–2380. doi: 10.1093/pcp/pcy160

Cui, H., Levesque, M. P., Vernoux, T., Jung, J. W., Paquette, A. J., Gallagher, K. L., et al. (2007). An evolutionarily conserved mechanism delimiting SHR movement defines a single layer of endodermis in plants. *Science* 316, 421–425. doi: 10.1126/science.1139531

Dello Ioio, R., Nakamura, K., Moubayidin, L., Perilli, S., Taniguchi, M., Morita, M. T., et al. (2008). A genetic framework for the control of cell division and differentiation in the root meristem. *Science* 322, 1380–1384. doi: 10.1126/science.1164147

Deveaux, Y., Toffano-Nioche, C., Claisse, G., Thareau, V., Morin, H., Laufs, P., et al. (2008). Genes of the most conserved WOX clade in plants affect root and flower development in Arabidopsis. *BMC Evol. Biol.* 8:291. doi: 10.1186/1471-2148-8-291

de Vega-Bartol, J. J., Simoes, M., Lorenz, W. W., Rodrigues, A. S., Alba, R., Dean, J. F., et al. (2013). Transcriptomic analysis highlights epigenetic and transcriptional regulation during zygotic embryo development of *Pinus pinaster*. *BMC Plant Biol.* 13:123. doi: 10.1186/1471-2229-13-123

de Vries, J., Fischer, A. M., Roettger, M., Rommel, S., Schluepmann, H., Brautigam, A., et al. (2016). Cytokinin-induced promotion of root meristem size in the fern *Azolla* supports a shoot-like origin of euphyllophyte roots. *New Phytol.* 209, 705–720. doi: 10.1111/nph.13630

Dharmasiri, N., Dharmasiri, S., and Estelle, M. (2005). The F-box protein TIR1 is an auxin receptor. *Nature* 435, 441–445. doi: 10.1038/nature03543

Di Mambro, R., De Ruvo, M., Pacifici, E., Salvi, E., Sozzani, R., Benfey, P. N., et al. (2017). Auxin minimum triggers the developmental switch from cell division to cell differentiation in the *Arabidopsis* root. *Proc. Natl. Acad. Sci. U. S. A.* 114, E7641–E7649. doi: 10.1073/pnas.1705833114

Ding, Z., and Friml, J. (2010). Auxin regulates distal stem cell differentiation in *Arabidopsis* roots. *Proc. Natl. Acad. Sci. U. S. A.* 107, 12046–12051. doi: 10.1073/pnas.1000672107

Dipp-Alvarez, M., and Cruz-Ramirez, A. (2019). A phylogenetic study of the ANT family points to a preANT gene as the ancestor of basal and euANT transcription factors in land plants. *Front. Plant Sci.* 10:17. doi: 10.3389/fpls.2019.00017

Dolan, L., Janmaat, K., Willemsen, V., Linstead, P., Poethig, S., Roberts, K., et al. (1993). Cellular organisation of the *Arabidopsis thaliana* root. *Development* 119, 71–84. doi: 10.1242/dev.119.1.71

Dolzblasz, A., Myskow, E., and Gola, E. M. (2018). "Meristems of seedless vascular plants: the state of the art," in *Current Advances in Fern Research*. ed. H. Fernandez (Berlin, Germany: Springer), 47–73.

Dolzblasz, A., Nardmann, J., Clerici, E., Causier, B., van der Graaff, E., Chen, J., et al. (2016). Stem cell regulation by *Arabidopsis WOX* genes. *Mol. Plant* 9, 1028–1039. doi: 10.1016/j.molp.2016.04.007

Dos Santos Maraschin, F., Memelink, J., and Offringa, R. (2009). Auxin-induced, SCF^{TIR1}-mediated poly-ubiquitination marks AUX/IAA proteins for degradation. *Plant J.* 59, 100–109. doi: 10.1111/j.1365-313X.2009.03854.x

Du, Y., and Scheres, B. (2017). PLETHORA transcription factors orchestrate de novo organ patterning during *Arabidopsis* lateral root outgrowth. *Proc. Natl. Acad. Sci. U. S. A.* 114, 11709–11714. doi: 10.1073/pnas.1714410114

Du, Y., and Scheres, B. (2018). Lateral root formation and the multiple roles of auxin. *J. Exp. Bot.* 69, 155–167. doi: 10.1093/jxb/erx223

Emms, D. M., and Kelly, S. (2015). OrthoFinder: solving fundamental biases in whole genome comparisons dramatically improves orthogroup inference accuracy. *Genome Biol.* 16:157. doi: 10.1186/s13059-015-0721-2

Emms, D. M., and Kelly, S. (2019). OrthoFinder: phylogenetic orthology inference for comparative genomics. *Genome Biol.* 20:238. doi: 10.1186/s13059-019-1832-y

Engstrom, E. M. (2011). Phylogenetic analysis of GRAS proteins from moss, lycophyte and vascular plant lineages reveals that GRAS genes arose and underwent substantial diversification in the ancestral lineage common to bryophytes and vascular plants. *Plant Signal. Behav.* 6, 850–854. doi: 10.4161/psb.6.6.15203

Fang, T., Motte, H., Parizot, B., and Beeckman, T. (2019). Root branching is not induced by auxins in *Selaginella moellendorffii*. *Front. Plant Sci.* 10:154. doi: 10.3389/fpls.2019.00154

Ferrari, C., Shivhare, D., Hansen, B. O., Pasha, A., Esteban, E., Provart, N. J., et al. (2020). Expression atlas of *Selaginella moellendorffii* provides insights into the evolution of vasculature, secondary metabolism, and roots. *Plant Cell* 32, 853–870. doi: 10.1105/tpc.19.00780

Floyd, S. K., and Bowman, J. L. (2007). The ancestral developmental tool kit of land plants. *Int. J. Plant Sci.* 168, 1–35. doi: 10.1086/509079

Friedman, W. E., Moore, R. C., and Purugganan, M. D. (2004). The evolution of plant development. *Am. J. Bot.* 91, 1726–1741. doi: 10.3732/ajb.91.10.1726

Friml, J., Vieten, A., Sauer, M., Weijers, D., Schwarz, H., Hamann, T., et al. (2003). Efflux-dependent auxin gradients establish the apical-basal axis of *Arabidopsis*. *Nature* 426, 147–153. doi: 10.1038/nature02085

Fujinami, R., Nakajima, A., Imaichi, R., and Yamada, T. (2021). *Lycopodium* root meristem dynamics support homology between shoots and roots in lycophytes. *New Phytol.* 229, 460–468. doi: 10.1111/nph.16814

Fujinami, R., Yamada, T., and Imaichi, R. (2020). Root apical meristem diversity and the origin of roots: insights from extant lycophytes. *J. Plant Res.* 133, 291–296. doi: 10.1007/s10265-020-01167-2

Fujinami, R., Yamada, T., Nakajima, A., Takagi, S., Idogawa, A., Kawakami, E., et al. (2017). Root apical meristem diversity in extant lycophytes and implications for root origins. *New Phytol.* 215, 1210–1220. doi: 10.1111/nph.14630

Gaillochet, C., and Lohmann, J. U. (2015). The never-ending story: from pluripotency to plant developmental plasticity. *Development* 142, 2237–2249. doi: 10.1242/dev.117614

Ge, Y., Liu, J., Zeng, M., He, J., Qin, P., Huang, H., et al. (2016). Identification of WOX family genes in *Selaginella kraussiana* for studies on stem cells and regeneration in lycophytes. *Front. Plant Sci.* 7:93. doi: 10.3389/fpls.2016.00093

Goh, T., Joi, S., Mimura, T., and Fukaki, H. (2012a). The establishment of asymmetry in *Arabidopsis* lateral root founder cells is regulated by LBD16/ASL18 and related LBD/ASL proteins. *Development* 139, 883–893. doi: 10.1242/dev.071928

Goh, T., Kasahara, H., Mimura, T., Kamiya, Y., and Fukaki, H. (2012b). Multiple AUX/IAA-ARF modules regulate lateral root formation: the role of *Arabidopsis* SHY2/IAA3-mediated auxin signalling. *Philos. Trans. R. Soc. Lond. Ser. B Biol. Sci.* 367, 1461–1468. doi: 10.1098/rstb.2011.0232

Goh, T., Toyokura, K., Wells, D. M., Swarup, K., Yamamoto, M., Mimura, T., et al. (2016). Quiescent center initiation in the *Arabidopsis* lateral root primordia is dependent on the *SCARECROW* transcription factor. *Development* 143, 3363–3371. doi: 10.1242/dev.135319

Gray, W. M., Kepinski, S., Rouse, D., Leyser, O., and Estelle, M. (2001). Auxin regulates SCF^{TIR1}-dependent degradation of AUX/IAA proteins. *Nature* 414, 271–276. doi: 10.1038/35104500

Gunning, B. E. S., Hughes, J. E., and Hardham, A. R. (1978). Formative and proliferative cell divisions, cell differentiation, and developmental changes in the meristem of *Azolla* roots. *Planta* 143, 121–144. doi: 10.1007/BF00387786

Hakoshima, T. (2018). Structural basis of the specific interactions of GRAS family proteins. *FEBS Lett.* 592, 489–501. doi: 10.1002/1873-3468.12987

Hao, S., Xue, J., Guo, D., and Wang, D. (2010). Earliest rooting system and root: shoot ratio from a new *Zosterophyllum* plant. *New Phytol.* 185, 217–225. doi: 10.1111/j.1469-8137.2009.03056.x

Helariutta, Y., Fukaki, H., Wysocka-Diller, J., Nakajima, K., Jung, J., Sena, G., et al. (2000). The *SHORT-ROOT* gene controls radial patterning of the *Arabidopsis* root through radial signaling. *Cell* 101, 555–567. doi: 10.1016/S0092-8674(00)80865-X

Hentrich, M., Bottcher, C., Duchting, P., Cheng, Y., Zhao, Y., Berkowitz, O., et al. (2013). The jasmonic acid signaling pathway is linked to auxin homeostasis through the modulation of *YUCCA8* and *YUCCA9* gene expression. *Plant J.* 74, 626–637. doi: 10.1111/tpj.12152

Hetherington, A. J. (2019). "Evolution of plant rooting systems," in *eLS*. Chichester: John Wiley & Sons, Ltd.

Hetherington, A. J., Berry, C. M., and Dolan, L. (2020). Multiple origins of dichotomous and lateral branching during root evolution. *Nat. Plants* 6, 454–459. doi: 10.1038/s41477-020-0646-y

Hetherington, A. J., and Dolan, L. (2017). The evolution of lycopsid rooting structures: conservatism and disparity. *New Phytol.* 215, 538–544. doi: 10.1111/nph.14324

Hetherington, A. J., and Dolan, L. (2018a). Bilaterally symmetric axes with rhizoids composed the rooting structure of the common ancestor of vascular plants. *Philos. Trans. R. Soc. Lond. Ser. B Biol. Sci.* 373:20170042. doi: 10.1098/rstb.2017.0042

Hetherington, A. J., and Dolan, L. (2018b). Stepwise and independent origins of roots among land plants. *Nature* 561, 235–238. doi: 10.1038/s41586-018-0445-z

Hetherington, A. J., and Dolan, L. (2019). Rhynie chert fossils demonstrate the independent origin and gradual evolution of lycophyte roots. *Curr. Opin. Plant Biol.* 47, 119–126. doi: 10.1016/j.pbi.2018.12.001

Hetherington, A. J., Dubrovsky, J. G., and Dolan, L. (2016). Unique cellular organization in the oldest root meristem. *Curr. Biol.* 26, 1629–1633. doi: 10.1016/j.cub.2016.04.072

Hirano, Y., Nakagawa, M., Suyama, T., Murase, K., Shirakawa, M., Takayama, S., et al. (2017). Structure of the SHR-SCR heterodimer bound to the BIRD/IDD transcriptional factor JKD. *Nat. Plants* 3:17010. doi: 10.1038/nplants.2017.10

Hou, G., and Blancaflor, E. B. (2018). "Fern root development," in *Annual Plant Reviews Online*. ed. J. A. Roberts (Hoboken, NJ: Blackwell Publishing Ltd.), 192–208.

Hou, G., and Hill, J. P. (2004). Developmental anatomy of the fifth shoot-borne root in young sporophytes of *Ceratopteris richardii*. *Planta* 219, 212–220. doi: 10.1007/s00425-004-1225-6

Hou, G., Hill, J. P., and Blancaflor, E. B. (2004). Developmental anatomy and auxin response of lateral root formation in *Ceratopteris richardii*. *J. Exp. Bot.* 55, 685–693. doi: 10.1093/jxb/erh068

Huang, L., and Schiefelbein, J. (2015). Conserved gene expression programs in developing roots from diverse plants. *Plant Cell* 27, 2119–2132. doi: 10.1105/tpc.15.00328

Imaichi, R., and Kato, M. (1989). Developmental anatomy of the shoot apical cell, rhizophore and root of *Selaginella Uncinata*. *Bot. Mag.* 102, 369–380. doi: 10.1007/BF02488120

Israeli, A., Reed, J. W., and Ori, N. (2020). Genetic dissection of the auxin response network. *Nat. Plants* 6, 1082–1090. doi: 10.1038/s41477-020-0739-7

Jernstedt, J. A., Cutter, E. G., Gifford, E. M., and Lu, P. (1992). Angle meristem origin and development in *Selaginella martensii*. *Ann. Bot.* 69, 351–363. doi: 10.1093/oxfordjournals.aob.a088352

Jha, T. b., Mukherjee, S., Basak, A., and Adhikari, J. (2013). In vitro morphogenesis in *Selaginella microphylla* (Kunth.) spring. *Plant Biotechnol. Rep.* 7, 239–245. doi: 10.1007/s11816-012-0255-y

Jones, V. A. S., and Dolan, L. (2012). The evolution of root hairs and rhizoids. *Ann. Bot.* 110, 205–212. doi: 10.1093/aob/mcs136

Kaneko, S., Cook, S. D., Aoi, Y., Watanabe, A., Hayashi, K.-I., and Kasahara, H. (2020). An evolutionarily primitive and distinct auxin metabolism in the lycophyte *Selaginella moellendorffii*. *Plant Cell Physiol.* 61, 1724–1732. doi: 10.1093/pcp/pcaa098

Kenrick, P. (2013). "The origin of roots," in *Plant Roots: The Hidden Half, Fourth Edition*. eds. A. Eshel and T. Beeckman (Boca Raton, FL: CRC Press), 1–13.

Kim, S., Soltis, P. S., Wall, K., and Soltis, D. E. (2005). Phylogeny and domain evolution in the *APETALA2*-like gene family. *Mol. Biol. Evol.* 23, 107–120. doi: 10.1093/molbev/msj014

Kong, X., Lu, S., Tian, H., and Ding, Z. (2015). WOX5 is shining in the root stem cell niche. *Trends Plant Sci.* 20, 601–603. doi: 10.1016/j.tplants.2015.08.009

Korasick, D. A., Westfall, C. S., Lee, S. G., Nanao, M. H., Dumas, R., Hagen, G., et al. (2014). Molecular basis for AUXIN RESPONSE FACTOR protein interaction and the control of auxin response repression. *Proc. Natl. Acad. Sci. U. S. A.* 111, 5427–5432. doi: 10.1073/pnas.1400074111

Leyser, O. (2018). Auxin signaling. *Plant Physiol.* 176, 465–479. doi: 10.1104/pp.17.00765

Ljung, K., Hull, A. K., Celenza, J., Yamada, M., Estelle, M., Normanly, J., et al. (2005). Sites and regulation of auxin biosynthesis in Arabidopsis roots. *Plant Cell* 17, 1090–1104. doi: 10.1105/tpc.104.029272

Long, Y., Goedhart, J., Schneijderberg, M., Terpstra, I., Shimotohno, A., Bouchet, B. P., et al. (2015). SCARECROW-LIKE23 and SCARECROW jointly specify endodermal cell fate but distinctly control SHORT-ROOT movement. *Plant J.* 84, 773–784. doi: 10.1111/tpj.13038

Lu, P., and Jernstedt, J. A. (1996). Rhizophore and root development in Selaginella martensii: meristem transitions and identity. *Int. J. Plant Sci.* 157, 180–194. doi: 10.1086/297337

Lucas, M., Swarup, R., Paponov, I. A., Swarup, K., Casimiro, I., Lake, D., et al. (2011). Short-root regulates primary, lateral, and adventitious root development in Arabidopsis. *Plant Physiol.* 155, 384–398. doi: 10.1104/pp.110.165126

Lv, B., Yu, Q., Liu, J., Wen, X., Yan, Z., Hu, K., et al. (2020). Non-canonical AUX/IAA protein IAA33 competes with canonical AUX/IAA repressor IAA5 to negatively regulate auxin signaling. *EMBO J.* 39:e101515. doi: 10.15252/embj.2019101515

Malamy, J. E., and Benfey, P. N. (1997). Organization and cell differentiation in lateral roots of *Arabidopsis thaliana*. *Development* 124, 33–44. doi: 10.1242/dev.124.1.33

Marhavy, P., Vanstraelen, M., De Rybel, B., Zhaojun, D., Bennett, M. J., Beeckman, T., et al. (2013). Auxin reflux between the endodermis and pericycle promotes lateral root initiation. *EMBO J.* 32, 149–158. doi: 10.1038/emboj.2012.303

Mashiguchi, K., Tanaka, K., Sakai, T., Sugawara, S., Kawaide, H., Natsume, M., et al. (2011). The main auxin biosynthesis pathway in *Arabidopsis*. *Proc. Natl. Acad. Sci. U. S. A.* 108, 18512–18517. doi: 10.1073/pnas.1108434108

Matsunaga, K. K. S., and Tomescu, A. M. F. (2016). Root evolution at the base of the lycophyte clade: insights from an early Devonian lycophyte. *Ann. Bot.* 117, 585–598. doi: 10.1093/aob/mcw006

Mello, A., Efroni, I., Rahni, R., and Birnbaum, K. D. (2019). The *Selaginella* rhizophore has a unique transcriptional identity compared with root and shoot meristems. *New Phytol.* 222, 882–894. doi: 10.1111/nph.15630

Motte, H., and Beeckman, T. (2019). The evolution of root branching: increasing the level of plasticity. *J. Exp. Bot.* 70, 785–793. doi: 10.1093/jxb/ery409

Motte, H., Parizot, B., Fang, T., and Beeckman, T. (2020). The evolutionary trajectory of root stem cells. *Curr. Opin. Plant Biol.* 53, 23–30. doi: 10.1016/j.pbi.2019.09.005

Motte, H., Vanneste, S., and Beeckman, T. (2019). Molecular and environmental regulation of root development. *Annu. Rev. Plant Biol.* 70, 465–488. doi: 10.1146/annurev-arplant-050718-100423

Mutte, S. K. (2020). Evolutionary analysis of a billion years of auxin biology. dissertation/doctoral thesis. [Wageningen (Netherlands)]: Wageningen University.

Mutte, S. K., Kato, H., Rothfels, C., Melkonian, M., Wong, G. K., and Weijers, D. (2018). Origin and evolution of the nuclear auxin response system. *elife* 7:e33399. doi: 10.7554/eLife.33399

Nageli, C., and Leitgeb, H. (1868). Entstehung und Wachstum der Wurzeln. *Beitr. Wiss. Bot.* 4, 124–158.

Nakajima, K., Sena, G., Nawy, T., and Benfey, P. N. (2001). Intercellular movement of the putative transcription factor SHR in root patterning. *Nature* 413, 307–311. doi: 10.1038/35095061

Nardmann, J., Reisewitz, P., and Werr, W. (2009). Discrete shoot and root stem cell-promoting *WUS/WOX5* functions are an evolutionary innovation of angiosperms. *Mol. Biol. Evol.* 26, 1745–1755. doi: 10.1093/molbev/msp084

Nardmann, J., and Werr, W. (2012). The invention of WUS-like stem cell-promoting functions in plants predates leptosporangiate ferns. *Plant Mol. Biol.* 78, 123–134. doi: 10.1007/s11103-011-9851-4

Olatunji, D., Geelen, D., and Verstraeten, I. (2017). Control of endogenous auxin levels in plant root development. *Int. J. Mol. Sci.* 18:2587. doi: 10.3390/ijms18122587

One Thousand Plant Transcriptomes Initiative, Leebens-Mack, J. H., Barker, M. S., Carpenter, E. J., Deyholos, M. K., Gitzendanner, M. A., et al. (2019). One thousand plant transcriptomes and the phylogenomics of green plants. *Nature* 574, 679–685. doi: 10.1038/s41586-019-1693-2

Otreba, P., and Gola, E. M. (2011). Specific intercalary growth of rhizophores and roots in *Selaginella kraussiana* (Selaginellaceae) is related to unique dichotomous branching. *Flora* 206, 227–232. doi: 10.1016/j.flora.2010.07.001

Palovaara, J., Zeeuw, T. D., and Weijers, D. (2016). Tissue and organ initiation in the plant embryo: a first time for everything. *Annu. Rev. Cell Dev. Biol.* 32, 47–75. doi: 10.1146/annurev-cellbio-111315-124929

Panchy, N., Lehti-Shiu, M., and Shiu, S. H. (2016). Evolution of gene duplication in plants. *Plant Physiol.* 171, 2294–2316. doi: 10.1104/pp.16.00523

Perrot-Rechenmann, C. (2014). "Auxin signaling in plants," in *Molecular Biology*. ed. S. Howell (Berlin, Germany: Springer), 245–268.

Piekarska-Stachowiak, A., and Nakielski, J. (2013). The simulation model of growth and cell divisions for the root apex with an apical cell in application to *Azolla pinnata*. *Planta* 238, 1051–1064. doi: 10.1007/s00425-013-1950-9

PPG I (2016). A community-derived classification for extant lycophytes and ferns. *J. Syst. Evol.* 54, 563–603. doi: 10.1111/jse.12229

Promchuea, S., Zhu, Y., Chen, Z., Zhang, J., and Gong, Z. (2017). ARF2 coordinates with PLETHORAs and PINs to orchestrate ABA-mediated root meristem activity in Arabidopsis. *J. Integr. Plant Biol.* 59, 30–43. doi: 10.1111/jipb.12506

Proost, S., and Mutwil, M. (2018). CoNekT: an open-source framework for comparative genomic and transcriptomic network analyses. *Nucleic Acids Res.* 46, W133–W140. doi: 10.1093/nar/gky336

Raven, J. A., and Edwards, D. (2001). Roots: evolutionary origins and biogeochemical significance. *J. Exp. Bot.* 52, 381–401. doi: 10.1093/jexbot/52.suppl_1.381

Rothwell, G. W., and Tomescu, A. M. F. (2018). "Structural fingerprints of development at the intersection of evo-devo and the fossil record," in *Evolutionary Developmental Biology*. eds. L. Nuno de la Rosa and G. Müller (Berlin, Germany: Springer), 1–30

Sabatini, S., Beis, D., Wolkenfelt, H., Murfett, J., Guilfoyle, T., Malamy, J., et al. (1999). An auxin-dependent distal organizer of pattern and polarity in the *Arabidopsis* root. *Cell* 99, 463–472. doi: 10.1016/S0092-8674(00)81535-4

Sabatini, S., Heidstra, R., Wildwater, M., and Scheres, B. (2003). SCARECROW is involved in positioning the stem cell niche in the *Arabidopsis* root meristem. *Genes Dev.* 17, 354–358. doi: 10.1101/gad.252503

Sanders, H. L., and Langdale, J. A. (2013). Conserved transport mechanisms but distinct auxin responses govern shoot patterning in *Selaginella kraussiana*. *New Phytol.* 198, 419–428. doi: 10.1111/nph.12183

Sarkar, A. K., Luijten, M., Miyashima, S., Lenhard, M., Hashimoto, T., Nakajima, K., et al. (2007). Conserved factors regulate signalling in *Arabidopsis thaliana* shoot and root stem cell organizers. *Nature* 446, 811–814. doi: 10.1038/nature05703

Shimotohno, A., Heidstra, R., Blilou, I., and Scheres, B. (2018). Root stem cell niche organizer specification by molecular convergence of PLETHORA and SCARECROW transcription factor modules. *Genes Dev.* 32, 1085–1100. doi: 10.1101/gad.314096.118

Shimotohno, A., and Scheres, B. (2019). Topology of regulatory networks that guide plant meristem activity: similarities and differences. *Curr. Opin. Plant Biol.* 51, 74–80. doi: 10.1016/j.pbi.2019.04.006

Song, X. M., Liu, T. K., Duan, W. K., Ma, Q. H., Ren, J., Wang, Z., et al. (2014). Genome-wide analysis of the GRAS gene family in Chinese cabbage (*Brassica rapa* ssp. *pekinensis*). *Genomics* 103, 135–146. doi: 10.1016/j.ygeno.2013.12.004

Stepanova, A. N., Robertson-Hoyt, J., Yun, J., Benavente, L. M., Xie, D. Y., Dolezal, K., et al. (2008). *TAA1*-mediated auxin biosynthesis is essential for hormone crosstalk and plant development. *Cell* 133, 177–191. doi: 10.1016/j.cell.2008.01.047

Tan, X., Calderon-Villalobos, L. I. A., Sharon, M., Zheng, C., Robinson, C. V., Estelle, M., et al. (2007). Mechanism of auxin perception by the TIR1 ubiquitin ligase. *Nature* 446, 640–645. doi: 10.1038/nature05731

Tang, L. P., Zhou, C., Wang, S. S., Yuan, J., Zhang, X. S., and Su, Y. H. (2017). FUSCA3 interacting with LEAFY COTYLEDON2 controls lateral root formation through regulating *YUCCA4* gene expression in *Arabidopsis thaliana*. *New Phytol.* 213, 1740–1754. doi: 10.1111/nph.14313

Torres-Martinez, H. H., Rodriguez-Alonso, G., Shishkova, S., and Dubrovsky, J. G. (2019). Lateral root primordium morphogenesis in angiosperms. *Front. Plant Sci.* 10:206. doi: 10.3389/fpls.2019.00206

Trewavas, A. (1986). "Resource allocation under poor growth conditions. A major role for growth substances in developmental plasticity." in *Symposia of the Society for Experimental Biology*. eds. D. H. Jennings and A. Trewavas; January 01, 1986 (Cambridge: Company of Biologists Ltd.).

Trinh, C. D., Laplaze, L., and Guyomarc'h, S. (2018). "Lateral root formation: building a meristem de novo," in *Annual Plant Reviews Online*. ed. J. A. Roberts (Hoboken, NJ: John Wiley & Sons, Ltd.), 847–890.

Troll, W. (1937). *Vergleichende Morphologie der höheren Pflanzen*. Berlin: Gebrüder Borntraeger.

VanBuren, R., Wai, C. M., Ou, S., Pardo, J., Bryant, D., Jiang, N., et al. (2018). Extreme haplotype variation in the desiccation-tolerant clubmoss *Selaginella lepidophylla*. *Nat. Commun.* 9:13. doi: 10.1038/s41467-017-02546-5

van den Berg, C., Willemsen, V., Hendriks, G., Weisbeek, P., and Scheres, B. (1997). Short-range control of cell differentiation in the *Arabidopsis* root meristem. *Nature* 390, 287–289. doi: 10.1038/36856

Vieten, A., Vanneste, S., Wisniewska, J., Benkova, E., Benjamins, R., Beeckman, T., et al. (2005). Functional redundancy of PIN proteins is accompanied by auxin-dependent cross-regulation of PIN expression. *Development* 132, 4521–4531. doi: 10.1242/dev.02027

Wang, Y., Shi, S., Zhou, Y., Zhou, Y., Yang, J., and Tang, X. (2016). Genome-wide identification and characterization of GRAS transcription factors in sacred lotus (*Nelumbo nucifera*). *PeerJ* 4:e2388. doi: 10.7717/peerj.2388

Webster, T. R. (1969). An investigation of angle-meristem development in excised stem segments of *Selaginella martensii*. *Can. J. Bot.* 47, 717–722. doi: 10.1139/b69-102

Went, F. W. (1929). On a substance, causing root formation. *Proc. K. Ned. Akad. Wet. C* 32, 35–39.

Williams, S. (1937). Correlation phenomena and hormones in *Selaginella*. *Nature* 139:966. doi: 10.1038/139966a0

Winter, D., Vinegar, B., Nahal, H., Ammar, R., Wilson, G. V., and Provart, N. J. (2007). An "electronic fluorescent pictograph" browser for exploring and analyzing large-scale biological data sets. *PLoS One* 2:e718. doi: 10.1371/journal.pone.0000718

Wochok, Z. S., and Sussex, I. M. (1974). Morphogenesis in *Selaginella*: II. Auxin transport in the root (rhizophore). *Plant Physiol.* 53, 738–741. doi: 10.1104/pp.53.5.738

Wochok, Z. S., and Sussex, I. M. (1975). Morphogenesis in *Selaginella*: III. Meristem determination and cell differentiation. *Dev. Biol.* 47, 376–383. doi: 10.1016/0012-1606(75)90291-2

Wochok, Z. S., and Sussex, I. M. (1976). Redetermination of cultured root tips to leafy shoots in *Selaginella willdenovii*. *Plant Sci. Lett.* 6, 185–192. doi: 10.1016/0304-4211(76)90071-7

Wong, G. K.-S., Soltis, D. E., Leebens-Mack, J., Wickett, N. J., Barker, M. S., Van de Peer, Y., et al. (2020). Sequencing and analyzing the transcriptomes of a thousand species across the tree of life for green plants. *Annu. Rev. Plant Biol.* 71, 741–765. doi: 10.1146/annurev-arplant-042916-041040

Wu, C. C., Li, F. W., and Kramer, E. M. (2019). Large-scale phylogenomic analysis suggests three ancient superclades of the WUSCHEL-RELATED HOMEOBOX transcription factor family in plants. *PLoS One* 14:e0223521. doi: 10.1371/journal.pone.0223521

Xu, Z., Xin, T., Bartels, D., Li, Y., Gu, W., Yao, H., et al. (2018). Genome analysis of the ancient tracheophyte *Selaginella tamariscina* reveals evolutionary features relevant to the acquisition of desiccation tolerance. *Mol. Plant* 11, 983–994. doi: 10.1016/j.molp.2018.05.003

Xuan, W., Audenaert, D., Parizot, B., Möller, B. K., Njo, M. F., De Rybel, B., et al. (2015). Root cap-derived auxin pre-patterns the longitudinal axis of the *Arabidopsis* root. *Curr. Biol.* 25, 1381–1388. doi: 10.1016/j.cub.2015.03.046

Yi, S. Y., and Kato, M. (2001). Basal meristem and root development in *Isoetes asiatica* and *Isoetes japonica*. *Int. J. Plant Sci.* 162, 1225–1235. doi: 10.1086/322942

Zhang, B., Liu, J., Yang, Z. E., Chen, E. Y., Zhang, C. J., Zhang, X. Y., et al. (2018). Genome-wide analysis of GRAS transcription factor gene family in *Gossypium hirsutum* L. *BMC Genomics* 19:348. doi: 10.1186/s12864-018-4722-x

Zhang, Y., Rodriguez, L., Li, L., Zhang, X., and Friml, J. (2020). Functional innovations of PIN auxin transporters mark crucial evolutionary transitions during rise of flowering plants. *Sci. Adv.* 6:eabc8895. doi: 10.1126/sciadv.abc8895

Zhang, Y., Xiao, G., Wang, X., Zhang, X., and Friml, J. (2019). Evolution of fast root gravitropism in seed plants. *Nat. Commun.* 10:3480. doi: 10.1038/s41467-019-11471-8

Zhou, X., Guo, Y., Zhao, P., and Sun, M.-X. (2018). Comparative analysis of WUSCHEL-related homeobox genes revealed their parent-of-origin and cell type-specific expression pattern during early embryogenesis in tobacco. *Front. Plant Sci.* 9:311. doi: 10.3389/fpls.2018.00311

Conflict of Interest: The authors declare that the research was conducted in the absence of any commercial or financial relationships that could be construed as a potential conflict of interest.

Publisher's Note: All claims expressed in this article are solely those of the authors and do not necessarily represent those of their affiliated organizations, or those of the publisher, the editors and the reviewers. Any product that may be evaluated in this article, or claim that may be made by its manufacturer, is not guaranteed or endorsed by the publisher.

frontiers in Plant Science

MINI REVIEW
published: 30 September 2021
doi: 10.3389/fpls.2021.745861

Root Patterning: Tuning SHORT ROOT Function Creates Diversity in Form

*Marcela Hernández-Coronado and Carlos Ortiz-Ramírez**

UGA Laboratorio Nacional de Genómica para la Biodiversidad, CINVESTAV Irapuato, Guanajuato, Mexico

Roots have a fundamental role in plant growth and adaptation to different environments. Diversity in root morphology and architecture enables plants to acquire water and nutrients in contrasting substrate conditions, resist biotic and abiotic stress, and develop symbiotic associations. At its most fundamental level, morphology is determined by discrete changes in tissue patterning. Differences in the number and arrangement of the cell layers in the root can change tissue structure, as well as root length and girth, affecting important productivity traits. Therefore, understanding the molecular mechanisms controlling variation in developmental patterning is an important goal in biology. The ground tissue (GT) system is an ideal model to study the genetic basis of morphological diversity because it displays great interspecific variability in cell layer number. In addition, the genetic circuit controlling GT patterning in *Arabidopsis thaliana* has been well described, although little is known about species with more complex root anatomies. In this review, we will describe the *Arabidopsis* model for root radial patterning and present recent progress in elucidating the genetic circuitry controlling GT patterning in monocots and the legume *Medicago truncatula (Mt)*, species that develop roots with more complex anatomies and multilayered cortex.

Keywords: root patterning, arabidopsis, short root, monocots, morphological diversity, root development, nodulation

OPEN ACCESS

Edited by:
Raffaele Dello Ioio,
Sapienza University of Rome, Italy

Reviewed by:
Hongchang Cui,
Florida State University, United States
Riccardo Di Mambro,
University of Pisa, Italy

***Correspondence:**
Carlos Ortiz-Ramírez
carlos.ortiz@cinvestav.mx

Specialty section:
This article was submitted to Plant Development and EvoDevo, a section of the journal Frontiers in Plant Science

Received: *22 July 2021*
Accepted: *08 September 2021*
Published: *30 September 2021*

Citation:
Hernández-Coronado M and Ortiz-Ramírez C (2021) Root Patterning: Tuning SHORT ROOT Function Creates Diversity in Form. Front. Plant Sci. 12:745861. doi: 10.3389/fpls.2021.745861

INTRODUCTION

Root morphological diversity can be studied at different scales: macroscopically (i.e., at the level of root architecture, length, branching angle, and number of secondary roots) and microscopically, as changes in tissue pattering, like the number and arrangement of cell layers. Although root system architecture has been studied extensively, the relationship between patterning and root phenotypic diversity and adaptation has seldom been explored. Recently, it was proposed that root morphological trait variation across species and across biomes is most strongly influenced by root diameter, a character that depends on tissue layer number and organization (Ma et al., 2018).

Roots consist of three fundamental tissue types arranged radially as concentric layers: the epidermis on the outside; the ground tissue at the middle, consisting of one layer of endodermis and one to many layers of cortex; and a core of vascular elements plus

pericycle called the stele (Dolan et al., 1993). Differences in the number and/or arrangement of these cell layers are not only relevant to explain diversity in root form, but they also give rise to important functional traits that have an impact on plant fitness and productivity (Lux et al., 2004). For example, plants living in waterlogged soils, such as rice, develop air filled cells from the cortex called aerenchyma (Yamauchi et al., 2018). Desert plants can accumulate water in their roots thanks to the proliferation of storage parenchyma from cortical cells, and a similar process allows plants to save starch to overwinter in difficult weather (Fahn, 1990; Lux and Inanaga, 1997). Halophyte plants growing in soils with toxic salt levels develop two suberized endodermis layers instead of one, which helps to isolate the root vasculature from the apoplast that is in direct contact with the soil (Inan et al., 2004).

At the basis of these developmental adaptations is the activity of genetic circuits that coordinate cell division activity and cell identity at the root apical meristem (RAM). Here, a set of stem cells, called initials, divide asymmetrically to produce daughter cells that give rise to epidermal, ground tissue, and vascular lineages (Esau, 1977; Benfey et al., 1993). While anticlinal divisions of initial cells will contribute to root length, periclinal divisions generate extra cell layers along the radial axis increasing girth. For example, in *Arabidopsis* a periclinal division of the cortex/endodermal initial gives rise to a single endodermis and a single cortex cell layer (Scheres et al., 1996). However, in species with roots that have multiple cortical layers the cortex/endodermal initial may undergo several divisions early in development producing thicker roots (Heimsch and Seago, 2008). There is limited information on the regulation of genetic circuits that produce different morphologies between closely related plant species, and even between roots from the same plant. Therefore, comparative intra- and interspecific developmental studies between roots with different morphologies are important for pinpointing the genetic basis of variation.

In this context, the ground tissue system is an ideal model to make such comparative studies since (1) it shows great variation in patterning, not only between closely related species, but also between root types from the same plant. e.g., rice roots can have between two to eleven ground tissue layers, depending on the root type (Clark and Harris, 1981). Maize develops between 8 and 15 layers (Bennetzen and Hake, 2009). (2) In many species, the ground tissue forms the bulk of the root; therefore, variations in the number of cortical cell layers have a significant effect on root form. (3) The genetic circuit controlling GT patterning in *Arabidopsis* is well described and serves as a model to search for modifications in the activity of homologous genes in species with more elaborated anatomies.

In this review, we will first describe the genetic circuit that controls development of the GT in *Arabidopsis*. Then, we will discuss the latest research in species with different anatomies and multilayered cortex. Finally, we will contrast the classical and new emergent models of root radial patterning and how they can be applied to explain morphological diversity.

DIFFERENCES IN GT DEVELOPMENT

Root tissue systems originate in the RAM, a region located near the tip of the root where cells remain undifferentiated. Here, a set of stem cell populations called initial cells undergo asymmetric cell division to produce different lineages. In *Arabidopsis*, there is four types of initials or stem cells: a population giving rise to vascular tissues, a population generating columella cells, a common initial producing the ground tissue (endodermis and cortex), and a common initial that originates root cap and epidermis (Pauluzzi et al., 2012). In the case of the ground tissue, the cortex/endodermis initials (CEIs) regenerate themselves by an anticlinal cell division, giving rise to the cortex endodermis initial daughter cell (CEID; **Figures 1A,B**). The CEID then undergoes one periclinal division to form two tissue layers: endodermis and cortex (Benfey et al., 1993). Thus, in primary development the *Arabidopsis* root has a single endodermal and a single cortex layer. Later in development an extra layer of cortex, called the middle cortex (MC), originates from the endodermis by an asymmetric periclinal division (Baum et al., 2002; Paquette and Benfey, 2005).

Important differences exist between root development in *Arabidopsis* and monocots, like rice and maize. In monocots, the epidermis and the ground tissue originate from the same initial cell. Therefore, a first asymmetrical division generates the CEI and the epidermis. Subsequently, the CEI will divide further giving rise to endodermis and cortex (Di Ruocco et al., 2018b; **Figure 1B**, left). Another important difference in the ability of most monocot roots to produce a multilayered cortex. It has been proposed that formation of several cortex layers is achieved by sustained periclinal cell divisions either of a single CEI or by divisions of multiple independent CEIs (Pauluzzi et al., 2012). In rice, there is a large variation in the number cortex cell layers depending on the root type. Small lateral roots have no cortex, while large laterals have 3; radical roots have 5, and crown roots have 10 (Clark and Harris, 1981). It is likely that precise modulation of the genetic circuit that controls CEI periclinal divisions underlies cortex layer number variation in rice, and this may be representative of a mechanism giving rise to interspecific ground tissue variation. Importantly, root diameter among rice root types is closely correlated with cortex cell layer number (Henry et al., 2015). Therefore, modulation of the CEI division program affects root size and function. Although this diversity in cortex development is most evident in monocots, it is not unique to this group. Some closely related dicot species also present differences in cortex layer number. For example, *Cardamine hirsuta,* a close *Arabidopsis* relative, has two cortex layers instead of one (Di Ruocco et al., 2018a). The wild tomato species *Solanum pennellii* has two cortex layers, while the domesticated *Solanum lycopersicum* has three, suggesting that differences in the genetic network controlling CEI divisions can evolve rapidly (Ron et al., 2013).

There is increasing evidence that the SHORT ROOT (*SHR*)/ SCARECROW (*SCR*) genetic pathway, initially described in *Arabidopsis*, also controls GT formation across species and that modifications in the activity of this pathway originate a multilayered cortex.

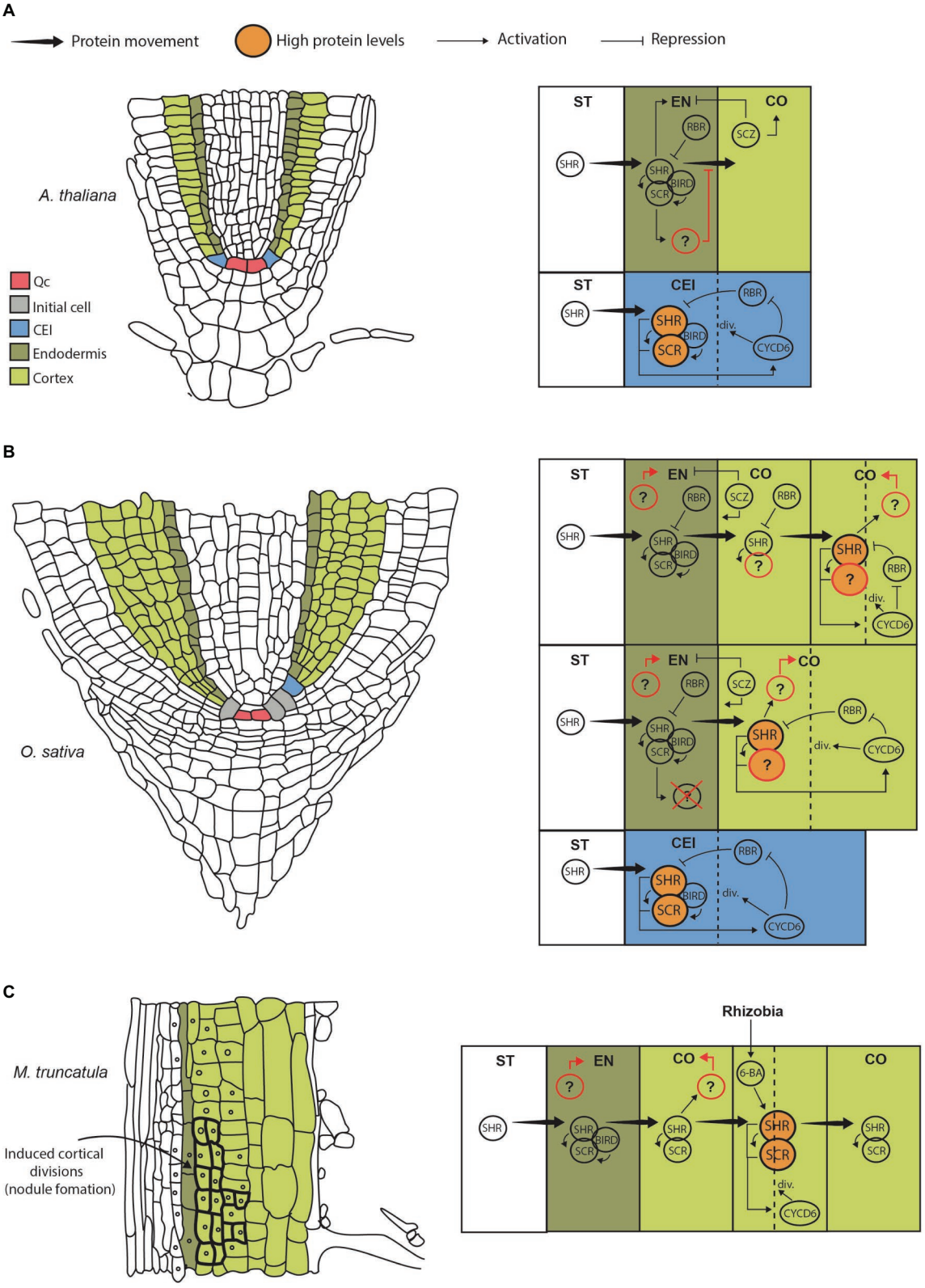

FIGURE 1 | Genetic models for GT formation and cortex expansion in different species. **(A)** Cartoon showing a longitudinal section from an Arabidopsis thaliana root highlighting initial and GT cells (left). Diagram representing the CEI, endodermis, cortex and stele, where the main genetic pathways contributing to GT formation are depicted (right). Briefly, SHR protein moves from the stele into the CEI where it induces SCR expression. SHR and SCR form a complex that moves

(*continued*)

FIGURE 1 | into the nucleus and activates CYCD6;1, which in turns prevents the negative regulator RBR from interacting with the SHR/SCR complex. This results in high levels of SHR (big circles), which trigger asymmetric cell division giving rise to cortex and endodermis. Cell division resets the circuit from its on state. Presumably, SHR/SCR complex levels are maintained low by RBR preventing further divisions. SCZ helps in establishing tissue boundaries by inducing cortical identity and repressing endodermal identity. Importantly, SHR protein movement is limited to the endodermis either directly by biding to SCR and BIRD proteins, or indirectly by a SCR-induced factor that has been hypothesized to limit its movement (Wu et al., 2014; question mark). **(B)** Cartoon of a longitudinal sectional from rice root (left). Diagram representing the putative pathways contributing to GT formation and multilayered cortex in monocots (right). Note that SHR movement is not restricted to the endodermis; hence, the factor limiting its movement in Arabidopsis is either not present or has modified activity. We propose that SHR moves into the cortex where it can accumulate at high levels (big circles) activating and flipping the SHR/SCR/CYCLIND6;1/RBR circuit to its "on" state. This movement and activation are maintained until several cortical layers are produced. This model also assumes that SHR does not induce endodermal differentiation. Therefore, the factors that specify endodermal and cortical cell fate in monocots are unknown (question marks). It is also unclear if SHR interacts with SCR in the cortex as SCR protein localization in rice and other monocots is unknown. **(C)** Cartoon of a longitudinal sectional from Medicago root differentiation zone (left). Diagram representing the putative pathway contributing to cortex formative divisions giving rise to the nodule primordium (right). This model assumes that SHR and SCR proteins are present and interact throughout the root cortex. This allows the expression of the SHR/SCR/CYCLIND6;1/RBR circuit in cortical cells; however, the circuit is kept in an "off" state in the absence of rhizobia (low SHR levels). When symbiont signals are perceived by individual cells, 6-BA triggers local SHR accumulation in those domains flipping the circuit to its "on" state and triggering divisions.

THE SHR/SCR PATHWAY CONTROLS GT FORMATIVE DIVISIONS

As mentioned before, the asymmetric division of the CEI is essential for GT formation. Genetically, this process is controlled by the activity of *SHR* and *SCR* transcription factors (TFs; Helariutta et al., 2000). These genes are members of the GRAS protein domain family, and together they activate the genetic pathway that determines radial patterning. Mechanistically, *SHR* functions as a mobile signal that regulates cell division and cell fate specification. *SHR* transcript is expressed in the stele; however, the protein moves intercellularly through plasmodesmata into the adjacent CEI, CEID, and endodermis layer where it induces the expression of the downstream target *SCR* (Nakajima et al., 2001). SHR and SCR then form a complex at the protein level that moves into the nucleus of the CEI inducing the expression of a D-type cyclin, *CYCLIND6;1* (*CYCD6;1*) in *Arabidopsis*. This triggers cell division allowing the differentiation of the clonally related cortex and endodermal cell layers (Sozzani et al., 2010; **Figure 1A**, right).

Importantly, this division of the CEI depends on a bistable circuit that functions as an on/off switch. Circuit stability is determined by *CYCD6;1* activity and the cell cycle regulator RETINOBLASTOMA-RELATED protein (*RBR*). Interaction of RBR with SCR reduces SHR/SCR complex formation, therefore decreasing SHR, SCR, and CYCD6;1 levels in a negative feedback loop that prevents cell division ("off" state; Cruz-Ramirez et al., 2012). At the same time, a positive feedback loop is encoded in this circuit because CYCD6;1 can negatively regulate RBR through phosphorylation (**Figure 1A**, right). Thus, increasing *CYCD6;1* activity shifts back the circuit to an "on" state. Simulations demonstrate that high levels of SHR influx into the CEI are needed to activate sufficient *CYCD6;1* and gain the potential for asymmetric cell division. Moreover, very high levels ensure flipping to the "on" state triggering division. Finally, the bistable switch is reset when the cell undergoes division and proteins are degraded (Cruz-Ramirez et al., 2012).

Because SHR levels determine the potential of GT initial cells to undergo asymmetric divisions, the movement and magnitude of SHR fluxes into adjacent tissues have to be tightly regulated during GT formation. A prediction that can be extrapolated from current models is that further movement into the adjacent cell layers or GT initials will cause further activation of *SCR* and *CYCD6;1* and thus cell division, increasing GT layer number. In *Arabidopsis,* it has been shown that SCR itself can regulate SHR movement by binding and sequestering SHR into the nucleus, which effectively limits the amount of protein that can move into the next layer (Heidstra et al., 2004; Cui et al., 2007). Therefore, SHR limits its own movement by inducing *SCR* expression forming another feedback loop. This has been demonstrated by the reduction of *SCR* expression *via* RNAi, which results in increased SHR mobility and production of more GT layers (Cui et al., 2007). In addition, the *SHR/SCR* pathway induces the expression of the *BIRD* zinc finger proteins JACKDAW (*JKD*), MAGPIE (*MGP*), BALDIBIS, and NUTCRACKER that together with SCR also reduce SHR mobility and contribute to maintain tissue boundaries (Welch et al., 2007; Long et al., 2017).

After CEI division, the daughter cells acquire either endodermis or cortex identity. *SHR* also has an essential role in this process since experiments in *Arabidopsis* show it is necessary for endodermis cell fate specification. *AtSHR* loss-of-function roots lack an endodermis and display a single GT layer with cortex identity. On the other hand, *SCR* mutants also display a single GT layer, but this has a mix of endodermal and cortex markers. Importantly, double mutants of *SCR* and its close homolog *SCARECROW-LIKE23* lack an endodermis similarly to SHR mutant, indicating that these TFs act together with *SHR* to specify cell identity. (Benfey et al., 1993; van den Berg et al., 1995; Long et al., 2015). Another transcription factor that is important for defining GT cell fate during formative divisions is SCHIZORIZA (*SCZ*), a member of the heat-shock TF family. SCZ is important for cortex fate specification, since loss-of-function mutants develop two ground tissue layers both with endodermis identity. Conversely, *SCZ* overexpression from the 35 s promoter results in ectopic cell divisions in epidermal and lateral root cap tissues in which high expression of the cortex marker Co2 is detected (ten Hove et al., 2010). Furthermore, *SCZ* has role in regulating correct cell fate separation and establishment of tissue boundaries across the root. Mutants show extra layers in ground, epidermal and lateral root cap tissues that express a mix of cell identity makers (Pernas et al., 2010).

MIDDLE CORTEX FORMATION

In addition to activating cell division and specifying cell identity, *SHR* has a role in post-embryonic development of cortical tissue. In *Arabidopsis* roots, an additional cortex layer, called the middle cortex (MC), develops approximately 10–14 days after germination. This layer does not originate from the CEI as described previously, but from an asynchronous division of the endodermis that generates one extra cell layer that rapidly acquires cortex identity (Paquette and Benfey, 2005). *SHR* and *PHABULOSA* trigger this formative division through the reactivation of *CYCD6;1* (Sozzani et al., 2010; Bertolotti et al., 2021). However, the timing of this division is important and is regulated by the hormone gibberellic acid (GA). High levels of GA inhibit MC formation early after germination in a *SHR*-dependent process (Paquette and Benfey, 2005; Cui and Benfey, 2009). Surprisingly, *SCR* acts antagonistically to *SHR* by repressing MC formation, as loss-of-function mutants initiate MC prematurely (Paquette and Benfey, 2005). Notably, the *SHR*, *SCR,* and *GA* pathways converge on the regulation of the transcription factor *SCARECROW LIKE 3*. This TF induces GA activity and itself is positively regulated by *SHR* and *SCR* forming a feedback loop that contributes to time MC formation (Heo et al., 2011; Koizumi et al., 2012; Gong et al., 2016).

SHR IN THE DEVELOPMENT OF MULTILAYERED CORTEX

In contrast to what has been reported in *Arabidopsis*, some functional aspects of *SHR* activity, such as mobility and fate specification, appear not to be conserved in other species. In recent years, compelling evidence has emerged for a role of *SHR* in the specification and control of cortex layer number. Most of this new evidence comes from the study of *SHR* homologs in monocots, which develop roots with a multilayered cortex (Rebouillat et al., 2008). Notably, it was found that two SHR homologues from rice (*Oryza sativa)* and one homolog from *Brachipodium distachyon* have increased intercellular movement compared to *Arabidopsis* SHR. When expressed heterologously in the stele of *Arabidopsis* roots, movement of the monocot SHR proteins was not limited to the adjacent endodermis but instead they moved 3 to 6 layers past the stele. All monocot SHR proteins were shown to strongly interact with *At*SCR, *At*JKD, and *At*MGP; hence, hypermobility could not be explained by a lack of interaction (and nuclear sequestration) between these transcription factors. The observed increase in SHR mobility was correlated with a similar increase in GT layer number. Therefore, SHR movement seems to be sufficient to activate the *SHR/SCR/CYCLIND6;1* circuit causing extra divisions and an enlarged GT (Wu et al., 2014; **Figure 1B**, right). Importantly, by performing a propidium iodide exclusion test and analyses of cell-type specific markers, Wu, et al. determined that the extra cell layers created by monocot SHR hypermobility had cortex identity. Hence, although monocot *SHR* homologs generate extra GT layers in *Arabidopsis*, just a single endodermis layer, the one in direct contact with the stele, was specified.

The fact that the experiments described before were performed in a heterologous system has both strengths and limitations. In this context, a recent study describing maize (*Zea mays*) endogenous *SHR* function provides valuable insight into root development. Both *ZmSHR* transcript and protein localization differ from what has been reported in *Arabidopsis*. The transcript was detected not in the stele but in the root endodermis. This was corroborated by tissue-specific RNA expression data (FACS-based tissue isolation), single-cell RNAseq, and translational reporter lines (Ortiz-Ramirez et al., 2021). Although it is unclear if this expression pattern affects protein localization, translational reporter lines showed *Zm*SHR protein is present in all cortical layers of the root (8–9 layers). This further confirms that SHR hypermobility is common in monocots. Moreover, generation of loss-of-function mutants in maize confirmed *Zm*SHR role in multilayered cortex development. Roots harboring CRISPR mutant alleles for two *Zm*SHR homologs lacked several cortex layers but maintained a functional endodermis (Ortiz-Ramirez et al., 2021). Importantly, authors demonstrated that this function was conserved in monocots by generating CRISPR mutants in *Setaria viridis*. Similar to maize, double mutants displayed a strong reduction in cortex layer number (Ortiz-Ramirez et al., 2021). Conversely, an independent study revealed that overexpression of *OsSHR2* in rice roots increases ground tissue layer number up to sixfold compared to wild type. Extra layers also had cortex identity (Henry et al., 2017).

In addition, there is evidence that *SHR* controls multilayer cortex formation in dicots as well. *Cardamine hirsuta (Ch)* is a close *Arabidopsis* relative that has been used as a model to study cortical expansion. Compared to *Arabidopsis, Cardamine* roots develop two cortex layers instead of one. *SHR* is also involved in cortex expansion in this species as heterologous expression of *ChSHR* in *Arabidopsis* produces roots with an additional cortex layer (Di Ruocco et al., 2018a). Therefore, a *SHR*-based mechanism to control cortex expansion seems to be conserved in many plant groups.

SHR ENABLES NODULATION BY TRIGGERING CORTICAL CELL DIVISIONS

Recently, *SHR* has been implicated in the development of root nodules, the structures that harbor the nitrogen fixing symbiont rhizobia. In *Medicago truncatula*, root nodule primordium is initiated upon rhizobia signals, which induce the dedifferentiation of cortical cells and its subsequent division (Timmers et al., 1999; **Figure 1C**, left). Both *SHR* and *SCR* were found to be necessary for rhizobia-induced cortex cell divisions. As shown for monocot homologs, *MtSHR* transcript and protein localization seem to be essential for cortex expansion. *SHR* expression in *Medicago* was found to be restricted to the stele, but the protein is present in the endodermis, cortex, and even the epidermis at low levels. Therefore, *Mt*SHR intercellular movement is also expanded

when compared to *Arabidopsis*. Notably, SCR protein was also observed in endodermis and cortex of *Medicago* roots (Dong et al., 2021).

Importantly, cortex-specific accumulation of SHR was found to be a key aspect of nodule formation. A decrease in nodule number was observed when *MtSHR* activity was specifically repressed in cortical cells using a *SHR* dominant repressor (*MtSHR1*-SRDX). In this line, inoculation with rhizobia did not trigger as many cell divisions as in wild type roots, which prevented formation of the nodule primordium. On the other hand, cortical cell-specific *MtSHR* overexpression induced divisions even in the absence of rhizobia (Dong et al., 2021). Thus, post-embryonic cortex expansion in *Medicago* is dependent on the local activation of the *SHR/SCR* pathway. Importantly, the hormone cytokinin (6-BA) is produced in response to symbiont signals and seems to be upstream of *SHR* in this local activation pathway. Authors showed that 6-BA triggered accumulation of *Mt*SHR-GUS and *Mt*SCR, and promoted cortex divisions leading to nodule formation (Murray et al., 2007; Tirichine et al., 2007; Gauthier-Coles et al., 2018; Dong et al., 2021).

Moreover, Dong et al. (2021) demonstrated that not only the presence, but also the amount of SHR protein is crucial in triggering these divisions. As revealed by transgenic reporter lines, *Mt*SHR and *Mt*SCR proteins are present in the cortex prior rhizobia inoculation and activation of divisions. Hence, it is only when *Mt*SHR is accumulated above a threshold level, either by symbiont-produced signals, hormones, or fusion to strong cortical-specific promoters (pro*MtNRT1.3*), that cell division occurs (**Figure 1C**, right). Furthermore, it was found that rhizobia inoculation increases *Mt*SHR protein in cortical cells without modifying its transcript levels. This suggests that *MtSHR* post-translational regulation in a cortex-specific context (e.g., by preventing protein degradation) represents a mechanism modulating cell division in *Medicago* roots.

A REVISED MODEL OF ROOT RADIAL PATTERNING

In the *Arabidopsis*-based model of root radial patterning, restriction of *SHR* movement through *SCR* interaction is a central regulatory aspect of the pathway that prevents development of more than one endodermal and one cortical cell layer. However, this function attributed to *SCR* do not seem to be conserved in other species. Both monocot and *Medicago* SCR homologs physically interact with SHR but do not limit its movement beyond the endodermis.

Alternatively, Wu et al. proposed that although *SCR* role in driving *SHR* nuclear localization is conserved, the control of SHR mobility is not. Experiments show that nuclear sequestration alone cannot explain restriction of SHR movement; thus, another factor must be involved. For example, in *Arabidopsis* roots expressing monocot homologs, ectopic expression of *AtSCR* in the stele dramatically increases *Os*SHR2 protein nuclear localization in this tissue. Because more protein is being held at the stele nuclei, a decrease in *Os*SHR2 intercellular movement should be observed. Nevertheless, no significant effect on the extent of protein mobility or decrease in cortex layer number was detected.

Another aspect of the model that requires further investigation is *SHR* role as an endodermal fate specification factor. In monocots and *Medicago,* the presence of SHR in the outer layers of the root does not result in the specification of endodermal identity. Rather, most of the GT layers where SHR protein is present have cortex identity according to their morphology and expression of genetic markers (Wu et al., 2014; Dong et al., 2021). Therefore, although *SHR* may be necessary, it is not sufficient to specify the root endodermis in these species.

A model for root radial patterning that incorporates the concept of SHR movement regulation as a central mechanism to control cortical layer number seems to be needed. In addition, work in *Medicago* suggest that local accumulation of SHR protein results in cell divisions and extra cortical layers, presumably by flipping the *SHR/SCR/CYCD6;1/RBR* circuit to its "on" state. Therefore, *SHR* can be conceptualized as a cell division trigger which can be tuned by regulating protein movement, accumulation, and degradation in a cell-type specific context. This regulation in space and time ultimately sets the asymmetric cell division program that shapes root form and function.

THE MISSING PIECES

Although recent studies have enabled the identification of new regulatory aspects of the *SHR/SCR* pathway, there are important questions regarding the identity of key regulatory components (see **Figure 1** question marks). For example, the identification and characterization of the factors that modulate the extent of intercellular movement is paramount. Furthermore, *SHR* is important for the specification of endodermal identity in *Arabidopsis*, but this function is not conserved in monocots and *Medicago*. Thus, identifying the developmental genetic network that specifies endodermis and cortex cell fate in other species than *Arabidopsis* will contribute to elaborate a more complete model of root radial patterning. Finally, it is unclear if SHR and SCR protein domains overlap in species with multilayered cortex, in which SHR domain is expanded to all GT layers (Wu et al., 2014; Dong et al., 2021; Ortiz-Ramirez et al., 2021). In *Medicago*, *SCR* is expressed in endodermis and cortex; hence, both transcription factors have expanded domains that overlap (Dong et al., 2021). Further analyses in monocots to determine if this expansion is conversed in complex roots will be valuable.

To achieve this, comparative high-resolution gene expression analysis and development of transgenic reporter lines in species with contrasting GT patterning is needed. Single-cell RNAseq would enable detection of differences

in gene activity at the level of individual cell layers, which is essential because many developmental regulators in the root act non-autonomously. In addition, generating high-resolution gene expression networks for multiple species and comparing their architectures will contribute to map changes in genetic circuits underlying morphological diversity. Finally, SHR loss-of-function mutants in different species are needed. They will aid in dissecting SHR function in cortex development and proliferation, which is essential for harboring symbiotic associations, resist biotic and abiotic stress, and generating morphological diversity.

AUTHOR CONTRIBUTIONS

MH-C and CO-R wrote the article and designed the figures. All authors contributed to the article and approved the submitted version.

FUNDING

MH-C and CO-R are supported by UGA-LANGEBIO Cinvestav early career funds.

REFERENCES

Baum, S. F., Dubrovsky, J. G., and Rost, T. L. (2002). Apical organization and maturation of the cortex and vascular cylinder in Arabidopsis thaliana (Brassicaceae) roots. *Am. J. Bot.* 89, 908–920. doi: 10.3732/ajb.89.6.908

Benfey, P. N., Linstead, P. J., Roberts, K., Schiefelbein, J. W., Hauser, M. T., and Aeschbacher, R. A. (1993). Root development in Arabidopsis: four mutants with dramatically altered root morphogenesis. *Development* 119, 57–70. doi: 10.1242/dev.119.1.57

Bennetzen, J.L., and Hake, S.C. (2009). *Handbook of Maize: Its Biology*. New York: Springer.

Bertolotti, G., Unterholzner, S. J., Scintu, D., Salvi, E., Svolacchia, N., Di Mambro, R., et al. (2021). A PHABULOSA-controlled genetic pathway regulates ground tissue patterning in the Arabidopsis root. *Curr. Biol.* 31, 420–426. doi: 10.1016/j.cub.2020.10.038

Clark, L. H., and Harris, W. H. (1981). Observations on the root anatomy of Rice (Oryza-Sativa-L). *Am. J. Bot.* 68, 154–161. doi: 10.1002/j.1537-2197.1981.tb12374.x

Cruz-Ramirez, A., Diaz-Trivino, S., Blilou, I., Grieneisen, V. A., Sozzani, R., Zamioudis, C., et al. (2012). A bistable circuit involving SCARECROW-RETINOBLASTOMA integrates cues to inform asymmetric stem cell division. *Cell* 150, 1002–1015. doi: 10.1016/j.cell.2012.07.017

Cui, H., and Benfey, P. N. (2009). Interplay between SCARECROW, GA and LIKE HETEROCHROMATIN PROTEIN 1 in ground tissue patterning in the Arabidopsis root. *Plant J.* 58, 1016–1027. doi: 10.1111/j.1365-313X.2009.03839.x

Cui, H., Levesque, M. P., Vernoux, T., Jung, J. W., Paquette, A. J., Gallagher, K. L., et al. (2007). An evolutionarily conserved mechanism delimiting SHR movement defines a single layer of endodermis in plants. *Science* 316, 421–425. doi: 10.1126/science.1139531

Di Ruocco, G., Bertolotti, G., Pacifici, E., Polverari, L., Tsiantis, M., Sabatini, S., et al. (2018a). Differential spatial distribution of miR165/6 determines variability in plant root anatomy. *Development* 145:dev.153858. doi: 10.1242/dev.153858

Di Ruocco, G., Di Mambro, R., and Dello Ioio, R. (2018b). Building the differences: a case for the ground tissue patterning in plants. *Proc. Biol. Sci.* 285:20181746. doi: 10.1098/rspb.2018.1746

Dolan, L., Janmaat, K., Willemsen, V., Linstead, P., Poethig, S., Roberts, K., et al. (1993). Cellular organisation of the Arabidopsis thaliana root. *Development* 119, 71–84. doi: 10.1242/dev.119.1.71

Dong, W. T., Zhu, Y. Y., Chang, H. Z., Wang, C. H., Yang, J., Shi, J. C., et al. (2021). An SHR-SCR module specifies legume cortical cell fate to enable nodulation. *Nature* 589, 586–590. doi: 10.1038/s41586-020-3016-z

Esau, K. (1977). *Anatomy of Seed Plants*. New York: John Wiley & Sons.

Fahn, A. (1990). *Plant Anatomy. 4th Edn*. Oxford: Pergamon.

Gauthier-Coles, C., White, R. G., and Mathesius, U. (2018). Nodulating legumes are distinguished by a sensitivity to Cytokinin in the root cortex leading to Pseudonodule development. *Front. Plant Sci.* 9:1901. doi: 10.3389/fpls.2018.01901

Gong, X., Flores-Vergara, M. A., Hong, J. H., Chu, H., Lim, J., Franks, R. G., et al. (2016). SEUSS integrates gibberellin Signaling with transcriptional inputs from the SHR-SCR-SCL3 module to regulate middle cortex formation in the Arabidopsis root. *Plant Physiol.* 170, 1675–1683. doi: 10.1104/pp.15.01501

Heidstra, R., Welch, D., and Scheres, B. (2004). Mosaic analyses using marked activation and deletion clones dissect Arabidopsis SCARECROW action in asymmetric cell division. *Genes Dev.* 18, 1964–1969. doi: 10.1101/gad.305504

Heimsch, C., and Seago, J. L. Jr. (2008). Organization of the root apical meristem in angiosperms. *Am. J. Bot.* 95, 1–21. doi: 10.3732/ajb.95.1.1

Helariutta, Y., Fukaki, H., Wysocka-Diller, J., Nakajima, K., Jung, J., Sena, G., et al. (2000). The SHORT-ROOT gene controls radial patterning of the Arabidopsis root through radial signaling. *Cell* 101, 555–567. doi: 10.1016/S0092-8674(00)80865-X

Henry, S., Dievart, A., Divol, F., Pauluzzi, G., Meynard, D., Swarup, R., et al. (2017). SHR overexpression induces the formation of supernumerary cell layers with cortex cell identity in rice. *Dev. Biol.* 425, 1–7. doi: 10.1016/j.ydbio.2017.03.001

Henry, S., Divol, F., Bettembourg, M., Bureau, C., Guiderdoni, E., Perin, C., et al. (2015). Immunoprofiling of Rice root cortex reveals two cortical subdomains. *Front. Plant Sci.* 6:1139. doi: 10.3389/fpls.2015.01139

Heo, J. O., Chang, K. S., Kim, I. A., Lee, M. H., Lee, S. A., Song, S. K., et al. (2011). Funneling of gibberellin signaling by the GRAS transcription regulator scarecrow-like 3 in the Arabidopsis root. *Proc. National Acad. Sci. U. S. A.* 108, 2166–2171. doi: 10.1073/pnas.1012215108

Inan, G., Zhang, Q., Li, P., Wang, Z., Cao, Z., Zhang, H., et al. (2004). Salt cress. A halophyte and cryophyte Arabidopsis relative model system and its applicability to molecular genetic analyses of growth and development of extremophiles. *Plant Physiol.* 135, 1718–1737. doi: 10.1104/pp.104.041723

Koizumi, K., Hayashi, T., Wu, S., and Gallagher, K. L. (2012). The SHORT-ROOT protein acts as a mobile, dose-dependent signal in patterning the ground tissue. *Proc. National Acad. Sci. U. S. A.* 109, 13010–13015. doi: 10.1073/pnas.1205579109

Long, Y., Goedhart, J., Schneijderberg, M., Terpstra, I., Shimotohno, A., Bouchet, B. P., et al. (2015). SCARECROW-LIKE23 and SCARECROW jointly specify endodermal cell fate but distinctly control SHORT-ROOT movement. *Plant J. Cell Mol. Biol.* 84, 773–784. doi: 10.1111/tpj.13038

Long, Y., Stahl, Y., Weidtkamp-Peters, S., Postma, M., Zhou, W., Goedhart, J., et al. (2017). In vivo FRET-FLIM reveals cell-type-specific protein interactions in Arabidopsis roots. *Nature* 548, 97–102. doi: 10.1038/nature23317

Lux, A., and Inanaga, S. (1997). Die atypische Struktur der jungen Wurzeln einer Wüstensukkulente Echinocactus platyacanthus. *Stapfia* 50:5.

Lux, A., Luxová, M., Abe, J., and Morita, S. (2004). Root cortex: structural and functional variability and responses to environmental stress. *Root Res.* 13, 117–131. doi: 10.3117/rootres.13.117

Ma, Z., Guo, D., Xu, X., Lu, M., Bardgett, R. D., Eissenstat, D. M., et al. (2018). Evolutionary history resolves global organization of root functional traits. *Nature* 555, 94–97. doi: 10.1038/nature25783

Murray, J. D., Karas, B. J., Sato, S., Tabata, S., Amyot, L., and Szczyglowski, K. (2007). A cytokinin perception mutant colonized by rhizobium in the absence of nodule organogenesis. *Science* 315, 101–104. doi: 10.1126/science.1132514

Nakajima, K., Sena, G., Nawy, T., and Benfey, P. N. (2001). Intercellular movement of the putative transcription factor SHR in root patterning. *Nature* 413, 307–311. doi: 10.1038/35095061

Ortiz-Ramirez, C., Dias-Araujo, P. C., Zhang, C., Demesa-Arevalo, E., Yan, Z., Xu, X., et al. (2021). Ground tissue circuitry regulates organ complexity in cereal roots. BioRxiv. doi: 10.1101/2021.04.28.441892

Paquette, A. J., and Benfey, P. N. (2005). Maturation of the ground tissue of the root is regulated by gibberellin and SCARECROW and requires SHORT-ROOT. *Plant Physiol.* 138, 636–640. doi: 10.1104/pp.104.058362

Pauluzzi, G., Divol, F., Puig, J., Guiderdoni, E., Dievart, A., and Perin, C. (2012). Surfing along the root ground tissue gene network. *Dev. Biol.* 365, 14–22. doi: 10.1016/j.ydbio.2012.02.007

Pernas, M., Ryan, E., and Dolan, L. (2010). SCHIZORIZA controls tissue system complexity in plants. *Curr. Biol.* 20, 818–823. doi: 10.1016/j.cub.2010.02.062

Rebouillat, J., Dievart, A., Verdeil, J. L., Escoute, J., Giese, G., Breitler, J. C., et al. (2008). Molecular genetics of Rice root development. *Rice* 2, 15–34. doi: 10.1007/s12284-008-9016-5

Ron, M., Dorrity, M. W., de Lucas, M., Toal, T., Hernandez, R. I., Little, S. A., et al. (2013). Identification of novel loci regulating interspecific variation in root morphology and cellular development in tomato. *Plant Physiol.* 162, 755–768. doi: 10.1104/pp.113.217802

Scheres, B., McKhann, H. I., and Van den Berg, C. (1996). Roots redefined: anatomical and Cenetic analysis of root development. *Plant Physiol.* 111, 959–964. doi: 10.1104/pp.111.4.959

Sozzani, R., Cui, H., Moreno-Risueno, M. A., Busch, W., Van Norman, J. M., Vernoux, T., et al. (2010). Spatiotemporal regulation of cell-cycle genes by SHORTROOT links patterning and growth. *Nature* 466, 128–132. doi: 10.1038/nature09143

ten Hove, C. A., Willemsen, V., de Vries, W. J., van Dijken, A., Scheres, B., and Heidstra, R. (2010). SCHIZORIZA encodes a nuclear factor regulating asymmetry of stem cell divisions in the Arabidopsis root. *Curr. Biol.* 20, 452–457. doi: 10.1016/j.cub.2010.01.018

Timmers, A. C., Auriac, M. C., and Truchet, G. (1999). Refined analysis of early symbiotic steps of the rhizobium-Medicago interaction in relationship with microtubular cytoskeleton rearrangements. *Development* 126, 3617–3628. doi: 10.1242/dev.126.16.3617

Tirichine, L., Sandal, N., Madsen, L. H., Radutoiu, S., Albrektsen, A. S., Sato, S., et al. (2007). A gain-of-function mutation in a cytokinin receptor triggers spontaneous root nodule organogenesis. *Science* 315, 104–107. doi: 10.1126/science.1132397

van den Berg, C., Willemsen, V., Hage, W., Weisbeek, P., and Scheres, B. (1995). Cell fate in the Arabidopsis root meristem determined by directional signalling. *Nature* 378, 62–65. doi: 10.1038/378062a0

Welch, D., Hassan, H., Blilou, I., Immink, R., Heidstra, R., and Scheres, B. (2007). Arabidopsis JACKDAW and MAGPIE zinc finger proteins delimit asymmetric cell division and stabilize tissue boundaries by restricting SHORT-ROOT action. *Genes Dev.* 21, 2196–2204. doi: 10.1101/gad.440307

Wu, S., Lee, C.-M., Hayashi, T., Price, S., Divol, F., Henry, S., et al. (2014). A plausible mechanism, based upon SHORT-ROOT movement, for regulating the number of cortex cell layers in roots. *Proc. National Acad. Sci. U. S. A.* 111, 16184–16189. doi: 10.1073/pnas.1407371111

Yamauchi, T., Colmer, T. D., Pedersen, O., and Nakazono, M. (2018). Regulation of root traits for internal aeration and tolerance to soil waterlogging-flooding stress. *Plant Physiol.* 176, 1118–1130. doi: 10.1104/pp.17.01157

Conflict of Interest: The authors declare that the research was conducted in the absence of any commercial or financial relationships that could be construed as a potential conflict of interest.

Publisher's Note: All claims expressed in this article are solely those of the authors and do not necessarily represent those of their affiliated organizations, or those of the publisher, the editors and the reviewers. Any product that may be evaluated in this article, or claim that may be made by its manufacturer, is not guaranteed or endorsed by the publisher.

frontiers in Plant Science

ORIGINAL RESEARCH
published: 08 October 2021
doi: 10.3389/fpls.2021.750623

Growth Patterns in Seedling Roots of the Pincushion Cactus *Mammillaria* Reveal Trends of Intra- and Inter-Specific Variation

José de Jesús González-Sánchez[1,2†], *Itzel Santiago-Sandoval*[1†], *José Antonio Lara-González*[1†], *Joel Colchado-López*[1,2], *Cristian R. Cervantes*[1,2], *Patricia Vélez*[3], *Jerónimo Reyes-Santiago*[1], *Salvador Arias*[1] *and Ulises Rosas*[1*]

[1] Jardín Botánico, Instituto de Biología, Universidad Nacional Autónoma de México, Mexico City, Mexico, [2] Posgrado en Ciencias Biológicas, Universidad Nacional Autónoma de México, Mexico City, Mexico, [3] Departamento de Botánica, Instituto de Biología, Universidad Nacional Autónoma de México, Mexico City, Mexico

Genetic mechanisms controlling root development are well-understood in plant model species, and emerging frontier research is currently dissecting how some of these mechanisms control root development in cacti. Here we show the patterns of root architecture development in a gradient of divergent lineages, from populations to species in *Mammillaria*. First, we show the patterns of variation in natural variants of the species *Mammillaria haageana*. Then we compare this variation to closely related species within the Series *Supertexta* in *Mammillaria* (diverging for the last 2.1 million years) in which *M. haageana* is inserted. Finally, we compared these patterns of variation to what is found in a set of *Mammillaria* species belonging to different Series (diverging for the last 8 million years). When plants were grown in controlled environments, we found that the variation in root architecture observed at the intra-specific level, partially recapitulates the variation observed at the inter-specific level. These phenotypic outcomes at different evolutionary time-scales can be interpreted as macroevolution being the cumulative outcome of microevolutionary phenotypic divergence, such as the one observed in *Mammillaria* accessions and species.

Keywords: Cactaceae, natural variation, root architecture, succulent plant, plant evolution, root development, evo-devo, microevolution

OPEN ACCESS

Edited by:
Ramiro Esteban Rodriguez, CONICET Instituto de Biología Molecular y Celular de Rosario (IBR), Argentina

Reviewed by:
María Laura Martínez, Universidad Nacional de Rosario, Argentina
María Victoria Rodriguez, Universidad Nacional de Rosario, Argentina

***Correspondence:**
Ulises Rosas
urosas@ib.unam.mx

†These authors have contributed equally to this work and share first authorship

Specialty section:
This article was submitted to Plant Development and EvoDevo, a section of the journal Frontiers in Plant Science

Received: *30 July 2021*
Accepted: *14 September 2021*
Published: *08 October 2021*

Citation:
González-Sánchez JJ, Santiago-Sandoval I, Lara-González JA, Colchado-López J, Cervantes CR, Vélez P, Reyes-Santiago J, Arias S and Rosas U (2021) Growth Patterns in Seedling Roots of the Pincushion Cactus Mammillaria Reveal Trends of Intra- and Inter-Specific Variation. Front. Plant Sci. 12:750623. doi: 10.3389/fpls.2021.750623

INTRODUCTION

A long standing debate in evolutionary biology is whether the nature of macroevolutionary change can be explained based on the principles and processes of microevolution. One possibility is that the macroevolutionary outcomes are the result of the cumulative microevolutionary processes, so the footprint of microevolution can be seen at higher levels of taxonomic divergence. This possibility has been tested in some organisms such as crocodiles, in which intraspecific crane variation (a highly robust trait) spans half of the extant species (Okamoto et al., 2015). Furthermore, in model species such as *Drosophila*, it has been experimentally shown that the genetic variation explaining

divergent pigmentation patterns among species, are shared with the genetic variation displayed within species (Wittkopp et al., 2009). On the other hand, it has been argued that morphological divergence between species is often non-adaptive, as compared to variation within species. This is because regardless of their adaptive value, phenotypic differentiation has been suggested to be frequently rapid, and random in direction, involving the evolution of gene regulation, pleiotropy, epistasis and canalization (Davis and Gilmartin, 1985), which in turn could result in different nature of the variation within and between species. Despite the relevance of the question for the understanding of evolution and development of breeding strategies, in plants, to our knowledge there are very few comprehensive cases where these ideas have been tested at the morphological or genetic level. One of the few examples is the case of cacti, in which the comparison of micro- vs. macro-evolutionary divergence has been indirectly addressed in the determinate primary growth of the root apex, a highly conserved trait in the subfamily Cactoideae (Shishkova et al., 2013; Rodriguez-Alonso et al., 2018) in which the timeframe of this apex determination is correlated with environmental factors, within and between species (Martino et al., 2018); however, the number of species and accessions are low to draw conclusions about the nature of evolutionary divergence. Therefore, we attempt to provide elements to this discussion in plant evolution, studying the root development of *Mammillaria* species.

Mammillaria is the most diverse genus within the Cactaceae family. It comprises 155–320 species mainly distributed in Mexico (Reppenhagen, 1992; Guzmán et al., 2003; Hunt et al., 2006; Hernández and Gómez-Hinostrosa, 2015; Villaseñor, 2016). The genus is characterized by plants with tubercles arranged in spiraled rows, the areola is dimorphic, that is, one part is at the base from where the flowers, bristles or branches arise, and another at the tip of the tubercles where spines grow (Bravo and Sánchez-Mejorada, 1991; Scheinvar, 2004). It has been proposed that *Mammillaria* s.l. is non-monophyletic (Butterworth and Wallace, 2004), and recently it was also proposed that the Mammiloid clade circumscribes three monophyletic genera: *Mammillaria* s.s., *Coryphantha* and *Cochemiea* s.l. (Breslin et al., 2021). The Mammilloid clade is estimated to have diverged for the last 8.62 million years (Hernández-Hernández et al., 2014). In addition, the *M. haageana* genome size has been estimated to be 1 C = 1.5 Gbp (Christian et al., 2006), and a plastid genome of 115 kbp (Hinojosa-Alvarez et al., 2020). Despite our current incomplete understanding of the phylogenetic relationships among *Mammillaria* species, a core *Mammillaria* set of species grouped into 8 subgenres and 16 series have been proposed (Butterworth and Wallace, 2004; Hernández and Gómez-Hinostrosa, 2015). Most species are distributed in arid or semi-arid lands, but some species are also found in deciduous forests, or even in oak-pine forests (Hernández and Gómez-Hinostrosa, 2015).

Among the series, *M.* ser. *Supertextae* is characterized by the presence of cuticular crystals (Lüthy, 1995) and flowers smaller than 15 mm (Hunt et al., 2006). The species that make up the series are distributed from Central Mexico to Central America (Pilbeam, 1999). It has been suggested that the sister series of *M.* ser. *Supertextae* is *M.* ser. *Polyachanthae,* supported by a deletion in *rpl16*; it was also found that *M.* ser. *Supertextae* started diverging about 2.1 million years ago. According to an accepted classification (Hunt, 1983; Hunt et al., 2006), the *Supertextae* series comprises 9 species: *M. albilanata* Backeb., *M. crucigera* Mart., *M. columbiana* Salm-Dyck, *M. dixanthocentron* Backeb. ex Mottram., *M. flavicentra* Backeb., *M. haageana*, *M. halbingeri* Boed., *M. huitzilopochtli* D.R.Hunt, and *M. supertexta* Mart. Ex Pfeiff. Within the *Supertextae* Series, *M. haageana* is a highly variable species, which seems to have a complex evolutionary history resulting in an ample distribution along the Mexican neovolcanic axis, inhabiting a wide range of environments from pine-oak forests to shrubs and deserts. These locations have been classified into subspecies according to their distribution, plant shape, spination patterns, flower color, among other traits (Guzmán et al., 2003). *M. haageana* is a highly charismatic species as ornamental, and it is one of the few cacti species to have been reported by the early expeditions to the New World of Sessé & Mociño during the XVIII Century (Mociño and Sessé, 2015). Currently it is one of the most representative flagships of the UNAM Jardín Botánico for conservation efforts. Despite its biodiversity, horticultural, historic and conservation importance, the evolutionary history of *M. haageana* is far from being fully understood. Thus, in this work we refer to the *M. haageana* natural variants as accessions.

In sessile organisms such as plants, resource foraging by roots, allocation of assimilates and growth are complex problems vital to maximize survival and reproductive success. Evolutionary processes have generated and tested biological trade-offs by optimizing urgent tasks, while allocating fewer resources to other non-imperative tasks. One could consider that species and populations are optimal to multitask in their native environment; however, their optimality is constrained by the previous best solutions for different tasks. During plant development some of the most imperative tasks that roots perform, and particularly for desert plants, are water uptake and nutrient foraging. This is why plants must decide how to grow to optimize resource uptake, but also some of these growth strategies might be fixed to maximize fitness. We currently have a comprehensive understanding of the molecular mechanisms controlling growth and drought stress responses in model plants. The challenge is to understand the genetic mechanisms on how desert plants uptake resources particularly by roots, grow and develop, in early stages when seedlings are highly sensitive to mortality.

In this work we present a comprehensive picture on how roots from the *Mammillaria* genus grow during early stages of development (first few months). We used three groups of *Mammillaria* stocks (*Mammillaria* species, *M.* ser. *Supertextae* species, and *M. haageana* accessions) representing an ample range of evolutionary divergence (up to 8 million years), and used this framework to ask the question whether natural variation recapitulates the diversity between species, and test the hypothesis whether microevolutionary phenotypic evolution resemble that from macroevolutionary processes.

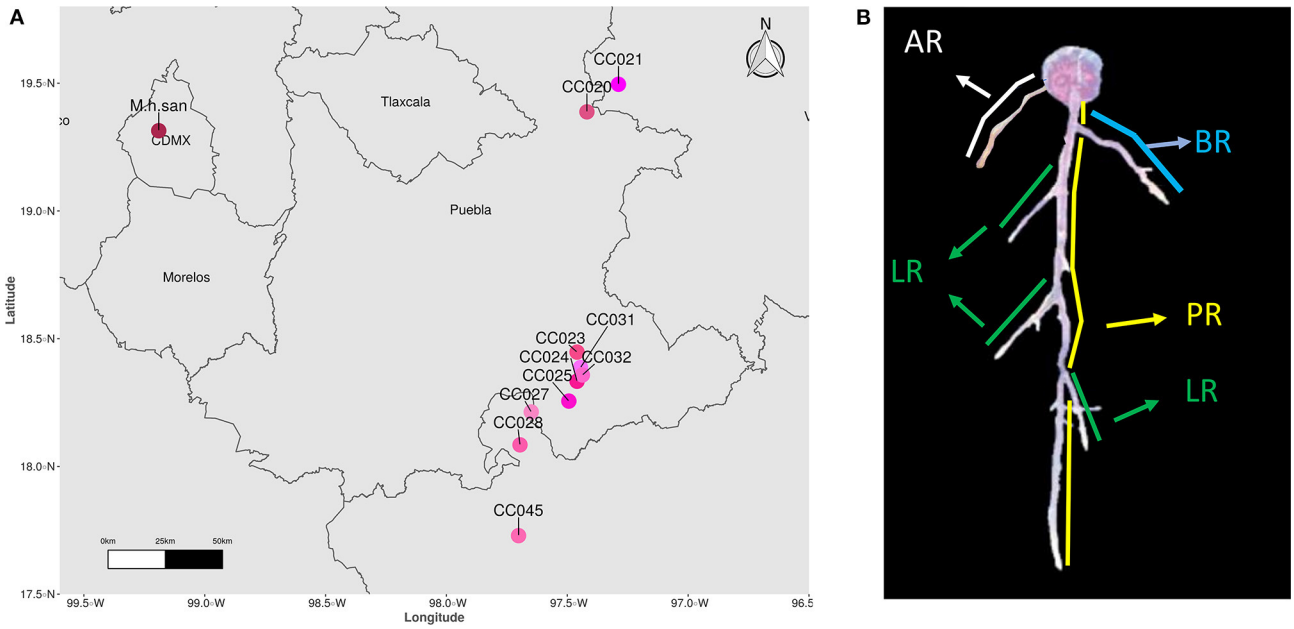

FIGURE 1 | (A) Geographical origin of *M. haageana* accessions. **(B)** Characterization of root attributes in a *Mammillaria* plant. PR, Principal Root; LR, Lateral Root; BR, Basal Root; AR, Adventitious Root.

MATERIALS AND METHODS

Plant Material

Seeds from *Mammillaria* species were obtained from the Jardín Botánico (UNAM) collections, harvested from the living cacti collections within 1–3 years prior germination. To represent species from the *Mammillaria* genus, we selected 16 species belonging to 8 series. For simplicity, acronyms of these species were created as follows: *M. carnea* Zucc. ex Pfeiff. (*M. car*), *M. coahuilensis* (Boed.) Moran (*M. coa*), *M. duwei* Rogoz. and P. J. Braun (*M. duw*), *M. formosa* Scheidw. (*M. for*), *M. hernandezii* Glass and R. A. Foster (*M. her*), *M. karwinskiana* Mart. (*M. kar*), *M. lasiacantha* Engelm. (*M. las*), *M. magnimamma* Haw. (*M. mag*), *M. pectinifera* F. A. C. Weber (*M. pec*). For *M.* ser. *Supertextae* species we could only obtain 7 species, and they were abbreviated as follow: *M. albilanata* (*M. alb*), *M. crucigera* (*M. cru*), *M. dixanthocentron* (*M. dix*), *M. flavicentra* (*M. fla*), *M. huitzilopochtli* (*M. hui*), and *M. supertexta* (*M. sup*). As for the *M. haageana* accessions, seeds were collected from the wild in 2018 (**Figure 1A**), assigned accession numbers according to our previous work (Cervantes et al., 2021), and their corresponding plants were deposited in the Jardín Botánico (Instituto de Biología, UNAM) collection (collection license SGPA/DGGFS/712/3690/10). For *M. haageana* subspecies *san-angelensis* (*M. h. san*) seeds were obtained from the Adoption Center Conservation Program for Endangered Species at Jardín Botánico (Instituto de Biología, UNAM).

Growth Conditions and Phenotyping

Seeds were disinfected by a wash in 70% commercial bleach for 5 mins, followed by three washes in sterile distilled water, within a laminar flow-hood with HEPA filter (Veco, México). The seeds were suspended in 0.1% agar to facilitate their manipulation and adhesion to the sowing plate. Seeds were sown in 12 × 12 cm petri dishes (Greiner Bio-One, Cat 688102), with 75 mL of 50% strength Murashige-Skoog media (Caisson Labs, Cat MSP09-1LT), added with 0.05 MES salts (MP Biomedicals, Cat 152454), adjusted to a pH of 5.7, and solidified with 1% agar (Sigma Life Science, Cat A1296-1KG). Each plate was sown with 49 evenly spaced seeds (7 by 7 disposition), and germinated in a growth chamber (Percival Scientific, Cat CU22L) at 28°C with a 16/8 long day photoperiod, as in our previously published experimental set up (Rosas et al., 2021). Germination was recorded every third day, for 45 days, after which we had plenty of healthy seedlings with 40–45 days after germination, and that is why we chose this age for further procedures. The seedlings were then transplanted to fresh plates prepared as mentioned above, and arranged in two rows of 5 seedlings in each plate. To adhere the roots to the plate, drops of 0.3% agar were added to the root, and plates were horizontally kept for 3 days, after which plates were switched to vertical position, and plants were kept in the same growth chamber at 28°C and 16/8 photoperiod. Digital images from plates were obtained using a scanner (EPSON Perfection v600 Photo) at a 600 dpi resolution in JPG format, at 45, 73, 101, 129, and 157 days post germination, corresponding to periods of 4 weeks, so the differences were noticeable. From each species or *M. haageana* accession we obtained 20–40 plants, which were considered as biological replicates (**Supplementary Table 1**). Because of the magnitude of the experiment, these plants were obtained in sequential batches. We used the free software ImageJ (version 1.52a), coupled to a measuring system previously used to

calculate the Rhizochron index (Colchado-López et al., 2019), and whose scripts calculated several attributes of the roots: Total Root Length (TRL), Principal Root Length (PRL), Total Lateral Root Length (TLRL), Adventitious Root Length (ARL), Basal Root Length (BRL), number of Lateral Roots (nLR), number of Adventitious Roots (nAR), and number of Basal Roots (nBR). We defined the principal root as the dominant root axis in the early stages (45 and 73 days), the lateral roots as any root branching out from another root, the adventitious roots as those originating from the shoot (the hypocotyl), and basal roots as those roots originating from the first millimeter from the root-shoot junction on the root side (**Figure 1B**). These measurements were done for individual plants over time, so it was always clear what type of root was being measured. All gathered data can be found in the **Supplementary Data Sheet 1**.

Data Processing and Clustering Analysis

Modified range plots for all genotypes were created using the package "ggplot2," in which the median value was expressed along with bars specifying the interquartile range, and atypic data points. For visualization purposes, all plots were done in $\log_{10}$ scale using the function "pseudo_log_trans()" from package "scales" to better appreciate the subtle differences toward low trait values in root variation. Cluster analysis for accession dissimilarity was performed on the medians of each group with euclidean distance, using the package "dendextend," normalizing for trait variance. PCA analysis was performed by scaling the variables, using a Spearman correlation, and eigenvectors and eigenvalues were obtained with "eigen()" from "base." Scree-plots and individual PCs boxplots were visualized using the "ggplot" and "ggrepel" packages, and the boxplots were aligned with the "plot_grid()" function from "cowplot." Statistical differences for the PCs were analyzed with a Kruskal-Wallis test performed with the "kruskal()" function from "agricolae." *Post-hoc* Dunn test was performed using the "dunnTest()," from "FSA" package and letters were obtained using the "cldList()" function from "rcompanion." All analyses were done in R version 4.0.1 (R Core Team, 2020).

RESULTS

Natural Variation in Root Architecture Within *Mammillaria haageana* Accessions

To characterize the natural variation in developmental dynamics in a *Mammillaria* species, we chose *M. haageana*, a widely distributed species along the Mexican neovolcanic axis (Hunt et al., 2006; Arias et al., 2012), whose diversity we are currently characterizing (Cervantes et al., 2021), and we have established a collection of natural accessions at the Jardín Botánico (Instituto de Biología, UNAM). Using seeds from the wild, first we performed germination in aseptic conditions in order to study the variation in root architecture in natural accessions under a controlled environment. However, these germination efforts of *M. haageana* revealed the consistent recovery of a dematiaceous filamentous fungus emerging from seeds in some accessions originating from oak-pine

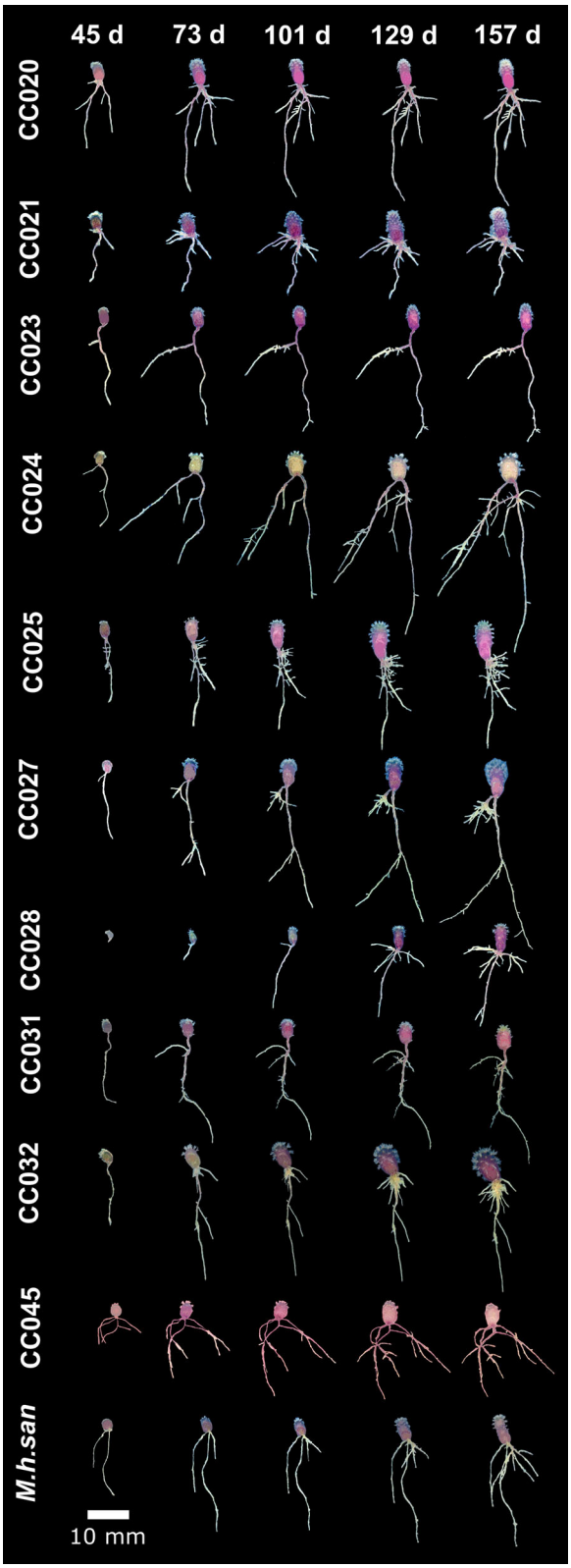

FIGURE 2 | Growth dynamics in *M. haageana* accessions over five developmental stages (45, 73, 101, 129, and 157 days after germination).

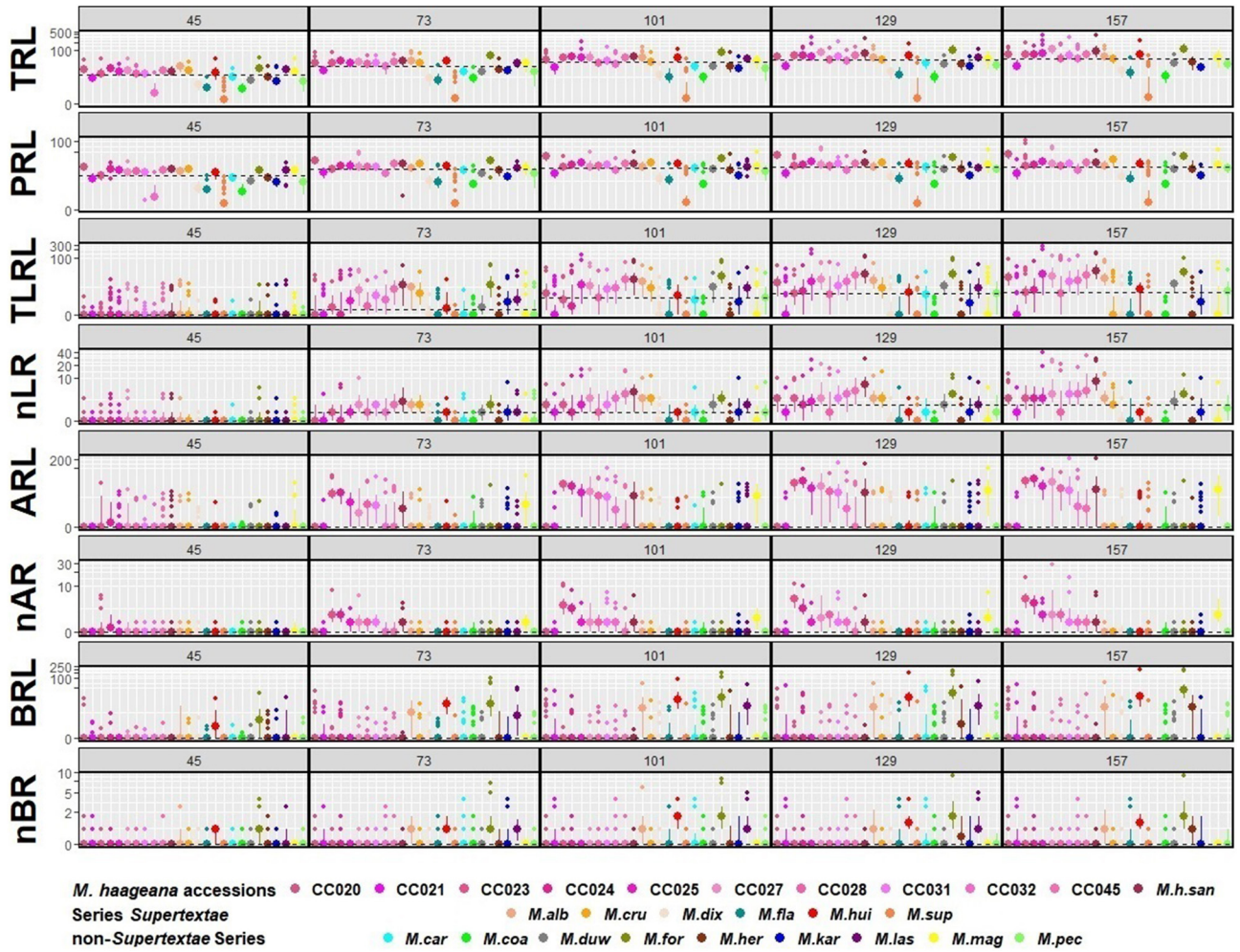

FIGURE 3 | Quantitative dynamics of root growth in *M. haageana* accessions, *Supertextae* series *Mammillaria* species, and non-*Supertextae* series *Mammillaria* species, at 45, 73, 101, 129, and 157 days after germination. Large dots represent the median of the accession, smaller dots represent the outliers, and bars represent the interquartile range. Horizontal dotted-lines represent the overall median for the entire developmental stage. TRL, Total Root Length; PRL, Principal Root Length; TLRL, Total Lateral Root Length; ARL, Adventitious Root Length; BRL, Basal Root Length; nLR, number of Lateral Roots; nAR, number of Adventitious Roots; nBR, number of Basal Roots. *y* axes are expressed in base 10 pseudo-log scale.

forests, despite superficial decontamination of the material and its incubation under controlled conditions in growth chambers. We isolated this fungus for future characterizations and experiments (**Supplementary Figure 1**). However, our observations suggest that the presence of this fungus enhanced the suitable germination and posterior development of the early root system in contrast to seeds where this fungus was not present. This agrees with former work reporting seed germination in *Opuntia* depends on the presence of fungi to reduce mechanical resistance of the testa (Delgado-Sánchez et al., 2013). Furthermore, success in the propagation of cacti infected with fungi and bacteria has been documented, with *Mammillaria* spp. being more amenable (Fay and Gratton, 1992). However, our observations of plant-fungus interactions in *M. haageana* deserve further examination in future work. For the purpose of the current experiment, those contaminated *M. haageana* accessions had to be discarded from the analysis (CC022, CC030, and CC035), and from the 20 accessions that we currently have in the *M. haageana* collection, we were able to assess root growth dynamics in 11 of them (**Figure 2**).

Regarding the growth dynamics in *M. haageana*, despite being variants of the so-called same species, there is plenty of variation on the root architectural system when comparing different accessions (**Figure 2**), as well as within each accession (**Figure 3**), and different types of roots emerge at distinct time frames. In general, the lateral roots had a sustained growth during the first 101 days, but later it stagnated toward the 129 and 157 days after germination. Among accessions, the presence and elongation of lateral roots was highly variable over time, with emerging lateral roots in CC024 and CC032 at 45 days, but in other accessions they

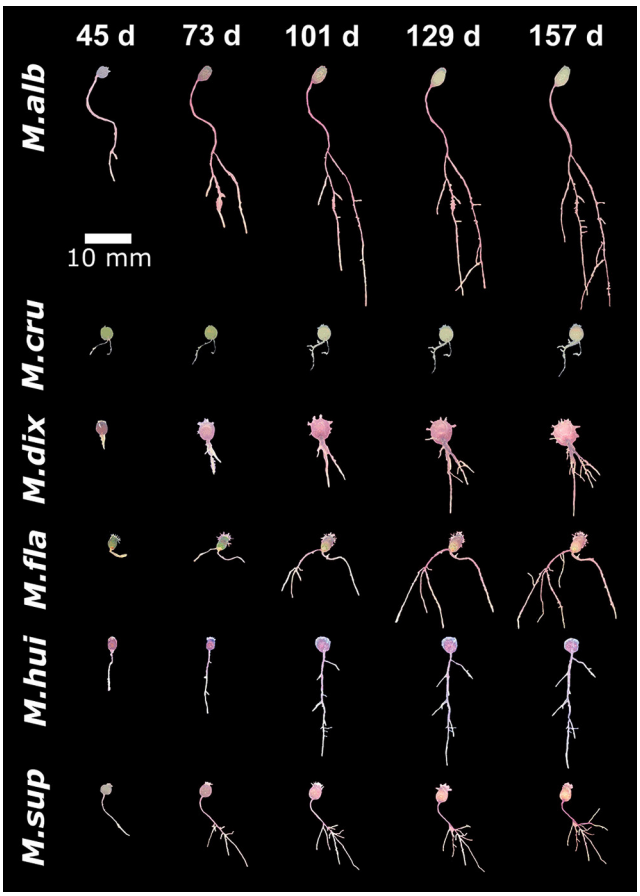

FIGURE 4 | Growth dynamics in *Mammillaria* species from the Series *Supertextae* over five developmental stages (45, 73, 101, 129, and 157 days after germination). For simplicity, acronyms of these species were created as follow: *M.alb*, *M. albilanata*; *M.cru*, *M.crucigera*; *M.dix*, *dixanthocentron*, *M.fla*, *M. flavicentra*; *M. hui*, *M. huitzilopochtli*; *M.sup*, *M. supertexta*.

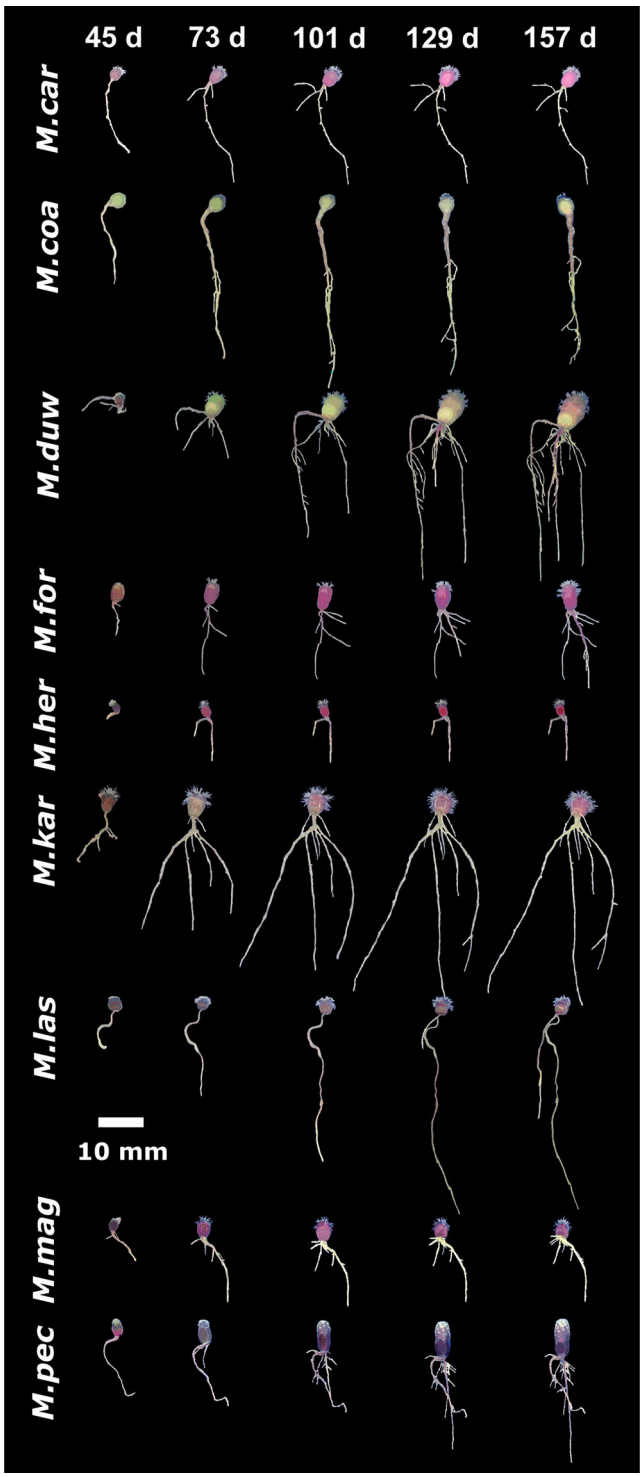

FIGURE 5 | Growth dynamics in *Mammillaria* species from series other than *Supertextae*, over five developmental stages (45, 73, 101, 129, and 157 days after germination). For simplicity, acronyms of these species were created as follow: *M. car*, *M. carnea*; *M. coa*, *M. coahuilensis*; *M. duw*, *M. duwei*; *M. for*, *M formosa*; *M. her*, *M. hernandezi*; *M. kar*, *M. karwinskiana*; *M. las*, *M. lasiacantha*; *M. mag*, *M. magnimama*; *M. pec*, *M. pectinifera*.

proliferated from day 73 onwards, except for the accession CC021 in which lateral roots were not visible before 101 days after germination.

Adventitious roots proliferated from day 73, and their growth was remarkable by day 129 and 157. However, in CC028 and CC031, a large proportion of the seedlings did not show adventitious roots before the day 129, suggesting that these two accessions have slower growth rates as compared to the rest of the accessions. Remarkably, CC024 and CC032 were the two accessions with the longest adventitious roots.

An interesting observation for *M. haageana* accessions is that in most seedlings we did not detect basal roots, however, in some exceptional plants, as in accessions CC021, CC025, and CC031, some adventitious roots emerged before the day 73, and elongated later on, but no new adventitious root emerged in later stages.

Diversity in Root Architecture Between Closely Related *Mammillaria* Species

To compare the growth dynamics of *M. haageana* to the set of sister species within the series *Supertextae*, we grew seedlings of *M. flavicentra*, *M. dixanthocentron*, *M. albilanata*, *M. supertexta*, *M. huitzilopochtli*, and *M. crucigera*, in the same controlled conditions (**Figure 4**). When observing these phenotypes, we detected more dramatic differences between *Supertextae* series as compared to the *M. haageana* accessions (**Figures 2–4**). For instance, *M. cru* or *M. fla* had limited growth as opposed to the prominent root growth of *M. alb*. On the other hand, *M. alb* and *M. haageana* accessions had the longest root systems, as compared to the other *Supertextae* species. Different to the rest of the *Supertextae* species and *M. haageana* accessions, lateral roots in *M. alb* and *M. sup* did not slow down their growth toward the later stages of development.

A compelling observation is that most *Supertextae* species did not develop adventitious roots, as was the case of *M. alb*, *M. dix*, and *M. sup*. Some plants had adventitious roots in *M. cru*, *M. hui*, and *M. fla*. This pattern was somehow similar to what was observed in *M. haageana* accessions, which might suggest that the absence or poor growth of adventitious roots, might be a defining morphological feature of *Supertextae* species. In addition, very few individuals in most *Supertextae* species develop basal roots, suggesting that basal roots might also be a characteristic feature of the series.

Diversity in Root Architecture Between *Mammillaria* Species

To compare the natural variation in root architecture in *M. haageana* accessions and *Supertextae* species to a higher order of evolutionary divergence, we grew a set of non-*Supertexta* Series *Mammillaria* species (**Figure 5**). Similar to what occurred in *M. haageana* accessions and *Supertextae* species, the overall root architecture grows at a sustained rate, but slows down in the later stages of development. Additionally, when comparing individuals from the same species, some of them are highly variable (i.e., *M. kar*) while others are pretty robust in their overall root size (i.e., *M. her*). When comparing among species, the clearest differences in overall root size were observed at 129 days after germination, in which time *M. kar* has the highest values, while *M. her*, *M. car*, and *M. cru* have the lowest values.

Regarding the principal root, it has an accelerated growth during the first developmental stages but later stagnates toward the later stages. None of the species principal roots exceeded the 60 mm of length. However, the principal root was one of the attributes with large variation among individuals of the same species, such as in *M. duw* and *M. kar*, while variation is tighter in *M. her*. A similar pattern was observed for the attributes of lateral roots.

Basal roots were present in all species, which was different to what occurs in *M. haageana*, in which basal roots are rare. In non-*Supertextae* species, basal root proliferation and growth was constant, having *M. kar* and *M. duw* the highest values. However, when observing the presence and length of adventitious roots, most species lacked them, being *M. her*, *M. cru*, and *M. duw* the species with the outstanding values. Moreover, the emergence of adventitious roots seems to be a stochastic event, in which some of the individuals within a species develop these types of roots while others do not. This was the case of *M. her*, in which adventitious roots can be observed in 50% of the plants. These two attributes, the presence of basal and adventitious roots can be interpreted as strategies to cope with stresses, as we reported for the cacti species *Echinocactus platyacanthus* grown under salt conditions (Rosas et al., 2021); but the fact that not all plants present these types of roots could also be interpreted as a pre-established bet-hedging strategy to cope with challenging environmental circumstances, as has been shown for other type of traits in model organisms such as yeast (Levy et al., 2012).

Comparing Trends of Natural Variation and Diversity in Root Architecture

In order to compare the trends of natural variation in *M. haageana* species, and the two levels of diversity in *Supertextae* Series and other non-*Supertextae* species, we performed a euclidean clustering analysis on the medians of eight root variables corresponding to TRL, PRL, TLRL, ARL, BRL, nLR, nAR, and nBR (**Figure 6A**). Performing the same clustering analysis using five root variables, excluding the number of different types of roots, gave a similar result (**Supplementary Figure 2**), recapitulating a similar clustering topography. We found four main clusters: the first cluster contains most *Supertextae* species (except for *M. cru*), as well as three non-*Supertextae* species (*M. for*, *M. pec*, and *M. las*); the cluster also includes three accessions of *M. haageana* (*M. h. san*, CC025 and CC045), which might be expected as *M. haageana* is one of the *Supertextae* species. Thus, this cluster shows a mixture of *Supertextae* species plus non-*Supertextae* species. The second cluster contains mostly non-*Supertextae* species in addition to *M. cru* which belongs to *Supertextae*, once again showing an asymmetric mixture *Supertextae* and non-*Supertextae* species. Interestingly, the third and fourth cluster grouped together most of the *M. haageana* accessions, leaving outside the cluster *M. h. san*, CC025, and CC045, which belonged to the first cluster. Within the fourth cluster, CC020 and CC021 grouped together, and this would be expected as these accessions were classified as *M. haageana* subsp. *haageana* (Guzmán et al., 2003), and their locations are within 10–12 km from one another. A similar case was observed on CC031 and CC032, grouping together in cluster three, which are classified as *M. haageana* subsp. *meissneri* (Guzmán et al., 2003), and whose populations are located 2 km away from one another. However, CC025 falls within cluster one, despite being within 5–6 kms from CC024 (in cluster three), both of them classified as *M. haageana* subsp. *meissneri*, but being CC025 more similar to *M. haageana* subsp. *san-angelensis*, which is located more than 230 km from those populations, inhabiting a completely different environment. Finally, *M. kar* does not cluster with any of the rest of the *Mammillaria* genotypes; this species is characterized by the prominent development of basal roots (**Figure 4**), which might be an adaptation to the environments where it is present. In addition, *M. kar* is the

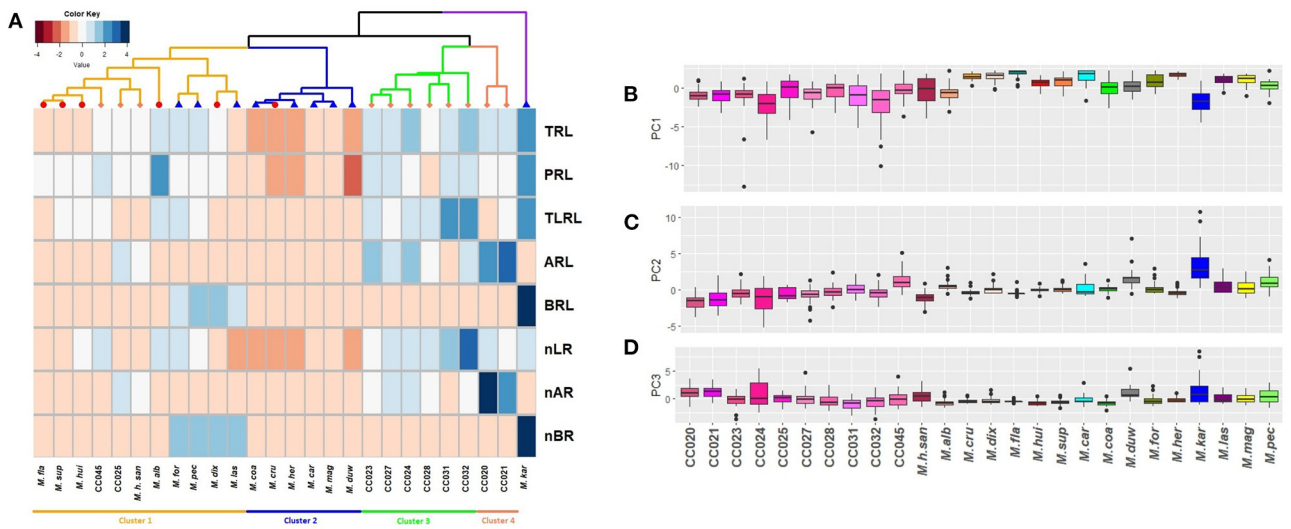

FIGURE 6 | Trends of phenotypic variation at different evolutionary levels. **(A)** Clustering (Euclidean distance) of *Mammillaria* accessions according to their root architecture phenotypes at 129 days after germination developmental stage. On dendrogram, coral rhomboids represent *M. haageana* accessions, red circles represent *Supertextae* series species, and blue triangles represent non-*Supertextae* series species. TRL, Total Root Length; PRL, Principal Root Length; TLRL, Total Lateral Root Length; ARL, Adventitious Root Length; BRL, Basal Root Length; nLR, number of Lateral Roots; nAR, number of Adventitious Roots; nBR, number of Basal Roots. **(B–D)** Boxplots of each of the 3 Principal Components that together captured 90.6% of the variation. Significant differences are shown with letters.

sister species of *M. car* (Butterworth and Wallace, 2004), and yet their root architecture was not as similar as it could be expected. However, *M. kar* has an ample distribution range, and it remains to be seen whether other *M. kar* accessions display phenotypic variation, similar to what we observed in *M. haageana*. An interesting observation is that, within the second cluster, which is dominated by non-*Supertextae* species, we found *M. cru*, which was not unexpected as *M. her* and *M. car* have a similar distribution as *M. cru*, mainly in the surroundings of the Tehuacan-Cuicatlan Valley (Arias et al., 2012; Hernández and Gómez-Hinostrosa, 2015), perhaps even in sympatry. The predominant rock type in this cited area is limestone, so it is possible that these species have similar adaptations to the substrate environmental conditions, reflected in their root architecture.

To double check this observation, we performed a Principal Component Analysis, using the above mentioned data (**Figures 6B–D**). We found that 3 PCs capture 90.6% of the variation, having PC1 40.6%, PC2 30.7%, and PC3 19.2% (**Supplementary Figure 3**). Each of the other 5 PCs individually captured <10% each, and therefore we did not further consider them. As for PC1, four root traits contributed to its variance (TRL, TLRL, nRL, and PRL), for PC2 the complementary root traits contributed to its variance (nRB, BRL, nRA, ARL), and the variance of PC3 was a mix of root trait contributions from our eight measured roots attributes (**Supplementary Tables 2, 3**). We then plotted each of the PC-calculated values according to our categories: *M. haageana* accessions, *Supertextae* species, and non-*Supertextae* species. We found that only PC1 was able to distinguish between these three levels of comparison and particularly *M. haageana* accessions from the other species. However, PC2, nor PC3 distinguish between the evolutionary categories, further confirming that the trends of variation between different levels of evolutionary divergence, partially overlap.

If microevolutionary processes recapitulate those of larger evolutionary time-scales, the accessible phenotypic space explored by natural variants within a species, might continuously overlap with the phenotypic space of closely related species, or distantly related species. This is, each of the species might find phenotypic solutions, but often finding the same solutions expressed in other closely related species; the phylogenetically closer the other species are, the more likely species are to find a similar solution. In our analysis, we found that cluster three and four distinguish most of the studied *M. haageana* accessions, showing that *M. haageana* might have found an exclusive phenotypic space for its root architecture; however, three of the accessions fell in cluster one, which in turn is dominated by *Supertextae* species, as well as having three non-*Supertextae* species. Meanwhile, one of the *Supertextae* species (*M. cru*), also fell within cluster two, which was dominated by non-*Supertextae* species. On the other hand, our PCA also showed a similar pattern, in which some trends of variation (i.e., PC1), allowed the distinction of the evolutionary categories, while in other PCs (i.e., PC2 and PC3) the distinction was not possible. This shows a reiterative partial overlap between the lower evolutionary hierarchy and its contiguous higher evolutionary hierarchy. In other words, during the evolutionary process and adaptation to novel environments, the root architecture phenotypes do not fall far from the evolutionary tree.

Despite our detailed root architecture characterization, it is possible that similar to *M. haageana*, other *Mammillaria* species

with wide distribution such as *M.car*, *M.alb*, *M. kar*, *M. mag*, *M. las*, *M. for*, and *M. hui*, might have local variants, and therefore their root phenotypes are only one small sample of the range of phenotypes the species can have. Thus, a similar approach to what was performed in *M. haageana* accessions is necessary for a more robust interpretation.

DISCUSSION

What originates macroevolutionary diversity has been for a long time the subject of discussion. One possibility is that the cumulative effects of microevolutionary processes within species give rise to the phenotypic diversity seen among species. Here we showed that when studying the root growth dynamics in root architecture, natural variants of *M. haageana* partially recapitulate the breath of diversity observed in a set of *Mammillaria* species at two different evolutionary time-scales. This might be because, as species evolve and diversify, their natural variants explore the phenotypic space, often reaching the same phenotypic spaces from other species, but also providing the grounds for diversification and speciation. In other words, the outcome of phenotypic microevolution partially recapitulates the patterns generated at the macroevolutionary level, in root architecture in *Mammillaria* species.

Understanding morphological variation is often focused on phenotypes that are relatively easy to observe. Despite being one half of the plant and having relevance for plant nutrition and establishment, plant roots are often overlooked. In cacti and other succulent species this is particularly important because plant roots are an essential organ in charge of foraging water and nutrients which are often scarce in their environments. Here we presented one of the first surveys of root development at different evolutionary time-scales. What remains to be studied is how and why these root phenotypic growth patterns have originated, either driven by stochastic or adaptive evolution, and what genomic footprints these processes have left behind. In this sense, we have started these studies at the genetic and phenotypic level (Hinojosa-Alvarez et al., 2020; Cervantes et al., 2021), which complement other studies on the population genetics and genomic constitution of *Mammillaria* species (Solórzano et al., 2014, 2019; Solórzano and Dávila, 2015; Chincoya et al., 2020). Our results indicate that there is ample variation within a single species, *M. haageana*, which is also present in a range of environments, allowing us to further study the associations between root phenotypes and their environmental conditions of origin. However, this also raises issues about the possible links that can be detected when studying associations of species with the environment, because it is usual (as was our case in non-*M. haageana* species) to take a single accession to represent the entire species, leaving aside the natural variation within each species.

According to our data, the root of *Mammillaria* species is short, because the length of the principal root does not exceed 80 mm in our evaluated time-frame. However, lateral and basal root branches are generated from the principal root, and some species also develop adventitious roots, leading us to think that the root system is shallow and extends horizontally. In fact, it has been proposed that the basal and adventitious roots in *E. platyacanthus* might play an important role during early growth of seedlings under salt stress (Rosas et al., 2021). It has been reported that in other cacti species the root system extends over the most superficial layers of the soil, and this might be an adaptation that allows roots to absorb rainwater quickly (Nobel, 1977; Gulmon et al., 1979; Hunt and Nobel, 1987; Niklas et al., 2002). In other plant species, it has been proposed through mathematical models and experimental validation, that genotypes with shallow and horizontally extended root systems improve the absorption of nutrients such as phosphorus, which has restricted mobility across the soil layers (Heppell et al., 2015; Camilo et al., 2021). Thus, we think that the *Mammillaria* (and perhaps other cacti) root system growth, might display strategies to cope with water stress and low phosphorus soils.

Our phenotypic characterization of root architecture growth was performed in controlled environmental conditions in order to minimize the environmental effects on the phenotype. This meant that our results might have interpretation limitations regarding our experimental environment, and perhaps these types of approaches should be done in multiple environments. However, jumping to a natural or semi natural condition poses a different set of limitations as previously shown in model species (Wilczek et al., 2009; Richards et al., 2012). Further research should be done to attempt bridging the gap between the lab and natural environments. Finally, in the wake of climate change and imminent prolonged droughts, we urge the community to draw more attention toward understanding drought tolerant plants such as cacti, and particularly roots in succulent plants, as this key organ might hold novel insights into water harvesting.

DATA AVAILABILITY STATEMENT

The datasets presented in this study can be found in online repositories. The names of the repository/repositories and accession number(s) can be found in the article/**Supplementary Material**.

AUTHOR CONTRIBUTIONS

JG-S, IS-S, JL-G, CC, JR-S, SA, and UR designed the research. SA and UR provided the research funds. JG-S, IS-S, and JL-G performed the experiments. IS-S, CC, SA, and UR collected seeds of *M. haageana* accessions. JR-S and SA provided seeds of non-*M. haageana* species. PV determined the identity of fungal contamination. JC-L and JG-S performed statistical analyses. JG-S, IS-S, JL-G, JC-L, and UR prepared the figures. UR and JG-S wrote the manuscript. JG-S, JC-L, and CC edited the manuscript. All authors contributed to the article and approved the submitted version.

FUNDING

This work was supported by UNAM-PAPIIT IN211319 to UR. JG-S and JC-L are MSc students, and CC is a doctoral student, all from Posgrado en Ciencias Biológicas, Universidad

Nacional Autónoma de México (UNAM), and received the fellowship 1085433, 1084692, and 631251, respectively, from Consejo Nacional de Ciencia y Tecnología (CONACyT-México). This work was done at Laboratorio Nacional de Biodiversidad (CONACyT-México), grant 268109 to UR.

SUPPLEMENTARY MATERIAL

The Supplementary Material for this article can be found online at: https://www.frontiersin.org/articles/10.3389/fpls.2021.750623/full#supplementary-material

REFERENCES

Arias, S., Gama-López, S., Guzmán-Cruz, L. U., and Vázquez-Benítez, B. (2012). "Flora del Valle de Tehuacán-Cuicatlán," in *Fasciculo 95. Cactaceae Juss,* 2nd Edn. eds. R. Medina Lemos, J. G. Sánchez Ken, A. García Mendoza, and S. Arias (Mexico City, Mexico: Intituto de Biología, UNAM).

Bravo, H., and Sánchez-Mejorada, H. (1991). *Las Cactáceas de México, Vol III*. 1st Edn. Mexico City, Mexico: UNAM.

Breslin, P. B., Wojciechowski, M. F., and Majure, L. C. (2021). Molecular phylogeny of the Mammilloid clade (Cactaceae) resolves the monophyly of *Mammillaria*. *Taxon* 70, 308–323. doi: 10.1002/tax.12451

Butterworth, C. A., and Wallace, R. S. (2004). Phylogenetic studies of *mammillaria* (CACTACEAE)—insights from chloroplast sequence variation and hypothesis testing using the parametric bootstrap. *Am. J. Bot.* 91, 1086–1098. doi: 10.3732/ajb.91.7.1086

Camilo, S., Odindo, A. O., Kondwakwenda, A., and Sibiya, J. (2021). Root traits related with drought and phosphorus tolerance in common bean (*Phaseolus vulgaris* L.). *Agronomy* 11, 1–14. doi: 10.3390/agronomy11030552

Cervantes, C. R., Hinojosa-Alvarez, S., Wegier, A., Rosas, U., and Arias, S. (2021). Evaluating the monophyly of *Mammillaria* series Supertextae (Cactaceae). *PhytoKeys* 177, 25–42. doi: 10.3897/phytokeys.177.62915

Chincoya, D. A., Sanchez-Flores, A., Estrada, K., Díaz-Velásquez, C. E., González-Rodríguez, A., Vaca-Paniagua, F., et al. (2020). Identification of high molecular variation loci in complete chloroplast genomes of *Mammillaria* (Cactaceae, caryophyllales). *Genes* 11, 1–11. doi: 10.3390/genes11070830

Christian, D. A., Palomino, G., García, A., and Méndez, I. (2006). Nuclear genome size and karyotype analysis in *Mammillaria* species (cactaceae). *Caryologia* 59, 177–186. doi: 10.1080/00087114.2006.10797914

Colchado-López, J., Cervantes, R. C., and Rosas, U. (2019). A linear model to describe branching and allometry in root architecture. *Plants* 8, 1–11. doi: 10.3390/plants8070218

Davis, J. I., and Gilmartin, A. J. (1985). Morphological variation and speciation. *Syst. Bot.* 10, 417–425. doi: 10.2307/2419135

Delgado-Sánchez, P., Jiménez-Bremont, J. F., Guerrero-González, M., de la, L., and Flores, J. (2013). Effect of fungi and light on seed germination of three Opuntia species from semiarid lands of central Mexico. *J. Plant Res.* 126, 643–649. doi: 10.1007/s10265-013-0558-2

Fay, M. F., and Gratton, J. (1992). Tissue culture of cacti and other succulents: a literature review and a report on micropropagation at Kew. *Bradleya* 10, 33–48. doi: 10.25223/brad.n10.1992.a4

Gulmon, S. L., Rundel, P. W., Ehleringer, J. R., and Mooney, H. A. (1979). Spatial relationships and competition in a chilean desert cactus. *Oecologia* 44, 40–43. doi: 10.1007/BF00346395

Guzmán, U., Salvador, A., and Dávila, P. (2003). *Catálogo de Cactéceas mexicanas*. 1st Edn. Mexico City, Mexico: CONABIO, UNAM.

Heppell, J., Talboys, P., Payvandi, S., Zygalakis, K. C., Fliege, J., Withers, P. J. A., et al. (2015). How changing root system architecture can help tackle a reduction in soil phosphate (P) levels for better plant P acquisition. *Plant Cell Environ.* 38, 118–128. doi: 10.1111/pce.12376

Hernández, H. M., and Gómez-Hinostrosa, C. (2015). *Mapping the Cacti of Mexico Part II: Mammillaria*. 1st Edn, ed. D. Hunt (Milborne Port, England: DH Books).

Hernández-Hernández, T., Brown, J. W., Schlumpberger, B. O., Eguiarte, L. E., and Magallón, S. (2014). Beyond aridification: multiple explanations for the elevated diversification of cacti in the new world succulent biome. *New Phytol.* 202, 1382–1397. doi: 10.1111/nph.12752

Hinojosa-Alvarez, S., Arias, S., Ferrand, S., Purugganan, M. D., Rozas, J., Rosas, U., et al. (2020). The chloroplast genome of the pincushion cactus *Mammilllaria haageana* subsp. san-angelensis, a Mexican endangered species. *Mitochondrial DNA Part B.* 5, 2038–2039. doi: 10.1080/23802359.2020.1757523

Hunt, D. (1983). A new review of *Mammillaria* names A-C. *Bradleya* 1, 105–128. doi: 10.25223/brad.n1.1983.a10

Hunt, D. R., Taylor, N. P., and Glass, H. (2006). *The new Cactus Lexicon: Descriptions and Illustrations of the Cactus Family*. 1st Edn. Milborne Port: DH Books.

Hunt, E. R., and Nobel, P. S. (1987). A two-dimensional model for water uptake by desert succulents: Implications of root distribution. *Ann. Bot.* 59, 559–569. doi: 10.1093/oxfordjournals.aob.a087350

Levy, S. F., Ziv, N., and Siegal, M. L. (2012). Bet hedging in yeast by heterogeneous, age-correlated expression of a stress protectant. *PLoS Biol.* 10:e1001325. doi: 10.1371/journal.pbio.1001325

Lüthy, J. M. (1995). *Taxonomische untersuchung der gattung Mammillaria Haw*. (dissertation/doctoral thesis). [Bern(Suiza)]:Universität Bern.

Martino, P. A., Bauk, K., Ferrero, M. C., Gurvich, D. E., and Las Peñas, M. L. (2018). Ecological significance of determinate primary root growth: inter- and intra-specific differences in two species of *Gymnocalycium* (Cactaceae) along elevation gradients. *Flora* 248, 70–75. doi: 10.1016/j.flora.2018.09.001

Mociño, J. M., and Sessé, M. (2015). *La Real Expedición Botánica a Nueva España Tomos I-XIII*. 1st Edn. Mexico City, Mexico: Coordinación de Humanidades, UNAM.

Niklas, K. J., Molina-Freaner, F., Tinoco-Ojanguren, C., and Paolillo, D. J. (2002). The biomechanics of *Pachycereus pringlei* root systems. *Am. J. Bot.* 89, 12–21. doi: 10.3732/ajb.89.1.12

Nobel, P. S. (1977). Water relations and photosynthesis of a barrel cactus, Ferocactus acanthodes, in the Colorado desert. *Oecologia* 27, 117–133. doi: 10.1007/BF00345817

Okamoto, K. W., Langerhans, R. B., Rashid, R., and Amarasekare, P. (2015). Microevolutionary patterns in the common caiman predict macroevolutionary trends across extant crocodilians. *Biol. J. Linn. Soc.* 116, 834–846. doi: 10.1111/bij.12641

Pilbeam, J. (1999). *Mammillaria*. 1st Edn. Oxford: Nuffield Press,.

R Core Team (2020). *R: A Language and Environment for Statistical Computing*. R Foundation for Statistical Computing. Available online at: https://www.r-project.org/ (accessed September 03, 2021).

Reppenhagen, W. (1992). *Die gattung Mammillaria. Monographie.* Vol. 2. Titisee-Neustadt, Germany: Druckerei Steinhart.

Richards, C. L., Rosas, U., Banta, J., Bhambhra, N., and Purugganan, M. D. (2012). Genome-wide patterns of Arabidopsis gene expression in nature. *PLoS Genet.* 8, 1–14. doi: 10.1371/journal.pgen.1002662

Rodriguez-Alonso, G., Matvienko, M., López-Valle, M. L., Lázaro-Mixteco, P. E., Napsucialy-Mendivil, S., Dubrovsky, J. G., et al. (2018). Transcriptomics insights into the genetic regulation of root apical meristem exhaustion and determinate primary root growth in Pachycereus pringlei (Cactaceae). *Sci. Rep.* 8, 1–11. doi: 10.1038/s41598-018-26897-1

Rosas, U., Lara-González, J. A., De-la-Rosa-Tilapa, A., and Terrazas, T. (2021). Persistent adventitious and basal root development during salt stress tolerance in *Echinocactus platyacanthus* (Cactaceae) seedlings. *J. Arid Environ.* 187, 1–5. doi: 10.1016/j.jaridenv.2020.104431

Scheinvar, L. (2004). *Flora cactológica del Estado de Querétaro Diversidad y Riqueza*. 1st Edn. Mexico City, Mexico: Fondo de Cultura Económica.

Shishkova, S., Las Peñas, M. L., Napsucialy-Mendivil, S., Matvienko, M., Kozik, A., Montiel, J., et al. (2013). Determinate primary root growth as an adaptation to aridity in Cactaceae: towards an understanding of the evolution and genetic control of the trait. *Ann. Bot.* 112, 239–252. doi: 10.1093/aob/mct100

Solórzano, S., Chincoya, D. A., Sanchez-Flores, A., Estrada, K., Díaz-Velásquez, C. E., González-Rodríguez, A., et al. (2019). *De novo* assembly discovered novel structures in genome of plastids and revealed divergent inverted

repeats in *Mammillaria* (Cactaceae, Caryophyllales). *Plants* 8, 1–16. doi: 10.3390/plants8100392

Solórzano, S., Cuevas-Alducin, P. D., García-Gómez, V., and Dávila, P. (2014). Genetic diversity and conservation of *Mammillaria huitzilopochtli* and *M. supertexta*, two threatened species endemic of the semiarid region of central Mexico. *Rev. Mex. Biodivers.* 85, 565–575. doi: 10.7550/rmb.39066

Solórzano, S., and Dávila, P. (2015). Identification of conservation units of *Mammillaria crucigera* (Cactaceae): perspectives for the conservation of rare species. *Plant Ecol. Divers.* 8, 559–569. doi: 10.1080/17550874.2015.1044581

Villaseñor, J. L. (2016). Checklist of the native vascular plants of Mexico. *Rev. Mex. Biodivers.* 87, 559–902. doi: 10.1016/j.rmb.2016.06.017

Wilczek, A. M., Roe, J. L., Knapp, M. C., Cooper, M. D., Lopez-Gallego, C., Martin, L. J., et al. (2009). Effects of genetic perturbation on seasonal life history plasticity. *Science* 323, 930–934. doi: 10.1126/science.1165826

Wittkopp, P. J., Stewart, E. E., Arnold, L. L., Neidert, A. H., Haerum, B. K., Thompson, E. M., et al. (2009). Intraspecific polymorphism to interspecific divergence: genetics of pigmentation in drosophila. *Science* 326, 540–544. doi: 10.1126/science.1176980

Conflict of Interest: The authors declare that the research was conducted in the absence of any commercial or financial relationships that could be construed as a potential conflict of interest.

frontiers in Plant Science

ORIGINAL RESEARCH
published: 28 January 2022
doi: 10.3389/fpls.2021.814110

Genetic Variability of *Arabidopsis thaliana* Mature Root System Architecture and Genome-Wide Association Study

*Agnieszka Deja-Muylle[1,2], Davy Opdenacker[1,2], Boris Parizot[1,2], Hans Motte[1,2], Guillaume Lobet[3], Veronique Storme[1,2], Pieter Clauw[4], Maria Njo[1,2] and Tom Beeckman[1,2]**

[1] Department of Plant Biotechnology and Bioinformatics, Ghent University, Ghent, Belgium, [2] VIB Center for Plant Systems Biology, Ghent, Belgium, [3] Forschungszentrum Jülich GmbH, Agrosphere (IBG-3), Jülich, Germany, [4] Gregor Mendel Institute of Molecular Plant Biology, Vienna, Austria

Root system architecture (RSA) has a direct influence on the efficiency of nutrient uptake and plant growth, but the genetics of RSA are often studied only at the seedling stage. To get an insight into the genetic blueprint of a more mature RSA, we exploited natural variation and performed a detailed *in vitro* study of 241 *Arabidopsis thaliana* accessions using large petri dishes. A comprehensive analysis of 17 RSA traits showed high variability among the different accessions, unveiling correlations between traits and conditions of the natural habitat of the plants. A sub-selection of these accessions was grown in water-limiting conditions in a rhizotron set-up, which revealed that especially the spatial distribution showed a high consistency between *in vitro* and *ex vitro* conditions, while in particular, a large root area in the lower zone favored drought tolerance. The collected RSA phenotype data were used to perform genome-wide association studies (GWAS), which stands out from the previous studies by its exhaustive measurements of RSA traits on more mature *Arabidopsis* accessions used for GWAS. As a result, we found not only several genes involved in the lateral root (LR) development or auxin signaling pathways to be associated with RSA traits but also new candidate genes that are potentially involved in the adaptation to the natural habitats.

Keywords: root systems architecture, genome-wide association study, *Arabidopsis thaliana*, ecotypes, accession, root development, rhizotron

OPEN ACCESS

Edited by:
Raffaele Dello Ioio, Sapienza University of Rome, Italy

Reviewed by:
Riccardo Di Mambro, University of Pisa, Italy
Peng Yu, University of Bonn, Germany

***Correspondence:**
Tom Beeckman
tom.beeckman@psb.vib-ugent.be

Specialty section:
This article was submitted to Plant Development and EvoDevo, a section of the journal Frontiers in Plant Science

Received: *12 November 2021*
Accepted: *15 December 2021*
Published: *28 January 2022*

Citation:
Deja-Muylle A, Opdenacker D, Parizot B, Motte H, Lobet G, Storme V, Clauw P, Njo M and Beeckman T (2022) Genetic Variability of Arabidopsis thaliana Mature Root System Architecture and Genome-Wide Association Study. Front. Plant Sci. 12:814110. doi: 10.3389/fpls.2021.814110

INTRODUCTION

Crops are in high need of improvement for higher yield and resistance to environmental stresses (Ray et al., 2013). The focus on the yield, however, makes it easy to forget that one of the most important parts of the plant cannot be seen: the hidden underground. Due to ongoing climate changes, all over the world, the breeders look for ways of modulating underground plant parts to improve the overall plant growth and yield efficiency (Rogers and Benfey, 2015; Chen et al., 2019). To obtain this goal, they focus on root system architecture (RSA) which is a concept used to summarize and calculate all aspects of root development. The RSA describes the spatial configuration of the overall root structure in the substrate it is growing in and includes the initiation and development of different subparts of the root and the speed of root growth. The RSA adapts to a changing environment and is responsible for the most optimal nutrient uptake depending on the conditions (Oldroyd and Leyser, 2020). *Arabidopsis thaliana* has been used as a model organism to

study all aspects of plant biology and the root has turned out to be a very elegant model organ for cell and developmental biology studies. Typically, roots are studied on young seedlings grown for a short period on vertical agar plates, commonly for 5 or 7 days (Zhao et al., 2017; Ogura et al., 2019), a developmental phase characterized by a still premature root system hardly showing higher order LRs. To our knowledge, up to date, only one study analyzed traits 16 days after sowing, but in this case, the roots were grown under different stresses which had a negative influence on their overall size (Rosas et al., 2013).

It is very well known that RSA can strongly vary depending on the environmental conditions that influence the three-dimensional distribution of the primary and LRs (Del Bianco and Kepinski, 2018). But plasticity of traits is also driven by genetic variation that shapes RSA. Within one species, local populations might have adapted their RSA to the prevailing environmental conditions which might have become a heritable trait. Such root types have obtained a genetic imprint and could be used to get insight into the genetic basis for root system adaptation to environmental conditions. A previous study demonstrated the wide natural variability in RSA among 12 *Arabidopsis* accessions that were collected originally from different geographical areas (Aceves-García et al., 2016).

In this study, we analyzed the RSA of 241 accessions incubated for 21 days in large Nunc plates (24 cm × 24 cm). The results show a broad range of variability for all parameters tested and represent a unique description of the existing natural variation in root system architecture in the *Arabidopsis* species. A selection of four accessions with a contrasting RSA was tested in rhizotrons and subjected to water limiting conditions to correlate root traits with plant performance in drought conditions. Finally, a GWA study was conducted, indicating potential genetic loci responsible for the implementation of specific root system architectures.

MATERIALS AND METHODS

Plant Material

A seed collection of 328 *A. thaliana* accessions has been selected from the Hap-Map population based on habitat, geographical information, or previously described interesting root or/and shoot phenotype. About 120 accessions were obtained from an in-house collection derived from the Nottingham Arabidopsis Stock Centre (NASC), the rest was retrieved directly from NASC (Scholl et al., 2000). The lines that did not germinate, flower, or perform poorly, were discarded from the analysis. The final set of plant material, that has been subjected to root analysis included 241 accessions (**Supplementary Table 1**). Seeds were gas-sterilized with chlorine (150 ml NaOCl with 8 ml HCl, overnight, in a closed container). Next, the seeds were vernalized at 4°C for 4 days. The values of climate temperature and precipitation have been collected for precise longitude and latitude locations, for the years: 1989–2019 from an online climate data source[1]. Soil types have also been noted based on the geographical localization of accessions, sourced from an online data source[2].

[1]https://climatecharts.net/

[2]https://data.isric.org/geonetwork/srv/pol/catalog.search#/home

Growth Conditions and Image Acquisition

Phenotyping occurred in 10 experimental repeats, each lasting 21 days. Seeds were stratified for 4 days and sown on small petri dish plates (12 cm × 12 cm, Novolab) on 1/2 MS medium with 0.6% Gelrite as a gelling agent according to the protocol (**Supplementary Word File 1**). Plates were placed in the growth chamber, with the following controlled conditions: 21°C and day/night light cycle (16h/8h), under 110 $\mu E/m^2/s$ photosynthetically active radiation (cool-white fluorescent tungsten tubes, Osram GmbH, Munich, Germany). After germination, the seedlings of similar size were transferred to large Nunc plates (24 cm × 24 cm) and placed back to the same conditions of growth. Placement of accessions on each plate and placement of plates in the growth chamber were randomized based on incomplete block design. According to this design, each accession was present in each repeat but with a variable number, different for each repeat and each accession. Each plate contained three plants from three different accessions. Col-0 was incorporated in the block design so that it was present in each repeat in a random number. At 14 days after germination, the plates were scanned on a high-resolution flatbed scanner, equipped with backlight illumination (Epson®Expression 11000XL, Seiko Epson Corporation, Nagano, Japan). First, the rosette was excised carefully to keep only the root on the plate for clear imaging. Shoot biomass was measured immediately after excision. The fresh weight of the root was measured instantly after image acquisition.

Image Analysis and Phenotyping

Each singular root image has been cut out from a plate picture, with an in-house written script for ImageJ. This program was also used manually to remove artifacts in the root images and maintain one root image per picture. Next, each root picture was analyzed with GiA Roots (Galkovskyi et al., 2012). About 15 traits were analyzed. Six spatial distribution traits have been measured for each image: length distribution, projected area, convex area, solidity, and total root length. Additional two traits, such as the root width and root depth, were analyzed with the use of an in-house written ImageJ script. The total number of LRs and the primary root length were calculated automatically *via* the Root Reader 2D plugin (Clark et al., 2013). The number of first order LRS were scored manually. Subsequently, the root biomass to shoot biomass ratio, width to depth ratio, and LR density were derived from the initial measurements. Additionally, Principal Component Analysis (PCA) was performed with ImageJ plugin routine: MariaJ (Bourne, 2010) on the root shape trait, with the help of the in-house build R script. The shape analysis was obtained by automatically placing pseudo landmarks along with the root profile and extracting their position. The position of the different landmarks was then analyzed using a PCA. This PCA allowed computing the average root system shape and the principal shape modifications observed in the dataset (represented by the different PCs). Altogether, 18 traits have been scored (**Figure 1** and **Table 1**). Correlation coefficients were calculated based on Pearson's correlation.

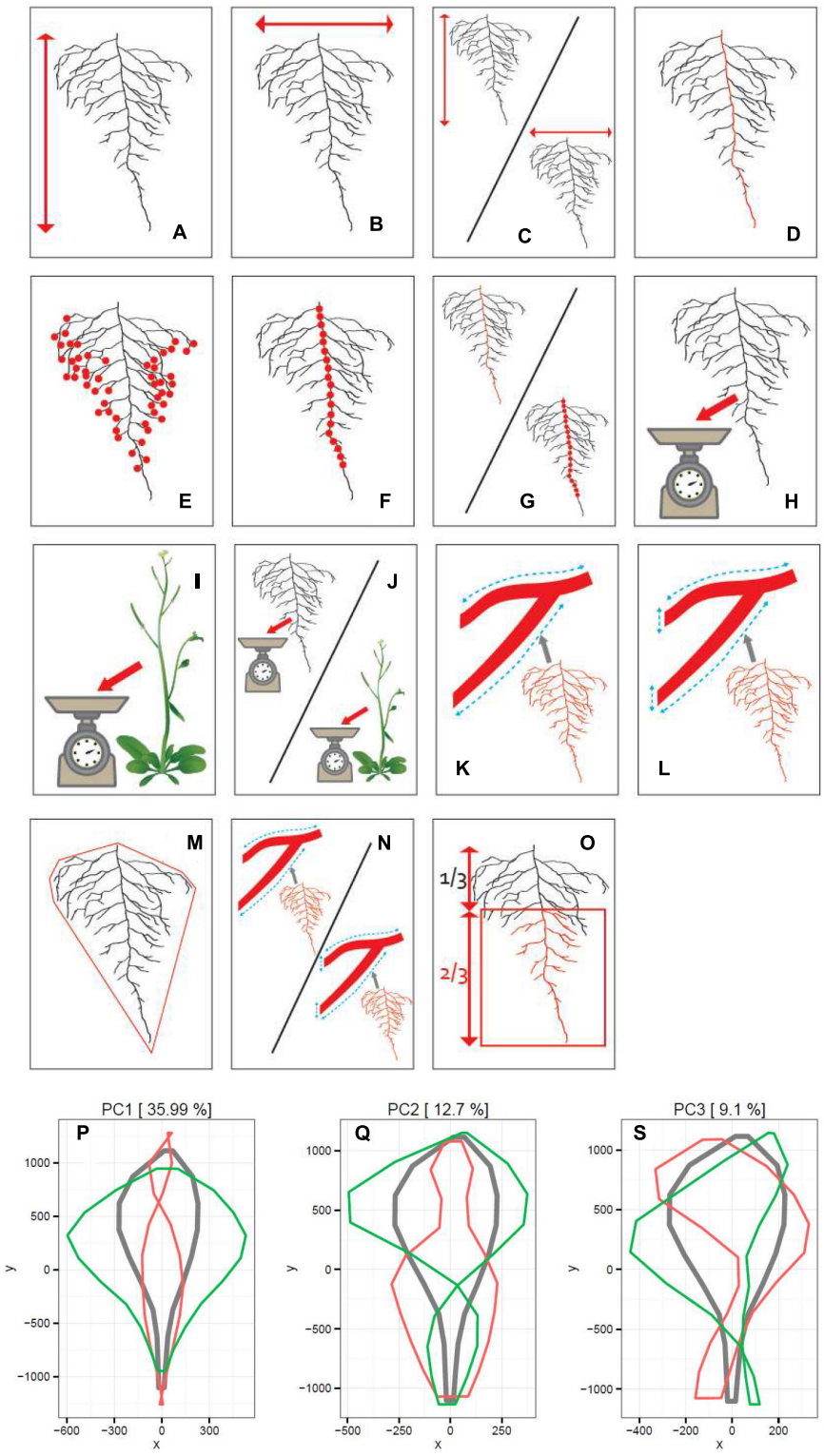

FIGURE 1 | Schematic representation of 15 RSA and 3 PC traits measured on 241 accessions. Panels from **(A–O)** correspond to 15 traits listed in **Table 1**. In Panels **(P,R,S)**, the results of the PCA are shown. The red line represents the maximum and the green line the minimum values observed. The gray line represents the average of all values for 241 accessions.

Rhizotron in Soil Study

To study the RSA in soil, we used an in-house built rhizotron set-up. The rhizotron system consists of flat boxes comprising two plastic sheets with a space of 4 mm filled with potting soil. A detailed protocol on the rhizotron assembly and preparation can be found in the study by Kerstens et al. (2021). The soil substrate in this study was a commercial mix (Aveve potting soil universal use 20L/bag). It was first sieved (Professional sieve; Model: nr 8, total diameter: 450 mm, total height: 100 mm, mesh size: 2.8 mm, diameter: 0.45 mm), dried, and loaded into the rhizotrons in a repeatable manner, allowing for equal density of soil. Next, rhizosheets were submerged into a water bath (2 ml/L Wuxal 8-8-6 solution, diluted with purified water) to ensure saturation of soil in the sheet before sowing. After 24 h, all rhizosheets were placed into scaffolding at an angle of 43 degrees, with the transparent wall facing downward. A micropore tape that was used to seal the top of each sheet during the water saturation period, was removed, and 5 seeds (stratified for 2 days) were placed in the middle of the soil surface. Saran foils were placed for the first 5 days to ensure humidity for germination. After this time, only one well-developed seedling was selected and the others were removed manually. About 5 ml of a diluted (2 ml/L) Wuxal solution[3] was applied each day to a set of 24 sheets in well-watered conditions. For drought experiments, watering was withdrawn to create mild water and nutrient stress in a parallel set of 24 sheets. Analysis of the root systems was performed 24 days after germination. Plates were scanned on a flatbed scanner (Epson®Expression 11000XL) and additionally, each sheet was photographed including the above-ground parts. Next, the shoots were excised and the length of the inflorescence stems was measured. The rosettes were imaged and the weight of the above-ground parts was determined. The rosette area and the dry and fresh weight of the stem and rosette were measured via an ImageJ in-house created script. The length measurements of roots were scored by hand: Root Width, Depth, PR Length, Convex Area, and Solidity. Additionally, an in-house written ImageJ script was used to determine how root growth is spatially distributed in the sheets. Two models were created. The first model consisted of 4 equal zones out of the whole length of the rhizosheet. The second model used 3 equal zones out of the whole length of the root system. The first model provides insight into the root development in function of the depth of the rhizosheet, while the second is more informative about the overall root development in function of root depth (**Supplementary Table 2**). Traits measured on both models included centroid, root area distribution, and root distribution.

Genome-Wide Association Study

Phenotype data were collected for all 15 root traits. Means were calculated for each of the traits, for each accession. Then, broad-sense heritability (H^2) for all RSA traits was calculated as the ratio of the genetic variation over the total phenotypic variation, with the total phenotypic variation being the sum of the genetic and environmental variation. Genetic variation was estimated as the variance explained by the genotype in a random effect model. The environmental variation was estimated as the residual variation from the random effect model. The random-effect model was constructed using the R package, "sommer" (4). To perform a genome-wide association study (GWAS), a publicly available collection of 250k single nucleotide polymorphism (SNP) array data was used (5). The QTCAT approach was chosen to perform the association analysis based on its in literature highlighted feature to outperform other methods *via* implementation of hierarchical testing to control the population structure (Klasen et al., 2016). As a first step, the means were log-transformed. Subsequently, QTCAT analysis was performed in the R-package program using codes available from the online freeware resource (6) (**Supplementary Word File 2**). The R analysis automatically records the positioning of significant associations and generates the results as a list and in a visual way as Manhattan plots. Significant SNPs are selected automatically based on family-wise error rate (FWER). Afterward, the genes in the 20kb window around the significant SNP (10 kb up and downward) were searched manually *via* the JBrowse platform (7) and listed (**Supplementary Table 5**) as genes of interest.

RESULTS

Natural Variation of the *Arabidopsis* Taproot System

To assess the natural variation of RSA parameters at an advanced stage, 241 *Arabidopsis* accessions were grown in large petri-dishes (24 cm × 24 cm). About 2,659 root pictures were collected and 15 RSA traits were measured (**Table 1**). Additionally, three traits have been established by means of PCA of root shape. All traits showed a broad variation (**Supplementary Figure 1**) over the different accessions. The spread of trait values is illustrated in **Figure 2**, where we selected the 11 contrasting accessions (chosen based on their score as among the 10 highest or lowest values for the following 5 traits: convex area, root depth and width, the total number of LRs, and/or total length) in terms of 9 RSA traits to make scatter plots. The plots directly point not only to accessions that have a similar RSA development but also to some that invest more in one trait over the other. For example, at the level of the convex area, the accessions, ICE-181, WC-1, ICE-70, and Stw-0 contrast with Ped-0, C24, Xan-1, Had-1b, Kondara, and Dr-0 with the first ones showing a much larger convex area (**Figure 2A**). Furthermore, Ped-0, Xan-1, C24, Kondara, and Stw-0 developed less deep root systems compared to the other accessions (**Figure 2B**). At the level of solidity, C24, Xan-1, Dr-0, and Stw-O excelled above the others (**Figure 2C**). All measurements can be found in **Supplementary Table 3**.

Several traits showed clear correlations (**Table 2**). Shoot biomass, for example, is strongly positively correlated to root biomass, projected area, and total root length, which confirms that there is an intimate relation between under- and above-ground organs. Other root traits are also positively correlated to shoot biomass, however, in a more moderate manner. The only negative correlation the shoot biomass had was with LR density.

[3]https://www.certiseurope.be/producten/productwijzer/productpage/product/wuxal-super-8-8-6/#skip-content

TABLE 1 | Root system architecture (RSA) traits measured on 241 *Arabidopsis thaliana* accessions and broad-sense heritability values (H^2) measured for 15 RSA traits.

Trait label	RSA trait	Description	Abbreviation	Broad-sense Heritability (H^2)
A	Root Depth	how deep the root grows	RD	0.4703
B	Root Width	how wide the root grows	RW	0.5412
C	Width to Depth Ratio	ratio of the two values	WDR	0.5347
D	Primary Root Length	length of the main root	PRL	0.4702
E	Total Number of Lateral Roots	amount of all lateral roots emerged	TNLR	0.4001
F	Number of 1st Order Lateral Roots	amount of lateral roots initiation on the primary root	NFLR	0.3322
G	Lateral Root Density	Primary Root Length/Number of 1st Order Lateral Roots	LRD	0.3084
H	Root Biomass	fresh weight of the root	RB	0.2903
I	Shoot Biomass	fresh weight of the shoot	SB	0.3920
J	Root Biomass to Shoot Biomass Ratio	ratio of the two values	RBSBR	0.3738
K	Total Root Length	all lengths of the root system	TRL	0.3474
L	Projected Area	sum whole root system length considering the thickness of root parts	PA	0.4027
M	Convex Area	the area of convex hull that encompasses the root by connecting its most outstanding ends	CA	0.5603
N	Solidity	Projected Area divided by Convex Area	S	0.4961
O	Length Distribution	the fraction of the root length found in lower 2/3 of the whole root system	LD	0.4287
P	Principal Component 1	–	PC1	–
R	Principal Component 2	–	PC2	–
S	Principal Component 3	–	PC3	–

Moreover, LR density appeared to be negatively correlated with several other root parameters, such as projected area, solidity, total root length, root biomass, number of first order LR, and the total number of LRs. Root biomass is positively correlated with the convex area, projected area, and total root length but, remarkably as indicated above, not with the lateral root density. This confirms that for an increase in convex area, the elongation of a limited number of root axes rather than the initiation of new ones is important. Overall, the negative correlation of LR density with several parameters suggests that increasing lateral root density may represent an energy-demanding process that occurs at the cost of other growth parameters which might be taken into account in future root-based breeding programs on crops.

The convex area represents the combination of both the depth and width of the root system. From the correlation data, we could observe that the root width has a stronger positive influence (one of the strongest correlations in the dataset) on shaping the convex area as compared to the root depth of which the positive correlation is rather modest.

Logically, root depth and primary root length are strongly correlated which aligns with a correlation between the convex area and primary root length. Convex area and length distribution were moderately negatively correlated with solidity. Solidity at the same time was strongly negatively correlated with parameters that relate to the width of the root system such as root width and width to depth ratio. In other words, the wider, the more diffuse root systems seem to develop. A similar strong negative correlation was observed between convex area and solidity indicating that reaching a larger area of soil can be accomplished by economizing on root growth in the central part of the root system.

Traits related to LR growth also clearly vary among accessions. Some accessions like ICE-70 and Sap-0, have long laterals that branch out mostly in the shootward region of the primary root and thus are growing in the topsoil levels. In contrast, some accessions, such as Knox-10 or ICE-106 are characterized by shorter but more condensed LRs distributed evenly along the primary root. The total number of LRs was much more variable than the order of LRs. Most of the accessions initiate LRs up to the second order. Only a few reached just the first level of branching. An increase in the number of LRs has a direct impact on how compacted a root system becomes. This relation emerges clearly from the correlation analysis (**Table 2**). The total number of LRs was positively correlated with solidity and with other traits such as projected area, total root length, shoot biomass, and root biomass.

Additionally, a PCA was used to explain the variation in the shape of the root system between accessions. Since the shape is different from the convex area and is insensible to size, orientation, not rotation, the most appropriate way of scoring the shape of the root system was to give vectoral artificial points to each root system and analyze the PCA. The analysis divided the shape into 3 PCs collectively explaining 58% of the total variation of that trait observed in this dataset. The PC1 was an indicator of the root system width in the upper half of the total root depth, explaining 36% of the whole root shape variation. The PC2 was influenced by the width of the bottom section of the root system, explaining 13% of the variation. The PC1 and PC2 components can be used to discriminate the different genotypes. The PC3 was responsible for about 9% of total shape variation and was indicative of a very peculiar trait representing the bending of the root system (**Figures 1O,P,R**).

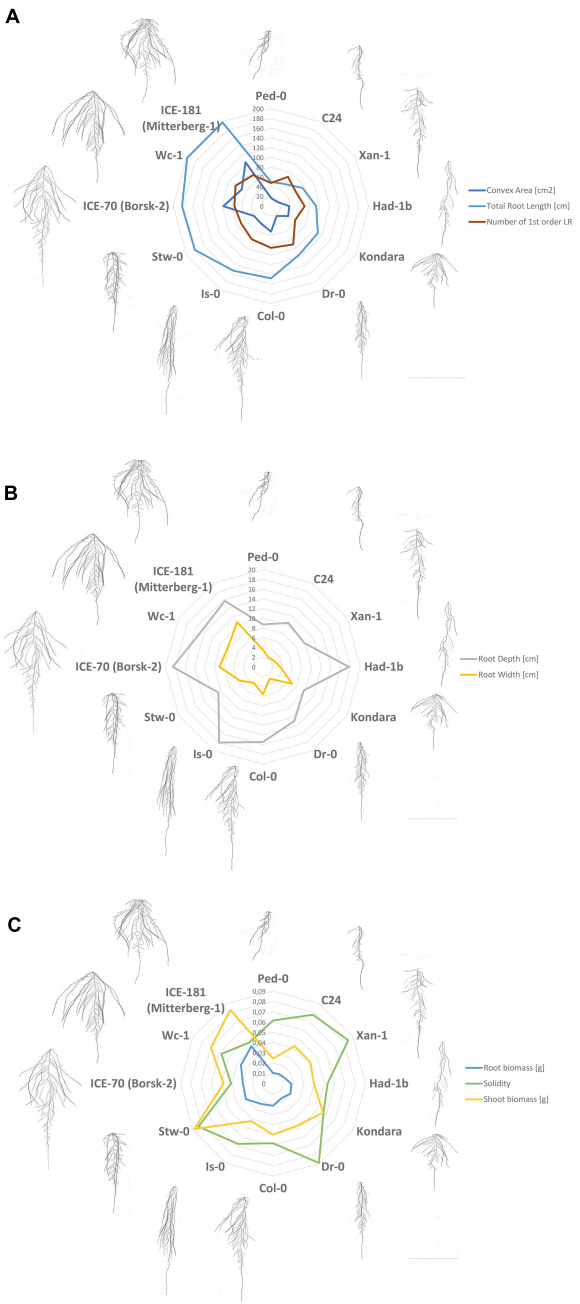

FIGURE 2 | Distribution of RSA traits values for 11 most contrasting accessions and Col-0, represented as scatter plots. **(A)** Convex area [cm^2], total root length [cm], number of first order lateral roots (LRs). **(B)** Root depth [cm] and root width [cm]. **(C)** root biomass [g], shoot biomass [g], and solidity.

For each accession, the sampling location data is known (longitude and latitude). Based on this data, climate-related parameters (yearly mean temperature and yearly mean rainfall), for each geographical location were assembled. This data collection aimed to analyze if habitat location and/or climate may have any influence on root traits. The influence of habitat conditions on root traits was analyzed as correlations and have also yielded striking dependencies (**Table 3**). The yearly mean temperature has a moderate negative influence on all analyzed root traits, indicating that higher temperatures might hamper root development. On the other hand, elevation above the sea level is in moderate positive correlation with most of the traits. Yearly precipitation sum has a moderate negative correlation not only with length distribution, convex area, and root biomass to shoot biomass ratio but also has a moderate positive correlation with solidity. This shows that rainfall seems to favor the development of the aboveground parts of the plant. In regions with limited rainfall, root systems appear less compacted thereby increasing the length distribution and area of soil to explore for underground water sources. To further investigate habitat influence on the root traits of the accessions, we have also obtained information about the type of soil occurring in each habitat. Soil types have been converted into numerical values based on the class of soil. Correlation of root traits to the type of soil was, however, not producing significant results, and thus, we could not draw correlations from this analysis (**Table 3** and **Supplementary Table 4**). This might be due to the fact that available taxonomies are not precise for a non-homogenous soil region (mixture of different types soil types).

Root System Architecture Identified on Plates Corresponds to Root System Architecture in Soil Conditions

To test whether contrasting phenotypes were stable in the genetically encoded traits or rather the expression of growth under artificial conditions in petri-dishes, we decided to grow a selection of contrasting accessions in soil conditions in a rhizotron set-up. For practical reasons (labor intensity and space limitations to handle the in-house built manual rhizotron system), an experimental setup of 4 accessions was considered feasible. First, we classified the 20 most contrasting accessions based on the width to depth ratio. Following, we narrowed down the selection to 3 accessions, Dr-0, Had-1b, and Wc-1, based on their contrast in primary root length and convex area (**Figure 3**). Those 3 accessions, and Col-0 as a control, were grown in 6 repetitions in rhizotron boxes (**Supplementary Figure 2**). Furthermore, we verified the stability of the RSA under high soil moisture content and mild drought conditions (refer to section "Materials and Methods").

In conditions of sufficient water availability, Col-0 and Dr-0 performed similarly to each other for all traits measured (**Figure 4**). For all 4 accessions, root width was similar but PR length and convex area were significantly larger in Had-1b (**Figures 4C,D**). To analyze how roots are distributed in soil, we have divided the rhizotron sheet surface into zones according to two models (refer to section "Materials and Methods"). The analysis of the distribution of roots in rhizosheets revealed additional characteristics of the Had-1b accession. Had-1b, being the longest accessions from the ones analyzed, represented low solidity indicative of a not densely compacted RSA (**Figure 5A**). If we look in more detail at the distribution of LRs in different zones, Had-1b had more LRs in the lower zones of the root system, which is represented by the root area in zones. In the

TABLE 2 | Correlation analysis between 15 RSA traits, based on *p*-Values.

	RSA Convex Area	RSA Solidity	RSA Total Length	Shoot biomass	Root biomass	Shoot/Root biomass	RSA Depth	RSA Width	Width/depth ratio	PR length	1st order LRs	Total number of LRs	LR density
RSA Length Distribution	0,256	–0,429			–0,133	0,141		0,301	0,257		–0,225	–0,22	0,368
RSA Area	0,757		0,952	0,725	0,918	–0,374	0,467	0,654	0,466	0,467	0,441	0,339	–0,15
RSA Convex Area		–0,641	0,636	0,444	0,581	–0,248	0,536	0,926	0,701	0,538	0,169		0,235
RSA Solidity					0,146		–0,334	–0,667	–0,546	–0,335	0,185	0,409	–0,503
RSA Total Length				0,718	0,88	–0,327	0,425	0,54	0,371	0,427	0,499	0,402	–0,243
Shoot biomass					0,756	0,234	0,219	0,385	0,304	0,218	0,409	0,387	–0,315
Root biomass						–0,431	0,349	0,487	0,344	0,345	0,412	0,47	–0,216
Shoot/Root biomass							–0,213	–0,199		–0,209		–0,183	
RSA Depth								0,274	–0,148	0,993	0,581		0,144
RSA Width									0,901	0,276			0,251
Width/depth ratio										–0,141	–0,269		0,188
PR length											0,584		0,145
1st order LRs												0,395	–0,696
Total number of LRs													–0,463

Light green and light red are weak positive and weak negative correlations, respectively. Dark green and dark red shadings represent strong positive and negative correlations, respectively.

TABLE 3 | Correlation analysis between 15 RSA traits and: A - geographical/climate features of their place of origin, B – soil types depending on the soil taxonomy (for the description of soil types, please refer to the **Supplementary Table 4**).

A	latitude (EW)	longitude (NS)	Country of origin	elevation	Temp Mean {C}	Precipitation sum {mm}
RSA Length Distribution				0,147		–0,198
RSA Area	0,165	0,236		0,239	–0,349	
RSA Convex Area		0,239		0,238	–0,288	–0,128
RSA Solidity						0,162
RSA Total Length	0,19	0,211		0,207	–0,338	
Shoot biomass		0,201	–0,163	0,322	–0,187	
Root biomass	0,145	0,205		0,211	–0,296	
Shoot/Root biomass	–0,242				0,222	–0,136
RSA Depth	0,188				–0,152	
RSA Width		0,287		0,3	–0,253	
Width/depth ratio		0,323		0,343	–0,178	
PR length	0,188				–0,153	
1st order LRs	0,149					
Total number of LRs						
LR density						
latitude (EW)				–0,425	–0,565	
longitude (NS)			–0,159	0,253	–0,221	–0,181
Country of origin						0,139
elevation					–0,297	
Temp Mean {C}						–0,178

B	soil type 1	soil type 2
RSA Length Distribution		
RSA Area	–0,196	
RSA Convex Area	–0,137	
RSA Solidity		
RSA Total Length	–0,238	–0,151
Shoot biomass		–0,18
Root biomass	–0,154	–0,17
Shoot/Root biomass		
RSA Depth	–0,181	
RSA Width		
Width/depth ratio		
PR length	–0,186	
1st order LRs	–0,16	
Total number of LRs	–0,153	–0,162
LR density		

Light green and light red shadings are weak positive and weak negative correlations, respectively. Dark green and dark red shadings represent strong positive and negative correlations, respectively.

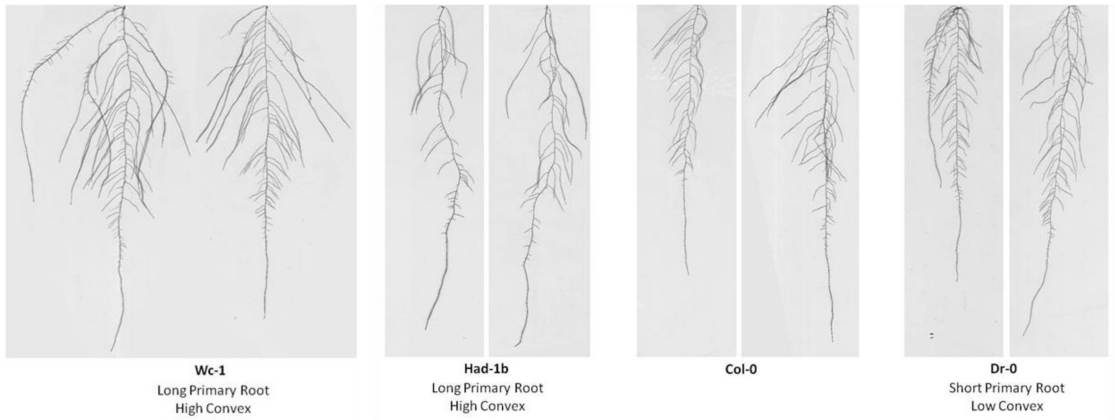

FIGURE 3 | Accessions contrasted width to depth ratio tested in the Rhizotron study. Wc-1 has a low width to depth ratio and a long primary root length and a high convex area. Had-1b has a high width to depth ratio, long primary root length, and a high convex area. Col-0 has an intermediate width to depth ratio, primary root length, and convex area. Dr-0 has a high width to depth ratio but shorter primary root length and a low convex area.

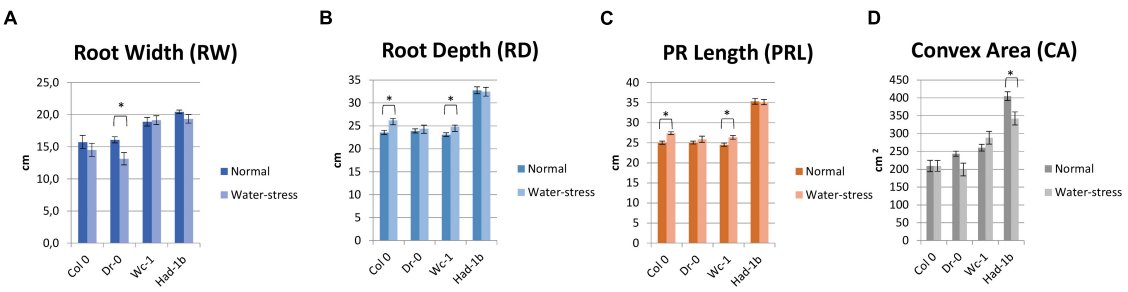

FIGURE 4 | (A–D) Results of measurements for root system architecture (RSA) traits, on four accessions tested in the rhizotron set-up, for normal and mild-stress conditions. *, $p < 0.05$ as analyzed by a Student's *t*-test.

case of Model 1 (division into 4 zones), Had-1b had more root area observed in the lower zones of the rhizosheet than Wc-1 (**Figure 5C**). This is less obvious if the rhizosheet is divided only into 3 zones (model 2) (**Figure 5D**). Measuring the centroid is an alternative way of getting insight into the spatial distribution of roots. Compared to other accessions, centroid value was higher in the case of Had-1b which seems to be influenced by the production of more LRs in the lower zones of the root system (**Figure 5B**). This pattern of Had-1b RSA development was observed in well-watered conditions suggesting this accession might be evolutionarily shaped as a water-seeking accession by its deep proliferation of its RSA at the cost of development of LRs and the shoot. Shoot development of plants grown in rhizotron was also scored for the following three parameters: rosette area, rosette dry, and fresh weight; and stem dry and fresh weight (**Figure 6**). Following its RSA, Had-1b also scored the highest values in the shoot traits. Both, the rosette fresh weight and rosette dry weight were the highest for this accession (**Figures 6A,B**). On the other hand, this was the only accession that in the period of the experiment did not develop an inflorescence stem (**Figure 6D**). Its investment into a well-established, deeper root system, prepared for deep water level exploration, influences the rosette area (**Figure 6C**) but, as a trade-off, it might postpone the progression into the flowering stage (**Figures 6D,E**). Alternatively, the more extensive root system of Had-1b could be the expression of its prolonged vegetative phase and suggests root traits might follow, in coordination with the shoot, phase-change transitions in plants.

Next, we compared the results obtained in petri-dish conditions with the observations made in the soil (**Figure 7**). While Had-1b presented the largest convex area in the rhizotrons, in plates it showed an intermediate CA which was much smaller than the one of Wc-1 (**Figures 7A,B**). Similarly, Had-1b on plates represented a much smaller root area (**Figures 7E,F**) in comparison with rhizotron conditions, in which it developed equally to Wc-1. Root area distribution for Had-1b and Wc-1, in

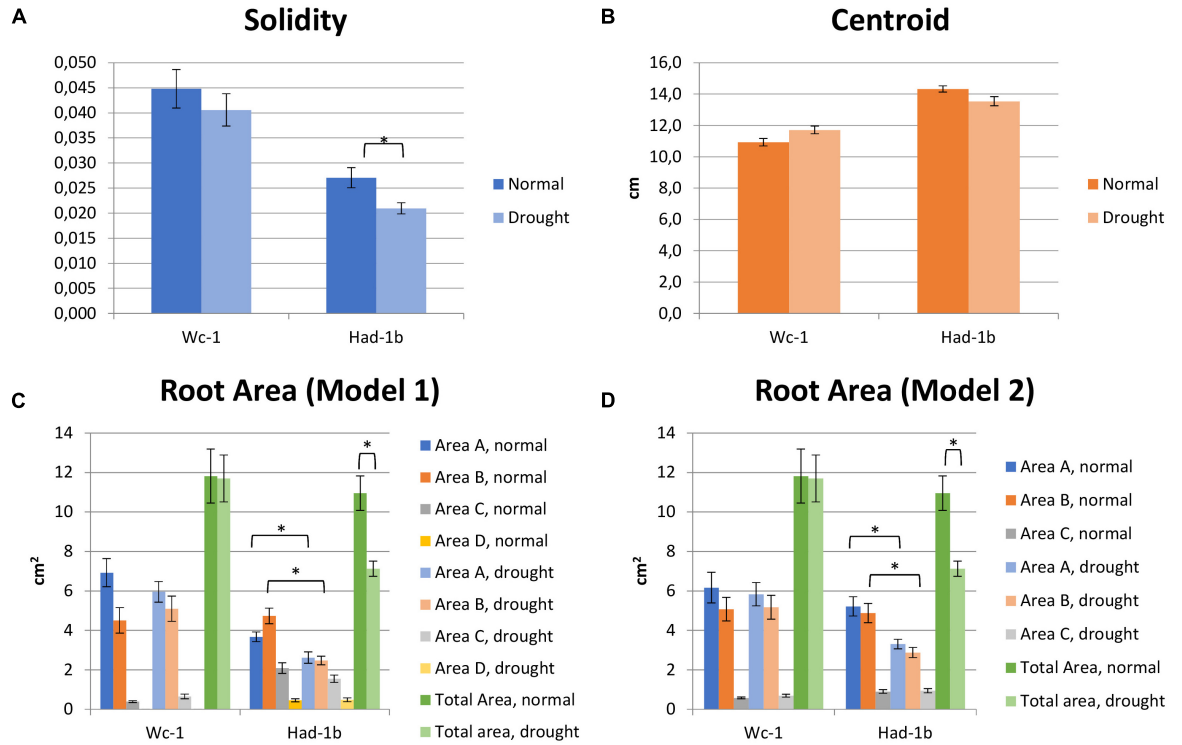

FIGURE 5 | (A–D) Results of measurements of RSA traits including root area in the zones of the rhizosheets, for two contrasting accessions. *, $p < 0.05$ as analyzed by a Student's *t*-test.

different zones, was similar on plates as in rhizotrons, indicating that the spatial distribution of the root stays the same over time, only the size can increase depending on growth medium, growth conditions, and stage of development. The different positions of Had-1b relative to the other accessions in soil vs. petri-dishes illustrate that some accessions respond differently and, thus, require more time to reveal their more mature root traits and urge some caution in making conclusions on RSA traits solely based on petri-dish conditions. On the other hand, relative differences of some traits between accessions, such as root distribution between Wc-1 and Had-1b were kept invariant between plates and rhizotron experiments.

Root System Architecture Parameters Are Influenced by Water Limiting Conditions

Limited water conditions had a visible influence on all accessions. Had-1b still scored the highest values for all parameters in water stress conditions while it showed also a significant reduction in convex area (**Figure 4D**), solidity, and root area distribution in the upper zones of the root system in comparison to normal conditions (**Figures 5A,C**). Primary root length did not change in Had-1b under limited water conditions while the other three accessions showed at least a trend in increasing PR length in water stress compared to normal, which was significant for Col-0 and Wc-1 (**Figure 4C**). On the other hand, Wc-1 did not show a reduction in root width while this was the case for the three other accessions (significant for Dro-0) (**Figure 4A**).

Concerning the shoot, for all accessions, a drop in values in shoot parameters was observed in water limiting conditions. The size and weight of the rosette were decreased (**Figures 6A-C**) and the inflorescence stem for the three flowering accessions also developed less as compared to well-watered conditions (**Figures 6D,E**) clearly showing the negative influence of suspended water treatment on the aboveground traits.

Genome-Wide Association Studies

For GWAS, a collection of 15 RSA traits was measured on plants grown in *in vitro* conditions, on gel-filled medium plates. The measurements and analysis of traits are described in the section "Materials and Methods." Broad-sense heritability (H^2) was calculated and the results varied from 21 to 56% (**Table 1**). This means that 21–56% of the observed variation for different phenotypes is due to genetic differences. Convex area, root width, and root to width ratio scored above 50% indicating them as the most heritable from our dataset of RSA traits. Root biomass was characterized as the least heritable RSA trait in the dataset. The GWAS analysis was performed with the QTCAT program and indicated 141 significant SNPs for a total of 15 root traits (**Table 4** and **Supplementary Table 6**). The only trait that did not deliver any significant results was root biomass. This is probably linked to low genetically inherited variation in this trait, which scored the lowest for our whole dataset (**Table 1**). Analysis of a 20 kb window

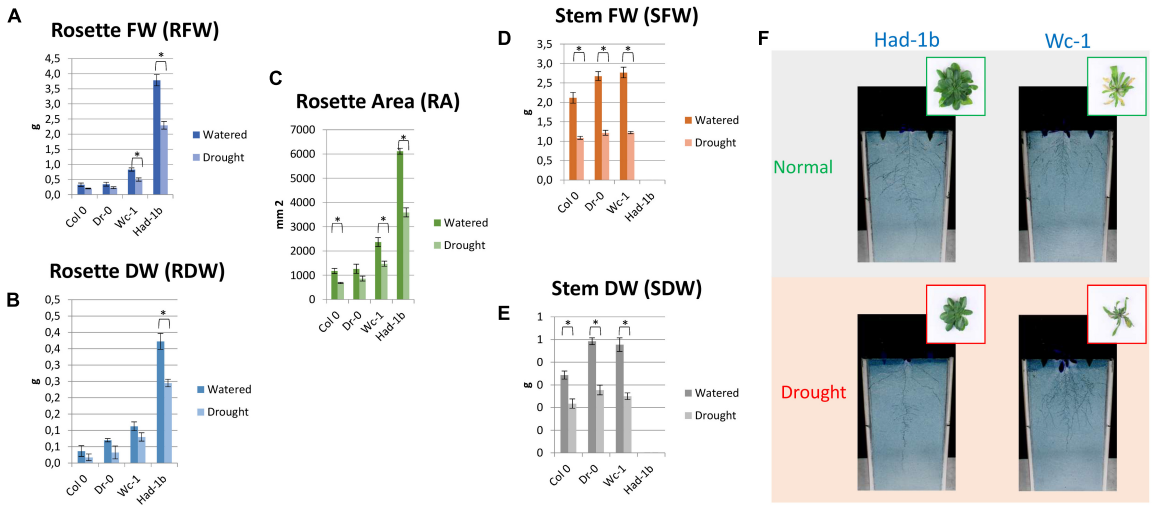

FIGURE 6 | Shoot trait measurements for rhizosheet experiments, for four accessions. **(A–E)** Results of shoot measurements. **(F)** Visualization of shoots of two accessions on 24 DAG in a rhizosheet. *, $p < 0.05$ as analyzed by a Student's *t*-test.

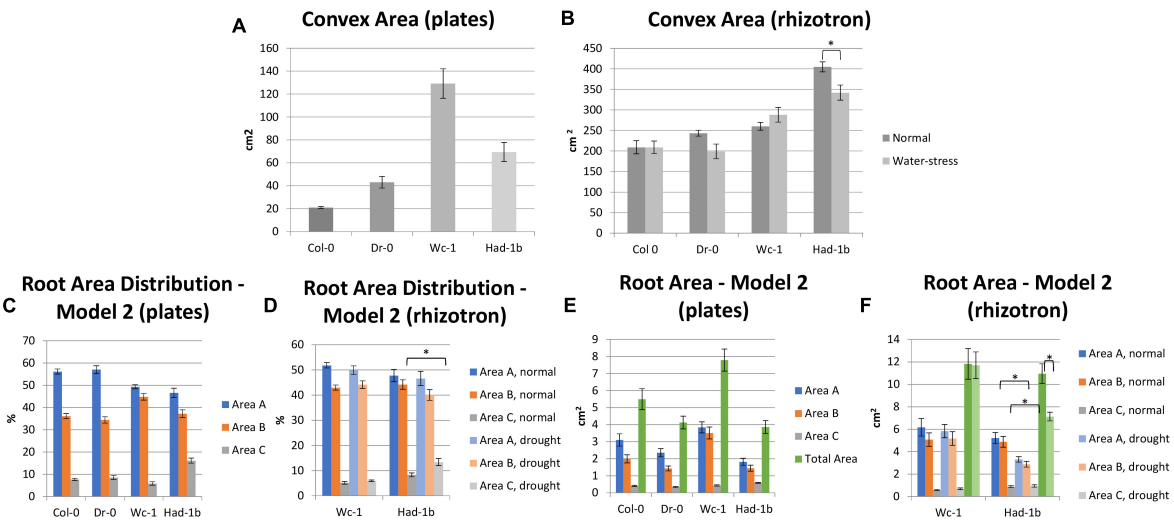

FIGURE 7 | (A–F) Comparison between the results of RSA trait measurements in plates (*in vitro*) and in rhizosheets. *, $p < 0.05$ as analyzed by a Student's *t*-test.

around each significant SNP allowed for collecting a dataset of 412 genes of interest (full list in **Supplementary Table 5**). The visual representation in the form of simplified Manhattan plots is shown in **Figure 8**. Some overlap between SNPs was detected for several traits. This was, however, expected due to the natural dependence between root traits. Shared SNPs were detected for the pairs of traits as follows: convex area—projected area, projected area—root biomass, projected area—total root length, root depth—primary root length, root width—convex area (**Supplementary Table 6**). Those relations are reflected in correlation analysis. A total of 26 genes have been chosen as genes of interest for further analysis (**Table 5**). The selection of those was narrowed down based on gene ontologies. *The suppressor of MAX 2 1 (SMAX1)* was one of the genes found in the 20 kb window around the SNP associated with shoot to root biomass ratio. The *SMAX1* is known to act downstream of MAX2 and is involved in response to strigolactones and karrikins (Stanga et al., 2016; Moturu et al., 2018). It has a role in germination and seedling morphogenesis but is also expressed in mature roots and axillary shoots. According to recent studies, *SMAX1*, together with the closely related *SMXL2*, plays a role in root and root hair development (Villaécija-Aguilar et al., 2019). In our study, this gene was detected for the shoot to root ratio trait linking the fact that it influences both below- and above-ground plant parts which would fit with the proposed role for strigolactones as coordinators of the shoot and root development. *PIN-LIKE 7 (PILS7)* was also detected for the root-to-shoot trait. It belongs to the known auxin efflux carrier protein family

TABLE 4 | Summary of single nucleotide polymorphisms (SNPs) and genes discovered by QTCAT analysis on 15 RSA traits on 241 *Arabidopsis* accessions.

No.	RSA Trait	QTCAT tool	
		SNPs	Genes
1	Root Depth	11	50
2	Root Width	6	35
3	Width to Depth ratio	28	60
4	Root Biomass	0	0
5	Shoot Biomass	33	36
6	Root Biomass to Shoot Biomass ratio	13	52
7	Projected Area	4	23
8	Convex Area	6	43
9	Solidity	6	45
10	Total Root Length	1	5
11	Length Distribution	4	29
12	Primary Root Length	9	39
13	Total Number of LRs	1	9
14	Number of 1st Order LRs	4	23
15	Lateral Root Density	7	27
	TOTAL	141	535
	TOTAL (after removing double genes)		412

(Rosquete et al., 2018) playing a role in auxin homeostasis which is an essential mechanism for root development. Another gene linked to this analyzed trait is *MILDEW RESISTANCE LOCUS O10*. It is a member of a large family of seven transmembrane domain proteins specific to plants that have a high level of functional redundancy, cofunction, or antagonistic function based on similar or overlapping tissue specificity and analogous responsiveness to external stimuli. It is expressed in root and cotyledon vascular system, in root–shoot junction, and LR primordia, which aligns with the result that was detected for root-to-shoot ratio trait (Chen et al., 2006). From our results, it seems that another resistance gene affects the overall root-to-shoot ratio. *ENHANCED DOWNY MILDEW 1, the* ENHANCER OF TIR1-1 AUXIN RESISTANCE 3 *(SGT1B)* that besides serving a role in plant immunity is also required for the SCF(TIR1)-mediated degradation of Aux/IAA proteins in the canonical auxin signaling pathway, linking it to RSA development (Gray et al., 2003). Two interesting associations for PR length and root depth were identified. One of them, *Root Meristem Growth Factor 6 (RGF6)* or *GOLVEN1*, can also be regarded as a proof of concept of the value of our GWAS as it is required for the maintenance of the root stem cell niche and transit amplifying cell proliferation in the root meristem which would be in agreement with its association with PR length (Ou et al., 2016; Song et al., 2016). The second gene, *C-Terminal Domain Phosphatase-Like 5 (CPL5)*, is involved in the regulation of abscisic acid (ABA) and drought responses of the root and was found in our study to be linked to vertical root growth as well (Jin et al., 2011). Association for convex area yielded a member of a family of LRR receptor-like kinases of which several members were shown to be involved in root growth and development (Ou et al., 2016), namely *RGF1 Insensitive 2 (RGI2)* that also plays role in the maintenance of root stem cell niche by influencing PLETHORA (PLT) transcription factors and is a receptor of RGFs. Association for shoot biomass also emerged as two interesting genes. One candidate gene is *Aberrant Lateral Root Formation 5 (ALF5)* (Diener et al., 2001). The *ALF5* encodes a multidrug efflux transporter gene family member, conferring resistance to toxins. Genes from the same family, *ALF1* and *ALF4* do have mutants with increased levels of endogenous auxin, promoting LR formation by maintaining the pericycle in a mitotically competent state leading to LR formation. ALF4 binds to RBX1 and inhibits the activity of SCFTIR1, an E3 ligase responsible for the degradation of the Aux/IAA transcriptional repressors (Bagchi et al., 2018). Because it was detected for shot biomass trait, it might indicate that influence on those pathways in root development has an influence on the above-ground development. The second gene with the association for shoot biomass is Scare Family Protein 4 (SCAR4) involved in microtubule organization and might again be responsible for shoot biomass increase due to a better root performance, as it was already linked to root elongation (Dyachok et al., 2011). Transcription factors (TFs) are known to take part in the maintenance of auxin signaling in root development. In our candidate gene list, a TF was linked to RSA depth trait: Kow Domain-Containing Transcription Factor 1 (KTF1) which is involved in regulating the transcription by RNA polymerase II (Köllen et al., 2015). Similarly, Basic transcription Factor **3 (BTF3)** was found for width to depth ratio and categorized as a gene of interest for further investigation. Among associations for RSA total length, Dioxygenase for Auxin Oxidation 1 (DAO1) was detected. This is the major indoleacetic acid (IAA) oxidase in plants, manipulating the levels of auxin degradation (Mellor et al., 2016). For this trait also, another oxidase was detected: Auxin Oxidase (DAO2) that is expressed in root caps and is, similarly to DAO1, responsible for auxin homeostasis. Overall, this indicates, as expected, that RSA length is directed by auxin homeostasis mechanisms. Our results of associations lead also to the detection of multiple unknown genes, such as calmodulin-binding protein, described from an auxin-treated complementary DNA (cDNA) library (Reddy et al., 2002). It is detected for the solidity trait, indicating that it might play a role in the initiation of new LRs that increase the compactness of the RSA. The molecular analysis of the genes of interest is beyond the scope of this study and awaits further investigations.

DISCUSSION

Root System Architecture Phenotyping: A Gateway to Underground Variability

With the current state of phenotyping of underground traits, common techniques can be upgraded and manipulated to fit more precisely to the investigation of desired root traits. In our case study, the exchange of a gelling agent from agar to Gelrite allowed for a limitation of root waving, due to its harder for a root to penetrate properties (Yan et al., 2017). This allowed us to obtain a less tangled RSA in more mature root systems and enabled the extraction of a long list of root traits, that can precisely describe RSA on a miniaturized scale. LR traits can

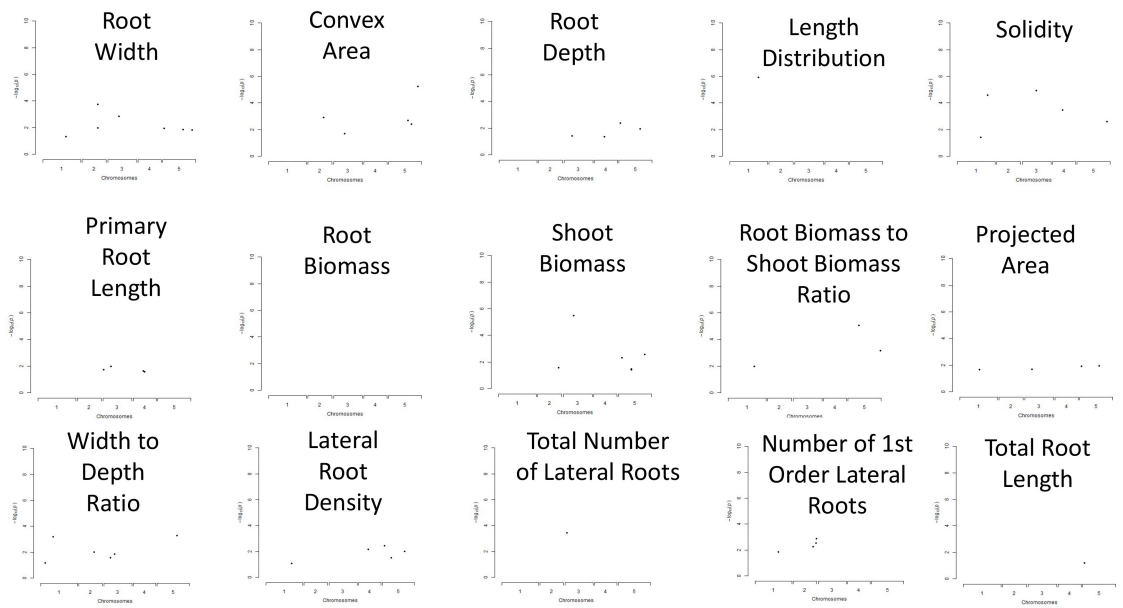

FIGURE 8 | Manhattan plot representation of associated single nucleotide polymorphisms (SNPs) detected for each of 15 RSA traits, plotted on the *x*-axis, based on their genomic position. Loci that are close to each other are averaged as one point in the scheme, for simplified visualization.

TABLE 5 | List of 26 genes selected based on their ontologies as genes of interest, together with information from which traits where those genes detected by QTCAT analysis.

Trait1	Trait2	Gene numbers	Gene name
Convex area		AT5G48940.1	RGF1 INSENSITIVE 2
Root_Shoot_ratio		AT4G11240.1	type I serine/threonine protein phosphatase
Root_Shoot_ratio		AT4G11260.1	ENHANCED DOWNY MILDEW 1, ENHANCER OF TIR1-1 AUXIN RESISTANCE 3
Root_Shoot_ratio		AT4G19120.1	EARLY-RESPONSIVE TO DEHYDRATION 3
Root_Shoot_ratio		AT4G20140.1	GASSHO1, GSO1, SCHENGEN 3, SGN3
RSA_depth		AT1G47056.1	VIER F-BOX PROTEINE 1
RSA_depth	PR_length	AT3G19600.1	C-TERMINAL DOMAIN PHOSPHATASE-LIKE 5
RSA_depth	PR_length	AT4G16515.1	ROOT MERISTEM GROWTH FACTOR 6
RSA_depth		AT5G04290.1	KOW DOMAIN-CONTAINING TRANSCRIPTION FACTOR 1
RSA_length		AT1G14120.1	ATDAO2, AUXIN OXIDASE
RSA_length		AT1G14130.1	DIOXYGENASE FOR AUXIN OXIDATION 1
RSA_length		AT1G62810.1	COPPER AMINE OXIDASE1
Shoot_Biomass		AT3G23560.1	ABERRANT LATERAL ROOT FORMATION 5
Shoot_Biomass		AT5G01730.1	SCAR FAMILY PROTEIN 4, WAVE3
Shoot_Root_ratio		AT5G57710.1	SUPPRESSOR OF MAX2 1
Shoot_Root_ratio	Root_Shoot_ratio	AT5G65970.1	MILDEW RESISTANCE LOCUS O 10
Shoot_Root_ratio	Root_Shoot_ratio	AT5G65980.1	PIN-LIKES 7
Solidity		AT5G40190.1	calmodulin-binding protein
Width_Depth_ratio		AT1G17880.1	BASIC TRANSCRIPTION FACTOR 3
Width_Depth_ratio		AT3G16690.1	SWEET16, Nodulin MtN3 family protein
Width_Depth_ratio		AT3G16785.1	PHOSPHOLIPASE D P1
1st order LRs		AT2G46920.1	Protein phosphatase 2C family protein
LR Density		AT4G13930.1	SHM4, serine hydroxymethyltransferase 4
RSA_depth		AT1G47128.1	RESPONSIVE TO DEHYDRATION 21
Root_Shoot_ratio		AT5G59240.1	Ribosomal protein S8e family protein
Root_Shoot_ratio		AT5G59290.2	UDP-GLUCURONIC ACID DECARBOXYLASE 3

be measured without having to sacrifice plants. Usually, root tracing in *in vitro* experiments is performed on very young seedlings compared to our study. At the end of the day, the phenotyping method, however, will always be a limiting factor as there is no single, universal method that allows for investigating all possible root traits at once (Deja-Muylle et al., 2021). The possibility to combine phenotyping techniques, despite time and cost consuming, allows for the extraction of additional information. In our case, a rhizotron study gave us information about differences between *in vitro* studies and soil growth on a selected group of accessions.

A high degree of RSA variability exists in the pool of the analyzed *Arabidopsis* accessions. Similar results of the high variability of RSA traits were described in a recent *Arabidopsis* root study in the "GLORoots" rhizo-systems (Larue et al., 2021). We have confirmed a strong relationship between the above and underground plant traits. An increase in shoot biomass had only one negative correlation to LR density, indicating that the overall increase in area that the root systems take, is due to a shift from the elongation of the primary root to the initiation of a new first order LRs. The LRs have an influence on total root length increasing the soil exploration zone for nutrients and thus influencing the shoot biomass as well. LR density is overall a trait that negatively correlates with many other measured traits, suggesting that LR density is a high energy demanding process, that occurs at a cost of other parameters. Overall, the LR density and dependencies with other traits should be considered while selecting root traits in breeding programs. Understanding the correlations between RSA traits and between under and aboveground parts should be considered as one of the best approaches for plant improvement (Paez-Garcia et al., 2015), especially as it can be linked to certain root ideotypes that aim at the improvement of nutrient and water uptake, leading to higher yield (Lynch, 2019).

Rhizosheets vs. Petri-Dishes and Water Deficit Stress

Recently, the study of the hidden half is gaining increased interest among researchers, resulting in various attempts to phenotype the root systems of plants. However, many of the developed techniques are destructive or inaccurate when being deployed in the field or being relatively expensive to install and space-consuming (Atkinson et al., 2019). Techniques also depend on which plant species is under evaluation (Deja-Muylle et al., 2021). Our aim was not only to test RSA observed on plates but also to provide a low-cost yet versatile root phenotyping system without the immediate requirement for sophisticated equipment allowing for easy implementation in any laboratory. Our experiments confirmed that ecotypes of *A. thaliana,* distinguished by specific root traits observed on gel media in *in vitro* studies, maintained their phenotypes in soil, but not for all four accessions. This means that there is a certain overlap between traits in *in vitro* studies at the small, young seedlings and later stages of plant development. This seems, however, to be sensitive to accession genetic build-up as, shown on accession Had-1b. Its differential performance between two phenotyping systems might be explained by the fact that for some accessions, certain root traits become more pronounced in the later stages of development. In such cases, the rhizotron has more benefits over *in vitro* techniques in plates as it allows for the plants to grow bigger, with fewer constraints of the physical system in which there are grown. Additionally, different phenotyping techniques bring versatile interference obstacles that cause variation in RSA. Possibly, in certain accessions, mechanically responsive genes might become activated only in defined conditions due to increased friction of soil medium compared to gelling agent, leading to differences in spatial distribution. Such a situation has been reported by Zhao et al. (2017), in experiments performed *in vitro* and in sand-filled rhizotrons on pea genotypes. Our results confirm the same result that seedling root traits are not *per se* predictive of mature RSA over time. Moreover, the plasticity in RSA is specific for each accession and, thus, represents a very interesting resource to study further to be used in crop breeding aiming at the production of crops that efficiently adapt to changing environments (Schneider and Lynch, 2020; Van Der Bom et al., 2020).

Rhizotron systems have also brought a valuable approach to test if and how RSA changes upon applied stress. We have tested a mild water stress setup on three contrasting accessions. Water stress did influence all RSA types tested. Among those accessions, there was one, Had-1b that seemed to be, however, less affected by water limitation than others, resulting in a more limited decrease in the observed root traits. The result of this experiment is that traits observed in *in vitro* conditions are not predictive of how plants will react to water stress. Had-1b and Wc-1 both had one trait that was not changed under water-limitation compared to the other two accessions. This result is corroborated by the study of Guimarães et al. (2020), based on a study of rice japonica accessions, which demonstrated that there was no indication of RSA traits on how plants, even the ones representing the same values of traits, react to water stress.

The Power of Genome-Wide Association Studies to Detect Genes Involved in the Overall Root System Architecture Development

In our study, we have detected a high amount of genes of interest, similar to many other root GWASs (Deja-Muylle et al., 2021). This might be explained partially due to the nature of the QTCAT program that was chosen for this analysis. It outperforms other algorithms, by specific correction of population structure leading to the identification of more loci while at the same time minimizing the amount of false-positive errors (Klasen et al., 2016). In this way, it efficiently counterparts the drawbacks that GWAS analysis struggles with currently (Alseekh et al., 2021). Another reason behind the high amount of SNPs detected is due to the intricate nature of RSA traits that are often intertwined and redundant, causing many genes to be responsible for one root trait (Motte et al., 2019). To narrow down the number of candidate genes, we have employed our prior knowledge over biological pathways and known gene ontologies, which is a common way of limiting GWAS results. In the case of

this study, 26 genes have been selected and, similarly to many other studies in *Arabidopsis* roots, further work is necessary, to uncover the pathways and molecular role in driving the RSA trait development of those genes (Kawa et al., 2016; Ristova et al., 2018). We have detected a few genes with known functions in the root development that are a good proof of concept for the chosen GWAS method. Additionally, the fact that some genes known to be involved in certain root development pathways have been identified in our study as responsible for another, distinct root trait, indicating that those will be an interesting subject in the further analysis as many genes are known to participate in multiple pathways. We have detected genes involved in different processes, for example, in hormonal signaling such as auxin, ABA, and strigolactones. Few of the indicated genes were linked to root–shoot interactions. We also retrieved genes involved in drought responses or genes that have roles in germination or disease resistance. This wide span can be indicative of GWAS detecting multiple casual variants. New methods are developed to further fine-tune this type of result (LaPierre et al., 2021). Based on our results, we can conclude that RSA is an interesting topic to study by means of GWAS, as it can reveal genes that would have not been linked to specific RSA traits by other means, such as forward genetics. There are two recent examples where GWAS appeared to be successful in pinpointing genes responsible for RSA expansion (Ogura et al., 2019; Waidmann et al., 2019). Additionally, a successful GWAS was performed on RSA traits measured in a rhizotron system called GLO-ROOTS, where roots are traced after fluorescent labeling of accessions by introducing a genetically encoded reporter system (Larue et al., 2021). This is because GWAS on RSA fulfills all requirements for a successful GWAS setup. With the correct phenotyping setup, a vast number of root traits can be mined. Second, the correct sample size will lead to increased GWAS power by saturating the dataset with the variability in the trait of interest. Based on our phenotyping experiment, it is clear that high variability in the root traits among the accessions for *Arabidopsis* is present. A trait with the lowest heritability (root biomass) yielded no significant SNPs, confirming that low heritability escapes the power of GWAS to detect causative regions of the genome.

Indeed, the GWAS produces a high amount of data that can be further exploited. For instance, in crops, marker-trait associations are used for breeding strategies (Gupta et al., 2020). Our resulting list of genes of interest is long and even after selection, it still requires molecular validation, which becomes a time-consuming drawback. It is, however, important to note that the GWAS technique, not only indicates association to the genes with mutations in gene expression but also can detect, for example, regions responsible for protein structure or post-transcriptional modifications. This opens up an excellent way of looking for gene-phenotype relationships and should be used in root studies to help undercover more of the still unknown gene pathways. Furthermore, the GWAS analysis is evolving yearly with new algorithms, techniques, and databases available (Togninalli et al., 2018). The phenotype data collected in this study is not of one-time use as it can, in the future, be implemented as a source for more advanced GWAS gene detection or as a part of metanalysis to link different GWAS studies in *Arabidopsis* enhancing our insight into genotype-phenotype relationships.

DATA AVAILABILITY STATEMENT

The datasets presented in this study can be found in online repositories. The names of the repository/repositories and accession number(s) can be found in the article/**Supplementary Material**.

AUTHOR CONTRIBUTIONS

AD-M and TB conceptualized the manuscript. AD-M performed the phenotyping and GWAS experiments. AD-M, BP, HM, and TB wrote the manuscript. AD-M and DO performed the rhizotron experiments. AD-M and MN made the figures. VS, GL, and PC shared their GWAS expertise and plant material. All authors contributed to the article.

FUNDING

This study was financially supported by a research grant (G024118N) from the Research Foundation-Flanders (FWO) and a BOF-ZAP to TB grant from the Special Research Fund of the Ghent University. This work was also partly supported by the German Research Foundation under Germany's Excellence Strategy, EXC-2070 - 390732324 (PhenoRob).

SUPPLEMENTARY MATERIAL

The Supplementary Material for this article can be found online at: https://www.frontiersin.org/articles/10.3389/fpls.2021.814110/full#supplementary-material

Supplementary Figure 1 | Natural distribution of RSA values measured on 241 accessions illustrated for 4 root traits, for example, **(A)** Length distribution, **(B)** solidity, **(C)** total root length. The position for Col-0 is indicated in red. X scale is in [cm] for TRL and in [cm^2] for Convex Area.

Supplementary Figure 2 | Four accessions grown in rhizosheets at 24 DAG (W-normal water conditions, D: mild drought conditions).

REFERENCES

Aceves-García, P., Álvarez-Buylla, E. R., Garay-Arroyo, A., García-Ponce, B., Muñoz, R., and Sánchez, M. P. (2016). Root architecture diversity and meristem dynamics in different populations of *Arabidopsis thaliana*. *Front. Plant Sci.* 7:858. doi: 10.3389/fpls.2016.00858

Alseekh, S., Kostova, D., Bulut, M., and Fernie, A. R. (2021). Genome-wide association studies: assessing trait characteristics in model and crop plants. *Cell. Mol. Life Sci.* 78, 5743–5754. doi: 10.1007/s00018-021-03868-w

Atkinson, J. A., Pound, M. P., Bennett, M. J., and Wells, D. M. (2019). Uncovering the hidden half of plants using new advances in root phenotyping. *Curr. Opin. Biotechnol.* 55, 1–8. doi: 10.1016/j.copbio.2018.06.002

Bagchi, R., Melnyk, C. W., Christ, G., Winkler, M., Kirchsteiner, K., Salehin, M., et al. (2018). The *Arabidopsis* ALF 4 protein is a regulator of SCF E3 ligases. *EMBO J.* 37, 255–268. doi: 10.15252/embj.201797159

Bourne, R. (2010). ImageJ. *Fund. Digit. Imaging Med.* 9, 185–188. doi: 10.1007/978-1-84882-087-6_9

Chen, Y., Palta, J. A., Wu, P., and Siddique, K. H. M. (2019). Crop root systems and rhizosphere interactions. *Plant Soil* 439, 1–5. doi: 10.1007/s11104-019-04154-2

Chen, Y., Takita, J., Hiwatari, M., Igarashi, T., Hanada, R., Kikuchi, A., et al. (2006). Mutations of the PTPN11 and RAS genes in rhabdomyosarcoma and pediatric hematological malignancies. *Genes Chromosom. Cancer* 45, 583–591. doi: 10.1007/s11103-005-5082-x

Clark, R. T., Famoso, A. N., Zhao, K., Shaff, J. E., Craft, E. J., Bustamante, C. D., et al. (2013). High-throughput two-dimensional root system phenotyping platform facilitates genetic analysis of root growth and development. *Plant Cell Environ.* 36, 454–466. doi: 10.1111/j.1365-3040.2012.02587.x

Deja-Muylle, A., Parizot, B., Motte, H., and Beeckman, T. (2021). Exploiting natural variation in root system architecture via genome-wide association studies. *J. Exp. Bot.* 71, 2379–2389. doi: 10.1093/JXB/ERAA029

Del Bianco, M., and Kepinski, S. (2018). Building a future with root architecture. *J. Exp. Bot.* 69, 5319–5323. doi: 10.1093/jxb/ery390

Diener, A. C., Gaxiola, R. A., and Fink, G. R. (2001). Arabidopsis *ALF5*, a multidrug efflux transporter gene family member, confers resistance to toxins. *Plant Cell* 13, 1625–1638. doi: 10.1105/tpc.010035

Dyachok, J., Zhu, L., Liao, F., He, J., Huq, E., and Blancaflor, E. B. (2011). SCAR mediates light-induced root elongation in *Arabidopsis* through photoreceptors and proteasomes. *Plant Cell* 23, 3610–3626. doi: 10.1105/tpc.111.088823

Galkovskyi, T., Mileyko, Y., Bucksch, A., Moore, B., Symonova, O., Price, C. A., et al. (2012). GiA Roots: software for the high throughput analysis of plant root system architecture. *BMC Plant Biol.* 12:116. doi: 10.1186/1471-2229-12-116

Gray, W. M., Muskett, P. R., Chuang, H., and Parker, J. E. (2003). *Arabidopsis* SGT1b Is Required for SCF(TIR1)-mediated auxin response. *Plant Cell* 15, 1310–1319. doi: 10.1105/tpc.010884.transcriptional

Guimarães, P. H. R., de Lima, I. P., de Castro, A. P., Lanna, A. C., Guimarães Santos Melo, P., and de Raïssac, M. (2020). Phenotyping root systems in a set of japonica rice accessions: can structural traits predict the response to drought? *Rice* 13:67. doi: 10.1186/s12284-020-00404-5

Gupta, A., Rico-Medina, A., and Caño-Delgado, A. I. (2020). The physiology of plant responses to drought. *Science* 368, 266–269. doi: 10.1126/science.aaz7614

Jin, Y. M., Jung, J., Jeon, H., Won, S. Y., Feng, Y., Kang, J. S., et al. (2011). AtCPL5, a novel Ser-2-specific RNA polymerase II C-terminal domain phosphatase, positively regulates ABA and drought responses in *Arabidopsis*. *New Phytol.* 190, 57–74. doi: 10.1111/j.1469-8137.2010.03601.x

Kawa, D., Julkowska, M. M., Sommerfeld, H. M., Ter Horst, A., Haring, M. A., and Testerink, C. (2016). Phosphate-dependent root system architecture responses to salt stress. *Plant Physiol.* 172, 690–706. doi: 10.1104/pp.16.00712

Kerstens, M., Hesen, V., Yalamanchili, K., Bimbo, A., Grigg, S., Opdenacker, D., et al. (2021). Nature and nurture: genotype-dependent differential responses of root architecture to agar and soil environments. *Genes* 12:1028. doi: 10.3390/genes12071028

Klasen, J. R., Barbez, E., Meier, L., Meinshausen, N., Bühlmann, P., Koornneef, M., et al. (2016). A multi-marker association method for genome-wide association studies without the need for population structure correction. *Nat. Commun.* 7, 1–8. doi: 10.1038/ncomms13299

Köllen, K., Dietz, L., Bies-Etheve, N., Lagrange, T., Grasser, M., and Grasser, K. D. (2015). The zinc-finger protein SPT4 interacts with SPT5L/KTF1 and modulates transcriptional silencing in *Arabidopsis*. *FEBS Lett.* 589, 3254–3257. doi: 10.1016/j.febslet.2015.09.017

LaPierre, N., Taraszka, K., Huang, H., He, R., Hormozdiari, F., and Eskin, E. (2021). Identifying causal variants by fine mapping across multiple studies. *PLoS Genet.* 17:e1009733. doi: 10.1371/journal.pgen.1009733

Larue, T., Lindner, H., Srinivas, A., Exposito-alonso, M., Lobet, G., and Dinneny, J. R. (2021). Uncovering natural variation in root system architecture and growth dynamics using a robotics-assisted phenomics platform. *Biorxiv* [Preprint]. doi: 10.1101/2021.11.13.468476v1

Lynch, J. P. (2019). Root phenotypes for improved nutrient capture: an underexploited opportunity for global agriculture. *New Phytol.* 223, 548–564. doi: 10.1111/nph.15738

Mellor, N., Band, L. R., Pìòík, A., Novák, O., Rashed, A., Holman, T., et al. (2016). Dynamic regulation of auxin oxidase and conjugating enzymes AtDAO1 and GH3 modulates auxin homeostasis. *Proc. Natl. Acad. Sci. U.S.A.* 113, 11022–11027. doi: 10.1073/pnas.1604458113

Motte, H., Vanneste, S., and Beeckman, T. (2019). Molecular and environmental regulation of root development. *Annu. Rev. Plant Biol.* 70, 465–488. doi: 10.1146/annurev-arplant-050718-100423

Moturu, T. R., Thula, S., Singh, R. K., Nodzyński, T., Vaøeková, R. S., Friml, J., et al. (2018). Molecular evolution and diversification of the SMXL gene family. *J. Exp. Bot.* 69, 2367–2378. doi: 10.1093/jxb/ery097

Ogura, T., Goeschl, C., Filiault, D., Mirea, M., Slovak, R., Wolhrab, B., et al. (2019). Root system depth in *Arabidopsis* is shaped by EXOCYST70A3 via the dynamic modulation of auxin transport. *Cell* 178, 400.e16–412.e16. doi: 10.1016/j.cell.2019.06.021

Oldroyd, G. E. D., and Leyser, O. (2020). A plant's diet, surviving in a variable nutrient environment. *Science* 368:eaba0196. doi: 10.1126/science.aba0196

Ou, Y., Lu, X., Zi, Q., Xun, Q., Zhang, J., Wu, Y., et al. (2016). RGF1 INSENSITIVE 1 to 5, a group of LRR receptor-like kinases, are essential for the perception of root meristem growth factor 1 in *Arabidopsis thaliana*. *Cell Res.* 26, 686–698. doi: 10.1038/cr.2016.63

Paez-Garcia, A., Motes, C. M., Scheible, W. R., Chen, R., Blancaflor, E. B., and Monteros, M. J. (2015). Root traits and phenotyping strategies for plant improvement. *Plants* 4, 334–355. doi: 10.3390/plants4020334

Ray, D. K., Mueller, N. D., West, P. C., and Foley, J. A. (2013). Yield trends are insufficient to double global crop production by 2050. *PLoS One* 8:e0066428. doi: 10.1371/journal.pone.0066428

Reddy, V. S., Ali, G. S., and Reddy, A. S. N. (2002). Genes encoding calmodulin-binding proteins in the *Arabidopsis* genome. *J. Biol. Chem.* 277, 9840–9852.

Ristova, D., Giovannetti, M., Metesch, K., and Busch, W. (2018). Natural genetic variation shapes root system responses to phytohormones in *Arabidopsis*. *Plant J.* 96, 468–481. doi: 10.1111/tpj.14034

Rogers, E. D., and Benfey, P. N. (2015). Regulation of plant root system architecture: implications for crop advancement. *Curr. Opin. Biotechnol.* 32, 93–98. doi: 10.1016/j.copbio.2014.11.015

Rosas, U., Cibrian-Jaramillo, A., Ristova, D., Banta, J. A., Gifford, M. L., Fan, A. H., et al. (2013). Integration of responses within and across *Arabidopsis* natural accessions uncovers loci controlling root systems architecture. *Proc. Natl. Acad. Sci. U.S.A.* 110, 15133–15138. doi: 10.1073/pnas.1305883110

Rosquete, M. R., Waidmann, S., and Kleine-Vehn, J. (2018). PIN7 auxin carrier has a preferential role in terminating radial root expansion in *Arabidopsis thaliana*. *Int. J. Mol. Sci.* 19, 1–11. doi: 10.3390/ijms19041238

Schneider, H. M., and Lynch, J. P. (2020). Should root plasticity be a crop breeding target? *Front. Plant Sci.* 11:546. doi: 10.3389/fpls.2020.00546

Scholl, R. L., May, S. T., and Ware, D. H. (2000). Resources and opportunities seed and molecular resources for *Arabidopsis*. *Society* 124, 1477–1480.

Song, W., Liu, L., Wang, J., Wu, Z., Zhang, H., Tang, J., et al. (2016). Signature motif-guided identification of receptors for peptide hormones essential for root meristem growth. *Cell Res.* 26, 674–685. doi: 10.1038/cr.2016.62

Stanga, J. P., Morffy, N., and Nelson, D. C. (2016). Functional redundancy in the control of seedling growth by the karrikin signaling pathway. *Planta* 243, 1397–1406. doi: 10.1007/s00425-015-2458-2

Togninalli, M., Seren, Ü, Meng, D., Fitz, J., Nordborg, M., Weigel, D., et al. (2018). The AraGWAS catalog: a curated and standardized *Arabidopsis thaliana* GWAS catalog. *Nucleic Acids Res.* 46, D1150–D1156. doi: 10.1093/nar/gkx954

Van Der Bom, F. J. T., Williams, A., and Bell, M. J. (2020). Root architecture for improved resource capture: trade-offs in complex environments. *J. Exp. Bot.* 71, 5752–5763. doi: 10.1093/jxb/eraa324

Villaécija-Aguilar, J. A., Hamon-Josse, M., Carbonnel, S., Kretschmar, A., Schmidt, C., Dawid, C., et al. (2019). SMAX1/SMXL2 regulate root and root hair development downstream of KAI2-mediated signalling in *Arabidopsis*. *PLoS Genet.* 15:e1008327. doi: 10.1371/journal.pgen.1008327

Waidmann, S., Ruiz Rosquete, M., Schöller, M., Sarkel, E., Lindner, H., LaRue, T., et al. (2019). Cytokinin functions as an asymmetric and anti-gravitropic signal in lateral roots. *Nat. Commun.* 10:3540. doi: 10.1038/s41467-019-11483-4

Yan, J., Wang, B., and Zhou, Y. (2017). A root penetration model of *Arabidopsis thaliana* in phytagel medium with different strength. *J. Plant Res.* 130, 941–950. doi: 10.1007/s10265-017-0926-4

Zhao, J., Bodner, G., Rewald, B., Leitner, D., Nagel, K. A., and Nakhforoosh, A. (2017). Root architecture simulation improves the inference from seedling root phenotyping towards mature root systems. *J. Exp. Bot.* 68, 965–982. doi: 10.1093/jxb/erw494

Conflict of Interest: The authors declare that the research was conducted in the absence of any commercial or financial relationships that could be construed as a potential conflict of interest.

Publisher's Note: All claims expressed in this article are solely those of the authors and do not necessarily represent those of their affiliated organizations, or those of the publisher, the editors and the reviewers. Any product that may be evaluated in this article, or claim that may be made by its manufacturer, is not guaranteed or endorsed by the publisher.

Frontiers in
Plant Science

Cultivates the science of plant biology and its applications

The most cited plant science journal, which advances our understanding of plant biology for sustainable food security, functional ecosystems and human health.

Discover the latest Research Topics

See more →

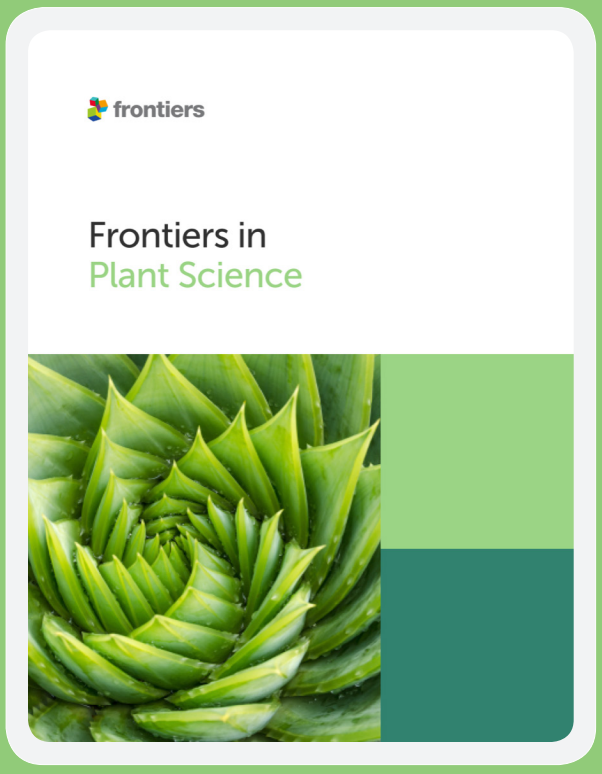

Frontiers

Avenue du Tribunal-Fédéral 34
1005 Lausanne, Switzerland
frontiersin.org

Contact us

+41 (0)21 510 17 00
frontiersin.org/about/contact